

03	01.03.2012	Final	EE	HH	KEK		EHH
02	25.01.2012	Draft for TNO					
01	06.01.2012	Draft					
Revision	Issue date	Issue description	Resp.	Verif.	Disc.	App	Project App.
Client:		Contract No.	Contractor:				
							
Document type description:		Project Phase:	Classification:				
Report			Confidential/Fortrolig/re-classified; open 2015				
Project no:	Project title:		Supplier document number:				
TL02	Transport and Storage of CO ₂ from Mongstad		5001-GTL-Z-RA-00003				
Discipline:	Document type:	Area:	System:				
Z	RA						
Document Title:							
Geological storage of CO ₂ from Mongstad. Interim report Johansen Formation							
Document no.:				Rev.:		Pages:	
TL02-GTL-Z-RA-0001				03		379	
Exempt from public disclosure, cf. regulations of the Free information Act sec. 1, 3rd subsection, litra f)							

Document authors:

Date	Authors	Authors signatures
01.03.2012	POA LH TR KLR MD GK TAT MV EE JH	Per Ola Andfossen Lise Horntvedt Trude Ravn Kari Lise Rørvik Morten Diesen Gemma Keaney Tor Arne Torgersen Morten Vetaas Espen Erichsen Johan Mohr

Revision record:

The revisions are denoted as follows:

i) By the symbol | with the revision number adjacent, located in left-hand column.

Revision	Description of Changes
01	Draft for Gassnova
02	Draft for TNO revision
03	Final version

Document summary:

The objective of the work summarised in this report was to assess the Johansen Formation as a storage site for CO₂. The work will form a basis for further maturation and qualification according to EU directive requirements. The report gives a status and indicates work still necessary, and may serve as the basis for transfer of technical work to a future operator. The evaluation requirement was a CO₂ stream of 3.2Mt/y for 50 years.

DOCUMENT NO.: TL02-GTL-Z-RA-0001	REVISION NO.: 03	REVISION DATE: 01.03.2012	APPROVED:
-------------------------------------	---------------------	------------------------------	-----------

TABLE OF CONTENTS

TABLE OF CONTENTS 3

1 EXECUTIVE SUMMARY 7

2 INTRODUCTION 10

2.1 Work objective 10

2.2 Capacity requirement 10

2.3 Location and licence information 10

2.4 Site description 11

2.5 Work schedule 12

2.6 Work structure 13

2.7 Report Structure 14

3 EVALUATION CRITERIA 16

4 DATA COLLECTION AND ASSESSMENT 18

4.1 Well database 18

4.2 Seismic database 19

4.3 Seismic inversion 22

4.4 Basin modelling 25

4.5 Petrophysical evaluation 25

4.5.1 Summary 25

4.5.2 Methodology and Modelling 27

4.5.3 Log Data Quality Check 27

4.5.4 Volume of Clay Analysis (VCI) 27

4.5.5 Porosity and Water Saturation Analysis 28

4.5.6 Permeability Analysis 28

4.5.7 Porosity and Permeability Calibration 28

4.6 Dynamic simulation parameter description 29

4.7 Lab testing of cores 29

4.7.1 Introduction 29

4.7.2 Storage formation 30

4.7.3 Cap rock 31

4.7.4 Geo-mechanical Testing 33

4.8 Fault seal assessment 34

4.9 Seismicity 36

4.10 Further data collection and assessment 39

5 STORAGE COMPLEX DESCRIPTION 40

5.1 Introduction 40

5.2 Seismic analysis 42

5.2.1 Well to seismic calibration 42

5.2.2 Seismic interpretation 44

5.2.3 Depth conversion 50

5.3 Geological development of storage formation 60

5.3.1 Storage formation presence 62

5.3.2 Storage formation quality 80

5.4 Geological development of sealing formations 95

5.4.1 Primary Seal 96

5.4.2 Secondary Seal - The Overburden 96

5.4.3 Sequence Stratigraphy and Regional setting 97

5.4.4 Biostratigraphy 98

5.4.5 Cap rock leakage assessment 99

5.4.6 Summary cap rock 110

5.5 Safe Pressure Evaluation 110

5.5.1 Introduction 110

DOCUMENT NO.: TL02-GTL-Z-RA-0001	REVISION NO.: 03	REVISION DATE: 01.03.2012	APPROVED:
-------------------------------------	---------------------	------------------------------	-----------

5.5.2	Structural geology relevant for safe pressure estimation.....	110
5.5.3	Fault Reactivation Study	110
5.5.4	Fracture Initiation	113
5.5.5	Summary.....	115
5.6	Development of Geological 3D model	116
5.6.1	Structural modelling	116
5.6.2	Property modelling	117
6	DYNAMIC STORAGE BEHAVIOUR	136
6.1	Preparation of dynamic model.....	136
6.1.1	CO ₂ phase behaviour and choice of simulation model.....	136
6.1.2	Model gridding	137
6.1.3	Property upscaling.....	137
6.1.4	Model initialization.....	138
6.2	Prediction of storage behaviour	141
6.2.1	Reference case	141
6.2.2	Simulation sensitivities.....	143
6.2.3	Grid sensitivities.....	144
6.2.4	Deterministic Low Case	145
6.2.5	CO ₂ trapping.....	147
6.2.6	Summary and discussions.....	148
6.3	Injectivity and permeability evaluation.....	149
6.3.1	Permeability uncertainty.....	149
6.3.2	Injectivity evaluation	151
6.3.3	Summary.....	153
6.4	Storage formation geochemistry	154
6.4.1	Geochemical influence of CO ₂ injection.....	154
7	Geological UNCERTAINTY EVALUATION	155
7.1	Geological uncertainty assessment	155
7.1.1	Storage formation presence	156
7.1.2	Storage formation quality – selection of CO ₂ injection point	160
7.1.3	Storage complex mapability	163
7.2	Pore volume connectivity	163
7.2.1	Dunlin Group.....	164
7.2.2	Brent Group.....	176
7.2.3	Viking Group.....	177
7.3	Pore volume assessment and uncertainties	178
7.3.1	Reference model.....	179
7.3.2	Johansen Formation sand presence.....	179
7.3.3	Johansen Formation sand quality	180
7.3.4	Interpretation uncertainty and depth conversion	181
7.3.5	Communication effects.....	181
7.3.6	Correlations	186
7.3.7	Total pore volume.....	187
7.4	Pressure build-up assessment.....	188
7.4.1	Compressibility.....	189
7.4.2	Permeability.....	190
7.4.3	Temperature and potential well damage effects	191
7.4.4	Total pressure build-ups	192
7.5	Risk of fracturing	193
7.6	Estimating the storage site capacity	194
7.7	Uncertainty summary.....	195
8	RISK OF LEAKAGE	196
8.1	Introduction.....	196

DOCUMENT NO.: TL02-GTL-Z-RA-0001	REVISION NO.: 03	REVISION DATE: 01.03.2012	APPROVED:
-------------------------------------	---------------------	------------------------------	-----------

8.2	Risk acceptance criteria	196
8.3	Analytical approach	197
	Leakage pathways	197
	Described further in.....	197
	Leakage risk depends on:	197
8.3.1	CO ₂ migration in the storage formation	200
8.3.2	Leakages through faults and fractures	201
8.3.3	Leakages through subseismic faults and paleo fractures	202
8.3.4	Leakage through injection wells.....	203
8.3.5	Leakage through abandoned wells.....	204
8.4	Probabilities and leakage rates.....	204
8.5	Leakage consequences	205
8.5.1	Human fatalities/injuries.....	206
8.5.2	Local environmental consequences	206
8.5.3	Global environmental consequences	207
8.6	Conclusion	207
9	STORAGE SITE DEVELOPMENT, TECHNICAL CONCEPT	209
9.1	Storage Site Development.....	209
9.2	Subsea Tie-back options	209
9.2.1	Host platform.....	210
9.2.2	Subsea Wells Controlled from Shore	210
9.3	Technical Concept	211
9.3.1	System overview.....	211
9.3.2	Template Structure	211
9.3.3	Cluster System.....	211
9.3.4	Manifold	212
9.3.5	Pig Receiver.....	212
9.3.6	Wellhead System	213
9.3.7	Xmas Tree System.....	213
9.3.8	Control System	213
9.3.9	Alternative Control system – All Electric	214
9.3.10	Umbilical System	214
9.3.11	Workover System	215
9.3.12	Drilling and Completion.....	215
9.3.13	CO ₂ Well Challenges	215
9.3.14	Pipeline	216
9.3.15	Environmental Consideration – Open Loop Hydraulic System	217
9.3.16	Leak/emission monitoring	217
9.3.17	Installation	218
9.3.18	Operation and Maintenance Strategy.....	218
9.4	Cost Estimate	219
9.4.1	Project Development Cost.....	219
9.4.2	Drilling and Completion of Injection Wells	220
9.4.3	Operation and Maintenance Cost.....	220
9.4.4	Storage cost	221
10	MONITORING	222
10.1	Definition of terms	222
10.2	Existing regulations	222
10.2.1	Monitoring.....	222
10.2.2	Metering	222
10.3	EU legislations applied to Johansen.....	223
10.3.1	Monitoring.....	223
10.3.2	Monitoring area	224

DOCUMENT NO.: TL02-GTL-Z-RA-0001	REVISION NO.: 03	REVISION DATE: 01.03.2012	APPROVED:
-------------------------------------	---------------------	------------------------------	-----------

10.4 Johansen specific monitoring needs..... 224

10.4.1 Identified leakage points..... 224

10.4.2 Monitoring for plume migration verification 224

10.4.3 Other operational monitoring techniques 228

10.4.4 Monitoring well 229

11 IMPACT ASSESSMENT 230

12 CONCLUSIONS AND RECOMMENDATIONS 231

REFERENCES 233

APPENDICES 238

A1 GAP Analysis..... 238

A2 Proposed Location and Formation Evaluation Programme for Exploration Well 245

A3 Well to Seismic Calibration – Figures 248

A4 Johansen Storage Complex Time and Depth Maps 262

A5 Velocity Modelling for Depth Conversion in Quadrant 31 299

A6 Content Johansen Storage Complex Petrel Projects 307

DOCUMENT NO.: TL02-GTL-Z-RA-0001	REVISION NO.: 03	REVISION DATE: 01.03.2012	APPROVED:
-------------------------------------	---------------------	------------------------------	-----------

1 EXECUTIVE SUMMARY

The objective of the work summarised in this report was to assess the Johansen Formation as a safe and operable storage site for CO₂ from Mongstad. Through extensive studies of seismic data and geological modelling it is concluded that the Johansen Formation in the area investigated is a good storage formation capable of storing at least the required CO₂ stream of 3.2Mt/y for 50 years.

The work may be basis for further maturation and qualification according to EU directive requirements. This report gives the status and indicates work necessary for final qualification. The main risk remaining is verification of reservoir properties through drilling of a well.

The area of main interest is south in quadrant 31, southwest of the Troll field. Based on the result of early studies, the possible injection area is found south on the structure. Additional seismic has been collected over this area in order to increase the level of maturity for the storage evaluations. The 3D seismic database covers 2500 km².

Conclusions

The evaluations documented in this report, lead to the following conclusions:

- The Johansen Formation has the reservoir properties, sufficient depth (2100 – 3100 m MSL) and seal to be used as a storage site for permanent storage of CO₂.
- The main uncertainty is found in the sand quality of the injection area. This is more critical for the injectivity than for the storage volume. The studies indicate, that the base case rate robustly can be accommodated
- An extensive seal; the Drake Formation, is in place over the plume migration area and simulations indicate that the Johansen Formation is expected to take an injection of 3.2Mt/y CO₂ for 50 years without any significant risk of leakage. The highest identified leakage risk is associated with the injection well. There are no high risk issues within the plume migration area for the base case volume of 160Mt (Figure 1-1). The model indicates that a doubling of the storage volume will be possible without migration into higher risk area for the first 500 years.
- A suggested selection of injection area is presented considering control of plume migration and confidence in reservoir properties.
- It is suggested that the storage site should be developed with a standard 4-slot template with two injection wells for redundancy purposes. With reservoir quality as predicted, one deviated or horizontal well will be adequate for daily injection.

Recommendations for further work

To qualify the defined Johansen Formation as a storage site, and to characterise the site according to requirements in the EU directive, the following is required:

- A well should be drilled to prove the quality of the storage formation and to collect core and fluid samples from the actual injection area. Core sampling, and subsequent testing and characterisation are required to fully comply with the requirements of the EU directive. Both the storage formation and the cap rock should be cored and investigated. Pressure measurements might detect potential depletion and area wide communication.
- Regional flow analysis should be done to form basis for possible surface leak monitoring.
- Full monitoring, metering and verification plans should be developed .

DOCUMENT NO.: TL02-GTL-Z-RA-0001	REVISION NO.: 03	REVISION DATE: 01.03.2012	APPROVED:
-------------------------------------	---------------------	------------------------------	-----------

Work described in this report:

In order to fulfil the objective of the study, the following main areas of work were undertaken:

- Construction of a static 3D earth model
- Petrophysical evaluation
- Seismic inversion and attribute study
- Construction of depositional model
- Fault study
- Geomechanical evaluation
- Core testing
- Dynamic simulation
- Leakage risk assessment

Two storage formations are included, Johansen and Cook, of which the Johansen Formation represents 85% of the volume. The Drake Formation is defined as the sealing cap rock. The storage complex is defined by faults to the north and east and pinch out of Johansen Formation sand to the south and west (see Figure 1-1). The top of the Johansen Formation varies between 2100m MSL in the north to 3200m MSL in the south.

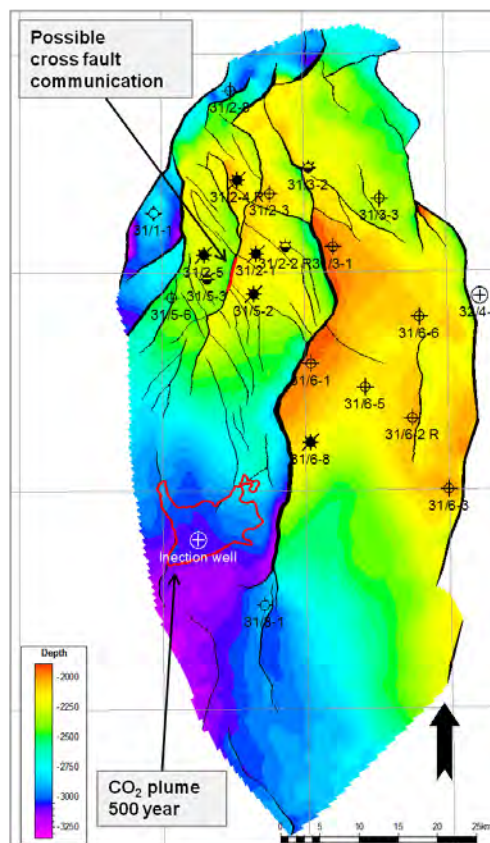


Figure 1-1: Plume migration and high risk areas (faults and wells).

Well coverage is good in the northern part, in the vicinity of the Troll field, while the southern part of the storage area is not penetrated by wells. A total of 21 wells penetrate the storage area. Due to the lack of well data in the southern part of the storage complex the maturation and evaluation are heavily based on seismic tools and methods. A seismic inversion study was done to predict formation properties in areas with little or no well data. They give high probability to

DOCUMENT NO.: TL02-GTL-Z-RA-0001	REVISION NO.: 03	REVISION DATE: 01.03.2012	APPROVED:
-------------------------------------	---------------------	------------------------------	-----------

the interpretation of a storage formation with adequate reservoir properties for CO₂ injection. Inversion and Attribute studies (SVI Pro) were also used to investigate the quality of the Lower Drake Formation cap rock and to look for any potential leakage paths through the seal.

The primary focus of the fault study was to investigate the sealing properties of the faults cutting through the storage formation and cap rock in areas where the CO₂ plume is likely to migrate (structural highs). An area with high leakage risk was found in the heavily faulted northern area, no faults were found that challenge storage site integrity in the southern area. The depositional proposes a system where the Johansen Formation was deposited as a delta sand. Strong wave influence and longshore transport have resulted in a spit system in the south with good homogeneous sands.

In order to assess what level of pressure increase would be safe for the storage complex, a geomechanical evaluation was performed. Three possible modes of failure due to pressure increase was considered. Data from wells in the area (leak-off tests), data from rock testing of cap rock and general knowledge about the stress state of the area were used. The results showed that a fracturing of the cap rock is most likely to happen first at a pressure increase at approximately 150 bar. The simulated pressure increase is well below this value.

A dynamic model was build and used to simulate CO₂ movement and pressure build-up within the geological structure. The injection area was chosen in order to avoid areas with leakage risk. The southern area is best suited for CO₂ storage with both good plume control and adequate formation properties. Long term simulations (500+ years) show that migration into the northern area is unlikely. Further, the simulations give an indication of the various methods by which the CO₂ is trapped and how much free and mobile CO₂ can be expected.

In an attempt to quantify the leakage risk and consequences of leakage from the storage complex, event trees were constructed for all identified leakage pathways. Examples of such pathways are: identified faults, legacy wells, injection wells, unidentified faults, unidentified sand bodies in cap rock, fracking of cap rock, etc.

The study concluded that the highest risk of leakage is associated with the blow-out risk of the injection well itself. The probability of such a blow-out is low and the same as for the hydrocarbon industry. The associated CO₂ release will be of limited duration (due to remedial actions) and does not pose any harm to the environment, even for the worst case situation. The leakage risk for the storage site is therefore concluded to be low.

DOCUMENT NO.: TL02-GTL-Z-RA-0001	REVISION NO.: 03	REVISION DATE: 01.03.2012	APPROVED:
-------------------------------------	---------------------	------------------------------	-----------

2 INTRODUCTION

Gassnova SF was established in January 2008 as a public enterprise under the Ministry of Petroleum and Energy (MPE). Prior to this date Gassnova existed as a government body acting as coordinator for a team consisting of Gassco, Norwegian Petroleum Directorate (NPD) and Norwegian Water Resources and Energy Directorate (NVE). The scope of work for the team was to perform a feasibility study for transport and storage of CO₂ to be captured at Mongstad and Kårstø, and to present a basis for investment decision. Initially the subsurface work was performed NPD (geological mapping) with contributions from SINTEF (simulation) Statoil and CGGVeritas. The transport part of the project was handled by Gassco. Two areas were investigated; Utsira Formation in block 16/11 and Johansen Formation in block 31/5. The work for this phase was reported in late 2008 as a DG2 (AP1) document. It was concluded that both sites might be suited to safe storage of CO₂, but this was not sufficiently documented. In this evaluation, Utsira was regarded as the most mature area and transport solutions were investigated for both capture plants. For Johansen Storage Complex, additional seismic was collected. Upon the conversion of Gassnova into a public enterprise in 2008, the subsurface activities, which earlier had been handled by Norwegian Petroleum Directorate (NPD) were moved in-house. A technical team consisting of 10-20 professionals were engaged through an Owner's Engineering Contract with Ross Offshore AS. The first task was to further mature the Utsira location for an investment decision in the second half of 2009. This project was, however, put on hold in May 2009 due to the cancellation of the capture plant project.

It has been a requirement to have a common investment decision point for both the capture plant and the transport/storage project. As such, the timeframes and associated deadlines have been affected by the activities related to the capture plant at both sites. Full focus on Johansen Storage Complex as a storage site was only started after cancellation of the capture project at Kårstø. Although the Utsira site would be suitable for storage of Mongstad volumes, the transport distance is considerable. Johansen Formation in block 31/5 is located immediately to the west of Mongstad and is better suited as a storage alternative due to this close proximity. With freshly acquired seismic collected in 2008, the aim was to have an investment decision regarding a storage site for Mongstad in 2012. This was later changed to 2014, and has recently been moved to 2016 due to delays related to the capture plant.

2.1 Work objective

The assessment of the Johansen Formation as a storage site for CO₂ from Mongstad has gone on for some years. The objective of the work summarized in this report was to mature the Johansen Formation as far as possible with the available data after seismic acquisition and to propose a location of verification well. The work will form a basis for further maturation and qualification according to EU directive requirements.

2.2 Capacity requirement

A capacity requirement of 3.2Mt/y over a period of 50 years was set by Gassnova as the desired capacity. This was based on 2.1Mt/y from Mongstad Power Station and Cracker with an extra 50% capacity.

2.3 Location and licence information

The Johansen Formation is located on the Horda Platform in the Northern North Sea (Figure 2-1). It is present in quadrant 31 but is also proven in quadrant 32 and 35. The part of the Johansen Formation located in the unlicensed areas of block 31/5 and 31/8 is only 80 km offshore Mongstad.

DOCUMENT NO.: TL02-GTL-Z-RA-0001	REVISION NO.: 03	REVISION DATE: 01.03.2012	APPROVED:
-------------------------------------	---------------------	------------------------------	-----------

The major part of block 31/5 is unlicensed, while activities in block 31/8 are controlled by PL416, with E.ON Ruhrgas Norge AS as operator. The license is valid until February 2013. The licensed area of 31/5 is held by PL085 with Statoil Petroleum AS as operator.

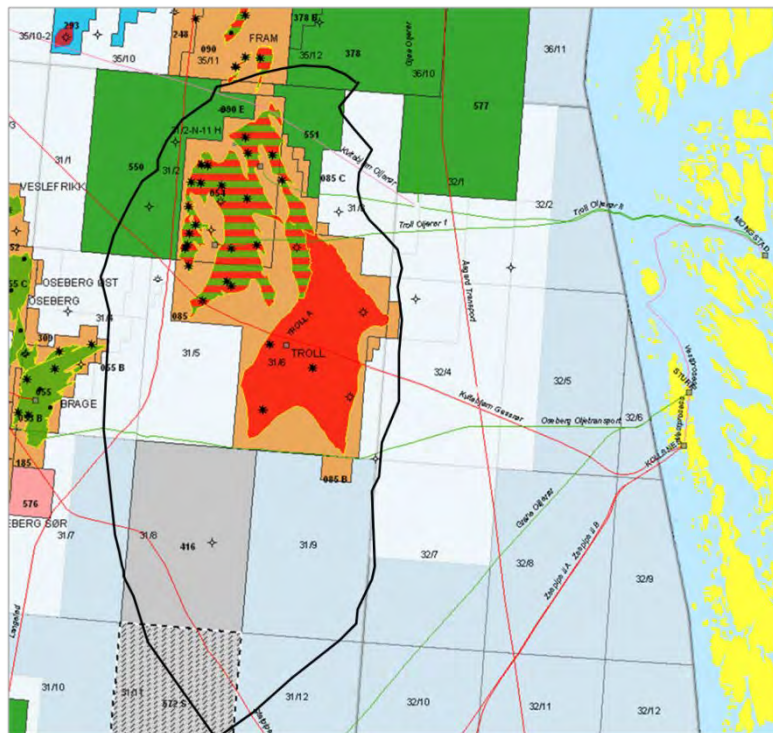


Figure 2-1: Outline of geological model (black line) and licences in area.

2.4 Site description

The Johansen Storage Complex is a saline aquifer with the Johansen Formation as the main storage formation. Some additional volume is found in the Cook Formation. The Johansen Formation is bound by faults to the east and north while a shale out is expected to the west. The southern limit is defined by a pinch out of the formation. The northern part of the complex is heavily faulted and has been given special attention regarding identification of possible communication points to overlying formations. The top of the storage complex is defined by the Drake Formation, of which the lower part (Lower Drake Formation) is defined as the primary seal (Figure 2-2).

DOCUMENT NO.: TL02-GTL-Z-RA-0001	REVISION NO.: 03	REVISION DATE: 01.03.2012	APPROVED:
-------------------------------------	---------------------	------------------------------	-----------

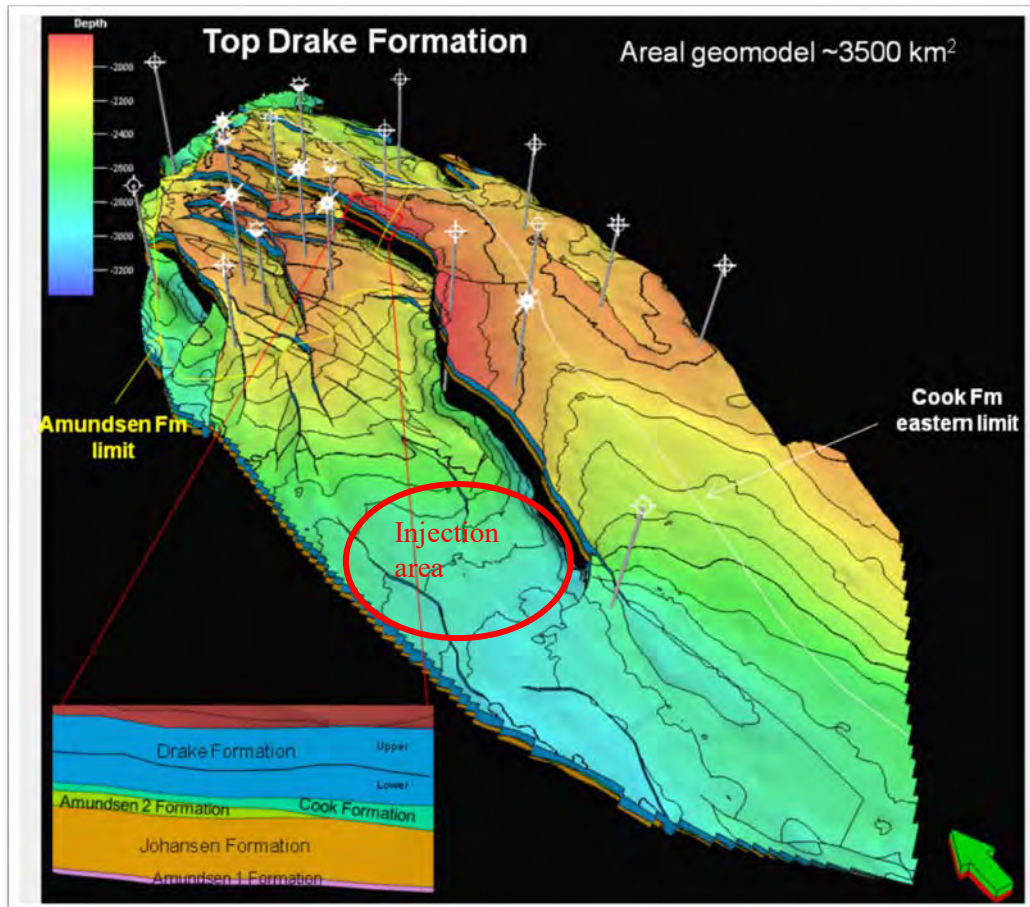


Figure 2-2: Overview of the Johansen Storage Complex.

2.5 Work schedule

The project started by interpretation of seismic 3D data collected by Statoil in 2008 in the unlicensed block 31/5. The initial aim was to drill an exploration well in 2010 in the southern part of the block based on this data. However, as work progressed it became evident that an injection point this far north on the structure could lead to a conflict with the Troll License. A possible leakage path had been identified and plume simulations showed migration below the Troll reservoirs. This could be avoided with a more southerly injection point in the north part of block 31/8 (south of the 3D area) as the 2D lines showed a flattening of the Johansen Formation structure in this area. Following postponement of the investment decision in late 2009 it was therefore recommended to shoot additional seismic south of block 31/5 and postpone the exploration well until a more suitable location was found. This was to avoid prematurely spending 400-500 million NOK on an exploration well in an area possibly unsuitable for CO₂ storage. It was more economical to attempt to mature the area as far as possible with additional seismic, and to use seismic attributes and special studies to the largest extent possible before a decision on the exploration well was taken. Additional 3D seismic was hence collected in 2010 and merged with available 3D seismic obtained from Statoil. This seismic was available for interpretation in late 2010 and formed the basis for the static 3D model and the dynamic model used for this investigation throughout 2011. This was supplemented with testing of the only available core for the Johansen Formation, together with cores of cap rock from wells closest to the area. All cores were unpreserved and had been stored under unfavourable conditions.

DOCUMENT NO.: TL02-GTL-Z-RA-0001	REVISION NO.: 03	REVISION DATE: 01.03.2012	APPROVED:
-------------------------------------	---------------------	------------------------------	-----------

The extensive evaluations throughout 2011 have matured and documented a high probability of good quality reservoir in the proposed injection area in block 31/8. Further, a location for an exploration well is proposed to confirm the depositional model and to collect additional well data necessary to fulfil characterisation of the storage complex according to EU guidelines.

Unfortunately the core testing was severely delayed and also the inversion study was delayed, impacting the completion of the geological 3D model. This delayed the start-up of the dynamic simulations. The consequence of this is that not all simulations have been run for 5000 years. The consequence of this is minimal and does not change any of the conclusions in the report.

Parallel to the technical work an effort was made to establish a formalised work process in-house at Gassnova. The aim of this was to make sure that the qualifying work was done according to the EU Storage Directive (Directive 2009/31/EC) and according to good industry practice. This process is further explained below. As part of that, a method to handle and communicate geological uncertainty was developed. This method is explained in chapter 7.

2.6 Work structure

Work was to be conducted according to EU Directive 2009/31/EC, as well as the latest edition of Gassnova’s internal document *Gassnova Work Processes for Geological Storage Qualifications*. The work process is risk based and ensures that good industry practice is used throughout the evaluation. While the maturing of geological storage sites uses many of the same tools and processes normally used in hydrocarbon exploration, there are also several differences. One of the main challenges for a typical main saline aquifer storage project is the lack of data and handling of the uncertainties this imposes on the final result. It is very important to be able to communicate these uncertainties in a structured manner. This leads to the development of a risk method which is used throughout the evaluation.

The work process can be divided into two process groups:

- Maturing processes which typically follow a phased approach
- Multidisciplinary iterative evaluation processes

These are illustrated in Figure 2-3 below.

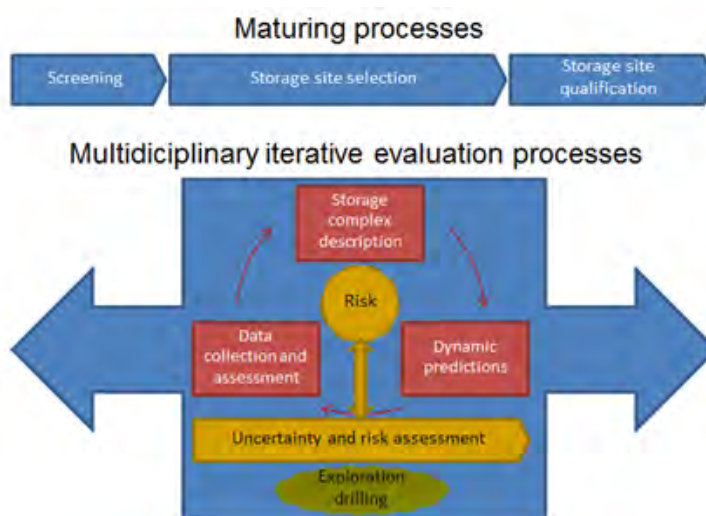


Figure 2-3: Work process description.

DOCUMENT NO.: TL02-GTL-Z-RA-0001	REVISION NO.: 03	REVISION DATE: 01.03.2012	APPROVED:
-------------------------------------	---------------------	------------------------------	-----------

The qualification process is risk driven, aiming to reduce uncertainty and increase the corresponding accuracy level of documentation. The iterative processes including uncertainty and risk assessment cover the multidisciplinary processes of qualifying a storage site. The main processes are:

- Continuous uncertainty and risk reduction/improvement
- Data collection and assessment
- Storage complex description
- Dynamic predictions

These processes were also reflected in the project plan and followed on into the documentation phase to ensure a consistent working structure. A more detailed explanation of the work process can be found in the GN work process document.

Throughout the project TNO has reviewed work processes, project plans and final report. This has been through a frame agreement with Gassnova SF. Results of these reviews can be found in (Gassnova - TNO/KEMA 2012).

2.7 Report Structure

The report layout follows, but expands the work structure outlined above. The main sections are as follows:

- **Evaluation criteria** provide an overview of the criteria used when evaluating the suitability of the selected area for CO₂ storage. This is a mix of both GN criteria (site specific) and general industry accepted criteria, and also provides a gap analysis between the current level of documentation and EU requirements.
- **Data collection and assessment** lists all the data the evaluation is based on, and any special studies that have been performed. These data are used both in construction of the static 3D geological model and in the dynamic model. A short explanation of the study scope is given together with a short conclusion of the result and its implementation in the evaluation. The chapter also summarises the additional data needed for a complete storage application.
- **Storage complex description** describes how the static geological 3D model was constructed using the data collected. The chapter includes seismic interpretation, development of depositional model, description of storage formation(s) and cap rock and an assessment of safe pressure build-up. An explanation of the volumetric uncertainty in the area is also given. The geological model constructed forms the basis for the dynamic model used to simulate plume movement. The safe pressure build-up assessment and volumetric uncertainty evaluation is used to estimate capacity of the storage complex using the dynamic simulation.
- **Dynamic behaviour and predictions** looks at plume migration for the given injection point and the associated pressure build-up of the reference case model. The dynamic model used is based on the geological model. The effect of uncertainty in the dynamic input parameters is explained and the consequence of a lack of well data in the injection area is discussed together with injectivity.
- **Uncertainty evaluation** explains how the uncertainty in modelled parameters and volumetric connectivity is handled and shows how the various parameters influence the capacity estimation. Output of this chapter gives a view of the confidence of the results and shows how the required capacity relates to the expected capacity of the site.
- **Leakage risk assessment** gives an estimation of the leakage risk and consequence of leakage from the storage complex. Event trees are constructed for all identified leakage pathways. Examples of such pathways are: identified faults, legacy wells, injection

DOCUMENT NO.: TL02-GTL-Z-RA-0001	REVISION NO.: 03	REVISION DATE: 01.03.2012	APPROVED:
-------------------------------------	---------------------	------------------------------	-----------

wells, unidentified faults, unidentified sand bodies in cap rock, fracking of cap rock, etc. Estimation of leakage rates and durations are also included.

- **Storage site development, technical concept** details how the storage site can be developed using traditional subsea equipment. This input is largely based on experience from a subsea FEED conducted for the Kårstø development in 2009 but is still highly relevant. A brief note on development wells are also included. No new work has been done for this part during 2011 apart from than done by Gassco regarding pipelines.
- **Monitoring** chapter highlights the requirements for monitoring according to the EU directive(s) and looks at the challenges related to monitoring the Johansen Storage Complex and possible monitoring solutions.
- **Impact assessment** gives an overview of potential areas of conflict related to CO₂ storage in the selected area.

DOCUMENT NO.: TL02-GTL-Z-RA-0001	REVISION NO.: 03	REVISION DATE: 01.03.2012	APPROVED:
-------------------------------------	---------------------	------------------------------	-----------

3 EVALUATION CRITERIA

Evaluation criteria given by Gassnova are listed in Table 3-1.

Table 3-1: Evaluation criteria.

Criterion	Requirement by Gassnova
Capacity	160 million tonnes of CO ₂
Injectivity	Sufficient to inject 3.2Mt/y for 50 years without compromising storage site integrity
Containment	Safe storage (without any significant risk of leakage) for 5000 years.
MMV	All CO ₂ stored shall be accounted for, plume shall be monitored, and stored and leaked CO ₂ shall be measured

Evaluation, qualification and characterisation are individual activities in developing storage site. While the EU directive lists extensive requirements regarding how to characterise a storage site, little is said regarding how to qualify or what qualification criteria should be used. Similarly, an evaluation can be done for certain storage complex characteristics or properties, where these are evaluated against certain given criteria needed for the site to fulfil the need of the site developer. Given that the site meets the evaluation criteria it may qualify for investment decision. Ultimate qualification as a storage site will be given by the Competent Authority (CA) through issuance of a storage permission, given that the site has been characterised according to the EU directive.

As the Johansen Storage Complex is a large area with varying characteristics, site selection should here be viewed more as injection site selection rather than area as a whole. The suitability of the injection site can be put into context using various criteria. A collection of criteria has been used by the Quest Carbon Capture and Storage Project (Gassnova-WGD 2011) and is perhaps the most recently used. In Table 3-2 the injection and Johansen Storage Complex is put into this context.

The assessment used shows that the selected injection site in the Johansen Storage Complex is appropriate. Perhaps the only limiting factor is the expected resolution on 4D seismic monitoring due to the depth of the formation. However, this is viewed as acceptable because there is an insignificant risk of leakage from the storage complex. Storage at shallower depths within the storage complex would lead to a higher leakage risk and potential conflicts with hydrocarbon interests in the area.

In addition to these initial screening criteria, the EU directive 2009/31/EC requires that the characterisation and assessment of the potential storage complex shall be carried out in three steps according to best practices at the time of assessment. A gap analysis of the reported work against the requirements in the EU Directive is included in appendix A1 GAP Analysis. From this it is evident that some of the gaps can only be closed by drilling of an exploration well. It is also evident that activities not directly related to storage site integrity and leakage risk, have not been described in the required detail. This is intentional as good project management requires good resource management to prevent doing tasks at too early a stage based on inadequate information. This has been especially important as the future of the project has always been uncertain.

DOCUMENT NO.: TL02-GTL-Z-RA-0001	REVISION NO.: 03	REVISION DATE: 01.03.2012	APPROVED:
-------------------------------------	---------------------	------------------------------	-----------

Table 3-2: Assessment of Johansen Storage Site suitability.

Criterion level	No	Criterion	Unfavourable	Preferred or favourable	Johansen Storage Site
Critical	1	Reservoir – seal pairs; extensive and competent barrier to vertical flow	Poor, discontinuous, faulted and /or breached	Intermediate and excellent; many pairs (multi-layered system)	Lower Drake Fm defined as seal with adequate thickness. Draupne Fm as secondary seal
	2	Pressure regime	Overpressured pressure gradient > 14 kPa/m	Pressure gradient < 12 kPa/m	Assumed hydrostatic
	3	Monitoring potential	Absent	Present	Present – but challenging for plume spread
	4	Affecting protected groundwater quality	Yes	No	No
Essential	5	Seismicity	High	<=Moderate	Low
	6	Faulting and fracturing intensity	Extensive	Limited to moderate	Limited. No faults penetrating major seal observed on 3D seismic
	7	Hydrogeology	Short flow systems, or compaction flow, saline aquifers in communication with protected groundwater aquifers	Intermediate and regional-scale flow	n/a. Offshore – no flow potential
Desirable	8	Depth	<750 – 800m	>800m	>2700m
	9	Located within fold belts	Yes	No	No
	10	Adverse diagenesis	Significant	Low	Low, chloride coating expected
	11	Geothermal regime	Gradients >35°C/km and low surface temperature	Gradients <35°C/km and low surface temperature	Gradients <35°C/km and low surface temperature
	12	Temperature	<35°C	>= 35°C	95 °C
	13	Pressure	<75 bara	>75 bara	305 bara
	14	Thickness	< 20m	>20m	>80m
	15	Porosity	<10%	>10%	21 % average
	16	Permeability	<20mD	>40mD	300mD
	17	Cap rock thickness	<10m	>10m	72 average
	18	Well density	High	Low	Low

DOCUMENT NO.: TL02-GTL-Z-RA-0001	REVISION NO.: 03	REVISION DATE: 01.03.2012	APPROVED:
-------------------------------------	---------------------	------------------------------	-----------

4 DATA COLLECTION AND ASSESSMENT

This section contains an overview of the databases used for the project. It also contains a short summary of the various special studies performed both in-house, and by the frame agreement contractors. A short summary of scope and further use of results is given.

4.1 Well database

The well database comprises released wells within the study area (Figure 4-1 and Table 4-1). The well database consists of all available data in terms of:

- Well logs
- Deviation survey
- Mud logs
- Check shot data
- Core analysis
- Core photos
- Lithostratigraphic tops

Well data have been investigated in order to recognise storage formation rocks and cap rocks. All wells penetrating the primary storage formation have been used for well to seismic calibration.

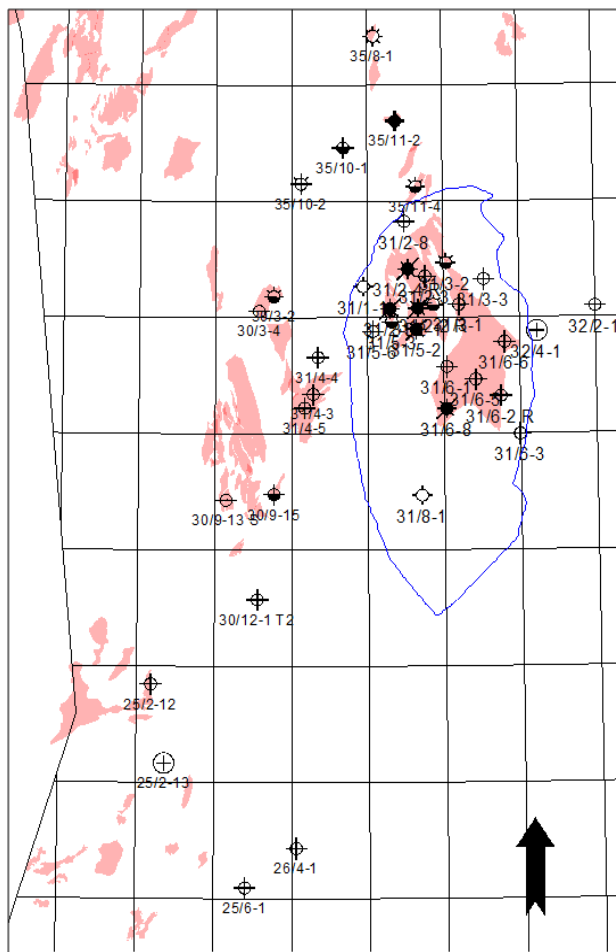


Figure 4-1: Johansen Storage Complex well database.

DOCUMENT NO.: TL02-GTL-Z-RA-0001	REVISION NO.: 03	REVISION DATE: 01.03.2012	APPROVED:
-------------------------------------	---------------------	------------------------------	-----------

Table 4-1: Johansen Storage Complex well database.

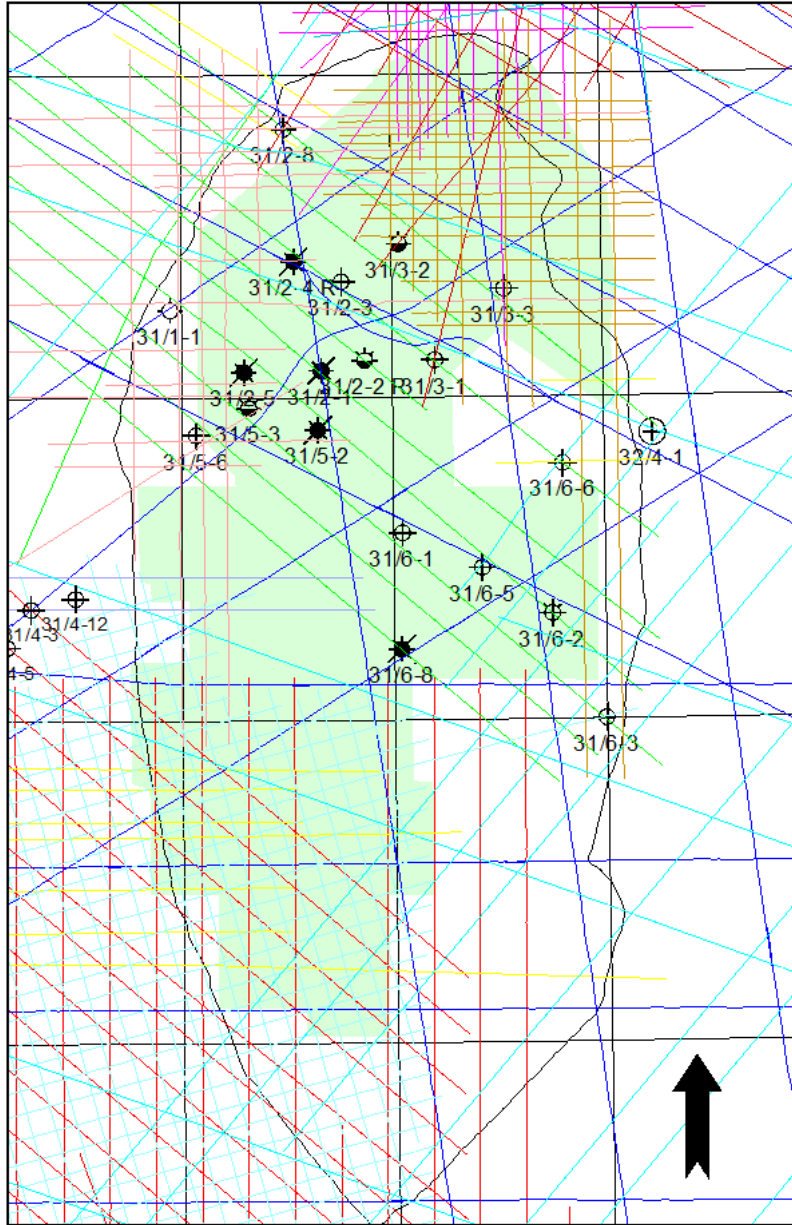
Well	Completion year	TD MD (m)	TD FORMATION	Operator
25/2-12	1988	4102	Middle Jurassic (Hugin Fm)	Elf Petroleum Norge AS
25/2-13	1990	3908	Late Triassic (Smith Bank Fm)	Elf Petroleum Norge AS
25/6-1	1986	2882	Pre-Devonian (Basement)	Saga Petroleum ASA
26/4-1	1987	3690	Triassic	BP Norway Limited U.A.
30/3-2R	1981	3567	Triassic (Hegre Gp)	Statoil AS
30/3-4	1985	3287	Early Jurassic (Statfjord Fm)	Statoil AS
30/9-13S	1991	4027	Early Jurassic (Statfjord Fm)	Norsk Hydro AS
30/9-15	1994	2764	Early Jurassic (Statfjord Fm)	Norsk Hydro AS
30/12-1	1994	3641	Early Jurassic (Statfjord Fm)	Norsk Hydro AS
31/1-1	2008	2920	Early Jurassic (Statfjord Fm)	Marathon Petroleum AS
31/2-1	1979	2433	Triassic (Hegre Gp)	A/S Norske Shell
31/2-2R	1980	2600	Triassic (Hegre Gp)	A/S Norske Shell
31/2-3	1980	2601	Triassic (Hegre Gp)	A/S Norske Shell
31/2-4R	1981	5035	Triassic (Hegre Gp)	A/S Norske Shell
31/2-5	1980	2532	Triassic (Hegre Gp)	A/S Norske Shell
31/2-8	1982	3375	Triassic (Hegre Gp)	A/S Norske Shell
31/3-1	1983	2374	Triassic (Hegre Gp)	Statoil AS
31/3-2	1984	2090	Early Jurassic (Drake Fm)	Norsk Hydro AS
31/3-3	1984	2573	Early Jurassic (Statfjord Fm)	Saga Petroleum ASA
31/4-3	1980	4981	Early Permian	Norsk Hydro AS
31/4-4	1981	3150	Early Jurassic (Statfjord Fm)	Norsk Hydro AS
31/4-5	1981	2930	Triassic	Norsk Hydro AS
31/5-2	1983	2500	Triassic (Hegre Gp)	Saga Petroleum ASA
31/5-3	1984	2250	Early Jurassic (Drake Fm)	Saga Petroleum ASA
31/5-6	2000	2370	Early Jurassic (Drake Fm)	Norsk Hydro AS
31/6-1	1983	4070	Pre-Devonian (Basement)	Norsk Hydro AS
31/6-2R	1984	2235	Triassic (Hegre Gp)	Statoil AS
31/6-3	1983	2250	Triassic (Hegre Gp)	Norsk Hydro AS
31/6-5	1984	2082	Early Jurassic (Drake Fm)	Statoil AS
31/6-6	1984	2293	Triassic (Hegre Gp)	Statoil AS
31/6-8	1985	2138	Early Jurassic (Cook Fm)	Norsk Hydro AS
31/8-1	2011	2629	Middle Jurassic (Brent Gp)	E.ON Ruhrgas AS
32/2-1	2008	1300	Triassic (Lunde Fm)	Talisman Energy AS
32/4-1	1996	3186	Pre-Devonian (Basement)	Phillips Petroleum AS
35/8-1	1981	445	Early Jurassic (Statfjord Fm)	Gulf Exploration AS
35/10-1	1992	3986	Early Jurassic (Statfjord Fm)	Statoil AS
35/10-2	1996	4677	Early Jurassic (Statfjord Fm)	Statoil AS
35/11-2	1987	4025	Early Jurassic (Statfjord Fm)	Mobil Exploration AS
35/11-4	1990	3127	Early Jurassic (Statfjord Fm)	Mobil Exploration AS

4.2

Seismic database

The seismic 3D data used in the evaluation is shown in Table 4-2 and Figure 4-2. The seismic 3D database consists of the six 3D seismic cubes; EO0801, GN1001, NPD-TW-08-4D-TROLLCO2 merged with SG9202, NH0301 and TNE01 (Figure 4-2 and Table 4-2). In addition, public 2D seismic (Figure 4-2) is being used in the areas not covered by 3D seismic.

DOCUMENT NO.: TL02-GTL-Z-RA-0001	REVISION NO.: 03	REVISION DATE: 01.03.2012	APPROVED:
-------------------------------------	---------------------	------------------------------	-----------



HRTRE00	MN88	MN9103	NSR
SG8043R91	SG9206	SH8001R92	SHP91
ST8408R91	ST8518	TE93	TW08

Figure 4-2: Map showing key wells and 2D database. 3D seismic coverage is shown in light green. The black polygon represents the outline of the Johansen reference geomodel.

To achieve a consistent seismic database for seismic interpretation, analysis and inversion, the seismic cubes GN1001, NPD-TW-08-4D-TROLLCO2 and NH0701 were merged together by processing from field data into a new seismic volume GN10M1. This also included change of the line direction for NH0301 from SW-NE to W-E (Figure 4-3).

DOCUMENT NO.: TL02-GTL-Z-RA-0001	REVISION NO.: 03	REVISION DATE: 01.03.2012	APPROVED:
-------------------------------------	---------------------	------------------------------	-----------

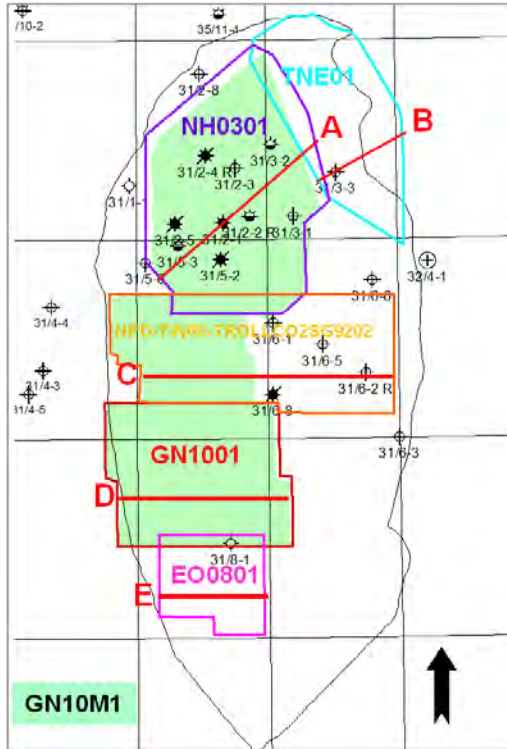


Figure 4-3: Map showing key wells and 3D database. The area of the merged 3D GN10M1 is shown in light green. The black polygon represents the outline of the Johansen reference geomodel.

The quality of the different seismic volumes is, except for the EO0801, generally good or very good (Table 4-2). The quality of the 2D data varies, but is generally good.

Table 4-2: The table shows the seismic 3D cubes, acquisition year, the area covered by seismic, inline direction (shot direction) and a comment concerning the seismic quality.

Seismic 3D	Acquisition year	Acreage km ²	Inline direction	Quality	Comments about quality
EO0801	2008	184	N-S	Medium/poor	Very difficult to interpret the north-south trending faults
GN1001	2010	503	E-W	Excellent	Especially from top Draupne Fm down to Statfjord Fm
NPD-TW08-4D-TROLLCO2	2008	293	E-W	Good	Large number of faults in northern part
SG9202	1992	346	E-W (N-S)	Good	Quality poorer below top Brent Gp
NH0301	2003	718	NE-SW	Good/very good	Excellent above top Brent Gp, large number of faults
TNE01	2001	399	NE-SW	Good	Problem interpreting small faults below top Brent Gp
GN10M1	2010	1370	E-W	Good/very good	Fault interpretation better on NH0301 in the Troll West area

DOCUMENT NO.: TL02-GTL-Z-RA-0001	REVISION NO.: 03	REVISION DATE: 01.03.2012	APPROVED:
-------------------------------------	---------------------	------------------------------	-----------

4.3 Seismic inversion

Reference is made to the report *3D AVO Seismic Inversion and Lithology Prediction West Troll Field, Norway* which is the final report encompassing the seismic inversion project (Gassnova-WGD 2011).

The objective of the seismic inversion study was to quantify the elastic properties, acoustic impedance and V_p/V_s ratio, over the West Troll area. The study relied on effective integration of all available information throughout well logs preparation, deterministic seismic pre-conditioning for AVO, global simultaneous inversion.

The seismic data provided to this seismic inversion consisted of migrated gathers processed by Western Geco in Cairo. The seismic survey inverted is the GN10M1 3D seismic dataset which is a pre-stack merge of the GN1001, NPD-TW-08 and NH0701 3D seismic surveys. Data for six wells and five interpreted seismic horizons covering the zone of interest were provided by the project team in Ross Offshore. This was all the data provided to this inversion work as input data.

The inversion primarily targeted the Dunlin Group, Cook Formation and Johansen Formation. The seismic data were inverted for acoustic impedance and V_p/V_s ratio using the ISIS simultaneous AVO inversion technology.

Prior to the inversion the provided logs were edited and calibrated in order to be prepared for synthetic generation, wavelet estimation and low frequency modelling. In addition a rock-physics model was defined to estimate shear velocity for all the wells as no measured shear logs were available in the field or a nearby one. The pre-stack migrated seismic gathers were stacked to form four angle stacks ($0^\circ - 10^\circ$, $10^\circ - 20^\circ$, $20^\circ - 30^\circ$ and $30^\circ - 40^\circ$). Successively the alignment of the angle stacks was optimized using a technique derived from the proprietary Non-Rigid Matching (NRM) algorithm.

The wavelets used in the final inversion were derived using a multi-well least squares wavelet estimation in the time domain. The wavelets were estimated from the seismic angle stacks at three well locations within the survey area. The optimum wavelets were close to zero-phase with positive amplitude corresponding to an increase in acoustic impedance. The frequency content and amplitude level of the final wavelets were varied with depth.

As the low-frequency components of the elastic properties are not present in the seismic data, the missing information was accounted for by introducing prior models for acoustic impedance, V_p/V_s ratio and density calculated by extrapolating the well calibrated properties throughout a structural model incorporating three horizons.

The main inversion results consist of:

- Four seismic aligned angle stacks
- Acoustic impedance and V_p/V_s ratio with low-frequency information
- Acoustic impedance and V_p/V_s ratio without low-frequency information

The final inversion modelled 83% of the seismic energy of the four inverted angle stack volumes.

DOCUMENT NO.: TL02-GTL-Z-RA-0001	REVISION NO.: 03	REVISION DATE: 01.03.2012	APPROVED:
-------------------------------------	---------------------	------------------------------	-----------

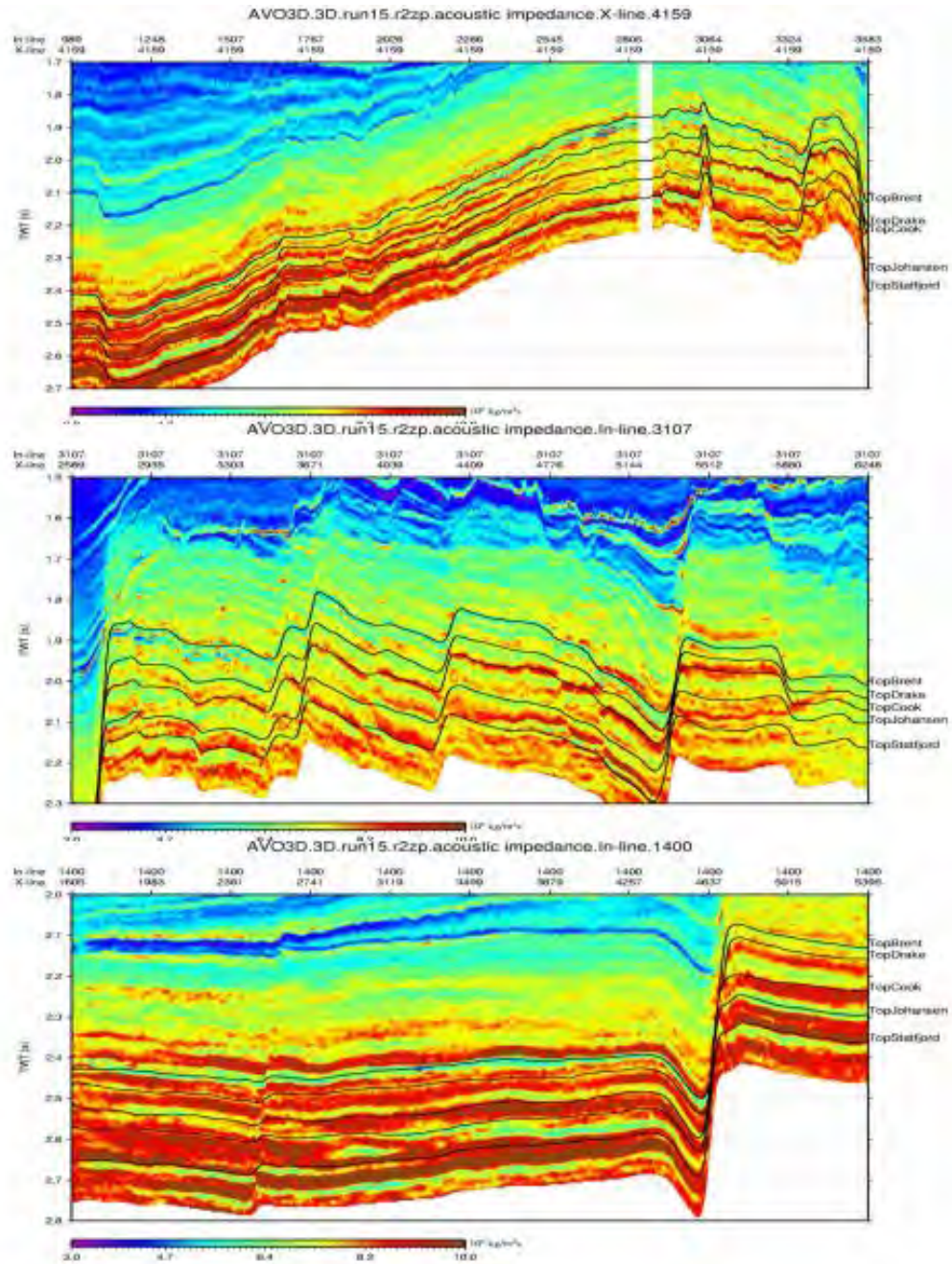


Figure 4-4: Acoustic impedance inversion result along cross-line 4159 (top), in-line 3107 (middle) and in-line 1400 (bottom).

The match between the absolute inversion results and the well logs was considered to be of good quality, both for acoustic impedance and V_p/V_s . For density the match between well logs and inversion results was considered to be average.

Comparing the results from the seismic inversion with the well logs shows that it is able to model most of the features of the well logs. For the primary target the acoustic impedance match is good. Comparing the V_p/V_s result with the V_p/V_s log based on synthetic shear has a more variable quality. In some of the wells the density inversion results display a good match. Overall, the inversion accurately modelled the seismic response, with 17% of the energy left in the residual seismic.

DOCUMENT NO.: TL02-GTL-Z-RA-0001	REVISION NO.: 03	REVISION DATE: 01.03.2012	APPROVED:
-------------------------------------	---------------------	------------------------------	-----------

The acoustic impedance and Vp/Vs inversion output was then used in a lithology classification, using two classes: Sand and Shale. A porosity volume was also estimated using the acoustic impedance inversion result to highlight the sands with the highest porosity values. From the lithology classification and porosity estimation, the following results were delivered:

- Probability for each class in the classification
- Combined class volume
- Porosity volume for the zone of interest (from the Brent Formation to the Statfjord Formation)

After a thorough evaluation of the entire inversion project it was decided to not use the lithology classification in the subsurface work. Well logs were shifted 25ms after an evaluation of the results from the inversion study and a revised evaluation of the well logs. The main result to be used further in the evaluation of the Johansen Formation was the acoustic impedance volume (Figure 4-5).

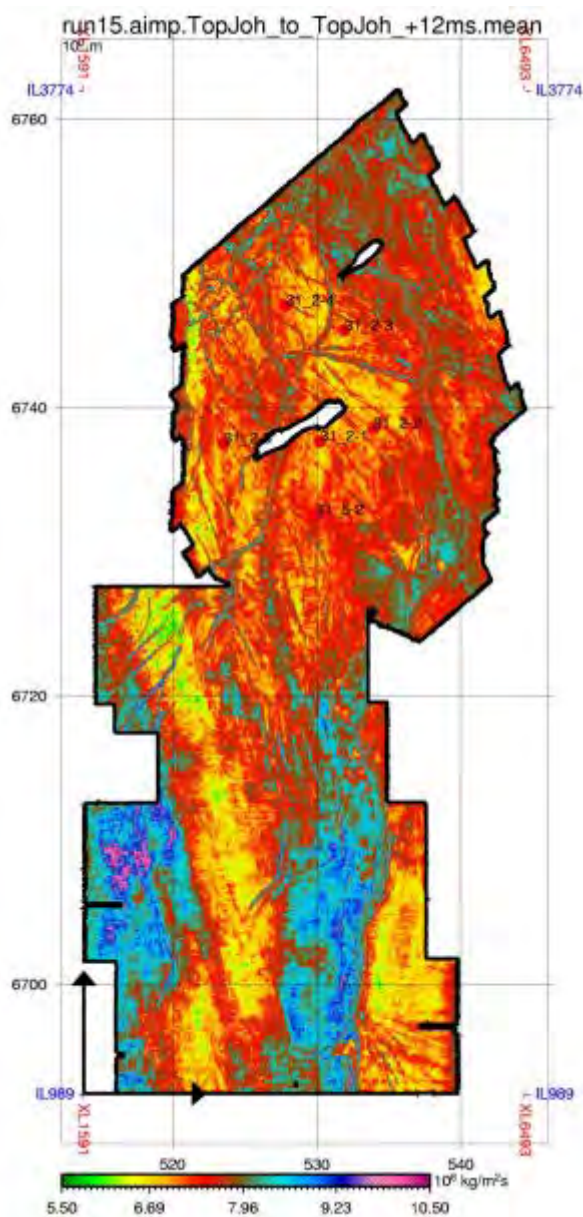


Figure 4-5: Acoustic impedance inversion results extracted in the interval Top Johansen 0.000s to Top Johansen +0.012s (mean value). The well locations are plotted as red circles.

DOCUMENT NO.: TL02-GTL-Z-RA-0001	REVISION NO.: 03	REVISION DATE: 01.03.2012	APPROVED:
-------------------------------------	---------------------	------------------------------	-----------

4.4 Basin modelling

A basin modelling study has been carried out at SINTEF for the sandy reservoir of the Lower Jurassic Johansen Formation within the Troll area (Gassnova-SIN 2011). The aim was to generate a porosity, thermal, shale gauge ratio (SGR) and overpressure model over geological times along three 2D lines. The 2D lines were used to create a pseudo-3D geomodel used in the modelling (e.g. heat modelling, pressure modelling). Missing segments (e.g. larger sections on the SE part of the area) were accounted for using linear interpolation.

The modelled porosities were built on standard curves for decompaction (Christie and Sclater 1980). The modelled porosity was compared to the observed porosity from wells in the northern area and the correlation was good. The modelled porosities are used in the evaluation of the storage formation quality in the non-well southern area of the storage complex.

The forward multi-1D heat flow modelling results show a very good match between predicted and measured temperatures in wells at present day. The lack of wells in the area of interest complicates the temperature model and hence the heat flow modelling.

The pressure modelling indicates hydrostatic pressure conditions in the shallow lying eastern area and high overpressure in the western area today. Modelled overpressure is too high with respect to present day calibration data within the deeper parts of the basin structure. These high overpressure results are related to pressure calculations being restricted along 2D lines only. The 2D model data set fails to account for lateral fluid flow and pressure dissipation out of the seismic section planes, and also lacks incorporation of erosion (uplift and cooling) events.

The SGR is calculated for all the 1st and 2nd order faults interpreted from the seismic lines using Volume shale data (Vsh) from 7 wells in the study area. The faults (large and intermediate sized) hold large pressures differences; e.g. 40 bar. The result is in accordance with the fault seal study evaluation (Gassnova-ROS 2011).

A 3D study will likely show that the fluid will flow around the faults (if possible) or go southwards and not build up such high pressure differences. Incorporating erosion events will likely reduce the presence of overpressure as it is expected that it will have bled off after the erosion events. On the upside, the high overpressures allow for checking the sealing properties of the faults under extreme conditions.

Lesson learned

In retrospect this study should have been conducted at a later stage with full 3D coverage and more input (interpreted fault sticks, depth maps) to advance the 3D geomodel. This is to better account for the missing segments in the 2D lines and to improve the pressure modelling (including erosion and allowing lateral flow).

4.5 Petrophysical evaluation

4.5.1 Summary

A petrophysical evaluation has been made from:

- Sognefjord Formation to the top of the Triassic Statfjord Formation for all Troll wells penetrating Johansen Formation (15 wells)
- Sognefjord Formation to Drake or Cook formations for wells with TD'd in Drake Formation/Cook Formation (6 Troll wells)
- Regional wells which penetrate Drake Formation, Cook Formation, Johansen Formation or time equivalents

DOCUMENT NO.: TL02-GTL-Z-RA-0001	REVISION NO.: 03	REVISION DATE: 01.03.2012	APPROVED:
-------------------------------------	---------------------	------------------------------	-----------

The wells are identified in Figure 4-6. The petrophysical interpretations are based on the general suite of logs including Gamma Ray, Resistivity, Sonic and Density/Neutron, and Spectral Gamma Ray.

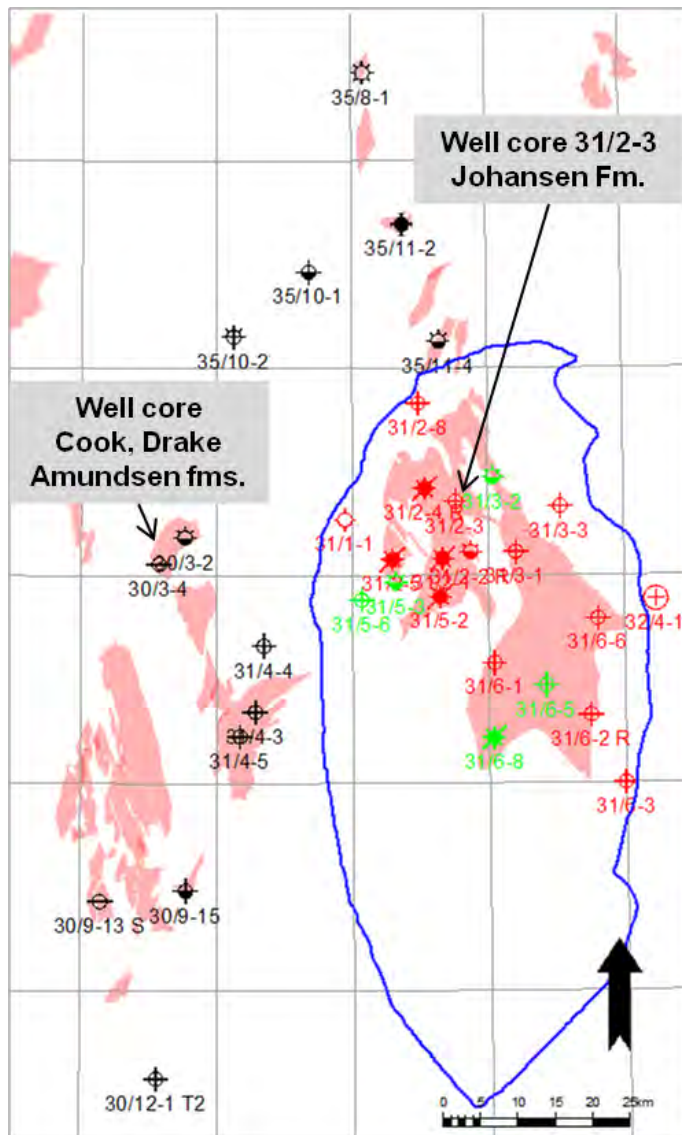


Figure 4-6: Map showing Troll area Johansen wells (red) studied in ResLab, additional wells penetrating Drake, Cook and Johansen formations, and regional wells incorporated in this study.

The volume of clay (VCI), porosity (PHIE) and permeability results for the Johansen Formation, according to the NPD and ResLab zonation are shown in Table 4-3. Note that in each case the results are calculated as a simple arithmetic mean. For each Johansen Formation zone (for example, Johansen Top, Johansen 2, Johansen 1, Johansen Shale) the property (VCI, PHIE, or permeability) was averaged as the mean from the log-derived curve. The ‘Average’ value of VCL, PHIE and permeability for each well is the arithmetic mean for the 5 Johansen Formation zones.

As part of the evaluation a review was conducted of an existing ResLab petrophysical study (Monaghan and Iskander 2009). Concerns regarding the ResLab study were addressed in this study, particularly to account for effects of mica on clay volume (VCI) and porosity estimates, and to address the lack of calibration to core porosity and permeability data. A comparison of

DOCUMENT NO.: TL02-GTL-Z-RA-0001	REVISION NO.: 03	REVISION DATE: 01.03.2012	APPROVED:
-------------------------------------	---------------------	------------------------------	-----------

the results from this study and ResLab’s study are shown in (Gassnova-ROS 2011). Porosity estimates through the clean sand and shaley sand zones (mainly Johansen Top, Johansen 2 and Johansen 1) are generally very similar in the two analyses. However, this study predicts significantly lower clay volumes and higher porosities in the lowest zone, called Johansen Shale. Much of this zone is now categorized as a prograding coarsening up sequence grading from shales (>40% VCI) to shaley sands (<30% VCI), the proportions of which vary from well to well (chapter 5.3).

Table 4-3: Summary of average volume of clay (VCI), porosity (PHIE), and permeability results for Johansen Formation by Johansen sub-zone.

Porosity Results																
	31/2-1	31/2-2	31/2-3	31/2-4	31/2-5	31/2-8	31/3-1	31/3-3	31/5-2	31/6-1	31/6-2	31/6-3	31/6-6	31/1-1	32/4-1	Average
Johansen Top	0,13	0,19	0,25	0,27	0,27	0,16	0,25	0,19	0,20	0,22	0,21	0,16	0,14	0,17	0,18	0,20
Johansen2	0,25	0,24	0,26	0,25	0,25	0,16			0,23	0,25	0,21	0,17	0,17	0,10	0,20	0,21
Johansen1	0,22	0,24	0,21	0,18	0,22	0,16	0,23	0,18	0,20	0,26	0,20	0,20	0,17	0,16	0,20	0,20
Johansen Shale	0,17	0,16	0,14	0,13		0,14				0,25	0,18	0,15	0,14	0,11		0,16
Average Porosity	0,19	0,21	0,21	0,21	0,25	0,16	0,24	0,19	0,21	0,25	0,20	0,17	0,15	0,13	0,19	0,20

Permeability Results (mD)																
	31/2-1	31/2-2	31/2-3	31/2-4	31/2-5	31/2-8	31/3-1	31/3-3	31/5-2	31/6-1	31/6-2	31/6-3	31/6-6	31/1-1	32/4-1	Average
Johansen Top	96,74	304,04	927,11	1168,40	1247,19	149,66	958,56	262,25	391,60	609,73	412,32	121,87	76,45	178,23		493,15
Johansen2	1042,21	893,04	1186,30	1065,96	1010,83	169,35			631,31	913,58	400,77	195,51	195,91	43,13		645,66
Johansen1	657,22	767,30	526,08	292,54	569,85	183,88	656,84	263,51	353,54	1210,52	412,29	316,86	158,32	194,11		468,77
Johansen Shale	76,55	64,66	21,10	28,30		23,01				308,42	68,32	35,92	31,12	14,74		67,21
Average Permeability	468,18	507,26	665,15	638,80	942,63	131,47	807,70	262,88	458,82	760,56	323,42	167,54	115,45	107,55		454,10

VCI Results																
	31/2-1	31/2-2	31/2-3	31/2-4	31/2-5	31/2-8	31/3-1	31/3-3	31/5-2	31/6-1	31/6-2	31/6-3	31/6-6	31/1-1	32/4-1	Average
TopJohansen	0,53	0,29	0,09	0,16	0,13	0,23	0,04	0,07	0,09	0,04	0,11	0,15	0,12	0,24	0,13	0,16
Johansen 2	0,12	0,11	0,05	0,08	0,08	0,07			0,03	0,06	0,11	0,08	0,19	0,45	0,08	0,12
Johansen 1	0,17	0,14	0,13	0,16	0,16	0,14	0,08	0,09	0,05	0,06	0,11	0,08	0,19	0,25	0,15	0,13
Johansen Shale	0,26	0,33	0,33	0,33		0,25				0,23	0,24	0,22	0,34	0,38		0,29
Average VCI	0,27	0,22	0,15	0,19	0,12	0,17	0,06	0,08	0,06	0,09	0,14	0,13	0,21	0,33	0,12	0,16

4.5.2 Methodology and Modelling

The Jurassic sequence consists of a number of predominantly sandstone units including Sognefjord, Fensfjord, Krossfjord, Cook and Johansen formations, and a number of more shaley intervals including the Drake Formation, Upper Amundsen Formation and Lower Amundsen Formation. The Jurassic sands are often micaceous, with tight calcareous streaks. The presence of mica is the main challenge in the interpretation.

The petrophysical zonation used is the NPD zonation, with 4 additional intra-Johansen zones referred to as the ResLab zonation. Additional zones were also added to separate gas and oil zones in the main Troll reservoir sections and within the Drake Formation to separate a generally more clay-rich Lower Drake Formation from the more mixed sand and shale in the Upper Drake Formation.

4.5.3 Log Data Quality Check

All log data was loaded into Interactive Petrophysics and QC'd to check logs were on-depth and other log effects due to hole problems. The IP model in each well was set up according to the logging tool vendor to ensure correct tool calibrations.

4.5.4 Volume of Clay Analysis (VCI)

A number of different volumes of clay (VCI) analysis methods were used, using Density and Neutron and Gamma Ray logs. Additionally, the thorium (Th) curve from the Spectral Gamma Ray, available through Johansen Formation in 4 Troll wells, was used to estimate VCI.

DOCUMENT NO.: TL02-GTL-Z-RA-0001	REVISION NO.: 03	REVISION DATE: 01.03.2012	APPROVED:
-------------------------------------	---------------------	------------------------------	-----------

The volume of clay analysis (VCl) was calibrated to a lithology description from various sources including lithology summaries in the ResLab report, well site lithology descriptions from the Completion Reports and core descriptions. Percentage estimates of sand/clay contents are very limited and so coarse estimates of clay content are made based on the lithology descriptions.

Results are summarized in Table 4-3 and the full method and results are documented in the Petrophysical Report (Gassnova-ROS 2011).

4.5.5 Porosity and Water Saturation Analysis

Porosity and water saturation model input parameters are described in detail in the Petrophysical Report (Gassnova-ROS 2011), and are summarized below.

Water saturation: for the evaluation the Indonesian equation has been used. Saturation parameters and water resistivity (R_w) were determined using Pickett Plots in the clean ($VCl < 0.15$) sands. Saturation parameters varied between wells and formations and ranged between $m = 1.95-2.2$, $n = 2 - 2.2$ and $a = 1$.

Reservoir temperature: For each well a generic temperature gradient of $3.46^\circ\text{C}/100\text{m}$ was used (Evans, et al. 2003) assuming a mudline temperature of 3.88°C .

True Formation Resistivity (R_t) was determined from crossplots of VCl vs deep resistivity.

Shale and Matrix Parameters: Shale and matrix parameters were derived from logs, histograms and crossplots. Generally a matrix density of 2.67g/cc was used to account for the presence of mica through much of the Jurassic sequence.

Porosity: Effective porosity (PHIE) was determined from the Density/Neutron model. Total porosity (PHIT) was corrected for volume of clay (VCl). Calculated PHIE was multiplied by 0.96 to correct the PHIE to reservoir stress conditions in accordance with laboratory data on Sognefjord Formation in 31/2-8.

4.5.6 Permeability Analysis

Since permeability was modelled throughout the entire Jurassic sequence, for convenience the Schlumberger Chart K3 porosity to permeability correlation was used, as in the ResLab study. The default Schlumberger parameters were used, with calibrations to honour core data, where available (Johansen 2, Upper Jurassic sands, Drake Formation and Cook Formation).

4.5.7 Porosity and Permeability Calibration

The porosity and permeability models were calibrated to laboratory porosity, permeability and grain density data from a combination of Sognefjord Formation, Heather Formation, Fensfjord Formation and Krossfjord Formation available in the following Troll wells: 31/2-2, 31/2-3, 31/2-4, 31/2-5, 31/2-8, 31/3-1, 31/3-2, 31/3-3, 31/5-2, 31/5-3, 31/6-2, 31/6-6.

The Johansen Formation porosity and permeability was calibrated to porosity/permeability data available from 31/2-3 in core reports from the operator's core testing programme in 1980 (referred to as the Johansen Reference Core Data (JRCD)), which was depth shifted by $+5.5\text{m}$ to better honour the log data. The core data from 31/2-3 was originally tested for K_h (horizontal permeability) at an effective confining pressure of 1.5MPa and is therefore not representative of in-situ stress conditions.

DOCUMENT NO.: TL02-GTL-Z-RA-0001	REVISION NO.: 03	REVISION DATE: 01.03.2012	APPROVED:
-------------------------------------	---------------------	------------------------------	-----------

The Drake Formation porosity and permeability was calibrated to laboratory data reported in (Yang and Aplin 2007). The Cook Formation was calibrated to publicly available data from BP (BP Petroleum Development Ltd 1983).

4.6 Dynamic simulation parameter description

The data and parameter values used for the dynamic modelling of CO₂ injection and storage in the Johansen/Cook Formation are summarized in Table 4-4. The table shows Base, Low and High values, and the main reference basis for the selected values. The Base values reflect the most likely (P50) values, and are values used in the reference Eclipse simulation case. The Low and High values reflect P90 and P10 values, and have been used in simulation sensitivities.

The Reservoir Parameter Study report presents and discusses the parameter value selection. Experimental laboratory data on cores from the storage formation were available towards the end of the parameter study. The result is presented in chapter 4.7 and in (Gassnova-IRI 2011). Where applicable, the experimental data have been evaluated against data from other sources. Generally, the experimental results carry more weight than other sources, but only after evaluation of the adequacy of the experiments in terms of core representation, core conditions, accuracy and relevancy of measurements etc. Results from the laboratory experiments showed good correspondence with the base values and were within the uncertainty span of the respective parameter.

The sensitivity to the variation in parameter values in simulated results is presented and discussed, with the main focus on CO₂ plume migration and pressure build-up. Parameters with a high effect on simulated results have received most attention in acquiring representative values.

Table 4-4: Summary of all input data in Reservoir Parameter study report.

Parameter	Low	Base	High	Chapter in Reservoir Parameter Report
Rock compressibility (bar ⁻¹)	1.6 x 10 ⁻⁶	4.0 x 10 ⁻⁵	1.6 x 10 ⁻⁴	Chapter 4
Physical properties of pure CO ₂ and brine	Properties calculated from "CO ₂ Thermodynamics". At P _{init} = 305 bar and T _{init} =94°C CO ₂ density = 688kg/m ³ , CO ₂ viscosity = 0.057 cP Brine density = 1009kg/m ³ , Brine viscosity = 0.344cP			Chapter 5.1
Rs value at initial pressure (305 bar) [Sm ³ /Sm ³]	0	25	31	Chapter 5.2
Rv value at initial pressure [Sm ³ /Sm ³]	0	1.47E-05	3.45E-05	Chapter 5.3
Formation water salinity [weight %]	0	5%	7%	Chapter 5.4
Reservoir temperature [°C]	92.5	94	106	Chapter 5.5
Residual CO ₂ saturation [fraction]	0.05	0.25	0.4	Chapter 6.2
Residual water saturation [fraction]	0.5	0.15	0	Chapter 6.3

4.7 Lab testing of cores

4.7.1 Introduction

Wells surrounding the storage complex were investigated to find those that had cores of the relevant formations. The following core plugs and cuttings were sampled:

- 30/3-2 – 9 Cook Fm plugs
- 30/3-4 – 2 Drake Fm plugs, 2 Amundsen Fm plugs, 6 Cook Fm plugs, cuttings Drake Fm
- 31/2-3 – 6 Johansen Fm plugs
- 31/5-2 – Cutting samples (Draupne Fm, Drake Fm, Amundsen Fm)
- 31/5-2 – Cutting samples
- 35/10-1 – Cuttings Amundsen Fm, Drake Fm

DOCUMENT NO.: TL02-GTL-Z-RA-0001	REVISION NO.: 03	REVISION DATE: 01.03.2012	APPROVED:
-------------------------------------	---------------------	------------------------------	-----------

Not all plugs were suitable for testing and a selection was made for laboratory testing. Laboratory experiments were carried out or managed by IRIS (Gassnova-IRI 2011), and the main results are discussed and summarized in this chapter. The purpose of conducting the laboratory experiments was to provide data for a better evaluation of Johansen/Cook formations as potential CO₂ storage formations, and to reduce uncertainties related to this evaluation.

The results from the laboratory experiments were available to Ross Offshore almost two months later than originally scheduled. That meant that there was no time to incorporate the results directly into the reservoir simulation work. However, the results and the expected effects on storage evaluation are discussed where appropriate.

The laboratory experiments and results can be grouped into three main categories, based on their usage:

1. Storage formation (relative permeability, permeability/porosity, compressibility etc)
2. Cap rock (permeability, break-through/capillary entry pressure, XRD and thin sections)
3. Geo-mechanical and mineralogy (Triax, UCS, XRD etc)

4.7.2 **Storage formation**

The core material from the Cook/Johansen formations was limited and some of it was of poor quality. This was particularly the case for the highly porous and permeable cores. Most of the preserved core material was from low permeable, cemented and laminated parts. Still, one core sample (no. 15) from the Cook Formation can be considered representative of porous, permeable sand. Also, the combined Johansen cores no. 1 & 6 used for relative permeability measurements can be viewed as representative of porous Johansen Formation sand.

4.7.2.1 *Permeability*

Permeability was one of the most important results from the laboratory experiments. Testing was done to evaluate the results previously available. The results from the testing are presented in chapter 6.3 where they are linked with injectivity. These results were not incorporated into the geomodel due to timing of results.

4.7.2.2 *Relative permeability*

Relative permeability experiments have been performed on 4 sets of core samples, as given in Table 4-5, along with measured residual end-point saturations and porosity/permeability. It should be noted that the cores are drilled vertically, and measurements are therefore in a vertical direction. Vertical permeability and relative permeability may differ significantly from the corresponding horizontal values, in particular for the low permeable laminated cores. However, residual end point saturations are not believed to be directionally dependent, and are therefore considered representative.

The experimental procedure involved initializing the cores at irreducible water saturation (Swir), then performing an imbibition cycle displacing CO₂ down to residual CO₂ saturation (Sgr). Finally, the CO₂ was removed, and a drainage process was carried out from 100% water down to Swir. This process is the opposite of that which the reservoir will experience (first drainage, then imbibition), and was chosen due to time limitation. The Swir from the drainage process was significantly different from the initial imbibition Swir, explained (by IRIS) by strong capillary end point effects, and perhaps change (damage) in core characteristics between the experiments. Therefore, only the imbibition results are used in the reservoir simulation model, and mainly the residual end point saturations. This is further discussed in (Gassnova-ROS 2011).

DOCUMENT NO.: TL02-GTL-Z-RA-0001	REVISION NO.: 03	REVISION DATE: 01.03.2012	APPROVED:
-------------------------------------	---------------------	------------------------------	-----------

Table 4-5: Relative permeability results.

Core No.	Swir	Sgr	Poro	Permz (mD)
1/6	0.337	0.298	0.281	398
5	0.291	0.268	0.302	6.5
13	0.377	0.197	0.191	1.1
15	0.34	0.218	0.271	41

4.7.2.3 *Permeability - directional*

Horizontal cores were drilled from three vertical cores from the Cook Formation, in order to also measure horizontal permeability. The results are given in Table 4-6. The Kv/Kh ratio is high for the high permeable core no. 15, and decreases to below 0.1 for the low permeable core no. 8. It is mainly the shaley/silty sequences that control flow in the reservoir, and the Kv/Kh ratios measured are in line with values used in the reservoir simulation model. None of the Johansen cores was in good enough condition to enable horizontal cores to be drilled.

Table 4-6: Permeability results.

Core No.	Kv (mD)	Kh (mD)	Kv/Kh
8	0.002	0.034	0.06
10	0.077	0.515	0.15
15	156	220	0.71

4.7.2.4 *Compressibility*

The most representative cores for rock (pore volume) compressibility values were core no. 5 from the Johansen Formation and core no. 15 from the Cook Formation. These were the only high porous cores with measurements up to reservoir pressure, and both had measured/calculated pore volume compressibility of 4.E-5, equal to the reference case value used since the Johansen simulations started.

4.7.3 **Cap rock**

The shale samples are from cuttings and core material. The test was conducted on samples collected from relevant well material at the NPD core storage facilities. The test programme was designed to support the selection and qualification of shale as the sealing layer in the Johansen Storage Complex. The lab analysis is summarized in Table 4-7 and in the external report (Gassnova-IRI 2011).

Several tests were performed on the samples:

1. Porosity and permeability measurements on core samples
2. Break through pressure testing on core samples
3. XRD and thin section analysis on core samples
4. Thin sections on core samples
5. Brine porosity and permeability
6. Triax and permeability
7. XRD on cuttings samples in the whole rock and clay size fraction

DOCUMENT NO.: TL02-GTL-Z-RA-0001	REVISION NO.: 03	REVISION DATE: 01.03.2012	APPROVED:
-------------------------------------	---------------------	------------------------------	-----------

Table 4-7: An overview of samples and tests conducted on shale samples from Amundsen Fm and Drake Fm.

Sample No.	Well Name	Depth	Lithology	Formation	Brazil Test	Por/ Perm	Breakthrough	Triax and permeability	XRD & TS Core	XRD Cuttings
16	3129,45	3129,45	Shale	Amundsen		x	x		x	
17	30/3-4	3129,8	Shale	Amundsen		x	x		x	
24	30/3-4	2969,2	Shale	Drake	x	x	x		x	
25	30/3-4	2963,5	Shale	Drake		x	x	x	x	
40	31/5-2	2037	Shale	Drake						x
41	31/5-2	2046	Shale	Drake						x
42	31/5-2	2061	Shale	Drake						x
43	31/5-2	2076	Shale	Drake						x
44	31/5-2	2091	Shale	Drake						x
45	31/5-2	2106	Shale	Drake						x
46	31/5-2	2121	Shale	Drake						x
47	31/5-2	2136	Shale	Drake						x
48	31/5-2	2151	Shale	Drake						x
49	31/5-2	2166	Shale	Drake						x
50	31/5-2	2172	Shale	Drake						x

Washed cuttings samples from the Drake Formation from well 31/5-2 were collected at the NPD storage facilities. The samples were subsequently XRD scanned in the < 2µm size fraction and for whole rock (Table 4-8).

The main clay types are Kaolinite, Illite+Mica and Chlorite. The dominating rock mineralogy is quartz and k-feldspar/plagioclase. The mineral distribution reflects a source area with igneous rocks. The Fenno-scandian shield is mainly constituted by igneous rocks in the granite-gneiss domain. The results are consistent with the mineralogy of the Norwegian mainland.

There is also a mean calcite content of 10% in the samples. This is derived from calcium carbonate (CaCO₂) in micro organisms feeding in ocean surface waters. It may also be contaminants from drilling fluid loss additives.

Capillary entry pressure was measured by lab oil and correlated to CO₂ entry pressure. It was found that entry pressure is >250 bar.

DOCUMENT NO.: TL02-GTL-Z-RA-0001	REVISION NO.: 03	REVISION DATE: 01.03.2012	APPROVED:
-------------------------------------	---------------------	------------------------------	-----------

Table 4-8: An overview of XRD analysis of whole rock of washed cuttings from well 31/5-2 through the Drake Fm.

Sample	Depth(m)	Illite/Smectite	Illite+Mica	Kaolinite	Chlorite	Quartz	K Feldspar	Plagioclase	Calcite	Dolomite	Siderite	Pyrite	Barite	Total
40	2037,00	0,0	3,2	8,6	2,9	62,0	5,7	1,2	8,4	0,9	4,1	3,0	0,0	100
41	2046,00	0,0	4,6	6,9	2,8	65,0	4,7	3,6	2,4	2,5	3,2	3,1	1,2	100
42	2061,00	0,6	4,5	14,0	4,9	47,1	13,3	2,0	4,4	0,0	2,2	1,6	5,4	100
43	2076,00	0,0	9,8	11,7	4,2	47,0	6,1	2,9	13,1	1,3	2,2	1,6	0,0	100
44	2091,00	TR	9,5	10,1	4,3	52,5	6,9	2,0	12,0	TR	1,1	1,6	0,0	100
45	2106,00	TR	8,5	9,4	4,8	44,5	8,1	3,1	17,3	0,6	1,4	2,2	0,0	100
46	2121,00	1,0	9,8	19,1	6,9	38,2	4,5	3,3	9,6	0,0	2,5	2,1	3,1	100
47	2136,00	0,0	11,6	21,0	7,3	29,8	2,9	2,1	13,2	0,8	1,6	6,7	3,0	100
48	2151,00	1,1	15,1	24,0	8,6	27,7	2,4	2,0	8,6	0,8	4,2	5,4	0,0	100
49	2166,00	1,3	13,2	17,9	7,6	31,7	4,0	1,7	12,3	0,0	6,9	3,4	0,0	100
50	2172,00	0,0	11,3	9,1	4,8	55,2	4,9	3,0	5,1	1,1	3,4	2,1	0,0	100

4.7.4 Geo-mechanical Testing

4.7.4.1 Tensile Strength from Brazil Tests

Brazil tests were conducted on discs sampled from 4 core plugs, two each from Amundsen Formation and Drake Formation. The tensile strengths are very similar, except for one relatively strong Drake sample (plug no. 25). Excluding this result the average tensile strength for Drake and Amundsen formations is 4.22MPa. Nine Brazil tests were conducted on Cook core (plugs no. 18 and 21). The average tensile strength for Cook Formation is 7.92MPa.

An average tensile strength of 4.22MPa has been used as input to the fracture initiation stress to define the safe pressure (see chapter 5.5.4).

Table 4-9: Tensile strength results for Amundsen, Drake and Cook Fm.

Plug No.	Formation and Well	Tensile Strength (MPa)
16	Amundsen Fm (30/3-4)	4.72
17	Amundsen Fm (30/3-4)	4.19
17	Amundsen Fm (30/3-4)	3.5
24	Drake (30/3-4)	4.25
24	Drake (30/3-4)	4.44
25	Drake (30/3-4)	9.74
18	Cook (30/3-4)	10.47
18	Cook (30/3-4)	8.15
18	Cook (30/3-4)	10.88
18	Cook (30/3-4)	8.9
21	Cook (30/3-4)	7.62
21	Cook (30/3-4)	6.64
21	Cook (30/3-4)	6.24
21	Cook (30/3-4)	6.55
21	Cook (30/3-4)	5.84
	Average	6.81

DOCUMENT NO.: TL02-GTL-Z-RA-0001	REVISION NO.: 03	REVISION DATE: 01.03.2012	APPROVED:
-------------------------------------	---------------------	------------------------------	-----------

4.7.4.2 *Stress Dependent Permeability*

Stress dependent permeability measurements from this study suggest a very high permeability reduction relative to that observed in the Upper Jurassic Sognefjord Formation (31/5-3). A description of the results and discussion of concerns regarding core quality follows in section 6.3.1.

4.7.4.3 *Permeability - Cap Rock*

Vertical permeability was measured on 2 cap rock formations, Amundsen Formation and Drake Formation. The results are 1.33×10^{-7} mD for Amundsen Formation and 3.56×10^{-7} mD for Drake Formation. These results are consistent with values based on (Yang and Aplin 2007) used to calibrate the permeability models.

4.7.4.4 *Rock Strength Parameters (Mohr Coulomb)*

Two sets of Mohr Coulomb strength parameters were established to represent shaley sand and clean sand. Plugs 9 and 11 from the Cook Formation, representing shaley sand, result in a friction angle of 30.05° and cohesive strength of 12.41MPa. Plugs 22 and 23 from Cook Formation represent clean sand (Table 4-9). Only 2 samples were available to establish the Mohr Coulomb parameters for each lithology type. No Mohr Coulomb parameters were established for the Johansen Formation, owing to the lack of appropriate core plugs.

The Mohr Coulomb parameters from plugs 9 and 11 have been applied in the fault reactivation assessment (Section 5.5.3), to define the strength characteristics of a sand/clay filled fault with low cohesive strength.

Table 4-10: Mohr Coulomb parameters for shaley and clean Cook sand.

Plug No.	Formation and Well	Friction Angle (degrees)	Cohesive Strength (MPa)	Lithology
9,11	Cook (30/3-2)	30.75	12.11	Shaley sand
22,23	Cook (30/3-4)	25.56	27.03	Clean sand

4.7.4.5 *Effective Stress Ratio, K0*

The ratio between the effective horizontal and effective vertical stress, K0, has been estimated from triaxial testing on plug no.2 (Johansen) and plug no.12 (Cook), giving $K_0 = 0.25$ and $K_0 = 0.43$ respectively. K0s between 0.43 – 0.48 are consistent with those reports from mini-frac data in the Sognefjord Formation in the Troll field (31/2-A-21) (Yielding and Bretan 2008), though these values are lower than those obtained from leak off tests in Drake and Johansen formations (K0s range from 0.53 – 0.61). Whilst leak off test data are prone to uncertainties, it is considered that the K0s from the laboratory tests underestimate in-situ stresses due to the presence of core damage during core retrieval and unloading, drying of core during storage, and the presence of calcite cementation in the Johansen core plug.

Given the uncertainty, K0 values ranging from 0.33 – 0.7 have been used as input to define the range of stress estimates for the fault reactivation study.

4.8 **Fault seal assessment**

A fault seal evaluation of the Dunlin Group on the Horda Platform has been performed (Gassnova-ROS 2011). The objective was to predict possible communication across and/or along faults within the storage complex area in order to find optimum injection point with low risk of leakage. This is important for both storage site seal integrity and for pore volume communication across faults within the storage site hydraulic unit. Faults have been evaluated

DOCUMENT NO.: TL02-GTL-Z-RA-0001	REVISION NO.: 03	REVISION DATE: 01.03.2012	APPROVED:
-------------------------------------	---------------------	------------------------------	-----------

using Shale Smear Factor (SSF) / Shale Gauge Ratio (SGR) and the Clay Smear Property (CSP) within each fault zone.

An area for possible communication was found in the area between the northern and the central area of the storage complex, along the main fault between the Troll West Gas Province (TWGP) and the Troll West Oil Province (TWOP). This is the only area where sand of the Dunlin Group and the Brent Group are in juxtaposition with each other. By defining both the lower and the upper Drake Formation as a clay-source thick enough for smearing the fault-zone, the coating along the fault planes is thick enough to prevent any communication. However, in two areas the offset along the fault is approximately 300m, and both the SSF/SGR and the CSP show that the thickness of the clay-coating is very thin. Here, the risk of communication across and along the fault-plane is rather high (see Figure 4-7). An injection point in the south where plume migration does not come into conflict with this area is therefore preferred.

Evaluation shows that the Amundsen 1 Formation is most likely too thin to create any secure seal along faults where the Statfjord Formation and the Johansen Formation are in juxtaposition towards each other. The Amundsen 2 Formation is interpreted to be extended only in the northern areas, and is here too thin to create an effective seal between the Johansen Formation and the Cook Formation in contact due to juxtaposition along faults. This indicates that there is a strong possibility of pressure communication in a much larger area than included in the reference case model. This does not indicate a leakage route for CO₂ as Statfjord Formation is below Johansen.

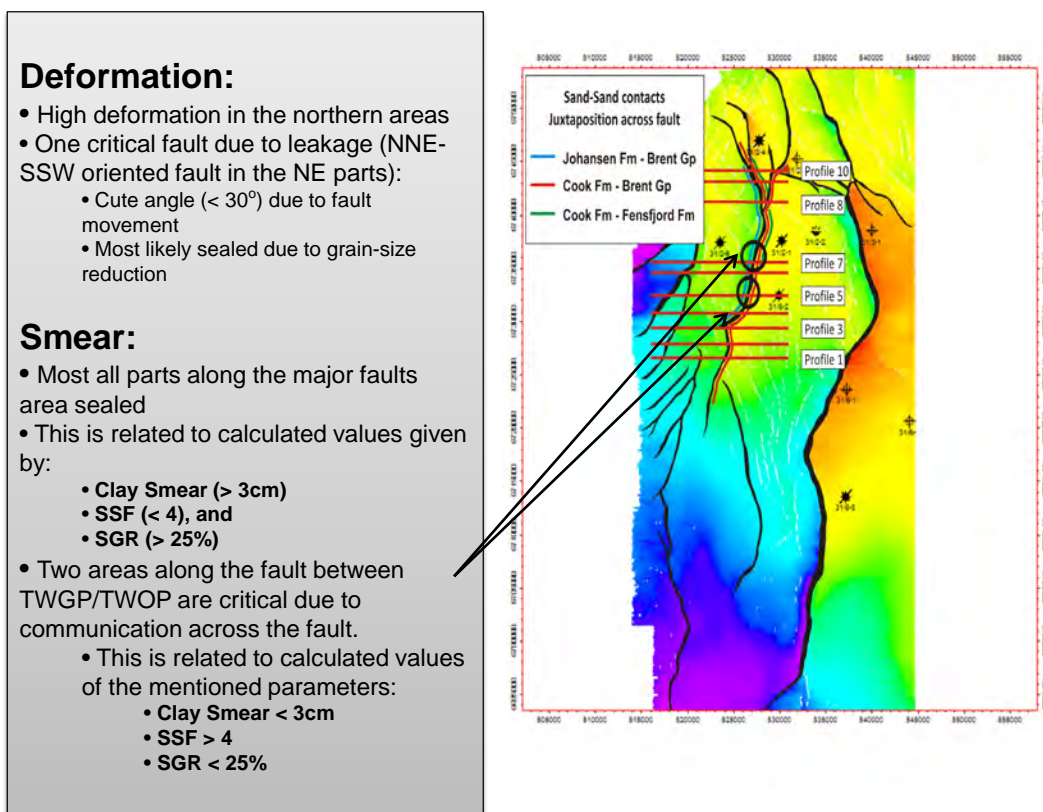


Figure 4-7: Results Fault Seal Evaluation - northern area.

DOCUMENT NO.: TL02-GTL-Z-RA-0001	REVISION NO.: 03	REVISION DATE: 01.03.2012	APPROVED:
-------------------------------------	---------------------	------------------------------	-----------

4.9 Seismicity

The seismotectonic of the North Sea, the Norwegian continental margin and the surrounding regions have been studied extensively over the last 30 years. Some of these studies show that, in the northern North Sea (Horda Platform), an area with quite anomalous stress orientations was identified, with strike-slip faulting, in a region transitional between normal and reverse faulting. The studied also clearly identified the Horda Platform (see Figure 4-8, Figure 4-9, Figure 4-10) as an aseismic region separating the Viking Graben, with indications of extension and normal faulting, from coastal areas to the east and the complex areas north of 61°N where the two zones are merged. While the focal mechanisms to the east and north are more mixed, the inferred stress directions are still dominantly NW-SE. Along the margin further north the mechanisms are more consistently reverse.

The best study was done by (Møllegård 2000) who also reviewed in detail all available earthquake focal mechanisms, indicating a complexity of sources of stress, at plate wide, regional and local scales, together with a heavily fractured crust (especially around 61°N where the number of mapped faults is also very high).

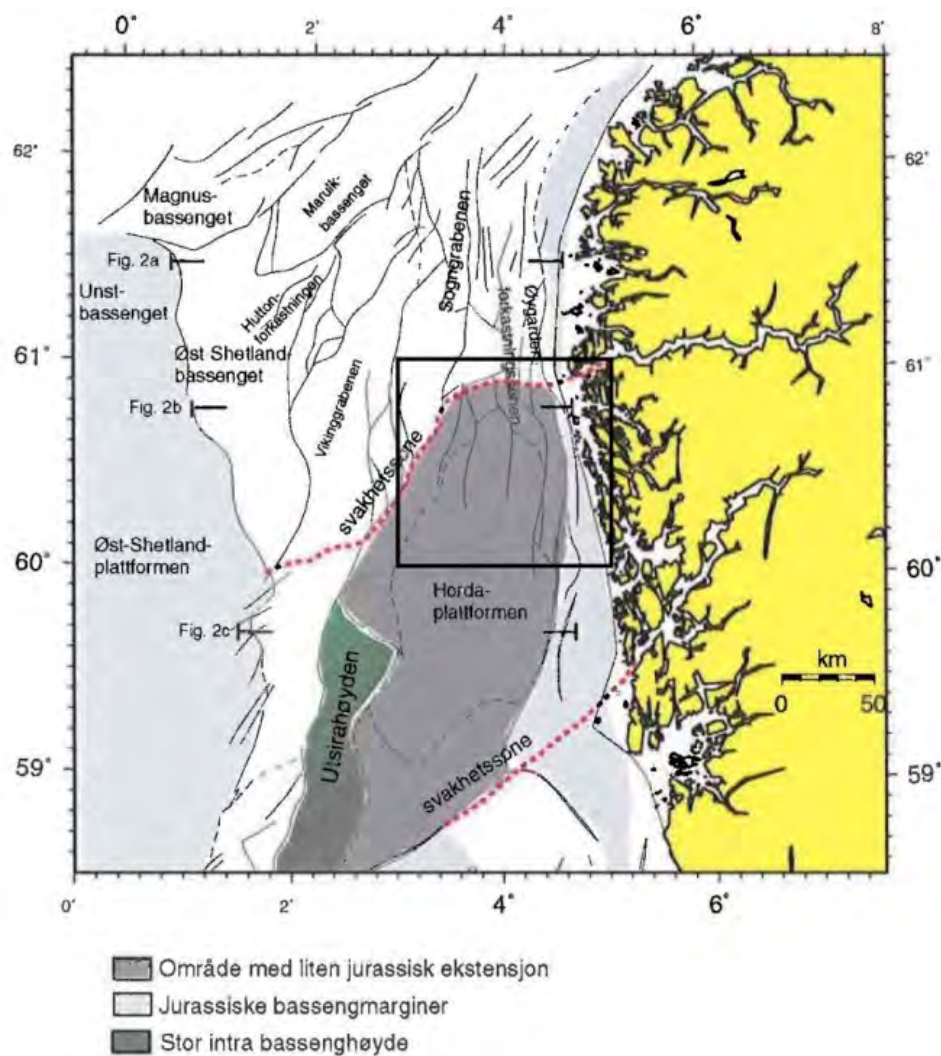


Figure 4-8: Overview of the Jurassic rift zone in the northern North Sea modified from (Møllegård 2000). The shaded area is the Horda Platform and the black box in the centre is the study region, covering 3-5°E and 60-61°N.

DOCUMENT NO.: TL02-GTL-Z-RA-0001	REVISION NO.: 03	REVISION DATE: 01.03.2012	APPROVED:
-------------------------------------	---------------------	------------------------------	-----------

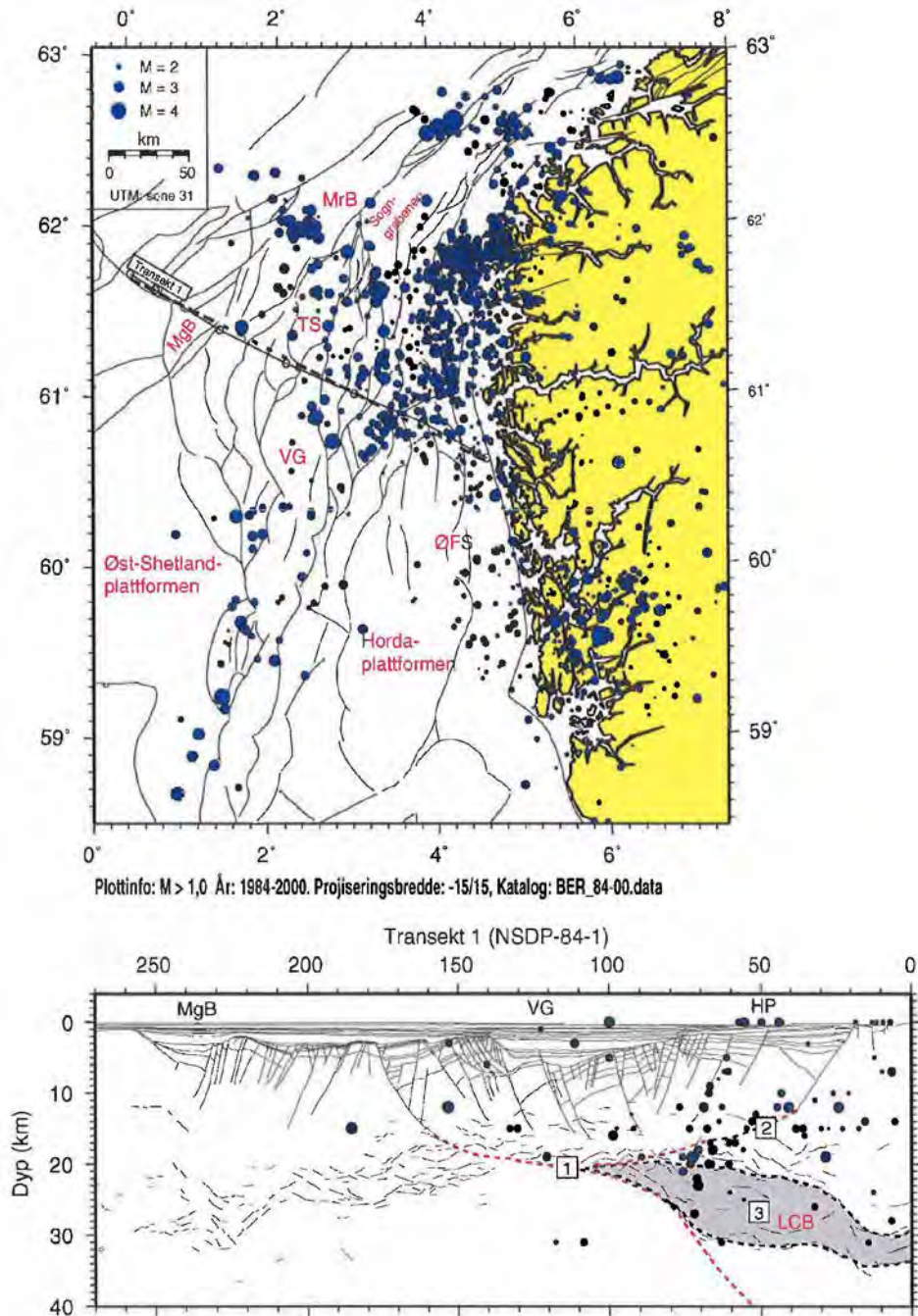


Figure 4-9: Earthquake distribution along profile NSDP-84-1, projecting events from 15km on both sides of the line. Line 1 indicates the continuation of a basement fault down to an old shear zone, while Line 2 indicates the continuation of the Øygarden Fault zone terminating on top of a lower crustal body (LCB, indicated by 3).

DOCUMENT NO.: TL02-GTL-Z-RA-0001	REVISION NO.: 03	REVISION DATE: 01.03.2012	APPROVED:
-------------------------------------	---------------------	------------------------------	-----------

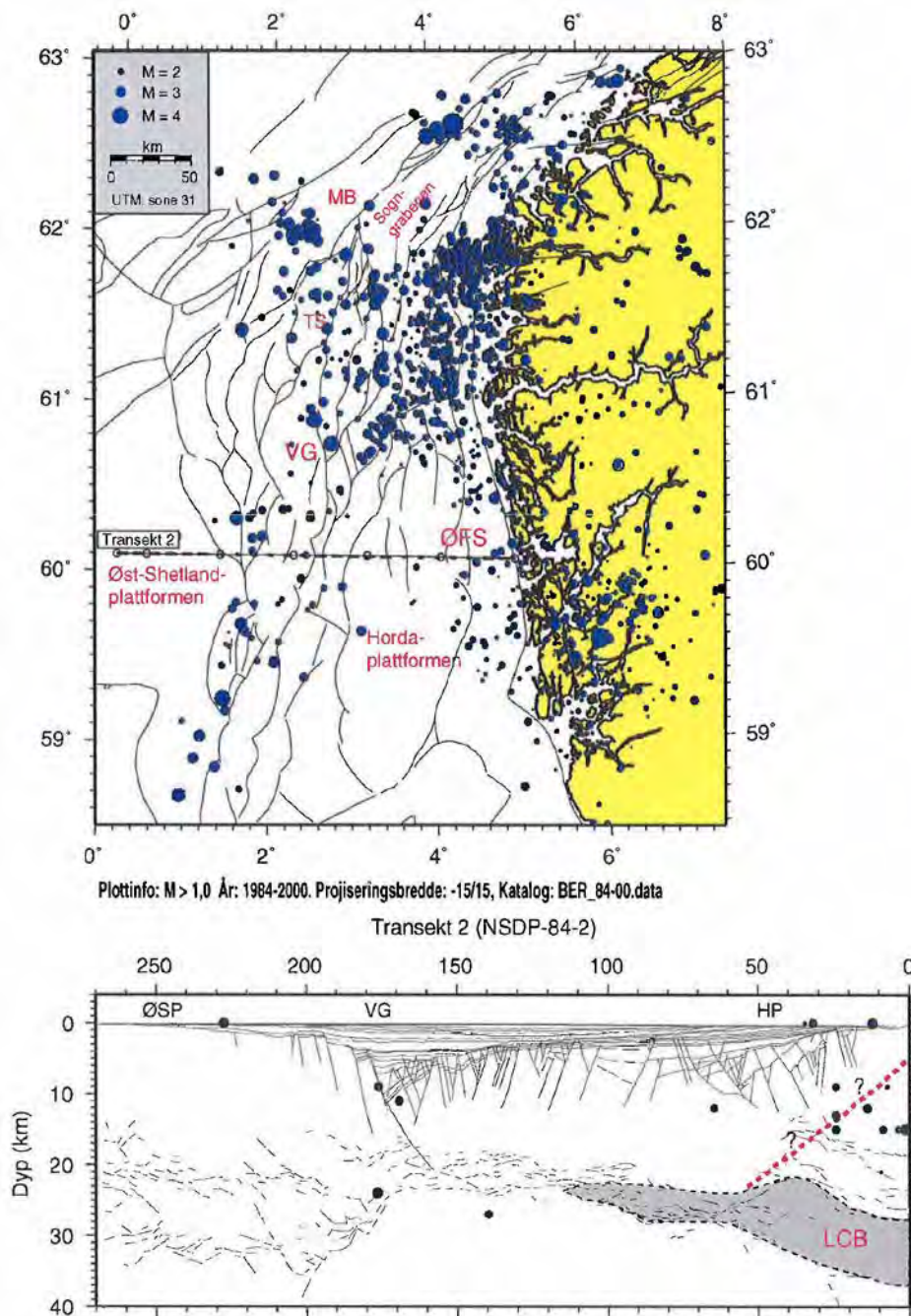


Figure 4-10: Earthquake distribution along profile NSP-84-2, projecting events from 15km on both sides of the line. See Figure xx for comparison. From (Møllegaard 2000).

There is an indication from Figure 4-9 that the earthquakes are quite deep and that they terminate at the top of the (high-velocity) lower crustal body (LCB), which should be expected. Around the southern transect (Figure 4-10) the seismicity is significantly lower and even more inconclusive, except that the hypocenters also seem to be quite deep here. This is expected to have minimal impact on storage site integrity.

DOCUMENT NO.: TL02-GTL-Z-RA-0001	REVISION NO.: 03	REVISION DATE: 01.03.2012	APPROVED:
-------------------------------------	---------------------	------------------------------	-----------

4.10 **Further data collection and assessment**

To fully characterize the Johansen Storage Complex according to EU requirements, a verification well is needed. This will provide both confirmation of formation presence and quality, and also give an opportunity to collect fresh core samples from both storage formation and cap rock. A well will further give the opportunity to provide in-situ stress data using a mini-frac as well as FIT/LOT. Reservoir properties in the near wellbore region and in a reasonable radius from the well should be investigated using a “dual packer” test. Ambitions regarding proving storage site performance through a long term injection test have been investigated and it is not recommended due to cost involved and the uncertainty related to the expected results obtained (ref injection well memo).

The fresh core and fluid samples should be used to perform a full suite of geochemical analysis to determine the long term fate of CO₂ and fully describe the trapping potential. It should further be used to narrow the uncertainties related to safe-pressure build-up. A proposed verification well location and formation evaluation programme can be found in appendix A2.

DOCUMENT NO.: TL02-GTL-Z-RA-0001	REVISION NO.: 03	REVISION DATE: 01.03.2012	APPROVED:
-------------------------------------	---------------------	------------------------------	-----------

5 STORAGE COMPLEX DESCRIPTION

5.1 Introduction

The storage complex evaluation is based on the Gassnova work processes for CO₂ storage. The main product from this evaluation is the generation and description of the Johansen Storage Complex geomodel. The main fundament in maturing the Johansen Storage Complex for safe CO₂ storage and identifying the geological risk is a thorough evaluation and understanding of the storage complex depositional and structural geological processes, based on all available data.

The main deliverables from this chapter are:

- **Storage Formations:**
 - Identification and evaluation of the presence and quality of all possible storage formations within the defined storage complex.
 - Results from the evaluation are the main input for the geomodel (chapter 5.6), identification of the geological risk (chapter 7.1) and assessment of the pore volume connectivity (chapter 7.2)
- **Sealing Formations:**
 - Identification of the sealing formations (thickness, extent and continuity) and cap rock quality assessment
 - Results from the evaluation are input to the geomodel (chapter 5.6) and the overall risk evaluation (chapter 7)
- **Safe Pressure Evaluation:**
 - Storage complex tectonic history and stress regime and any implications on the CO₂ storage
 - Results are main input to overall risk evaluation (chapter 7)
- **Geomodel:**
 - Construct 3D static geomodels with valid rock properties for the development of the dynamic model.
 - Geomodel is the main input for development of the dynamic model (simulation model) (chapter 6)

The main criterion for the definition of the storage complex is that no CO₂ will migrate out of the storage complex. Figure 5-1 shows the definition of the Johansen Storage Complex reference case based on the evaluation done in this chapter.

The top of the storage complex is defined by top Drake Formation and the bottom is defined by top Statfjord Formation. The storage complex is defined by major faults to the north, and major faults and data availability to the east (Figure 5-1 and Figure 4-2). The interpreted pinch out of the Johansen Formation defines the western and most southern boundary of the storage complex. The data availability in the southeastern part of the storage complex is low, only a very coarse grid of 2D data exists (Figure 5-1). This is not important as it will only have effect for storage volume/possible extent of the Johansen Formation. This area is not suitable for injection as migration towards Troll East is expected.

DOCUMENT NO.: TL02-GTL-Z-RA-0001	REVISION NO.: 03	REVISION DATE: 01.03.2012	APPROVED:
-------------------------------------	---------------------	------------------------------	-----------

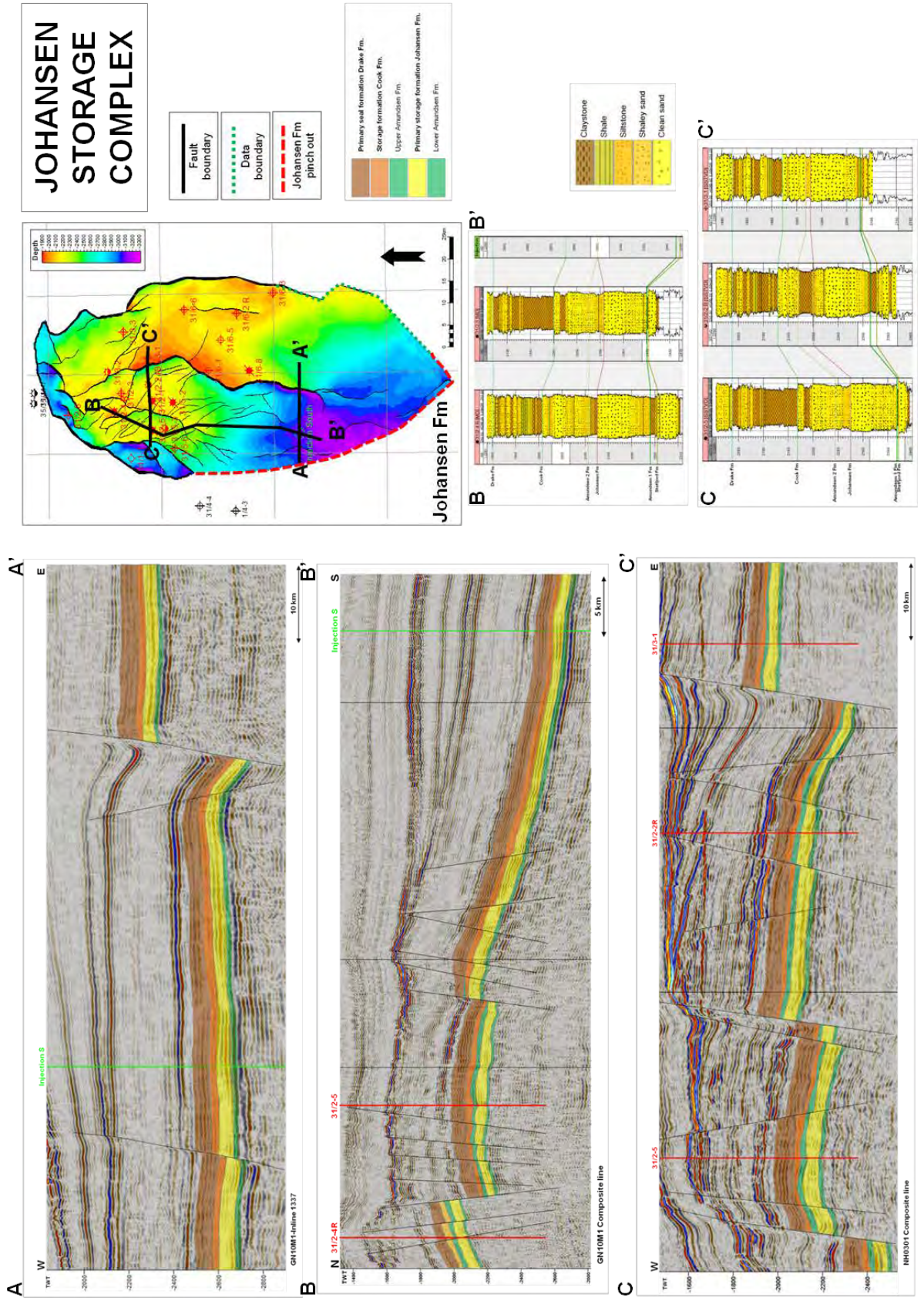


Figure 5-1: Regional geo-seismic lines and well correlations showing the defined storage complex seal and storage formations.

DOCUMENT NO.: TL02-GTL-Z-RA-0001	REVISION NO.: 03	REVISION DATE: 01.03.2012	APPROVED:
-------------------------------------	---------------------	------------------------------	-----------

5.2 Seismic analysis

One of the main tasks in storage complex description is the interpretation and analysis of seismic data. The purpose is to establish the stratigraphic and structural framework for the Johansen Storage Complex. The Petrel E&P software platform (Schlumberger) is the main tool used in the analysis. In addition the SVI Pro software has been used (Gassnova-ROS 2011).

The main activities in the seismic analysis are;

- Well to seismic calibration
- Interpretation of faults/horizons
- Depth conversion
- Seismic attributes analysis

The seismic attribute analysis will not be described in this chapter. The interpretation and use of the attributes will be described in chapters 5.3 and 5.4 which cover the geological development of the storage formations and sealing formations.

5.2.1 Well to seismic calibration

Input data for the well to seismic calibration process can be seen in Figure 5-2.

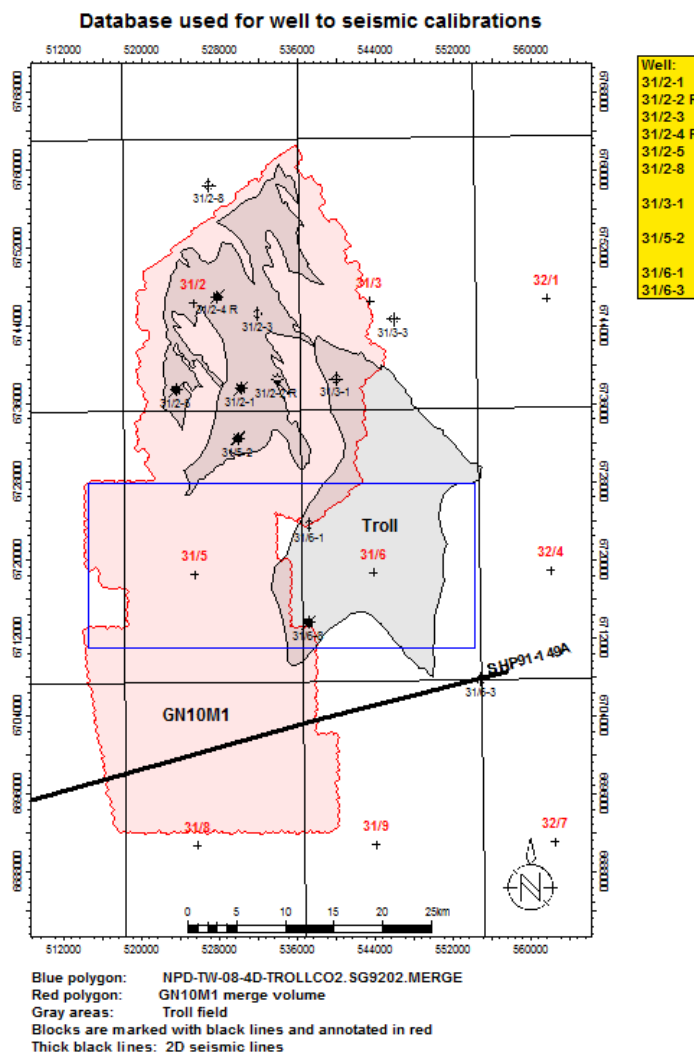


Figure 5-2: Wells and seismic data used in well to seismic calibrations process.

DOCUMENT NO.: TL02-GTL-Z-RA-0001	REVISION NO.: 03	REVISION DATE: 01.03.2012	APPROVED:
-------------------------------------	---------------------	------------------------------	-----------

Seismic data: NPD-TW-08-4D-TROLLCO2.SG9202.MERGE (3D survey)
 GN10M1 merge survey (3D survey)
 SHP91-149A (2D line)

Wells: 31/2-1, 31/2-2 R, 31/2-3, 31/2-4 R, 31/2-5, 31/2-8
 31/3-1
 31/5-2
 31/6-1, 31/6-3

Well logs: HDT (P-sonic, $\mu\text{s}/\text{ft}$), check shots, HRHOB (density, g/cm^3)

The workflow comprises:

1. QC/edit of input logs (de-spiking, missing data interval interpolation, check shot outliers)
2. Sonic – check shot calibration
3. Synthetic seismogram generation (wavelet extraction and reflection coefficient log calculations based on acoustic impedance \rightarrow Density \times V_p)
4. QC/Edit of input logs

Input well log panels are shown in appendix A3 Well to Seismic Calibration(Figure 1 to Figure 3).

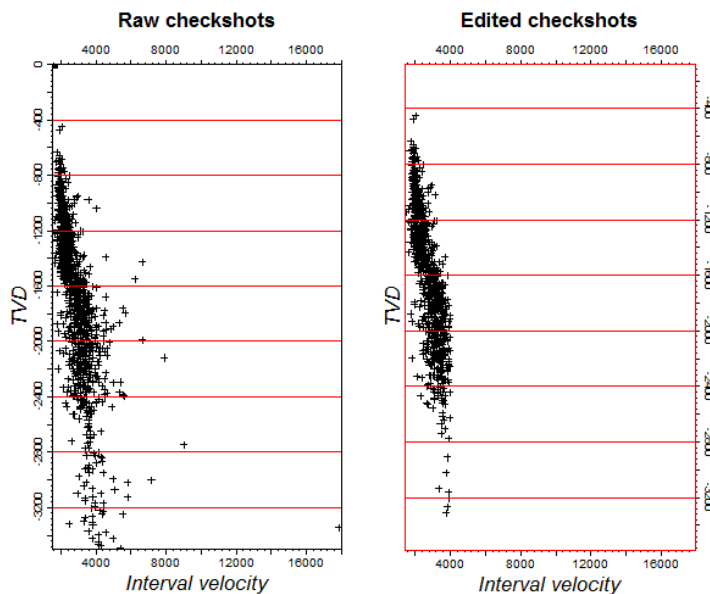


Figure 5-3: Raw check shots before editing (left) and after editing (right).

Sonic calibration

Sonic logs give a detailed picture in velocity along the borehole, as the depth sampling is dense (typically depth steps of 6 inches). However, to be used as a time-depth relationship (TDR) between seismic data and the well, the sonic log needs to be integrated. This process amplifies any inaccuracies in the log, and can cause a significant drift from the true TDR along the length of the borehole. For this reason, check shots are used to create a new calibrated sonic log that minimizes this drift. Before creating these calibrated sonic logs, the check shots need to be checked for outliers and if need be also edited (Figure 5-3). The calibrated sonic logs are subsequently used as TDR for the wells and well markers as a guide for the seismic interpretation (see appendix A3 Well to Seismic Calibration, Figure 4 and Figure 5).

DOCUMENT NO.: TL02-GTL-Z-RA-0001	REVISION NO.: 03	REVISION DATE: 01.03.2012	APPROVED:
-------------------------------------	---------------------	------------------------------	-----------

Synthetic seismogram generation

From the sonic and density logs an acoustic impedance log is calculated which in turn can be converted into a reflection coefficient log. A wavelet is then extracted from seismic (2D or 3D) around the well position and is convolved with the reflection coefficient log to produce the synthetic seismic traces used for calibrating wells (depth) to seismic (time) data. (See appendix A3 Well to Seismic Calibration for resulting well seismograms).

Well tie summary

- Least square constant zero phase wavelets extracted for each well position reveals good consistency except for well 31/2-4.
- Minor corrections to the time-depth relationships were made using small shift corrections between well markers and seismic horizons.

5.2.2 **Seismic interpretation**

5.2.2.1 *Horizon interpretation*

To obtain a consistent interpretation of the Johansen storage formation, seal units and faults, the following horizons were interpreted:

- Seabed
- Base Quaternary
- Base Pliocene
- Mid Oligocene
- Top Green Clay
- Top Balder Formation
- Top Shetland Group
- Top Draupne Formation
- Top Sognefjord Formation
- Top Fensfjord Formation
- Top Brent Group
- Top Drake Formation
- Top Lower Drake Formation
- Top Cook Formation
- Top Amundsen 2 Formation
- Top Johansen Formation
- Top Amundsen 1 Formation
- Top Statfjord Formation

Time and depth horizon maps are presented in appendix A4 Johansen Storage Complex Time and Depth Maps. The well calibration performed in chapter 5.2.1 is the basis for the seismic interpretation.

Prior to interpretation of the different horizons the different seismic cubes were tied in with the NPD-TW-08-4D-TROLLCO2 as master. The time difference between the cubes was in the region of 4-8ms. Due to different mismatch with the new merged cube GN10M1 from the south (GN1001, 0ms) to the north (NH0301, 4-8ms) in addition to a tie-in of 5ms, an adjustment/reinterpretation of the different horizons was necessary. The southernmost survey, EO0901, was received in February 2011 and needed a downward shift of 10.5ms.

Originally the different cubes were interpreted with an inline spacing of 16 which corresponds to 400m for GN1001 and NPD-TW-08-4D-TROLLCO2 and 300m for NH0307. Due to the

DOCUMENT NO.: TL02-GTL-Z-RA-0001	REVISION NO.: 03	REVISION DATE: 01.03.2012	APPROVED:
-------------------------------------	---------------------	------------------------------	-----------

more heavily faulted Troll West area (NH0301) this line spacing seemed too large beneath this area. Therefore, by the surface adjustment/reinterpretation on GN10M1 the line spacing was reduced to 8 (200m). A denser interpretation was performed in the injection area (GN1001 cube).

The geomodel gridding space is 200 x 200m which is the same as an inline spacing of 4. 3D interpretation would mean a 25 x 25m spacing of the grid and this would lead to a simulation model difficult to manage. The effect of gridding space vs. migration has been tested in chapter 6.1. 3D interpretation has however been performed to evaluate the presence and quality of both the storage and sealing formations.

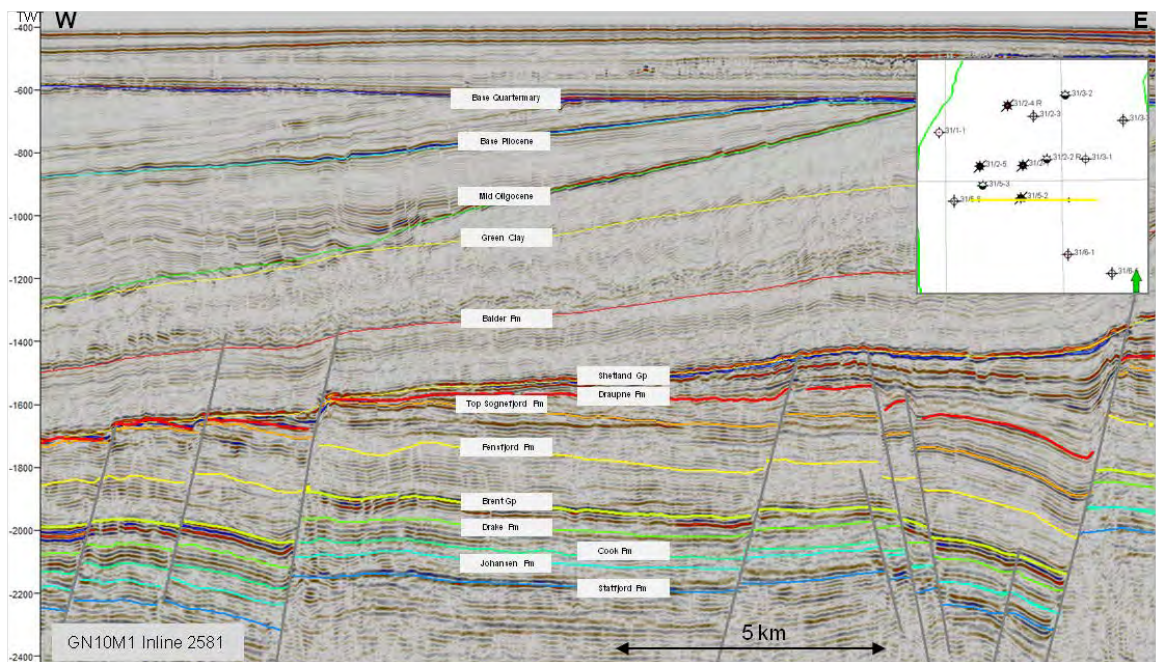


Figure 5-4: Seismic line showing interpreted key horizons.

During the interpretation the surfaces were divided into three patches; six surfaces in the upper part (above top Shetland) were mainly used in depth conversion and well planning, four surfaces between top Shetland Formation and top Brent Group to be used in fault analysis and the final complete (large) reservoir model, and five surfaces from top Brent Group down to top Statfjord Formation were interpreted for use in the storage reservoir model, primary and secondary storage volume and primary/secondary seal. The Dunlin Group horizons, top Drake Formation, top Cook Formation and top Johannsen Formation are relatively weak reflectors and were therefore interpreted on zero crossing instead of peak trough respectively. In Table 5-1 the interpreted horizons are listed together with the pick and comments.

The observed mismatch between the picked reflectors and the horizons tops from logs in the well to seismic calibration chapter are in part due to the pick of zero crossing instead of peak/trough and in part because the wells were originally matched to the 2D seismic available at the time of drilling of the wells. The uncertainty in Table 5-1 is, except middle Oligocene and top Green Clay, to be anticipated given that the picked reflector is correct. For middle Oligocene in the west and top Green Clay the reflector may be incorrectly picked. The effect of the uncertainty associated with the pick of the reflectors is described and discussed in chapter 7.1.

DOCUMENT NO.: TL02-GTL-Z-RA-0001	REVISION NO.: 03	REVISION DATE: 01.03.2012	APPROVED:
-------------------------------------	---------------------	------------------------------	-----------

With the exception of base Pliocene, mid Oligocene, and top Green Clay which are all eroded by base Quaternary in the east and top Cook Formation which is absent in the east, the surfaces are interpreted over the entire investigation area (2D and 3D areas).

An overview of the interpreted horizons is given in Table 5-1 and interpretation examples from the different seismic 3D volumes are shown in Figure 5-5 - Figure 5-9.

Table 5-1: The table shows the interpreted horizons, seismic pick, uncertainty related to the horizon pick and a comment about the quality of the reflector.

Horizon	Pick	Uncertainty	Comment
Sea-floor	Peak	+/- 5ms	Good reflector
Base Quaternary	Peak	+/- 10ms	Variable reflector, picked at top of eroded strata below
Base Pliocene	Trough	+/- 10ms	Strong reflector, some difficulties in the southwest in connection with clay diapirism
Mid Oligocene	Peak	+/- 10ms +/- 30ms	Mostly strong and consistent reflector, weak and difficult to pick in the west
Top Green Clay	Trough	+/- 30ms	Chaotic reflector broken by numerous small faults and clay diapirism
Top Balder Fm	Trough	+/- 10ms	Relatively weak but consistent reflector, broken by small faults
Top Shetland Gp	Peak	+/- 15ms	Strong and mainly consistent reflector, broken by small faults and erosion
Top Draupne Fm	Trough	+/- 5ms	Strong and consistent reflector
Top Sognefjord Fm	Trough/ Peak	+/- 5ms	Strong and consistent reflector, trough in hydrocarbon zone and peak in water zone
Top Fensfjord Fm	S-crossing	+/- 15ms	Very weak but relatively consistent reflector
Top Brent Gp	S-crossing	+/- 10ms	Mainly strong and consistent reflector, especially where top Brent Gr is eroded
Top Drake Fm	S-crossing	+/- 10ms	Weak, but relatively consistent reflector
Top Lower Drake Fm	Trough	+/- 10ms	Strong, consistent reflector
Top Cook Fm	Z-crossing	+/- 10ms	Weak, but relatively consistent reflector
Top Amundsen 2 Fm	Trough	+/- 10ms	Weak reflector, sometimes difficult to track
Top Johansen Fm	S-crossing	+/- 10ms	Weak, but relatively consistent reflector
Top Amundsen 1 Fm	S-crossing	+/- 10ms	Strong, consistent reflector
Top Statfjord Fm	Z-crossing	+/- 5ms	Strong, consistent reflector

DOCUMENT NO.: TL02-GTL-Z-RA-0001	REVISION NO.: 03	REVISION DATE: 01.03.2012	APPROVED:
-------------------------------------	---------------------	------------------------------	-----------

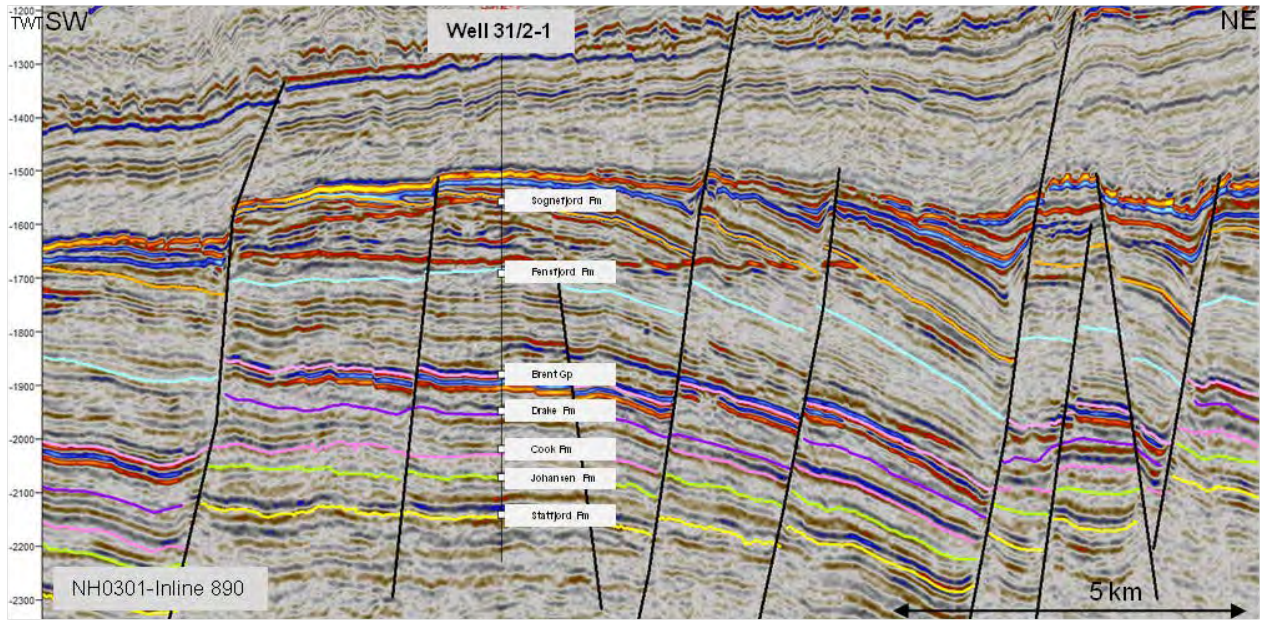


Figure 5-5: Seismic well tie (NH0301 Inline 890 and well 31/2-1). See Figure 5-6 for seismic line (A) location.

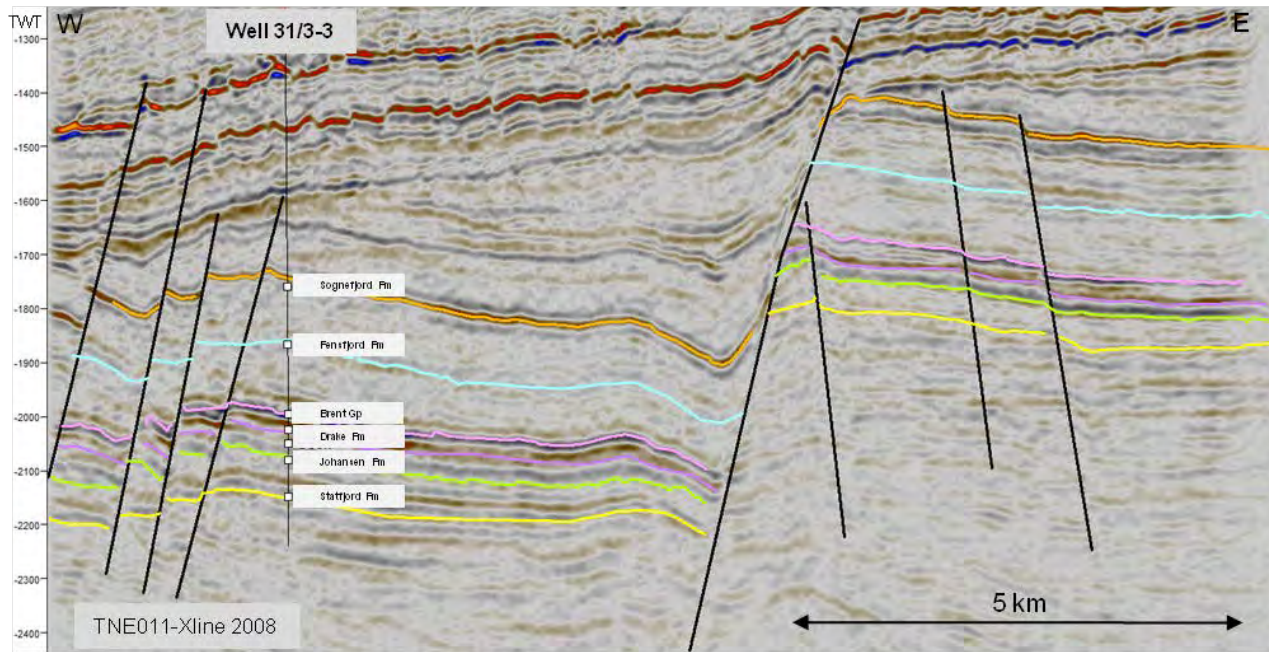


Figure 5-6: Seismic well tie (TNE01 Xline 2008 and well 31/3-3). See Figure 5-7 for seismic line (B) location.

DOCUMENT NO.: TL02-GTL-Z-RA-0001	REVISION NO.: 03	REVISION DATE: 01.03.2012	APPROVED:
-------------------------------------	---------------------	------------------------------	-----------

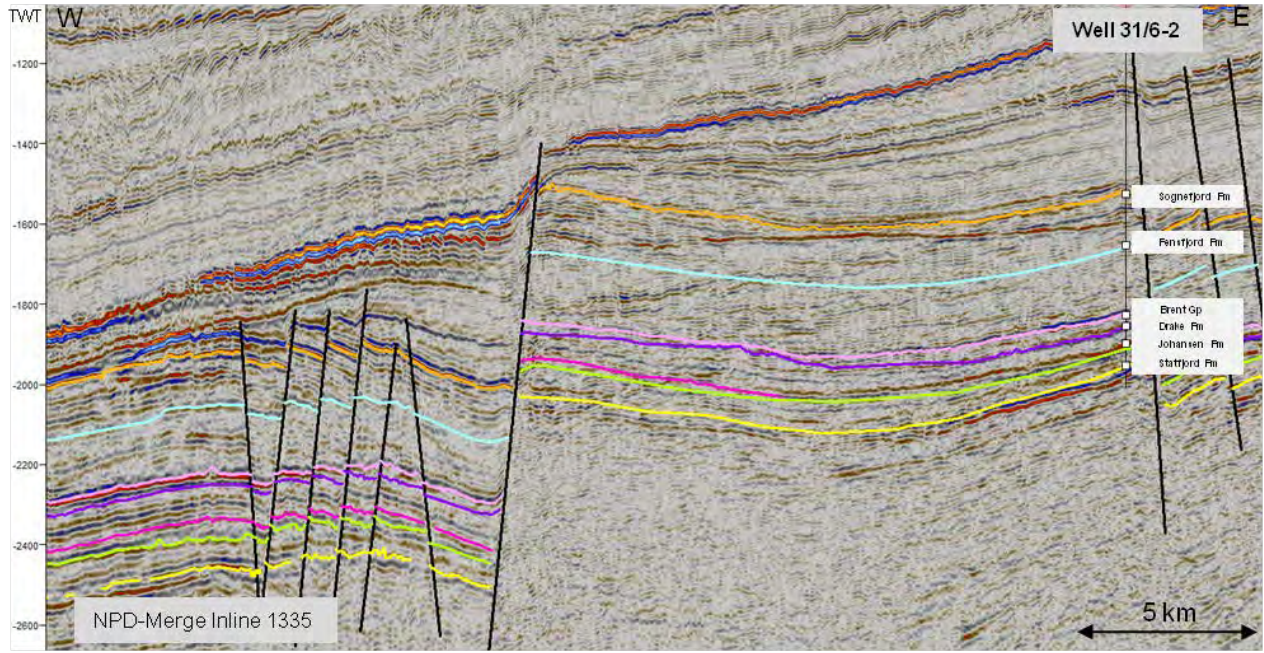


Figure 5-7: Seismic well tie (NPD-Merge Inline 1335 and well 31/6-2). See Figure 5-8 for seismic line (C) location.

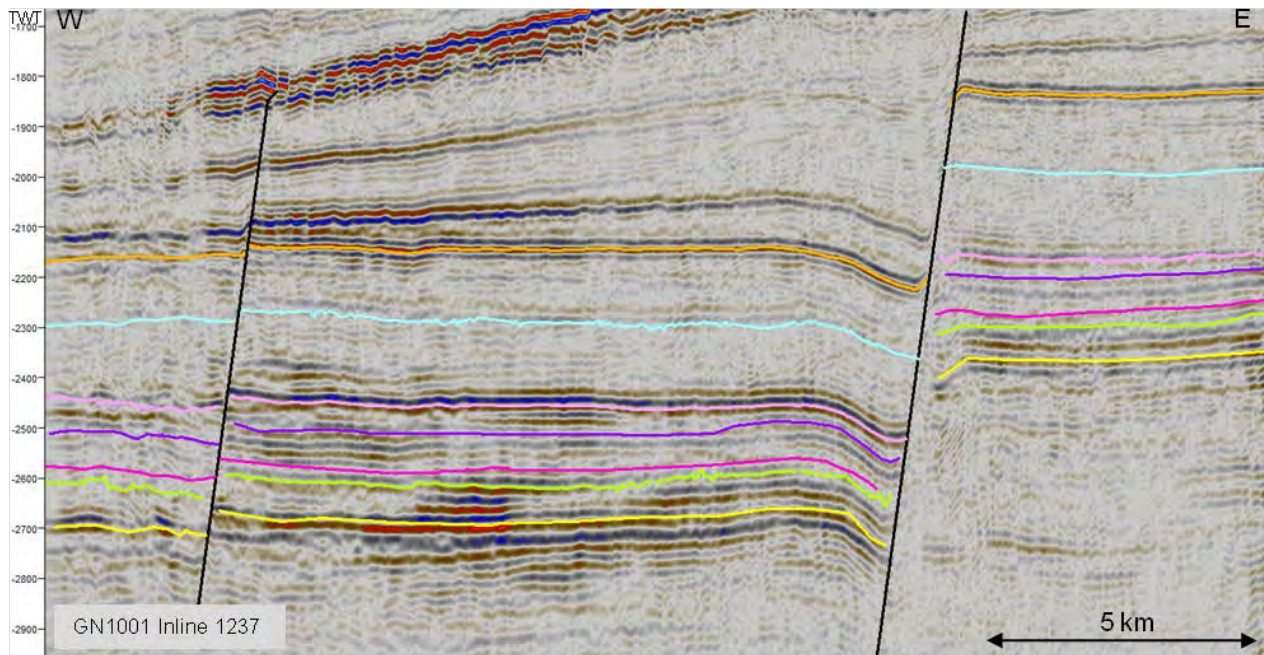


Figure 5-8: Seismic inline 1243 from the seismic survey GN10M1. See Figure 5-9 for seismic line (D) location.

DOCUMENT NO.: TL02-GTL-Z-RA-0001	REVISION NO.: 03	REVISION DATE: 01.03.2012	APPROVED:
-------------------------------------	---------------------	------------------------------	-----------

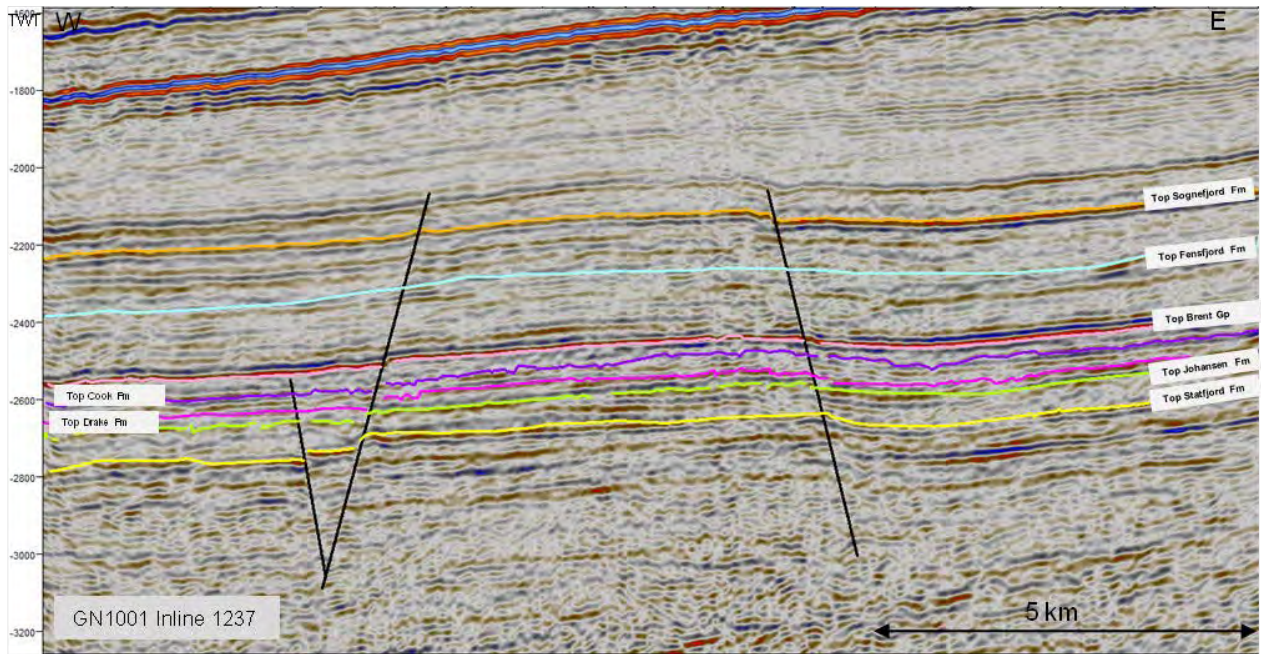


Figure 5-9: Seismic cross-line 4436 from the seismic survey EO0801. See Figure 4-3 for seismic line (E) location.

5.2.2.2 *Fault interpretation*

Virtually no faults are found above the base Pliocene surface (Figure 5-4). Between base Pliocene and top Balder numerous small faults are present. These faults in part form polygonal patterns and are probably induced by compaction and water escape from the clay rich strata between. These small faults are impossible to map and have no significance for the model building except for the information they contain about the change of stress system/direction in lower/middle Triassic compared with the Jurassic faulting.

The Jurassic faulting mainly commenced post Sognefjord deposition. Most of these faults can easily be interpreted throughout the entire Jurassic strata and are mapped and used in the model building.

The Troll area is depicted by three north-south trending and westward dipping main faults, one to the west of Troll and one dividing the Troll West into two different provinces, Troll West Oil Province (TWOP) and Troll West Gas Province (TWGP). Those two faults die out approximately 10km south of Troll. The third north-south trending main fault parts the Troll West from the Troll East and continues southwards to the southern part of GN1001 survey where north-south trending and eastward dipping fault takes over. East of Troll East two more north-south trending and westward dipping main faults are found. All those main faults are parallel / semi-parallel with the Øygarden Fault Zone further east. The Troll West is further divided by a large amount of northwest-southeast trending faults. Those faults do not seem to have any preferred dip direction. The northwest-southeast trending faults are also present but not so dense in Troll East. South of Troll West some of these faults seem to bend into a more north-southerly trend, i.e. in the area covered by the NPD-TW-08-4D-TROLLCO2 survey. In the area covered by the GN1001 survey few faults are seen.

Due to the close to 90 degree inline direction of the NH0301 towards the northwest-southeast trending faults, interpretation and mapping of these faults is easier on the NH0301 seismic

DOCUMENT NO.: TL02-GTL-Z-RA-0001	REVISION NO.: 03	REVISION DATE: 01.03.2012	APPROVED:
-------------------------------------	---------------------	------------------------------	-----------

survey than on the merged GN10M1 survey. For the main north-south trending faults the GN10M1 survey is better.

5.2.3 **Depth conversion**

Before any depth conversion can be performed, a velocity model needs to be generated. For this study 4 different velocity models were generated;

- 1) A Linvel velocity model based on time-depth relationships (TDR) for available wells in the study area and seismic interpreted horizons from time domain seismic.
- 2-3) An interval and average velocity model based on seismic stacking velocities from the GN10M1 survey using the Dix formula (Sheriff and Geldhart 1987), seismic interpreted horizons from time domain seismic and well velocities based on TDR for available wells.
- 4) A hiQbe® average velocity model generated. Input to this velocity model was the GN10M1 survey, 2D velocity trend lines from the NVGT-88 & NVGTI-3-92 surveys and well velocities based on TDR for available wells.

5.2.3.1 *Database*

The data base consists of checkshots from available wells and selected seismic surveys (Figure 5-10). The primary data set is a stacking velocity volume (50 x 50m grid) from the **GN10M1** survey (Figure 5-10) In addition velocity data on selected 2D lines from the *nvgt-88* and *nvgti-3-92* surveys were used as trend data in generating the hiQbe® average velocity model (Figure 5-10, and appendix A5 Velocity Modelling for Depth Conversion in Quadrant 31).

DOCUMENT NO.: TL02-GTL-Z-RA-0001	REVISION NO.: 03	REVISION DATE: 01.03.2012	APPROVED:
-------------------------------------	---------------------	------------------------------	-----------

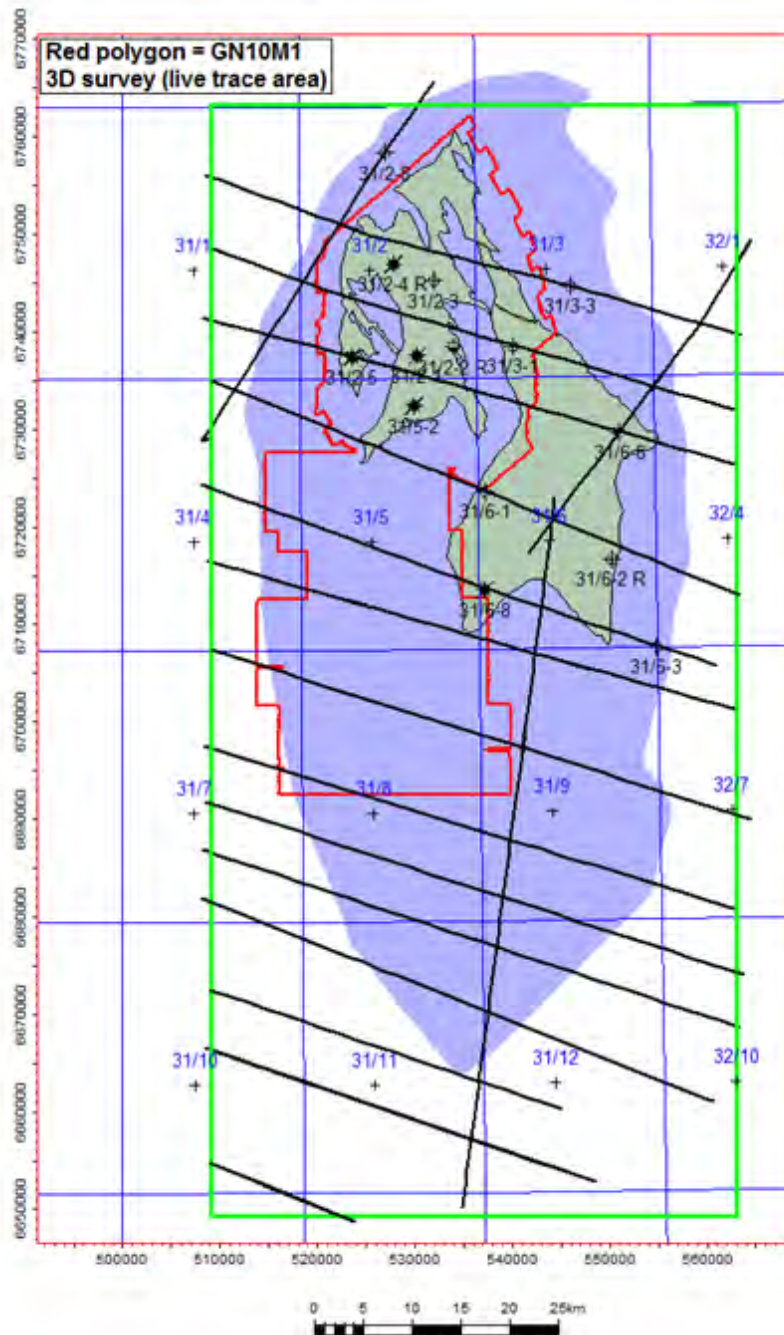


Figure 5-10: Blue filled polygon shows extent of Johansen model, and the red polygon is the live data extension of the GN10M1 3D survey. Wells used for velocity model building are plotted on the map. Seismic 2D lines from the NVGT-88 & NVGTI-3-92 lines used for velocity trend data are plotted as black lines.

DOCUMENT NO.: TL02-GTL-Z-RA-0001	REVISION NO.: 03	REVISION DATE: 01.03.2012	APPROVED:
-------------------------------------	---------------------	------------------------------	-----------

Table 5-2: Overview over NVGT-88 and NVGTI-3-92 lines used as trend data in generating the hiQbe® average velocity model.

Line name	Shotpoint range
NVGT-88-01	7867 - 10562
NVGT-88-02	5708 - 8028
NVGT-88-03	1210 - 5510
NVGT-88-04	2880 - 11145
NVGT-88-05	1210 - 4471
NVGT-88-06	9310 - 12606
NVGT-88-21	5317 - 8045
NVGT-88-23	10 - 9245
NVGTI-3-92-201	10 - 653
NVGTI-3-92-202	10 - 1533
NVGTI-3-92-203 A	5365 - 7350
NVGTI-3-92-204	253 - 2573
NVGTI-3-92-205 A	3813 - 4200
NVGTI-3-92-205 B	5201 - 5990
NVGTI-3-92-205 C	7987 - 9133
NVGTI-3-92-206	10 - 1685
NVGTI-3-92-206 A	2686 - 3253
NVGTI-3-92-207 A	6592 - 7577
NVGTI-3-92-207 B	7882 - 8734
NVGTI-3-92-207 C	10735 - 11236
NVGTI-3-92-208	493 - 2733

5.2.3.2 *1. Linvel velocity model*

The Linvel velocity model is based on linear velocity trends within each zone: $V=V_0+kZ$: At each XY location, the velocity changes in the vertical direction by a factor of k. V_0 represents the velocity at datum, and Z the distance (in length units, not time) of the point from datum. NB V_0 represents the velocity at Z=0 (datum) and not the top of each zone. In Petrel both V_0 and k can be calculated in well positions using the TDR for each well. Petrel uses a **minimum depth error** method to estimate these values. After calculating V_0 and k there are two options available; either to use a constant value based on an average of the calculated values or to generate a 2D grid surface based on the different values at well positions. For this velocity model a gridded (50 x 50m) V_0 surface and constant k was used.

The following time surfaces from seismic interpretation were used for zone definitions in this velocity model: Seafloor, Top Shetland Formation, Top Sognefjord Formation, Top Brent Group, Top Johansen Formation and Top Statfjord Formation. Constant velocities were used for the water layer (1480m/s, Datum - Seafloor) and Johansen zone (3534m/s, Top Johansen - Top Statfjord formations). Well tops (in depth) for each lithological zone top in the model were used as correction.

5.2.3.3 *2. Interval and average velocity models based on seismic stacking velocities (GN10M1) and Dix formula*

First the GN10M1 stacking velocity field, loaded into Petrel as a SEG Y volume, was converted into a point dataset (a point for each velocity sample value in the volume).

Using the Petrel “Settings” window and “Operations” tab for this point data set, both interval and average velocity volumes were calculated applying the “Dix conversion” option.

Before applying seismic derived velocities for velocity models it is necessary to perform some lateral smoothing of the input data to remove high frequency noise. This was done by re-gridding the original stacking velocity volume from a 50 x 50m grid into a larger 250 x 250m grid size. Subsequent to the lateral smoothing, a reduction of the seismic derived velocities needs to be done to match velocities observed in the wells. The reason for this is that the seismic velocities are generated by finding the optimal velocities for Normal Move Out corrections of

DOCUMENT NO.: TL02-GTL-Z-RA-0001	REVISION NO.: 03	REVISION DATE: 01.03.2012	APPROVED:
-------------------------------------	---------------------	------------------------------	-----------

events representing contrast in Acoustic Impedance (AI). These events are often associated with lithological changes in the sub surface earth model. However, these NMO correction velocities, often called stacking velocities, represent a horizontal measure along lithological boundaries whereas the velocities measured in wells are vertical. Therefore, as a rule of thumb, it is necessary to apply a reduction factor to the seismic derived velocities to get a match with the velocities from the wells over the same area. This process is sometimes referred to as anisotropy modelling. For the velocity reduction two approaches were used.

- 1) Point data were generated from the smoothed 250 x 250m gridded stacking velocity volume and average and interval velocities were calculated from this point dataset applying the Dix formula. The calculated average point data were subsequently upscaled into a 250 x 250m structural grid. A moving average interpolation/extrapolation algorithm was applied to calculated velocity field in cells outside the GN10M1 area of the total Johansen model (Figure 5-10). Velocities from this model were extracted along the available wells in the area (Figure 5-10) and compared with the average velocities measured in the wells. A reduction factor log was calculated for each well to match the converted stacking velocities in the model with the wells (Figure 5-11).

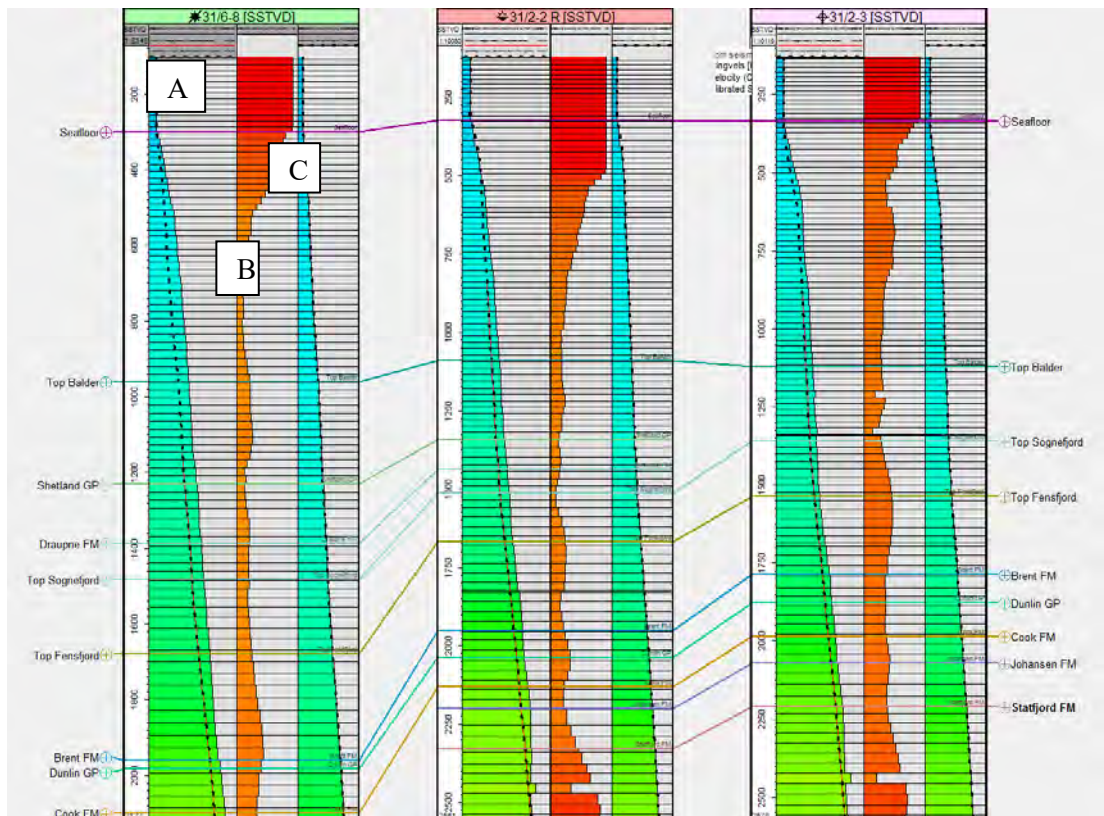


Figure 5-11: The seismic derived average velocities can be reduced by a scalar log computed to each well. Average velocity from seismic (A) * scalar log (B) = average velocity from wells (C). Examples above taken from wells 31/6-8, 31/2-2 & 31/2-3.

The scalar logs were upscaled/blocked into the structural grid and interpolated/extrapolated over the Johansen model area as described above for the seismic derived average velocities. The resulting average velocity model and scalar

DOCUMENT NO.: TL02-GTL-Z-RA-0001	REVISION NO.: 03	REVISION DATE: 01.03.2012	APPROVED:
-------------------------------------	---------------------	------------------------------	-----------

model were then multiplied to give the resulting well adjusted average velocity model property used for depth conversion.

- 2) From the same point data, mentioned in the section above, an interval velocities point dataset was calculated. Interval velocities from selected zones were extracted and gridded to velocity maps. For the interval velocities fixed reduction factors were applied. The reduction factors giving the best match with well tops were selected.

The following time horizons and intervals were used for the two velocity models. For both models a constant velocity of 3534m/s was used for the deepest horizon (Top Statfjord Formation);

Average Dix velocity model: Top Shetland Formation – Top Brent Group – Top Johansen Formation – Top Statfjord Formation

Interval Dix velocity model: Datum – Seafloor – Top Shetland Formation – Top Sognefjord Formation – Top Johansen Formation – Top Statfjord Formation

For the interval velocity model the following reduction factors were applied:

Datum - Seafloor	1480m/s (constant velocity in water)
Seafloor - Top Shetland Formation	94%
Top Shetland - Top Sognefjord formations	92%
Top Sognefjord - Top Johansen formations	99%
Top Johansen - Top Statfjord formations	3534m/s (constant velocity through layer)

5.2.3.4 3. Proprietary hiQbe®

To perform a quality assurance on the velocity model generated using the stacking velocity field on the GN10M1 merge survey, Aker Geo was consulted. It was decided to look at the average velocity model only, since this could be generated without an input model (seismic horizons). Also it was assumed that there were not large enough velocity contrasts between thick layers in the underground, that the well scaling (anisotropy modelling) needed to be modelled per layer as in an interval velocity model.

Some steps were changed from the previously made average velocity model;

- 1) A stronger smoothing of the input stacking velocity field (Figure 5-12).
- 2) Since Dix formula is based on the assumption that all layers (with correct properties) that bend the sound signal are present in the model, it was not used for this updated velocity model. General advice is not to use Dix formula, but only perform smoothing before scaling of the stacking velocities directly to get a good match with well tops (Figure 5-14).
- 3) Velocities from some 2D lines were used to get a better control of the velocity extrapolation into the 2D areas outside the velocity field covered by the GN10m1 merge survey (Figure 5-10 and Table 5-2). These overlapping velocity data needed to be balanced with the original GN10M1 data to be used as guide data (Figure 5-13).

Based on the suggested changes above, a proprietary hiQbe© was generated using the Aker Geo software. The generation of this average velocity cube is described in detail in a separate report (appendix A5 Velocity Modelling for Depth Conversion in Quadrant 31). Due to the improved extrapolation guide control in this velocity cube, it is the preferred velocity model used for depth conversion of the Johansen geomodel.

DOCUMENT NO.: TL02-GTL-Z-RA-0001	REVISION NO.: 03	REVISION DATE: 01.03.2012	APPROVED:
-------------------------------------	---------------------	------------------------------	-----------

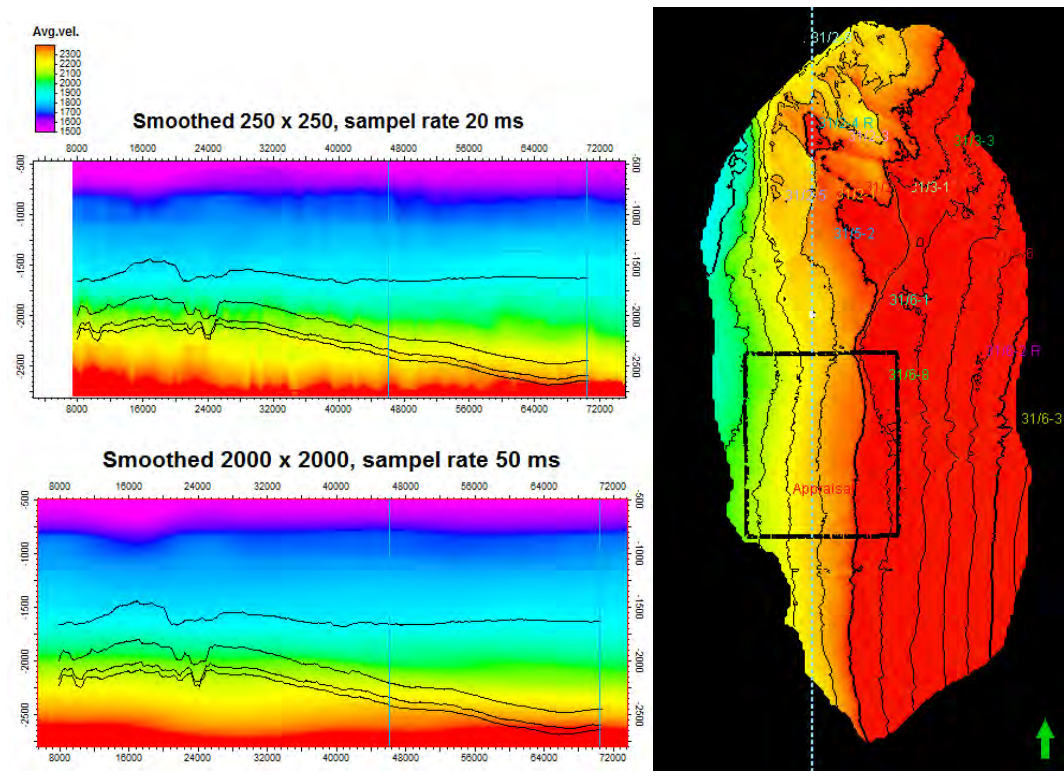


Figure 5-12: Upper left image shows an intersection through the 250m x 250m gridded stacking velocity volume compared with the much smoother velocity field in the 2000m x 2000m grid shown in the lower left image. The image on the right shows the position of the intersections to the left.

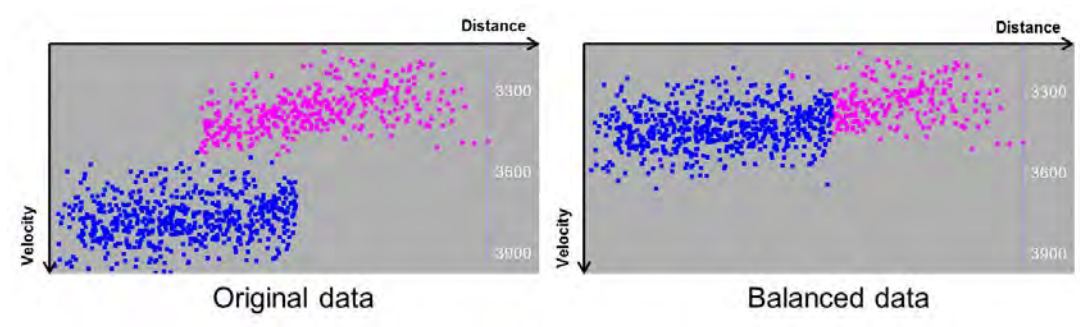


Figure 5-13: Survey to survey balancing.

DOCUMENT NO.: TL02-GTL-Z-RA-0001	REVISION NO.: 03	REVISION DATE: 01.03.2012	APPROVED:
-------------------------------------	---------------------	------------------------------	-----------

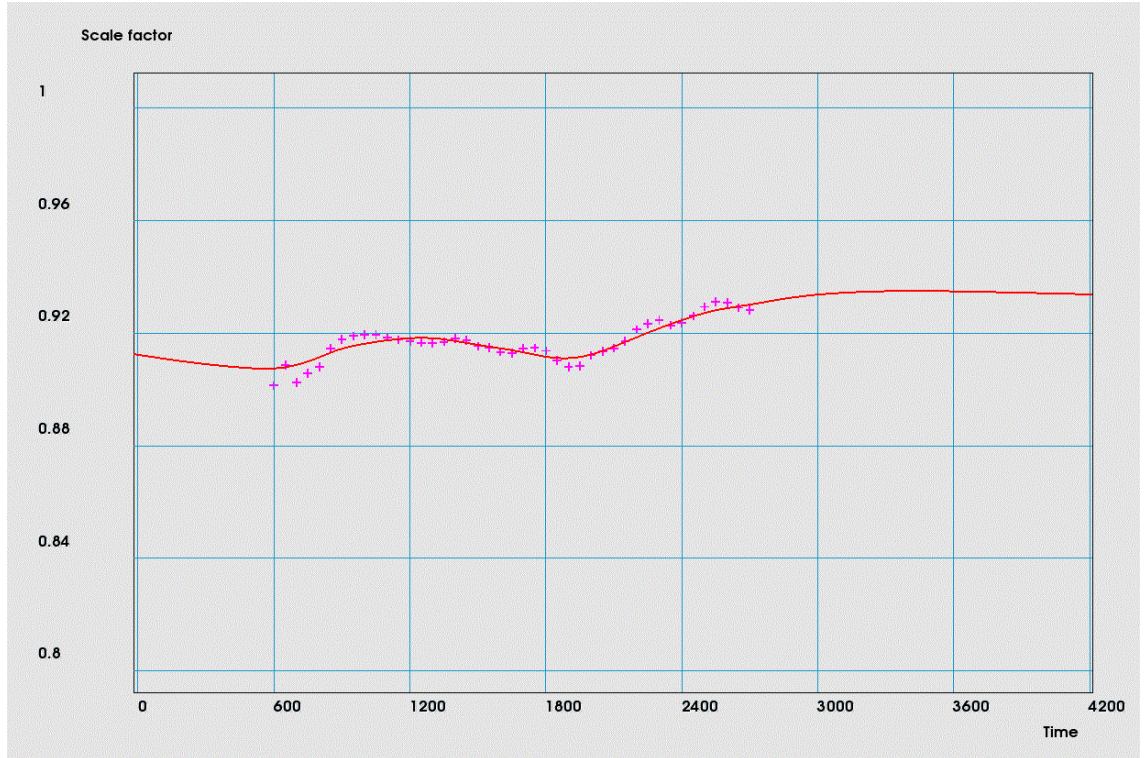


Figure 5-14: General scaling factor curve (anisotropy model) used to convert stacking velocity cube to the average velocity domain. The red line is the digitized function used for the scaling and applied below seabed since the water layer is isotropic (constant 1480m/s).

5.2.3.5

N-S trend comparisons between depth conversions using different velocity models

A comparison between the preferred updated average velocity model (section 3 above) with the former generated velocity models (sections 1 & 2 above). It shows small differences inside the area covered by GN10M1 where the well control is good, which is to be expected. However, as the distance to well control increases southwards, differences occur. The general picture is that the updated velocity model gives larger depths on the depth converted time horizons compared with the former models (Figure 5-15). This might be due to the fact that the Dix conversion was used for the older versions, and that this method is less valid in areas with dipping reflectors. The generation of the various velocity models was done as sensibility testing for CO₂ plume migration northwards towards the Troll field. Although the updated average velocity model is preferred for depth conversion, results from the recent 31/8-1 well indicate that this velocity field is slightly too high in the deeper parts of the model (Figure 5-17 & Table 5-3).

DOCUMENT NO.: TL02-GTL-Z-RA-0001	REVISION NO.: 03	REVISION DATE: 01.03.2012	APPROVED:
-------------------------------------	---------------------	------------------------------	-----------

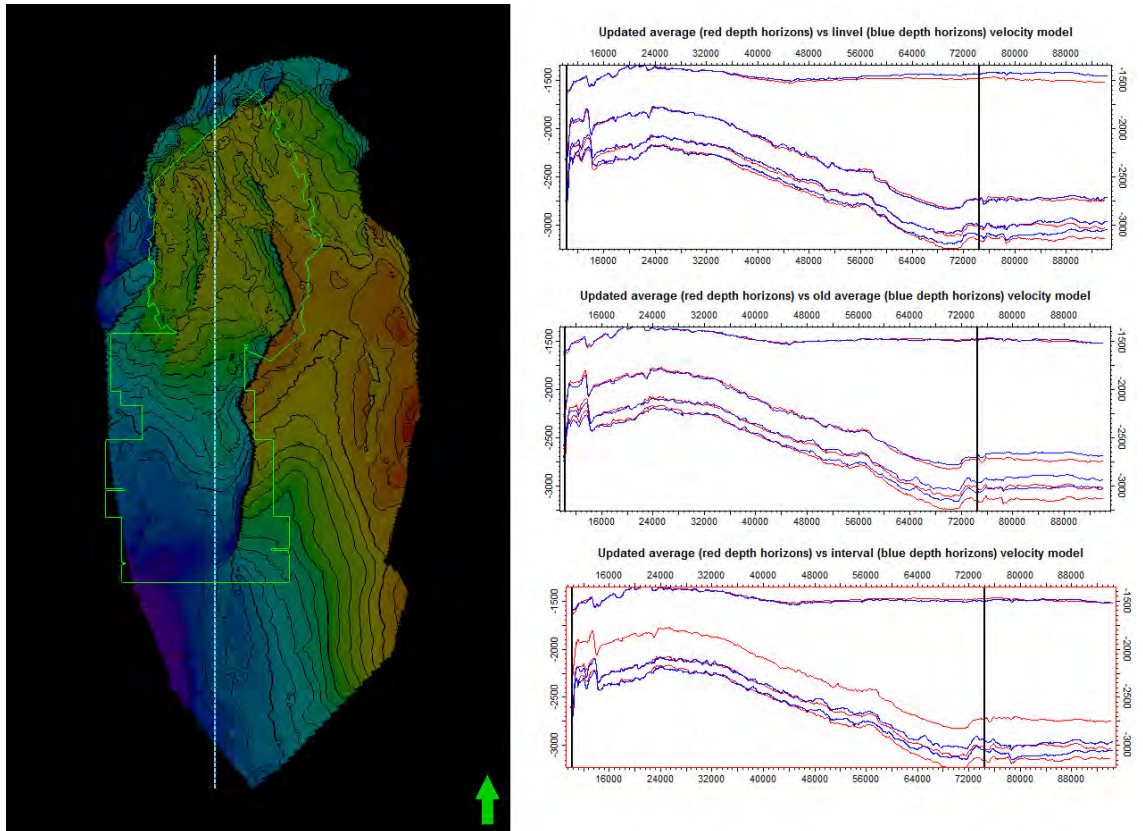


Figure 5-15: N-S oriented intersection through model (left image). On the 3 intersection images to the right the vertical black lines shows extent of GN10M1 survey area shown as green polygon on left image. From top to bottom on the right image; Depth horizons from updated average vs Linvel velocity model, updated average vs old average velocity model and updated average vs interval velocity model.

5.2.3.6 *Depth conversion uncertainty*

In this area of the North Sea, the velocity related depth conversion uncertainty can be expected to be within $\pm 1\%$ where the seismic data quality and coverage is good. By rule of thumb, this should apply to the 3D area above the level of Top Statfjord Formation. In the 2D area, or at deeper levels, or in parts of the 3D area with poor seismic data quality (if any), the uncertainty will be two to three times as large.

In a depth conversion there will also be uncertainty related to the seismic time interpretation and the well ties. This should be estimated by the interpreter and added to the velocity uncertainty (see chapter 5.4.3).

5.2.3.7 *Results from E.ON Ruhrgas well 31/8-1 on PL416*

E.ON Ruhrgas Norge drilled in June/July 2011 an exploration well in the production licence 416. This well had its deepest penetration age down to middle Jurassic, and could therefore unfortunately neither confirm nor deny the presence of Johansen sand which is anticipated to exist in this area (Figure 5-16).

DOCUMENT NO.: TL02-GTL-Z-RA-0001	REVISION NO.: 03	REVISION DATE: 01.03.2012	APPROVED:
-------------------------------------	---------------------	------------------------------	-----------

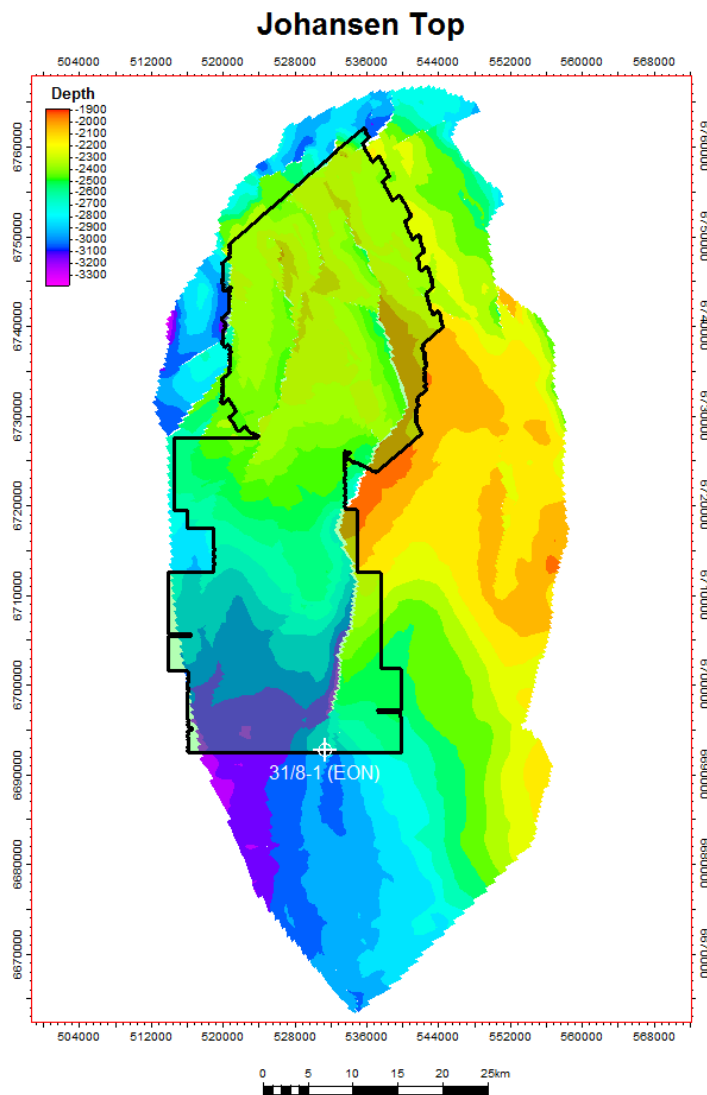


Figure 5-16: Top Johansen depth map with GN10M1 polygon (black) and the 31/8-1 E.ON Ruhrgas well drilled in the production licence 416.

The interpreted well tops for this well match with E.ON's own interpretations down to Top Sognefjord. However, E.ON's pre-drill seismic time horizon interpretations are also in accordance with interpretations of the deeper lithology below Top Sognefjord Formation. Therefore E.ON's well top interpretations of these deeper markers (Top Fensfjord Formation, Top Krossfjord Formation and Top Brent Group) should be questioned. From the differences between the depth converted horizons and well markers shown in Figure 5-17 and Table 5-3, it can be concluded that the velocity model is representative for this area. The errors for some of the deeper horizons (Top Draupne Formation, Top Sognefjord Formation and Top Fensfjord Formation) are larger than anticipated ($\pm 1\%$ inside GN10M1 area), however this well is some distance away from the wells used for anisotropy correction when generating the velocity model used for depth conversion. A suggestion for future work would therefore be to adjust the velocity model with the new checkshot survey from the 31/8-1 well.

DOCUMENT NO.: TL02-GTL-Z-RA-0001	REVISION NO.: 03	REVISION DATE: 01.03.2012	APPROVED:
-------------------------------------	---------------------	------------------------------	-----------

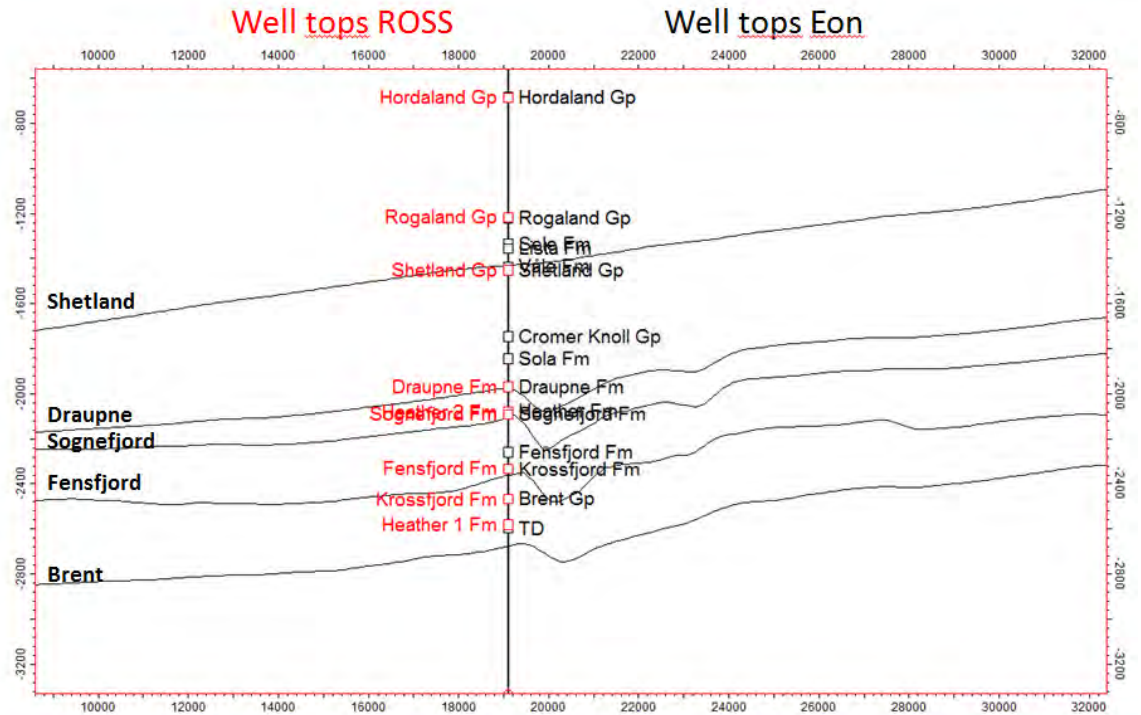


Figure 5-17: W-E intersection through well 31/8-1 with depth lines converted seismic interpreted horizons (black lines) and well markers interpreted by Gassnova (plotted as red boxes) and E.ON's well markers (plotted as black boxes).

Table 5-3: Statistics from well 31/8-1. The Δ DEPTH column is the difference between true vertical depth (Z) of well top and Depth map column value in well position, and Δ TIME is difference between TWT Auto (time value of well marker from time-depth relationship for the well) and Time maps column values.

Well	Surface	Z	MD	Depth Maps	Δ Depth	Depth Error %	TWT auto	Time maps	Δ Time
31/8-1	Hordaland Gp	-684.8	715.02	689.02	-4.22	0.62	812.13	791.87	20.26
31/8-1	Rogaland Gp	-1217	1248.00	1234.49	-17.49	1.44	1338.60	1339.08	-0.48
31/8-1	Shetland Gp	-1452	1483.00	1461.48	-9.48	0.65	1534.60	1558.26	-24.03
31/8-1	Draupne Fm	-1969	2000.00	2003.02	-34.02	1.73	1978.97	1972.40	6.57
31/8-1	Heather 2 Fm	-2079	2110.00	N/A	N/A	N/A	2068.08	N/A	N/A
31/8-1	Sognefjord Fm	-2092	2123.00	2135.71	-43.71	2.09	2076.58	2060.24	16.34
31/8-1	Fensfjord Fm	-2333	2364.00	2373.00	-40.00	1.71	2221.19	2209.10	12.09
31/8-1	Krossfjord Fm	-2468	2499.00	N/A	N/A	N/A	2293.29	N/A	N/A
31/8-1	Heather 1 Fm	-2581	2612.00	N/A	N/A	N/A	2355.94	N/A	N/A

5.2.3.8 Summary

Four velocity models were generated for depth conversion of the Johansen geo-model. The purpose of generating these velocity models was to investigate any sensitivity in dips of the Johansen zone. This could have implications for migration time of the CO₂ plume towards the Troll field to the north of the suggested injection well (cross reference). The general challenge for a good depth conversion of the Johansen geo-model is its large extension and lack of well control – especially in the southernmost area of the model. The Linvel model gives a good depth fit with the stratigraphical geomarkers in the wells. This is to be expected since the velocities are calculated in the well positions. However, the weakness with this velocity model is the uneven distribution of wells over the entire modelled area. Hence an increasing uncertainty in the

DOCUMENT NO.: TL02-GTL-Z-RA-0001	REVISION NO.: 03	REVISION DATE: 01.03.2012	APPROVED:
-------------------------------------	---------------------	------------------------------	-----------

velocity field with distance to area with well control. The average and interval velocity models based on Dix conversion of stacking velocities is expected to give better lateral trends compared with the Linvel velocity model. However, the validity of the application of the Dix formula is questionable (see 5.2.3.4, step 2). Therefore an updated velocity model (*hiQbe*®) was generated and used as the preferred input to depth conversion of the Johansen geo-model. The reasons for this are;

1. Dix conversion was not applied
2. Additional 2D data was used to improve the velocity field outside the 3D area (GN10M1)
3. A stricter smoothing of the velocity model was applied

The stratigraphical well markers from the new E.ON Ruhrgas well 31/8-1 show that the *hiQbe*® velocity model appears to be representative also for the area of the planned injection well. However, for future work, a correction of the velocity field with the checkshot survey from the 31/8-1 well is recommended.

5.3 Geological development of storage formation

The storage formation descriptions are based on integrated seismic analysis, well log and core analysis in order to build the depositional models. In the southern part of the storage complex the descriptions are mainly based on seismic analysis.

Two storage formations (Figure 5-18 and Figure 5-19) of early Jurassic age are identified for the Johansen Storage Complex:

- The Johansen Formation
- The Cook Formation

The Johansen Formation is defined as the primary storage formation and the Cook Formation is included as a storage formation due to the probable communication with the Johansen Formation. The Johansen and Cook formations are separated by shales and siltstones of the Upper Amundsen Formation in the northern part. Due to the lack of Upper Amundsen Formation in the southern and to cross fault communication the formations will be treated as one storage formation. This communication will be described in chapter 7.2. The Cook Formation represents approximately 15% of total storage complex pore volume.

DOCUMENT NO.: TL02-GTL-Z-RA-0001	REVISION NO.: 03	REVISION DATE: 01.03.2012	APPROVED:
-------------------------------------	---------------------	------------------------------	-----------

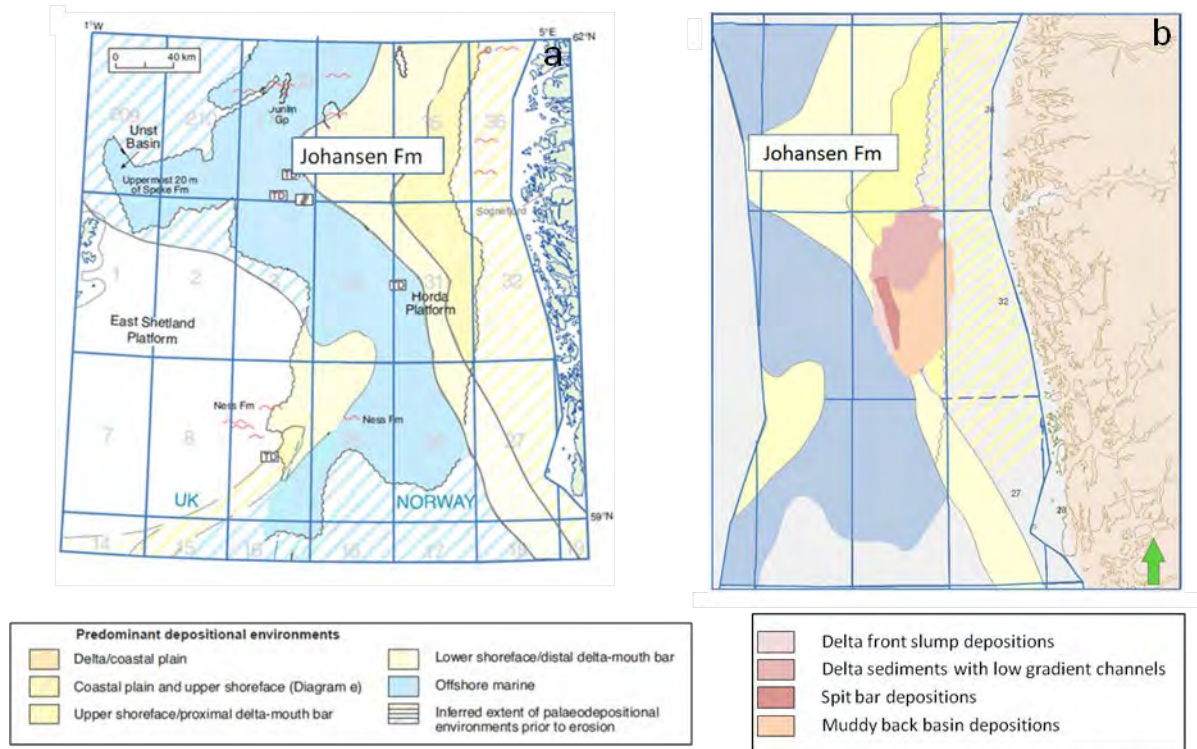


Figure 5-18: a) Johansen Formation depositional map (modified from Millennium Atlas), b) Paleoenvironmental depositional map for the Johansen Formation based on new evaluation (modified map from the Millennium Atlas).

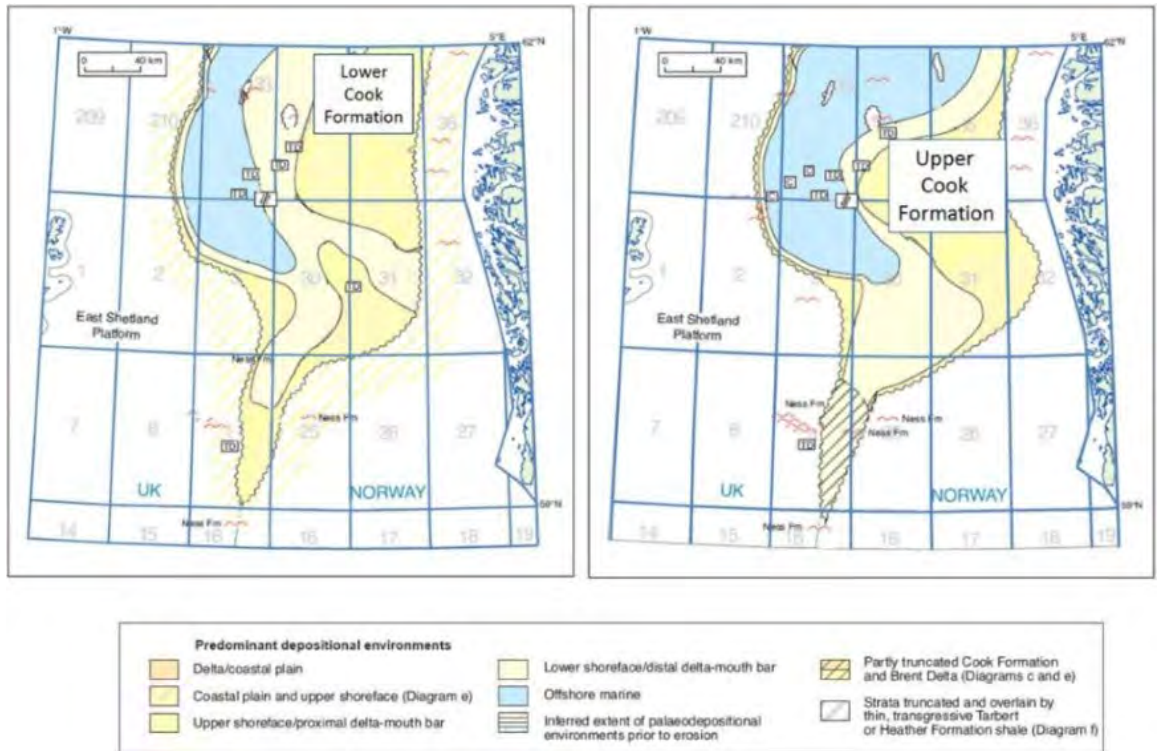


Figure 5-19: Cook Formation depositional map (modified from Millennium Atlas).

DOCUMENT NO.: TL02-GTL-Z-RA-0001	REVISION NO.: 03	REVISION DATE: 01.03.2012	APPROVED:
-------------------------------------	---------------------	------------------------------	-----------

5.3.1 **Storage formation presence**

5.3.1.1 *The Johansen Formation*

A new depositional model (Figure 5-18 and Figure 5-20) for the Johansen Formation based on new well analysis, new seismic analysis and previous stratigraphic work, i.e. (Charnock, et al. 2001) (Marjanac 1995) (Marjanac and Steel 1997) (Steel 1993) is presented in this chapter.

The Johansen Formation is interpreted to have been deposited as delta sand where strong wave influence and long shore transport have resulted in spit system deposits and a large difference in morphology and facies architecture which may indicate delta asymmetry. Recent asymmetric deltas which consist in general of sandier shoreface deposits on the updrift side and mixed riverine and wave/storm-reworked deposits on the downdrift side with significant paralic, lagoonal and bay-fill facies (Weiguo, et al. 2010), may be analogues to the Johansen Formation. The hydrocarbon reservoirs of the Troll Field are interpreted to be analogue to Johansen Formation based on similar facies development.

Previous studies based on well logs describe the Early Jurassic Johansen Formation as a deltaic deposit of Sinemurian to Pliensbachian age belonging to the Dunlin Group (Figure 5-18). The Dunlin Group consists mainly of dark to black argillaceous marine sediments, however in marginal areas of the basin marine sandstones are well developed at several stratigraphic levels. The sandstones are white to light grey, very fine to medium grained and generally well sorted. The group tends to be more calcareous in the Norwegian sector, and in places limestone beds, some of which contain chamosite and siderite oolites, are found. The Johansen Formation has been interpreted to be deposited in a near shore to inner-shelf environment with high energy and there were indications of brackish water (Vollset and Doré 1984).

Definition of the Johansen Formation

The presence of the Johansen Formation is proven by a number of wells in the northern part of the evaluation area (

Table 5-4, Figure 5-21), and the formation is interpreted to be present all over the investigated area. This is based on the observed seismic characters of the Johansen Formation (Figure 5-22). In the well type 31/2-1 the Johansen Formation consists of sandstones with thin calcite cemented streaks and is 95.5m thick.

The top Johansen Formation is defined in the seismic at the 31/2-1 well location as an onset on a peak reflection (S-crossing) (chapter 5.2.2). This seismic definition is consistent for the Top Johansen interpretation throughout the storage complex (Figure 5-22). The Figure shows the seismic characteristics of the Johansen Formation sequence for the northern part and the southern part of the storage complex. The seismic definition of the new Johansen Formation zonation is shown at the 31/2-1 well location. In the southwestern part of the storage complex, at the injection area, the Johansen Formation sequence is associated with a strong amplitude anomaly (Figure 5-22 and Figure 5-23). This anomaly is interpreted to represent sand development in connection with the Johansen Formation delta system.

The total storage formation thickness is interpreted to reach up to approximately 200m in the mapped area and between 80m to 180m in the CO₂ plume area (Figure 5-24). Well 31/2-3 from the Troll West area with 117m Johansen Formation is the only well with core samples of the formation.

DOCUMENT NO.: TL02-GTL-Z-RA-0001	REVISION NO.: 03	REVISION DATE: 01.03.2012	APPROVED:
-------------------------------------	---------------------	------------------------------	-----------

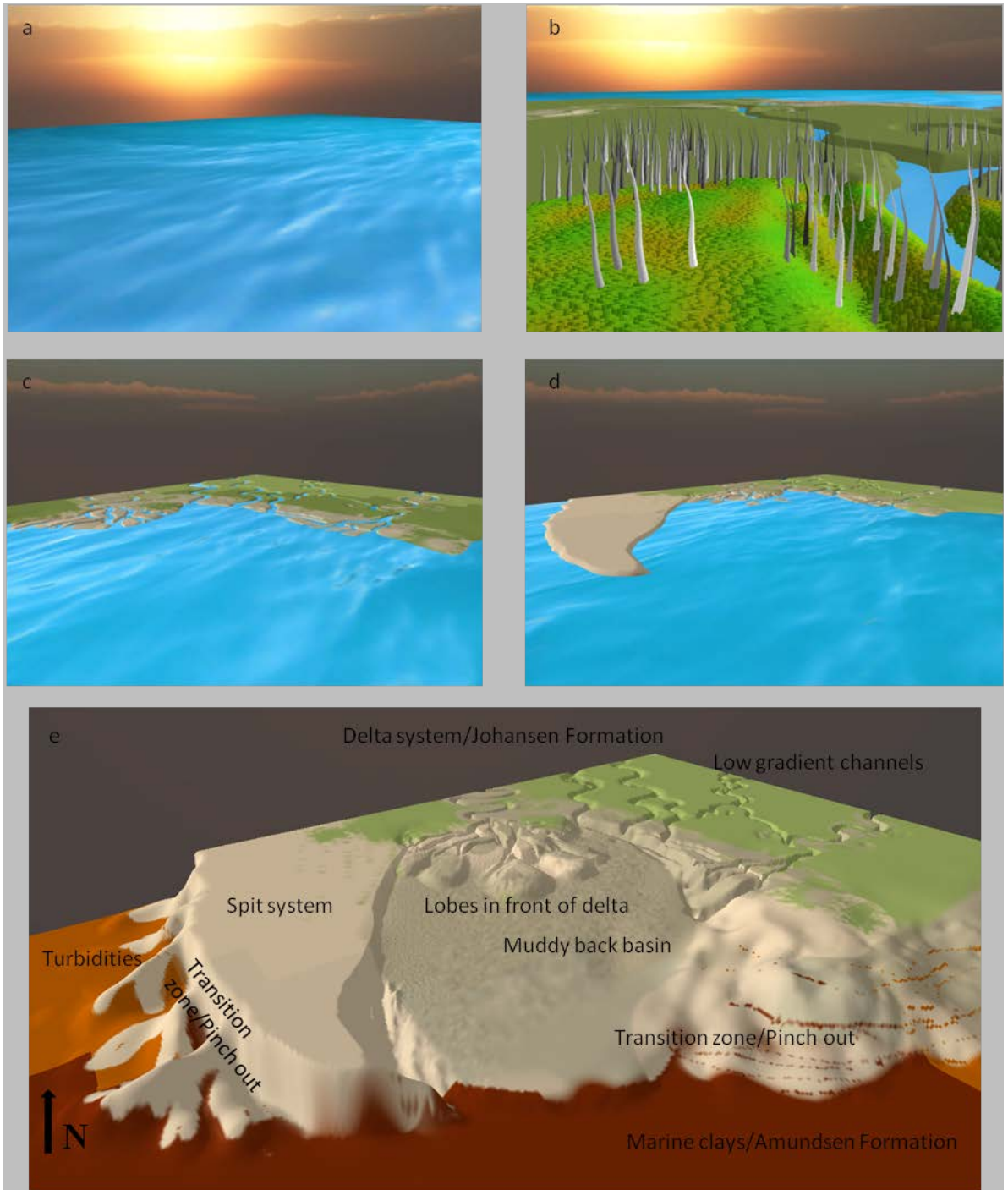


Figure 5-20: a) Deposition of the marine Amundsen Fm 1, b-d) prograding and building up face of the Johansen Fm, e) different depositional environments dominating the formation in the study area.

DOCUMENT NO.: TL02-GTL-Z-RA-0001	REVISION NO.: 03	REVISION DATE: 01.03.2012	APPROVED:
-------------------------------------	---------------------	------------------------------	-----------

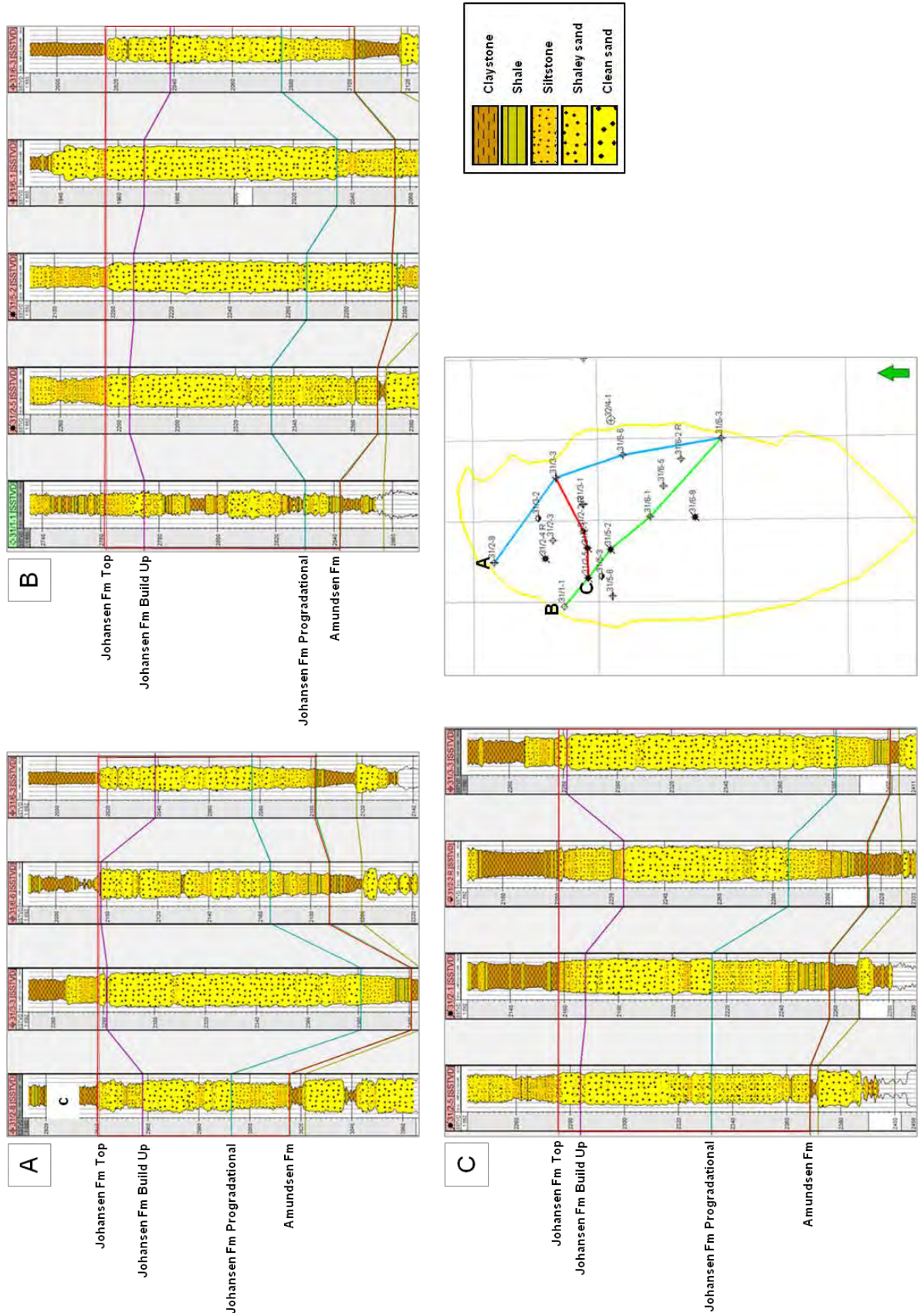


Figure 5-21: Well correlations showing the Johansen Fm development from A) northwest to southeast (blue), B) west to southeast (green) and C) west to east (red).

DOCUMENT NO.: TL02-GTL-Z-RA-0001	REVISION NO.: 03	REVISION DATE: 01.03.2012	APPROVED:
-------------------------------------	---------------------	------------------------------	-----------

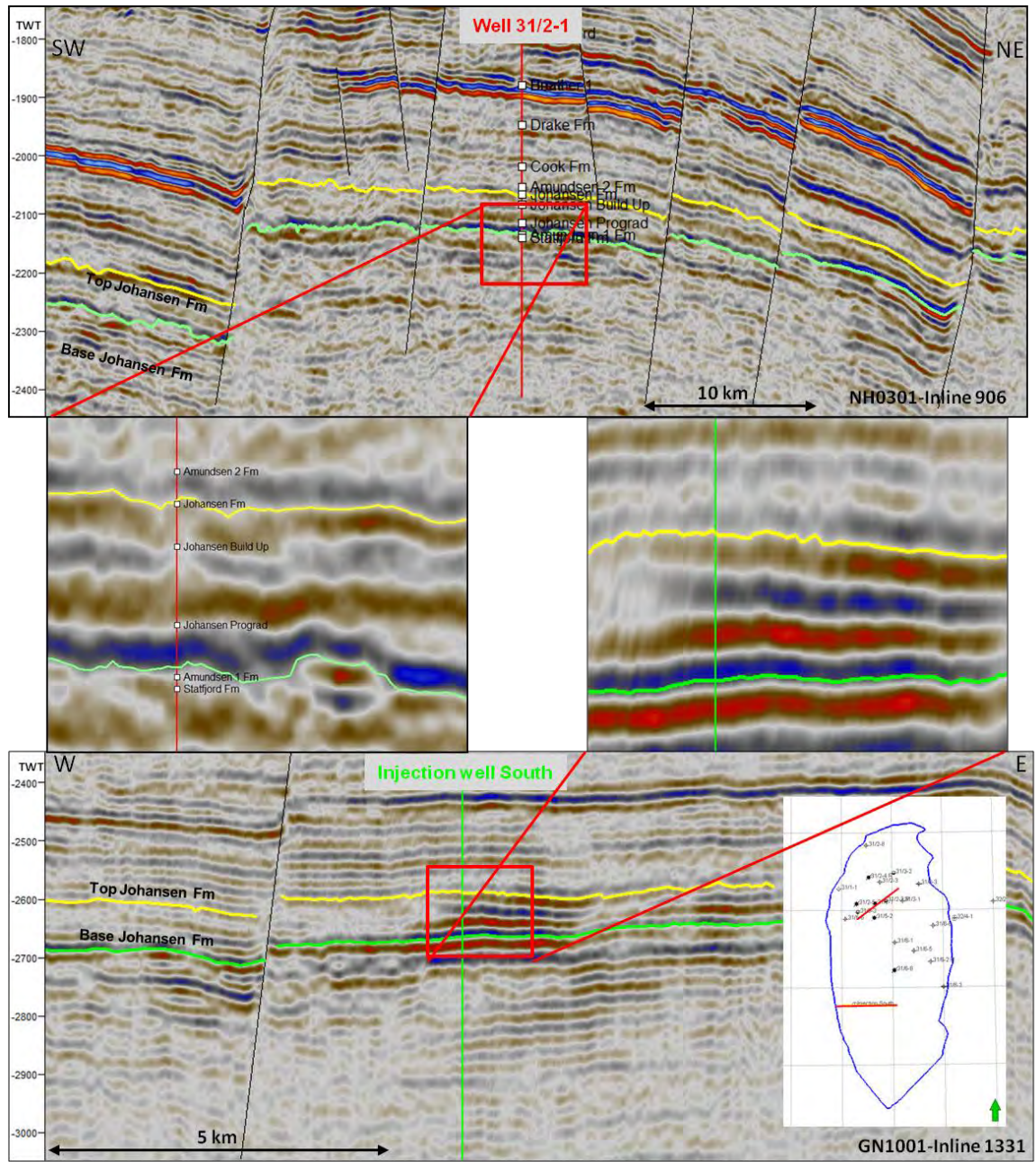


Figure 5-22: Seismic character and definition of the Johansen Fm sequence. New Johansen Fm zonation shown at well location.

DOCUMENT NO.: TL02-GTL-Z-RA-0001	REVISION NO.: 03	REVISION DATE: 01.03.2012	APPROVED:
-------------------------------------	---------------------	------------------------------	-----------

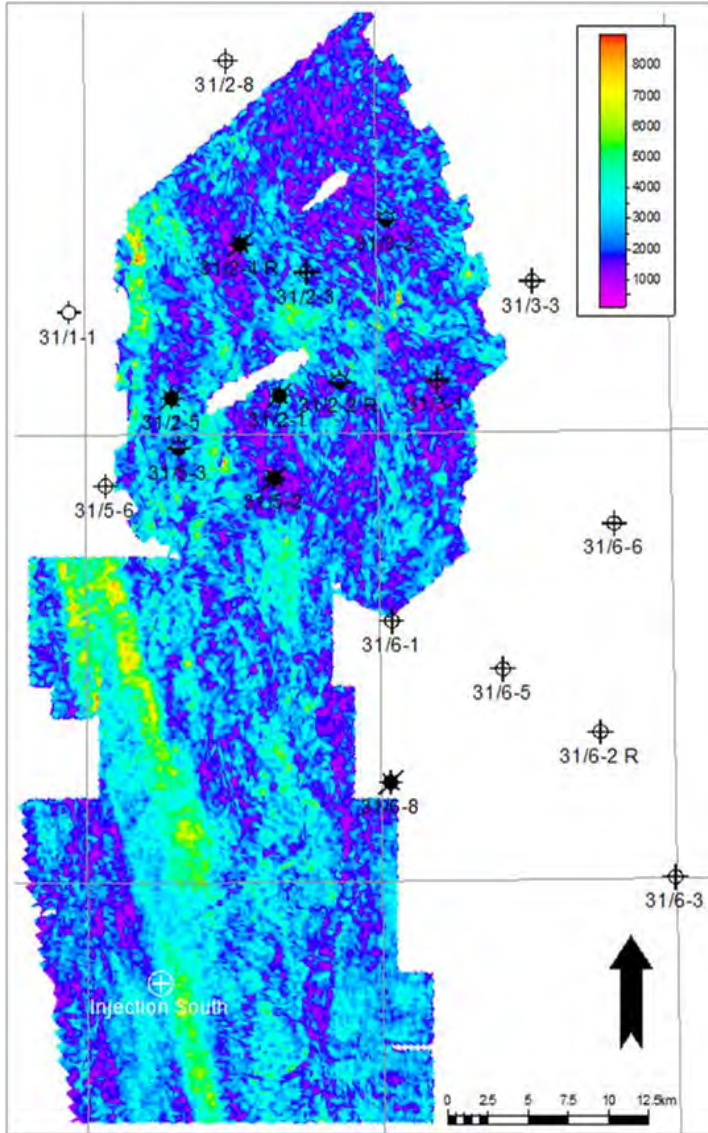


Figure 5-23: RMS surface attribute for the Johansen Fm (25m from Top Johansen) showing amplitude anomaly interpreted to represent sand system.

DOCUMENT NO.: TL02-GTL-Z-RA-0001	REVISION NO.: 03	REVISION DATE: 01.03.2012	APPROVED:
-------------------------------------	---------------------	------------------------------	-----------

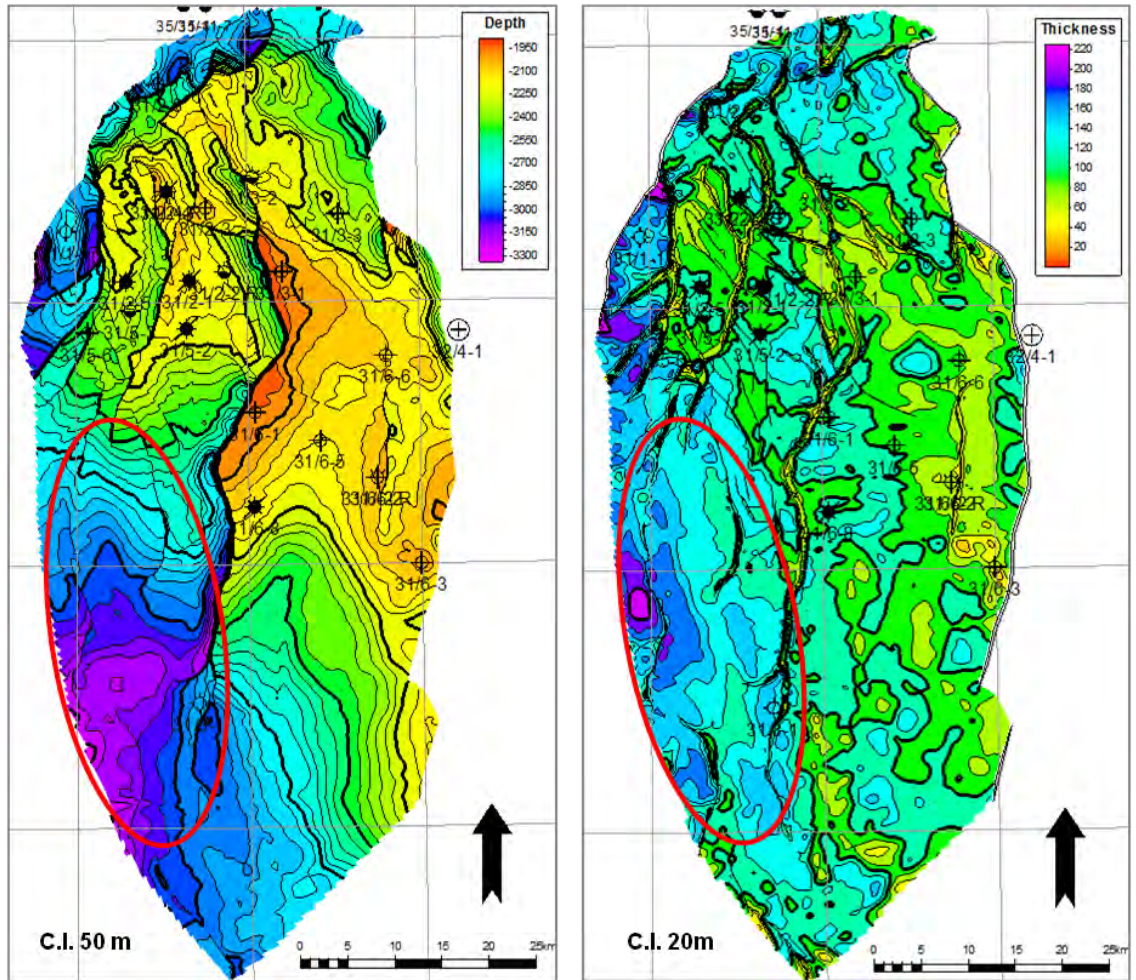


Figure 5-24: Johansen Fm depth map and thickness map. Red polygon represents plume injection and plume migration area.

Petrophysical and well log analysis

Using well logs and recently acquired 3D seismic the architecture and growth history of the Johansen Formation have been reviewed and reconstructed in more detail to better constrain geological processes controlling and affecting the growth history and evolution of the formation.

Sequence stratigraphic framework based on previous studies of the formation (Vollset and Doré 1984) (Marjanac 1995) (Marjanac and Steel 1997), NPD descriptions and well tops have been used as guidelines. However, new observations in this study show no consistency in the description of each of the different parts of the formation (i.e. Johansen Shale, Johansen 1, Johansen 2, Johansen Top) (Table 5-4, Table 5-5 and Figure 5-21). Based on these observations an evaluation has been performed on each well to identify and to refine the definitions of the different parts of the formation.

The method used for the Johansen wells is based on the description of the VCI (volume of clay) and the gamma ray signal (Gassnova-ROS 2011). Criteria which define clean sand, shaley sand, siltstone, shale and claystone were set based on VCI. These criteria together with gamma ray logs (see Table 5-6, Table 5-7, and Figure 5-21) were used to describe the formation as upward fining, upward coarsening or stacking referring to different sedimentary environments (prograding, stacking or transgressive).

DOCUMENT NO.: TL02-GTL-Z-RA-0001	REVISION NO.: 03	REVISION DATE: 01.03.2012	APPROVED:
-------------------------------------	---------------------	------------------------------	-----------

Table 5-4: Definition of the Johansen Fm based on average % of volume of clay (VCI), % of sand and silt based on gamma ray form well logs.

	31/1-1	31/2-5	31/2-1	31/5-2	31/6-1	31/2-4	31/2-2	31/3-1	31/6-2	31/6-3	31/3-3	31/2-3	31/2-8	32/4-1	
Cook															
% VCL	40	29	27	7	11	25	20	10	not present	not present	not present	57	26	23	21
% SAND	31	45	45	52	56	47	50	54				18	47	41	43
% SILT	17	4	9	21	11	8	9	14	17	8	19	18			

Amundsen 2														
% VCL	46	29	44	30	not present	49	66	30	not present	not present	31	53	44	not present
% SAND	28	46	34	37		33	17	37			31	26	23	
% SILT	14	1	8	20	4	10	18	26	9	23				

Johansen Top														
% VCL	24	12	53	9	4	17	37	4	11	15	7	9	23	13
% SAND	42	61	30	49	55	56	38	62	51	38	46	59	40	43
% SILT	17	0	4	22	18	0	9	9	17	32	28	7	21	25

Johansen 2														
% VCL	45	9	12	3	6	8	11	not present	11	8	not present	5	7	8
% SAND	24	59	59	56	62	58	58		51	42		62	39	48
% SILT	21	7	4	19	8	9	8	17	32	6	38	24		

Johansen 1														
% VCL	25	16	17	5	5	16	13	8	11	8	9	13	14	14
% SAND	40	53	53	51	62	44	60	57	50	48	46	53	41	49
% SILT	20	9	8	24	6	21	3	12	19	24	27	13	29	17

Johansen Shale														
% VCL	38	not present	26	not present	23	33	33	not present	24	22	not present	32	25	not present
% SAND	27		42		52	33	39		43	36		30	34	
% SILT	25		15		0	21	12		15	27		25	27	

Amundsen 1														
% VCL	52	27	56	31	38	61	61	39	59	63	32	52	42	43
% SAND	20	40	20	26	37	18	18	29	20	14	32	24	23	26
% SILT	20	17	16	12	10	13	13	20	13	17	23	14	26	20

Claystone: VCI > 0.5
Shale: VCI > 0.4
Siltstone: VCI < 0.4
Shaley sand: VCI 0.15- 0.3
Clean sand: VCI < 0.15

Western Troll wells
Eastern Troll wells
Troll kystnær well

DOCUMENT NO.: TL02-GTL-Z-RA-0001	REVISION NO.: 03	REVISION DATE: 01.03.2012	APPROVED:
-------------------------------------	---------------------	------------------------------	-----------

Table 5-5: Description of the Johansen Formation.

	31/1-1	31/2-5	31/2-1	31/5-2	31/6-1	31/2-4	31/2-2	31/3-1	31/6-2	31/6-3	31/3-3	31/2-3	31/2-8
Johansen Top													
Depth	2787-2800	2308-2316	2176-2184	2224-2238	1981-1994	2126-2130	2233-2257	2001-2034	2055-2066	2042-2064	2306-2351	2097-2113	2967-2984
Thickness	13	8	8	14	13	5	24	33	11	22	45	16	17
Lithology	Shaly sand	Clean sand	Claystone	Clean sand	Clean sand	Shaly sand	Shaly sand slightly upward fining/ upward coarsening top	Clean sand	Clean sand	Shaly sand	Clean sand	Clean sand	Shaly sand
	Upward fining from clean sand to shaly sand	Stacking/upward fining top	Upward fining	Stacking	Stacking	Stacking/finer than Johansen 2			Upward coarsening/ stacking		Stacking	Upward coarsening/ clean sand	Upward fining to MFS/upward coarsening/ finer than Johansen 2
Maximum flooding surface (MFS)/Erosional surface	At base/at top								At base				
Facies	Retrograding	Aggrading	Retrograding	Aggrading	Aggrading	Aggrading	Slightly retrograding, mostly aggrading, prograding top		Prograding/ aggrading		Aggrading	Prograding	Retrograding/ prograding
Calcite horizons	4 (0,5-2m)	0	0	3(0,2-1m)	2(0,2-1m)	0	?		2(0,5m)		10 (?)	2 (0,5m)	5 (0,5m)
Johansen 2													
Depth	2800-2821	2316-2350	2164-2223	2238-2280	1994-2028	2130-2190	2257-2304	Not present	2066-2099	2064-2087	Not present	2113-2168	2984-3000
Thickness	21	34	33	42	34	60	48		33	23		56	16
Lithology	Shale	Clean sand	Clean sand	Clean sand	Clean sand	Clean Sand	Clean sand		Clean sand	Clean sand		Clean sand	Clean sand
	Upward coarsening	Stacking/ coarser than Johansen 1	Stacking/ upward fining	Stacking	Stacking	Upward coarsening at base/stacking/ upward fining	Stacking		Stacking/ upward fining			Stacking	Stacking/ silty sand, coarser than Johansen 1
Maximum flooding surface (MFS)/Erosional surface	At base/at top												
Facies	Prograding	Aggrading	Aggrading/ retrograding	Aggrading	Aggrading	Prograding/ aggrading/ retrograding	Aggrading		Aggrading/ stepward shift, minor retrograding toward top			Aggrading	Aggrading (Prograding from Johansen Shale to Johansen 2)
Calcite horizons	4 (0,5-1,5m)	5 (0,5-1m)	4 (?m)	7 (<0,5-0,5m)	4 (<0,5m)	13 (0,5-1m)			2(0,5m)			8 (0,5m)	6 (0,5-2m)
Johansen 1													
Depth	2821-2847	2350-2387	2223-2255	2280-2335	2028-2060	2190-2200	2304-2318	2034-2088	2039-2130	2087-2102	2351-2407	2168-2180	3000-3019
Thickness	26	37	32	42	32	9	13	54	31	15	56	11	19
Lithology	Shaly sand	Shaly sand	Shaly sand	Clean sand	Clean sand	Shaly sand	Clean sand	Clean sand	Clean sand	Clean sand	Clean sand	Clean sand	Clean sand
	Upward coarsening/stacking (one shale horizon)	Upward coarsening /stacking, one shale horizon	Upward coarsening from shaly sand to clean sand intervals	Stacking	Very good sand, slightly upward coarsening toward flooding event	Upward fining from shaly sand to shaly silt	Upward coarsening after mfs		Slightly upward coarsening		Stacking	Upward coarsening	Stacking
Maximum flooding surface (MFS)/Erosional surface	Toward top	Near top	Flooding at top of a possible channel deposition system		Small flooding event at top		At base		Toward top				
Facies	Prograding/ aggrading	Prograding/ aggrading/ prograding	Prograding	Aggrading	Prograding/ aggrading	Retrograding	Prograding		Slightly prograding/ mostly aggrading		Aggrading	Prograding	Aggrading
Calcite horizons	4(0,5-1,5m)	3 (0,5m)	5 (0,5m)	6 (0,5m)	4(0,5-1m)	3 (1-1,5m)			4(0,2-1m)		8 (0,5-1m)	1 (2,5m)	4 (1-1,5m)
Johansen Shale													
Depth	2847-2867	Not present	2255-2293	Not present	2060-2111	2200-2241	2318-2344	Not present	2130-2138	2102-2125	Not present	2180-2214	3019-3035
Thickness	20		15		20	41	26		8	23		34	16
Lithology	Siltstone		Shaly sand		Shaly sand	Siltstone	Siltstone		Shaly sand	Shaly sand		Siltstone	Shaly sand
	3 coarsening upward cycles of shale to shaly sand		Upward coarsening from shale to shaly sand		Good sand	Upward coarsening from shale to shaly sand	Upward coarsening		Upward coarsening towards top	Upward coarsening		Upward coarsening	Upward coarsening from shaly silt to silty sand
Facies	Stacking/aggrading		Prograding		Aggrading	Prograding	Prograding		Aggrading	Prograding		Prograding	Prograding
Calcite horizons	6 (0,5-1m)		3 (0,5m)		0	8 (1-1,5m)			2 (0,5m)	2(0,2-1,5m)		?	2 (0,5m)
Thickness Total Johansen	80	79	34	38	39	115	111	87	83	83	101	117	68

All of the Johansen wells were refined as shown in Table 5-4, now divided into Johansen Progradation, Johansen Build-Up and Johansen Top. The lower boundary of the Johansen Formation is distinguished by a low response, gamma ray profile, comparable to top Amundsen 1 Formation, and marks the start of an apparent prograding deltaic environment named Johansen Progradation.

DOCUMENT NO.: TL02-GTL-Z-RA-0001	REVISION NO.: 03	REVISION DATE: 01.03.2012	APPROVED:
-------------------------------------	---------------------	------------------------------	-----------

Amundsen 1 Formation is in all wells defined as claystones and shales whereas Johansen Progradation sediments range from siltstones to shaley sands and show in several wells upward coarsening trends. General stacking and aggrading facies characterize the Johansen Build-Up with clean sand in all wells. Sediments in Johansen Top range from shaley sands to clean sand and are the transgressive part of the formation.

Table 5-6: New definition of the Johansen Fm based on average % of volume of clay (VCL), % of sand and silt based on gamma ray from well logs.

	31/1-1	31/2-5	31/2-1	31/5-2	31/6-1	31/2-4	31/2-2	31/3-1	31/6-2	31/6-3	31/3-3	31/2-3	31/2-8	32/4-1
Cook														
% VCL	40	29	27	7	11	25	20	10	not present	not present	31	26	23	25
% SAND	31	45	45	52	56	47	50	54			28	47	41	47
% SILT	17	4	9	21	11	8	9	14			30	8	19	8
Amundsen 2														
% VCL	46	29	46	30	not present	49	66	30	not present	not present	63	53	44	49
% SAND	28	46	33	37		33	17	37			16	26	23	33
% SILT	14	1	8	20		4	10	18			14	9	23	4
Johansen Top														
% VCL	24	12	27	11	4	17	29	1	11	15	29	9	23	13
% SAND	42	61	48	49	55	56	45	57	51	38	32	59	40	43
% SILT	17	0	3	20	18	0	7	18	17	32	27	7	21	25
Johansen Build Up														
% VCL	35	11	11	4	5	9	11	5	11	8	8	7	11	9
% SAND	32	58	59	54	62	56	58	61	51	45	46	60	40	56
% SILT	20	7	5	21	7	10	7	9	17	29	27	8	33	10
Johansen Progradation														
% VCL	32	18	29	5	23	33	35	20	24	23	29	36	27	33
% SAND	29	49	41	50	52	33	38	44	42	35	33	29	32	33
% SILT	27	13	13	24	0	21	12	17	17	27	24	23	29	21
Amundsen 1														
% VCL	52	56	70	32	38	61	64	58	71	66	55	63	42	61
% SAND	20	18	10	26	37	18	17	17	12	13	22	20	23	18
% SILT	20	18	16	31	10	13	13	18	12	15	13	9	26	13

Claystone: VCL > 0.5	Western Troll wells Eastern Troll wells Troll kystnær well
Shale: VCL > 0.4	
Siltstone: VCL < 0.4	
Shaley sand: VCL 0.15- 0.3	
Clean sand: VCL < 0.15	

Table 5-7: New division and description of the Johansen Fm.

	31/1-1	31/2-5	31/2-1	31/5-2	31/6-1	31/2-4	31/2-2	31/3-1	31/6-2	31/6-3	31/3-3	31/2-3	31/2-8
Johansen Top													
Depth	2787-2800	2308-2316	2182-2192	2224-2233	1981-1994	2126-2130	2233-2257	2001-2007	2055-2066	2042-2064	2293-2309	2097-2113	2967-2984
Thickness	13	8	10	9	13	5	24	6	11	22	16	16	17
Lithology	Shaley sand	Clean sand	Shaley sand	Clean sand	Clean sand	Shaley sand	Shaley sand	Clean sand	Clean sand	Shaley sand	Shaley sand	Clean sand	Shaley sand
Johansen Build Up													
Depth	2800-2855	2316-2364	2192-2239	2233-2292	1994-2060	2130-2200	2257-2318	2007-2069	2066-2120	2064-2102	2309-2408	2113-2181	2984-3019
Thickness	55	48	47	59	66	69	61	61	54	38	99	68	35
Lithology	Siltstone	Clean sand	Clean sand	Clean sand	Clean sand	Clean sand	Clean sand	Clean sand	Clean sand	Clean sand	Clean sand	Clean sand	Clean sand
Johansen Progradin													
Depth	2855-2867	2364-2401	2239-2282	2292-2323	2060-2111	2200-2241	2318-2348	2069-2100	2120-2148	2102-2127	2408-2428	2181-2227	3019-3042
Thickness	12	36	43	30	20	41	30	31	28	25	20	45	23
Lithology	Siltstone	Shaley sand	Shaley sand	Clean sand	Shaley sand	Siltstone	Siltstone	Shaley sand	Shaley sand	Shaley sand	Shaley sand	Siltstone	Shaley sand
Total thickness	80	92	100	98	99	115	115	98	93	85	135	129	75

DOCUMENT NO.: TL02-GTL-Z-RA-0001	REVISION NO.: 03	REVISION DATE: 01.03.2012	APPROVED:
-------------------------------------	---------------------	------------------------------	-----------

Deposition pattern is dependent on delta type and location within delta. There are four major groups of deltas; fluvial-dominated, wave-dominated, tide-dominated and undifferentiated deltas, where each of these has distinct fluid flow patterns due to their internal architecture. From well 31/2-3 aqueous fluid inclusions from the Johansen Formation trapped in late quartz overgrowths or cemented fractures confirm a dominating low saline NaCl-H₂O system, i.e. mixed fresh water and sea water.

Seismic analysis

Results of well analysis are supported by the seismic analysis. The new seismic and well evaluation of the Johansen Formation indicates a complex depositional pattern and several facies successions are recognized; river dominated delta front, distributary channels and wave dominated shoreface. In the northern part of the investigated area, channels are recognized both within the well logs (Figure 5-25) and as sinusoidal features apparent in seismic attribute mapping (Figure 5-26).

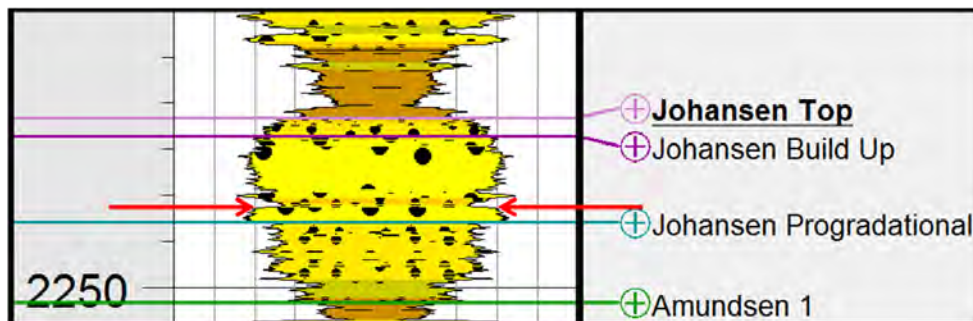


Figure 5-25: Well evidence (31/2-1). Indication of channel-point bar deposition in the gamma ray well log response.

In the delta of the northeastern area, mapped changes in well logs and seismic facies are now considered to reflect delta flats with channel-like features. The channels observed in the seismic and well logs may be described as anastomosing systems, meaning that channels were fixed in the same place, that accommodation of space was very close to supply of sediments, and hence that there was aggradation of sand bodies (Table 5-5). This resulted in thick sequences of sand depositions but with limited lateral extent. Aggradation represents delta top with flood plain facies in between. In general the Johansen Formation is enclosed by transgressive succession on top (Amundsen Formation).

Seismic attributes and interpretation suggest lateral change southwards and westwards, outside the area with well control (Figure 5-23 and Figure 5-27). These changes are reflected as elongated, coast-parallel features in the southwestern part with high reflectivity and have been interpreted as deposited in a high wave energy environment such as an open coast, probably with strong longshore currents.

Wave-dominated delta environments are associated with waves that run over the top of sand spits and bars. The sand will be reworked into coastal barriers oriented roughly parallel to the shoreline. There are indications of down laps (Figure 5-28), however (forced) regression of the delta may have prevented preservation of topsets. Where shoreface is dominated by strong longshore currents, sediments deposited at a river mouth can be transported along the coastline instead of forming a well-defined delta. From modern analogues it is documented that with sediment distribution in this type of system with longshore currents, both landward and seaward sediment transport can dominate (Duke 1990). Longshore currents result in sediment sorting of sediment bodies and the longshore sediment distribution results in elongated distribution of sand

DOCUMENT NO.: TL02-GTL-Z-RA-0001	REVISION NO.: 03	REVISION DATE: 01.03.2012	APPROVED:
-------------------------------------	---------------------	------------------------------	-----------

bodies, a feature which is recognized by seismic attributes in this study (Figure 5-27). This elongated feature is interpreted as better developed (cleaner) Johansen Formation sand compared to the Johansen Formation depositions in the northeastern areas.

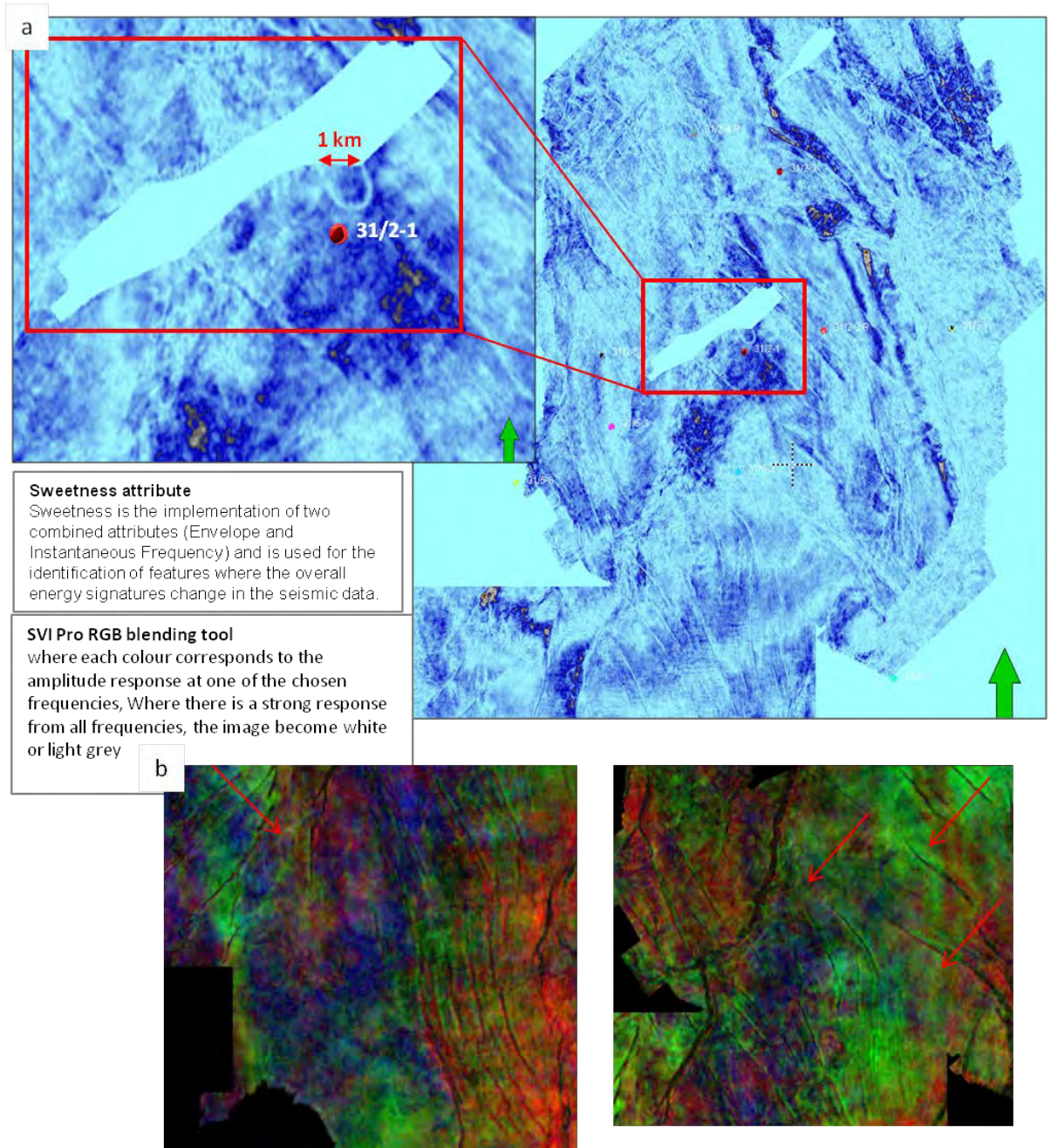


Figure 5-26: a) Sweetness attribute showing channel features at 2171m in the Johansen Fm, b) RGB-blend pictures showing channel features 56m below the top Johansen Fm.

DOCUMENT NO.: TL02-GTL-Z-RA-0001	REVISION NO.: 03	REVISION DATE: 01.03.2012	APPROVED:
-------------------------------------	---------------------	------------------------------	-----------

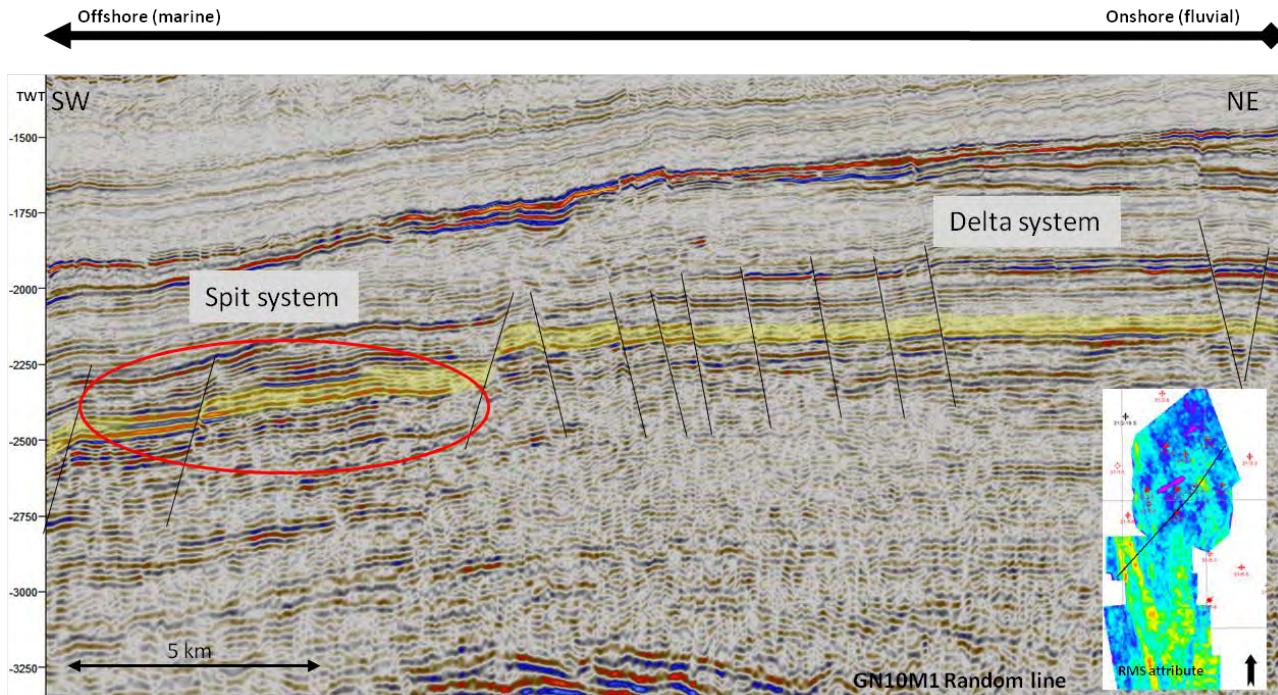


Figure 5-27: Seismic line showing the development of the Johansen depositional system from northwest to southwest. Amplitude anomalies (red polygon) are seen in the southwestern part. These are interpreted to constitute spit bar deposits.

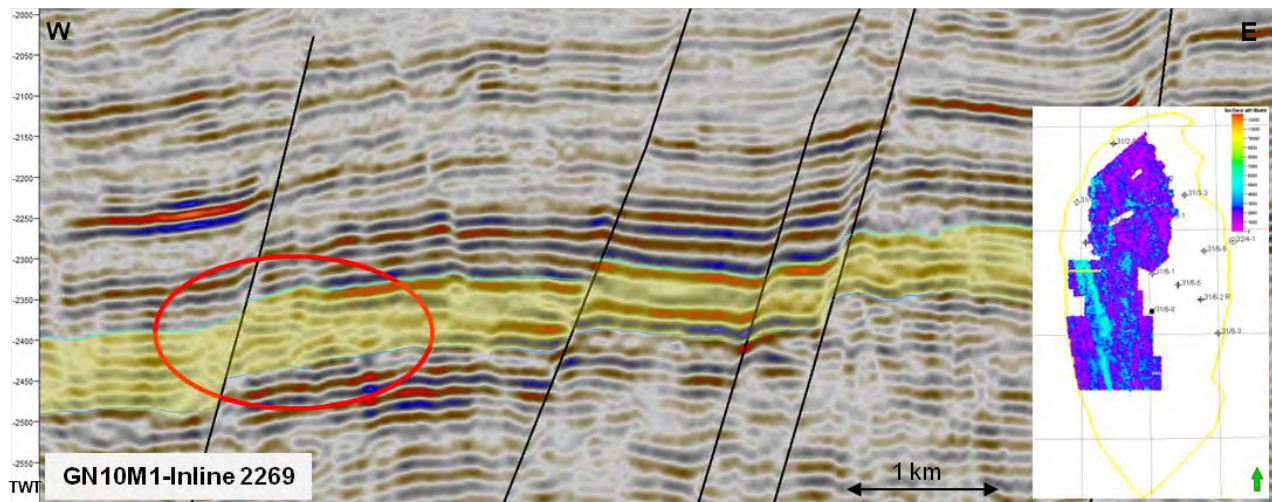


Figure 5-28: East-west trending seismic line showing clinoforms (down lap) in connection with Johansen Fm spit bar deposits (yellow).

The storage formation sand system is interpreted to pinch out southward and westward (Figure 5-30). Southward there is a pronounced change in the thickness seen on seismic data and on the associated thickness map (Figure 5-23). Similarities in extent and pinch out to the overlying Sognefjord Formation may be due to underlying structural control on this delta's development. There is a distinct westward change in seismic character from strong reflectivity to a more transparent seismic facies. A westward thickness change is observed, interpreted to represent delta front slump sediments and reworking.

The increase in accommodation of space basinward would allow for infilling of a thick sequence, explaining the observed thickened Johansen. A spit system model would also explain

DOCUMENT NO.: TL02-GTL-Z-RA-0001	REVISION NO.: 03	REVISION DATE: 01.03.2012	APPROVED:
-------------------------------------	---------------------	------------------------------	-----------

relatively high porosity and permeability caused by reworking. The spit system, i.e. wave reworked delta front sediments, is consistent with basinward migration (as seen in seismic time sequence) of the delta. The coastal spit system of the Johansen Formation is interpreted to be flanked to the east by a tidal back basin as in the Sognefjord Formation.

Depositional analogues

A spit system may have a high preservation potential since it may be enveloped and sealed by offshore mudstones as observed in the recent Skagen Odde, which is a sand-dominated spit-system (Johannessen and Nielsen 2006). The thickness of a spit system depends on water depth in which it progrades; it will be thick above topographic lows and thin over highs. In general spit systems prograde on top of elevated areas and preferentially prograde on the plunging crest of fault blocks (Johannessen and Nielsen 2006).

From studies of the Sognefjord Formation similar elongated features are highlighted by seismic mapping (Dreyer, et al. 2005) and may as well be an analogue to the observed features in the Johansen Formation (Figure 5-29). Both modern analogues such as the Skagen Odde, Denmark, and the Cape Lopez, Gabon, and paleo-analogues such as the Sognefjord Formation (Dreyer, et al. 2005) have elongated sandbars up to 35km long and 2-4km wide enclosed by offshore mud as recognized in the Johansen Formation. The coastal spit system of the Johansen Formation is interpreted to be flanked to the east by a tidal backbasin as in the Sognefjord Formation.

DOCUMENT NO.: TL02-GTL-Z-RA-0001	REVISION NO.: 03	REVISION DATE: 01.03.2012	APPROVED:
-------------------------------------	---------------------	------------------------------	-----------

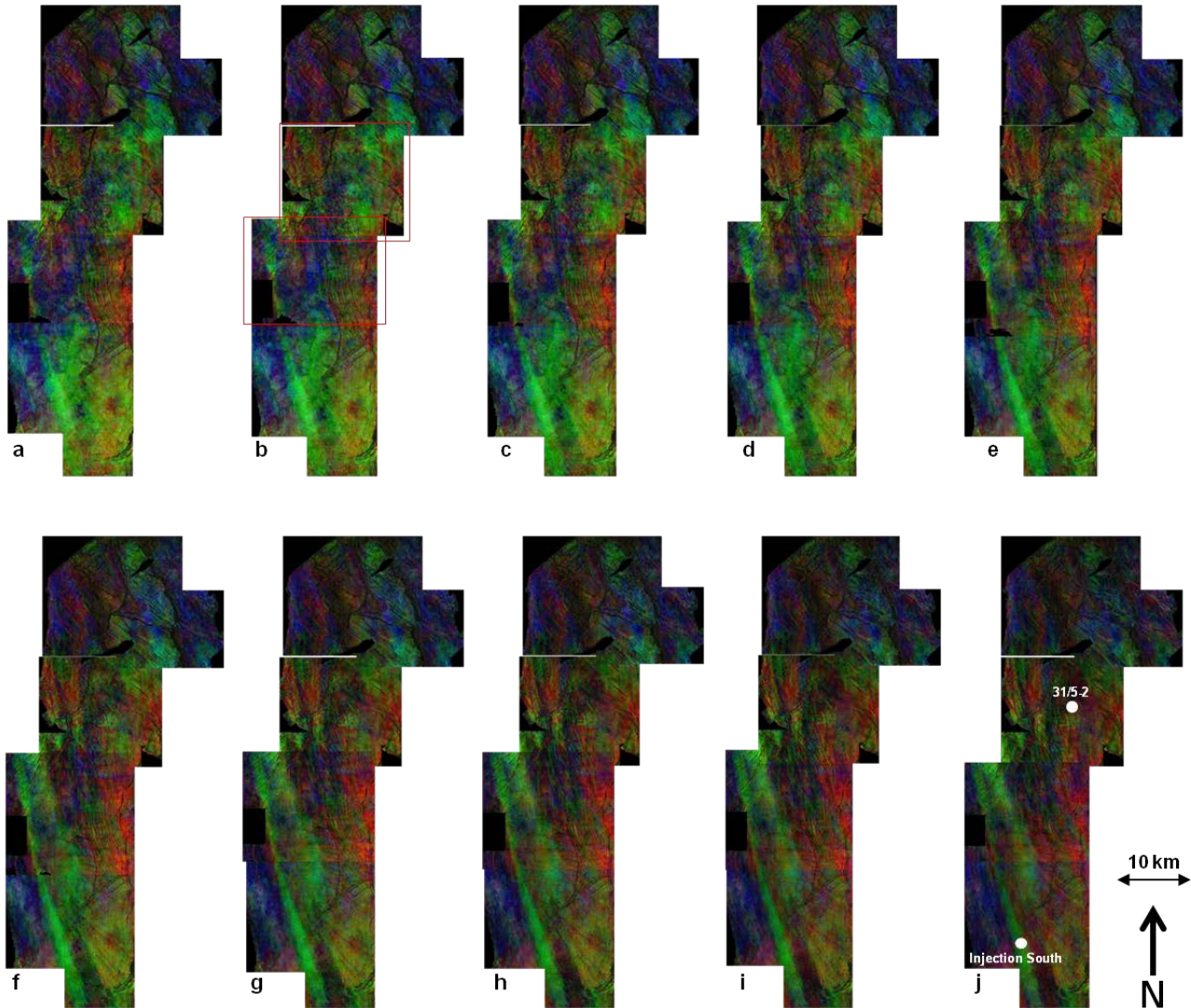


Figure 5-29: RGB-blend pictures from 7 cubes giving overview of the formation in study area. The pictures are taken within the formation, ie from Top Staffjord Fm (a) to Top Johansen (j) to depict the development of the formation; a) 72m below Top Johansen, b) 64m below Top Johansen, c) 56m below Top Johansen, d) 48m below Top Johansen, e) 40m below Top Johansen, f) 32m below Top Johansen, g) 24m below Top Johansen, h) 16m below Top Johansen, i) 8m below Top Johansen and j) Top Johansen.

DOCUMENT NO.: TL02-GTL-Z-RA-0001	REVISION NO.: 03	REVISION DATE: 01.03.2012	APPROVED:
-------------------------------------	---------------------	------------------------------	-----------

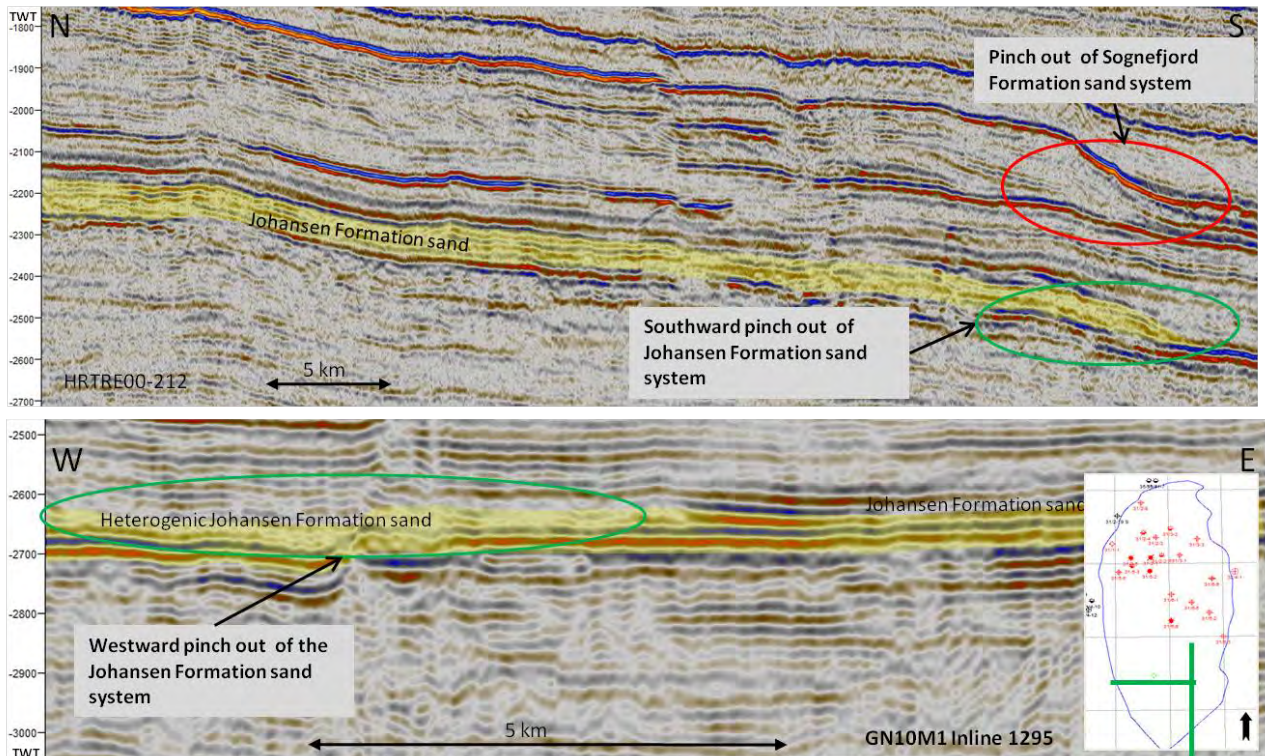


Figure 5-30: North-south and east-west trending seismic lines showing the pinch out of the Johansen Fm sand system. Note the concurrence with the pinch out of the Sognefjord Fm sand system.

5.3.1.2 *The Cook Formation*

On the Horda Platform and along its western margin the Cook Formation sandstone represents prograding shelf sands, and is dated as Pliensbachian (Deegan and Scull 1977) (Vollset and Doré 1984) (Figure 5-19). Several cycles are identified within the formation. The Cook Formation is part of the Cook megasequence developed as a consistent, upward-coarsening sandy unit or a series of stacked upward-coarsening trends. It is deposited contemporary with the laterally equivalent, shaley Burton Formation (Steel 1993). The Cook megasequence has an extensive distribution in the northernmost North Sea, with the uppermost Cook Formation sandstones extending well across the north Viking Graben into the Tampen Spur region.

All of the sand bodies between the basal Burton Formation, which is the lower boundary of the megasequence, and the overlying shaley part of the Drake Formation, are referred to as the Cook Formation (Steel 1993). The Norwegian hinterlands are believed to be the source of the Cook Formation sands. The formation is thought to represent a wave/storm-dominated shelf sand system, however locally tidal-shelf sand ridges have also been described (Livbjerg and Mjøs 1989). (Parkinson and Hines 1995) suggest that a late Pliensbachian regressive event corresponds in part to the Cook Formation and can be documented all over western Europe. This indicates a regional relative sea-level fall at this stratigraphic position (Charnock, et al. 2001).

The presence of the Cook Formation is proven by a number of wells in the northern part of the evaluation area (Table 5-8). The formation is interpreted to be present in the northwestern and southern part of the storage complex. In the southern part where the Amundsen Formation is absent the Cook Formation is interpreted to communicate directly with the Johansen Formation (chapter 7.2).

DOCUMENT NO.: TL02-GTL-Z-RA-0001	REVISION NO.: 03	REVISION DATE: 01.03.2012	APPROVED:
-------------------------------------	---------------------	------------------------------	-----------

In well 31/6-2R and 31/6-6, two eastern Troll wells, the Cook formation is absent (Figure 5-31 - wells marked with red circles). In well 31/3-3 (green circle) a thin (10m) Cook Formation is interpreted to be present. The well correlation (Figure 5-31) shows the lithology interpretation based on the Cook Formation VCI calculation from the key well petrophysical study performed (Table 5-9). The evaluation shows the presence of a heterogenic Cook Formation ranging from siltstone to clean sand. Claystone and shale layers are also developed in some wells (i.e. 31/2-5 and 31/2-1). The average Cook Formation thickness from the wells is approximately 50m. An eastward thinning of the Cook Formation is observed in the wells from 76m in well 31/2-5 to 11m in the most eastern well 31/3-3 (Figure 5-31).

Table 5-8: Well description of the Cook Formation.

	31/1-1	31/2-5	31/2-1	31/5-2	31/6-1	31/2-4	31/2-2	31/3-1	31/6-2	31/6-3	31/3-3	31/2-3	31/2-8
Cook													
Depth	2691-2767	2201-2277	2093-2134	2175-2193	1962-1981	2008-2107	2162-2202	1945-1992	Not present	Not present	2251-2293	2010-2055	2825-2896
Thickness	76	76	41	18	19	99	40	47			11	45	71
Lithology	Siltstone	Shaley sand	Shaley sand	Clean sand	Clean sand	Shaley sand	Shaley sand	Clean sand			Siltstone	Shaley sand	Shaley sand

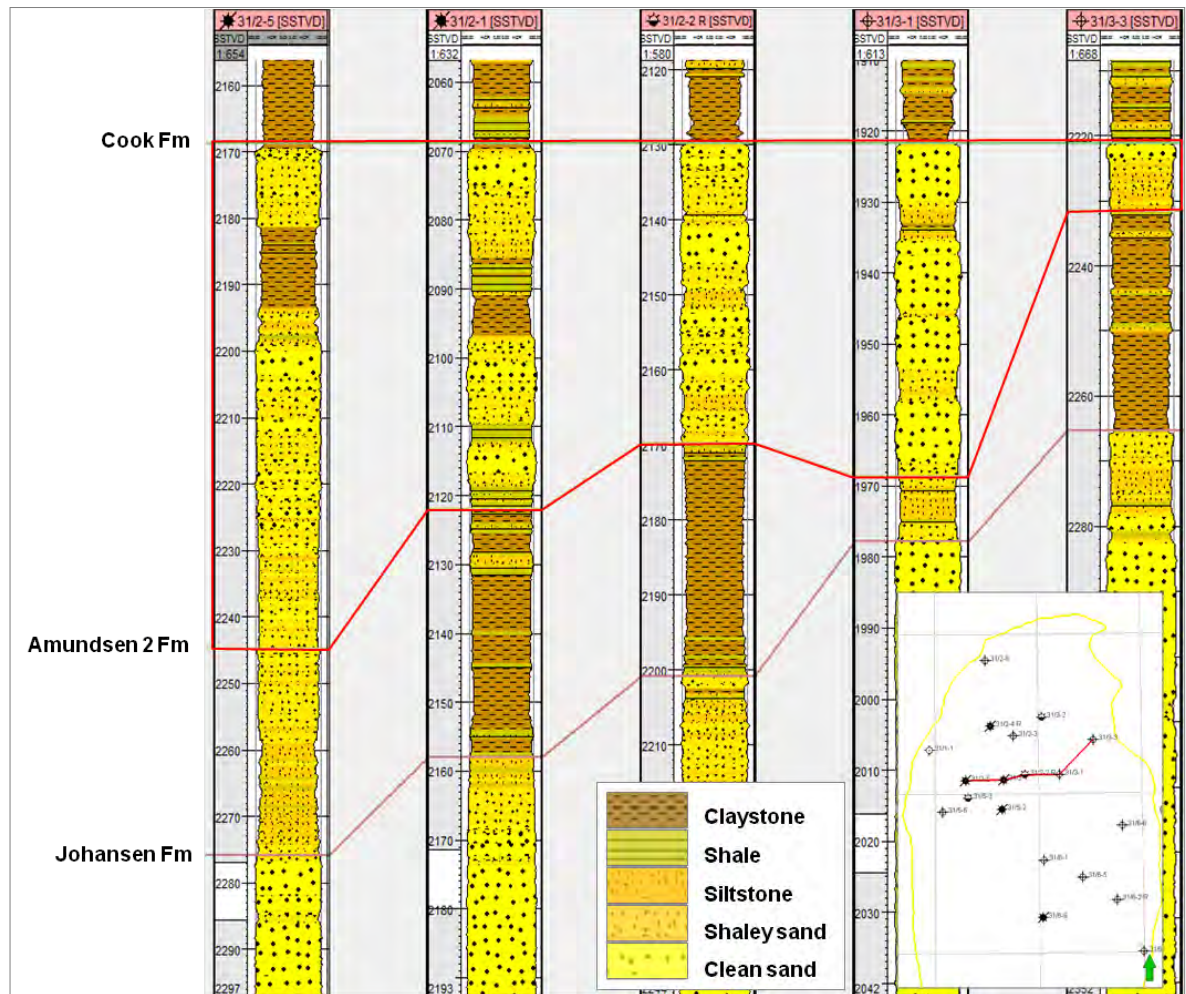


Figure 5-31: Well correlation from west to east showing the Cook Fm development. The lithology results are based on formation VCI interpretation.

DOCUMENT NO.: TL02-GTL-Z-RA-0001	REVISION NO.: 03	REVISION DATE: 01.03.2012	APPROVED:
-------------------------------------	---------------------	------------------------------	-----------

Table 5-9: Definition of the Cook Fm based on average % of volume of clay (VCI), % of sand and silt based on gamma ray form well logs.

	31/1-1	31/2-5	31/2-1	31/5-2	31/6-1	31/2-4	31/2-2	31/3-1	31/6-2	31/6-3	31/3-3	31/2-3	31/2-8	32/4-1
Cook														
% VCL	40	29	27	7	11	25	20	10	not present	not present	31	26	23	25
% SAND	31	45	45	52	56	47	50	54			28	47	41	47
% SILT	17	4	9	21	11	8	9	14			30	8	19	8

Claystone: VCI > 0.5	Western Troll wells Eastern Troll wells Troll kystnaer well
Shale: VCI > 0.4	
Siltstone: VCI < 0.4	
Shaley sand: VCI 0.15- 0.3	
Clean sand: VCI < 0.15	

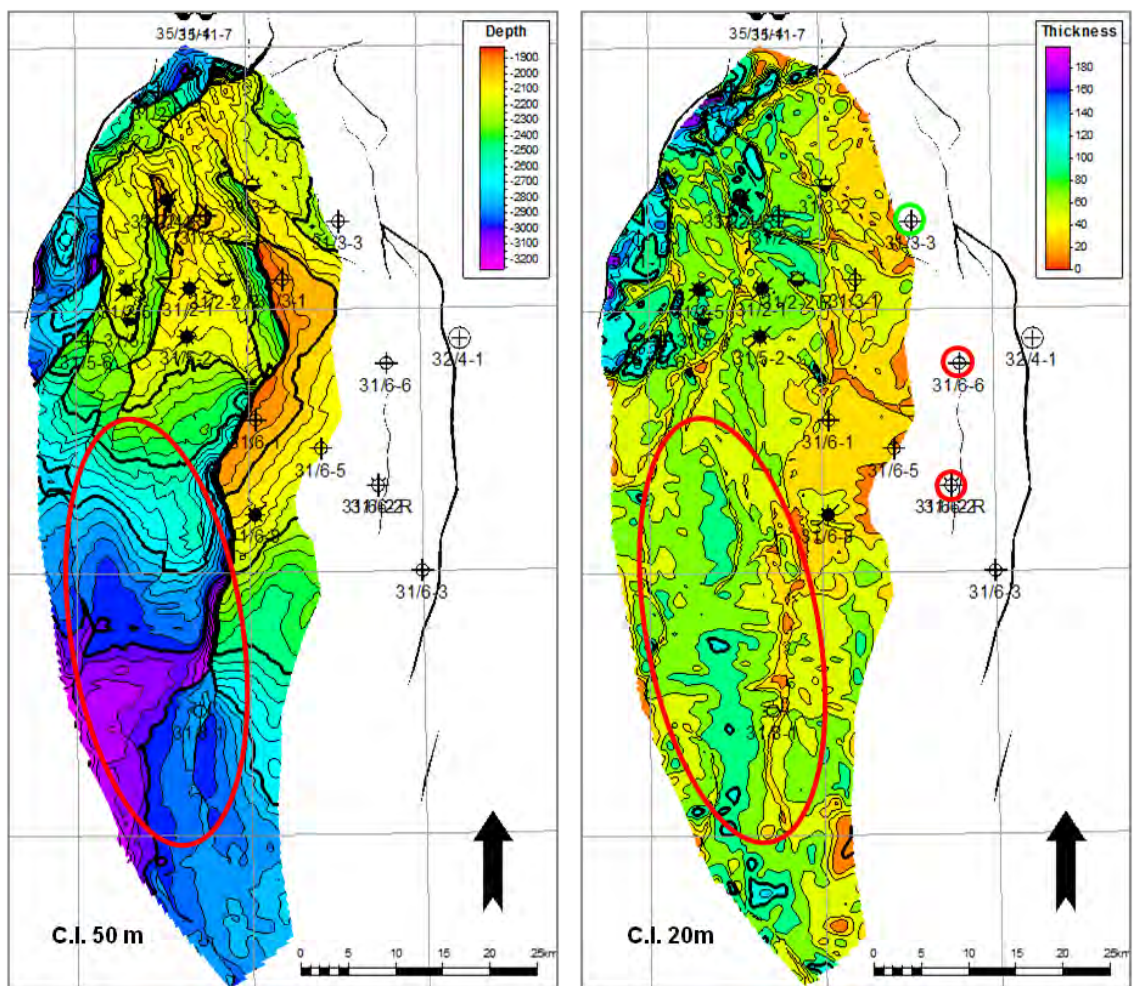


Figure 5-32: Cook Fm depth map and thickness map. Red polygons represent plume injection and plume migration area.

The Cook Formation depth map and thickness map are presented in Figure 5-32, with the red boundary representing the outline of the injection and plume migration area. The Cook Formation depth varies from approximately 1800m in the northeastern part to over 3000m in the most southern part. The average Cook Formation thickness, based on the seismic interpretation, is approximately 60m. The total storage formation thicknesses reach up to 120m in the mapped area and are between 60m to 100m in the CO₂ plume area (Figure 5-32).

DOCUMENT NO.: TL02-GTL-Z-RA-0001	REVISION NO.: 03	REVISION DATE: 01.03.2012	APPROVED:
-------------------------------------	---------------------	------------------------------	-----------

The thickness map (Figure 5-32) shows an eastward thinning of the Cook formation. This is especially clear in the northern part of the storage complex. This distinct change in thickness is also clear in the seismic data (Figure 5-33). In the southern part, the Cook Formation pinch out is defined on 2D seismic data of variable quality and thinning is therefore not so distinct.

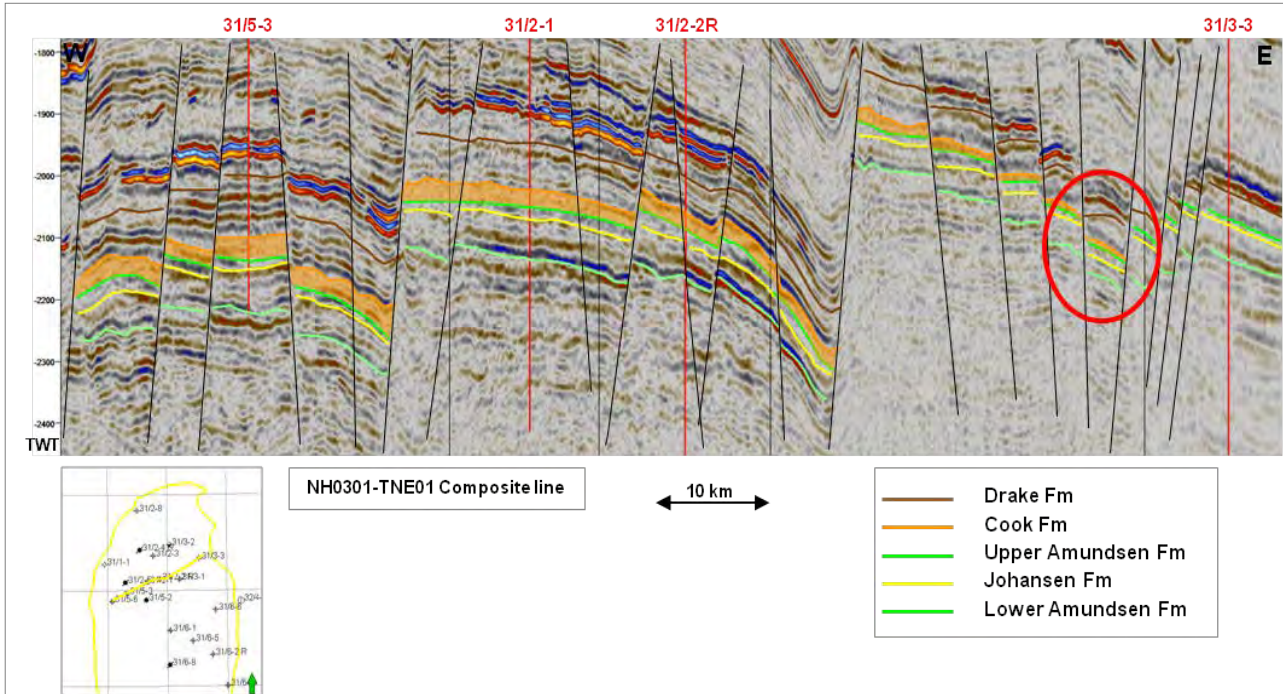


Figure 5-33: East-west trending seismic line showing the eastward thinning and pinch out of the Cook Fm. Red circle indicates pinch out zone.

The Cook Formation RMS attribute map (Figure 5-34) shows no distinct anomaly that could be interpreted as cleaner sand and there is no concurrence between clean sand well observations (i.e. well 31/3-1 and well 31/5-2, Table 5-9) and the attribute map. There is, however, some conformity between the Cook Formation thickness map (Figure 5-32) and the RMS (high) attribute values.

DOCUMENT NO.: TL02-GTL-Z-RA-0001	REVISION NO.: 03	REVISION DATE: 01.03.2012	APPROVED:
-------------------------------------	---------------------	------------------------------	-----------

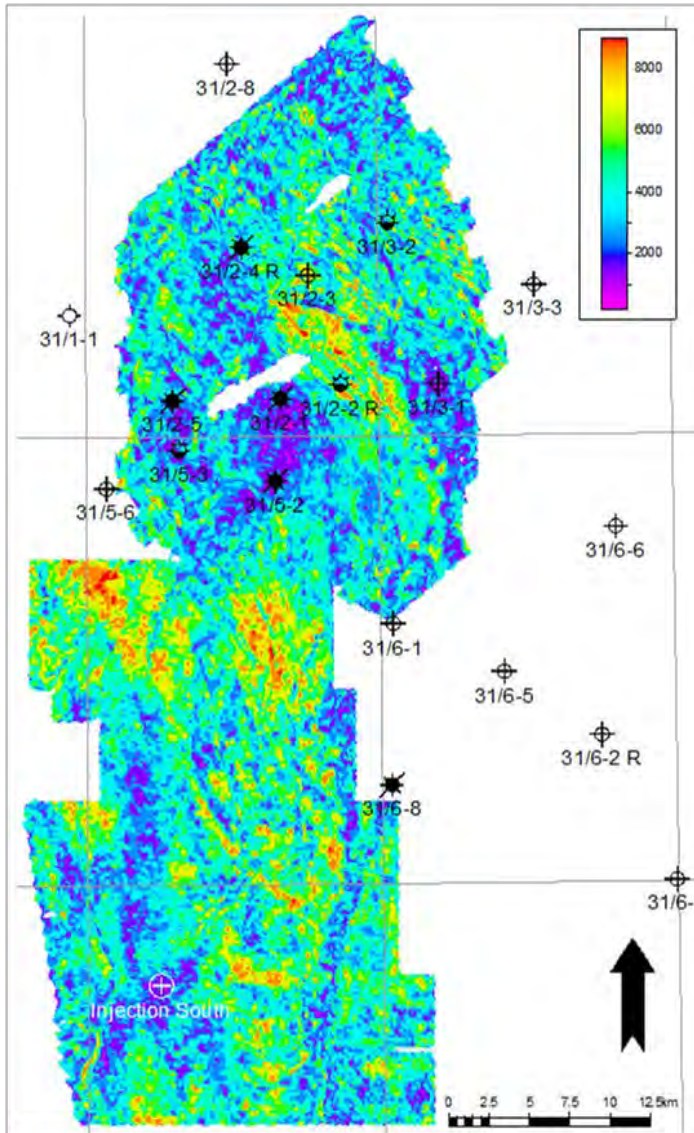


Figure 5-34: RMS surface attribute for the Cook Fm.

5.3.2 Storage formation quality

The main challenge when evaluating the Johansen Storage Complex is the lack of well data in the southern part of the storage complex. All Johansen Formation well data are concentrated around the Troll Field. The storage formation quality assessment in the northern part of the storage complex is based on the key well petrophysical and laboratory evaluation together with the proposed depositional model (Johansen Formation). An implication of lack of well control in the southern part is that the seismic analysis (seismic inversion) has a high degree of control over the storage formation properties in major parts of the storage complex. A description of the storage complex property building is found in chapter 5.6.2.

Several different geological factors are controlling the storage formation quality and the most important factors for the southern part of the Johansen Storage Complex are:

- storage formation facies
- diagenesis

The burial depth of the storage formations are increasing significantly southward to over 3000m for the Johansen Formation. This will induce several possible diagenetic risk factors. The

DOCUMENT NO.: TL02-GTL-Z-RA-0001	REVISION NO.: 03	REVISION DATE: 01.03.2012	APPROVED:
-------------------------------------	---------------------	------------------------------	-----------

potential influence sub seismic faults may have on the storage formation quality is not regarded in this study.

Mechanical compaction and quartz cementation are the most important porosity reducing processes in sandstones. Mechanical compaction is the controlling process down to 80°C (Figure 5-35). The mechanical compaction of sandstones is mainly controlled by depth of burial and clay content (Bjørkum and Nadeau 1998).

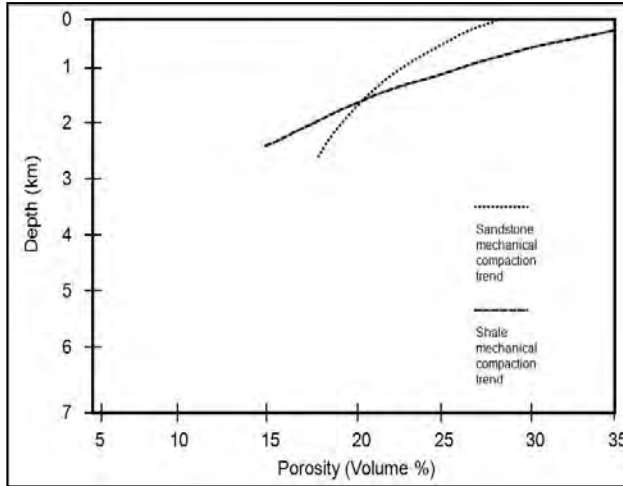


Figure 5-35: Porosity trends for sandstone and shale as result of mechanical compaction. Thermally driven cementation dominates at temperatures over 80°C (modified from (Bjørkum and Nadeau 1998)).

Some 3000m-3500m below the North Sea, reservoir quality is variable due to variations in porosity and permeability reduction as a result of compaction, quartz cementation and formation of fibrous illite. However, good permeability may be preserved in depths greater than 4000m if the porosity is preserved by a high overpressure or chlorite coating and if illitization is hindered by a limited potassium supply (Ramm and Ryseth 1996).

Cementation

Preservation of porosities in storage formation sandstones may be controlled by cementation. The main clays of the North Sea are illite and kaolin (Wilkinson, Haszeldine and Fallick 2006). Chlorite is only locally important.

Illitization

This occurs almost all over within clastic sediments of the North Sea. Illite is a fibrous shale mineral that covers pore throats. Illite does not affect the overall porosity much, but may severely reduce permeability. In the North Sea Basin, the main phase of illite precipitation reducing the quality of Jurassic reservoirs take place at 130-140°C (at depths close to 4km) but the quantity of illite depends on the presence of both kaolinite and K-feldspar (Bjørlykke 1998). Kaolin is found within a wide range of sedimentary settings. Even in marine sands kaolin is found suggesting that these locations have been flushed with meteoric water (Wilkinson, Haszeldine and Fallick 2006). At temperatures above 120°C illite diagenesis in sandstone becomes an important permeability reducing process due to the reaction of K-feldspars and kaolinite (Ehrenberg 1990).

Quartz cementation

Quartz cementation growth starts precipitating at burial depths around 2-2.5km (70-80°C), and once the process starts it will continue until all porosity is lost. The total amount of quartz cement and porosity reduction increases exponentially with increasing temperature, and decreases with increasing grain size and a reduction in quartz content.

DOCUMENT NO.: TL02-GTL-Z-RA-0001	REVISION NO.: 03	REVISION DATE: 01.03.2012	APPROVED:
-------------------------------------	---------------------	------------------------------	-----------

Chlorite

May form diagenetically from smectite and from kaolinite when a source of Fe and Mg is present (Bjørlykke 1998). A wide range of nearshore/marginal marine sand-body types is susceptible to chlorite mineralization formed during diagenesis from precursor Fe-rich clays such as berthierine or verdine (Wilkinson, Haszeldine and Fallick 2006). Distribution of anomalous porosity and proportion of net sand depends upon sedimentary facies architecture and pattern of discharge of Fe-rich river water during sand deposition. Chlorite coatings enhance reservoir quality by inhibiting quartz cementation, thereby preserving primary intergranular porosity (Ehrenberg 1993). Grain-coating Fe-rich chlorite cements can thus preserve exceptional porosity during burial. It is well known from literature that chlorite coatings prevent quartz cementation, but observations show that illite and illite/chlorite coatings can also be effective in preventing quartz precipitation (Storvoll, et al. 2002).

5.3.2.1 *Johansen Formation*

The Johansen Formation is deposited with large differences in morphology and facies (chapter 5.3). These differences in the depositional system give changes in storage formation facies (sand quality) and are shown in the well correlations (Figure 5-21) and in Table 5-6. All wells show a wide range of porosities indicating a heterogenic Johansen Formation which give large changes in storage formation quality (Figure 5-36). This is also shown by the porosity model based on inversion data.

Based on the evaluation of % volume of clay, all parts of the Johansen Formation, i.e. Johansen Progradation, Johansen Build-Up and Johansen Top show typical deltaic sediments ranging from clay to clean sand (Figure 5-21 and Table 5-6) in the northern part of the storage complex. In general, composition of deltaic depositions range from course sand in channel bottoms to fine clay in flood plains.

Porosity and depth trends from key wells (Figure 5-36) within this study show systematic trends versus burial depth. The Johansen Formation average porosities vary from 21% in the main Troll wells to 8 in the northern deep wells (Figure 5-36).

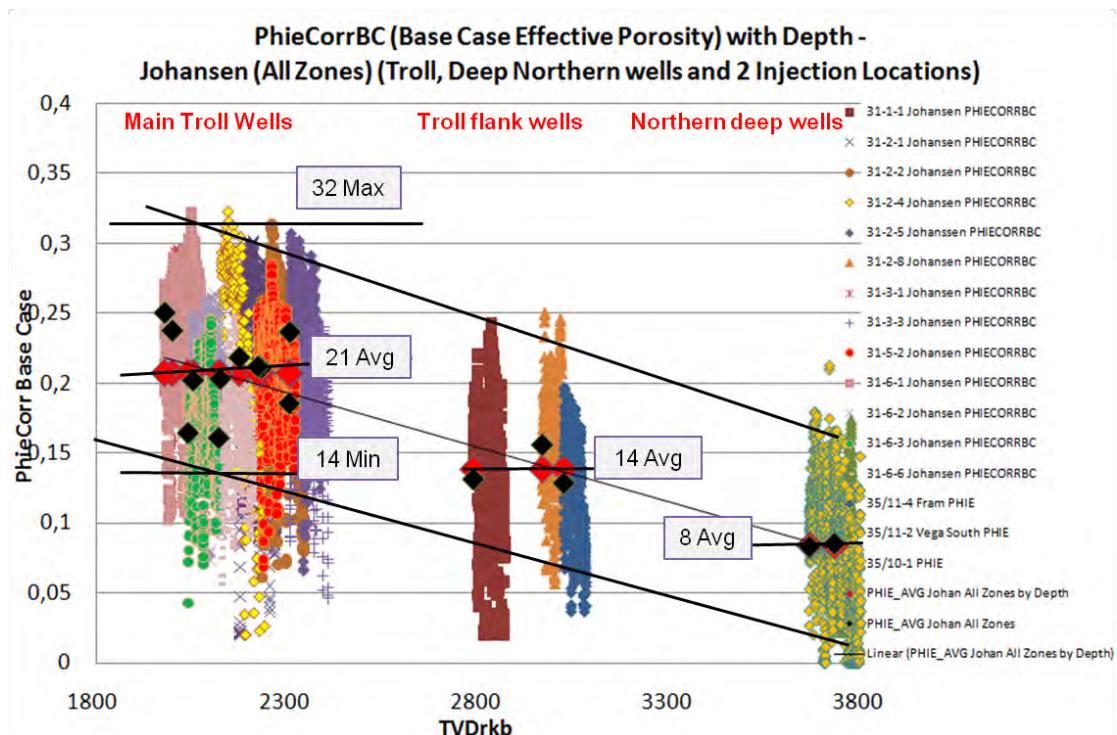


Figure 5-36: Johansen Fm porosity/depth trends from key wells and inversion.

DOCUMENT NO.: TL02-GTL-Z-RA-0001	REVISION NO.: 03	REVISION DATE: 01.03.2012	APPROVED:
-------------------------------------	---------------------	------------------------------	-----------

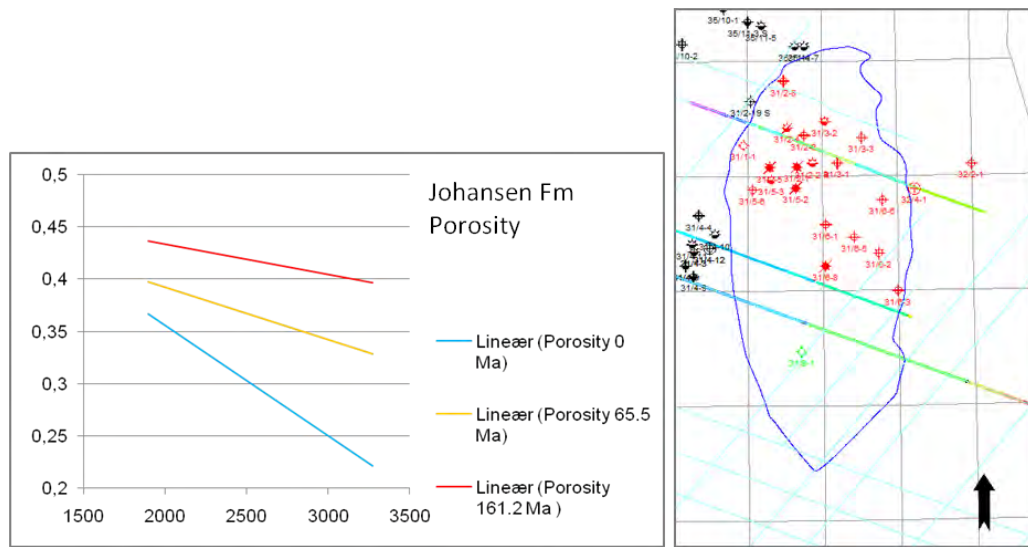


Figure 5-37: Johansen Fm porosity development from basin modelling result from three 2D lines over the JSC.

A 2D basin modelling study has been performed (Gassnova-SIN 2011). The basin burial history can be used to predict the storage formation quality, especially for the southern part where no data from wells are available. Figure 5-37 shows the Johansen Formation porosity development versus depth over geological time. At present (0Ma) porosities presumably range from 0.36-0.23, at 65.5Ma porosities presumably range from 0.39-0.33, and at 161.2Ma porosities presumably range from 0.44-0.39 which demonstrates the result of sediment compaction over time. The present day porosity trend from the basin modelling study differs from key well porosity/depth trends and shows overall higher values. The basin modelling porosity depth trend is more in accordance with porosities from the inversion study (Gassnova-WGD 2011) and hence supports the proposed Johansen Formation depositional model.

The observed calcite layers in the Johansen Formation are interpreted to have only limited lateral correlation and hence to have limited flow blocking effect. Calcite horizons, which may influence the quality of the storage formation, have been detected in the 14 wells investigated and their thickness measured indirectly by well logs. Maximum thickness measured is in all wells approximately 2m. These calcite horizons (Table 5-5), originally biogenic, have not been possible to correlate from well to well. This may be due to the fact that calcite horizons occurred in central delta sequences where delta lobes moved and shifted positions. Generally, shallow marine sandstones are often enriched in biogenic carbonates which promote calcite precipitation as a cement source during burial (Bjørkum and Walderhaug 1990). Deposition of calcite enriched sandstones take place in wave and storm dominated, shallow marine environments, and to a smaller degree in muddy, fair weather sediments, tidal channels and tidal point bars (Morad 1998).

The Johansen Formation samples from 31/2-3 show chlorite coating (Figure 5-38) which suggests that porosity variation is not only a function of depth and facies but also controlled by grain coatings preventing quartz overgrowth and preserving porosities. Such chlorite cementation is typically found in marginal marine sandstones (Wilkinson, Haszeldine and Fallick 2006).

DOCUMENT NO.: TL02-GTL-Z-RA-0001	REVISION NO.: 03	REVISION DATE: 01.03.2012	APPROVED:
-------------------------------------	---------------------	------------------------------	-----------

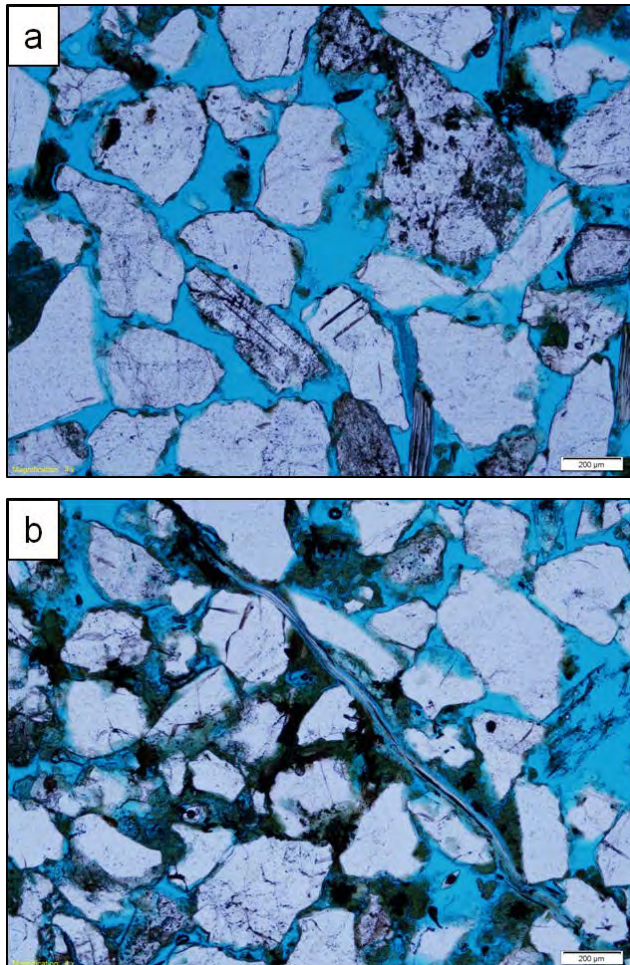


Figure 5-38: Highly porous sandstone from the Johansen Fm. Note the poor grain contact, angular grains and scattered pore filling clays. The greenish clay material suggests iron rich chlorite or glauconite. Mica is partly packed in between quartz grains, but do not form continuous layers (Gassnova-IRI 2011).

Key wells 31/2-1 and 31/2-2R have modelled porosity values up to 30% with matching permeabilities up to 5000mD. The quality increases from the Johansen Progradational part to maximum values within the Johansen Build-Up part, however there are marked changes within all parts of the formation. Average porosity modelled for well 31/2-1 is 25% and 24% for well 31/2-2R. The Johansen Formation average porosity model based on the inversion data confirms the heterogenic signature from the wells (Figure 5-36).

DOCUMENT NO.: TL02-GTL-Z-RA-0001	REVISION NO.: 03	REVISION DATE: 01.03.2012	APPROVED:
-------------------------------------	---------------------	------------------------------	-----------

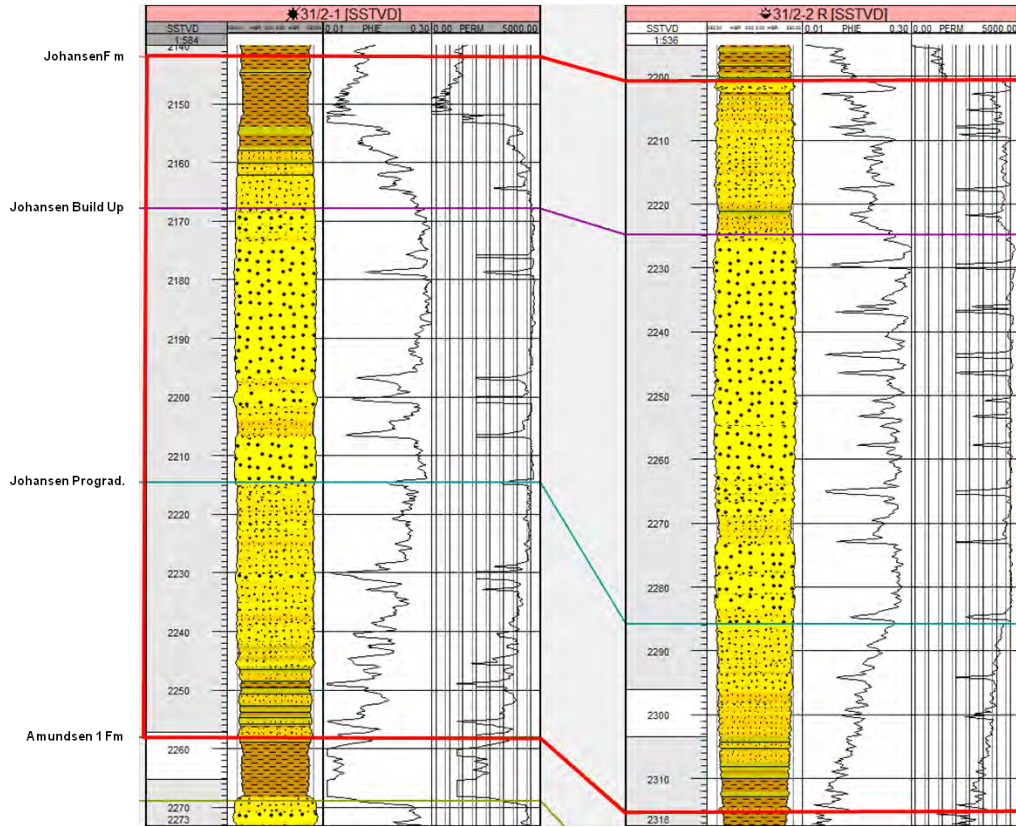


Figure 5-39: Well panels showing key well Johansen Fm lithology with porosity and permeability (log) results from the petrophysical modelling for well 31/2-1 and 31/2-2R. See Figure 5-31 for lithology legend and Figure 5-45 for well locations.

DOCUMENT NO.: TL02-GTL-Z-RA-0001	REVISION NO.: 03	REVISION DATE: 01.03.2012	APPROVED:
-------------------------------------	---------------------	------------------------------	-----------

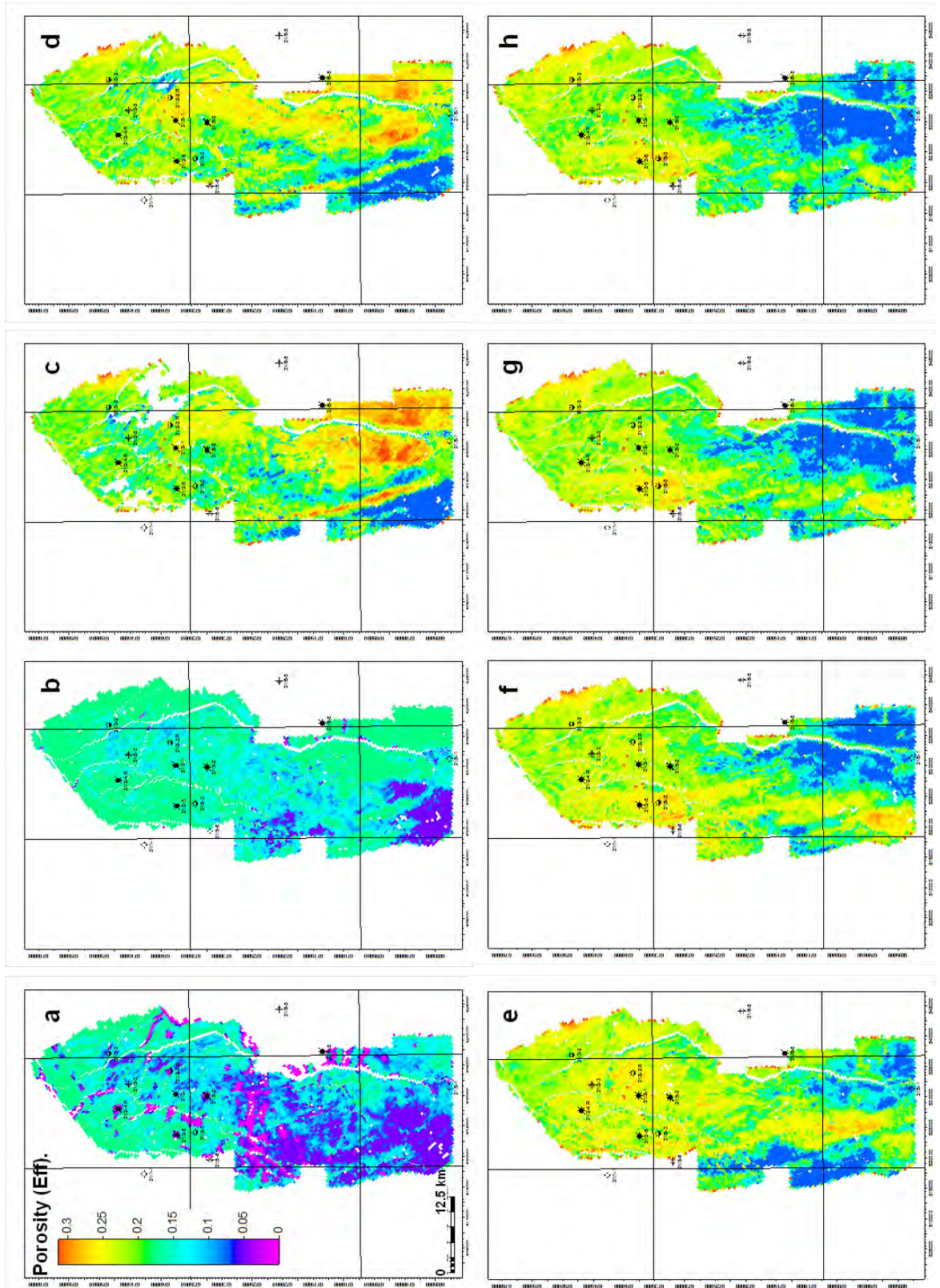


Figure 5-40: Porosity trends in the Johansen Fm. a) Amundsen Fm. mid, b) Top Amundsen Fm, c) Johansen Progradational mid, d) Johansen Progradational, e) Top Johansen Build-Up mid, f) Top Johansen Build-Up, g) Top Johansen mid, h) Top Johansen.

DOCUMENT NO.: TL02-GTL-Z-RA-0001	REVISION NO.: 03	REVISION DATE: 01.03.2012	APPROVED:
-------------------------------------	---------------------	------------------------------	-----------

Figure 5-40 shows the development of the Johansen Formation over geological time, starting with the deposition of the marine shale Amundsen Formation with very low porosities, to a clear progradational stage of the Johansen Delta with increasing porosities and the following build-up stage reaching maximum porosities. In time slice Johansen Progradational mid, the Johansen Formation average porosities change from an average of 20% in the northern part of the storage complex up to 30% in the most southern parts (Figure 5-40, c). The time slices show a shift in good quality sands from southeastern parts from the early progradational phase to southwestern parts during the build-up phase and this east-west trend indicates higher porosities in the western part of the formation. This may depict the development and basinward movement of the described spit-system of the Johansen Formation.

In general, the property model suggests good quality sands with high porosities developed in the west and south. However, this southward change in the storage formation quality with increasing porosities contradicts the porosity/depth trend observed in the wells. In spite of this contradiction, the trends from the property model are assumed to be realistic indicating that different facies of the apparent asymmetrical delta may act as the most important factor controlling quality properties.

There are few well data in the storage complex available for evaluation of possible cementation processes. Table 5-10 shows temperature data from key wells for Jurassic and Triassic deposits indicating that cementation processes such as quartz cementation are not dominant in the Johansen formation in the northern area. For the southern part the depth for the Johansen Formation is over 3000m (Figure 5-24) and possible quartz cementation may occur. However, the observation of a high amount of chlorite in the Johansen Formation (Figure 5-38) and thus chlorite coating of the sand grains is believed to have preserved the porosities.

Table 5-10: Jurassic and Triassic key well temperature measurements.

Well	Depth (m)	Temperature (°C)	Age
31/2-4R	5035	61	Triassic
31/2-5	2500	66	Triassic
31/3-3	2573	64	Triassic
31/3-3	2493	77	Triassic
31/6-2	2020	63	Jurassic
31/6-2	2235	72	Triassic
31/6-3	2250	70	Triassic
32/2-1	1300	33	Triassic

The average density data from the seismic inversion (Figure 5-41) illustrate density trends versus depth in agreement with the porosity trends in Figure 5-40 as the density of the Johansen Formation decreases where porosities increase. The acoustic impedance data, which is the main input for property modelling, show anomalous low values in the southwestern part (the apparent spit system), suggesting sand development in the injection area. This is also depicted in intersection A-A' (Figure 5-41).

The quality evaluation indicates variable storage formation quality for the Johansen Formation, but seismic inversion data indicates development of good quality sand in the southwestern part of the storage complex. The property modelling based on the seismic inversion data indicates average Johansen Formation porosity values around 20% at the proposed injection area, ranging from 10% at the latest stage of the storage formation development to 30% in the progradational part of the deposits (Figure 5-40). These values are, however, dependent upon the development of a sand spit system in the injection area.

The storage formation presence and quality evaluation suggests that there is reason to believe that porosities could be preserved due to both depositional facies and grain coating processes.

DOCUMENT NO.: TL02-GTL-Z-RA-0001	REVISION NO.: 03	REVISION DATE: 01.03.2012	APPROVED:
-------------------------------------	---------------------	------------------------------	-----------

However, the largest uncertainties are found in the southern part of the storage complex due to the lack of well data for calibration of the seismic inversion data used for the property modelling and to prove the suggested depositional model.

5.3.2.2 Storage formation quality - disregarding inversion data.

To evaluate the consequences of not having developed a spit system in the southern injection area, porosity and permeability maps (Figure 5-42 A&C) using the Johansen Formation porosity vs. depth trend from the northern key wells (Figure 5-36) were generated for comparison with the porosity model based on the seismic inversion (Figure 5-42 B&D). In this model the depth is the only controlling factor of the storage formation quality.

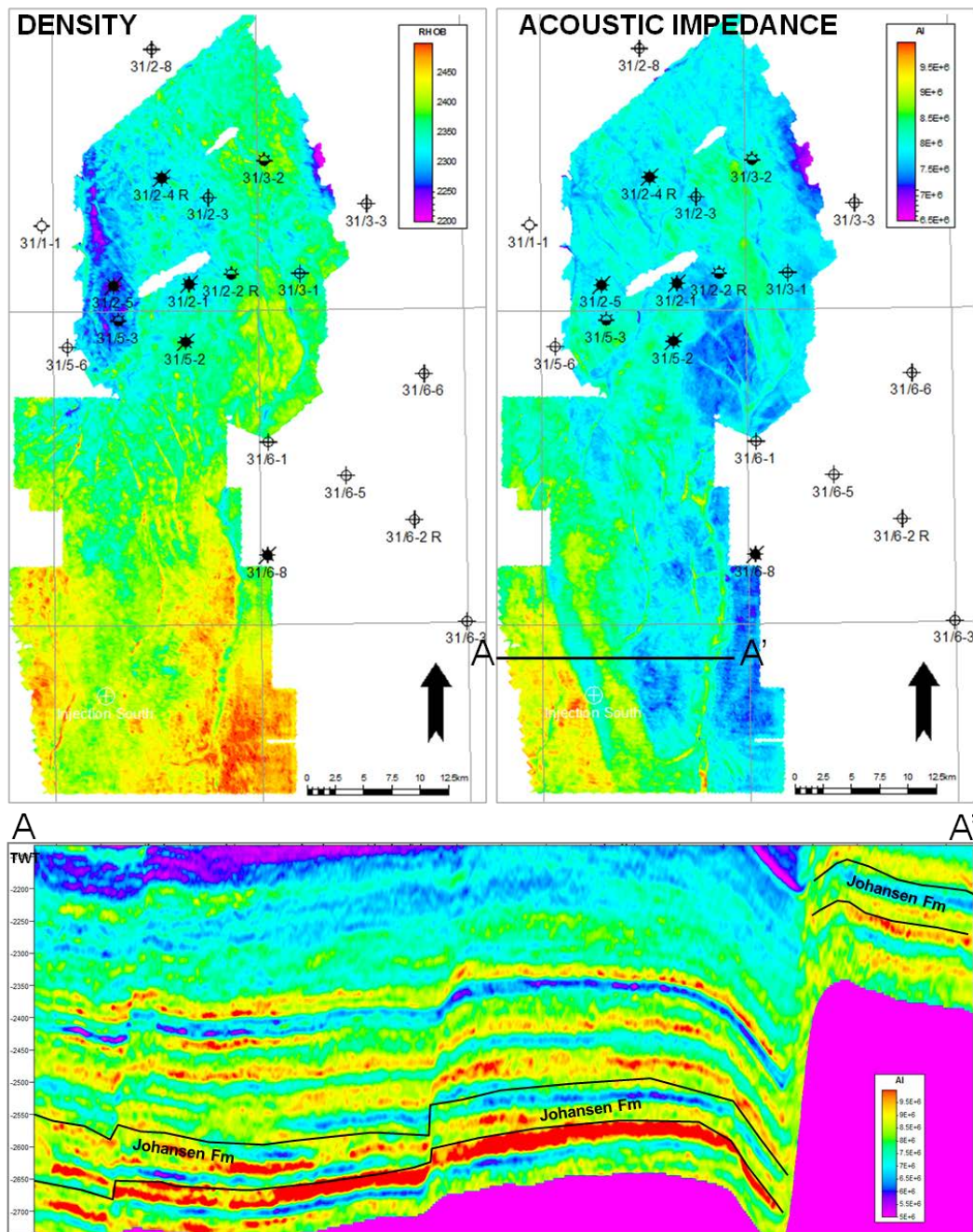


Figure 5-41: Density and Acoustic impedance RMS attribute map for the Johansen Fm. Acoustic impedance section is showing AI values indicating Johansen Fm sand development in the injection area.

DOCUMENT NO.: TL02-GTL-Z-RA-0001	REVISION NO.: 03	REVISION DATE: 01.03.2012	APPROVED:
-------------------------------------	---------------------	------------------------------	-----------

The porosity map A shows an average porosity at approximately 14% for the injection area, whereas the porosity map B shows average porosity values over 21%. An average permeability map was generated using porosity-permeability correlation from key wells (see chapter 5.6.2.4). The corresponding permeability maps show a significant difference in the average permeability for the two different porosity models for the injection area; approximately 60mD (Figure 5-42C) and 600mD (Figure 5-42D). This reduction in permeability will have an impact on the storage complex injectivity. The consequence of this is further evaluated in chapter 6.3. There is no significant change in the Johansen Formation reference case pore volume using the depth trend based porosities.

DOCUMENT NO.: TL02-GTL-Z-RA-0001	REVISION NO.: 03	REVISION DATE: 01.03.2012	APPROVED:
-------------------------------------	---------------------	------------------------------	-----------

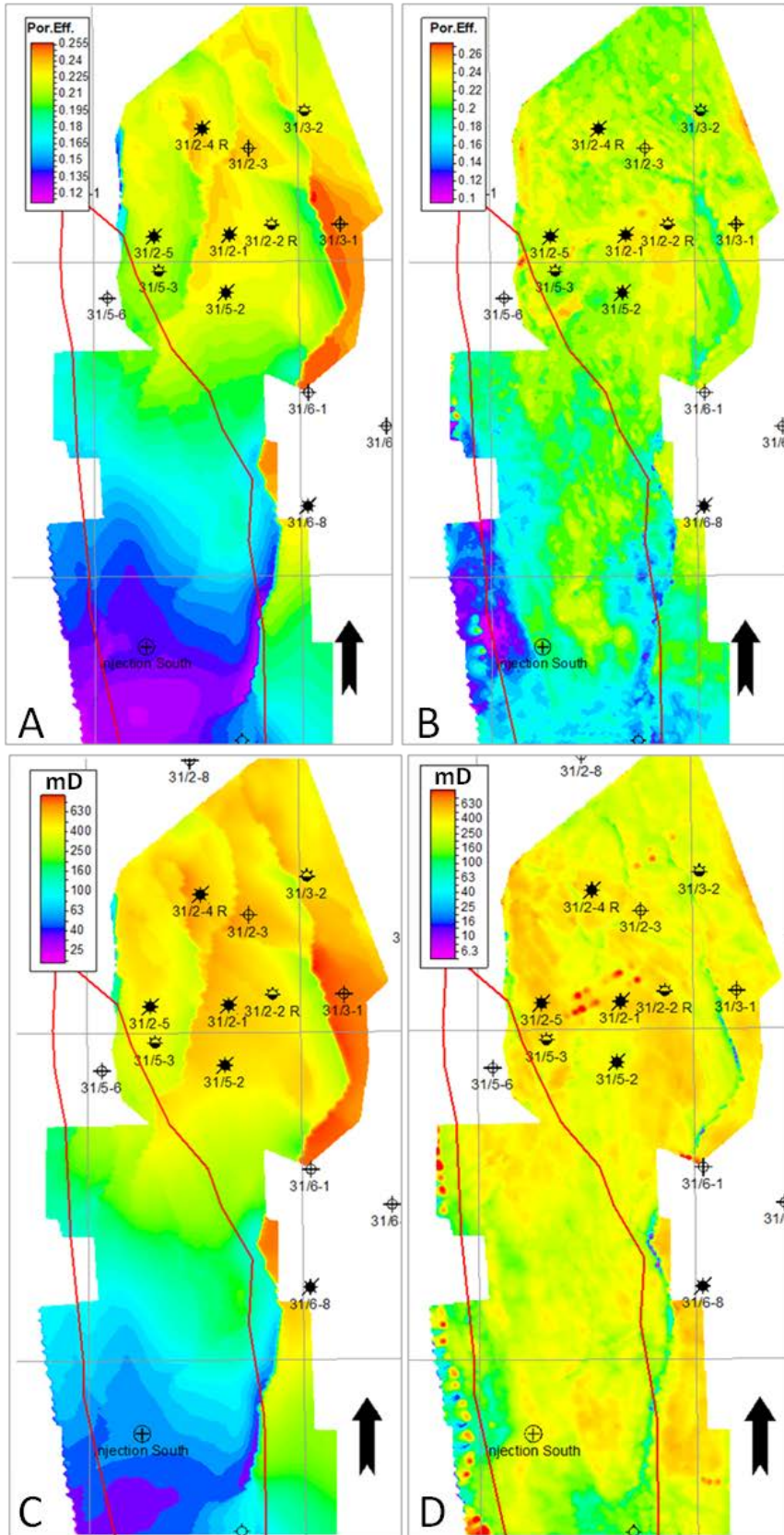


Figure 5-42: Johansen Fm porosity and permeability maps based on porosity vs. depth trends from wells (A&C - non-spit system) and seismic inversion data (B&D - spit system). Red boundary indicates area where spit system sand is interpreted to be developed.

DOCUMENT NO.: TL02-GTL-Z-RA-0001	REVISION NO.: 03	REVISION DATE: 01.03.2012	APPROVED:
-------------------------------------	---------------------	------------------------------	-----------

5.3.2.3 Cook Formation

The Cook Formation is deposited as prograding shelf sands (chapter 5.3.1.2). The changes in storage formation facies (sand quality) are shown in the well correlations. Based on the evaluation of % volume of clay, the Cook Formation varies from siltstone to clean sand (Figure 5-33 and Table 5-6) in the northern part of the storage complex.

Porosity and depth trends from key wells (Figure 5-43) show systematic trends versus burial depth for the Cook Formation. The porosity data from the wells show a variable storage formation quality probably controlled both by facies and burial depth. The Cook Formation average porosities vary from approximately 23% in the main Troll wells down to 10% in the northern deep wells (Figure 5-43).

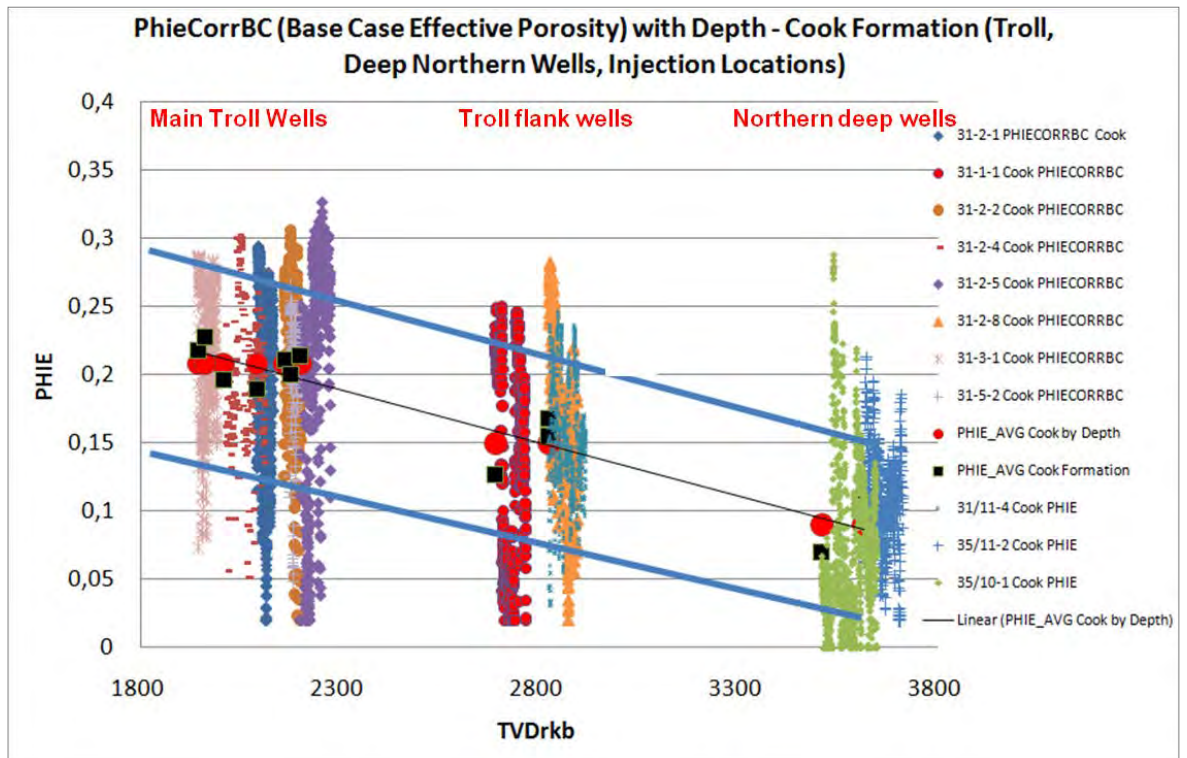


Figure 5-43: Cook Fm porosity/depth trends from key wells.

The northern wells show a heterogenic Cook Formation sand development with a significant degree of change in storage formation quality. Key wells 31/2-1 and 31/2-2R show modelled porosity values up to 30% for the best part of the Cook Formation deposits (Figure 5-44) with corresponding modelled permeabilities up to 2000mD, but as shown in the well panel the quality changes quite rapidly. The average modelled porosity for well 31/2-1 and well 31/2-2R is 21% and 17%, respectively.

The Cook Formation average porosity model (Figure 5-45) based on the inversion data (chapter 5.6.2) substantiates the Cook Formation heterogeneity shown in the northern wells. The southward changes in storage formation quality due to depth are also clearly observable in the porosity model. A change in the Cook Formation quality from west to east is also shown in the model, concurrent with the observed eastward thinning of the Cook Formation (Figure 5-31).

DOCUMENT NO.: TL02-GTL-Z-RA-0001	REVISION NO.: 03	REVISION DATE: 01.03.2012	APPROVED:
-------------------------------------	---------------------	------------------------------	-----------

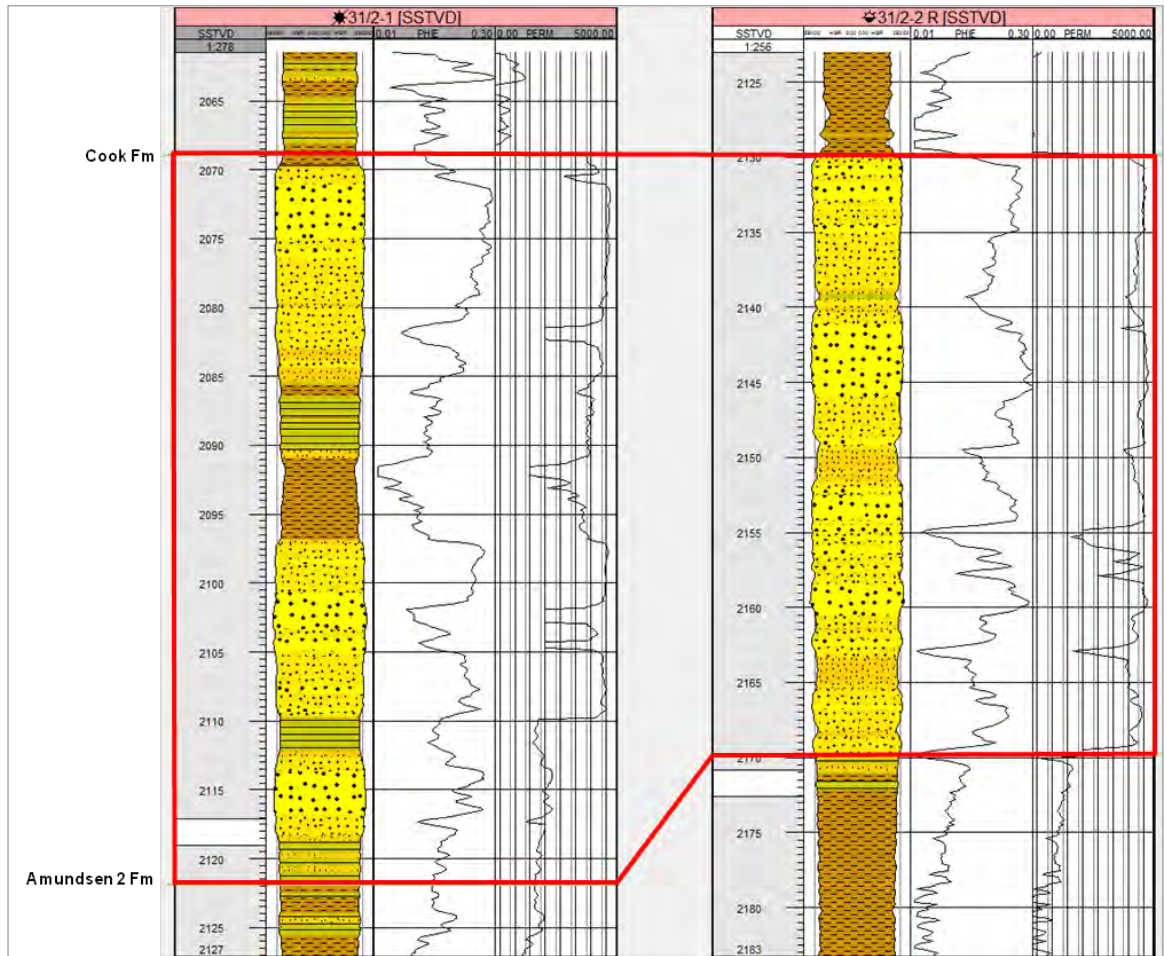


Figure 5-44: Well panels showing key well Cook Fm lithology with porosity and permeability (log) results from the petrophysical modelling for well 31/2-1 and 31/2-2R. See Figure 5-31 for lithology legend and Figure 5-45 for well locations.

DOCUMENT NO.: TL02-GTL-Z-RA-0001	REVISION NO.: 03	REVISION DATE: 01.03.2012	APPROVED:
-------------------------------------	---------------------	------------------------------	-----------

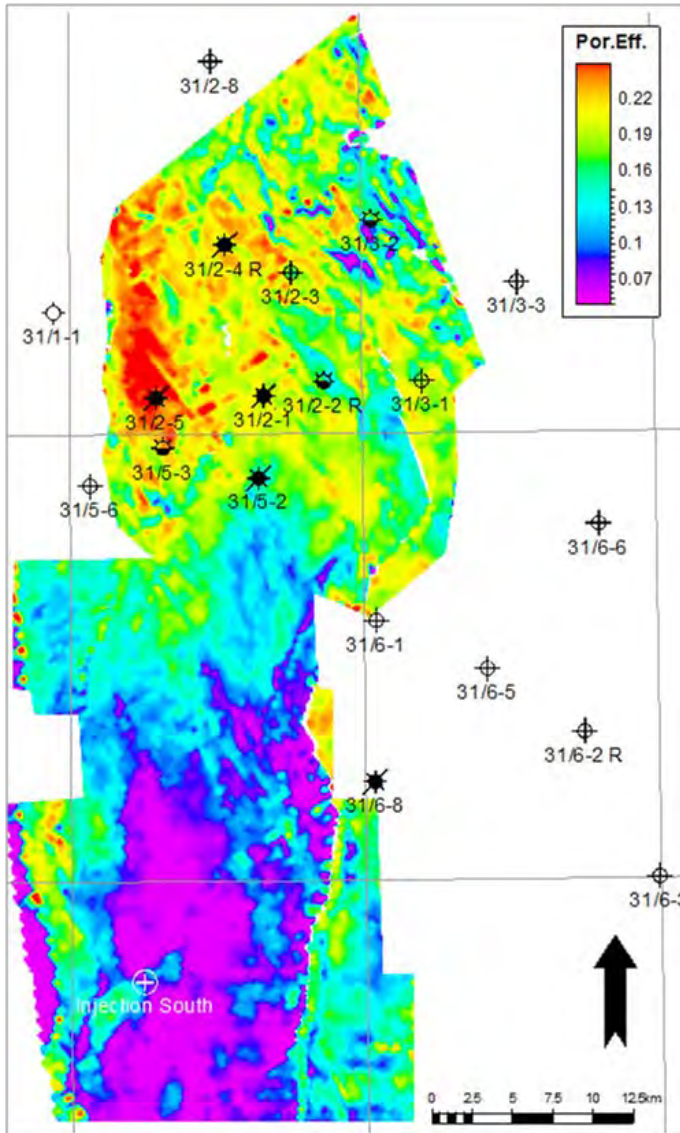


Figure 5-45: Average porosity property map for the Cook Fm based on GN10M1 acoustic impedance (AI) cube from the seismic inversion and the porosity/AI correlation.

The Cook Formation average porosities change from approximately 25% in the northwestern part of the storage complex down to shale values in the most southern parts (Figure 5-45). Sand porosities, however, seem to be developed in the western and eastern parts of the southern area of the storage complex. The average porosity for the Cook Formation (Figure 5-45) throughout the model is approximately 14%.

The average density data from the seismic inversion (Figure 5-46) shows density trends versus depth in accordance with the porosity trends shown in Figure 5-43. The density of the Cook Formation is gradually increasing southwards. The acoustic impedance data, which is the main input for property modelling, show anomalous low (sand) values in the southern part, indicating sand development in the injection area. This is also shown in intersection A-A' shown in Figure 5-46. The blue colour (low AI values) through the injection site is interpreted to represent Cook Formation sand.

DOCUMENT NO.: TL02-GTL-Z-RA-0001	REVISION NO.: 03	REVISION DATE: 01.03.2012	APPROVED:
-------------------------------------	---------------------	------------------------------	-----------

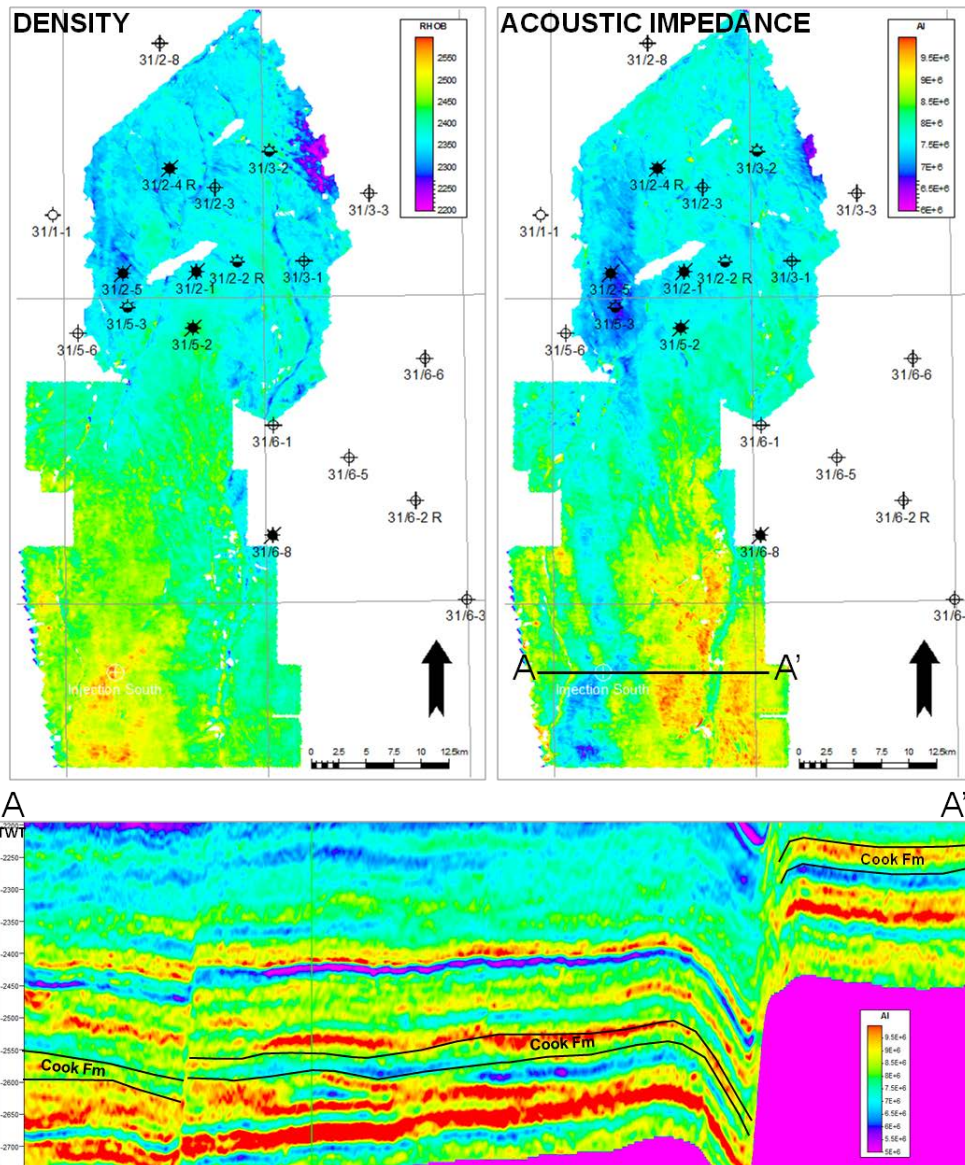


Figure 5-46: Average density and Acoustic impedance RMS attribute map for the Cook Fm. Acoustic impedance section is showing AI values indication Cook Fm sand development in the injection area.

There are few well data in the storage complex available for evaluation of possible cementation processes for the Cook Formation. Temperature data from key wells (Table 5-10) for Jurassic and Triassic deposits do not indicate that cementation processes such as quartz cementation is dominant in the storage formation in the northern area. For the southern part the depth for the Cook Formation is over 3000m (Figure 5-24) and quartz cementation is therefore likely to occur in the southern area. Anomalous high porosities are, however, recorded in wells 30/3-2 and well 30/3-A1 in sandstones interpreted to be equivalent (Intra-Dunlin) with the Cook Formation (Ehrenberg, 1996). The wells are located in the Veslefrikk Field west of the Johansen Storage Complex. The Intra-Dunlin Formation depth is over 3000m (Figure 5-47). The preservation of the porosities is caused by chlorite coating of the sand grains (Ehrenberg, 1996).

Mechanical storage formation processes in connection with burial depth is believed to be the main controlling factor for the reservoir quality in the northern part and possible preservation of porosities in the southern part, due to chlorite coating.

DOCUMENT NO.: TL02-GTL-Z-RA-0001	REVISION NO.: 03	REVISION DATE: 01.03.2012	APPROVED:
-------------------------------------	---------------------	------------------------------	-----------

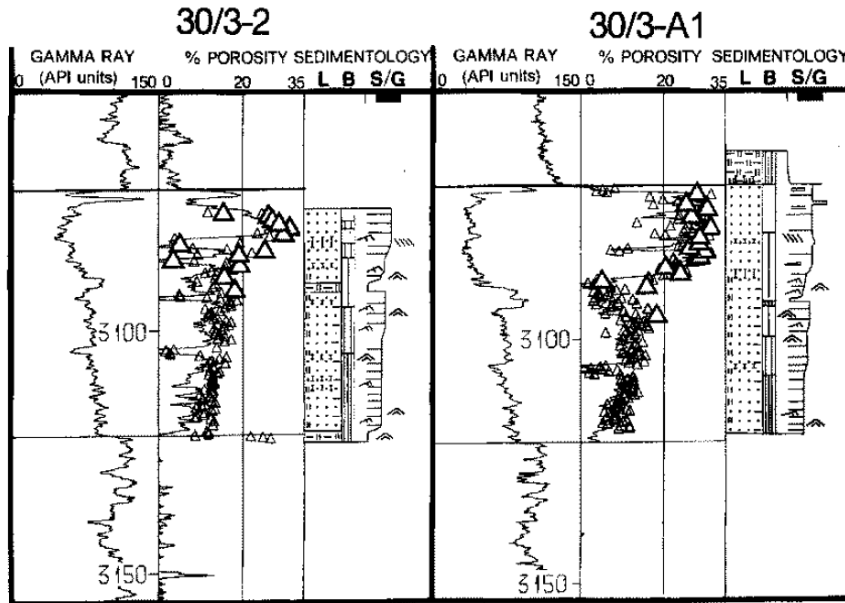


Figure 5-47: Intra-Dunlin (Cook Fm) sandstone: gamma-ray log, porosity variation, and sedimentological description for well 30/3-1 and well 30/3-A1 (Ehrenberg, 1996).

The quality assessment shows variable storage formation quality for the Cook Formation. Uncertainties and risk are associated with the southern part of the storage complex, both associated with burial depth and the lack of well data for calibration of the seismic inversion data used in the property modelling.

5.4 Geological development of sealing formations

This section describes the shales of the Dunlin Group that have been assessed in terms of CO₂ containment in a storage complex. The Dunlin Group is of Lower Jurassic age and includes the Amundsen, Johansen, Burton, Cook and Drake formations. Burton Formation is not present on the Horda platform. Both the Drake Formation and the Amundsen 2 Formation have been assessed. However, the Amundsen 2 Formation is not present over the entire evaluation area and has thus only been described in the sections covering lithological description and sequence stratigraphy. The Johansen Formation is time equivalent to the Amundsen Formation and is only present on the Horda Platform (Figure 5-48).

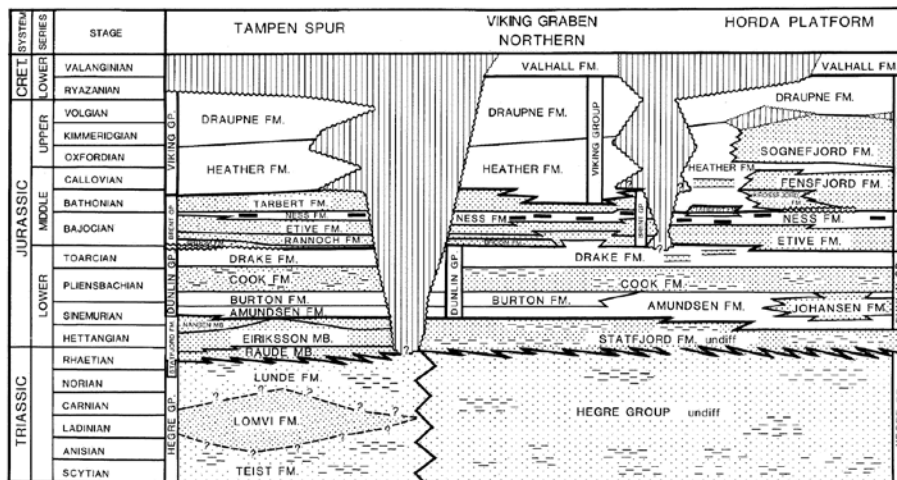


Figure 5-48: Triassic and Jurassic lithostratigraphic nomenclature in the northern North Sea (Vollset and Doré 1984)

DOCUMENT NO.: TL02-GTL-Z-RA-0001	REVISION NO.: 03	REVISION DATE: 01.03.2012	APPROVED:
-------------------------------------	---------------------	------------------------------	-----------

In petroleum exploration activities the existence of an effective seal is proven by a hydrocarbon accumulation. In CO₂ storage proving an effective seal must be done by first verifying the existence of a sealing formation, and then looking for evidence of leakage through the formation.

5.4.1 Primary Seal

The main sealing section for the Johansen storage complex is the lower Drake Formation. However, the upper Drake Formation is considered a contributing layer. The documentation described in this section covers the evaluation performed on the Drake Formation in general. The regional description of the Drake Formation analogues is mainly connected to the lower Drake Formation.

Drake Formation

The Drake Formation consists of mainly marine shales within the basins, while there are sand deposits on the margins (Vollset and Doré 1984). The Horda Platform has inputs of sand transported from the Norwegian Hinterland (Steel 1993). Such sand development is believed to be derived from long-lived sediment input routes (Parkinson and Hines 1995). In well 31/5-2 on the Horda Platform the Drake Formation is divided into an upper and a lower part. The upper part consists of sandstone alternating with siltstone and claystone. The lower part consists of claystone (Norsk Saga 1985).

Amundsen Formation

The Amundsen Formation was deposited in the Lower Jurassic Hettangian to Sinemurian or Early Pliensbachian (Vollset and Doré 1984). The formation is recognized as a heterolithic unit, with sandstone interbeds within siltstones and shales distributed in the East Shetland basin and Viking Graben. On the Horda platform the formation is partially spilt by the Johansen Formation. The upper Amundsen Formation is also referred to as Amundsen 2 Formation.

5.4.2 Secondary Seal - The Overburden

The secondary seal for the storage complex is the complete record of impermeable layers in the overburden. This consists of shales and sandstones of Jurassic, Cretaceous, Tertiary and Quaternary age (Figure 5-49). The assessment of sealing formations for the Johansen CO₂ storage has not included the overburden. However, the overburden has been mapped from seismic and is a part of the geological and geophysical assessment.

DOCUMENT NO.: TL02-GTL-Z-RA-0001	REVISION NO.: 03	REVISION DATE: 01.03.2012	APPROVED:
-------------------------------------	---------------------	------------------------------	-----------

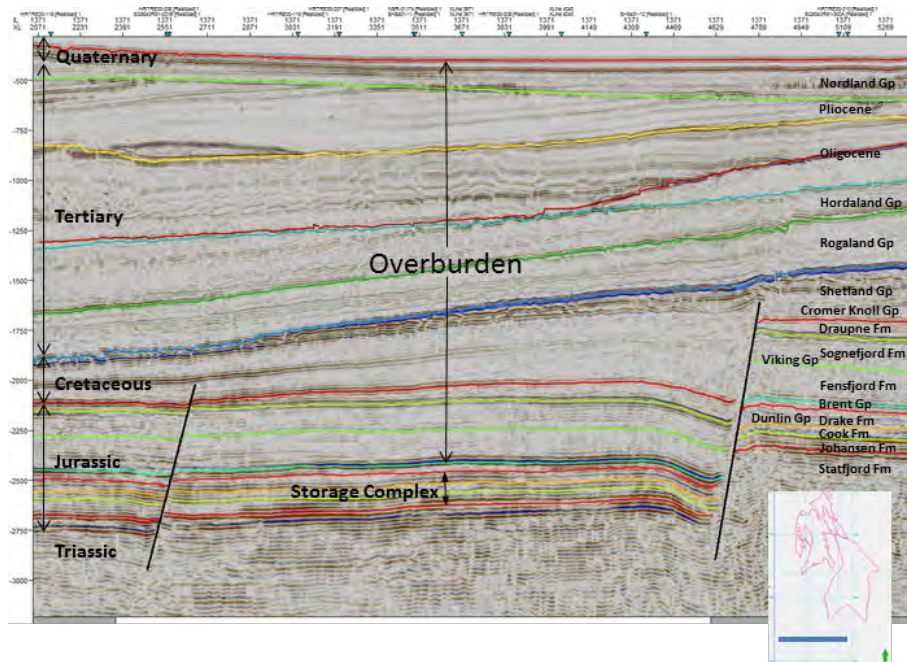


Figure 5-49: A seismic profile with the main stratigraphical units. Inline 1371 from GN10M01. The left column indicates the age, whereas the right hand column formation and group names. The storage complex geometry includes Johansen - Amundsen - Cook - Drake Fm in this figure. The overburden is defined as the rocks overlaying the storage complex.

Jurassic

These rocks are constituted by the Brent and Viking Groups of the middle and upper Jurassic. Both groups have mixed lithologies, but are mainly labelled as sandstones with origins related to major delta environments of regional scale. Shales with sealing properties occur within these zones and the most known is the Draupne Formation shales which is the main sealing formation for the majority of petroleum fields in the North Sea.

Cretaceous

The Cretaceous interval consists of the Cromer Knoll and Shetland Groups. These are dominated by lithologies of shaley and calcareous rocks.

Tertiary and Quaternary

The Tertiary and Quaternary package has the greatest thickness of the formations on the Horda platform. It is divided into the Rogaland and Hordaland and Nordland Groups. The Rogaland Group has a predominant shaley lithology on the Horda platform. The Hordaland Group consists of shale and sandstones. The upper Nordland Group is of Quaternary age. The Quaternary sediments are the youngest sediments in the overburden. They can be characterized as fresh unconsolidated claystones.

5.4.3 **Sequence Stratigraphy and Regional setting**

This section describes the Dunlin Group shales in a regional setting. Several workers have described this sedimentary succession and it has been correlated to the framework established for similar events in Europe (Steel 1993) (Parkinson and Hines 1995) (Charnock, et al. 2001).

The shales of the Dunlin Group have been defined as the retrograding shaley counterparts to prograding sands in lower Jurassic mega-sequences 4, 5 and 6 corresponding respectively to Drake Formation - Rannock / Drake formations sands, Burton - Cook formations and Upper & Lower Amundsen - Johansen formations (Figure 5-50). In this terminology both the Amundsen Formation and Drake Formation are defined as maximum transgressions based on well logs. Such events are indicative of high sea levels with marine clay deposits (Steel 1993).

DOCUMENT NO.: TL02-GTL-Z-RA-0001	REVISION NO.: 03	REVISION DATE: 01.03.2012	APPROVED:
-------------------------------------	---------------------	------------------------------	-----------

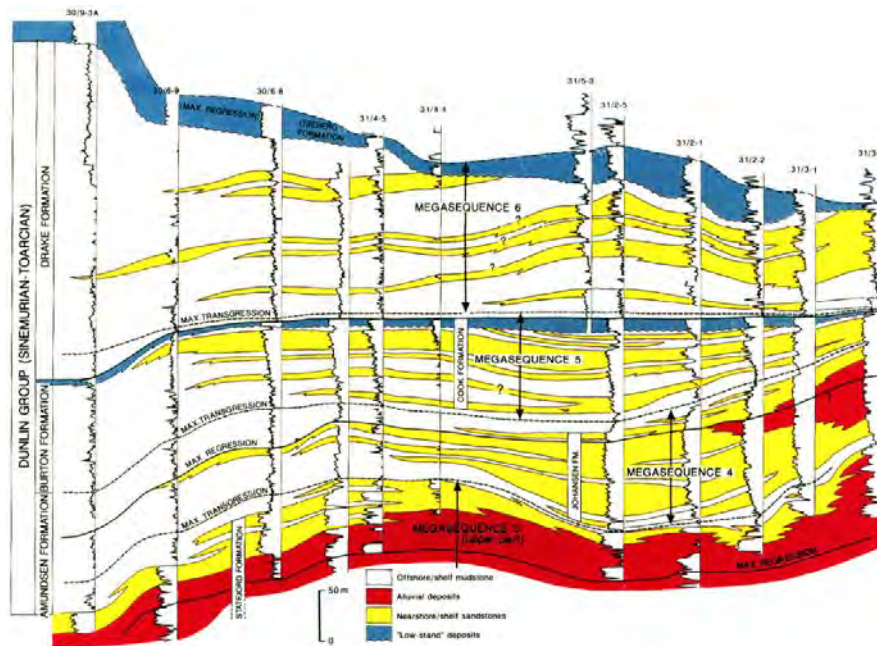


Figure 5-50: Sub-regional architecture of the Johansen, Cook and Drake mega-sequences in an ENE-WSW traverse across the Horda Platform. The Early Toarcian age Lower Drake Fm corresponds to the max transgression near the base of mega sequence 6.

The base of the Drake Formation is of Early Toarcian stage (Figure 5-48) at approximately 190Ma. It marks the onset of a global eustatic sea level rise and belongs to the Exaratum Subzone (Morton 1993) and global warming (Ilyina 1985). Several shales have been identified of this age and it is described as dark to black, clean, marine, organic rich (TOC 1-5) and with typical Gamma Ray values of GR > 100 API (Marjanac 1995).

The anoxic bottom conditions associated with this sea-level rise resulted in deposition of the widespread hydrocarbon source rock, the Posi-donischiefer in Germany and Schistes cartons elsewhere in Europe (Hallam 1963).

Shales of this character are very similar to lower Toarcian shales identified in Russia, Europe, and the North Americas (Nikitenko and Shurygin 1992). In Russia it has source rock potential indicating high TOC and anoxic conditions. This may also apply to the Oseberg area (Thomas, et al. 1985). Shales of the Drake Formation in the Oseberg field have TOC values of 0.8 to 2.4% (Yang and Aplin 2007). In Russia the deposits have a typical thickness of 25m (Shurygin 1978).

5.4.4 Biostratigraphy

The Drake Formation belongs to the J18 max transgressive surface defined by (Parkinson and Hines 1995). This correlation supports the interpretation of the lower Drake Formation as belonging to the global anoxic event (Jenkyns 1988) associated with the deposition of marine mudstones (Charnock, et al. 2001). The event belongs to the Exaratum Subzone (Hallam 1963) (Copestake, et al. 1993).

DOCUMENT NO.: TL02-GTL-Z-RA-0001	REVISION NO.: 03	REVISION DATE: 01.03.2012	APPROVED:
-------------------------------------	---------------------	------------------------------	-----------

5.4.5 **Cap rock leakage assessment**

There are four main leakage mechanisms through a cap-rock;

- Leakage through porous layers
- Through juxtaposed porous layers
- Through weak palaeo-leakage paths
- Through dissolution of calcite cemented fractures or faults

Other mechanisms include leakage through capillary migration and diffusion. This has been evaluated through the analysis of well samples (Gassnova-IRI 2011).

In order to evaluate these risks in the study area the work was organized in key subjects; porous layers, faults and fractures and deformed zones to identify palaeo leakage signatures.

A cap rock covering the storage site may leak given the existence of critical initial conditions that may affect cap rock functionality. Such conditions can cause migration into the cap rock and subsequent leakage to formations outside the storage complex.

5.4.5.1 *Porous Layers*

The most significant risk of leakage through a cap rock is via porous layers. Leakage through porous sand bodies within the cap rock may function as conduits for fluid flow (Friedmann and Nummedal 2003). Such sand bodies may exist as a singular or multiple point deposit. They may be deposited as submarine fans or channels transported in turbidic or mass movement processes (Boggs Jr 1995). In some cases they can be subjected to subaerial processes where the clay or shale deposit is followed by tectonic uplift with subsequent erosion and sand deposition from rivers or deltas.

Sand intervals in shales are very common, and may be a significant risk in cap rocks (Daniel and Kaldi 2008). Due to the possible sub-seismic nature of such deposits they may be very difficult to track on seismic data.

Porous Layers in Juxtaposition

Sand layers may increase the cap rock leakage risk additionally in faulted areas (Ingram, Urai and Naylor 1997). Normal faults can cause a juxtaposition situation (Figure 5-51) where porous zones are aligned allowing cross-fault communication (Yielding, Lykakis and Underhill 2011) (Friedmann and Nummedal 2003). Porous zones in faulted areas may be subject to effective leaking through a network of faults adding significant risk in CO₂ storage purposes. See also diffusion and capillary migration further on in this chapter. For seal assessment studies it is suggested that a fault seal study is necessary if fault throw is greater than seal thickness. If the throw is less than seal thickness, further assessment is suggested to focus on stresses and lithology prediction (Ingram, Urai and Naylor 1997).

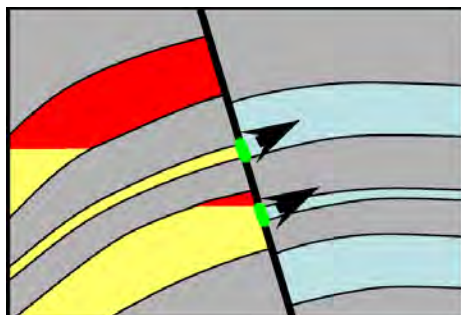


Figure 5-51: Scenario of juxtaposed strata along a fault. Red shows the trapped volume, and green shows the areas in contact with porous layers that fluids migrate to (modified from (Friedmann and Nummedal 2003)).

DOCUMENT NO.: TL02-GTL-Z-RA-0001	REVISION NO.: 03	REVISION DATE: 01.03.2012	APPROVED:
-------------------------------------	---------------------	------------------------------	-----------

The permeability of deeply buried shale is a function of depth, temperature and pressure. Rocks with normal pressure are considered to be ductile due to the progressive burial (Hager and Handin 1957). Migration through such shales therefore probably requires high over-pressures and hydro-fracturing to provide sufficient vertical fracture permeability (Bjørlykke, Karlsen and Olstad 1997).

The upper Drake Formation is considered to have higher risk due to the proven sand development in Troll Wells in Quadrant 31. However, the sands are believed to have local extent with a horizontal distribution and are not believed to pose any large risk in the study area south of the Troll field.

The lower Drake Formation is treated as the main seal with the upper Drake Formation as a contributing layer. The Drake Formation was mapped on seismic (Figure 5-52) which was used to generate thickness maps (Figure 5-53 and Figure 5-54) of both the upper and lower part of the formation.

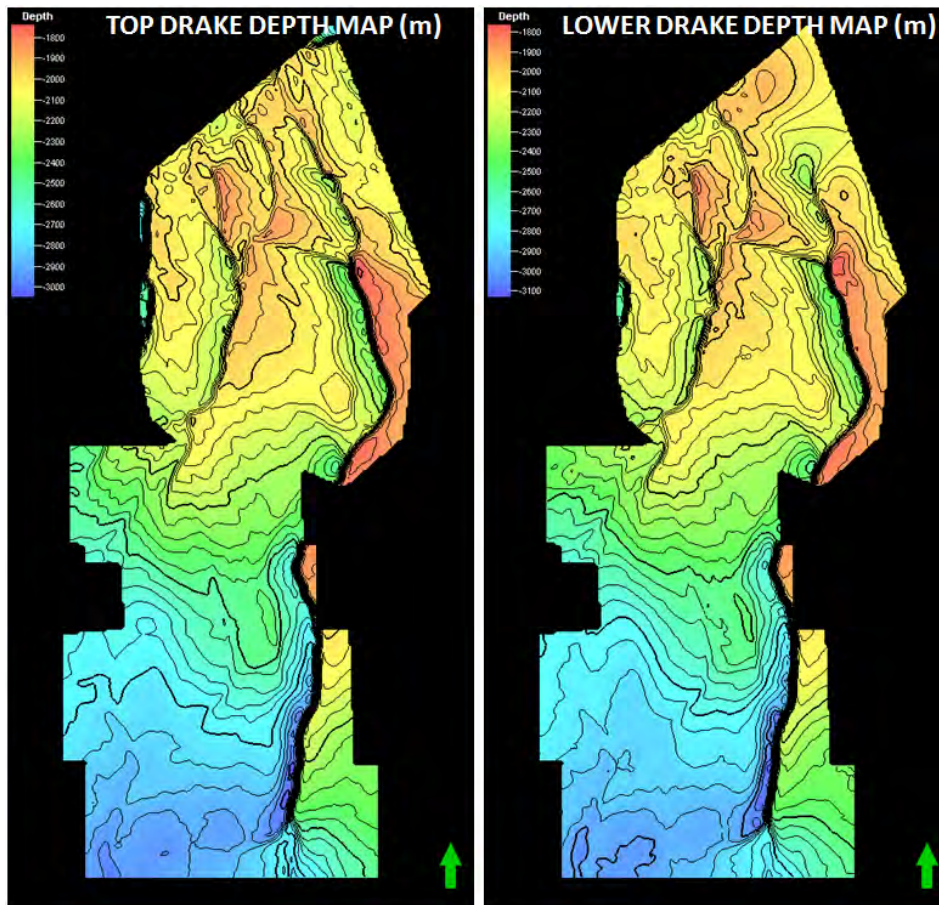


Figure 5-52: Depth maps over Top Drake and top Lower Drake Fm.

DOCUMENT NO.: TL02-GTL-Z-RA-0001	REVISION NO.: 03	REVISION DATE: 01.03.2012	APPROVED:
-------------------------------------	---------------------	------------------------------	-----------

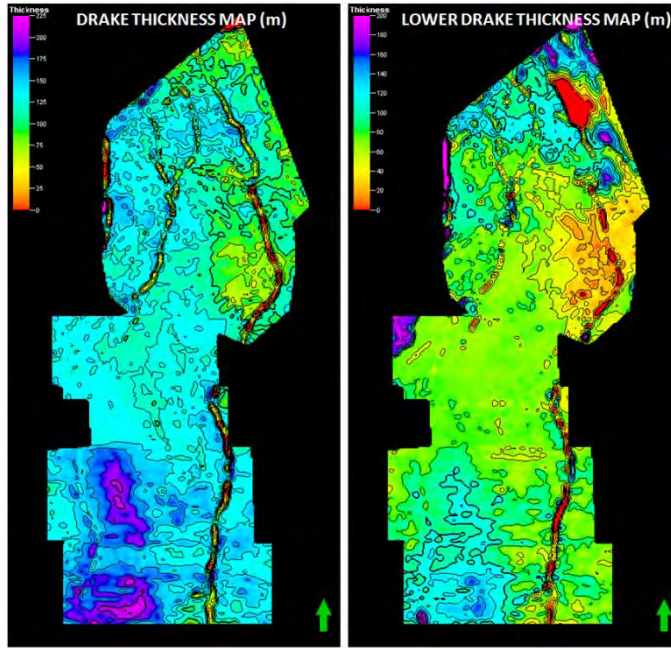


Figure 5-53: Thickness maps over the Drake Fm and the Lower Drake Fm.

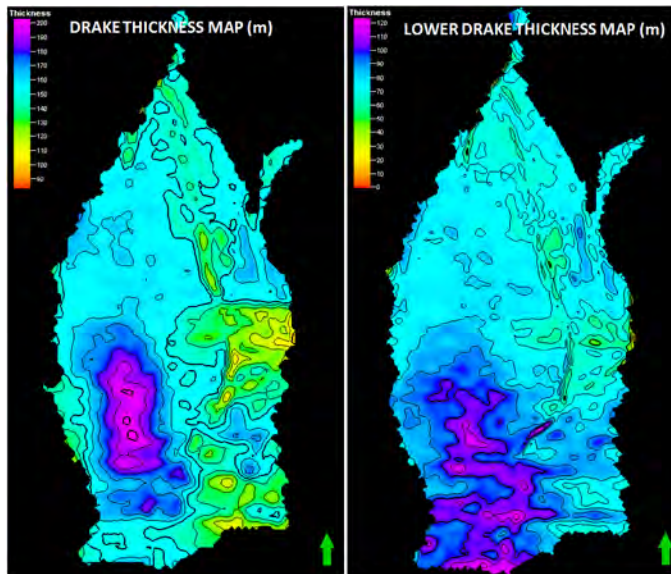


Figure 5-54: Thickness maps over Drake and Lower Drake Fm. The shape represents the maximum simulated CO₂ plume extent. Mean thicknesses are 153m for the entire Drake Fm and 72m for the Lower Drake Fm.

Well Evaluation

The well evaluation was performed by analysing reports and interpretations from the well drilled in the Troll field. The results from the analysis allowed a further definition of the two parts constituting the Drake Formation. A general description of the Drake Formation is given in chapter 5.4. A petrophysical evaluation (Gassnova-ROS 2011) was performed with respect to cap rock properties and cap rock potential. Relevant wells on the Horda platform and adjacent area were investigated.

DOCUMENT NO.: TL02-GTL-Z-RA-0001	REVISION NO.: 03	REVISION DATE: 01.03.2012	APPROVED:
-------------------------------------	---------------------	------------------------------	-----------

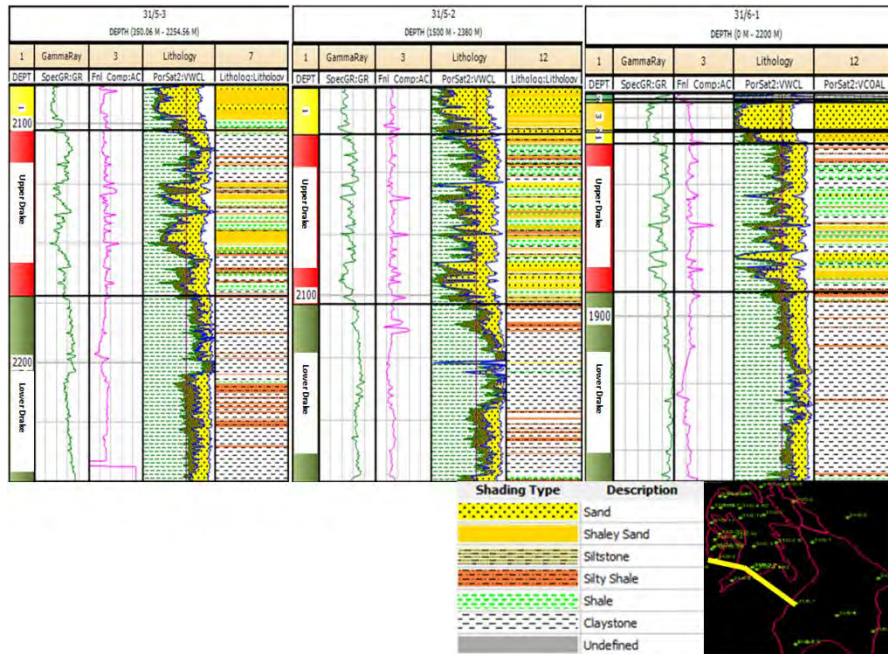


Figure 5-55: Well Log Panel from wells 31/5-3, 31/5-2 and 31/6-1 of the Drake Fm in a cross-section over the Troll field on the Horda Platform. The well logs give a good indication of the two-fold nature of Drake; an upper and lower part. The upper part is characterized as shale with thin sand layers. The lower part is mainly clean claystone and shale with a few thin layers of silty shale. The legend refers to the Lithology columns 7, 12 and 12.

Table 5-11: Formation thicknesses of the Drake and the Lower Drake Fm from wells. The mean thickness of the Drake Fm is 105m. The mean thickness in the Lower Drake Fm is 55m.

	31/2-1	31/2-2	31/2-3	31/2-4	31/2-5	31/2-8	31/3-1	31/3-3	31/5-2	31/6-1	31/6-2	31/6-6
Drake Fm	108	92	108	106	131	105	101	84	140	127	80	77
Lower Drake Fm	30	55	70	105	70	55	35	42	60	58	40	40

Seismic Attributes

In this study seismic attributes have been generated to assess the various parameters identified as the main risks for the cap rock. A combination of software tools have been used individually or in combination. In addition the acoustic impedance attribute is a product of the AVO based seismic inversion study conducted as a part of the project (Gassnova-WGD 2011).

In reflection seismology, a seismic attribute is any quantity derived from seismic data using measured time, amplitude, frequency, attenuation or any combination of these. It intends to output a subset of the data that quantifies rock and fluid properties and/or allows the recognition of geological patterns and features.

Acoustic Impedance - Porosity Distribution

There is a relationship between acoustic impedance (AI) and porosity (Maver, Odegaard and Rasmussen 1996) where low AI is correlated with high porosity and vice versa (Aleman 2004). In the inversion project (Gassnova-WGD 2011) an acoustic impedance cube was generated based on wavelet estimation.

The data from the inversion were imported to Petrel and subsequently used to perform further qualification of the cap rock (Figure 5-56).

DOCUMENT NO.: TL02-GTL-Z-RA-0001	REVISION NO.: 03	REVISION DATE: 01.03.2012	APPROVED:
-------------------------------------	---------------------	------------------------------	-----------

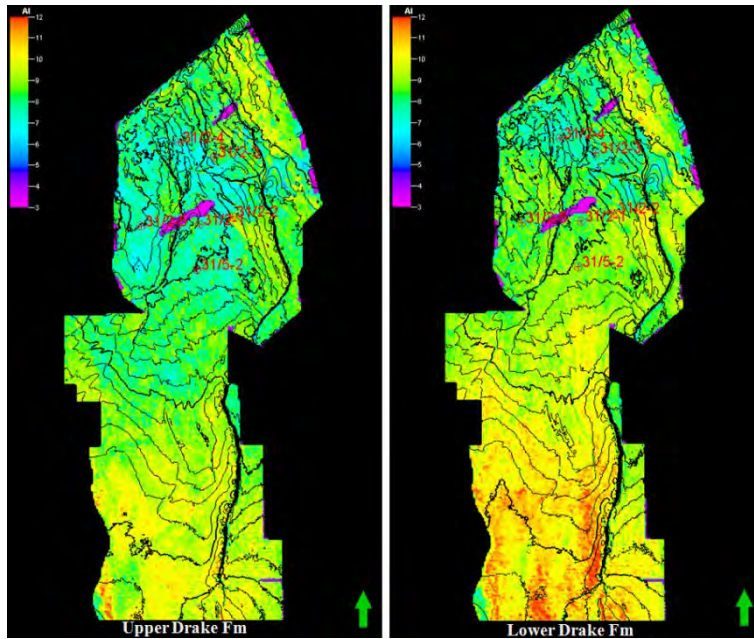


Figure 5-56: Inversion derived Acoustic impedance on Upper and Lower Drake Fm time grid. The inverse relationship between porosity and acoustic impedance has been used to indicate shale facies of the sealing layers in the Drake Fm. These two-way time maps indicate a southward decrease in porosity in both maps.

5.4.5.2 Gas Chimney evaluation

A possible gas chimney is observed below a dome-like feature at the Utsira level. It is seen as a vertical disruption through the whole seismic section (Figure 5-57). Amplitude observations at Utsira Formation level could indicate accumulation of gas in this sand unit.

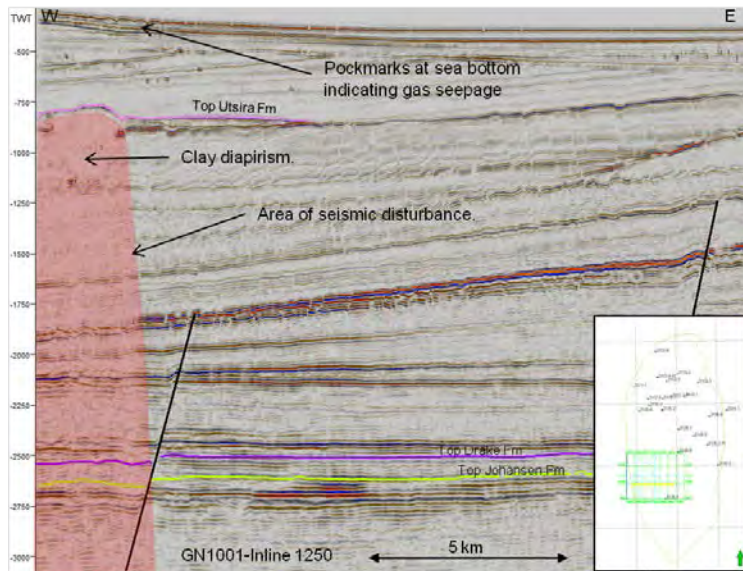


Figure 5-57: Seismic section showing disturbance that could be caused by gas leakage from the Jurassic section.

Gas leakage from the Jurassic section could indicate a weak zone in the identified Johansen Storage Complex cap rock. Alternatively, the disturbance could be due to clay diapirism in the upper section.

DOCUMENT NO.: TL02-GTL-Z-RA-0001	REVISION NO.: 03	REVISION DATE: 01.03.2012	APPROVED:
-------------------------------------	---------------------	------------------------------	-----------

Several independent studies with different approaches have been implemented to assess this possible leakage risk. A summary presentation has been made based on the different study results (Gassnova-ROS 2011).

Gas chimney assessment studies:

- Western Geco - AVO Study (Gassnova-WGD 2011)
- AkerGeo - Apparent Gas Chimney in Block 31/8 (Gassnova-AKS 2011)
- Weatherford - Assessment of Gas Chimney (Gassnova-WPC 2011)
- VBPR (Sverre Planke) - Quick Assessment of Seismic Evidence of Leakage of the Johansen Formation (Gassnova-VBPR 2011)

Conclusions

The main conclusion from the above studies is that there is no conclusive evidence of the presence of a deep gas chimney in block 31/8 (Gassnova-ROS 2011).

The main argument against the presence of a deep gas chimney is that the main migration path for hydrocarbons from the oil fields in the west towards the Troll field exists at least 20-30km further north (Oseberg, Brage). The dry well 31/8-1 also reinforces this conclusion.

5.4.5.3 *Faults and Fractures*

This subsection describes the assessment of faults and fractures in the cap rock study. In general the faults are described in the report *Structure Geology of the Horda Platform* (Gassnova-ROS 2011). However, most of the faults have also been interpreted in the cap rock study. The major fault features in the study area have fault throws greater than seal thickness. The small faults have throws less than the seal thickness and are thus not subject to cross-fault leakage scenarios. Small faults have been mapped where continuous and possible.

Sub-seismic faults (~10m) are not considered a risk in terms of cross-fault leakage as the throws are of corresponding size. Fractures have not been mapped due to their non-continuous nature. Instead the fractures have been assessed from attribute maps where fault patterns are indicators of origin and properties.

In principle the deformation of clays and shale may occur in two stages; during sediment deformation after deposition or through growth faulting (Bjørlykke 2010). These may be induced by tectonic stresses or by pressure build-up caused by compaction. For the latter fluid movement may occur, creating fractures in the rock (Bjørlykke 2010). This process commences when fluid is expelled due to increasing pressure in a progressive burial. In situations where fast burial is seen the pressure will not escape resulting in extreme overpressures.

Plastic deformation behaviour is mostly related to shallower clay sediments with low rheologies (Ingram, Urai and Naylor 1997). As the sediments reach greater depths, deformation exhibits a more brittle character. However, in most cases shale will more readily deform than its sandstone counterparts in adjacent layers. This relationship is typically seen in faulted sandstones, where faults and fractures often terminate in shales due to the lower shear strength of such rocks (Hildebrand-Mittlefehldt 1979).

Natural fractures are derived from pressure release processes related to burial and fluid escape. As clay layers are compressed the pore pressure will increase until the shear strength is reached. The excess pore fluids escape through vertical fractures within the layer. The fracture permeability decreases after fluid expulsion due to shale creep and cementation (Cuisiat, Grande and Høeg 2002).

DOCUMENT NO.: TL02-GTL-Z-RA-0001	REVISION NO.: 03	REVISION DATE: 01.03.2012	APPROVED:
-------------------------------------	---------------------	------------------------------	-----------

Petrel Variance Attribute

The structural attribute variance was generated in Petrel in order to map faults and fractures in the 3D seismic cube (Figure 5-58). Based on the fault presence and density the study area was divided into four main areas of interest; North (N), North-West (NW), South-West (SW) and South-East (SE). These four areas were cropped and exported for further evaluation in the SVI Pro software (Figure 5-58).

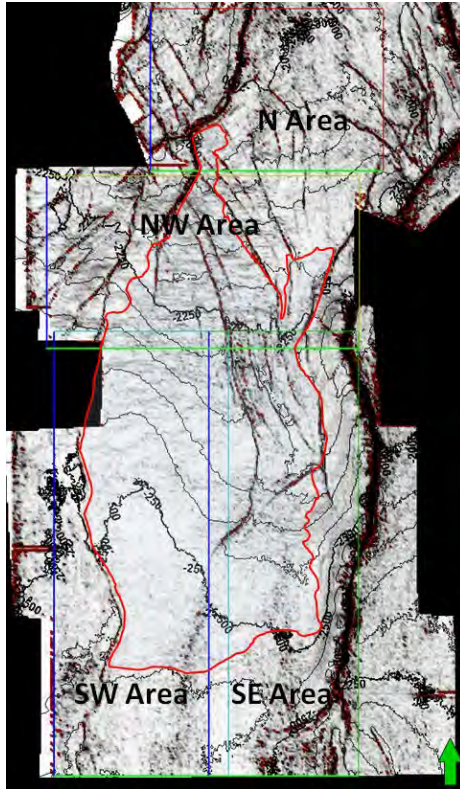


Figure 5-58: Variance Attribute map on Lower Drake Fm grid with red plume extent polygon in the year 3200 BP. Areas SW, SE, NW and N have been designed based on main faults areas within the plume extent. The Troll Field “Triple Point” (Gassnova-ROS 2011) is located just north of the northernmost tip of the plume extent. The four study areas have been studied for faults and fractures in SVI Pro and Petrel.

SVI Pro

SVI Pro is a seismic analysis software optimized to perform simple data processing for noise reduction and attribute extraction. The software contains several modules and workflows that allow a further evaluation of structural, stratigraphical and depositional features. One of the most useful modules is the frequency decomposition and RGB blending tool allowing an efficient “x-ray” examination of the data. SVI Pro is fully integrated with most data formats and has an import/export friendly interface. It can import seismic cubes, seismic grids, well data and well tops.

For a further description of the SVI Pro software and project results refer to the SVI Pro result (Gassnova-ROS 2011).

For data import applications the cube size is limited to 800Mb. For large areas the 3D cubes must be cropped in three dimensions to fit this constraint. The merged seismic 3D cube GN10M01 was used as the main data input (Figure 5-59).

DOCUMENT NO.: TL02-GTL-Z-RA-0001	REVISION NO.: 03	REVISION DATE: 01.03.2012	APPROVED:
-------------------------------------	---------------------	------------------------------	-----------

FaultIn Attribute

This attribute is an end product of a workflow including noise filtering as well as structural and fault attributes. The fault identifications are combined with the noise filtered cube. The output volume from FaultIn has all the fault information stored in the top bin (highest value) giving them a single colour. The FaultIn volume can be a useful interpretation tool providing a template for fault picking (www.ffa-geosciences.com).

From the seismic variance attribute analysis (Figure 5-58) the assessment area was divided into four areas based on fault density and plume extension. All cubes were limited to < 800Mb.

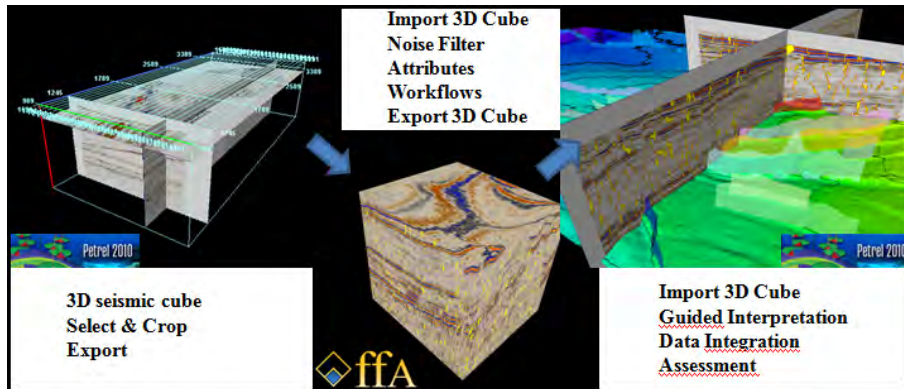


Figure 5-59: Workflow description for the leakage risk assessment.

Evaluation of faults and fractures in the cap rock

The cap rock is characterized by a low gradient and hummocky layer with a low fault density. The layer exhibits high angle fractures with a non-continuous nature. The fractures do not display any predominant orientation, indicating that they have an origin related to local pressure changes due to burial, compaction and pressure relief.

The irregular pattern is interpreted to represent polygonal faults (Figure 5-61). Such faults are linked to processes related to burial and compaction, with no significant tectonic extension.

The absence of tectonic extension is inferred from two observations: the layer-bound fractures do not extend into underlying or overlying strata; and where the regional dip is less than 1°, there is no preferred orientation of fault strike (Goultly and Swarbrick 2005).

The fractures are formed by de-watering due to pressure relief, where fluid is expelled from the shale layer as when the shear strength of the layer is overridden. It is assumed that the de-watering processes starts immediately after burial (Berndt, Bunz and Mienert 2003) (Bolton, Cartwright and James 2003).

The faults (Figure 5-60) in the study area are divided into two categories;

1. Fault throw > seal thickness
2. Fault throw < seal thickness

The faults in the first category have been interpreted in the fault seal evaluation (Gassnova-ROS 2011) and will not be covered here. The second category faults are considered to be safe in terms of communication to shallow layers (Yang and Aplin 2007). However, these faults may have a potential for hydraulic fracturing if injection pressures override fault reactivation threshold levels. Still, cemented fractures have proven to be stronger than the adjacent rock in laboratory tests.

DOCUMENT NO.: TL02-GTL-Z-RA-0001	REVISION NO.: 03	REVISION DATE: 01.03.2012	APPROVED:
-------------------------------------	---------------------	------------------------------	-----------

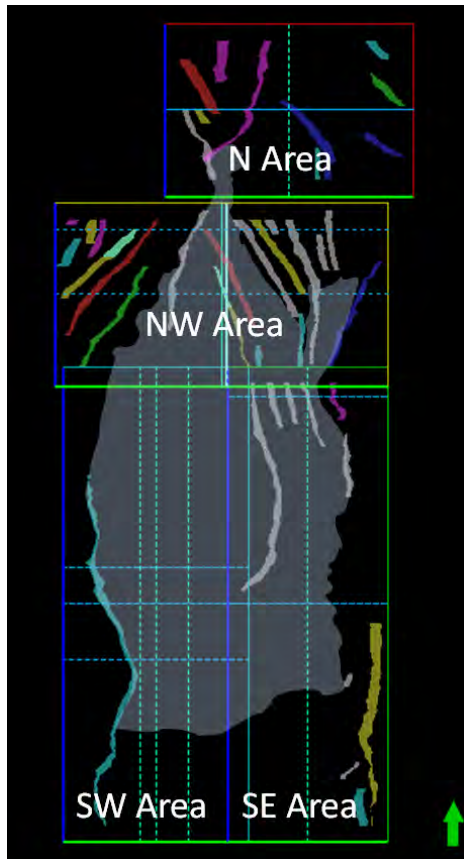


Figure 5-60: An overview of the areas assessed in the fault evaluation. The plume extent is illustrated by the light grey area. The interpreted faults are shown as fault surfaces with undefined colour scale.

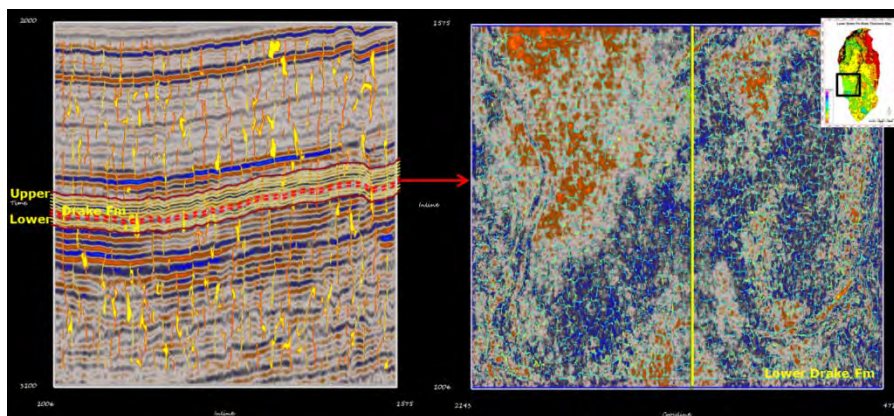


Figure 5-61: FaultIn Attribute from SVI Pro. The left-hand seismic section shows the discontinuities and the right-hand map is a time interval of ~12ms illustrated by the red dotted lines on the Lower Drake Fm seismic section. The map view supports the interpretation of a polygonal fault system.

DOCUMENT NO.: TL02-GTL-Z-RA-0001	REVISION NO.: 03	REVISION DATE: 01.03.2012	APPROVED:
-------------------------------------	---------------------	------------------------------	-----------

Assessment Areas

North Area

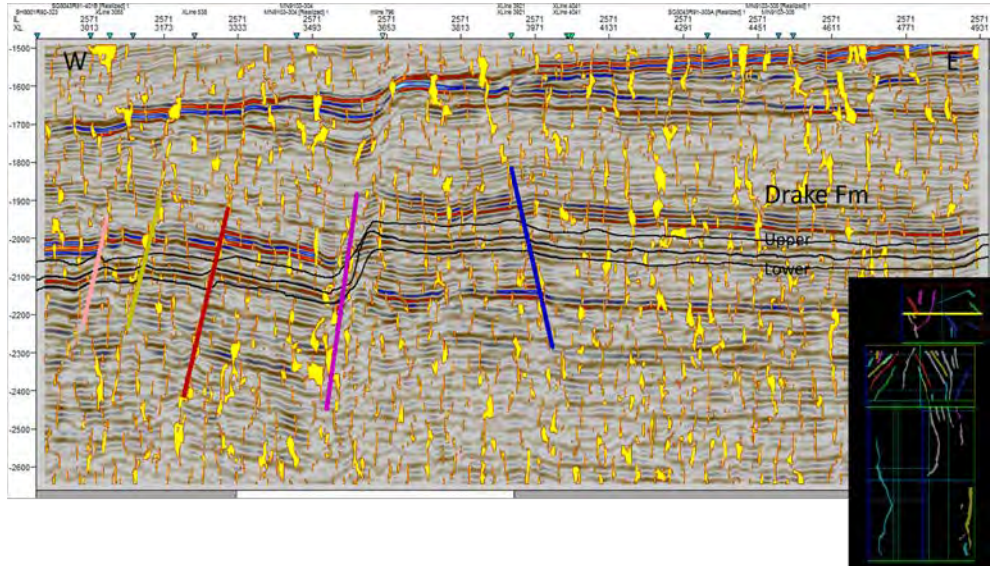


Figure 5-62: InLine 2571 in Area N. SVI Pro FaultIn attribute on noise filtered seismic. The area is characterized as being dominated by the controlling faults of the Troll field. The Drake Fm has fault throws > cap rock thickness and are subject to clay smear (Gassnova-ROS 2011). The fractures indicated by yellow-red fields indicate a high activity in the west. However, no indication of seal disintegration.

The North-West Area

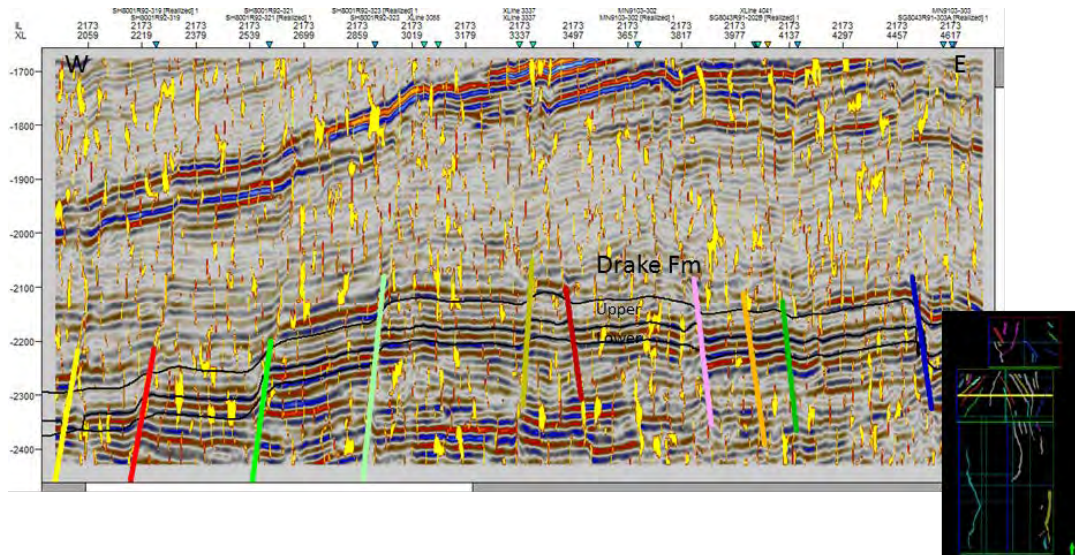


Figure 5-63: InLine 2173 in the NW Area. SVI Pro FaultIn attribute on noise filtered seismic. Situated directly under the Troll Flat-Spot. The controlling structures are the main faults of the Troll field, but the throws are limited and do not exceed the cap rock thickness. The fractures are influenced by the stress field set up by the rotated fault blocks, but are not disintegrated and do not show signs of palaeo leakage paths.

DOCUMENT NO.: TL02-GTL-Z-RA-0001	REVISION NO.: 03	REVISION DATE: 01.03.2012	APPROVED:
-------------------------------------	---------------------	------------------------------	-----------

The South West Area

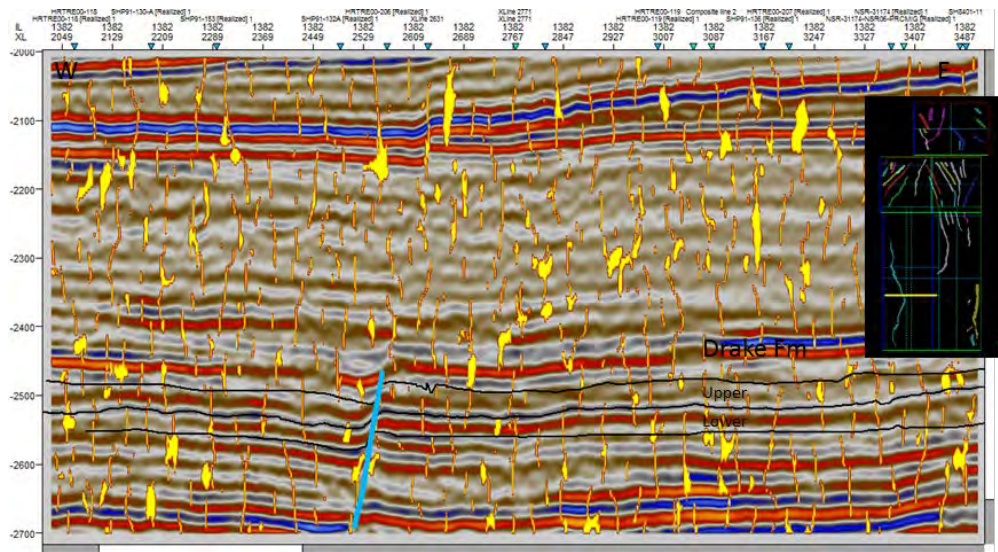


Figure 5-64: Inline 1382 in the SW Area. SVI Pro FaultIn attribute on noise filtered seismic. The area displays low fault and fracture activity. Most fractures terminate in the shale and there are no signs of disintegration or palaeo leakage.

The South-East Area

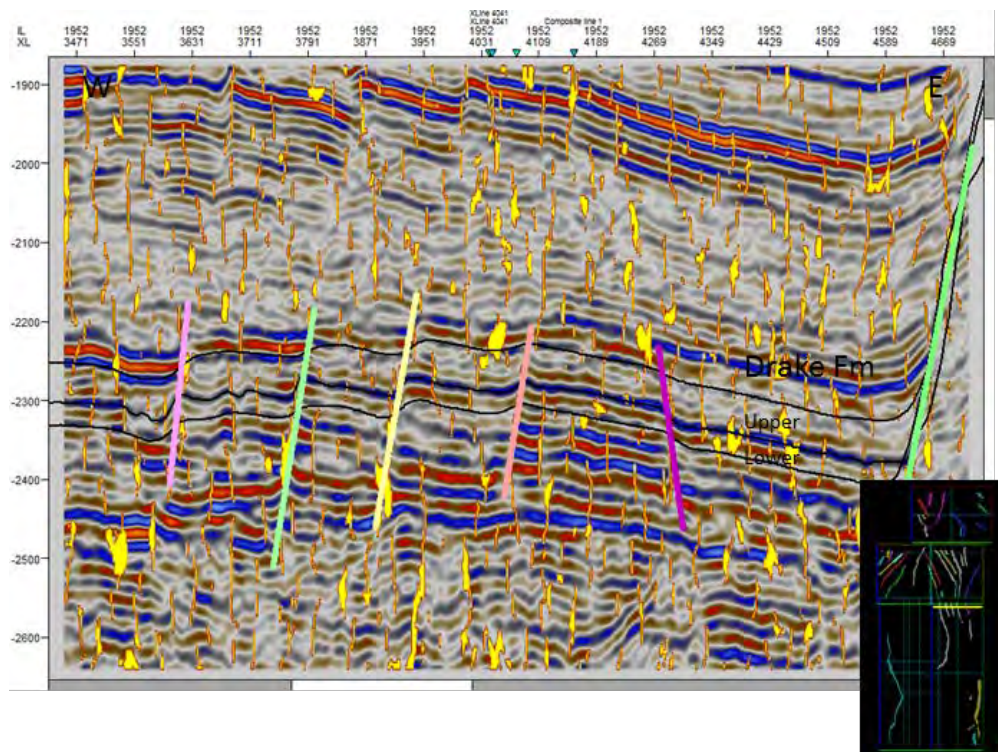


Figure 5-65: Inline 1952 SE Area. SVI Pro FaultIn attribute on noise filtered seismic. The area displays low fault and fracture activity. Most fractures terminate in the shale and there are no signs of disintegration or palaeo leakage.

DOCUMENT NO.: TL02-GTL-Z-RA-0001	REVISION NO.: 03	REVISION DATE: 01.03.2012	APPROVED:
-------------------------------------	---------------------	------------------------------	-----------

De-watering Structures in Shallower Sections

The assessment of features that may cause leakage through the cap rock are dewatering structures formed by migrating fluids. These features are often seen in sands above a polygonal fault system indicative of a palaeo-leakage system. Such a system has not been identified in the seismic data. As these features are formed at early stages of a clay burial they can be difficult to detect due to the healing properties of young and mobile clays. Another possibility is that they may be under the limit of seismic resolution.

Mineral Dissolution

A further leakage scenario is through acidic CO₂-brine dissolution of calcite cemented fractures in the shale constituting the cap rock (Bromhal, et al. 2010). Such cementation is common and may open natural fractures formed during compaction and diagenesis. It is not possible to detect such features in conventional data analysis.

In the well sample testing conducted by Iris (Gassnova-IRI 2011), a mean calcite percentage of 10% was measured by XRD analysis of bulk rock. This level is comparable to calcite percentages measured on Utsira cap rock (Kemp, Bouch and Murphy 2001). The calcite is present in the natural mineral assemblage of the rock and is not believed to represent a major risk to seal suitability.

5.4.6 Summary cap rock

Lower Drake Formation is defined as the cap rock for the storage complex. The formation has ample thickness throughout and no evidence of leakage has been found in the plume migration area.

5.5 Safe Pressure Evaluation

5.5.1 Introduction

The risk for CO₂ leakage through three geological processes has been evaluated. These are summarized as:

- Fault sealing – CO₂ leakage through existing non-sealing faults
- Fault reactivation – leakage through re-activation of existing faults or initiation of new faults due to changes in the stress regime resulting from pressure build due to CO₂ injection
- Fracture opening and/or initiation – leakage through flow into pre-existing fractures or the initiation of new tensile fractures.

5.5.2 Structural geology relevant for safe pressure estimation

The stress field and its orientation with respect to the investigated fault are important when assessing the leakage potential of a fault. The present day stress regime in the investigated area is ambiguous as it moves from a compressional stress regime with an NW/SE orientation west of the Viking Graben, to a more normal stress regime closer to the Norwegian coast with a direction of ENE/WSW in the Troll area. Both these stress regimes are therefore investigated with respect to fault reactivation.

5.5.3 Fault Reactivation Study

A study was undertaken by Schlumberger to evaluate the allowable pressure increase from CO₂ injection before a pre-existing fault would reactivate. Full details are given in (Schlumberger 2011). Two fault locations were considered: one close to the injection location (Fault 8 GN1001 1+2) and one in the Troll field close to wells 31/5-2, 31/2-5 and 31/2-1 (Figure 5-66).

DOCUMENT NO.: TL02-GTL-Z-RA-0001	REVISION NO.: 03	REVISION DATE: 01.03.2012	APPROVED:
-------------------------------------	---------------------	------------------------------	-----------

The in-situ stress magnitudes at these two locations are quite different owing to the different depths of the modelled faults.

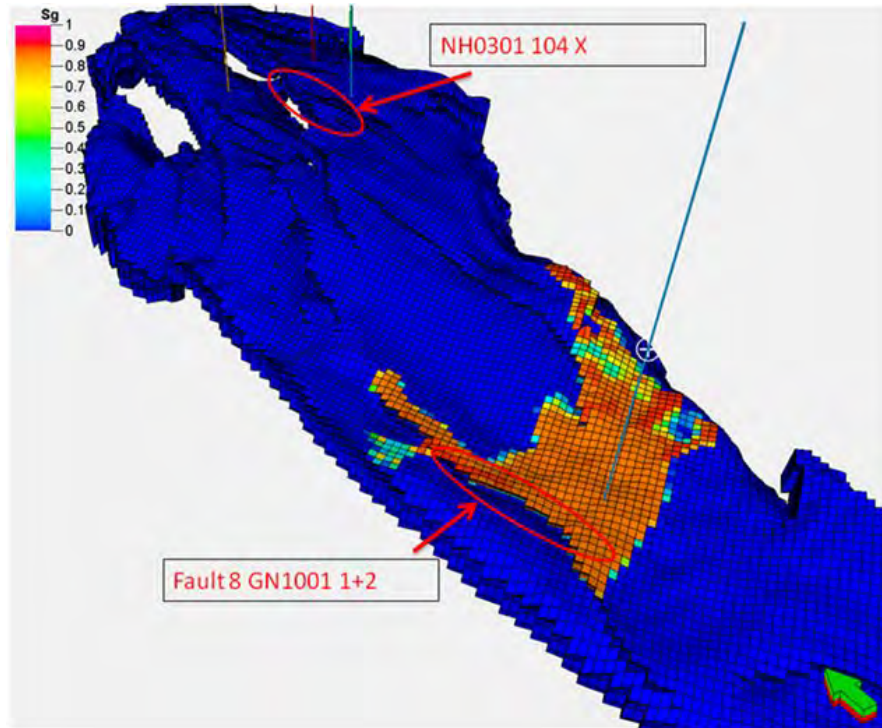


Figure 5-66: Faults modelling in Fault Reactivation Study.

A wide range of scenarios were simulated to account for the following at each of the fault locations (Troll and injection well location) and are summarized in Table 5-12:

- Stress magnitudes and stress regime (normal vs strike slip)
- Maximum horizontal stress direction
- Fault orientation and fault dip
- Fault rock strength parameters (for weak fault, a weak clay-filled fault and strong cemented fault)

Table 5-12: Model parameters and variables in Fault Reactivation Study.

Model Variables	Injection Area Fault	Troll Location Fault (near 31/2-1)
Fault/Top Johansen Depth	3080.5mTVDrkb	2176nTVDrkb
Stress Regimes	Normal (NS) and Strike Slip (SS)	Normal (NS) and Strike Slip (SS)
Vertical Stress Sv	611 bar	416 bar
Min Horizontal Stress Sh	495 bar and 436 bar	336 bar and 302 bar
Max Horizontal Stress Sh	553 bar (NS) and 672 bar (SS)	376 bar (NS) and 458 bar (SS)
Initial Pore Pressure	310 bar	216 bar
SH Azimuth	081 (most likely), 013 (least likely)	081 (most likely), 013 (least likely)
Fault azimuth and dip (average and max) for faults in figure 5-66)	270/58° and 270/82°	288/55° and 288/74°
Fault dip azimuth and dip – theoretical weak fault orientation	171° dip azimuth, 45° dip angle	171° dip azimuth, 45° dip angle
Fault Strength Parameters (Cohesion (MPa) and Friction Angle)	0/20° Very weak fault 0/30° Weak fault (base case) 5 MPa/20° Moderate Strength Fault 12.4/20° Clay filled fault 40/30° Strong fault	0/20° Very weak fault 0/30° Weak fault (base case) 5 MPa/20° Moderate Strength Fault 12.4/20° Clay filled fault 40/30° Strong fault
Poisson's Ratio	0.25	0.25

DOCUMENT NO.: TL02-GTL-Z-RA-0001	REVISION NO.: 03	REVISION DATE: 01.03.2012	APPROVED:
-------------------------------------	---------------------	------------------------------	-----------

Fault reactivation was modelled using an analytical shear slip analysis, using the Mohr Coulomb failure criterion, and accounting for two cases, where:

- Total stresses equal pre-injection stresses and injection pressure reduces effective stresses
- Total stresses increase with injection pressure (poro-elastic stress)

In each case the model assumes that if the failure criteria are reached the fault will initiate and/or re-activate and, if CO₂ is present, CO₂ containment will be breached. If the failure criteria are not reached, the fault is assumed to be sealing.

For the poro-elastic model, total stress increase was assumed to be equal to 2/3 of the pressure increase from CO₂ injection, according to a Poisson’s Ratio of 0.25.

Vertical stress was estimated at a number of Troll wells by integrating density logs, where available. The stress gradient established at the Troll wells was applied to the injection well location, accounting for differences in water depth. Various horizontal stress models were tested and are summarized in section 5.5.4.

Default values for rock strength for a very weak fault, a base case fault, moderate strength and strong fault were assumed as in Table 5-12. The clay-filled fault strength parameters were based on the NGI Mohr Coulomb results available at the time of modelling and reflect the cohesion and friction angle of intact clay laminated Cook Formation samples. Fault geometries for Fault NH0301 104 1 and Fault 8 GN1001 1+2 (Table 5-12) were reviewed and simulations run for the average and maximum fault dips. To determine a worst case for risk assessment, simulations were also run for theoretical faults oriented optimally for shear slip.

The failure model is sensitive to the modelling method (fluid pressure effects alone or poro-elastic effects), fault orientation, and to rock strength parameters. A distribution of results for various scenarios is summarized in Table 5-13.

Poro-elastic modelling results in more stable fault conditions, whereas the case in which injection pressure only reduces the effective stresses results in much less stable conditions. In reality, the stress state will be somewhere between these two modelled cases.

Modelling a theoretical pre-existing fault oriented optimally for shear slip and with zero cohesive strength and a friction angle of 20° would be unstable at current in-situ stress conditions. Increasing the friction angle to 30° increases the allowable pressure build up to 65 bar and 40 bar for the injection and Troll locations, respectively. Adding a nominal rock strength of 5MPa cohesive strength to the unstable scenario greatly increases the fault strength, allowing for injection pressures of 90 bar and 95 bar for the injection and Troll locations, respectively.

Modelling the actual faults with zero cohesion and 20° friction angle shows allowable injection pressures of 100 bar and 50 bar for the injection and Troll field locations, respectively. Modelling the base case with a friction angle of 30° allows for 150 bar injection pressure at the injection location.

DOCUMENT NO.: TL02-GTL-Z-RA-0001	REVISION NO.: 03	REVISION DATE: 01.03.2012	APPROVED:
-------------------------------------	---------------------	------------------------------	-----------

Table 5-13: Results of allowable CO₂ pressure build-up before fault reactivation for various fault scenarios.

	Minimum allowable pressure build-up (bar)					
	Theoretical Unrealistic	Theoretical Worst Case	Theoretical Low Case	Actual Fault Low Case	Actual Fault Base Case	Actual Fault High Case
	Theoretical Fault Orientation, Very Weak Fault, Zero Cohesion, 20° FANG, Normal Stress Regime	Theoretical Fault Orientation, Weak Fault, Zero Cohesion, 30° FANG, Normal Stress Regime	Theoretical Fault Orientation, Weak Fault, 5MPa Cohesion, 20° FANG, Normal Stress Regime	Actual Fault Orientation, Very Weak Fault, zero Cohesion, 20° FANG, Normal Stress Regime	Actual Fault Orientation, Weak Fault, zero Cohesion, 30° FANG, Normal Stress Regime	Actual Fault Orientation, Very Weak Fault, zero Cohesion, 20° FANG, Strike Slip Regime, Poro-Elastic Modelling
Injection Area Fault at Top Johansen Formation	0	65	90	100	150	200
Troll Area Fault at Top Johansen Formation	0	40	95	50	80	120

In summary, a theoretical model shows a very weak fault optimally oriented for shear slip is unstable at current in-situ stress conditions. However, relatively small increases in rock strength parameters increase stability. Modelling the actual fault orientations shows that the minimum allowable pressure build-up at the injection well and Troll area is 100 bar and 50 bar, respectively, before the faults reactivate. Allowable injection pressure increases as fault strength increases.

5.5.4 Fracture Initiation

Estimates were made to determine the allowable CO₂ pressure build-up before leakage occurs into the overlying Drake Formation cap rock, owing to processes of opening pre-existing fractures and/or initiating new tensile fractures.

Conservative estimates are based on minimum horizontal stress (Sh) models, assuming leakage will occur when the pressure build-up exceeds Sh. A range of minimum horizontal stress models were tested, assuming a theoretical minimum and calibrations to a combination of mini-frac data and leak-off tests, see Figure 5-67. This figure summarizes the various leak-off test (LOT) data from Troll field wells used to define the minimum horizontal stress models, together with the overburden, pore pressure and base and low case minimum horizontal stress (Sh) models for 31/2-1. Note that the LOT data are plotted versus TVD but have not been corrected for water depth and air gap effects. The base case minimum horizontal stress model honours the lower bound of the majority of LOTs and the low case minimum stress model honours a mini-frac Sh estimate from 31/6-A-21 reported in (Bretan, et al. 2011). The theoretical lower bound of minimum horizontal stress is not shown here, but has been used to estimate the worst case scenario for allowable pressure build up as shown in the first column of results in Table 5-14.

DOCUMENT NO.: TL02-GTL-Z-RA-0001	REVISION NO.: 03	REVISION DATE: 01.03.2012	APPROVED:
-------------------------------------	---------------------	------------------------------	-----------

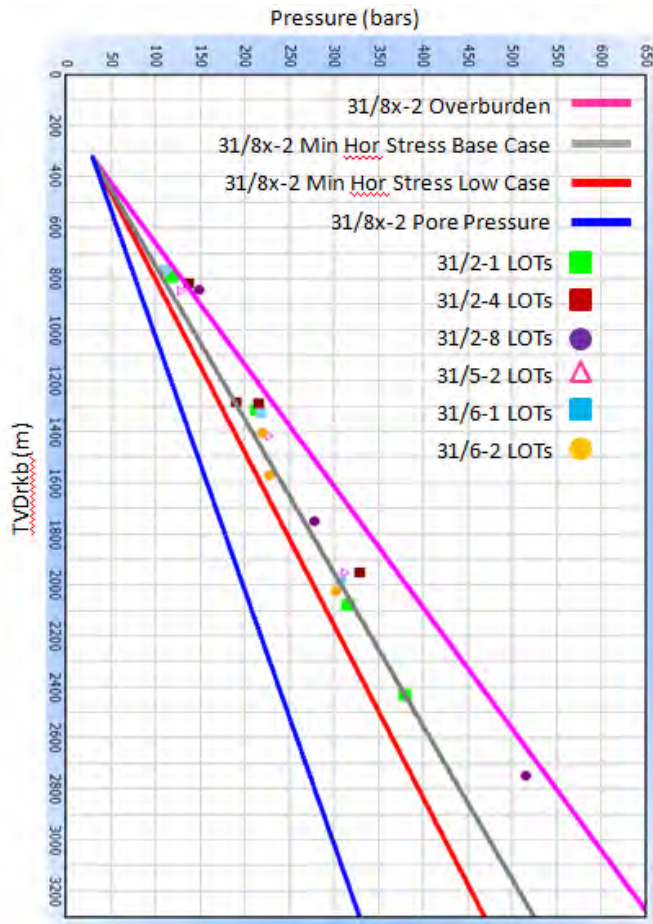


Figure 5-67: Overburden, base and low case minimum horizontal stress models, and pore pressure for 31/2-1, together with LOT data from various Troll field wells.

Higher allowable pressure build-up was seen using Fracture Initiation models, assuming the formations are not fractured and have some inherent tensile strength, calibrated to Brazil test tensile strengths from Drake and Upper Amundsen formations. An average tensile strength of 4.22MPa was established for these formations.

Thermal stress modelling was conducted to estimate potential stress reduction due to thermal effects as colder CO₂ is injected into the reservoir. Theoretical models accounting for short term near wellbore and longer term far field thermal stress reduction, and a model from field data from a depleted reservoir water injection field were run (Santarelli, Havmøller and Naumann 2008). The values from Table 5-14 were used as the input stress model.

Poisson’s Ratio was varied from 0.2 – 0.3, and Young’s Modulus was varied from 1 – 9 GPa, estimated based on values from the NGI triaxial test data from the clay laminated Cook Formation (Poisson’s Ratio 0.27, Youngs Modulus 9.53GPa), and publicly available data for the Draupne Formation and similar formations. A thermal expansion coefficient of $5 \times 10^{-6} \text{ } ^\circ\text{C}$ was used (Santarelli, Havmøller and Naumann 2008).

The model assumes CO₂ injection near the base of the Johansen Formation and models the thermal stresses at the base Drake Formation, approximately 190m above the injection zone. The injected CO₂ may be in the range of 23 - 30°C at the wellbore, and formation temperature at the base Drake Formation is assumed to be 30°C below in-situ temperature. The results in

DOCUMENT NO.: TL02-GTL-Z-RA-0001	REVISION NO.: 03	REVISION DATE: 01.03.2012	APPROVED:
-------------------------------------	---------------------	------------------------------	-----------

Table 5-15 summarize the lower values of allowable injection pressure, given the range of variables stated above.

Table 5-14: Results of allowable CO₂ pressure build-ups before leakage of CO₂ into cap rock, for various minimum stress and fracture initiation models.

	Minimum allowable pressure build-up (bar) accounting for minimum horizontal stress and tensile strength				
	Min Stress - Theoretical Minimum	Min Stress - Low/Possible	Frac Initiation – Low Case	Min Stress – Base Case	Frac Initiation – High Case
Injection Area (base Drake Formation)	97	127	169	177	218
Troll Field (31/2-1) (base Drake Formation)	63	82	124	114	156

Table 5-15: Results of allowable CO₂ pressure build-ups before leakage of CO₂ into cap rock, accounting for thermal effects.

	Minimum allowable pressure build-up (bar) accounting for thermal effects				
	Min Stress + Thermal Theoretical Minimum	Min Stress + Thermal - Low	Frac Initiation + Thermal – Low Case	Min Stress + Thermal – Base	Frac Initiation + Thermal – High Case
Injection Area (base Drake Formation)	77	107	149	157	198
Troll Field (31/2-1) (base Drake Formation)	44	63	105	95	137

5.5.5 Summary

Assuming no thermal stress effects due to the injection of cold CO₂, it is considered that the lowest likely pressures build-up before leakage into the overburden is represented by the ‘Min Stress – Low Case’ column (127 bar and 82 bar at the injection location and 31/2-1 well location, respectively). The theoretical minimum case is not supported by field data and therefore is considered to be too conservative for both the thermal and non-thermal stress modelling. It is equally likely that injection pressures of 169-177 bar and 114-124 bar are allowable at the injection and 31/2-1 well locations, respectively, before CO₂ leakage occurs.

Accounting for thermal stress effects, the lowest likely safe pressure before leakage is again represented by the ‘Min Stress – Low Case’ column (107 bar and 63 bar for the injection and Troll locations, respectively). It is equally likely that injection pressures of 149-157 bar and 95-105 bar are allowable at the injection and 31/2-1 well locations, respectively, accounting for thermal effects.

This is also below the capillary entry pressure (> 250 bar) for the Drake Formation found through lab testing (Gassnova-IRI 2011).

Chapter 7 will use the result of this study to evaluate it towards the expected and the uncertainty distribution of pressure build-up in the storage complex. Table 5-14 will then be represented as

DOCUMENT NO.: TL02-GTL-Z-RA-0001	REVISION NO.: 03	REVISION DATE: 01.03.2012	APPROVED:
-------------------------------------	---------------------	------------------------------	-----------

an uncertainty distribution (Figure 7-36). The pressure build-up will be affected by the total pore volume connectivity, rock compressibility and permeability in the injection area.

5.6 Development of Geological 3D model

The geomodel is the main input for the CO₂ storage complex dynamic simulations. The models are derived from a structural model based on the interpreted storage complex faults and horizons. Well data interpretation and seismic inversion data are the basis and the main input for the 3D geomodels property modelling. Several geomodels are built for different purposes, to be discussed in chapter 6.

5.6.1 Structural modelling

The fault and horizon interpretations described in chapter 5.2.2 are the main input to geomodel prior to the property modelling. Figure 5-68 shows the interpreted faults defining the structural time models. During the gridding process faults that are interpreted to have no impact on the dynamic simulations were removed to simplify the gridding process.

The Johansen Storage Complex geomodel (Figure 5-69) is defined by both sealing and storage formations and includes the following interpreted horizons:

- Drake Formation Primary seal
- Cook Formation Secondary storage formation
- Amundsen 2 Formation Seal/Storage
- Johansen Formation Primary storage
- Amundsen 1 Formation Seal/Storage
- Statfjord Formation Base storage complex formation

The reference geomodel grid resolution is 400m x 400m grid with zigzag faults. The areal extent of the geomodel is approximately 3500km². The time geomodel is depth converted by the method described in chapter 5.2.3.

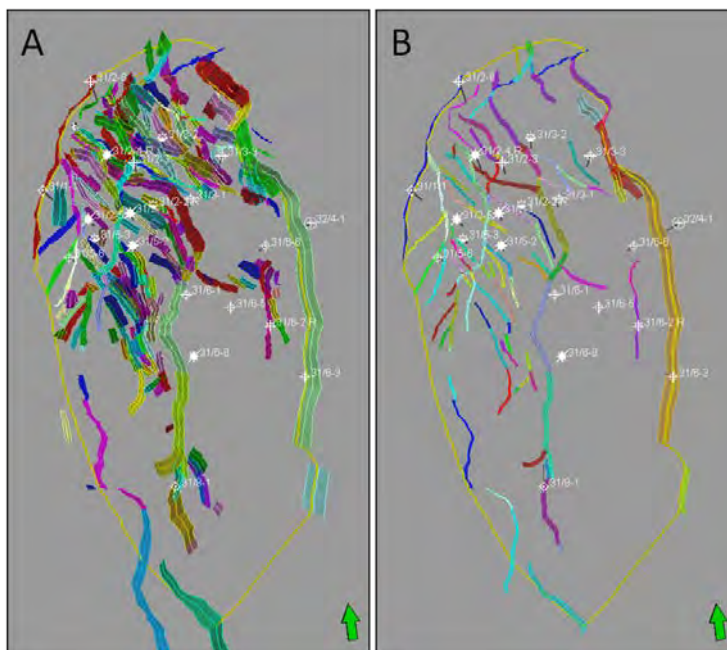


Figure 5-68: Interpreted fault planes used in the structural modelling of the JSC. Figure A is showing the original fault model. Figure B is showing the fault model that constitutes the reference geomodel.

DOCUMENT NO.: TL02-GTL-Z-RA-0001	REVISION NO.: 03	REVISION DATE: 01.03.2012	APPROVED:
-------------------------------------	---------------------	------------------------------	-----------

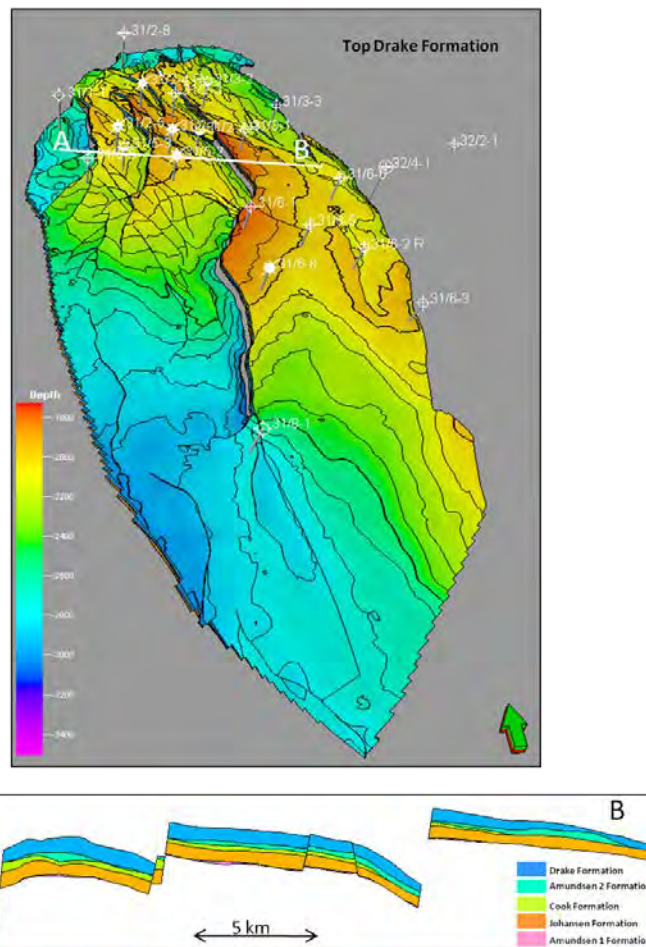


Figure 5-69: Reference JSC geomodel.

5.6.2 Property modelling

The depositional model for primary storage formation (Johansen Formation) is interpreted to be an asymmetric delta (chapter 5.3.1.1) hence the wells in the northern part of the storage complex do not represent the Johansen Formation deposits in the western and southern parts (non-well areas). To build a geomodel with applicable lithological properties, a seismic inversion study (chapter 4.3) based on the GN10M1 3D (Figure 5-70) survey was performed (Gassnova-WGD 2011). Seismic inversion is the process of transforming seismic reflection data into a quantitative rock-property description of a reservoir and will increase the resolution and reliability of the seismic data.

There is a clear relationship between acoustic impedance and porosity and this relationship is especially useful in the prediction of sand deposits (Aleman 2004). The seismic inversion data is used for prediction of sand quality both for the Johansen and Cook formations and is, together with the petrophysical evaluation, the main input for storage complex porosity and permeability assessment.

DOCUMENT NO.: TL02-GTL-Z-RA-0001	REVISION NO.: 03	REVISION DATE: 01.03.2012	APPROVED:
-------------------------------------	---------------------	------------------------------	-----------

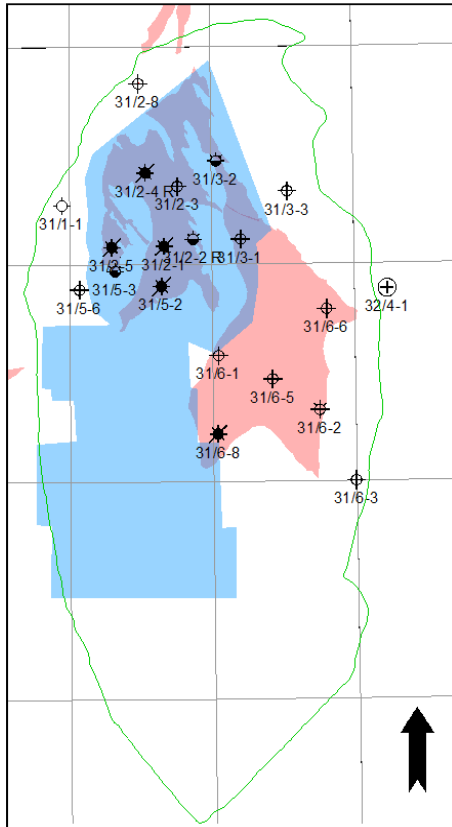


Figure 5-70: Map showing key wells and storage complex area (blue) covered by the GN10M1 seismic inversion study. The green polygon represents outline of the Johansen reference geomodel.

5.6.2.1 Seismic inversion

The seismic inversion data are used to predict the lithology of the storage formations in the southern part of the Johansen Storage Complex and it is assumed that this is a better and more accurate method of reflecting the lithological changes of the storage formations, than building the property models based on the well data from the northern part.

The main deliveries from the seismic inversion study are two acoustic impedance cubes (Gassnova-WGD 2011). The acoustic impedance cube with a low-frequency model was used to account for the increasing southward storage complex depth (lack of well calibration).

Comparison of the low-frequency background models (LFM) with the absolute (acoustic impedance with LFM) and relative inversion results (acoustic impedance without LFM) is important during the interpretation of the inversion results. In particular in the southern area where there is no well control, and only guidance from the 3D velocity model (Gassnova-WGD 2011).

5.6.2.2 Input from Petrophysical Evaluation

The porosity data to be used in the geomodel is generated by using the acoustic impedance cube from the seismic inversion and the correlation between effective porosity and acoustic impedance from the well logs. High, base and low case correlations (Figure 5-71 to Figure 5-74) for each zone (formation) are in the geomodel.

Sand/shale cut-off values were interpreted for all zones except for the Johansen Formation where no shale is interpreted to be present. The lowest sand porosity was 9% (Figure 5-73).

DOCUMENT NO.: TL02-GTL-Z-RA-0001	REVISION NO.: 03	REVISION DATE: 01.03.2012	APPROVED:
-------------------------------------	---------------------	------------------------------	-----------

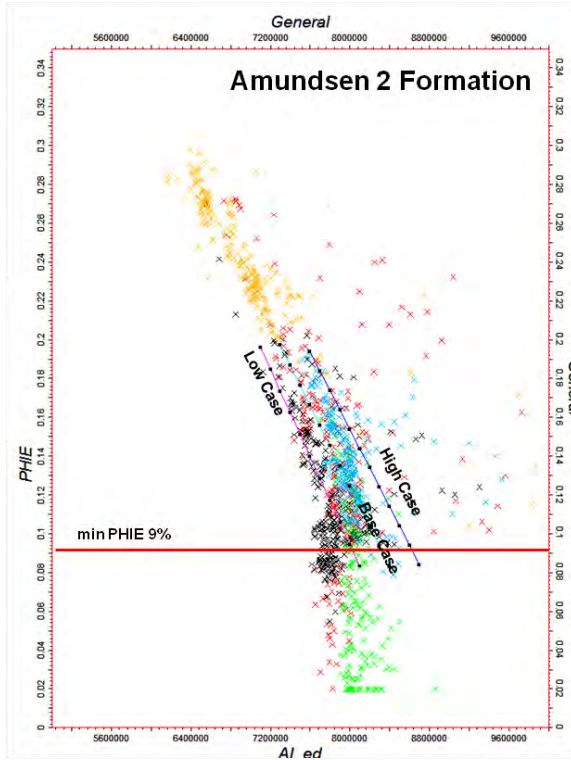


Figure 5-71: Amundsen 2 Fm porosity (PHIE) vs acoustic impedance (AI) high, base and low case correlations from key wells.

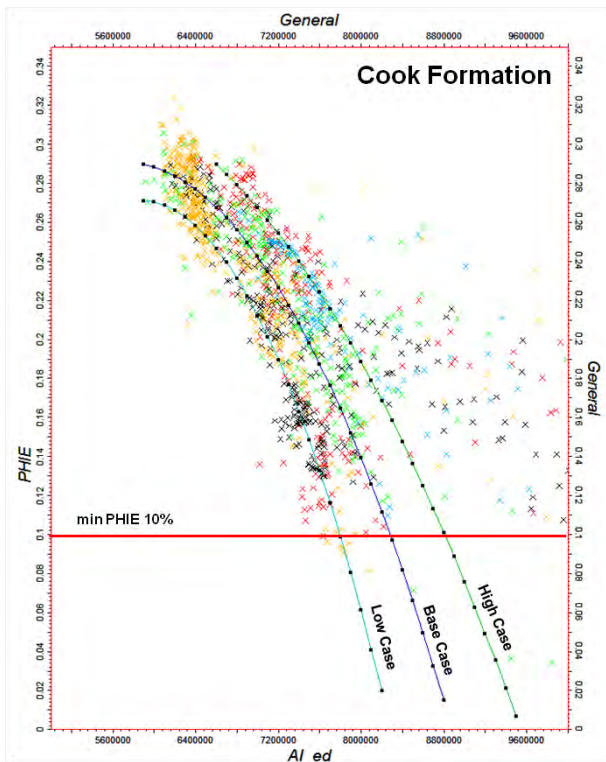


Figure 5-72: Cook Fm porosity (PHIE) vs acoustic impedance (AI) high, base and low case correlations from key wells.

DOCUMENT NO.: TL02-GTL-Z-RA-0001	REVISION NO.: 03	REVISION DATE: 01.03.2012	APPROVED:
-------------------------------------	---------------------	------------------------------	-----------

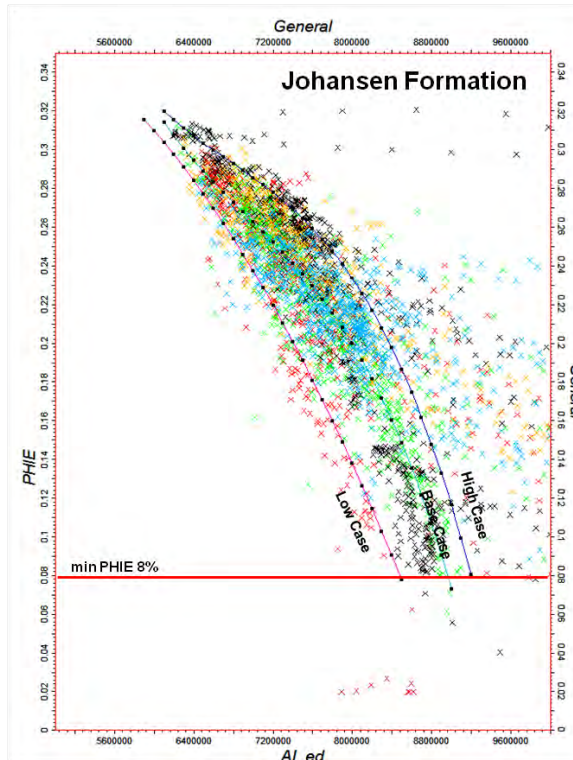


Figure 5-73: Johansen Fm porosity (PHIE) vs acoustic impedance (AI) high, base and low case correlations from key wells.

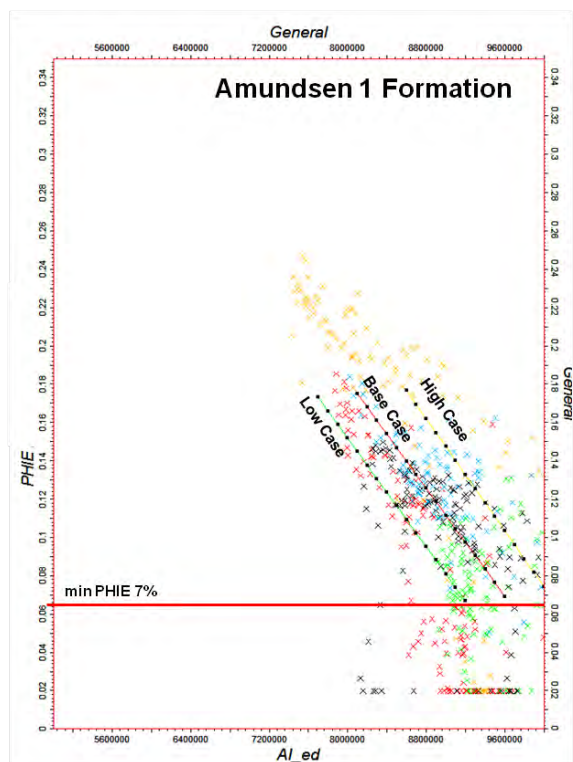


Figure 5-74: Amundsen 1 Fm porosity (PHIE) vs acoustic impedance (AI) high, base and low case correlations from key wells.

DOCUMENT NO.: TL02-GTL-Z-RA-0001	REVISION NO.: 03	REVISION DATE: 01.03.2012	APPROVED:
-------------------------------------	---------------------	------------------------------	-----------

Table 5-16: Summary table over AI base case cut-offs used for the zones in the model. For AI values beyond the maximum cut of values, a constant shale porosity was used (except for the Johansen Fm zone where no shale is anticipated to be present).

Formation	Max PHIE	Corresponding AI	Min PHIE	Corresponding AI	Shale Porosity
Cook	0.2897	5900000	0.0969	8300000	0.055
Amundsen 2	0.1972	7300000	0.0829	8400000	0.055
Johansen	0.3140	6100000	0.0731	9000000	No shale
Amundsen 1	0.1750	8100000	0.0692	9600000	0.050

Table 5-17: Summary table over AI high case cut-offs used for the zones in the model. For AI values beyond the maximum cut of values, a constant shale porosity was used (except for the Johansen Fm zone where no shale is anticipated to be present).

Formation	Max PHIE	Corresponding AI	Min PHIE	Corresponding AI	Shale Porosity
Cook	0.2896	6600000	0.1009	8800000	0.09
Amundsen 2	0.1936	7600000	0.0840	8700000	0.083
Johansen	0.3199	6100000	0.0804	9200000	No shale
Amundsen 1	0.1766	8600000	0.0741	10000000	0.065

Table 5-18: Summary table over AI low case cut-offs used for the zones in the model. For AI values beyond the maximum cut of values, a constant shale porosity was used (except for the Johansen Fm zone where no shale is anticipated to be present).

Formation	Max PHIE	Corresponding AI	Min PHIE	Corresponding AI	Shale Porosity
Cook	0.2710	5900000	0.0987	7800000	0.02
Amundsen 2	0.1959	7100000	0.0832	8100000	0.02
Johansen	0.3155	5900000	0.0777	8500000	No shale
Amundsen 1	0.1730	7700000	0.0668	9200000	0.02

5.6.2.3 Porosity modelling

The property models were generated over the lithological interval Cook Formation - Statfjord Formation. The horizons defining the zones are; Cook Formation, Amundsen 2 Formation, Johansen Formation, Amundsen 1 Formation and Statfjord Formation. The zones in the model are named; Cook, Amundsen 2, Johansen and Amundsen 1. The internal layering in the zones is generated as type proportional, which means that the zone is divided into a given number of layers of proportionally equal thickness (Figure 5-75, Figure 5-76, Figure 5-77 and Table 5-19). The number of layers in the model is calculated to give maximal cell thicknesses around of 5m on average.

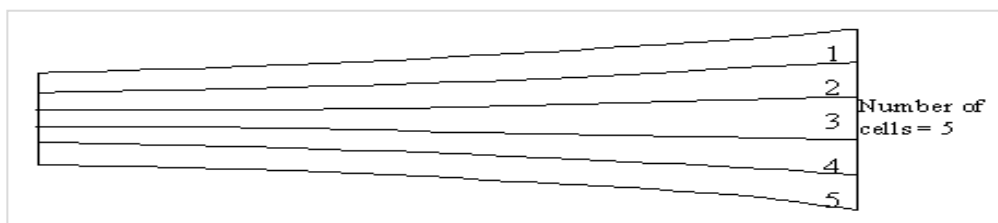


Figure 5-75: Divides the zone into a given number of layers of equal thickness. The example shown in the figure above shows a zone subdivision into 5 proportional layers using the Petrel Layering process.

DOCUMENT NO.: TL02-GTL-Z-RA-0001	REVISION NO.: 03	REVISION DATE: 01.03.2012	APPROVED:
-------------------------------------	---------------------	------------------------------	-----------

	Name	Color	Calculate	Zone division		
	Cook		<input checked="" type="checkbox"/> Yes	Proportional	Number of layers:	30
	Amundsen 2		<input checked="" type="checkbox"/> Yes	Proportional	Number of layers:	30
	Johansen		<input checked="" type="checkbox"/> Yes	Proportional	Number of layers:	100
	Amundsen 1		<input checked="" type="checkbox"/> Yes	Proportional	Number of layers:	50

Figure 5-76: Layering settings applied for each zone in the model.

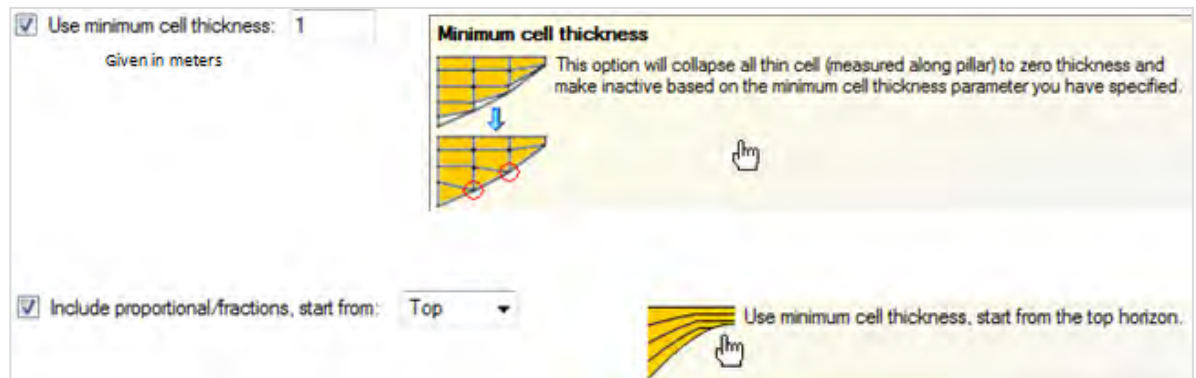


Figure 5-77: Detailed options used in the Layering process.

Table 5-19: Cell thicknesses in model zones after the Layering process.

Zone	Max stratigraphic cell thickness (m)	Average stratigraphic cell thickness (m)
Cook	7	1.82
Amundsen 2	5.63	1.22
Johansen	5	1.16
Amundsen 1	5.40	0.95

The porosity property model was calculated from acoustic impedance (AI) data generated by AVO inversion of the GN10M1 3D merge survey. A shift of +25m was applied to the inversion data to achieve an optimal match with well logs.

The effective porosity (PHIE) model was generated in two stages. The first stage was calculating porosities over the 3D area using the inversion data, and the second stage was a pixel based stochastic (Sequential Gaussian Simulation) modelling over the 2D area honouring the value distributions in the 3D area (Figure 5-78).

DOCUMENT NO.: TL02-GTL-Z-RA-0001	REVISION NO.: 03	REVISION DATE: 01.03.2012	APPROVED:
-------------------------------------	---------------------	------------------------------	-----------

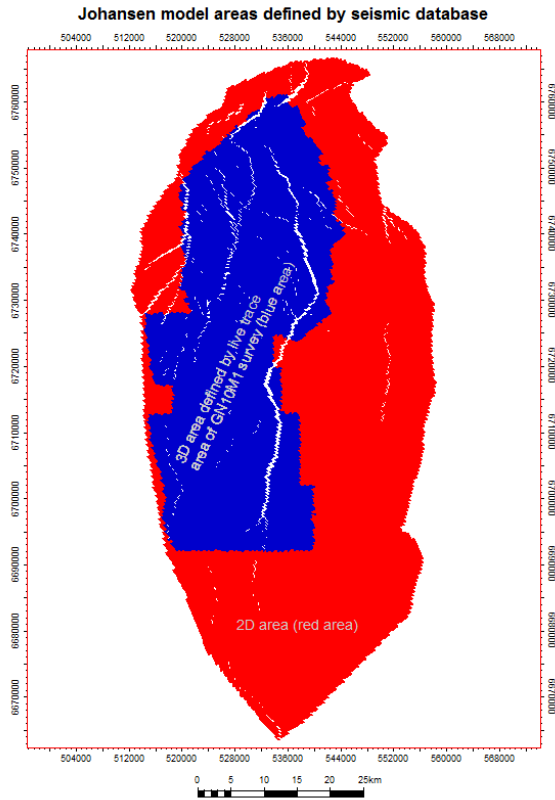


Figure 5-78: 3D (blue) and 2D area (Red) of the total model defined by the seismic database.

In the first stage, porosity values were calculated using AI vs PHIE look-up functions from well log cross plots and the acoustic impedance values from the AVO inversion (Figure 5-79). These look-up functions were generated for each zone in the model and for three cases (High, Base and Low case) (Figure 5-71 to Figure 5-74).

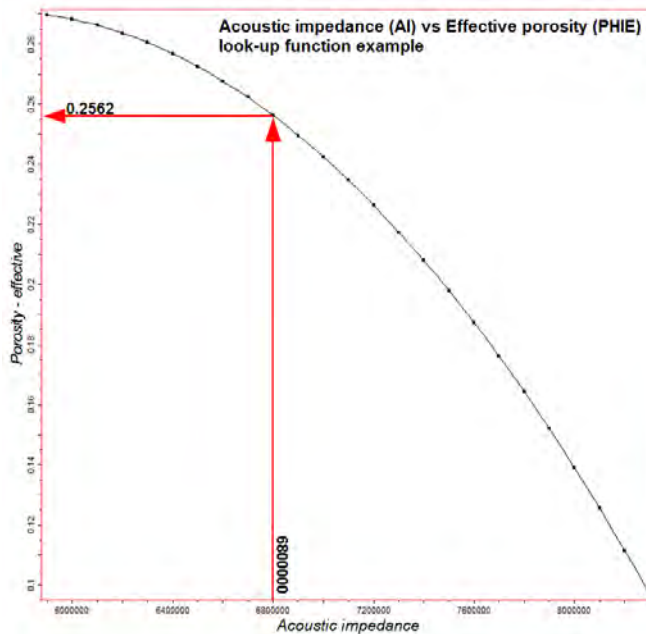


Figure 5-79: Acoustic impedance (AI) vs Effective porosity (PHIE) look-up function example.

DOCUMENT NO.: TL02-GTL-Z-RA-0001	REVISION NO.: 03	REVISION DATE: 01.03.2012	APPROVED:
-------------------------------------	---------------------	------------------------------	-----------

The first stage (3D area) workflow;

1. Up scaling (blocking) of AI values from inversion into the structural model. Setting the AI ranges for each zone to match the min/max ranges in the look-up curves to ensure PHIE values within acceptable ranges based on well logs and conceptual understanding of depositional model. AI values lower or higher than min/max are set to min/max.
2. Table 5-17 Calculation of PHIE values applying AI vs PHIE look-up curves. For all zones except Johansen, where no shale is anticipated, a range of AI representing sand was used for the look-up calculations. For AI values beyond this range, a constant shale porosity was used (Table 5-16, Table 5-17 and Table 5-18).

The resulting 3D porosity maps for the different zones are shown in Figure 5-80 (base case), Figure 5-81 (high case) and Figure 5-82 (low case).

The second stage is running pixel based stochastic modelling (Petrel: Sequential Gaussian Simulation) to expand the model into the areas defined by 2D seismic data (2D area) (Figure 5-78). This modelling scheme honours the input data distribution from the 3D area generated in the first stage. Information related to the stochastic simulation options can be found in the Geostatistical Software Library (GSLIB) manual (Deutsch and Journel 1998).

The resulting porosity 3D and 2D maps, Figure 5-83 (base case), Figure 5-83 (high case) and Figure 5-85 (low case), show a non-realistic transition between the 3D and 2D areas. This is a result of difference in input data density between the 3D and 2D areas. In the 3D area the data is sampled with the same density as the seismic data, but in the 2D area only sparse well data are available and stochastic modelling was used to compute values for the cells in the no-data areas. The model inside the 3D area will therefore have a smoother appearance compared to the heterogenic appearance of the data in the 2D area where the stochastic computation of values is dominant. This will have no significant effect on the CO₂ migration which occurs only in the 3D area.

DOCUMENT NO.: TL02-GTL-Z-RA-0001	REVISION NO.: 03	REVISION DATE: 01.03.2012	APPROVED:
-------------------------------------	---------------------	------------------------------	-----------

PHIE base case model (3D area)

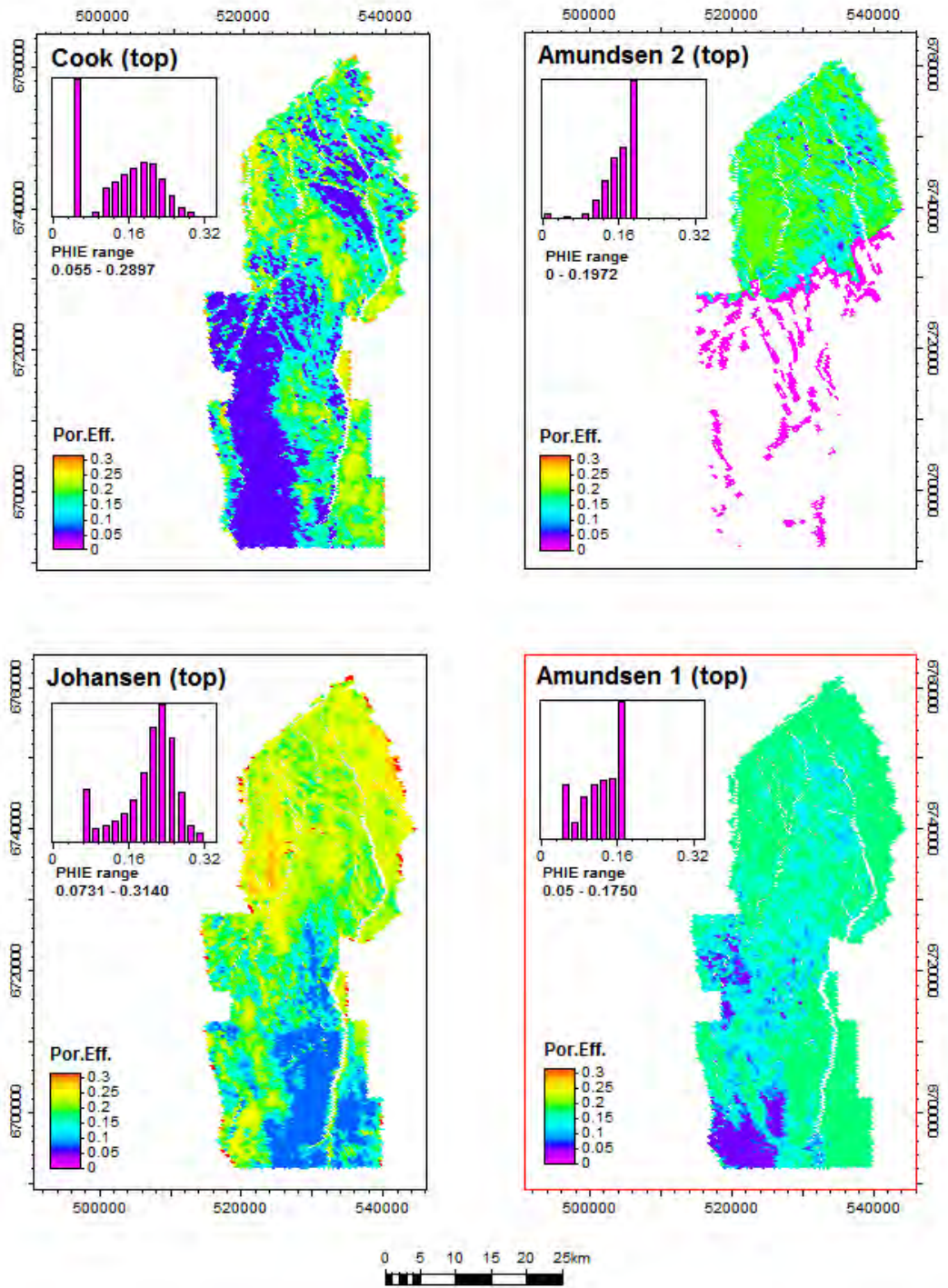


Figure 5-80: PHIE base case model (3D area) viewed on top of each zone.

DOCUMENT NO.: TL02-GTL-Z-RA-0001	REVISION NO.: 03	REVISION DATE: 01.03.2012	APPROVED:
-------------------------------------	---------------------	------------------------------	-----------

PHIE high case model (3D area)

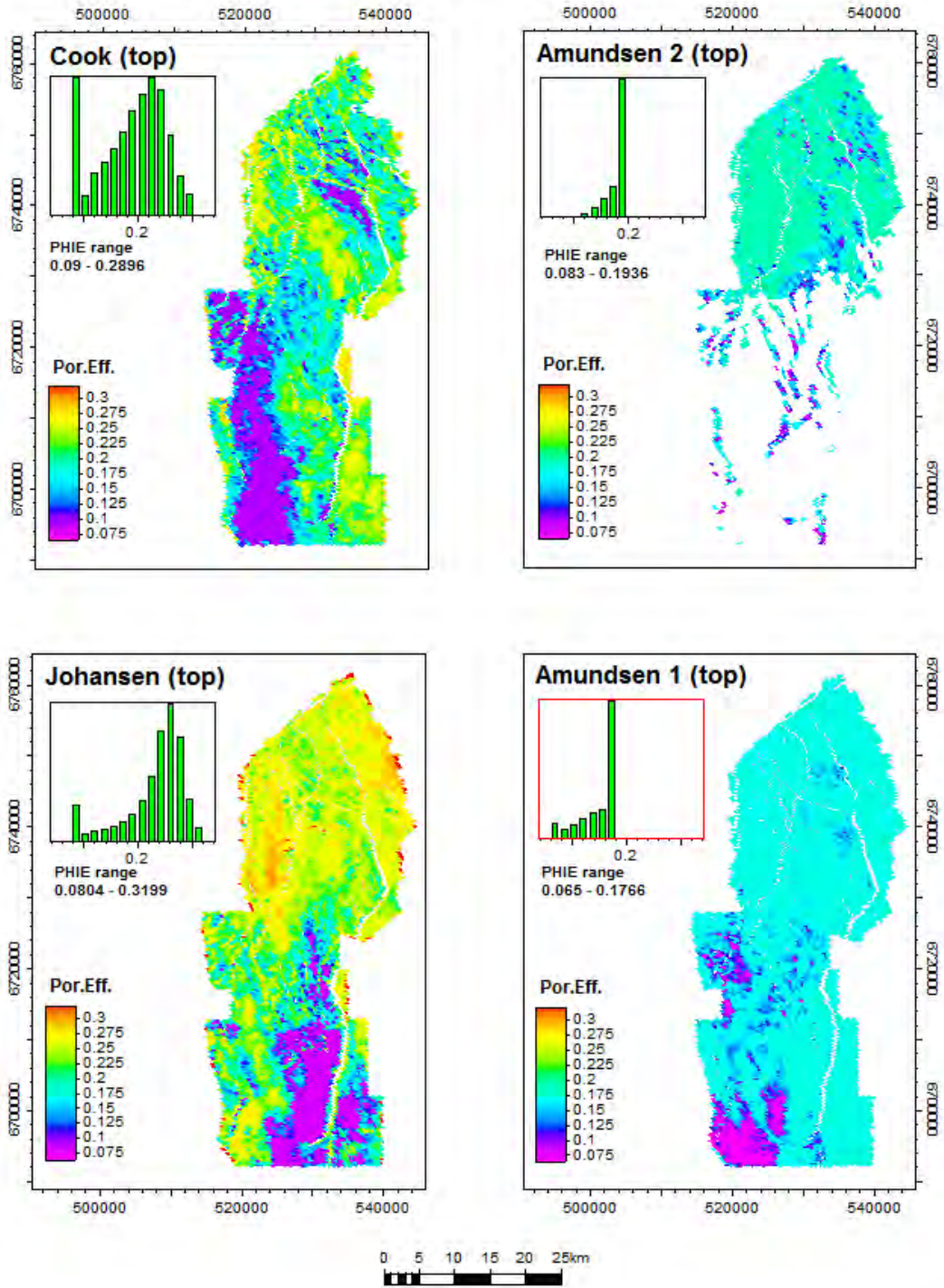


Figure 5-81: PHIE high case model (3D area) viewed on top of each zone.

DOCUMENT NO.: TL02-GTL-Z-RA-0001	REVISION NO.: 03	REVISION DATE: 01.03.2012	APPROVED:
-------------------------------------	---------------------	------------------------------	-----------

PHIE low case model (3D area)

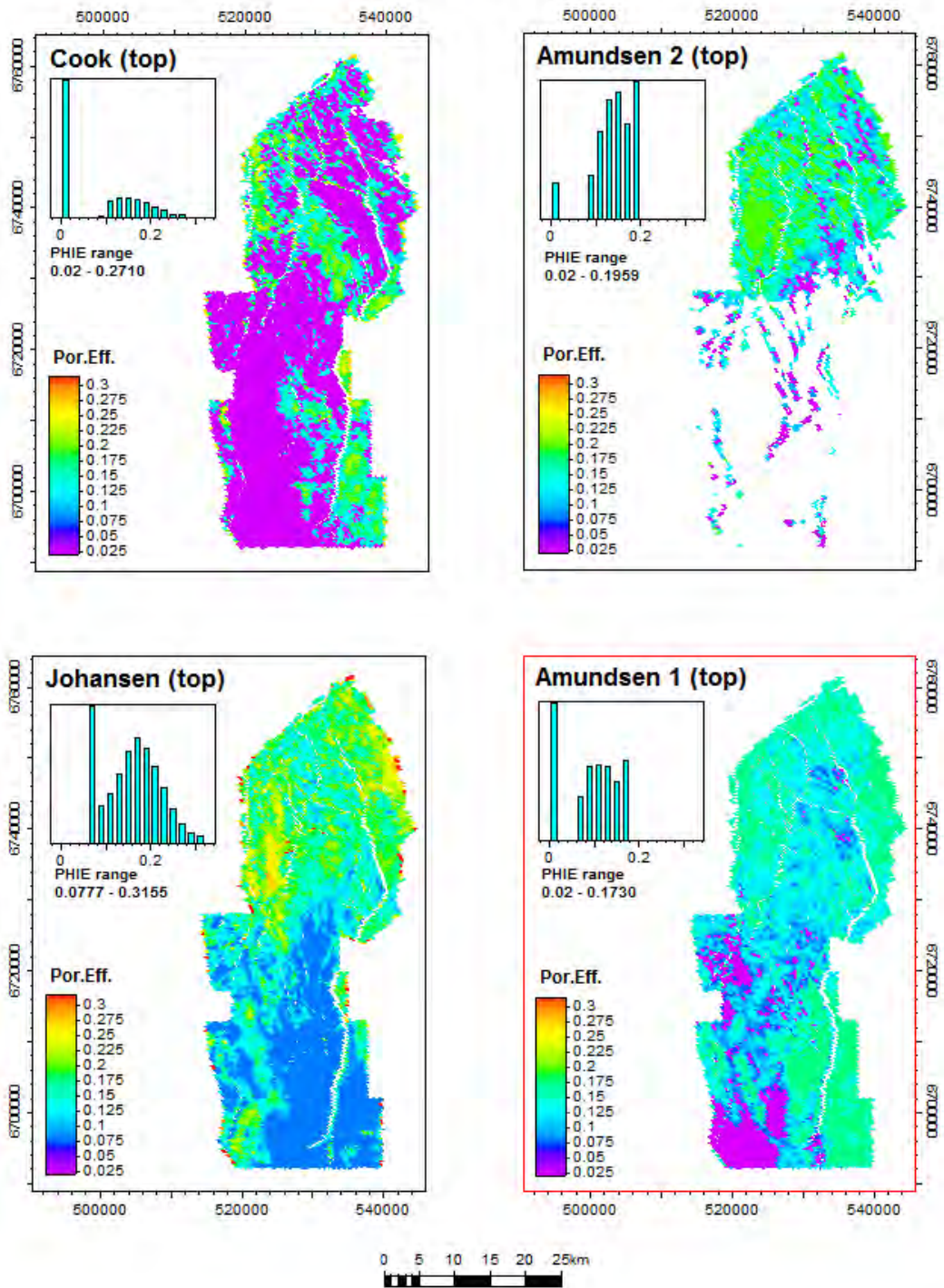


Figure 5-82: PHIE low case model (3D area) viewed on top of each zone.

DOCUMENT NO.: TL02-GTL-Z-RA-0001	REVISION NO.: 03	REVISION DATE: 01.03.2012	APPROVED:
-------------------------------------	---------------------	------------------------------	-----------

PHIE base case model (total model: 3D & 2D area)

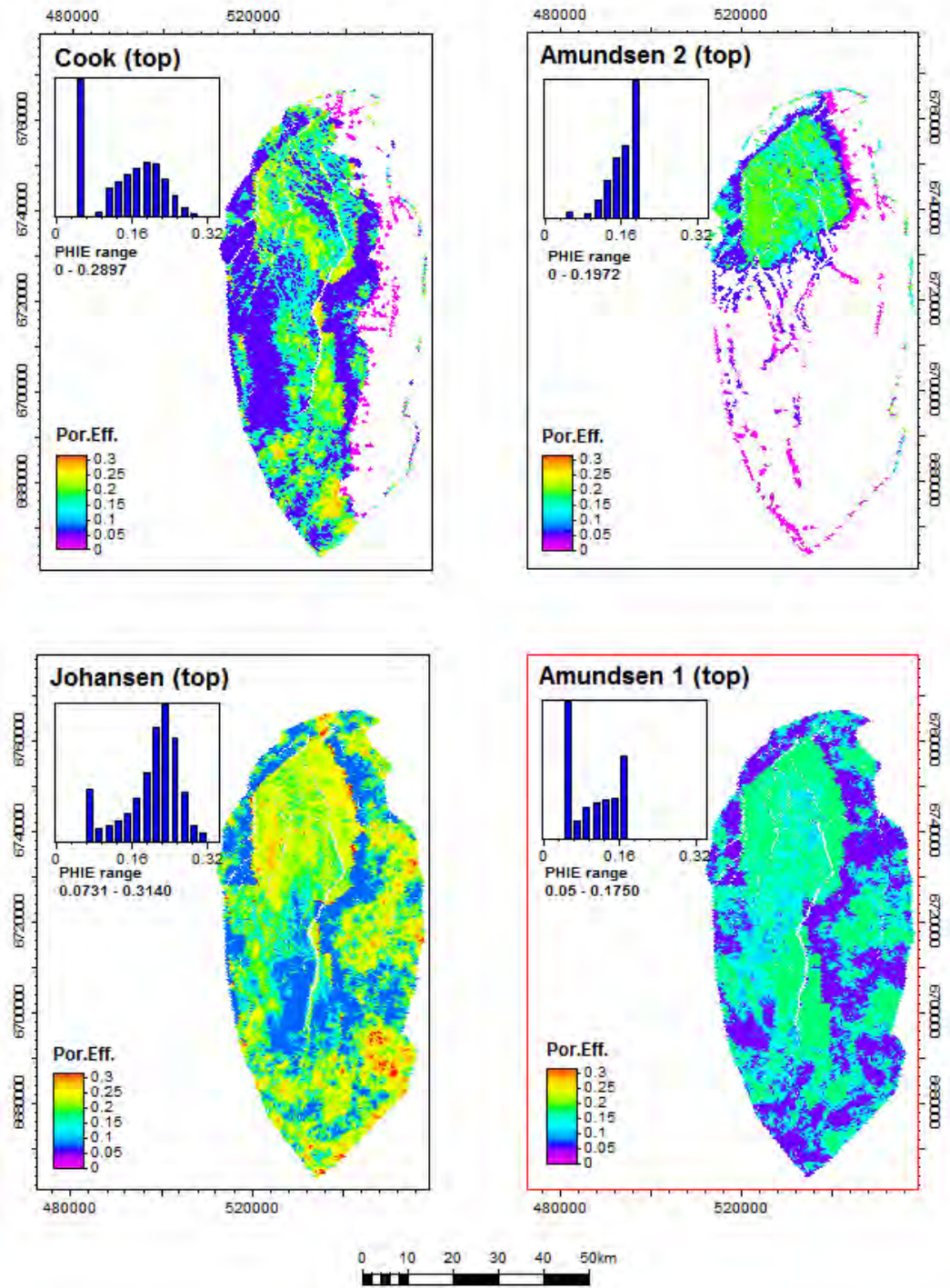


Figure 5-83: PHIE base case model (2D & 3D area) viewed on top of each zone.

DOCUMENT NO.: TL02-GTL-Z-RA-0001	REVISION NO.: 03	REVISION DATE: 01.03.2012	APPROVED:
-------------------------------------	---------------------	------------------------------	-----------

PHIE high case model (total model: 3D & 2D area)

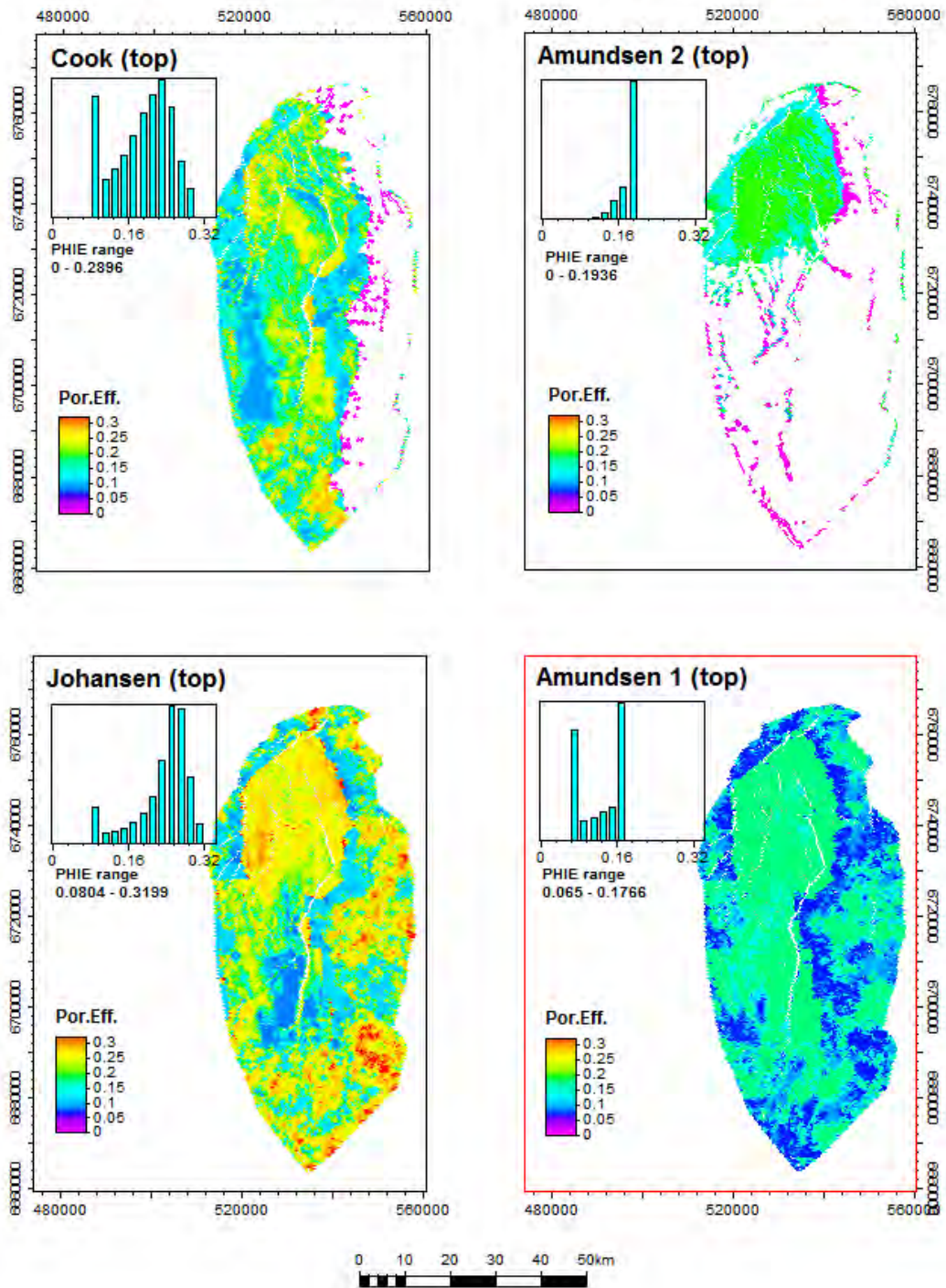


Figure 5-84: PHIE high case model (2D & 3D area) viewed on top of each zone.

DOCUMENT NO.: TL02-GTL-Z-RA-0001	REVISION NO.: 03	REVISION DATE: 01.03.2012	APPROVED:
-------------------------------------	---------------------	------------------------------	-----------

PHIE low case model (total model: 3D & 2D area)

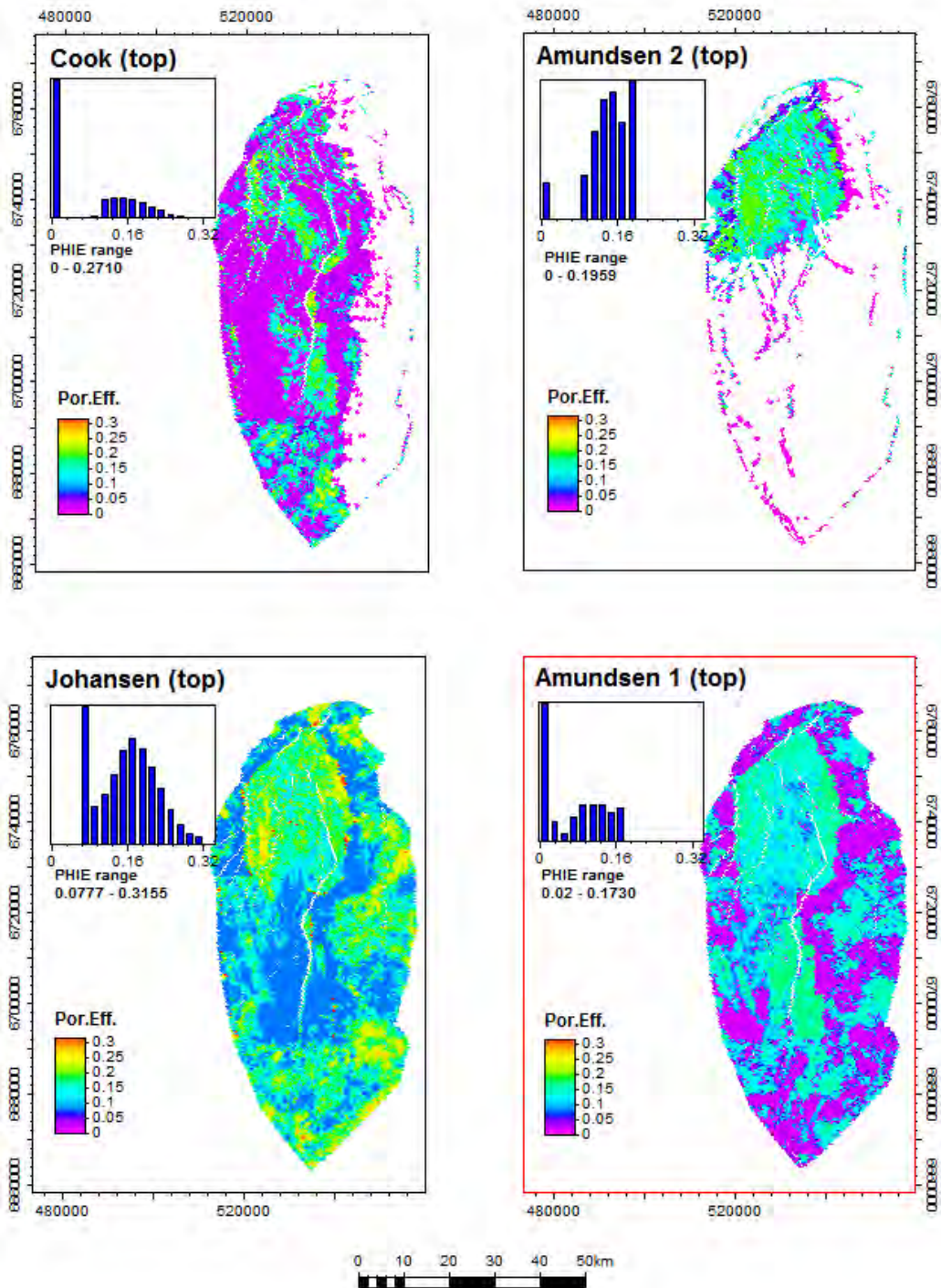


Figure 5-85: PHIE low case model (2D & 3D area) viewed on top of each zone.

DOCUMENT NO.: TL02-GTL-Z-RA-0001	REVISION NO.: 03	REVISION DATE: 01.03.2012	APPROVED:
-------------------------------------	---------------------	------------------------------	-----------

5.6.2.4 Permeability modelling

The permeability modelling is based on effective porosity (PHIE) versus permeability (Perm) cross plots based on well logs from the petrophysical evaluation (Gassnova-ROS 2011).

The look-up functions used in the modelling (Figure 5-32) were generated for each zone in the model. Based on these look-up functions the permeability models, Figure 5-87 (base case), Figure 5-88 (high case) and Figure 5-89 (low case), were calculated from the porosity property models described in the previous chapter.

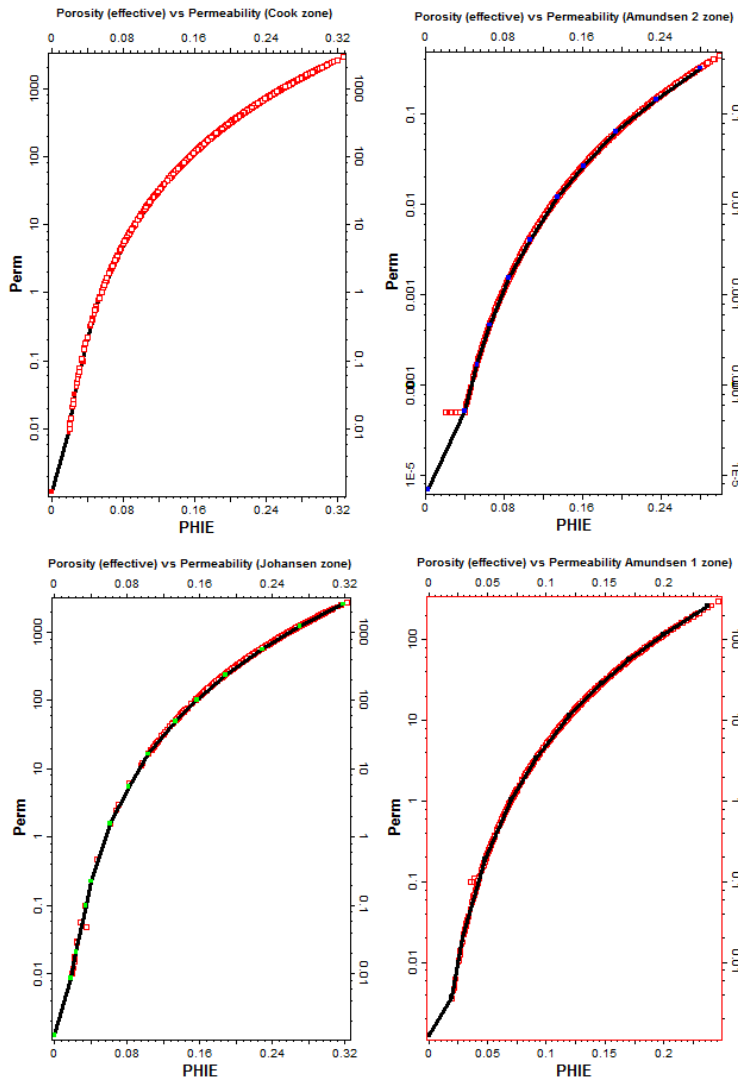


Figure 5-86: Look-up functions (black curves) made from PHIE vs Perm crossplots from wells (red squares).

DOCUMENT NO.: TL02-GTL-Z-RA-0001	REVISION NO.: 03	REVISION DATE: 01.03.2012	APPROVED:
-------------------------------------	---------------------	------------------------------	-----------

Perm base case model (total model: 3D & 2D area)

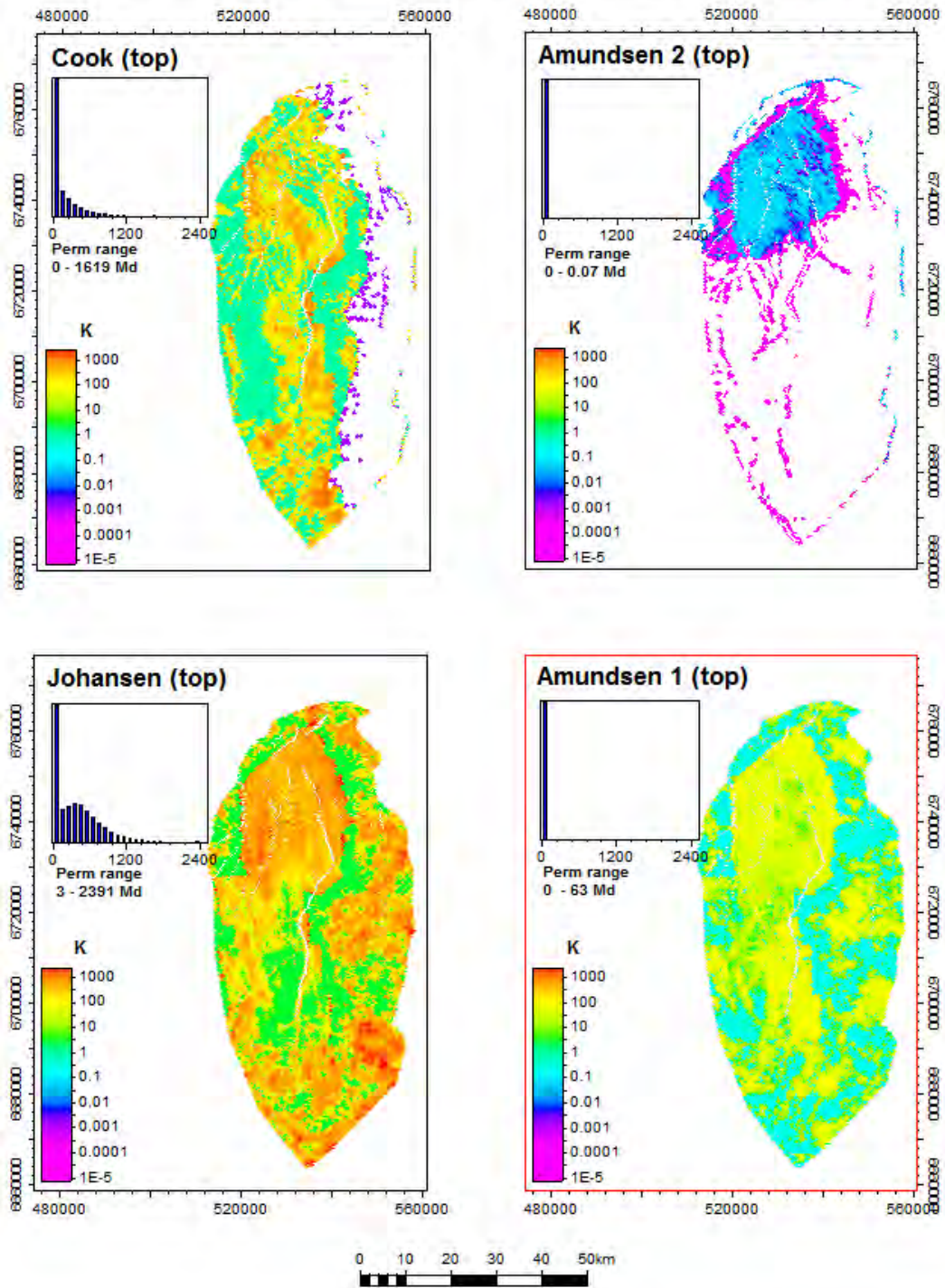


Figure 5-87: Perm base case model (2D & 3D area) viewed on top of each zone.

DOCUMENT NO.: TL02-GTL-Z-RA-0001	REVISION NO.: 03	REVISION DATE: 01.03.2012	APPROVED:
-------------------------------------	---------------------	------------------------------	-----------

Perm high case model (total model: 3D & 2D area)

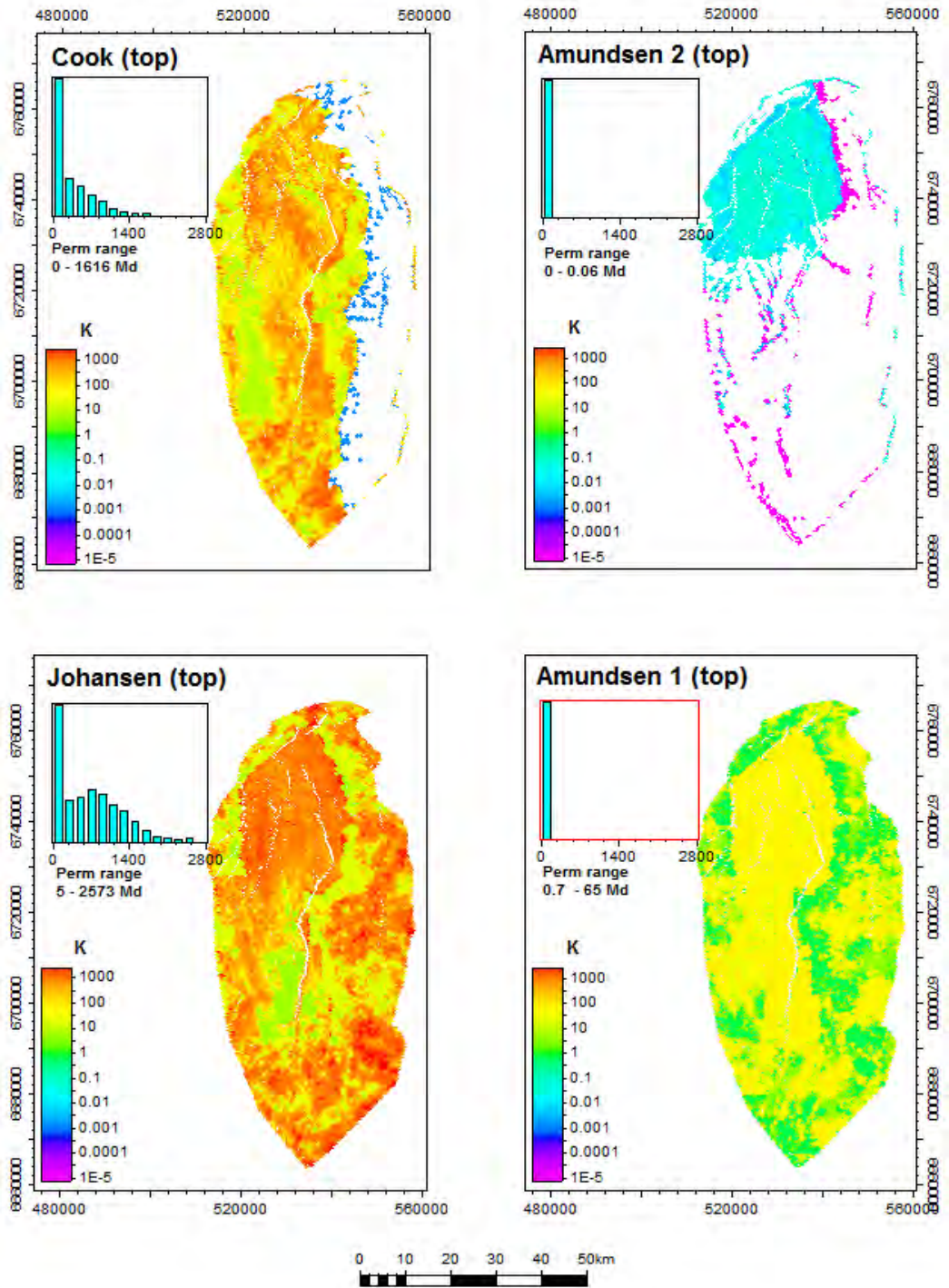


Figure 5-88: Perm high case model (2D & 3D area) viewed on top of each zone.

DOCUMENT NO.: TL02-GTL-Z-RA-0001	REVISION NO.: 03	REVISION DATE: 01.03.2012	APPROVED:
-------------------------------------	---------------------	------------------------------	-----------

Perm low case model (total model: 3D & 2D area)

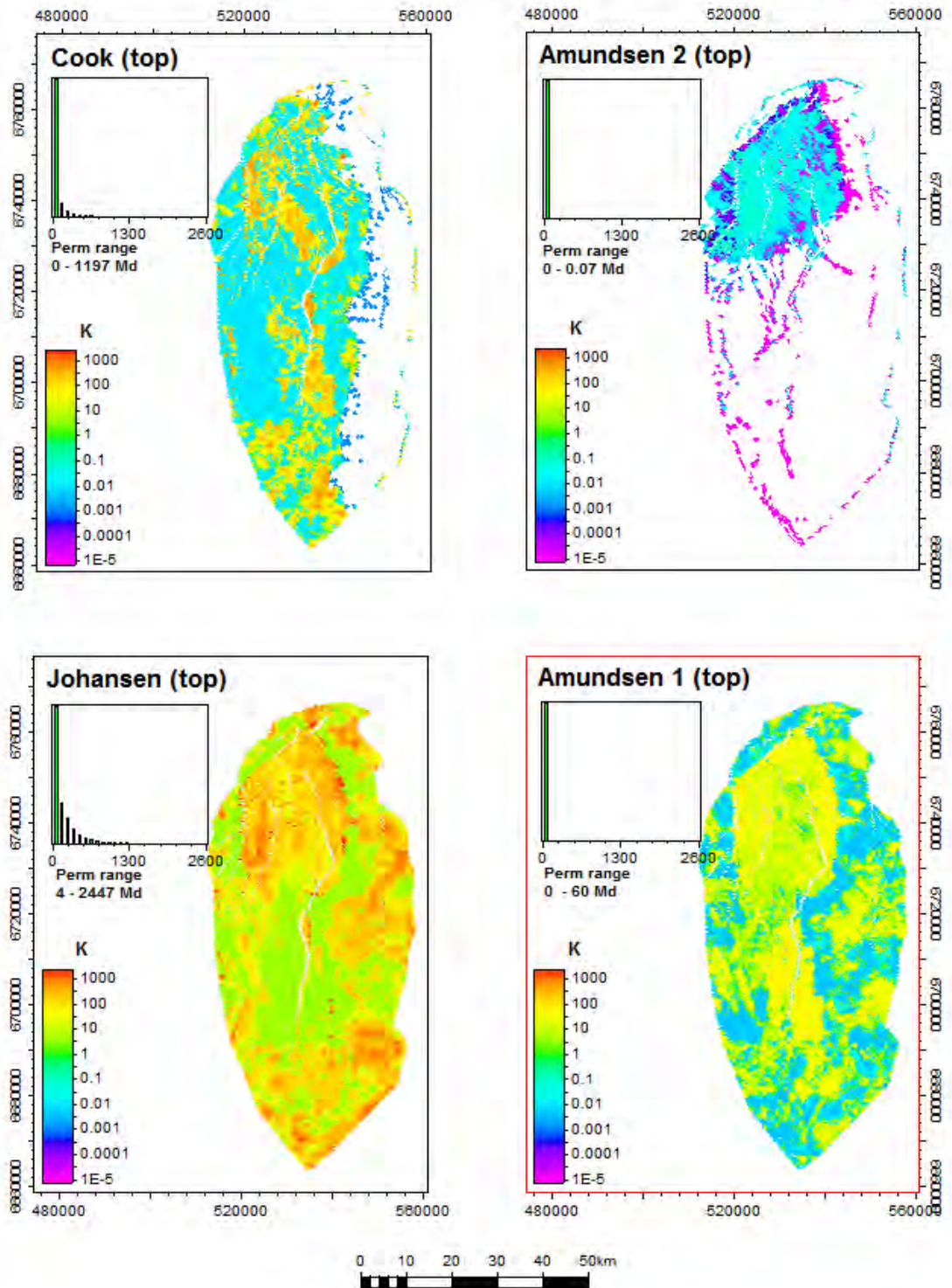


Figure 5-89: Perm low case model (2D & 3D area) viewed on top of each zone.

DOCUMENT NO.: TL02-GTL-Z-RA-0001	REVISION NO.: 03	REVISION DATE: 01.03.2012	APPROVED:
-------------------------------------	---------------------	------------------------------	-----------

5.6.2.5 *Uncertainties*

There are different approaches to obtain a property model depending on available data. In the most basic case, where no hard data (wells) are available, the only option is to use constant porperm values based on the conceptual knowledge of the depositional model for the area. If well data exist, and are believed to be representative for the area, a stochastic model can be calculated based on the variable (e.g. porosity) distributions in the wells and an estimate of a variogram of the variable to be modelled. A variogram is a statistical function that describes the increasing difference (or decreasing correlation) between sample values as separation distance between them increases. Such a statistical model has clear uncertainties based on the areal validity of the variable (e.g. porosity) to be modelled shown in wells, and how representative the variogram model is for the area to be modelled. Most often a sparse areal distribution of wells gives too few data points to identify any clear variogram model representing the area. Therefore, the best results may be achieved when hard data (wells) are combined with soft data (seismic data). The well data gives in-situ porosity values measured in a borehole, but are usually valid only for a smaller area around the well. The seismic data provides areal structural and lithological information, and if closely tied with the wells, may in good cases reveal an areal model of the measured values observed in the well positions.

In this study a combination of available well data and 3D seismic data is used to calculate the porosity model. In an AVO inversion study (elastic impedance modelling and inversion from angle band cubes) an Acoustic Impedance volume was generated and used as an areal guide for the porosity values. The match between the absolute inversion results and the well logs was considered to be of good quality for the acoustic impedance data (Gassnova-WGD 2011). However, the lack of wells for calibration of the seismic inversion data in the southern part of the 3D area constitutes an uncertainty on the lithology prediction here.

DOCUMENT NO.: TL02-GTL-Z-RA-0001	REVISION NO.: 03	REVISION DATE: 01.03.2012	APPROVED:
-------------------------------------	---------------------	------------------------------	-----------

6 DYNAMIC STORAGE BEHAVIOUR

This section deals with the dynamic behaviour of the Johansen Storage Complex when CO₂ is injected into it. The reservoir model is based on the geo model described in Chapter 5.6. The first part deals with model set-up and initiation, the second part discusses results and dynamic behaviour and investigates the effect of the uncertainty of various parameters. The final part follows a discussion around the uncertainty in permeability in the injection location.

6.1 Preparation of dynamic model

6.1.1 CO₂ phase behaviour and choice of simulation model

The CO₂ phase diagram is shown in Figure 6-1. The CO₂ injected into the Johansen Formation will be in a liquid or supercritical state.

Simulation of storage behaviour requires accurate modelling of the CO₂ phase behaviour, in particular the CO₂ density and viscosity, and its mutual solubility with brine/water at the range of reservoir conditions. There are several types of commercial reservoir simulation model that can be used, and the main choice is between compositional Equation of State (EOS) and Black Oil (BO) modelling. In additions, there exist variations within these model types that account for special features like geochemical effects (Gassnova-ROS 2011).

Eclipse 300 (E300) is Schlumberger's EOS compositional simulation model. This model treats CO₂ and water as separate components. The CO₂ density is calculated by an EOS (a two-parameter EOS) and its mutual solubility with water follows predefined correlations.

Eclipse 100 (E100) is Schumberger's BO model. The CO₂ and water can also here be considered separate components, but the properties and mutual solubility are given as pressure dependent tables rather than being calculated. The pressure dependent tables are calculated by an advanced EOS in a SINTEF proprietary PVT programme "CO2Thermodynamics" (Gassnova-IRI 2011). As suggested by SINTEF, it is necessary to model water as "oil" and CO₂ as "gas", to make this method work in E100.

Although compositional simulation in this context may sound more advanced, the opposite is in fact the case. The simpler EOS used by E300 is less accurate than the more advanced EOS used to generate table values used by E100. Also, while the solubility correlation is "hardwired" into E300, the tables used by E100 can be generated by any correlation. It was therefore decided to use E100 for the major part of this study.

Eclipse 100 is a finite difference based simulator that due to the spatial and time discretisation, are prone to certain numerical dispersion effects. One such effect of relevance here is that the CO₂ solubility rate will be overestimated, unless the rate is explicitly reduced.

DOCUMENT NO.: TL02-GTL-Z-RA-0001	REVISION NO.: 03	REVISION DATE: 01.03.2012	APPROVED:
-------------------------------------	---------------------	------------------------------	-----------

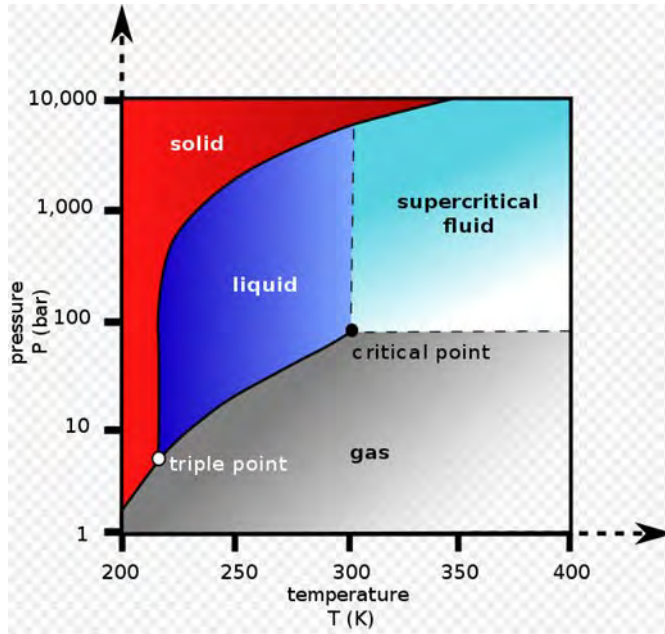


Figure 6-1: Phase envelope for CO₂ (Wikipedia). Critical point for CO₂ is at 304.18K and 7.38MPa (Suehiro, et al. 1996).

6.1.2 **Model gridding**

The reference simulation model grid is based on the geomodel grid, but has been both coarsened and refined. Coarsening and refinement have been done to minimize numerical dispersion effects, while attaining practical computer running times. The areal grid of the geomodel has been kept at 400m by 400m for the reference model. The vertical geomodel grid is coarsened and refined as shown in Table 6-1. The geo to simulation model grid conversion was performed to i) reduce the number of layers and grid cells in regions with relatively homogeneous properties and that will not be swept by CO₂, and ii) to sufficiently refine the grid dimensions in top layers that are swept by CO₂. Sensitivities to the reference model gridding were performed, and the results of these are presented and discussed in chapter 6.2.3.

Table 6-1: Layering in geo and reservoir model.

Layering in well area		Geomodel			Reservoir model		
Formation	Formation thickness (m)	Layering	No. of layers	Average thickness	Layering	No. of layers	Thickness (m)
Cook	66.6	1-30	30	1.8	1-8	8	0.4, 0.7, 2.2, 3.7, 7.4, 11.1, 23.3, 17.8
Amundsen 2	33	31-60	30	1.2	9	1	33
Johansen	168.1	61-160	100	1.2	10-16	6	0.6, 1.3, 3.9, 11.0, 33.6, 16.8, 100.8
Amundsen 1	45.8	161-210	50	1.0	17-18	2	18.3, 27.5

6.1.3 **Property upscaling**

Porosity and directional permeability has been converted from the geo-grid to the simulation grid. Figure 6-2 shows an east-west cross section of permeability in the well area, where the fine scaled geomodel is shown to the left and the upscaled reservoir model is shown to the right.

DOCUMENT NO.: TL02-GTL-Z-RA-0001	REVISION NO.: 03	REVISION DATE: 01.03.2012	APPROVED:
-------------------------------------	---------------------	------------------------------	-----------

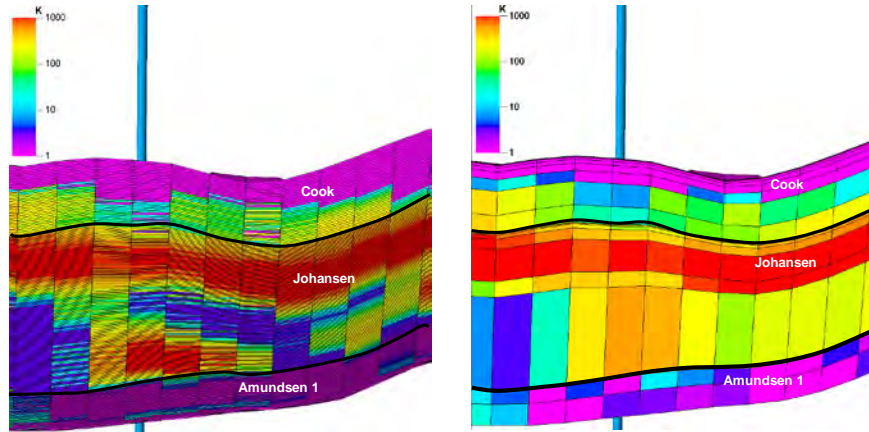


Figure 6-2: E-W cross section of permeability in injection well area, geomodel layering (left) and reservoir model (right).

When a geomodel layer has been refined into several simulation model layers, each simulation model layer keeps the property values of the original geo-layer. When several geo-layers are combined into fewer simulation layers, the porosity and the areal permeability is arithmetically weighted. The vertical permeability is upscaled harmonically, and in addition based on detailed log intervals of 15cm. An illustration of the vertical permeability upscaling is shown in Figure 6-2.

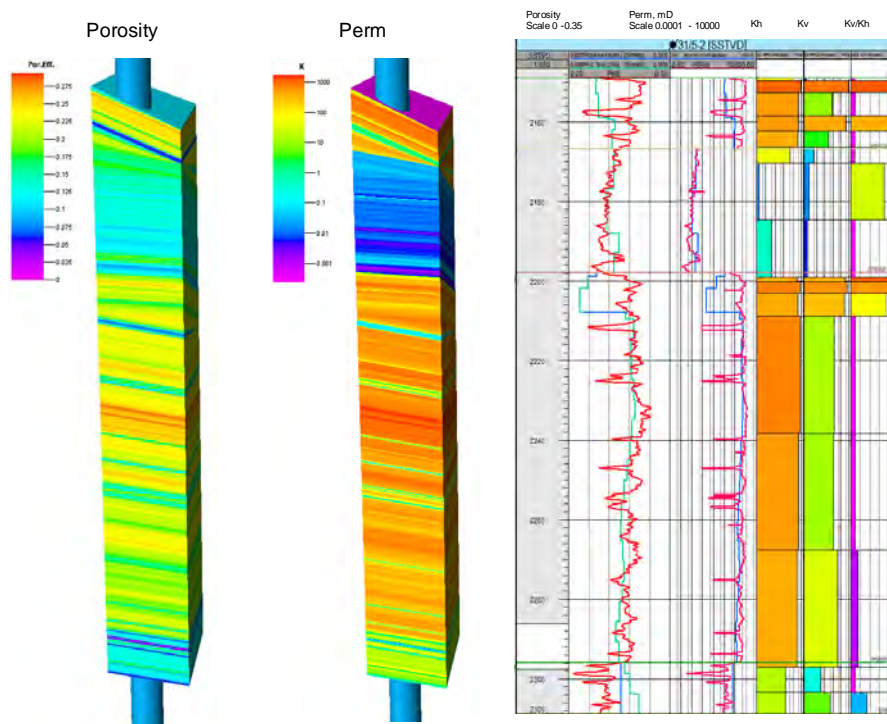


Figure 6-3: Vertical permeability upscaling from well logs for well 31/5-2.

6.1.4 Model initialization

The reference model input data are described and discussed in detail in the Reservoir Parameter report (Gassnova-ROS 2011), and a summary of these are given in Table 4-4 in chapter 4. With the structural geomodel as the basis, the most important other data are petrophysical data, rock

DOCUMENT NO.: TL02-GTL-Z-RA-0001	REVISION NO.: 03	REVISION DATE: 01.03.2012	APPROVED:
-------------------------------------	---------------------	------------------------------	-----------

and fluid data, and relative permeability data. Laboratory measurements were carried out with the aim of reducing the uncertainty in some of these data, but the results were available too late to be fully incorporated into this study. Also, poor core material and inconsistent measurements have done little to reduce uncertainty in some of these data. However, two important parameter values used were confirmed by the laboratory measurements; rock compressibility and residual CO₂ saturations from imbibitions. The laboratory reports are attached in (Gassnova-IRI 2011), and a summary of our early interpretations are found in chapter 4.7.

The Johansen and Cook formations are expected to be at hydrostatic pressure, and at datum depth of 3050m the pressure is 305 bar and the reservoir temperature is 94⁰C.

The modelled reference case aquifer volume is 91.4 GS_m3. This is the total aquifer volume in a closed Johansen/Cook system, and does not take into account any possible communication to adjacent structures. This is considered in the uncertainty and risk analysis described in chapter 7.

The outline of the simulation model top structure is shown in Figure 6-4, and the areal variation of some main properties are listed in Table 6-2. The regions referred to in Table 6-2 are shown in Figure 6-5.

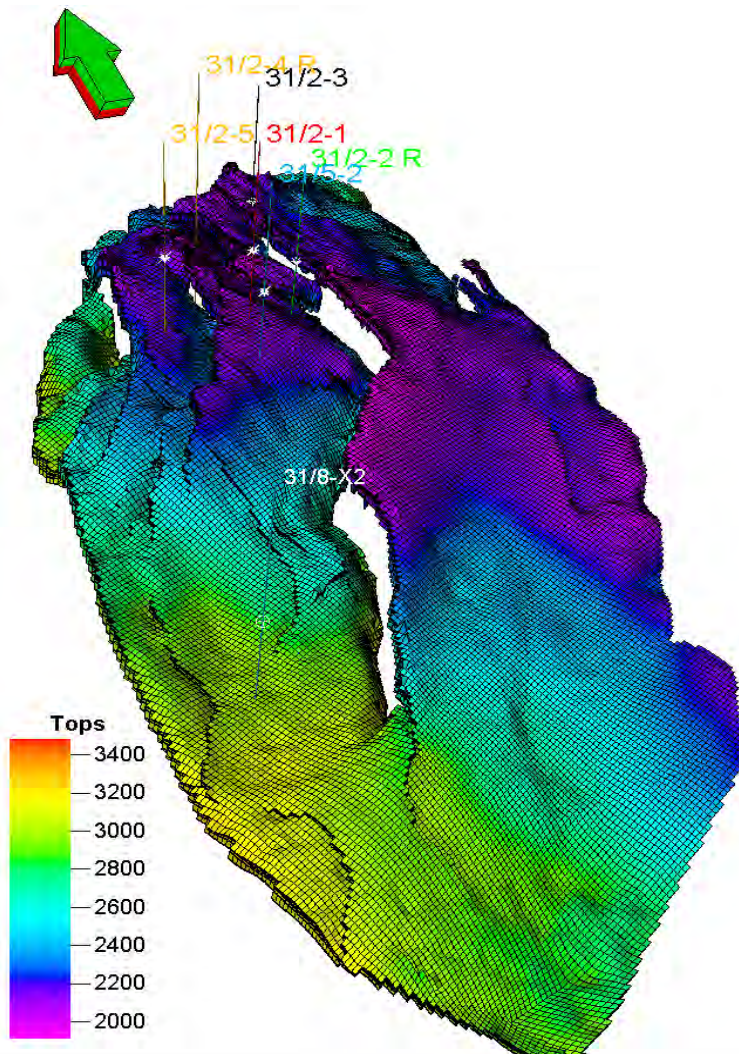


Figure 6-4: Top structure (Cook Fm) of reservoir model.

DOCUMENT NO.: TL02-GTL-Z-RA-0001	REVISION NO.: 03	REVISION DATE: 01.03.2012	APPROVED:
-------------------------------------	---------------------	------------------------------	-----------

Table 6-2: Areal variation of porosity and permeability separated into 5 regions.

Average Depths	Region 1 North	Region 2	Region 3	Region 4	Region 5 South
Cook	2074	2279	2694	2990	2930
Amundsen 2	2088	2296	Not Present	Not Present	Not Present
Johansen	2139	2328	2778	3050	2980
Amundsen 1	2218	2441	2920	3220	3150
Porosity	Region 1 North	Region 2	Region 3	Region 4	Region 5 South
Cook	0.14	0.13	0.10	0.10	0.13
Amundsen 2	0.14	0.12	Not Present	Not Present	Not Present
Johansen	0.18	0.19	0.16	0.17	0.18
Amundsen 1	0.15	0.10	0.10	0.10	0.10
Permeability	Region 1 North	Region 2	Region 3	Region 4	Region 5 South
Cook	239	152	92	85	175
Amundsen 2	7	29	Not Present	Not Present	Not Present
Johansen	421	402	290	337	400
Amundsen 1	25	15	18	15	17

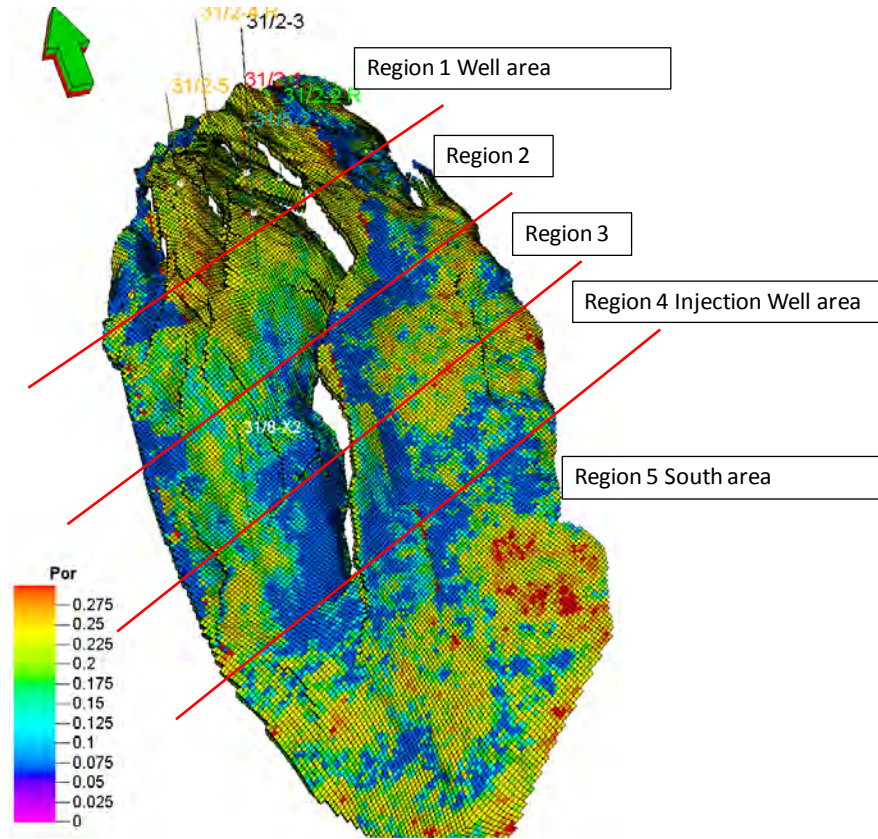


Figure 6-5: Porosity map of Johansen Fm showing 5 regions for overview of porosity and permeability.

DOCUMENT NO.: TL02-GTL-Z-RA-0001	REVISION NO.: 03	REVISION DATE: 01.03.2012	APPROVED:
-------------------------------------	---------------------	------------------------------	-----------

6.2 Prediction of storage behaviour

6.2.1 Reference case

Injection well location

The CO₂ injection well location is indicated in Figure 6-4 with the well 31/8-X2. This location is a suggested preliminary location which is a compromise between being far enough south to avoid CO₂ plume migration into the faulted area discussed in chapter 5.3, and to avoid penetrating the reservoir too deeply. Locating the CO₂ injection well this far south also increases the volumetric sweep, hence reducing the volume of free mobile CO₂. The injection location is also located away from the mapped faults. At the reference location, the well penetrates the Johansen Formation at 3050m (msl) in an area which is estimated to have good porosity and permeability. Model parameters at injection location are 625mD and 20% porosity.

Injection rates and duration

The reference case injection rate is 3.2Mt CO₂/y, and the injection period lasts for 50 years. Total CO₂ injection volume is then 160Mt. Simulation continues after injection stops, to follow the migration of the CO₂ plume, although it has not been possible to run all cases to 5000 years due to time constraints.

CO₂ plume migration and pressure build-up

The most relevant results from the reservoir simulations are the migration of the CO₂ plume, and the reservoir and near-well pressure build-up.

The migration of the CO₂ plume after 50 years of injection is shown in Figure 6-6, showing both top Cook Formation and top Johansen Formation. Figure 6-7 shows the plume after 500 years. The figure shows the fractional pore volume occupied with free CO₂ as the parameter S_g (gas saturation). This is done for all figures showing CO₂ migration. The plume does not migrate into any potentially high risk faults or leakage areas. A vertical cross-section of the CO₂ plume is shown in Figure 6-8.

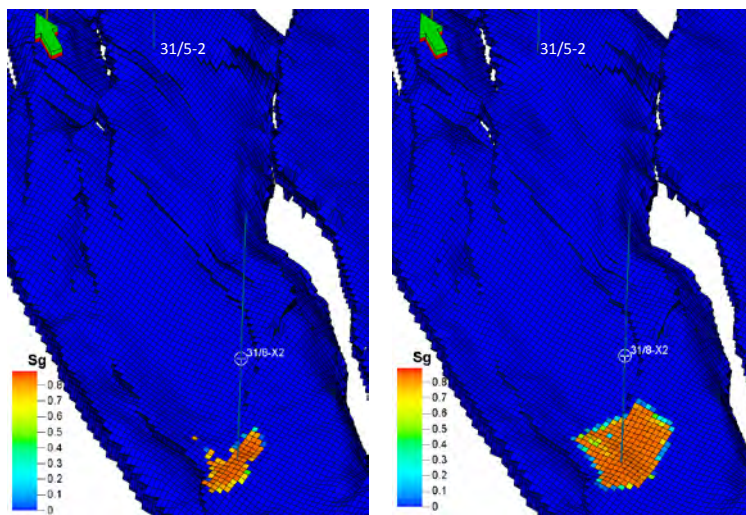


Figure 6-6: CO₂ plume after 50 years of injection (2064) at top Cook Fm (left) and top Johansen Fm (right). S_g is saturation of CO₂ in free phase.

DOCUMENT NO.: TL02-GTL-Z-RA-0001	REVISION NO.: 03	REVISION DATE: 01.03.2012	APPROVED:
-------------------------------------	---------------------	------------------------------	-----------

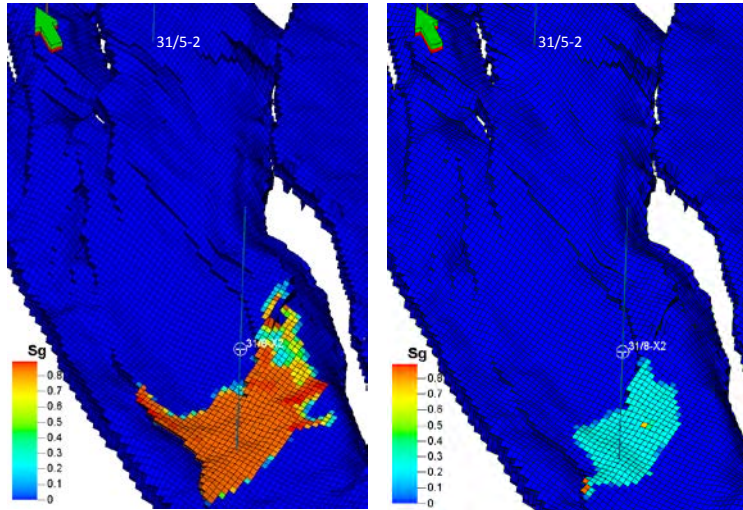


Figure 6-7: CO₂ plume after 500 years of injection (2514) at top Cook Fm (left) and top Johansen Fm (right).

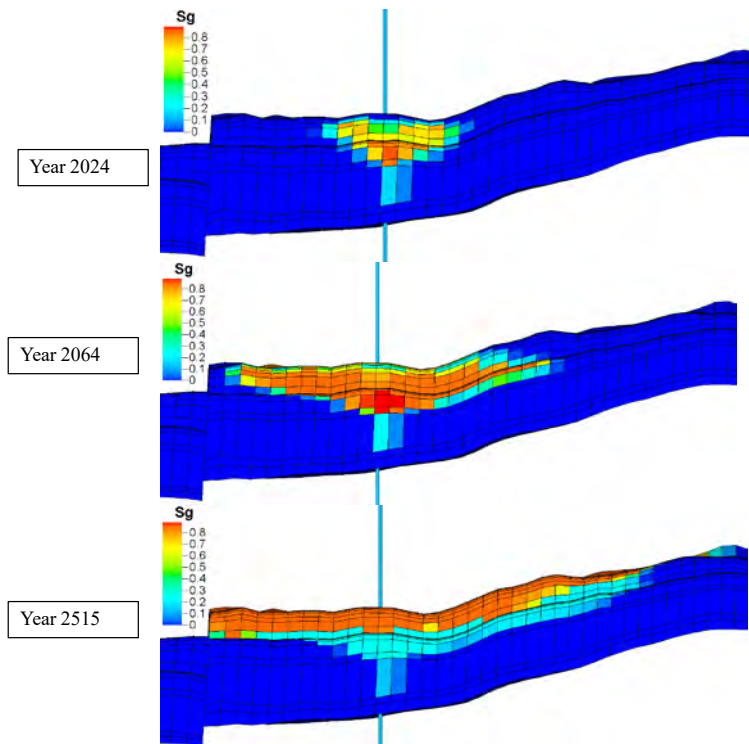


Figure 6-8: Vertical cross section of plume after 10, 50 and 500 years.

The pressure build-ups in the near well area and “inside” the reservoir are shown in Figure 6-9. These pressure increases are significantly below what has been evaluated to be “safe” pressure increase (chapter 5.5). The near well pressure build-up is about 10 bar higher than the average reservoir build-up. The near well pressure build-up is mainly dependent on permeability/injectivity, while the average reservoir pressure is mainly dependent on total compressibility.

DOCUMENT NO.: TL02-GTL-Z-RA-0001	REVISION NO.: 03	REVISION DATE: 01.03.2012	APPROVED:
-------------------------------------	---------------------	------------------------------	-----------

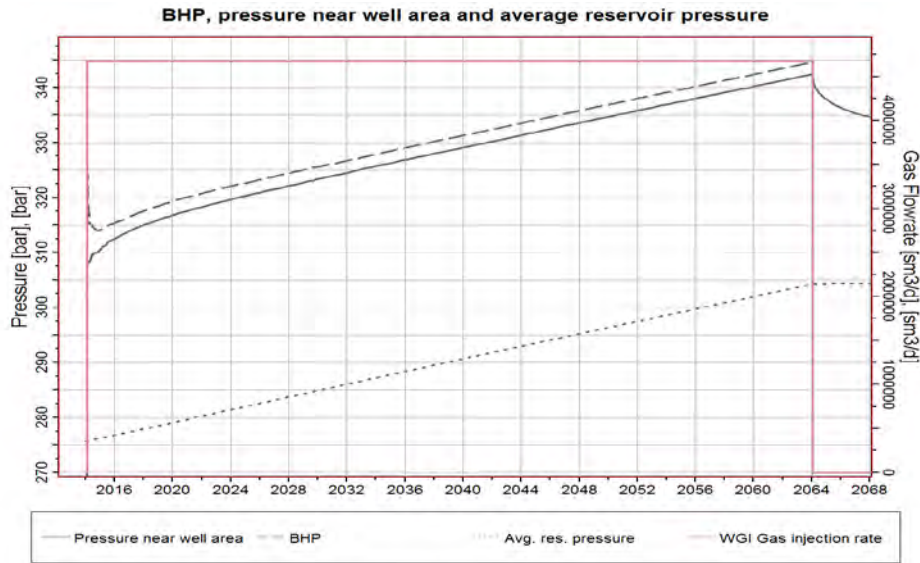


Figure 6-9: Pressure build-up in near well area, reservoir and bottom hole.

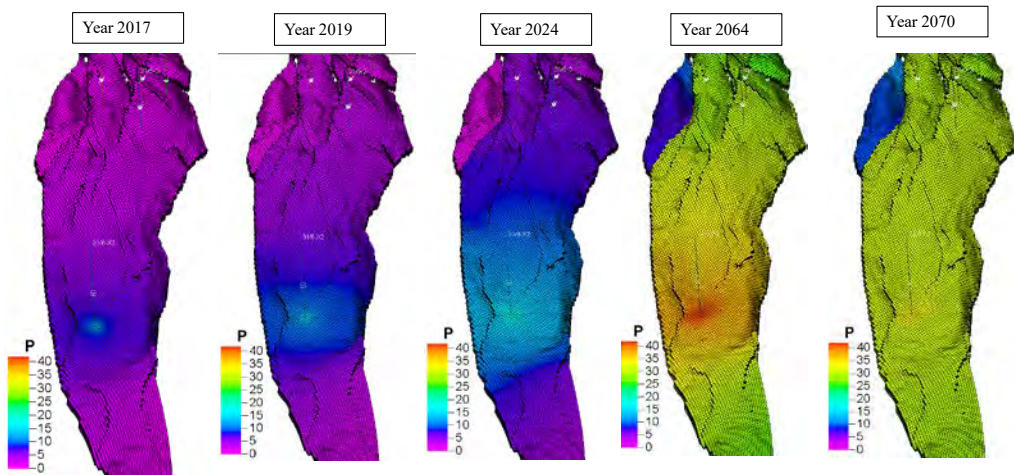


Figure 6-10: Areal pressure development over time.

6.2.2 Simulation sensitivities

Most simulation sensitivities are covered in the Reservoir Parameter Study (Gassnova-ROS 2011). These sensitivities include variations in:

- Compressibility
- Mutual solubility between CO₂ and brine
- Relative permeability endpoints

None of the parameter variations alone in these sensitivities has an effect that causes significantly different plume migration or unacceptable pressure increase. However, low permeability sensitivities are borderline cases, but remedies can be more and/or longer injection well(s).

In addition to the parameter value sensitivities, the uncertainty related to the geological model and the connected pore volume is covered in the overall risk assessment explained in chapter 7.

DOCUMENT NO.: TL02-GTL-Z-RA-0001	REVISION NO.: 03	REVISION DATE: 01.03.2012	APPROVED:
-------------------------------------	---------------------	------------------------------	-----------

6.2.3 **Grid sensitivities**

The main objective of grid sensitivity simulations is to evaluate whether the reference case grid is sufficiently detailed and refined, and this relates to both the areal and vertical gridding.

The areal reference gridding is 400m by 400m. This gridding may not fully capture structural variations. Sensitivity to more refined gridding (100m by 100m) is not yet completed. This is not expected to have a large effect on the CO₂ plume migration, but is listed under further work. There are two opposite effects that fine structural variation could give. One effect is an “upside down” river effect, meaning that rather than uniformly filling in a large grid cell, the CO₂ would follow narrow structural variations, and therefore progress more rapidly. The other effect is that fine structural variations would give local traps. No effort has been made to quantify these effects.

The vertical gridding of the reference grid is rather detailed, and the thickness of the top layer (Cook) is only about 0.5m. This is significantly thinner than the thickness of the CO₂ plume, and sufficiently refined. The top Johansen Formation layer is of similar thickness. A possible simulated optimistic effect may be caused by the low permeability of the top Cook layers. Low permeable top layers with high permeable layers below will give a positive vertical spreading effect of the CO₂, since the viscous and gravitational forces will be more balanced. A sensitivity simulation with high permeability in the top layer (or alternatively where the top layers were impermeable) was carried out to check if the gridding is then acceptable. Figure 6-11 shows an east-west cross section in the well area comparing reference model gridding with a finer upscaling of Cook Formation. The results were different (faster spreading in the top layers) but the gridding is still sufficiently refined.

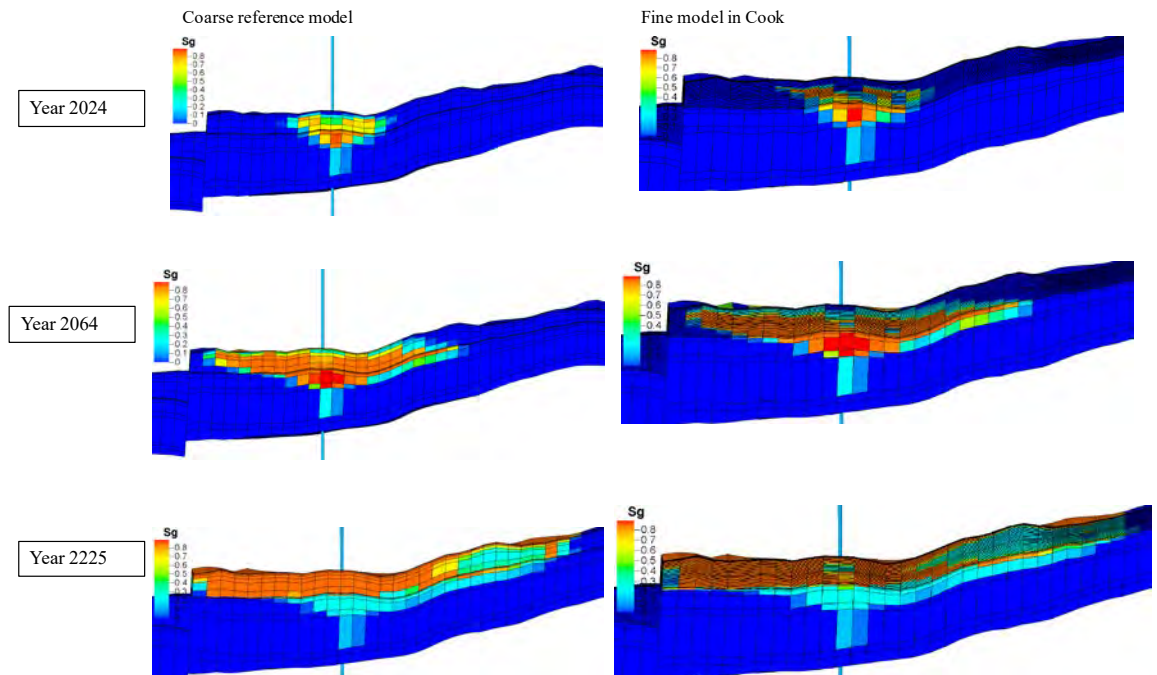


Figure 6-11: E-W cross section of CO₂ saturation in well area over time, reference gridding (left) and finer upscaling (right).

DOCUMENT NO.: TL02-GTL-Z-RA-0001	REVISION NO.: 03	REVISION DATE: 01.03.2012	APPROVED:
-------------------------------------	---------------------	------------------------------	-----------

6.2.4 **Deterministic Low Case**

6.2.4.1 *CO₂ plume spread low case*

A deterministic low case from a simulation point of view has been constructed with the following changes to the reference case:

- No solubility of CO₂ in water (DRSDT = 0)
- High top layers permeability (200mD)
- High vertical communication (kv/kh = 1)

The purpose of this deterministic low case is to check the spreading of the CO₂ plume under such adverse simulation assumptions, with the most pessimistic assumptions on the most important simulation parameters. The CO₂ plume is shown in Figure 6-12. The CO₂ plume does not reach the high risk fault areas underneath the Troll area (marked with a white line) even under such adverse simulation assumption. However, after 250 years, the plume gets close to this area. Although this deterministic low case contains the most pessimistic simulation parameters it should not be considered an absolute low case (P100) since there are other modelling issues (geology) that could cause even quicker spreading of the CO₂ plume.

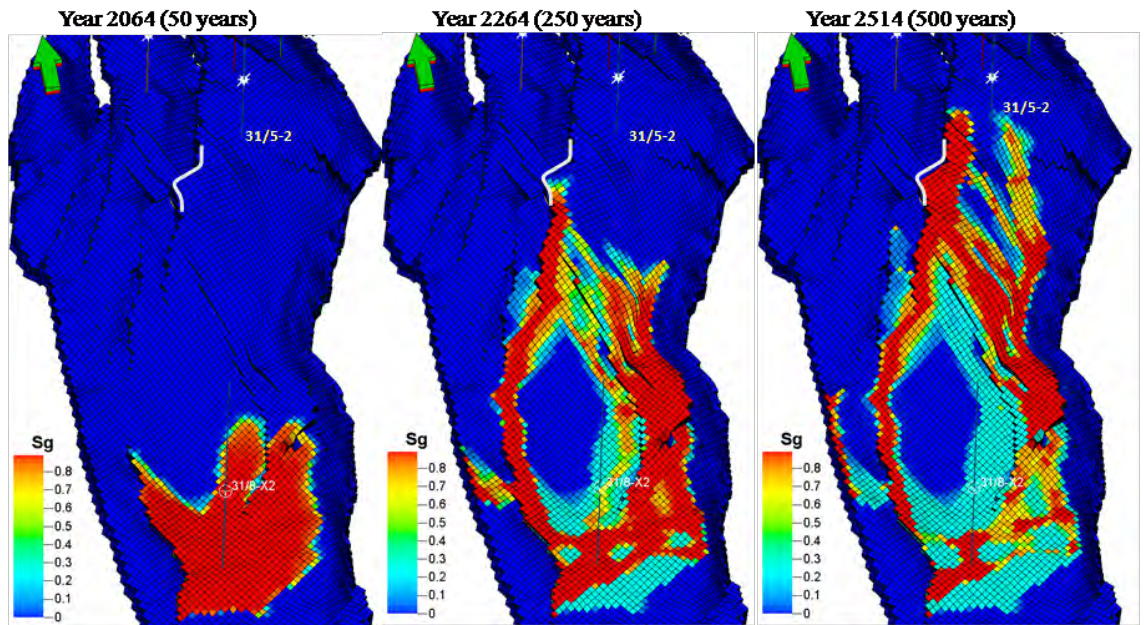


Figure 6-12: CO₂ plume migration low deterministic, top Cook – 50, 250 and 500 years after start injection.

6.2.4.2 *Pressure build-up low case*

The reference case permeability has been reduced by factors of 5 and 10 to check the effect on near well pressure increase in the case that permeability should be significantly lower than estimated. When permeability is reduced by a factor of 10 (average reservoir permeability reduced from 600 to 60mD), the near well pressure increase is 105 bar. This is below the estimated P90 fracture pressure of 113 bar (chapter 7.5). Figure 6-13 shows the pressure build-up for the bottom hole, near well area and average reservoir pressure with varying permeability. A remedy to this pressure increase is to inject in more than one well and/or drill more deviated/horizontal wells that penetrate longer reservoir sections. Permeability reduction and its effect on injectivity and injection pressure limitation are also discussed in chapter 6.3.

DOCUMENT NO.: TL02-GTL-Z-RA-0001	REVISION NO.: 03	REVISION DATE: 01.03.2012	APPROVED:
-------------------------------------	---------------------	------------------------------	-----------

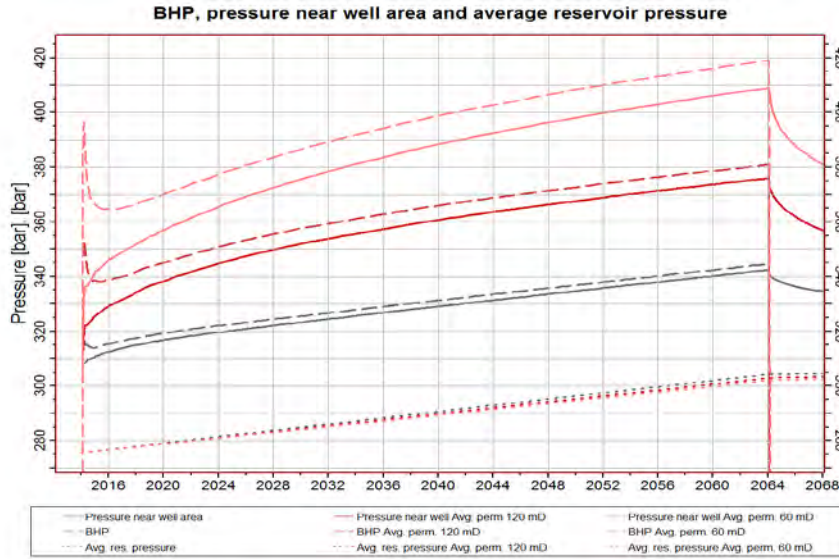


Figure 6-13: Pressure build-up in near well area, reservoir and bottom hole for reference model and permeability reductions by factor of 5 and 10.

The effects of the low permeability on the plume spread are shown in Figure 6-14 . Lower permeability gives lower areal, but higher vertical spreading of the CO₂ plume. Lower permeability increases the viscous forces, and therefore reduces the relative significance of gravity.

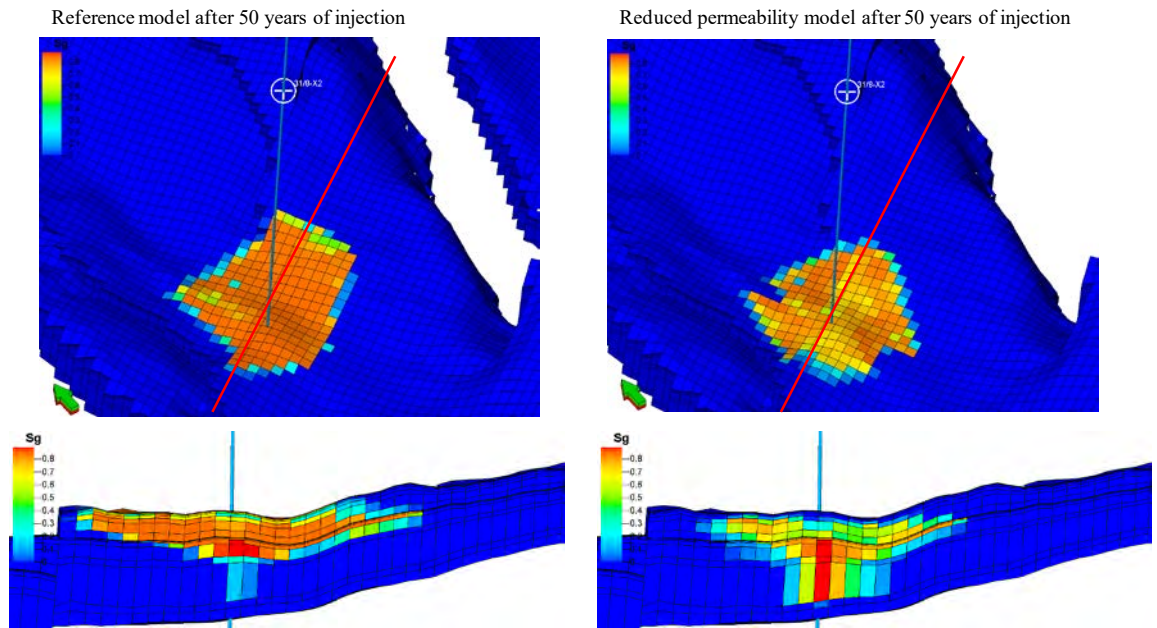


Figure 6-14: Permeability low case (factor 10) plume migration. Lower figures are vertical cross sections as indicated in the top figures.

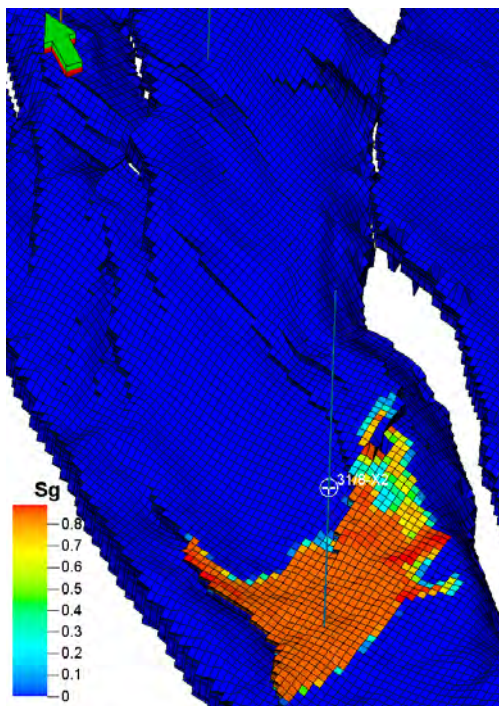
Geological volume uncertainty is not included in this low case. Lower connected reservoir volume will cause an additional increase in pressure. This is included in the risk analysis (chapter 7).

DOCUMENT NO.: TL02-GTL-Z-RA-0001	REVISION NO.: 03	REVISION DATE: 01.03.2012	APPROVED:
-------------------------------------	---------------------	------------------------------	-----------

6.2.4.3 *Depth trend model- disregard of inversion data*

An alternative simulation model was made from the geomodel explained in section 5.3.2.2, where inversion data is disregarded when populating the model. Similarly to the model explained above this model has an average permeability of approximately 60mD in the injection area. The model is however, totally homogeneous. Pressure build-ups are therefore lower than those found in section 6.2.4.2. Plume spread in such a homogeneous model can be seen in Figure 6-15, and it is evident that effect on plume spread is marginal as it is largely controlled by buoyancy and within the safe area.

Reference model



Model based on depth

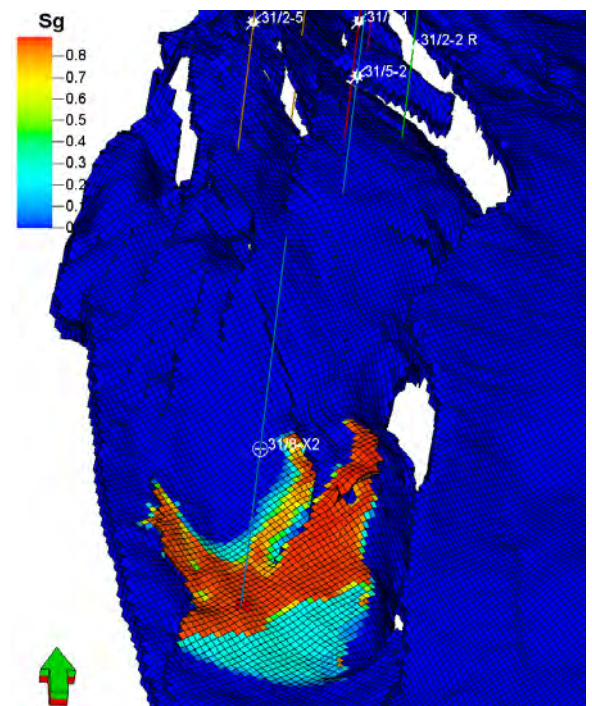


Figure 6-15: Plume spread in depth trend model after 500 years (2515).

6.2.5 **CO₂ trapping**

The injected CO₂ will be stored and trapped in the reservoir by different mechanisms, dependent on place and time. This is illustrated in Figure 6-16 (mineralization not included).

The main states of CO₂ are:

- Free mobile CO₂ (free phase and free to flow)
- CO₂ in solution with water (can only flow with water phase)
- Residually trapped CO₂ (free CO₂ phase, but trapped)
- Mineralised of CO₂ (caused by slow chemical reactions)

When CO₂ makes contact with water, that water becomes saturated by CO₂. The remaining, free CO₂ will flow and saturate new, fresh water. The proportion of CO₂ that goes into solution is small compared to the total amount of CO₂ injected, but increases with time. The increase with time is caused by several effects. One effect is diffusion within the water phase since different solution gradients will gradually be equilibrated. Another effect is convection within the water phase. Since water saturated with CO₂ is slightly heavier than pure water, the shallow water (in contact with CO₂) will tend to sink downwards, thus replacing and trading places with the CO₂-free, lighter water underneath. This stirring effect will cause CO₂ to contact more fresh

DOCUMENT NO.: TL02-GTL-Z-RA-0001	REVISION NO.: 03	REVISION DATE: 01.03.2012	APPROVED:
-------------------------------------	---------------------	------------------------------	-----------

water and therefore increase the potential for solubility storage. These effects are not explicitly modelled, but numerical dispersion effects in the simulation model will give similar effects. However, it is difficult to estimate whether the numerical dispersion effects are higher or lower than the real physical effects.

The residually trapped CO₂ becomes noticeable after injection stops, and the imbibition process with water displacing CO₂ starts. A portion of approximately 40% of the CO₂ will then be trapped in the smallest rock pores, and thus become immobile.

Mineralisation is a slow process, and is described in the Reservoir Parameter Study Report (Gassnova-ROS 2011).

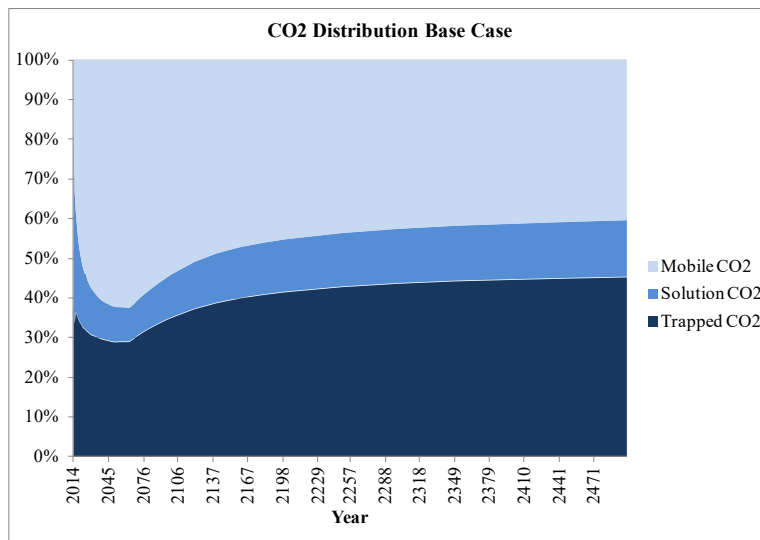


Figure 6-16: Fractional distribution of injected CO₂ for Base case (top), Low case (middle) and High case (bottom) residual CO₂ saturation.

6.2.6 Summary and discussions

The dynamic reservoir behaviour under CO₂ injection can be summarized as follows:

- For the reference case model CO₂ will not reach areas of communication to surrounding formation or potential leakage to surface areas within the first 500 years.
- For the reference case model the pressure build-up due to injection is below safe pressure build-up.
- Geological uncertainties are not fully incorporated in the reservoir simulation sensitivities, and may impact dynamic behaviour. Geological uncertainties are combined with dynamic reservoir uncertainties in chapter 7.

Some planned reservoir engineering work was not possible to complete within the time frame of this project. These tasks may be completed at a later stage, and include:

- Evaluation and implementation of laboratory core measurements
- Alternative geomodels
- Fine areal grid dimension (100m x 100m) model

In general, the reservoir engineering work concludes that the planned CO₂ injection volumes of 160Mt can be injected and safely stored in the Johansen Formation. There is, however, uncertainty associated with this conclusion, both regarding injection volumes/pressure and spreading and containment of the CO₂ plume. This uncertainty was not reduced by the laboratory core experiments, and can only be reduced by conducting proper laboratory

DOCUMENT NO.: TL02-GTL-Z-RA-0001	REVISION NO.: 03	REVISION DATE: 01.03.2012	APPROVED:
-------------------------------------	---------------------	------------------------------	-----------

experiments on cores from a new well in the planned injection area. Even further reduction may be achieved by performing an injection test. This is further elaborated on in the injectivity section.

6.3 Injectivity and permeability evaluation

One of the main evaluation criteria for the Johansen Storage Complex is that it should have sufficient injectivity for the desired rates. CO₂ injection into the Johansen Formation will mainly be limited by the permeability, reservoir thickness and reservoir pressure. This study evaluates the impact of all these parameters except for temperature effects, which will be evaluated at a later point.

6.3.1 Permeability uncertainty

As discussed in chapter 5.3.2, regarding sand quality in the Johansen Formation, there are large uncertainties related to the permeability in the injection area. The geomodel is based on petrophysical results and older core data from the available wells. A core analysis was initiated to evaluate the porosity and permeability data. Chapter 4.7 describes these tests in further detail, but the results from the core measurements related to permeability are discussed below.

Absolute permeability measurements can be seen in Figure 6-17, showing log permeability versus linear porosity, together with the porosity/permeability data available in core reports from the operator’s core testing programme in 1980 (referred to as the Johansen Reference Core Data (JRCD), and the permeability/porosity trend used in the reference simulation model. Note that the JRCD tests are Klinkenberg corrected horizontal permeability (Kh) measured at ambient conditions of 1.5MPa net confining pressure. Also, from the current testing programme, the measured permeability reductions going from ambient to reservoir pressure/stress condition are indicated.

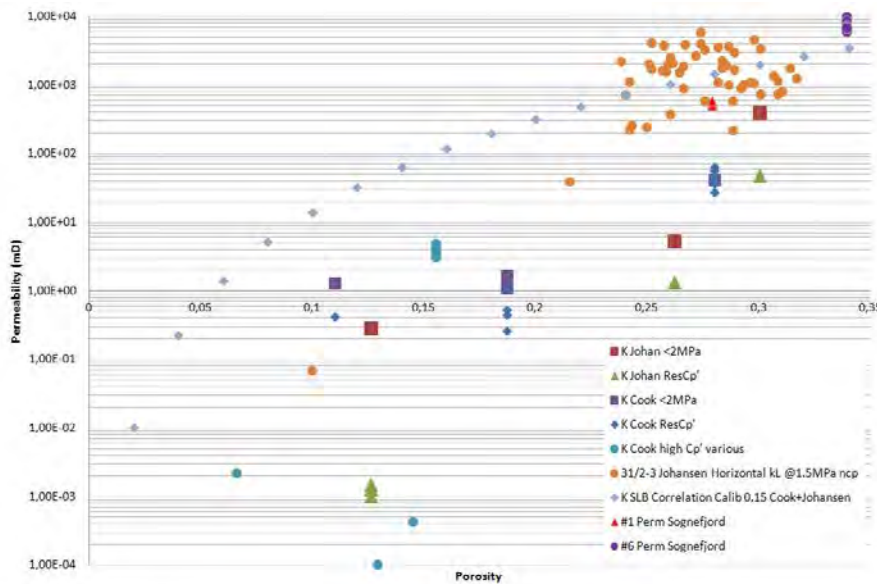


Figure 6-17: Core laboratory measurements of permeability of Cook and Johansen Fm cores.

The figure shows that the JRCD permeability measurements and the correlation used are significantly higher than the new laboratory measurements. The difference can be split into two main components; a general lower ambient permeability and the ambient to reservoir conditions reduction factor. The apparent difference between old and new data requires analysis, explanation and possibly conclusion. First, a summary of what the old and new measurements represent is presented.

DOCUMENT NO.: TL02-GTL-Z-RA-0001	REVISION NO.: 03	REVISION DATE: 01.03.2012	APPROVED:
-------------------------------------	---------------------	------------------------------	-----------

The JRCD measurements are performed on what is believed to be fresh, representative cores, and there is no apparent reason why these measurements should be discredited. They are however, performed at ambient conditions (1.5MPa net confining pressure), and the correlation used to generate reservoir simulation model permeability is not adjusted to reservoir conditions. Old measurements indicate that this reduction factor is about 2/3, and this correction should be applied. Measurements conducted on the Sognefjord Formation from 31/5-2 indicate that this permeability reduction factor ranges between 0.6-0.83 for 35%-28% porosity Sognefjord samples. This correction should be applied to the JRCD. The new permeability measurements are mostly performed on vertical cores, and the vertical permeability is lower than the corresponding horizontal permeability. Measurements of Kv and Kh on three Cook Formation cores in this study show that the ratio decreases with lower permeability and a higher degree of heterogeneity. Of the relatively high permeable cores, only core plug 15 (Cook) had both vertical and horizontal permeability measured, with a ratio of about 0.7. The only high Johansen

Formation porosity/permeability core is the combined core 1 and core 6. The measured ambient vertical permeability on core 1/6 is about 400mD, and applying the kv/kh ratio of core 15, the ambient horizontal permeability of core 1/6 is almost 600mD. Still, this permeability is somewhat outside the JRCD experimental correlation cloud. Also, the measured stress effect (from ambient to reservoir condition) is very high relative to analogue data from Sognefjord Formation (31/5-2), and reduces the permeability from about 400 to 50mD. This effect is suggested by NGI to be unrealistically high, but it is unclear whether that means the ambient measurement is too high or the reservoir measurement is too low (or a combination of the two).

The new experiments have been carried out on cores that have been exposed to adverse core conditions for many years, and may have changed characteristics.

The measurements also show inconsistencies between different experiments (carried out by different laboratories), and also within the same experiment. The core plug that has undergone most experiments and “travel” is probably the Cook Formation plug 15, and examples of different permeability measurements on this core plug are given in Table 6-3 below:

Table 6-3: Permeabilities from lab.

Core 15 measurements	Perm mD	Direction	Conditions	Lab	Comment
1	156	Vertical	Ambient, k_L^*	IRIS	
2	220	Horizontal	Ambient, k_L^*	IRIS	
3	75	Vertical	Ambient, k_L^*	IRIS	compares with 1, but before ends of plug cut off
4	41	Vertical	Ambient, k_w	IRIS	compares with 3, water vs Klinkenberg corrected Helium
5	27	Vertical	Reservoir, k_w	IRIS	compares with 4, reservoir vs Ambient
6	9	Vertical	Ambient	NGI	compares with 1
7	30	Vertical	Reservoir	NGI	compares with 6, higher measured perm at higher stress

Considering these results, the permeability correlation used to generate input to the reservoir simulation model (based on the old measurements) still stands as representative of a most likely estimate, but should be corrected by a reservoir/ambient correction factor of between 0.6 and 0.83. This has not been implemented into the current work, but the estimated effect in injectivity has been simulated in 6.3.2. The new measurements are questionable due to the overall condition of the cores, the few representative high permeability cores, and some apparent inconsistencies between measurements. However, the new lower permeability measurements cannot be completely discarded. The risk of lower reservoir permeability has

DOCUMENT NO.: TL02-GTL-Z-RA-0001	REVISION NO.: 03	REVISION DATE: 01.03.2012	APPROVED:
-------------------------------------	---------------------	------------------------------	-----------

increased, with the consequence of lower injectivity and higher pressure increase. This uncertainty will be present until any new measurements from a new well become available.

6.3.2 Injectivity evaluation

Pipesim 2011.1 nodal analysis software has been utilized to evaluate the injectivity of the Johansen Formation prospect for CO₂ storage. The simulations are based on the reference geological model and assuming injection in a single vertical well. Unfortunately at the time of writing it has not been possible to investigate the effect of horizontal wells due to software constraints. The following injection rates have been evaluated:

Yearly injection rate MT/yr	Yearly injection rate including 95% uptime MT/hr)	Hourly injection rate T/hr	Hourly injection rate including 95% uptime T/hr
3.2	3.37	370	384.5

Available wellhead injection pressure is governed by the onshore pump and pipeline design pressure. Maximum pipeline pressure is set to 245 barg at MSL and pump pressure is 200 bar which gives a wellhead pressure of approximately 145 barg at 3.2Mt/y (see section 9.3.14). Figure 6-18 shows the results of massflow vs permeability. Injection pressure here is defined as wellhead pressure. With the base reservoir thickness of 151m and reservoir pressure of 305 bar, it will require an injection pressure (at wellhead) of approximately 130 bar to inject 3.2Mt/y, assuming an average permeability of 625mD which is the average permeability in the well area according to the geomodel. Reducing the average permeability by a factor of 0.6 (as may be suggested from core measurements) will give a permeability of 375mD. This will be marginally achievable with the current injection pressure and a vertical well. Longer reservoir exposure obtained with horizontal well will lower required injection pressure. For a permeability down to 50 mD a 300-400m horizontal well will be necessary (Figure 6-19).

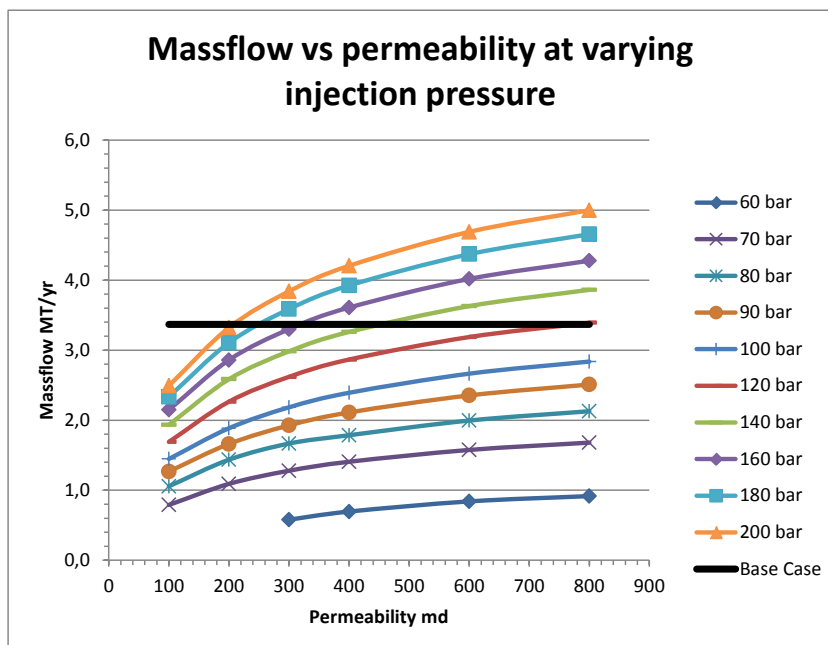


Figure 6-18: Injection pressure sensitivity, mass flow vs permeability.

DOCUMENT NO.: TL02-GTL-Z-RA-0001	REVISION NO.: 03	REVISION DATE: 01.03.2012	APPROVED:
-------------------------------------	---------------------	------------------------------	-----------

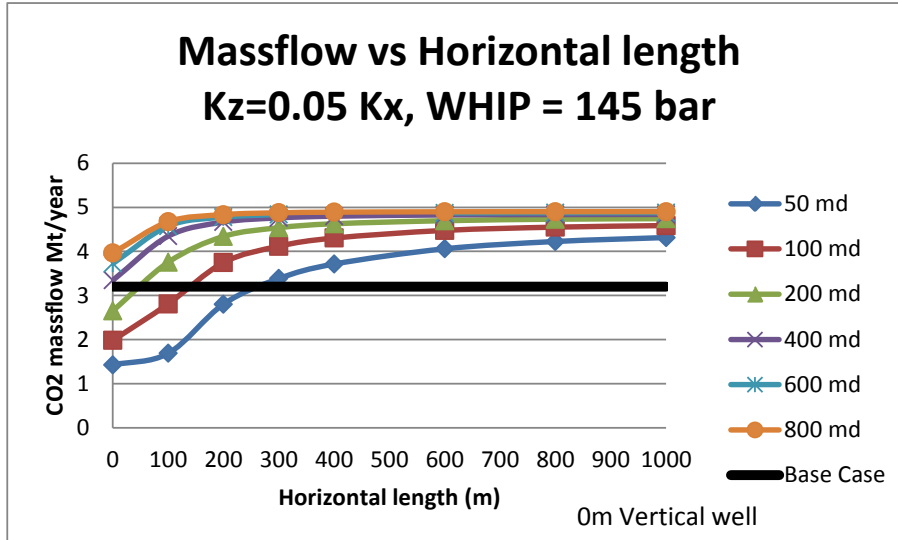


Figure 6-19 Injection rate with horizontal well vs permeability

6.3.2.1 Effect of increased reservoir pressure

Figure 6-20 shows the result with increasing reservoir pressure, again with mass flow vs permeability. The simulations are done with the base case reservoir thickness, permeability and 145 bar injection pressure. It can be seen that more than one well is needed when reservoir pressure reaches 320 bar with base case permeability for a vertical well.

Increasing the injection pressure, sand exposure through horizontal well or having several wells available for injection will compensate for the increasing reservoir pressure.

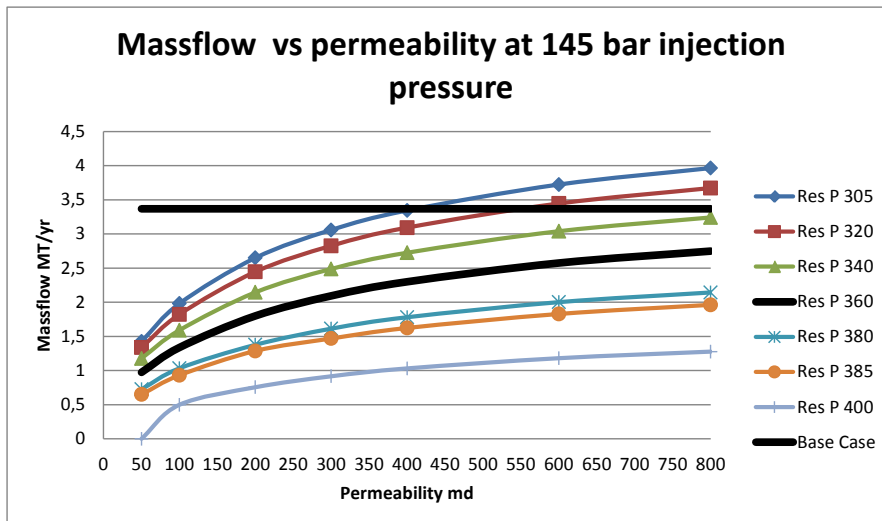


Figure 6-20: Reservoir pressure sensitivity, mass flow vs permeability.

6.3.2.2 Skin

Increasing skin only gives a limited effect on the injectivity; approximately 16 t/hr, increasing the skin from 0 to 40. This limited effect is mainly due to the low viscosity of the CO₂.

DOCUMENT NO.: TL02-GTL-Z-RA-0001	REVISION NO.: 03	REVISION DATE: 01.03.2012	APPROVED:
-------------------------------------	---------------------	------------------------------	-----------

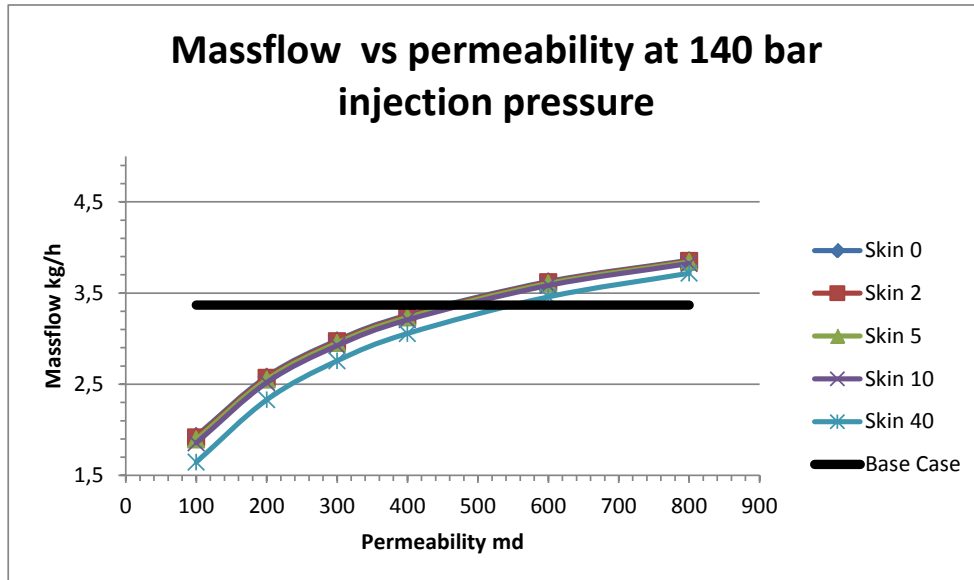


Figure 6-21: Skin sensitivity, mass flow vs permeability.

6.3.2.3 Further work

The study has identified a few areas that should be further investigated. These are as follows:

- Since the CO₂ injection temperature at wellhead is expected to be the same temperature as the seabed temperature it is expected that the cool injection CO₂ liquid will gradually cool down near wellbore temperature, i.e. it is expected that thermal fracturing may occur in the reservoir, potentially improving the injectivity of the Johansen Formation. This will have to be further investigated in the next phase of the project.
- Horizontal injection well, horizontal length effects on injectivity.
- Salt deposition in the reservoir, the injection of dry supercritical CO₂ into brine aquifers has the potential to dry saline formation waters due to evaporation effects, leading to severe increases in salinity and salt precipitation. This can significantly impair injection rates, as has been noted in gas-storage reservoirs. This is of interest for CO₂ storage in saline aquifers, but can be solved by fresh water injection.

6.3.3 Summary

Permeability is the main controlling factor for injectivity. Uncertainty in the permeability has been evaluated through the core laboratory experiments, and the results show that they differ from the original core measurements. Since the correlations used to generate porosity and permeability maps in the geomodel are based on core results, the predicted permeability in the well area is also affected. Rather than reducing the uncertainty in permeability, the core results highlighted the need for fresh and relevant sample material from an exploration well in the injection area.

Based on the reference geomodel, the simulations using Pipesim showed that the injectivity of the Johansen Formation is expected to be sufficiently good with the base case reservoir parameters and achieving the target rate is expected to be possible with one well. Even with less reservoir thickness or less permeability, the target injection rate of 384.5 T/hr (3.2 Mt/y) should be achievable with more and/or horizontal wells. It is also expected that the cool CO₂ will cause some thermal fracture effects, potentially improving the injectivity.

DOCUMENT NO.: TL02-GTL-Z-RA-0001	REVISION NO.: 03	REVISION DATE: 01.03.2012	APPROVED:
-------------------------------------	---------------------	------------------------------	-----------

6.4 Storage formation geochemistry

A petrographic study of core samples has been conducted by IRIS to provide geochemical insight to the storage formation rocks (Gassnova-IRI 2011). The study is based on analyses of thin sections using microscope and X-ray diffraction (XRD). Whole rock chemistry (powder) analyses were also performed using XRD. The results of this study are drawn from very few samples collected from wells located in the periphery of the target area.

The Johansen Formation consists of quartz, feldspar, plagioclase, mica, kaolinite, and chlorite/smectite, and is found to have very high porosity ranging from 25% to 35% in the samples. The high porosity is partly allocated to the quartz grains having a thin layer of chlorite coating, which inhibits overgrowth of quartz. Carbonate cement is mostly absent, but is recognized (on macro inspection) in one sample, probably due to localized shell accumulation. The Cook Formation consists of quartz, feldspar, plagioclase, mica and clays. It has a lower porosity than the Johansen Formation and it varies greatly between samples, ranging from 2% to 15-20%. This is owing to quartz overgrowth (lack of chlorite coating) and higher clay content. A varying degree of flaser and lenticular bedding is also observed.

6.4.1 Geochemical influence of CO₂ injection

A petrographic study on core samples from wells that penetrate the storage rocks has been performed by IRIS (Gassnova-IRI 2011). Their concluding remark on the geochemistry of the different formations with respect to CO₂ injection is that despite its poor cementation it is not expected that injection will destabilize the storage due to dissolution. However, the study is performed on few samples and it is recommended that all available samples are studied in thin sections and preferably also samples from new wells in the target area.

A study on the effect of O₂ contamination in CO₂ for CO₂ storage has been conducted by IRIS (Gassnova-IRI 2010). As part of the study they have performed an in-depth literature search on the subject of CO₂ storage and chemical reactions and bi-products resulting from CO₂ injection. There is very little written on the effect of O₂ contamination of CO₂, but pilot testing on CO₂ contaminated with O₂ and NO_x has not reported any damage during injection or storage. Field experience from water injection (without O₂ removal) into oil reservoirs shows no complication from the O₂ in the injection water.

All the CO₂ projects reviewed in the study (e.g. in Salah, Sleipner, Snøhvit, Ketzin etc) report no formation deformation resulting from the injection. These reports do not include the level of O₂ contamination, but are worth mentioning.

One major concern pointed out in the report is that O₂ can lead to oxidation of pyrite and form low solubility ferric iron hydroxide (Fe(OH)₃) and sulphur (S₈). Such low solubility minerals can reduce porosity and lead to deformation of the formation or reduced injectivity.

In the petrographic study one sample from the Cook Formation indicated high pyrite content in CRD, but was not supported by visual inspection. The other samples from the storage formations and the cap rocks did not reveal any content of pyrite.

DOCUMENT NO.: TL02-GTL-Z-RA-0001	REVISION NO.: 03	REVISION DATE: 01.03.2012	APPROVED:
-------------------------------------	---------------------	------------------------------	-----------

7 GEOLOGICAL UNCERTAINTY EVALUATION

The evaluation criteria for the Johansen Storage site in chapter 3 states that capacity and containment related to safe storage has to be evaluated. There are currently no set requirements as far as acceptable uncertainty levels for the evaluation criteria. Capacity is therefore communicated in a risk-based approach where the uncertainty in pore volume connectivity and resulting pressure build-up is viewed against the confidence in estimation of safe pressure build-up.

The aim of this uncertainty evaluation is to set up a systematic overview so that the uncertainty factors are comparable and the uncertainty range and significance of each factor can be visualized. Further, it uses a statistical approach to calculate the range and the expected pore volume connectivity for the storage complex. Combined with other factors influencing the pressure build-up, a range and expected pressure build-up is calculated.

The sand presence and quality of the formations within the storage complex have been evaluated in chapter 5.3. The results from these evaluations form the main fundament for the geological uncertainty assessment.

Chapter 7.1 describes the geological risk assessment where the uncertainties related to the presence and quality of the Johansen Formation are assessed. The evaluation of the quality of the Johansen Formation is performed from the viewpoint of the selection of the storage complex CO₂ injection point. Chapter 7.2 describes pore volume connectivity to other surrounding formations. All these evaluations form the basis for the input to the risk model, where the risk model ties them to the main capacity parameters; pore volume and pressure build-up. The results are presented as *leakage risk*, but can equally be considered a commercial risk, i.e. a risk that the target injection rate cannot be maintained (in order to prevent leakage).

7.1 Geological uncertainty assessment

The main focus for the geological uncertainty assessment has been the presence and quality of the Johansen Formation, which is the primary storage formation for the storage complex. The Johansen Formation deposits are proven by wells in and northwest of the Troll Field (Figure 7-1 and Figure 5-18), but in the southern part the extent of the Johansen Formation is defined by seismic analysis (seismic interpretation, seismic inversion and seismic attributes).

A result of this is that the probability of the storage formation presence and quality is lower in the southern part of the storage complex. The lack of 3D data in the most southern and eastern parts of the storage complex also substantiates this. Both the storage formation presence and storage formation quality have a significant impact on the volume calculation. The latter will also influence the storage formation injectivity. This will again have an impact on the storage complex pressure build-up and development scenario.

Three main geological uncertainty factors have been identified in the geological evaluation of the Johansen Formation:

- Storage formation presence - probability of lack of storage formation
- Storage formation quality - probability of poorly developed storage formation
- Storage complex mapability - risk associated with incorrect mapping, mainly seismic interpretation and depth conversion

The main geological uncertainty factors will be assessed separately, with each probability input to the overall storage complex risk model (chapter 7), where the end result is expected storage complex pressure build-up.

DOCUMENT NO.: TL02-GTL-Z-RA-0001	REVISION NO.: 03	REVISION DATE: 01.03.2012	APPROVED:
-------------------------------------	---------------------	------------------------------	-----------

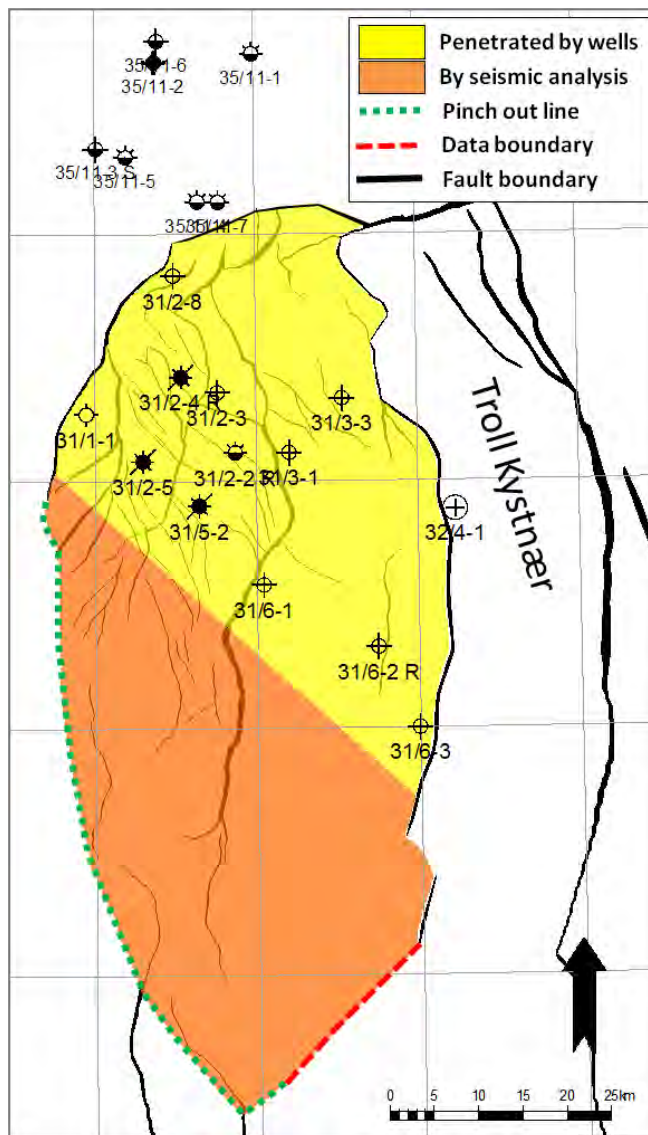


Figure 7-1: The JSC. The presence of the Johansen Fm in the southern part of the storage complex is defined by seismic interpretation, seismic inversion and different seismic attributes.

7.1.1 Storage formation presence

The Johansen Formation depositional system and storage complex definition is described in chapter 5.3. The boundary of the Johansen Storage Complex is defined by primary storage formation pinch out zones, fault zones and data availability (Figure 7-1). The eastern Troll Kystnær (Figure 7-1) area of the storage complex is not included in the geomodel due to the low seismic data availability.

The main question in the risking of the storage formation presence assessment is:

- What is the probability that the volume calculations are incorrect due to lack of storage formation development?

In order to answer this question, several geological risk factors which are considered important for this storage complex have been evaluated:

DOCUMENT NO.: TL02-GTL-Z-RA-0001	REVISION NO.: 03	REVISION DATE: 01.03.2012	APPROVED:
-------------------------------------	---------------------	------------------------------	-----------

1. Well control

To prove the presence of the storage formation, nearby wells have to penetrate a sufficient amount of sand stones of the same geological age within the storage complex. If the wells only prove thin storage formation sands, the quality of the sand stones and the well location has to be considered. For example, if the well is located optimally on the depositional system showing thin, low quality sand stones, the uncertainty should be considered high.

The distance from the wells to injection area has to be considered; in principle the storage formation presence and quality uncertainty should increase with distance. Other data must be evaluated for a potential de-risk of the area.

2. Storage formation sand source area

Knowledge of the possible source areas for the storage formation sand depositions is important. The number and petrophysical compositions of the possible source areas have to be taken into consideration.

3. Depositional barriers

Observation of barriers that could have prevented sand depositions inside the storage complex is of importance. Such barriers could be faults, ridges and highs.

4. Regional accumulation space

Accumulation space has to be available at the time of deposition. The regional isopach thick is used for this evaluation.

5. Regional geological shapes

Observation of seismic facies indicating depositional environment and possible types of sedimentological facies (e.g. channels, clinofolds, mounds) has to be evaluated.

6. Analogue

The knowledge of possible analogues to the storage formation depositional system is essential in the risk evaluation. Several analogues are possible; same age/facies at a different location, different age/same facies at same/different location and present day analogue (same/different location).

The Johansen Storage Complex has been divided in to four different areas based on distance to wells and data availability (Figure 7-2), and these areas are risked separately. The consequence of this is the probability of presence change within the different areas.

DOCUMENT NO.: TL02-GTL-Z-RA-0001	REVISION NO.: 03	REVISION DATE: 01.03.2012	APPROVED:
-------------------------------------	---------------------	------------------------------	-----------

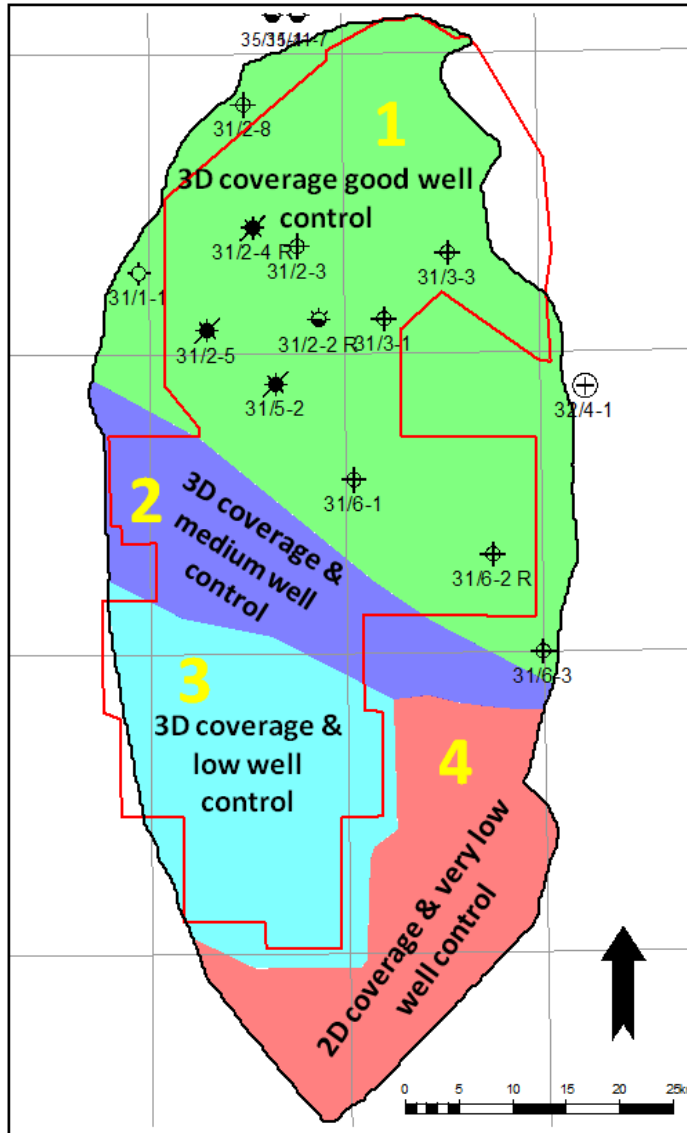


Figure 7-2: The JSC divided in four different risk areas. The red polygon is the outline of the 3D coverage.

The probabilities are estimated between 0.0 and 1.0 for each risk factor. The uncertainty assessment is based on observations, evaluations and conclusions described in chapter 5.3. The results of the storage formation presence uncertainty assessment are shown in Table 7-1.

DOCUMENT NO.: TL02-GTL-Z-RA-0001	REVISION NO.: 03	REVISION DATE: 01.03.2012	APPROVED:
-------------------------------------	---------------------	------------------------------	-----------

Table 7-1: Risk assessment scheme for the Johansen Fm presence evaluation.

RISK ASSESSMENT - STORAGE FORMATION PRESENCE							
Area	Well control	Sand source	Depositional barriers	Accumulation space	Regional geological shapes	Analogue	Probability
1	Area tested and proved by several wells. All wells penetrating sufficient amount of Johansen Formation sandstone. Probability 1.0	The hinterland to the east of the storage complex was the provenance area, the Sognefjord was the main feeder channel. Probability 1.0	No indications of barriers. Probability 1.0	The Johansen Formation thickness map support available accumulation space for sand depositions. Probability 1.0	Sesimic attributes are showing channels in the Johansen Formation. Probability 1.0	Adjacent depositional systems exist with the same facies (Sognefjord delta). Probability 1.0	1.0
2	Area tested by wells. Distance to wells is between 5 km and 15 km. Probability 0.8	The hinterland to the east of the storage complex was the provenance area, the Sognefjord was the main feeder channel. Probability 1.0	No indications of barriers. Probability 1.0	The Johansen Formation thickness map support available accumulation space for sand depositions. Probability 1.0	Sesimic attributes are showing channels in the Johansen Formation. Clinofolds observed in the western part of area 2. Probability 1.0	Adjacent depositional systems exist with the same facies (Sognefjord delta). Probability 1.0	0.8
3	Area tested by wells. Distance to nearest wells are over 15 km. Probability 0.7	The hinterland to the east of the storage complex was the provenance area, the Sognefjord was the main feeder channel. Probability 1.0	No indications of barriers. Probability 1.0	The Johansen Formation thickness map support available accumulation space for sand depositions. Probability 1.0	Sesimic attributes are showing channels in the Johansen Formation. Clinofolds observed in the western part of area 3. Probability 1.0	Adjacent depositional systems exist with the same facies (Sognefjord delta). Probability 1.0	0.7
4	Area not tested by wells (only 2D data). Probability 0.6	The hinterland to the east of the storage complex was the provenance area, the Sognefjord was the main feeder channel. Probability 1.0	No indications of barriers. Probability 1.0	The Johansen Formation thickness map support available accumulation space for sand depositions. Probability 1.0	No clear observations. Probability 0.8	Adjacent depositional systems exist with the same facies (Sognefjord delta). Probability 1.0	0.5

There is no significant uncertainty for Area 1 associated with the presence of the storage formation (Table 7-1) and therefore very high probability of correct pore volume calculations. The extent and thickness of the storage formation is proven by several wells. Area 1 constitutes approximately 46% of the total Johansen Formation pore volume in the geomodel.

Area 2 constitutes approximately 15% of the total Johansen Formation pore volume. There is a slightly higher uncertainty associated with storage formation presence for this area, due to well distance (Table 7-1). The probability for an incorrect Johansen Formation pore volume for this area is still low (20%).

The probability for incorrect pore volume calculations for Area 3 is 30% (Table 7-1). Area 3 comprises approximately 23% of the total Johansen Formation pore volume. This is due to the distance to the northern wells; over 15km to nearest well point.

DOCUMENT NO.: TL02-GTL-Z-RA-0001	REVISION NO.: 03	REVISION DATE: 01.03.2012	APPROVED:
-------------------------------------	---------------------	------------------------------	-----------

Area 4 is regarded as “not proven by wells” due to a very long distance to wells that penetrate the storage formation (Table 7-1). The lack of high quality 3D data also enhances the risk and makes it difficult to observe indications of sand stone depositions in this area. The area constitutes approximately 16% of the total pore volume and the probability for incorrect calculations is 50% (Table 7-1).

The overall probability for the presence of the Johansen Formation in the storage complex based on the above calculations is 80%.

Summary

The above uncertainty summary (Table 7-1) has shown that probabilities in connection with the presence of Johansen Formation sand vary throughout the storage complex and this is mainly due to the variable data availability. The long distance to wells proving the Johansen Formation constitutes the highest risk for the storage formation. There are no well data directly confirming the depositional system presented for the southern part (spit system).

A non- or poorly developed and strongly depth dependent Johansen Formation sand system would have significant impact on the Johansen Formation pore volumes. The pore volume reduction could be over 60% (Figure 5-42, Figure 7-6 and Table 7-3).

The results of the geological risk evaluation on storage formation presence will be further addressed in the main risk and uncertainty evaluation in chapter 7. The storage formation presence uncertainty is reflected in the sand presence probabilities for the different model cases (high, reference and low) used in the uncertainty evaluation (chapter 7.3.2). The different model cases for the Johansen Formation are defined in chapter 7.2.1.

7.1.2 Storage formation quality – selection of CO₂ injection point

The assessment of Johansen Formation quality is described in chapter 5.3.2. The injection area storage formation quality assessment is based on observations, evaluations and conclusions described in this chapter. The selection of the injection point is based mainly on the two most important criteria as a sealing layer is present throughout the injection area: CO₂ plume migration and the storage formation quality in the injection area. The latter, which is the focus in this chapter, will influence both the injectivity and the capacity (pore volume) of the storage complex.

The injection point is selected evaluating the following factors:

- CO₂ plume migration
 - No migration into high risk area
- Storage formation quality
 - Storage formation facies
 - Local accumulation space
 - Geological shapes
 - Diagenesis

CO₂ plume migration

The injection point chosen is located in the southern part of the storage complex (Figure 7-3 and Figure 7-4). The most important reason for the southern injection area is the distance to the Troll Field. The fault seal study (Gassnova-ROS 2011) has shown possible cross fault communication between the Johansen Formation and the Troll Field reservoir. CO₂ migration results from several injection points have been evaluated before selecting the optimal point (chapter 6.1).

DOCUMENT NO.: TL02-GTL-Z-RA-0001	REVISION NO.: 03	REVISION DATE: 01.03.2012	APPROVED:
-------------------------------------	---------------------	------------------------------	-----------

Storage formation facies

The proximity of the injection area within the depositional system is important. There is a good understanding of the depositional system in the non-well areas which is necessary to avoid injection in low porosity areas. The selected injection point is positioned in the part of the depositional system where the storage formation facies is expected to be well developed sandstones (spit system) (chapter 5.3.1.1).

Figure 7-3 shows a generalized depositional map for the Johansen Formation. The figure shows the selected injection point in the western part of the storage complex.

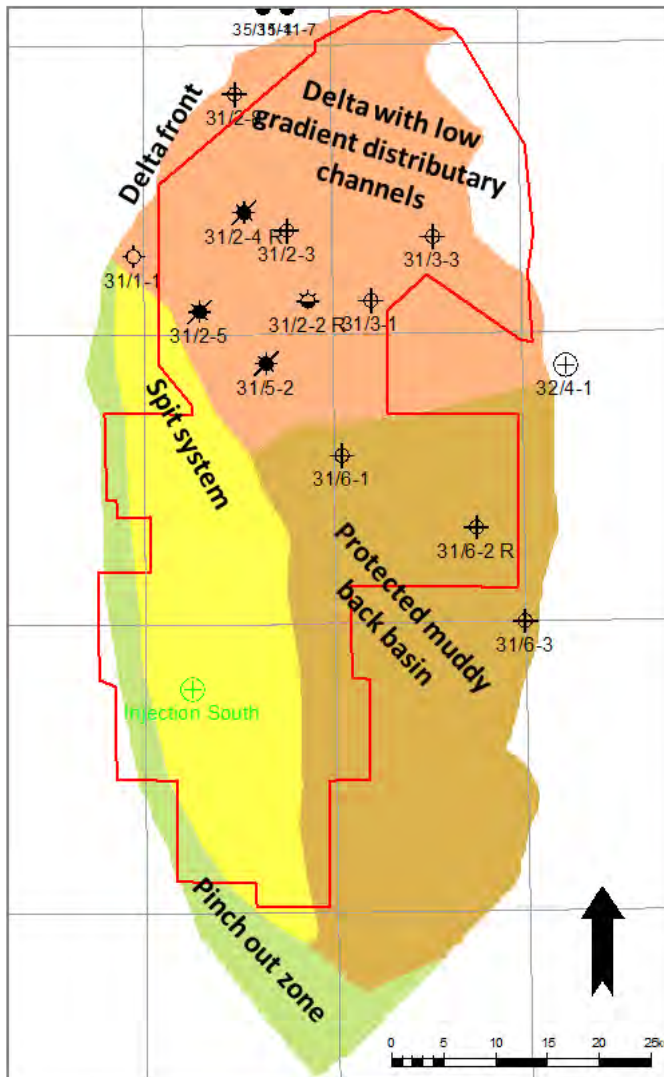


Figure 7-3: Generalized depositional model for the Johansen Fm with proposed injection location. The red polygon is the outline of the 3D coverage.

Local accumulation space

Accumulation space has to be available for the injection area at the time of deposition. Isopach thick is used for this evaluation, a positive isopach anomaly could support sand deposition. The Johansen Formation isopach map (Figure 7-4) shows a clear thickening towards the western part of the storage complex. This is a good indication of available accumulation space at the time of deposition, and this also supports the interpretation of a spit bar depositional environment. The injection point is within the isopach thick.

DOCUMENT NO.: TL02-GTL-Z-RA-0001	REVISION NO.: 03	REVISION DATE: 01.03.2012	APPROVED:
-------------------------------------	---------------------	------------------------------	-----------

Geological shapes

Observations of seismic facies indicate the presence of sand deposition within the injection area (chapter 5.2.2). The Johansen Formation depositional models are in the southern part mainly based on seismic analysis; interpretation, seismic inversion and seismic attributes, due to the lack of well data penetrating the spit bar area. There are a few seismic facies observations interpreted as clinoforms (Figure 5-28). Clinoforms are typical depositional features within delta systems and in spit systems.

Diagenesis

Possible diagenetic effects on storage formation quality due to storage formation lithology, burial depth (temperature) versus quartz cementation, and illitization have been evaluated (chapter 5.3.2). The storage formation depth for the injection point is 3051m. At this depth, processes other than compaction can influence the storage formation quality. Quartz cementation processes in sandstone are becoming more predominant at burial depths over 2500m. However, evidence of chlorite coating is seen in the Johansen Formation cores (Figure 5-38). Chlorite coating can prohibit cementation and preserve porosity in the storage formation. Temperature and lithology are controlling the diagenetic processes in the storage formation such as cementation and illitization. Storage formation temperatures over 120°C and heterogenic sands could considerably damage storage formation properties. Available Johansen Formation well temperature data are all lower than 120°C (Table 5-10).

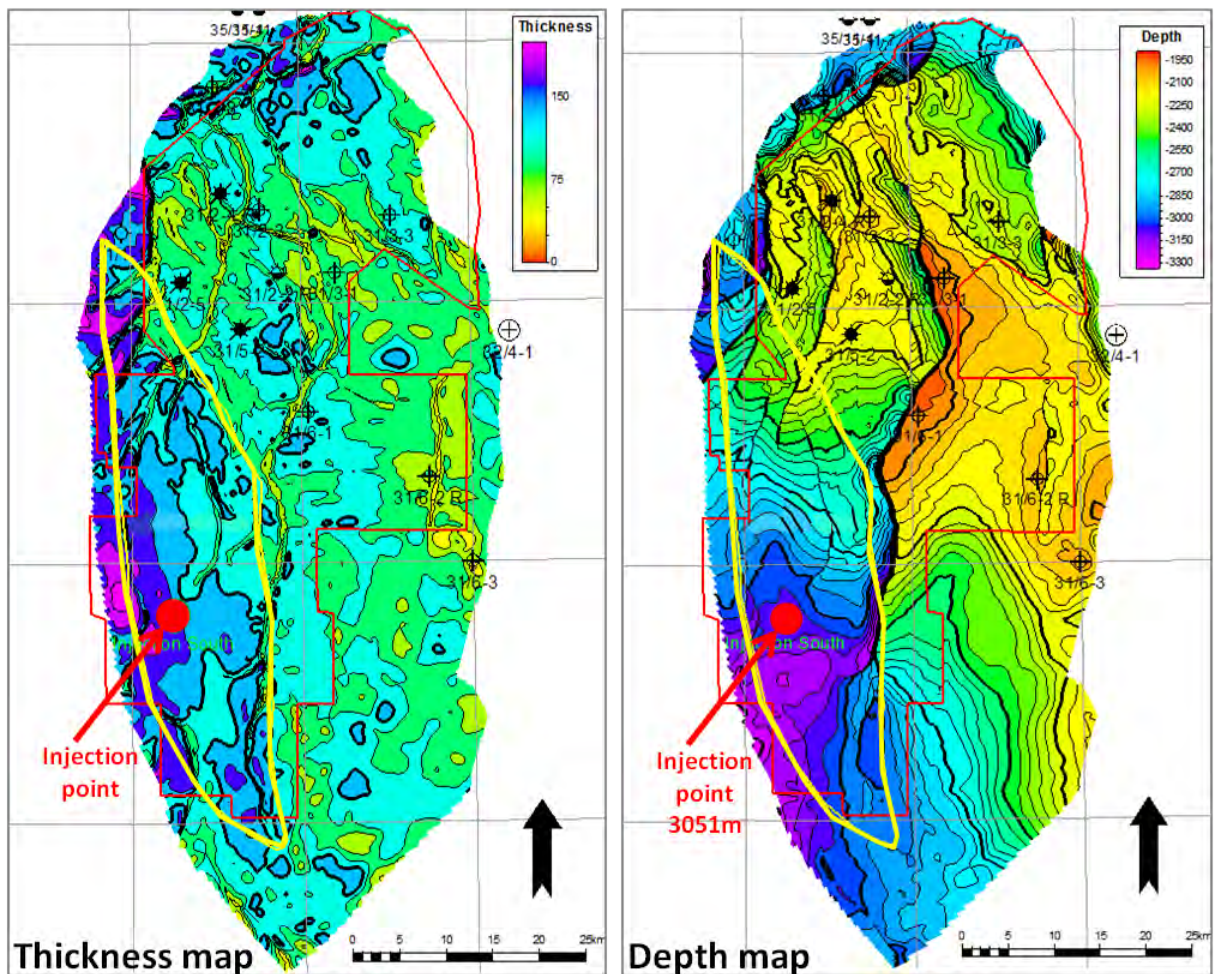


Figure 7-4: Johansen Fm thickness map (c. 25m) and depth map (c. 50m). Yellow polygon is outline of spit bar depositions and red polygon is the outline of the 3D coverage.

DOCUMENT NO.: TL02-GTL-Z-RA-0001	REVISION NO.: 03	REVISION DATE: 01.03.2012	APPROVED:
-------------------------------------	---------------------	------------------------------	-----------

Sealing layers

The selected area has well developed seals consisting of a laterally extensive primary seal represented by the Drake Formation and a secondary sealing package consisting of shale layers of Jurassic, Cretaceous, Tertiary and Quaternary shales. The shales are impermeable and are not considered to represent significant risk of migration into the cap rock and subsequent leakage to shallower layers and the atmosphere. The primary seal is described in chapter 5.4.1 and the secondary seal in chapter 5.4.2.

Summary

The selected injection point is considered applicable when assessing the storage formation quality. However, the injection point is located in the storage complex non-well area and this lack of well confirmation on the storage formation (sand) presence (chapter 7.1.2) constitutes an additional risk on the storage formation quality.

7.1.3 **Storage complex mapability**

The uncertainty associated with incorrect mapping of the storage complex could be significant. There are risks associated with the top and base seismic interpretations of the storage formations. Table 5-1 shows that the uncertainty for the horizon pick is between 5ms and 10ms. In the depth domain an average would be approximately +/- 25ms uncertainty on the Cook and Johansen Formation maps.

Table 7-2 shows the implications on the pore volume calculations based on the above uncertainty.

Table 7-2: Sand volume uncertainties for the storage formations due to incorrect seismic mapping.

Cook-Johansen	Sand volume GSm ³	Overestimated sand volume GSm ³	Increase volume GSm ³	Underestimated sand volume GSm ³	Decrease volume GSm ³	
Reference Case	509.73	677.97	168.24	343.55	166.18	+/- 32%
Low Case 2	291.65	504.48	212.83	247.43	44.22	+/- 34%
Low Case 1	162.3	208.73	46.43	117.89	44.41	+/- 28%

Uncertainties in connection with depth conversion could also have implication on both storage formation quality and the storage complex volume calculations. The implications on the volume calculations are considered low. The depth conversion uncertainty in connection with burial depth is +/-60ms (chapter 5.2.3). This will only have a small effect on the storage formation quality. The uncertainties in connection with mapability are used in the overall risk evaluation (chapter 7.3.4).

7.2 **Pore volume connectivity**

To understand and calculate the pressure build-up in the storage formation due to CO₂ injection, it is important to understand the storage formation pore volume communication with the surrounding formations.

Figure 7-5 shows the area (yellow) and the definition of the Johansen Storage Complex and outlines of the potential formations that communicate with the storage complex. The following chapters will describe, define and calculate the pore volume of each communicating formation. The calculations are input to the overall storage complex risking (chapter 7).

DOCUMENT NO.: TL02-GTL-Z-RA-0001	REVISION NO.: 03	REVISION DATE: 01.03.2012	APPROVED:
-------------------------------------	---------------------	------------------------------	-----------

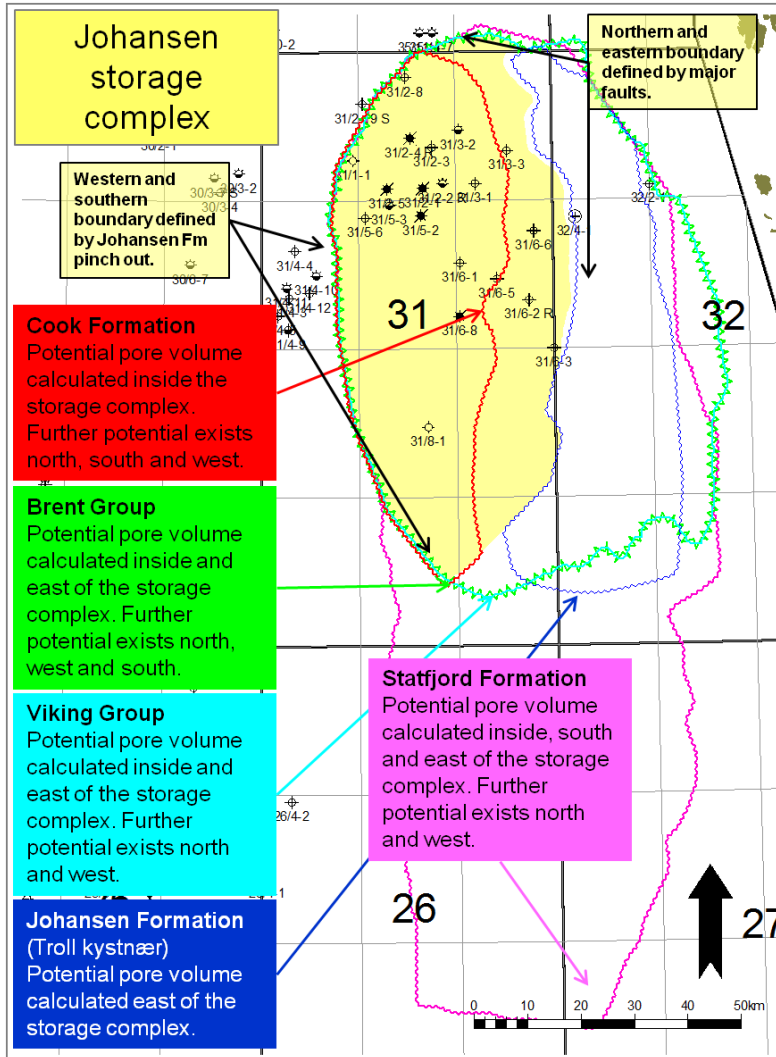


Figure 7-5: Overview map showing the outline of the JSC and the potential communicating formations.

7.2.1 Dunlin Group

Johansen Formation

The Johansen Formation is the primary storage formation for the Johansen Storage Complex. The yellow area (Figure 7-5) is defined as the reference (base) case. The boundary is defined by pinch out lines and major faults, see chapter 5.3 (storage formation) for a detailed description. To develop a more dynamic risk model for the Johansen Storage Complex, high and low pore volume cases were calculated (Figure 7-6). In addition the Johansen Formation pore volume potential for the Troll Kystnær area (Figure 7-6) east of the storage complex, was calculated.

DOCUMENT NO.: TL02-GTL-Z-RA-0001	REVISION NO.: 03	REVISION DATE: 01.03.2012	APPROVED:
-------------------------------------	---------------------	------------------------------	-----------

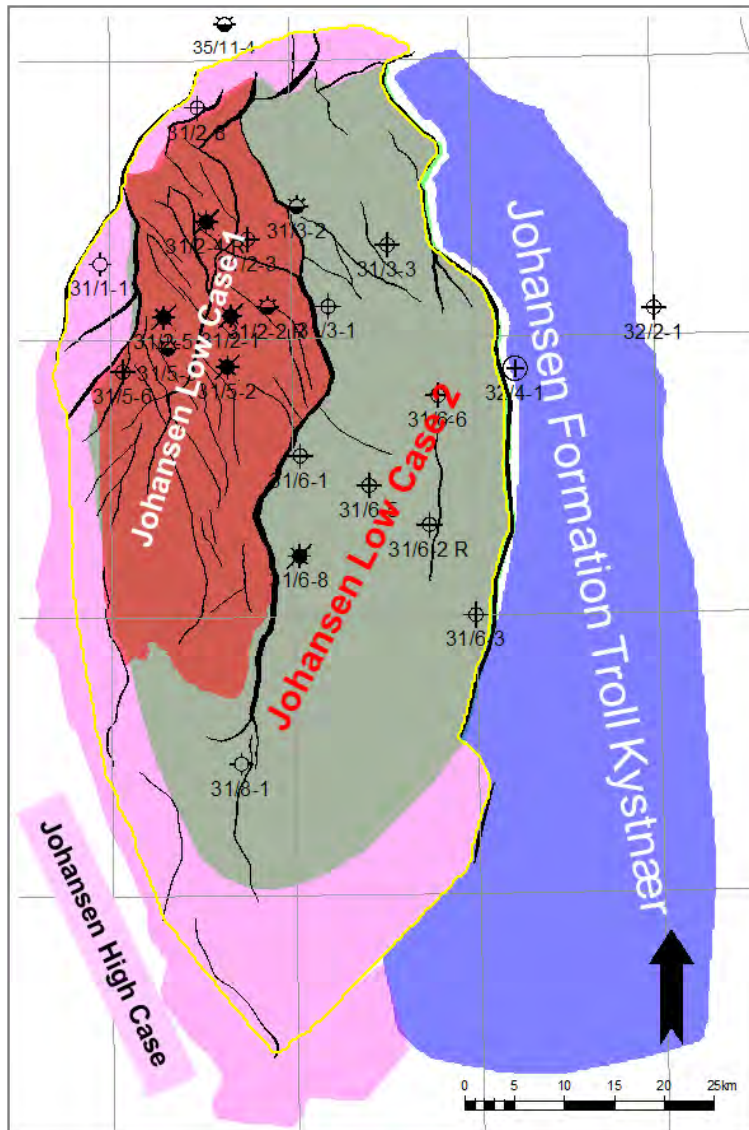


Figure 7-6: Map showing Johansen Fm low and high pore volume cases and the Troll Kystnær potential. The Johansen reference model (base case) is shown by the yellow polygon.

The high case was defined by extending the pinch out lines both west and southwards. The extended pinch out line is based on the 2D seismic reflectivity of the Johansen Formation, an example is presented in Figure 7-7. The western base case pinch out boundary is mainly based on 3D interpretation. To calculate the Johansen Formation high case, an average porosity of 19% was used (Table 7-3). The pore volume increase is calculated to be $6 \times 10^9 \text{ Sm}^3$.

The Johansen Formation Low case 1 (Figure 7-6) represents the most dramatic volume reduction for storage formation, the estimated bulk rock reduction is approximately 70%. The Johansen Formation bulk rock volume is approximately $360 \times 10^9 \text{ Sm}^3$.

DOCUMENT NO.: TL02-GTL-Z-RA-0001	REVISION NO.: 03	REVISION DATE: 01.03.2012	APPROVED:
-------------------------------------	---------------------	------------------------------	-----------

Table 7-3: Johansen Fm average porosities used in pore volume calculations.

Well	Thickness (m)	Mean
31/1-1	80.16	0.133
31/2-1	100.30	0.212
31/2-2	114.40	0.207
31/2-3	130.50	0.204
31/2-4	115.00	0.204
31/2-5	93.26	0.223
31/2-8	75.28	0.151
31/3-1	99.62	0.223
31/3-3	131.15	0.172
31/5-2	99.87	0.210
31/6-1	99.12	0.250
31/6-2	92.87	0.195
31/6-3	85.12	0.162
31/6-6	93.00	0.157
31/2-4	51.20	0.193
Average	97.71	0.193

In this scenario the southward extension of Johansen Formation is limited and the communication to the eastern part of the storage complex is prohibited due to a major fault dividing the western and eastern part. Communication between the western and eastern part is likely at approximately well 31/8-1 (Figure 7-6). The Johansen Formation Low case 2 (Figure 7-6) represents the most probable low case; the pinch out lines are based on seismic reflectivity (Figure 7-8), where the high amplitudes represent sand deposition.

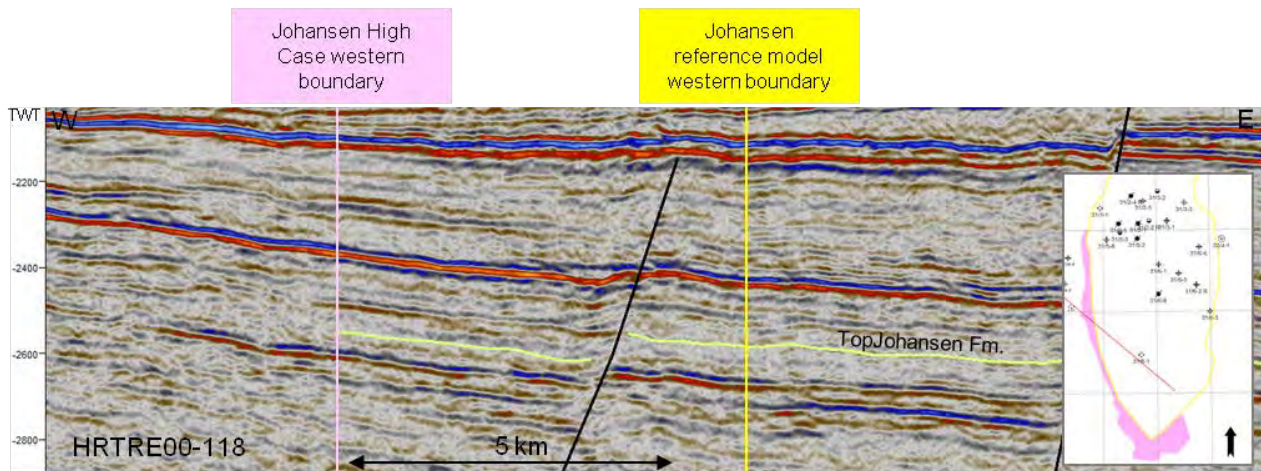


Figure 7-7: Seismic line showing high and reference (base) case boundaries for the Johansen Fm. The high case pinch out boundary is determined by change of intra Johansen Fm internal reflectivity.

DOCUMENT NO.: TL02-GTL-Z-RA-0001	REVISION NO.: 03	REVISION DATE: 01.03.2012	APPROVED:
-------------------------------------	---------------------	------------------------------	-----------

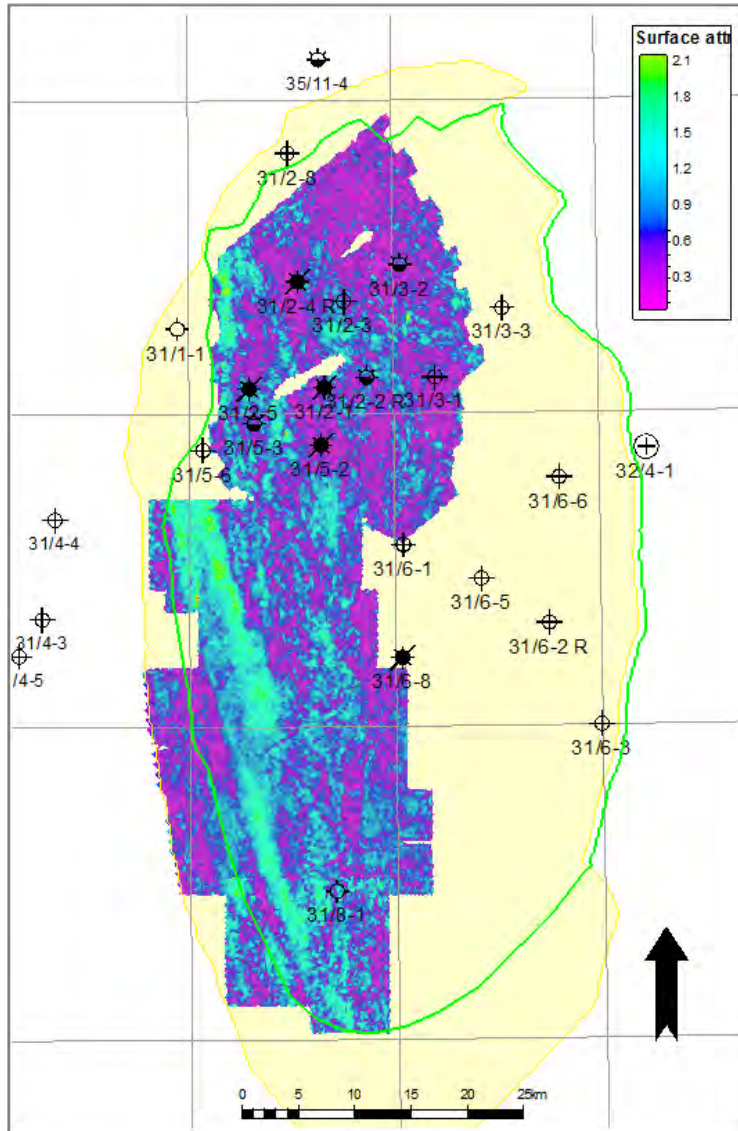


Figure 7-8: Amplitude RMS attribute on Top Johansen Fm level. Yellow area is representing Johansen reference model and green boundary is Johansen Low case 2.

The Johansen Storage Complex porosity property model (described in chapter 5.6.2) is used for the Johansen Low case 1 and 2 pore volume calculations.

The Johansen Troll Kystnær area is located east of the Johansen Storage Complex (Figure 7-6). The area is not included in the storage complex due to the low data availability. The Johansen Formation Troll Kystnær depth map is shown in Figure 7-9. The Johansen Formation pinches out to east and is not present in well 32/2-1 (Figure 7-9). The southern boundary is interpreted as a pinch out line, but with higher uncertainty, due to the low data availability (Figure 4-2).

The pore volume calculation result for the Johansen Troll Kystnær is $41 \times 10^9 \text{ Sm}^3$. An average porosity of 19% is used and the base of the formation is the Top Lower Amundsen.

DOCUMENT NO.: TL02-GTL-Z-RA-0001	REVISION NO.: 03	REVISION DATE: 01.03.2012	APPROVED:
-------------------------------------	---------------------	------------------------------	-----------

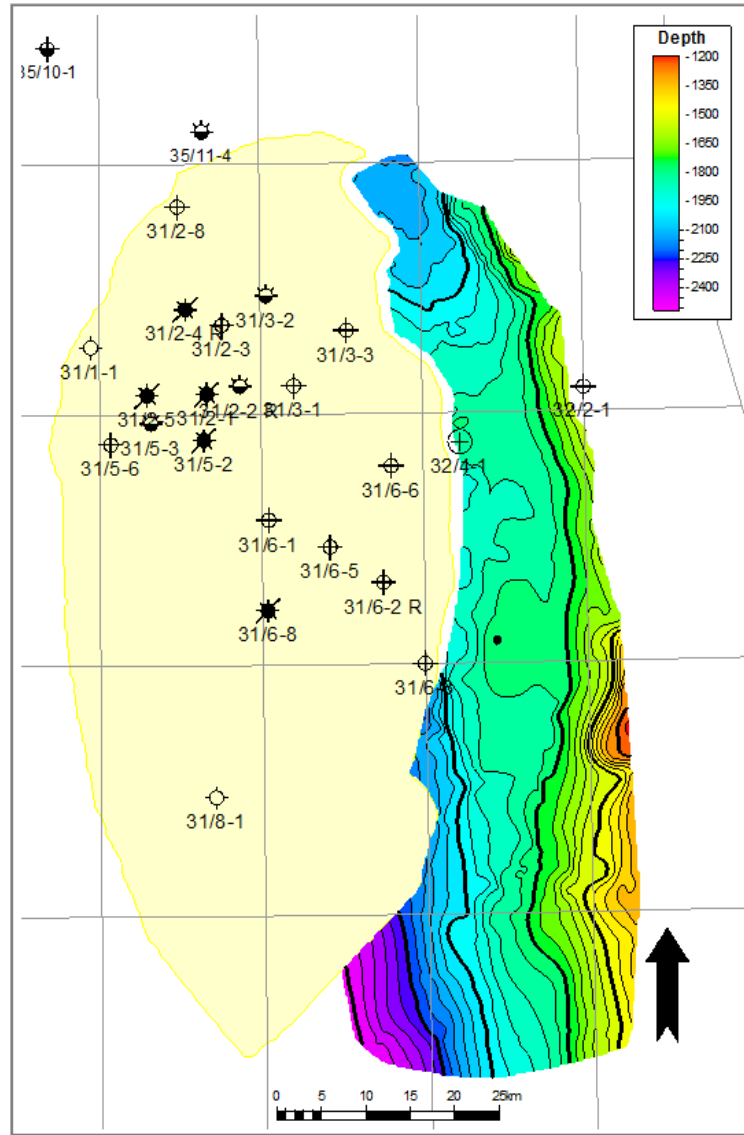


Figure 7-9: Johansen Fm Troll Kystnær depth map c. 50m. Light yellow area is JSC.

Cook Formation

The Cook Formation is interpreted to be a part of the primary storage formation. The red boundary (Figure 7-5) is defined as the reference (base) case. The boundary is defined by a pinch out line to the east and major faults to the north. The western and southern depositional boundaries are defined by the storage complex. This is due to the lack of seismic data in these areas. The Cook Formation exits both in western and southern wells outside the storage complex. The Cook Formation pore volume potential is therefore probably underestimated.

The Cook Formation is interpreted to overlie the Johansen Formation directly in the southern part of the storage complex. The upper Amundsen Formation pinches out in the northern part (Figure 7-10) and vertical pore volume communication between the two storage formations is substantiated. Seismic inversion and well data (Figure 7-11) supports vertical pore volume communications between the Cook Formation and the Johansen Formation.

See chapter 5.3 for a detailed description of the Cook Formation depositional system.

DOCUMENT NO.: TL02-GTL-Z-RA-0001	REVISION NO.: 03	REVISION DATE: 01.03.2012	APPROVED:
-------------------------------------	---------------------	------------------------------	-----------

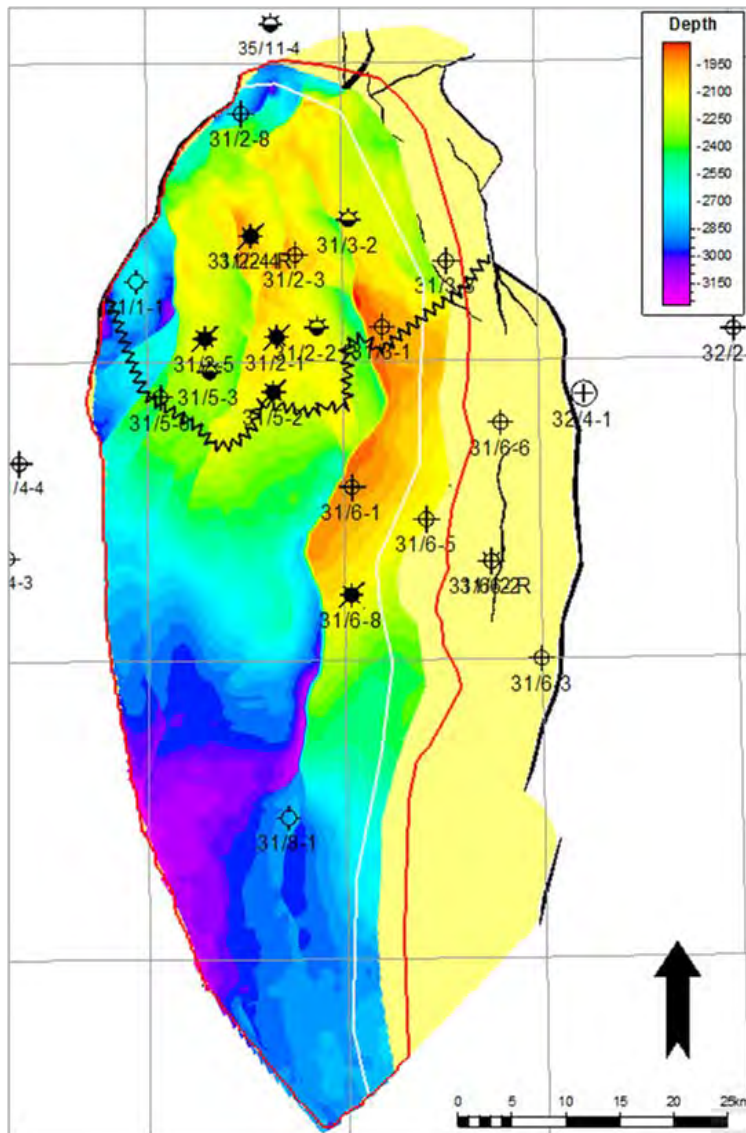


Figure 7-10: Cook Fm depth map. C.I. 50 m. Light yellow area is JSC. White boundary is Cook Fm Low case and red boundary is Cook Fm High case. The black zigzag line represents the Upper Amundsen Fm pinch out line.

The Cook Formation pore volume results are presented in Table 7-4. The Johansen Storage Complex porosity property model (described in chapter 5.6.2) is used for the Cook Low and High case pore volume calculations.

DOCUMENT NO.: TL02-GTL-Z-RA-0001	REVISION NO.: 03	REVISION DATE: 01.03.2012	APPROVED:
-------------------------------------	---------------------	------------------------------	-----------

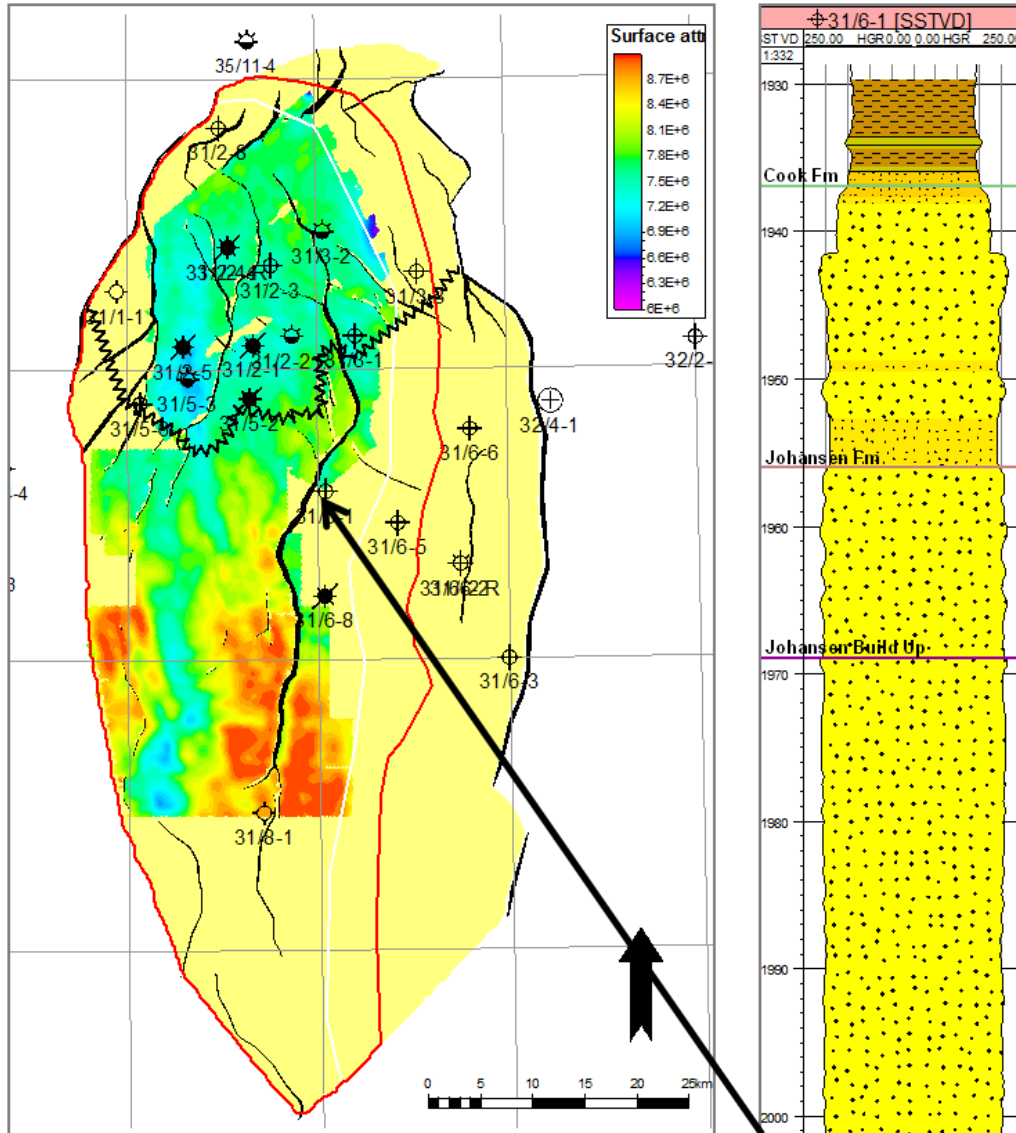


Figure 7-11: Acoustic Impedance RMS attribute through the Cook Fm. Low values (blue) indicate permeable sand depositions. Lithology interpretation based on Vshale for well 31/6-1 showing permeable Cook Fm. Deposited on Johansen Fm sand. Yellow area represents Johansen reference model, red boundary is Cook Fm High case and white boundary is Cook Low case. Black zigzag line is Upper Amundsen Fm pinch out line.

Table 7-4: Cook Fm High and Low case pore volume results. * Pore volume calculated using storage complex porosity model.

Cook Formation	Bulk Rock x 10 ³ Sm ³	Pore Volume
High Case	125	10% volume increase*
Low Case	111	5% volume reduction*

Statfjord Formation

The Statfjord Formation is the main reservoir unit in many Norwegian hydrocarbon fields and has proven excellent reservoir properties, e.g. Statfjord, Snorre and Gullfaks South. The pink boundary (Figure 7-5) is the outline of mapped Statfjord Formation used in the pore volume calculation. The map is based on the available well and seismic data base. The Statfjord Formation has been proved present by wells from Q35 down to Q26 (Figure 7-12).

DOCUMENT NO.: TL02-GTL-Z-RA-0001	REVISION NO.: 03	REVISION DATE: 01.03.2012	APPROVED:
-------------------------------------	---------------------	------------------------------	-----------

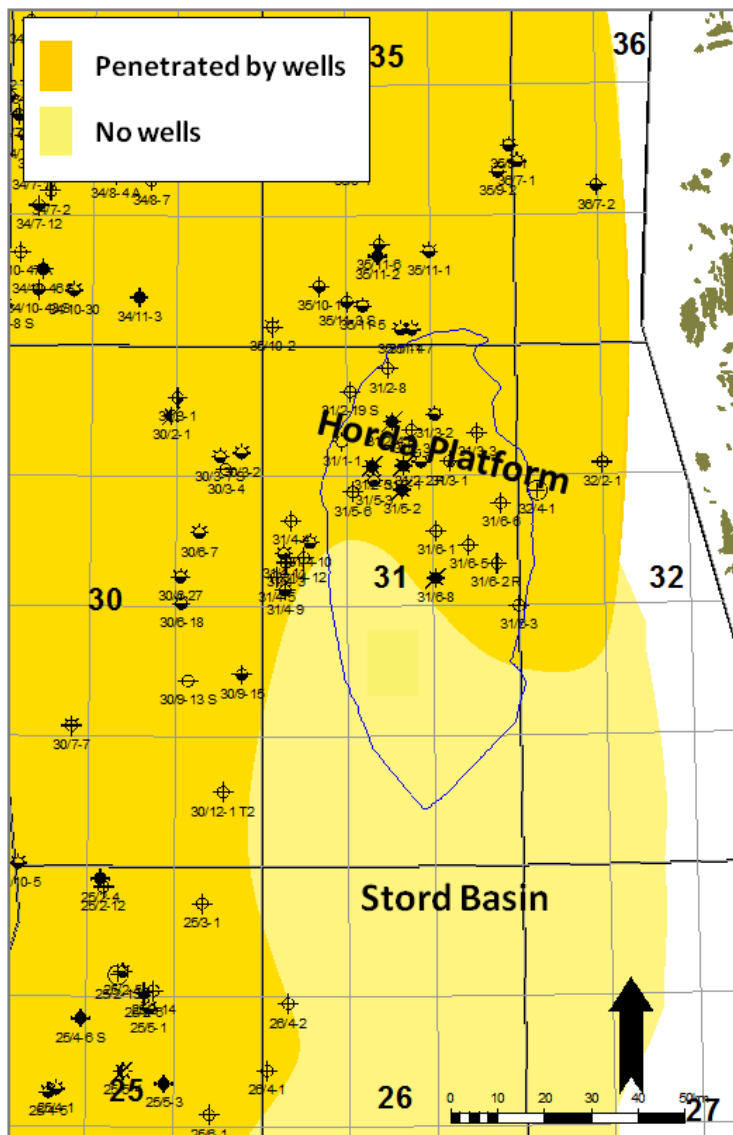


Figure 7-12: Generalised distribution of the Statfjord Fm. The presence of the Statfjord Fm in Stord Basin is defined by seismic interpretation. Blue polygon represents the JSC.

The Statfjord Formation deposits vary from continental to shallow marine sediments. The amount of sandstone varies from less than 40% to more than 80% (Ramm and Ryseth 1996). On the Horda Platform the Statfjord Formation consists of massive sandstones inter-bedded with shales. The Statfjord Formation could have the potential for significant storage capacity.

The pore volume communication from the Statfjord Formation to the Johansen Formation could potentially occur vertically through the Lower Amundsen Formation and via sand/sand contacts in fault zones. Both are made probable by the storage complex evaluation. The fault seal evaluation of cross fault communication between the Statfjord Formation and Johansen Formation shows several fault zones with probable pore volume communication between the formations (Gassnova-ROS 2011). Figure 7-15 shows several profiles from the north to the south of the Johansen Storage Complex.

Wells in the northern part of the storage complex (Figure 7-13) and seismic inversion data (density) (Figure 7-14) show the development of a sandier Lower Amundsen Formation. The

DOCUMENT NO.: TL02-GTL-Z-RA-0001	REVISION NO.: 03	REVISION DATE: 01.03.2012	APPROVED:
-------------------------------------	---------------------	------------------------------	-----------

density data (Figure 7-14) shows sandy areas both north and south of the formation. These observations substantiate direct vertical pore volume communication between the Statfjord Formation and Johansen Formation in several areas in the storage complex.

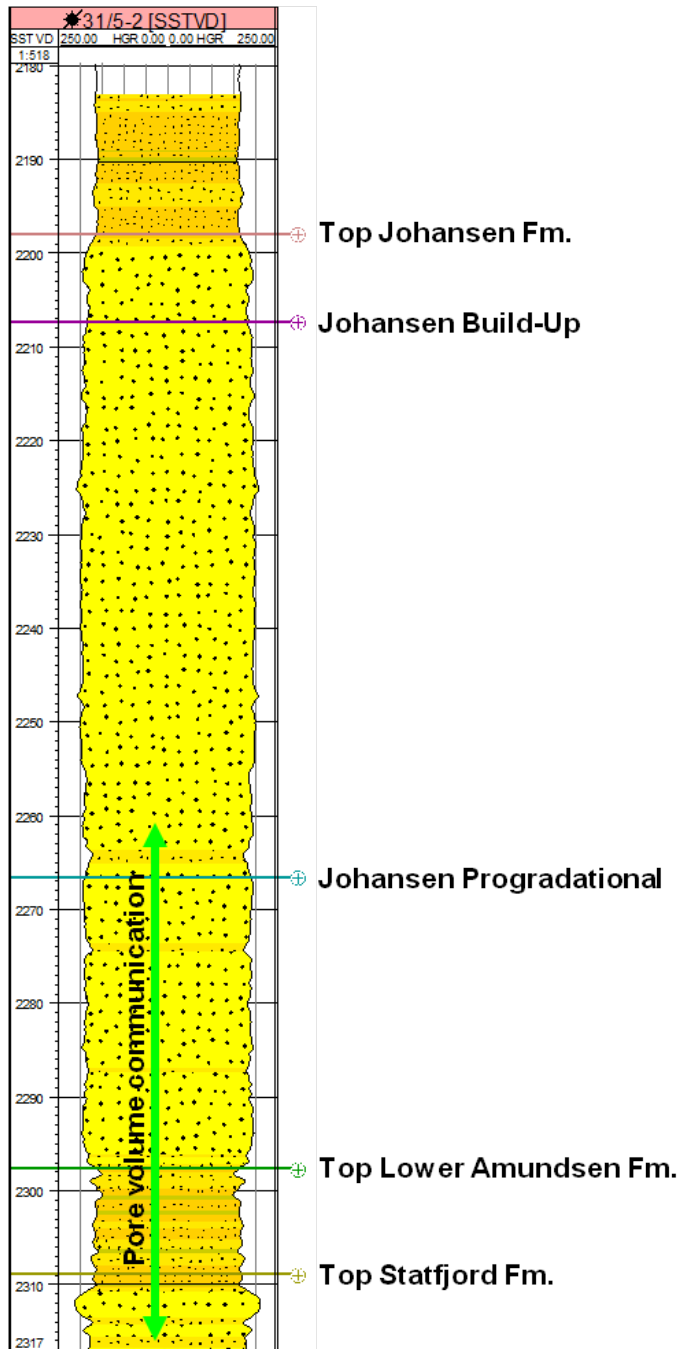


Figure 7-13: Well panel showing sandy/silty developed Lower Amundsen Fm in well 31/5-2. See Figure 7-5 for well location.

DOCUMENT NO.: TL02-GTL-Z-RA-0001	REVISION NO.: 03	REVISION DATE: 01.03.2012	APPROVED:
-------------------------------------	---------------------	------------------------------	-----------

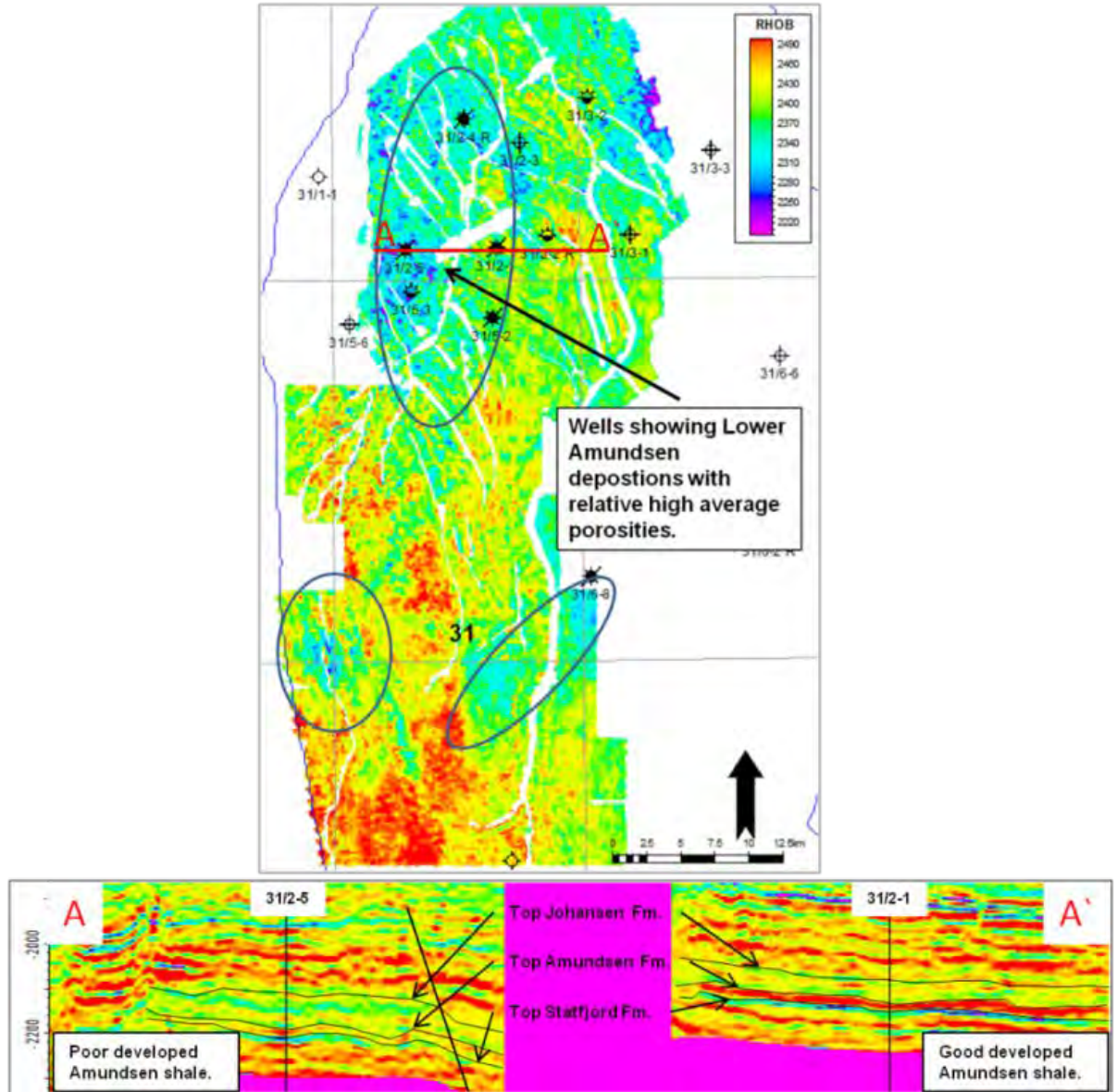


Figure 7-14: Density maps for Lower Amundsen. Circled areas are areas with possible pore volume communication from Johansen Fm to the Staffjord Fm where blue/green colours are showing low porosities (sandy shale) and yellow red colours are high porosities (clean shale).

The Top Staffjord Formation depth map used in the calculation of the potential pore volume is shown in Figure 7-16 and the results are listed in Table 7-5. The depth map is based on seismic interpretation and is limited due to data availability. Compared to the generalized depositional map (Figure 7-12) the Staffjord Formation potential is probably underestimated. The base of the Staffjord Formation is not interpreted, instead average thicknesses are used for the pore volume calculations. The average (mean) porosity for the Staffjord Formation is 17% using the Troll Field wells (Table 7-5). This porosity is used for all the Staffjord Formation pore volume calculations.

DOCUMENT NO.: TL02-GTL-Z-RA-0001	REVISION NO.: 03	REVISION DATE: 01.03.2012	APPROVED:
-------------------------------------	---------------------	------------------------------	-----------

Cross communication fault zones

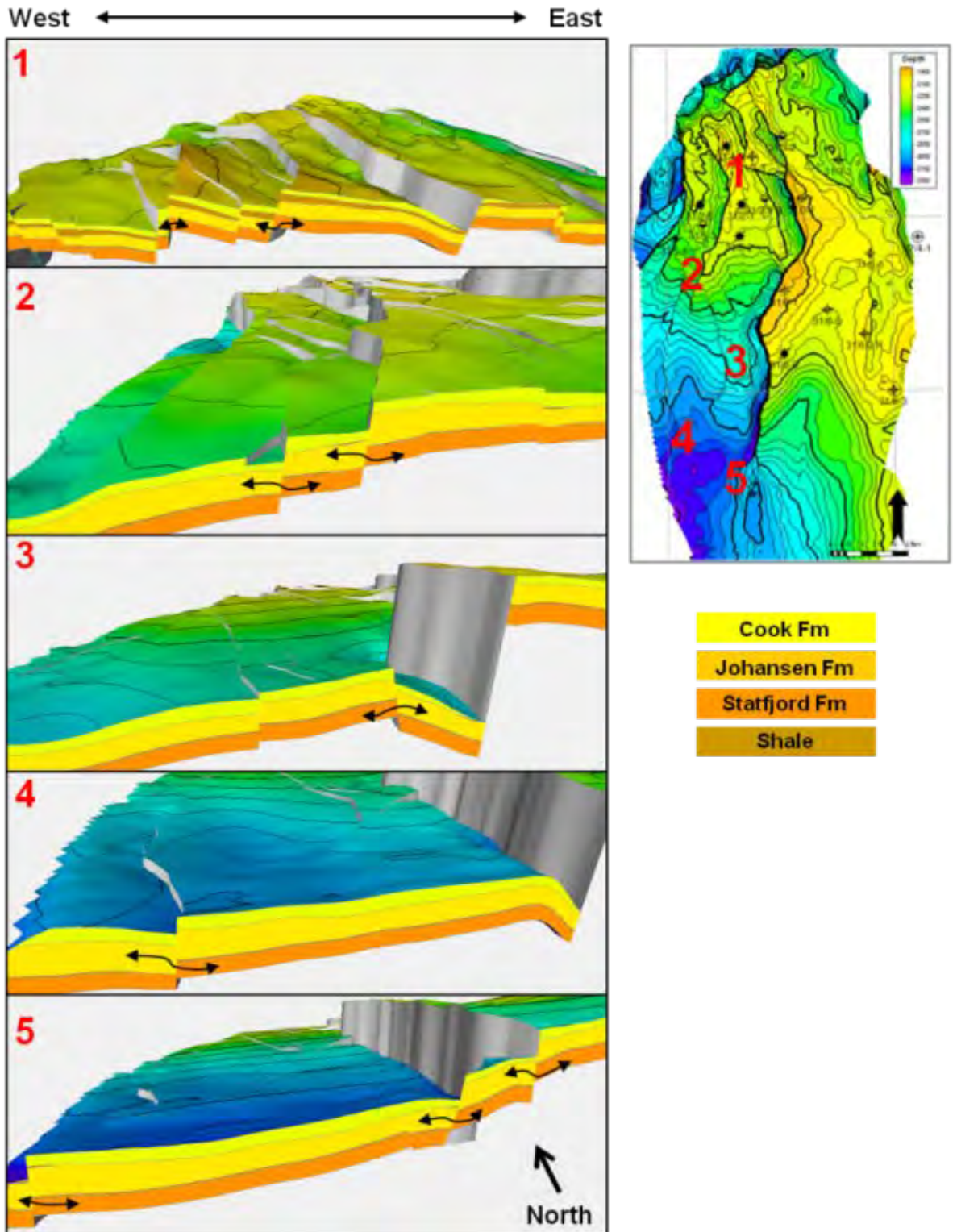


Figure 7-15: E-W profiles showing examples of pore volume communication between primary storage formation Johansen and Statfjord due to sand/sand juxtaposition and lack of clay smear.

DOCUMENT NO.: TL02-GTL-Z-RA-0001	REVISION NO.: 03	REVISION DATE: 01.03.2012	APPROVED:
-------------------------------------	---------------------	------------------------------	-----------

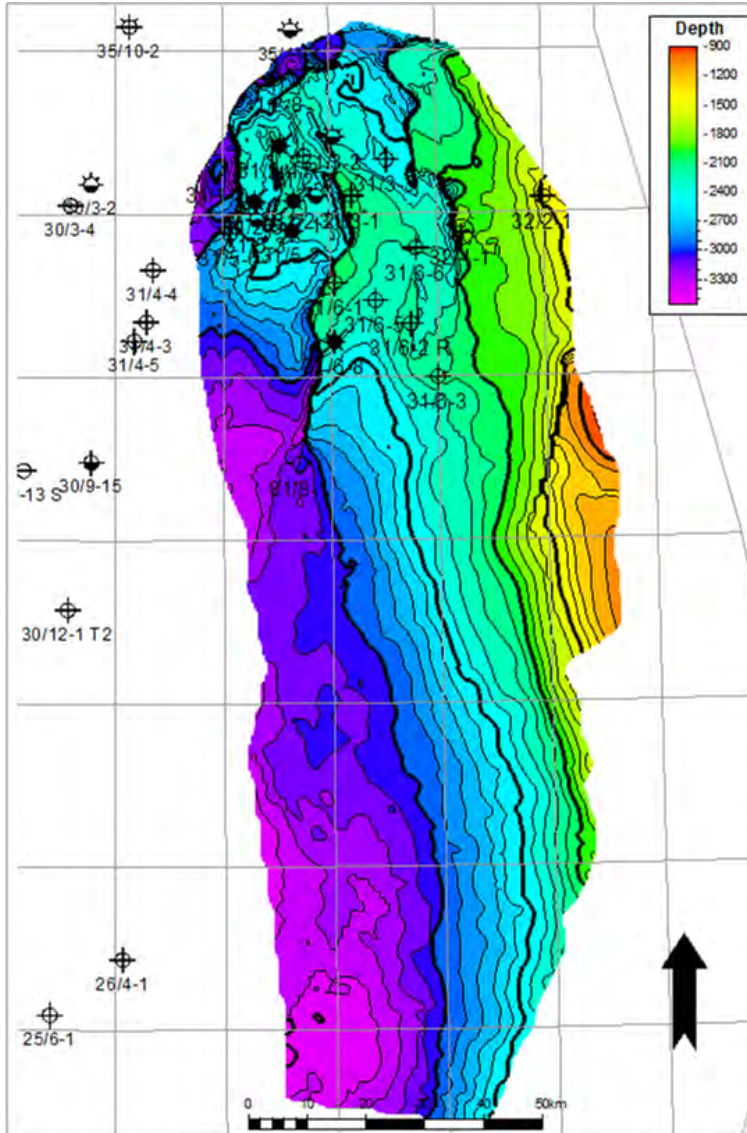


Figure 7-16: Statfjord Fm depth map. C. 100m.

Table 7-5: Statfjord Fm average porosities used in pore volume calculations and results.

Well	Thickness (m)	Mean
31/2-1	106.56	0.187
31/2-2	100.43	0.186
31/2-3	47.00	0.146
31/2-4	100.00	0.198
31/2-5	108.66	0.162
31/2-8	91.74	0.169
31/3-1	54.63	0.170
31/3-3	102.50	0.185
31/5-2	105.13	0.160
31/6-1	45.13	0.189
31/6-2	53.88	0.172
31/6-3	51.88	0.159
31/6-6	43.25	0.159
Average	77.75	0.172

Statfjord Fm	Bulk Rock x 10 ⁹ Sm ³	Pore Volume x 10 ⁹ Sm ³
Low Case (50m)	504	86
Base Case (75m)	751	171
High Case (150m)	1512	257

DOCUMENT NO.: TL02-GTL-Z-RA-0001	REVISION NO.: 03	REVISION DATE: 01.03.2012	APPROVED:
-------------------------------------	---------------------	------------------------------	-----------

A comprehensive investigation, including both seismic (extension and thickness) and well data (reservoir properties) is necessary to fully understand the Statfjord Formation pore volume contribution.

7.2.2 **Brent Group**

The Brent Group depositions on the Horda Platform consist of fine to coarse sandstones, siltstones, shale and claystones. Coal beds and calcareous bands are also observed in the wells. The green boundary (Figure 7-5) is the outline of the mapped Brent Group used in the pore volume calculation. The map is based on the available well and seismic data base. Brent Group depositions exist in wells south, west and north of the Johansen Storage Complex, further pore volume potential probably exists in these areas. The Brent Group depth map is shown in Figure 7-17.

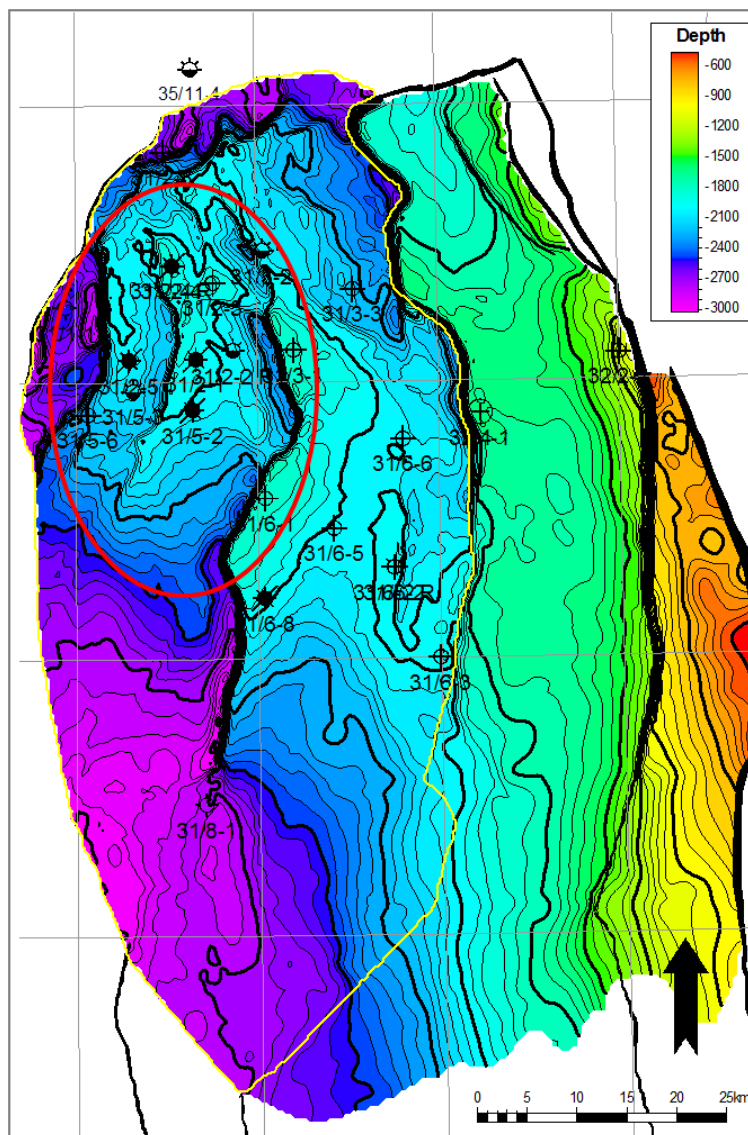


Figure 7-17: Brent Gp depth map. C. 50 m. Red circle shows area with possible cross fault communications between Johansen Fm and the Brent Gp. Yellow polygon represents Johansen reference case.

DOCUMENT NO.: TL02-GTL-Z-RA-0001	REVISION NO.: 03	REVISION DATE: 01.03.2012	APPROVED:
-------------------------------------	---------------------	------------------------------	-----------

The average porosity for the Brent Group in the Horda Platform (Troll) wells is 18%. This is used for the pore volume calculation. The base of the Brent Group is the mapped Top Dunlin Group (Top Drake Formation). The potential pore volume for the Brent Group using the average porosity from key wells is $68 \times 10^9 \text{ Sm}^3$.

The Brent Group pore volume potential is dependent upon cross fault communication in the northern (Troll West) area (Gassnova-ROS 2011).

7.2.3

Viking Group

The Viking Group depositions on the Horda Platform consist mainly of reservoir quality sandstones. These sandstones (Sognefjord, Fensfjord and Krossfjord formations) comprise the reservoir units of the Troll Field. The turquoise boundary (Figure 7-5) represents the outline of the mapped Viking Group used in the pore volume calculation. The map is based on the available well and seismic database. The Viking Group sandstone depositions also exist in wells northwest of the Johansen Storage Complex, further pore volume potential probably exists in this area. The Viking Group depth map is shown in Figure 7-18.

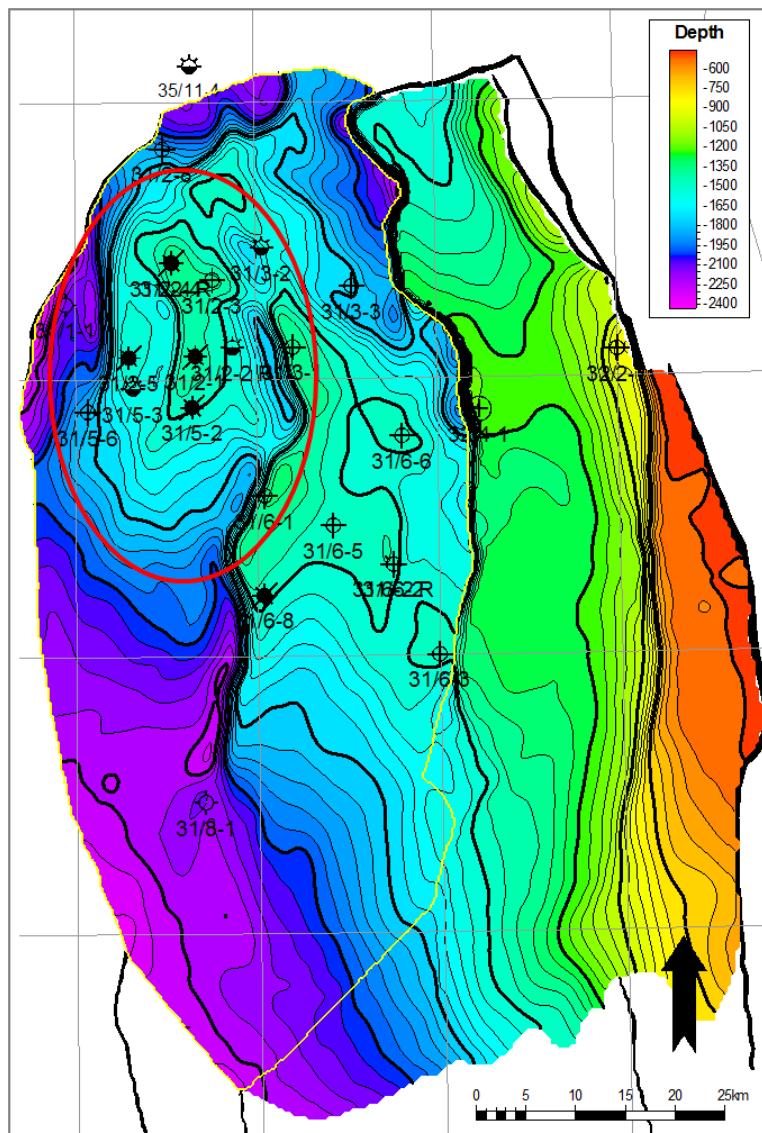


Figure 7-18: Viking Gp depth map. C50 m. Red circle shows area with possible cross fault communications between Johansen Fm and the Viking Gp. Yellow polygon represents Johansen reference case.

DOCUMENT NO.: TL02-GTL-Z-RA-0001	REVISION NO.: 03	REVISION DATE: 01.03.2012	APPROVED:
-------------------------------------	---------------------	------------------------------	-----------

The average porosity for the Viking Group on the Horda Platform (Troll) wells is 21%. This is based on all the Troll Field wells. This average is used for the pore volume calculation. The base of the Viking Group is the mapped Brent Group (Figure 7-17). The potential pore volume for the Viking Group using the average porosity from key wells is $512 \times 10^9 \text{ Sm}^3$. The Viking Group is also deposited further north and this is not included in the calculation and the calculated volume is regarded as conservative. A regional study performed by Statoil (van Wijngaarden, Tjøstheim and Torp 2007) shows aquifer communication between the Troll Field and the northern Viking Group deposits.

The Viking Group pore volume potential is dependent on cross fault communication in the northern area. Communication routes from the Johansen Formation to the Viking Group are probable. Results from the fault seal study and previous study made by the NPD (Bretan, et al. 2011) support cross fault communication on several of the Troll Field faults. Communication between the Johansen Formation and Viking Group would deplete the Johansen Formation due to the Troll Field production (Gassnova-ROS 2011). A verification well would prove the possible communication. The latest exploration well (31/8-1) did not penetrate the Johansen Formation, but showed a depleted Sognefjord Formation and confirms the regional aquifer communication from the Troll production (van Wijngaarden, Tjøstheim and Torp 2007).

7.3 Pore volume assessment and uncertainties

Pore volume in this chapter relates to *total connected pore volume*, and is the total pore volume accessible through the planned injection well.

The pore volume is calculated from the geomodel using the most likely parameters for storage formation quality and extension, average porosity and communication with other formations. The basis for the geomodel is described in chapter 5.3 and 5.4. This is the reference model to be used for base case dynamic predictions.

By starting with the reference geomodel and its calculated pore volume, each uncertainty parameter could increase or decrease the pore volume with a particular uncertainty distribution. Some parameters influence the pore volume with a factor, and some with an absolute volume. This is done to avoid double booking of downsides and upsides. All the uncertainty distributions are summaries to a result distribution of pore volume. Table 7-6 lists the included uncertainty parameters and shows the setup of the uncertainty model. The parameter in 1) in the left-most column, is volume included in the reference model and that has a continued uncertainty with a given range. Parameters within 2) are also included in the reference model, but have an “on-or-off” communication effect. The probability of connectivity is listed in the column “Communication assessment” and range of the contributing pore volume is presented in “Volume estimates”, where “Distribution percentile” describes what the values represent in the distribution. Parameters within 3) represent communication to adjacent formation and segments which are not included in the reference model. These will increase the expected connecting pore volume. The parameter input is found in chapter 5.3.

DOCUMENT NO.: TL02-GTL-Z-RA-0001	REVISION NO.: 03	REVISION DATE: 01.03.2012	APPROVED:
-------------------------------------	---------------------	------------------------------	-----------

Table 7-6: Risk model for pore volume uncertainties.

	Volume/Containment	Volumes estimates			Distribution percentiles			Pinch out Johansen		Communication assessment	
		Low	Base	High	Low	Base	High	p	factor value	p(yes)	p(no)
	Reference model, GSm ³		91.4								
1.1)	Johansen sand presence, factor	0.813	1.000	1.074	10%	Most likely	95%				
1.2)	Johansen sand quality, factor	0.809	1.000	1.124	10%	Most likely	90%				
1.3)	Interpretation uncertainty and depth conversion, factor	0.674	1.000	1.330	Min	Most likely	Max				
2.1)	Communication to Cook, factor		0.15							0.90	0.1
2.1.1)	Cook sand presence	0.94	1.00	1.51	5%	Most likely	Max				
2.1.2)	Cook sand quality	0.58	1.00	1.42	10%	Most likely	90%				
2.2)	Communication to Johansen East, GSm ³		-20.56					5%	0.771		
2.3)	Volume contribution in Amundsen 1, GSm ³	-9.5	-7.7	-5.8	10%	Most likely	90%			0.90	0.1
3.1)	Communication to Johansen East Troll Kystnær, GSm ³	25.86	44.21	66.11	5%	Most likely	95%			0.90	0.1
3.2)	Communication to Statfjord, GSm ³	90.72	181.44	272.16	10%	Most likely	90%			0.00	1
3.3)	Communication to Brent, GSm ³	23.05	68.40	106.15	5%	Most likely	95%			0.50	0.5
3.4)	Volume contribution in Viking group, GSm ³	164.40	512.24	713.75	5%	Most likely	90%			0.00	1

7.3.1

Reference model

The reference model is based on the geomodel presented in chapter 5.6. Figure 5-83 shows both the outer boundary of the geomodel and the top porosity maps for each formation in the model. The reasoning for the outer boundary of the model is described in chapter 7.2.1 and the basis for the porosity maps are described in chapter 5.6.2. Table 7-7 shows the reference volumes within each formation.

Table 7-7: Bulk and pore volume within each formation.

Formation	Bulk volume [Gm3]	Pore volume [Grm3]
Cook	118.42	14.25
Amundsen 2	22.53	3.36
Johansen	373.81	66.32
Amundsen 1	76.63	7.74

7.3.2

Johansen Formation sand presence

The parameter, Johansen Formation sand presence, represents the uncertainty in the pinch out of the Johansen Formation sand. The presence of the Johansen Formation sand is highlighted as one of the main uncertainties for the Johansen Storage Complex due to lack of well control in the south. The data basis and estimates of how the Johansen Formation sand pinch out could be mapped more optimistically or pessimistically than the reference model as described in chapter 7.2.1. A more optimistic estimate increases the pore volume relative to the reference case and vice versa with the pessimistic estimate. The pinch out of Johansen Formation is a continuous uncertainty between pessimistic and optimistic estimate and the uncertainty distribution is therefore also continuous. Figure 7-19 shows the distribution, where the X-axis shows the pore volume change of Johansen (66.3 GSm³ in the reference model) and the Y-axis shows the relative probability. P5 and P95 are marked. In accordance with the polygons presented in chapter 7.2.1, Johansen Formation sand presence has a higher downside potential than upside potential.

DOCUMENT NO.: TL02-GTL-Z-RA-0001	REVISION NO.: 03	REVISION DATE: 01.03.2012	APPROVED:
-------------------------------------	---------------------	------------------------------	-----------

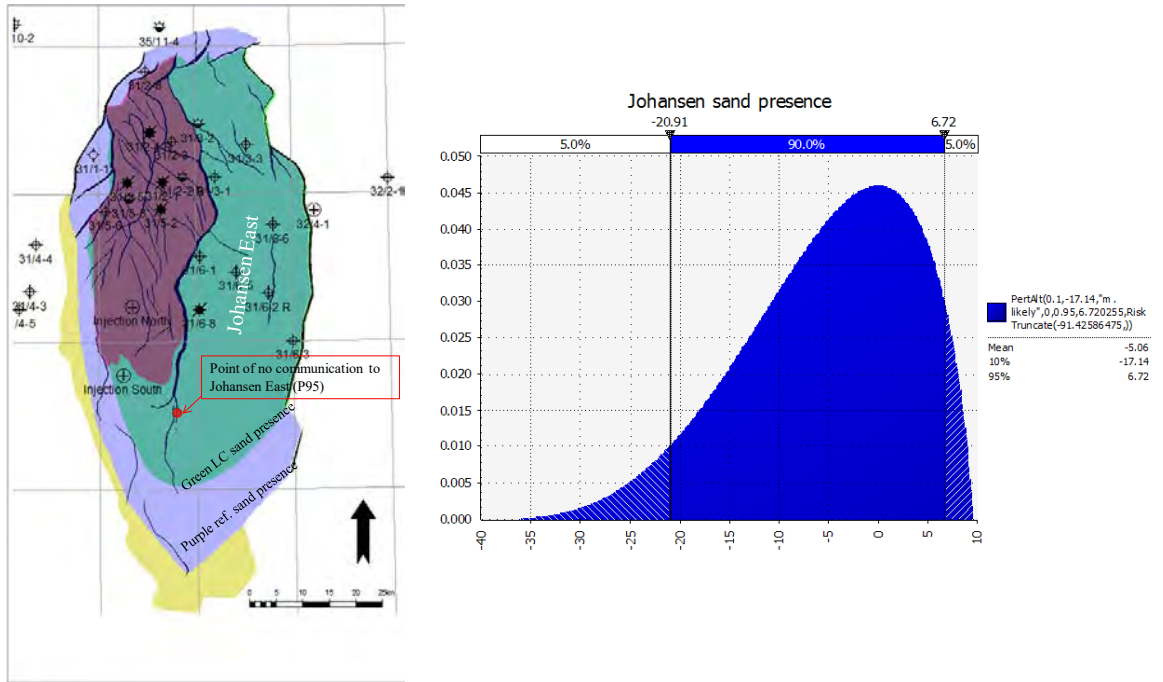


Figure 7-19: Johansen Fm sand presence uncertainty distribution.

7.3.3

Johansen Formation sand quality

This parameter describes how the sand quality can affect the total pore volume connectivity. The property modelling of porosity maps for the geomodel is described in chapter 5.6.2, but uncertainty in porosity modelling is a collection of uncertainties and results from several models and correlations. This includes well log data, core laboratory data and seismic data. The data basis should also be included when evaluating the uncertainty span of the porosity map. Figure 7-20 shows the uncertainty distribution of the quality of the Johansen Formation sand (GSm³). The downside in the 2D area is risked more highly due to uncertainties in a stronger depth trend.

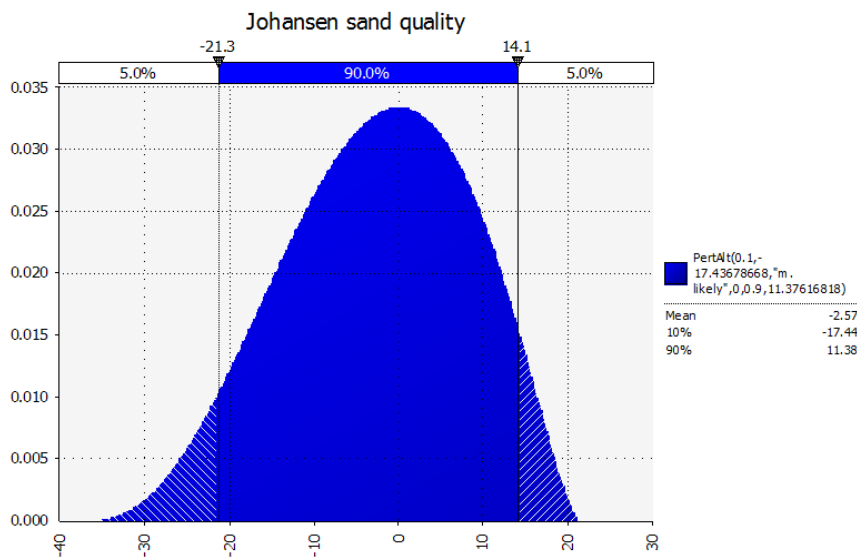


Figure 7-20: Johansen Fm sand quality uncertainty distribution.

DOCUMENT NO.: TL02-GTL-Z-RA-0001	REVISION NO.: 03	REVISION DATE: 01.03.2012	APPROVED:
-------------------------------------	---------------------	------------------------------	-----------

7.3.4 Interpretation uncertainty and depth conversion

Interpretation uncertainty and depth conversion represents the uncertainty in the seismic pick of top and bottom horizon of Cook and Johansen formations. The range shown in Figure 7-21 is calculated from bulk rock volume change described in chapter 7.1. This distribution also continues and shows the increasing and reducing volumes (GSm³) relative to the reference pore volume of 91.4 GSm³. The uncertainty is symmetrical.

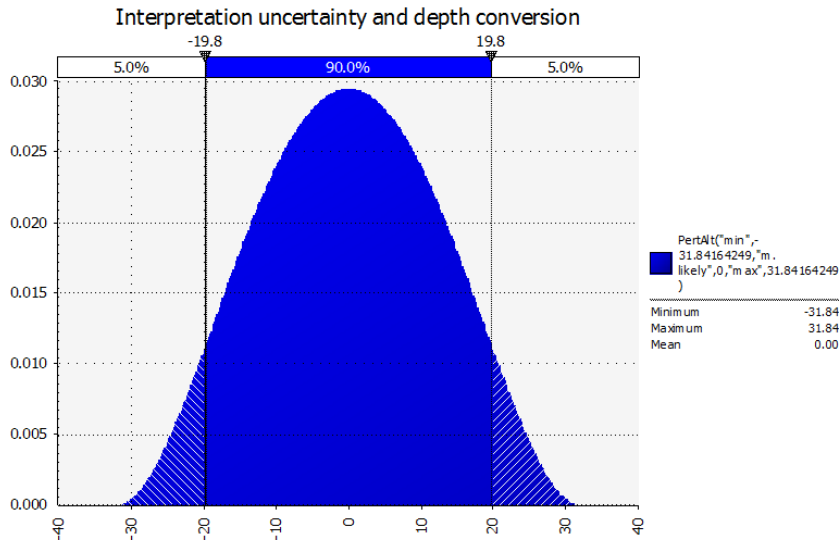


Figure 7-21: Interpretation and depth conversion uncertainty distribution.

7.3.5 Communication effects

Communication effect means the pore volume available in formations other than the primary storage formation. These volumes may or may not be available, depending on the communication properties. There are two considerations for the possible communicating volumes:

1. Amount of available pore volume (value and range)
2. Probability of communication

Probability of communication is modelled as a discrete variable, which means that either there is communication, giving access to the whole of the pore volume, or there is no communication, and thereby the additional available pore volume is zero.

In Table 6.1, the uncertainty distributions noted are 2) reduce the reference volume and 3) parameters increasing the pore volume.

7.3.5.1 Communication effects reducing connecting pore volume

Cook Formation

The Cook Formation is the overlaying formation of Johansen and Amundsen 2 formations. In the reference model, the Cook Formation is assumed to be in pressure communication with the Johansen Formation and the pore volume of 14 GSm³.

The estimation of total volume of the Cook Formation is separated into sand presence and sand quality, similar to the Johansen Formation. The uncertainty in Cook Formation sand presence is based on interpretation uncertainty in the Cook Formation sand pinch out polygon. This is described in chapter 7.2.1. See also Figure 7-10. Figure 7-22 shows the uncertainty distribution where X-axis is the volume (GSm³) contribution relative to the reference volume.

DOCUMENT NO.: TL02-GTL-Z-RA-0001	REVISION NO.: 03	REVISION DATE: 01.03.2012	APPROVED:
-------------------------------------	---------------------	------------------------------	-----------

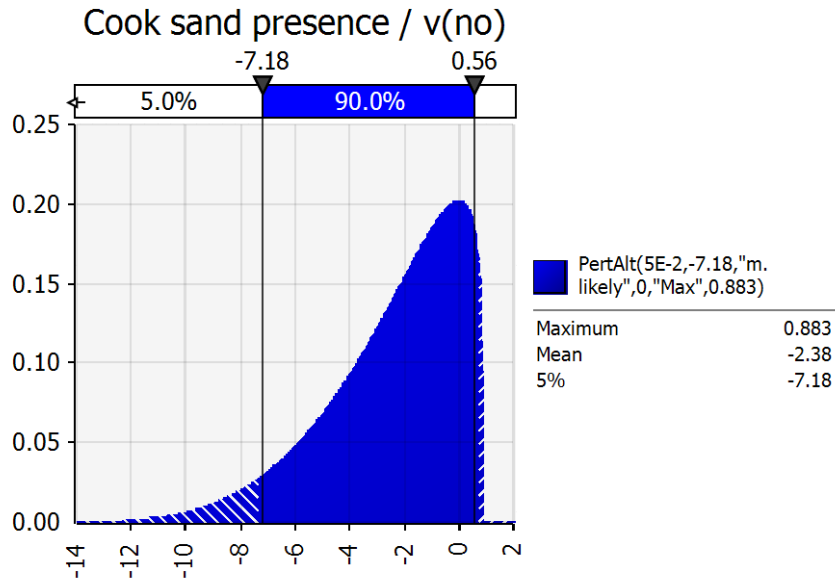


Figure 7-22: Cook Fm sand presence uncertainty distribution.

Further on is the parameter with Cook Formation sand quality based on the uncertainty in porosity mapping and lithology modelling of Cook Formation. This is described in chapter 5.6.2. Figure 7-23 shows the uncertainty distribution where X-axis is the volume (GSm³) contribution relative to the reference volume.

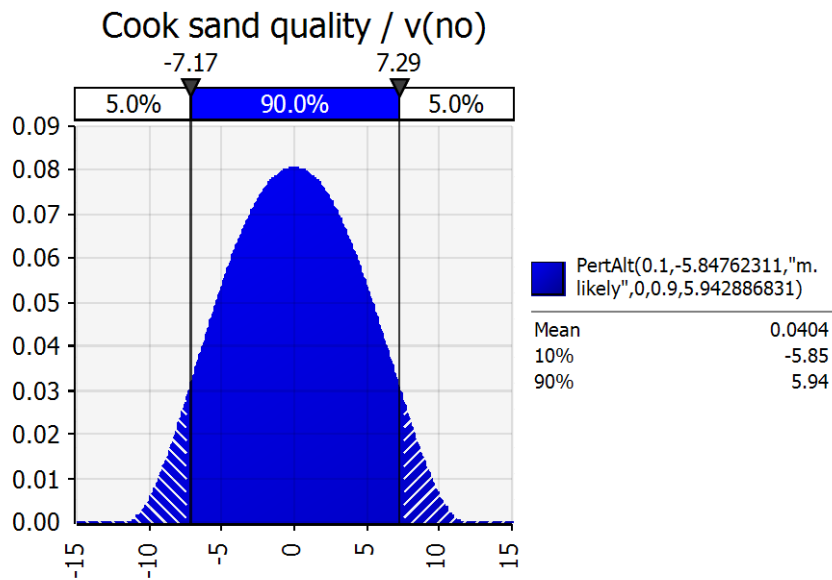


Figure 7-23: Cook Fm sand quality uncertainty distribution.

Adding these two uncertainty distributions together gives a total distribution for the Cook volume. The distribution is shown in Figure 7-24. The volume is converted to a factor of the reference volume to avoid double booking of volume.

DOCUMENT NO.: TL02-GTL-Z-RA-0001	REVISION NO.: 03	REVISION DATE: 01.03.2012	APPROVED:
-------------------------------------	---------------------	------------------------------	-----------

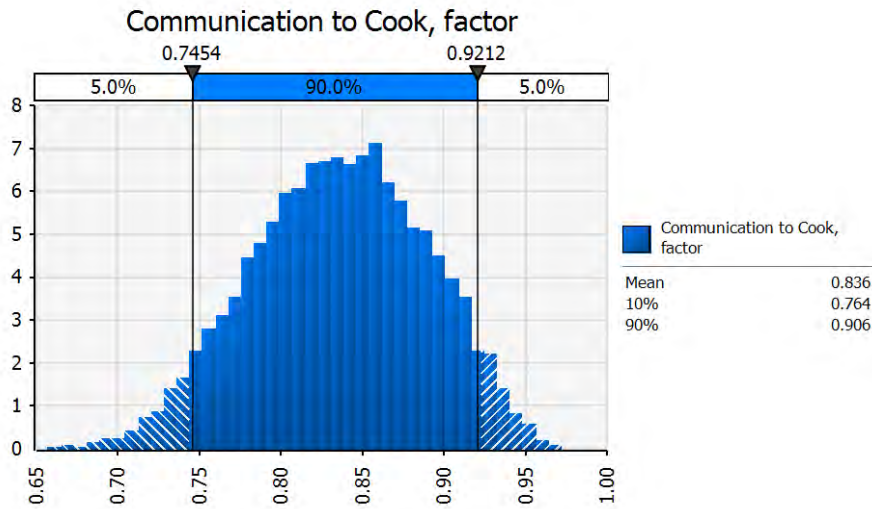


Figure 7-24: Cook Fm total uncertainty distribution as a factor.

The probability of the Johansen Formation being in pressure communication with the Cook Formation is set to 0.9. This is based on confidence in the interpretation of the Amundsen 2 Formation and the sand presence of the Johansen Formation towards the south.

Communication to Johansen East

Johansen East is the segment east of the main fault in the Johansen Formation. Chapter 7.2.1 describes uncertainty in the Johansen Formation sand presence towards the south and the red polygon in Figure 7-6 shows how pessimistic the sand distribution of the Johansen Formation must be to avoid pressure communication with the Johansen Formation East segment. The volume of Johansen Formation East in the reference model is 20.56 GSm³. The risk model is set up so that the Johansen Formation East volume is subtracted from the reference volume only when the outcome of the Johansen Formation sand presence is on P5 or below.

Communication to Johansen Formation East is the uncertainty parameter that could reduce the reference pore volume the most, but its probability is low.

Amundsen 1 Formation

The Amundsen 1 Formation is characterized as shaley and is stratigraphically below the Johansen Formation. Even low permeable shale can contribute to volume for pressure relief during injection. Hence the pore volume of the shale is included in the reference pore volume. The properties of the Amundsen 1 Formation shales are uncertain due to the lack of well and core data. The probability of communication to the shale volume is set to 0.9. Figure 7-25 shows the uncertainty range in the contributing pore volume (GSm³) from the Amundsen 1 Formation based on the property modelling described in chapter 5.6.2.

DOCUMENT NO.: TL02-GTL-Z-RA-0001	REVISION NO.: 03	REVISION DATE: 01.03.2012	APPROVED:
-------------------------------------	---------------------	------------------------------	-----------

Volume contribution in Amundsen 1, GSm³ / v(no)

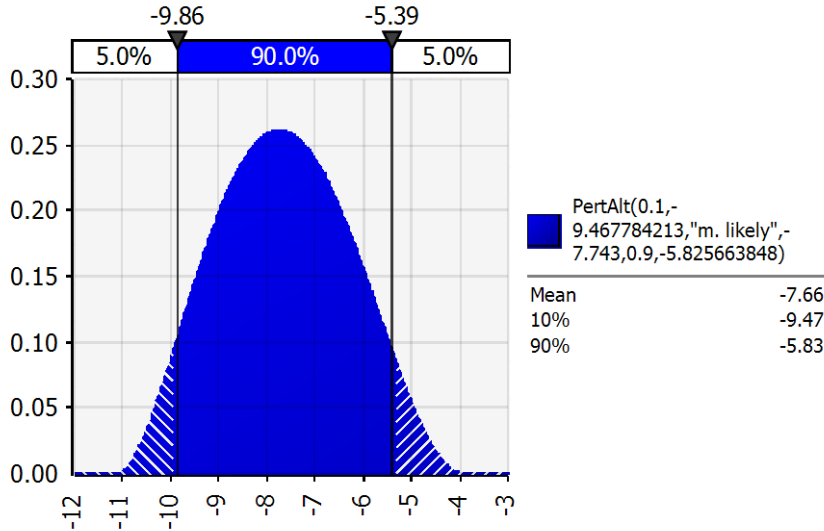


Figure 7-25: Amundsen 1 Fm shale quality uncertainty distribution.

7.3.5.2 Communication effects increasing connecting pore volume

Johansen Formation East Troll Kystnær

This segment is located to the east of Johansen Formation East. Figure 7-9 shows the polygon of the estimated contributing pore volume and chapter 7.2.1 describes background for the volume calculation. This uncertainty parameter has only a positive contribution of volume. Figure 7-26 shows the uncertainty distribution of the contributing pore volume (GSm³). The volume distribution is based on uncertainty in both porosity quality and interpretation (33%), similar to the uncertainty included in chapter 7.3.4. The probability of communication to the Johansen Formation East Troll Kystnær is estimated to be 0.9. This is based on confidence in the Johansen Formation sand distribution to be sufficient for communication towards the east.

Communication to Johansen East Troll Kystnær, GSm³ / v(yes)

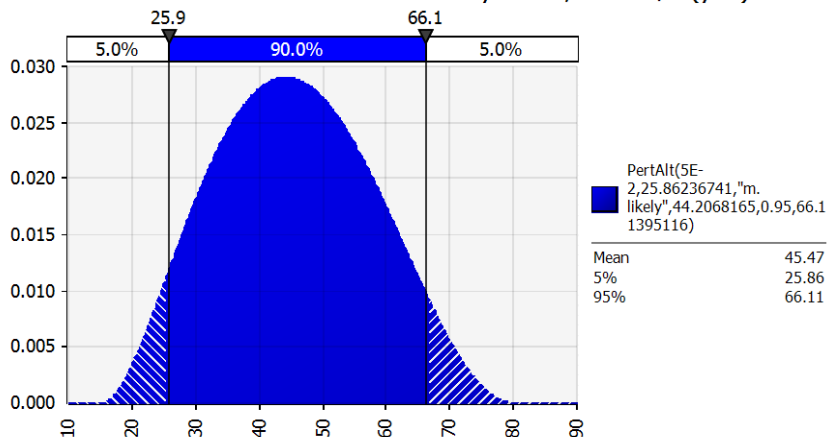


Figure 7-26: Johansen Fm East Troll Kystnær additional volume distribution.

DOCUMENT NO.: TL02-GTL-Z-RA-0001	REVISION NO.: 03	REVISION DATE: 01.03.2012	APPROVED:
-------------------------------------	---------------------	------------------------------	-----------

Statfjord Formation

The Statfjord Formation constitutes widespread deposits located stratigraphically below the Johansen and Amundsen 1 formations. Communication with the Statfjord Formation could occur both over a sand-sand contact over a non sealing fault or through permeable areas of Amundsen 1 Formation. Estimation of the potential contributing Statfjord Formation volume is described in chapter 7.2.1. Figure 7-27 shows the distribution in the volume (GSm³) uncertainty of the Statfjord Formation. The volume is significantly larger than the volume in the reference model. The probability of communication to Statfjord Formation is set to 0 in the Risk model. This is done to highlight the main uncertainty parameters within the storage complex. If a high probability of communication with the Statfjord Formation was included, it would have overruled the other uncertainties in the model. The parameter is still included in the Risk model for sensitivity testing of the potential upside of including the volume.

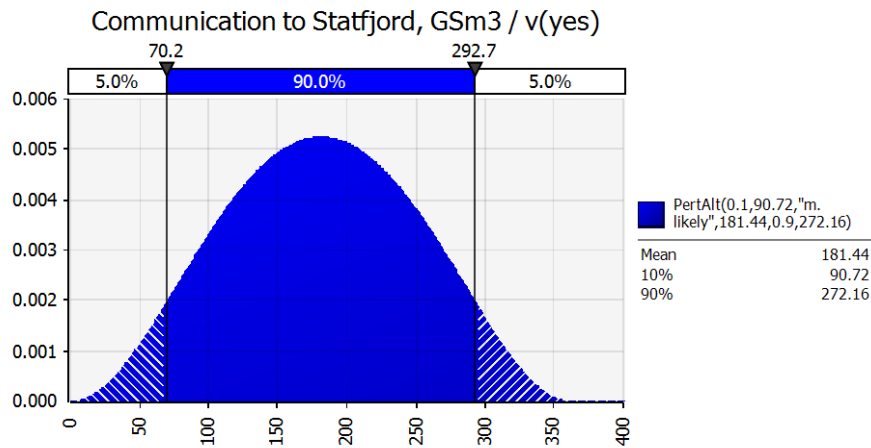


Figure 7-27: Statfjord Fm additional volume distribution.

Brent Group

Brent Group is stratigraphically located above Drake Formation, and is a set of various formations. The estimation of potential contributing pore volume in Brent Group is described in chapter 7.2.2, and Figure 7-28 shows the distribution in the volume (GSm³) uncertainty. Brent Group might be in pressure communication with Johansen Formation and Cook Formation in a sand-sand juxtaposition over a fault in the north, west of well 31/5-2. (Gassnova-ROS 2011) describes the fault seal potential in further detail.

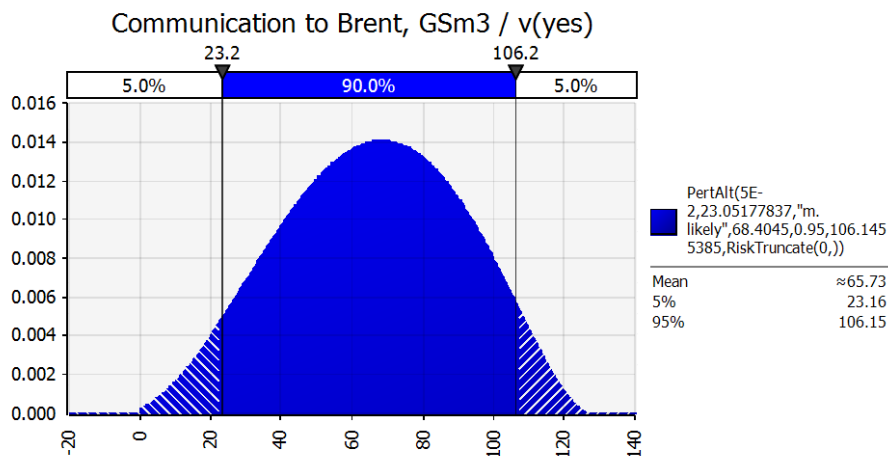


Figure 7-28: Brent Gp additional volume distribution.

DOCUMENT NO.: TL02-GTL-Z-RA-0001	REVISION NO.: 03	REVISION DATE: 01.03.2012	APPROVED:
-------------------------------------	---------------------	------------------------------	-----------

Viking Group

The Viking Group is stratigraphically located above the Brent Group and consists of formations like Sognefjord, Fensfjord and Krossfjord in the area above the storage complex. The estimation of potential contributing pore volume in the Viking Group is described in chapter 7.2.3 and Figure 7-29 shows the distribution in the volume (GSm³) uncertainty. Again, the volume is significantly higher than the reference volume, and the probability of communication is set to 0. As with Statfjord Formation, this is done to focus the Risk model relevant for the main uncertainties within the storage complex and including probability for communication to Viking Group would overrule all other uncertainties. However, it is included for upside sensitivities purposes. Communication with Viking Group would be via sand formations of the Brent Group.

Volume contribution in Viking group, GSm³ / v(%)

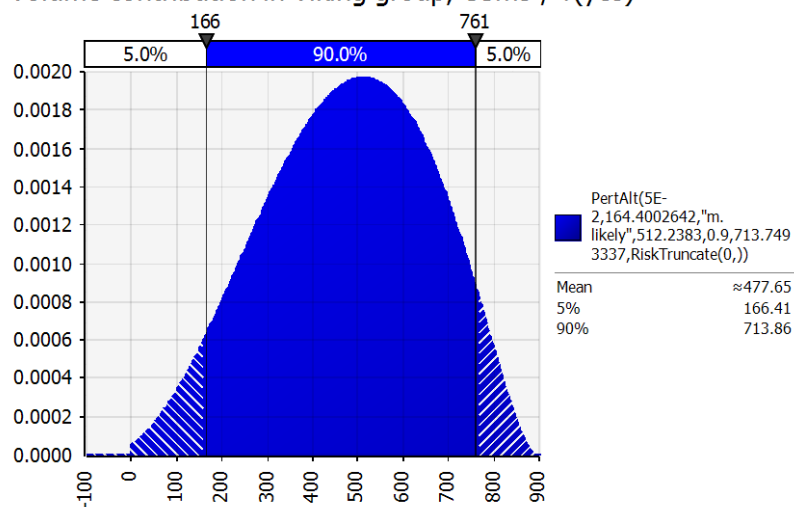


Figure 7-29: Viking Gp additional volume distribution.

7.3.6

Correlations

For the Risk model to be as realistic as possible, correlations between the input parameters must be defined. Defining the relevant correlations ensures that the scenarios used are logical (Table 7-8). The most obvious correlations are defined as follows:

- Johansen Formation sand presence / Communication to Johansen East Troll Kystnær
 - Communication to Johansen East Troll Kystnær requires a minimum presence of sand in the Johansen Formation.
 - Monte –Carlo simulation will never combine low Johansen Formation sand presence with high likelihood of communication with Johansen East Troll Kystnær – and vice versa.
- Johansen Formation sand quality / volume in Johansen East Troll Kystnær
 - The sand quality in Johansen Formation and Johansen East Troll Kystnær must be correlated as this is the same sand system.
 - Monte –Carlo simulation will never combine low Johansen Formation sand quality with high Johansen East Troll Kystnær volume – and vice versa.
- Johansen Formation sand quality / Rock compressibility factor
 - The sand quality in the Johansen Formation must be inversely correlated to the compressibility effect on reservoir build-up pressure. This is based on shale having a higher rock compressibility than a high porous sandstone.

DOCUMENT NO.: TL02-GTL-Z-RA-0001	REVISION NO.: 03	REVISION DATE: 01.03.2012	APPROVED:
-------------------------------------	---------------------	------------------------------	-----------

- Monte –Carlo simulation will never combine low Johansen Formation sand quality with a low compressibility factor.
- Johansen Formation sand quality / Permeability factor for near well pressure
 - The sand quality in the Johansen Formation must be correlated to the permeability effect on well build-up. These are correlated in the model through a porosity-permeability correlation.
 - Monte –Carlo simulation will never combine low Johansen Formation sand quality with high permeability.

Table 7-8: Pore volume correlation matrix.

@RISK Correlations	Johansen sand presence, factor	Johansen sand quality, factor	Communication to Johansen East Troll Kystnaer, GSm3	Communication to Johansen East Troll Kystnaer, GSm3 / v(yes)	Compressibility effects factor	Permeability added pressure build up
Johansen sand presence, factor	1					
Johansen sand quality, factor	0	1				
Communication to Johansen East Troll Kystnaer, GSm3	1	0	1			
Communication to Johansen East Troll Kystnaer, GSm3 / v(yes)	0	1	0	1		
Compressibility effects factor	0	-1	0	-1	1	
Permeability added pressure build up	0	1	0	1	-1	1

There is no direct correlation including Cook and Amundsen formations.

7.3.7

Total pore volume

The output of all the volume uncertainties is a representation of the total pore volume (GSm³) available for CO₂ injection pressure connectivity as a probability distribution. Figure 7-30 shows the uncertainty range for the total pore volume and a descending cumulative probability function. Table 7-9 shows the statistical results of the uncertainty range.

DOCUMENT NO.: TL02-GTL-Z-RA-0001	REVISION NO.: 03	REVISION DATE: 01.03.2012	APPROVED:
-------------------------------------	---------------------	------------------------------	-----------

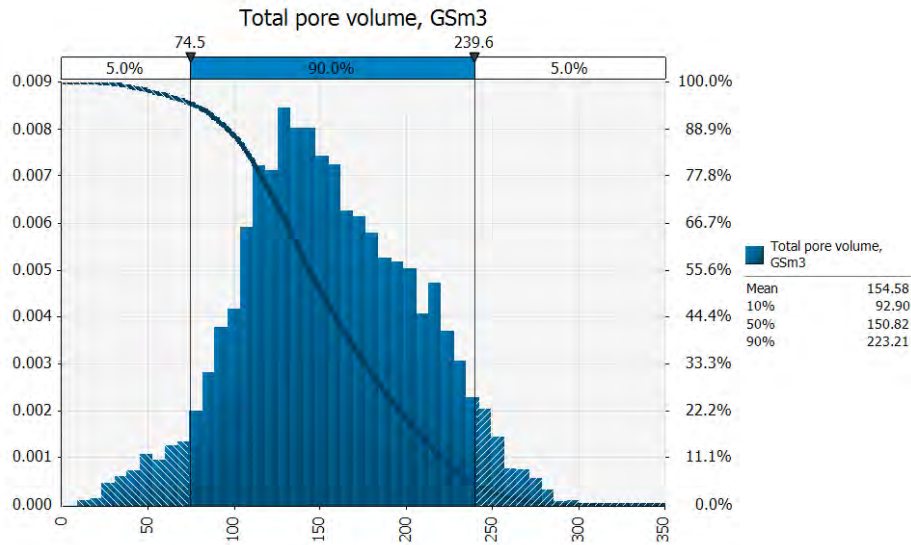


Figure 7-30: Total pore volume distribution.

Table 7-9: Total pore volume results.

Total pore volume	Low	Base	High
Percentile	10%	Most likely	90%
Pore volume (GSm³)	93	155	223

The reference model of 91.4GSm³, is the volume of the closed Johansen/Cook system. Taking the main uncertainty parameters into account, and assigning possible communication to adjacent formations, the expected pore volume is increased by 69% to 155GSm³. This means that the uncertainty parameters have a greater upside potential than downside, and the reference model is a conservative estimate of pore volume.

The following chapters will describe how the uncertainty range in volume will affect the risk for Johansen Storage Complex.

7.4 Pressure build-up assessment

The pressure build-up in the storage complex as a result of Base case CO₂ injection is calculated in the dynamic simulations – along with a representation of the CO₂ plume migration. Base case CO₂ injection is defined as 3.2Mt/y for 50 years, giving a total of 160Mt total injected CO₂. In this chapter the pressure build up is always referred to the highest pressure during injection which will be at the end of the injection period.

The main parameter affecting the pressure build-up is the total pore volume. As described in the previous chapter, the total pore volume is represented as a probability distribution, containing relevant uncertainties. The reservoir pressure build-up is a function of the total pore volume following the basic compressibility equation:

$$C = -\frac{1}{V} \times \frac{dV}{dP}$$

DOCUMENT NO.: TL02-GTL-Z-RA-0001	REVISION NO.: 03	REVISION DATE: 01.03.2012	APPROVED:
-------------------------------------	---------------------	------------------------------	-----------

From this, a probability distribution for the pressure build-up can be directly derived. As the pressure build-up will vary across the storage formation, the focus here is on the probability distributions for pressure build-up in the following areas:

- Reservoir (pbu_{res})
- Near well area (pbu_{nw})
- Bottom hole (pbu_{BH})

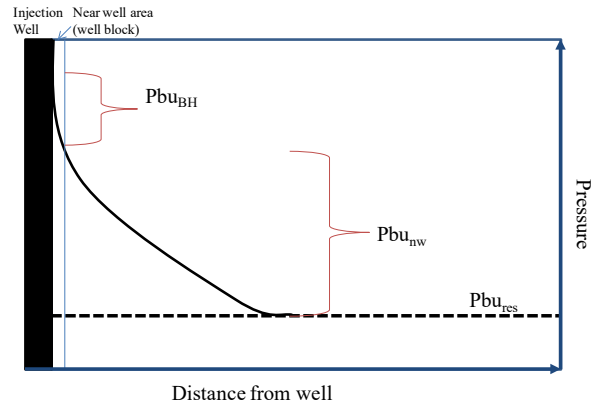


Figure 7-31: Pressure components in an injection reservoir.

Additional to the pore volume parameter are other uncertainty parameters influencing the pressure build-up. Table 7-10 sets up how these various parameters influence the chosen pressure build-ups.

Table 7-10: Build-up pressure influencing parameters.

Build-up pressure influencing parameters	Reservoir (pbures)	Near Well (pbunw)	Bottom Hole (pbuBH)
Pore volume	X	X	X
Compressibility	X	X	X
Permeability		X	X
Temperature effects and potential well damage			X

These last three parameters influencing pressure build-up are described in the following chapters.

7.4.1

Compressibility

Rock compressibility is the largest compressibility uncertainty of the system. Sensitivities and description of compressibility can be found in the Reservoir Parameter Study, chapter 4 (Gassnova-ROS 2011). Rock compressibility is inversely proportional to pressure build-up. Table 7-11 shows the estimated range in rock compressibility and the corresponding factor on pressure build-up relative to the base rock compressibility. Figure 7-32 shows the uncertainty range with the corresponding factor on pressure build-up.

DOCUMENT NO.: TL02-GTL-Z-RA-0001	REVISION NO.: 03	REVISION DATE: 01.03.2012	APPROVED:
-------------------------------------	---------------------	------------------------------	-----------

Table 7-11: Compressibility uncertainty range.

	Low	Base	High
Rock compressibility [bar^{-1}]	1.6×10^{-6}	4.0×10^{-5}	1.6×10^{-4}
Compressibility factor to pressure build-up	1.63	1	0.57
Percentile	5%	Most likely	95%

Core laboratory results from Johansen and Cook cores support an expected rock compressibility of $4.0 \times 10^{-5} \text{ bar}^{-1}$. This is described in chapter 4.7 and (Gassnova-IRI 2011). Due to the confidence in the expected rock compressibility value, the percentiles of High and Low case are set to 5% and 95%.

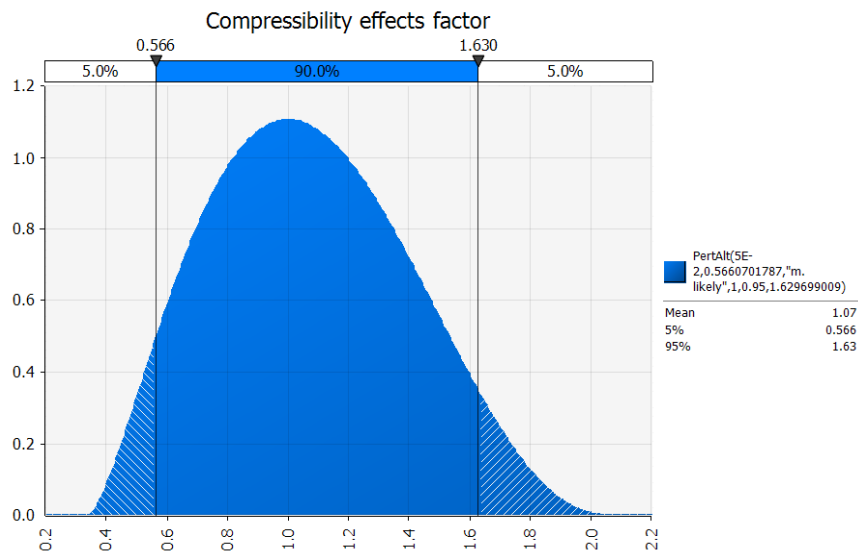


Figure 7-32: Compressibility factor distribution.

Note that high and low is here swapped due to definition of low case always to be negative for the potential for CO₂ storage.

7.4.2

Permeability

As described in chapter 6.3, permeability in the injection well area is an important uncertainty for the Johansen Storage Complex. Uncertainty in the permeability will affect the near well, bottom hole pressure etc, and also the injection pressure at well head described in chapter 6.3. Permeability in the reservoir model is based on the property modelling described in chapter 5.6.2. It is generated from the porosity maps by applying a porosity - perm semi log linear correlation. The correlations are based on core and log data from the well. This is also described in chapter 5.6.2. Table 7-12 shows the range in permeability represented with average permeability in the near well area and its effect on pressure build-up. The reference model has a near well pressure build-up (See Figure 7-31, $\text{pbu}_{\text{nw}} - \text{pbu}_{\text{res}}$) of 9.8 bar. Due to a lack of well data in the injection well area, the percentiles of high and low estimates of permeability effect are set to 10% and 90%. This uncertainty will be narrowed with an exploration well. Figure 7-33 shows the uncertainty distribution of the pressure effect (bar) relative to the reference model.

DOCUMENT NO.: TL02-GTL-Z-RA-0001	REVISION NO.: 03	REVISION DATE: 01.03.2012	APPROVED:
-------------------------------------	---------------------	------------------------------	-----------

Table 7-12: Permeability uncertainty range.

	Low	Base	High
Average permeability in near well area (well block), [mD]	382	625	940
Near well pressure build-up, [bar]	21.0	9.8	7.4
Percentile	10%	Most likely	90%

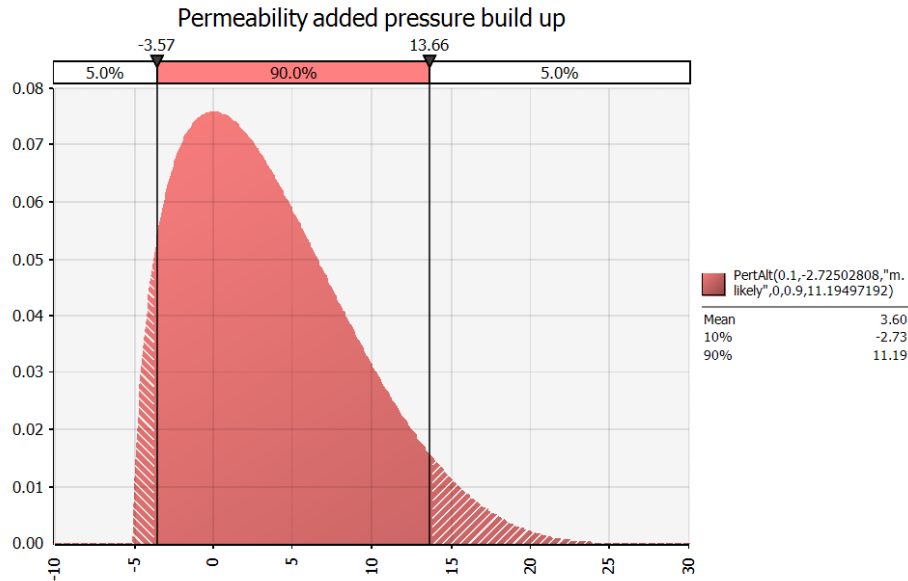


Figure 7-33: Permeability effect distribution on near well pressure build-up.

7.4.3 Temperature and potential well damage effects

The pressure difference between the well and near reservoir is approximately 4 bar in the reference model. This is $pbu_{BH} - pbu_{nw}$ from Figure 7-31. Viscosity of CO₂ increases with decreasing temperature. If CO₂ has a higher viscosity than estimated, well pressure build-up could increase. Well damage during drilling or perforations could also increase well build-up. If injection of CO₂ causes small fractures in the near well area, injectivity could increase, and there will be a reduction in well build-up. The estimated range is listed in Table 7-13 and Figure 7-34 shows the parameter distribution (bar). As shown in Table 7-10, this parameter will only affect the pbu_{BH} and sand interface pressure.

Table 7-13: Additional well pressure build-up due to temperature and potential well damage.

	Low	Base	High
Additional pressure well pressure build-up, [bar]	8	4	2
Percentile	10%	Most likely	90%

DOCUMENT NO.: TL02-GTL-Z-RA-0001	REVISION NO.: 03	REVISION DATE: 01.03.2012	APPROVED:
-------------------------------------	---------------------	------------------------------	-----------

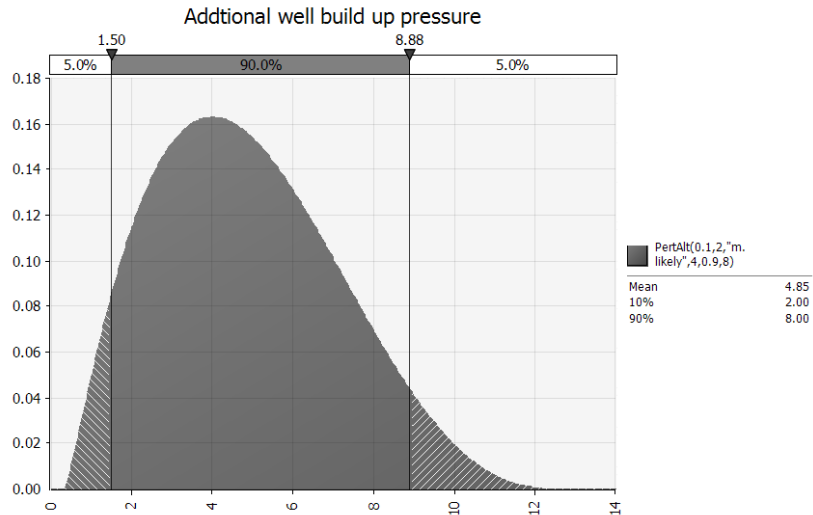


Figure 7-34: Well pressure build-up distribution.

7.4.4 Total pressure build-ups

By establishing these four uncertainty parameters influencing the pressure build-up and combining them statistically in a Monte-Carlo simulation, result distributions for all the three pressure build-ups ($p_{bu_{BH}}$, $p_{bu_{nw}}$, $p_{bu_{res}}$) can be obtained. Figure 7-35 shows the probability distribution of the pressure build-ups. The X-axis represents the pressure build-up above initial pressure in bar and the Y-axis represents the relative probability. Table 7-14 summarises the results. Expected (mean) value of the pressure build-up is higher for bottom hole than near well area and reservoir (Figure 7-31).

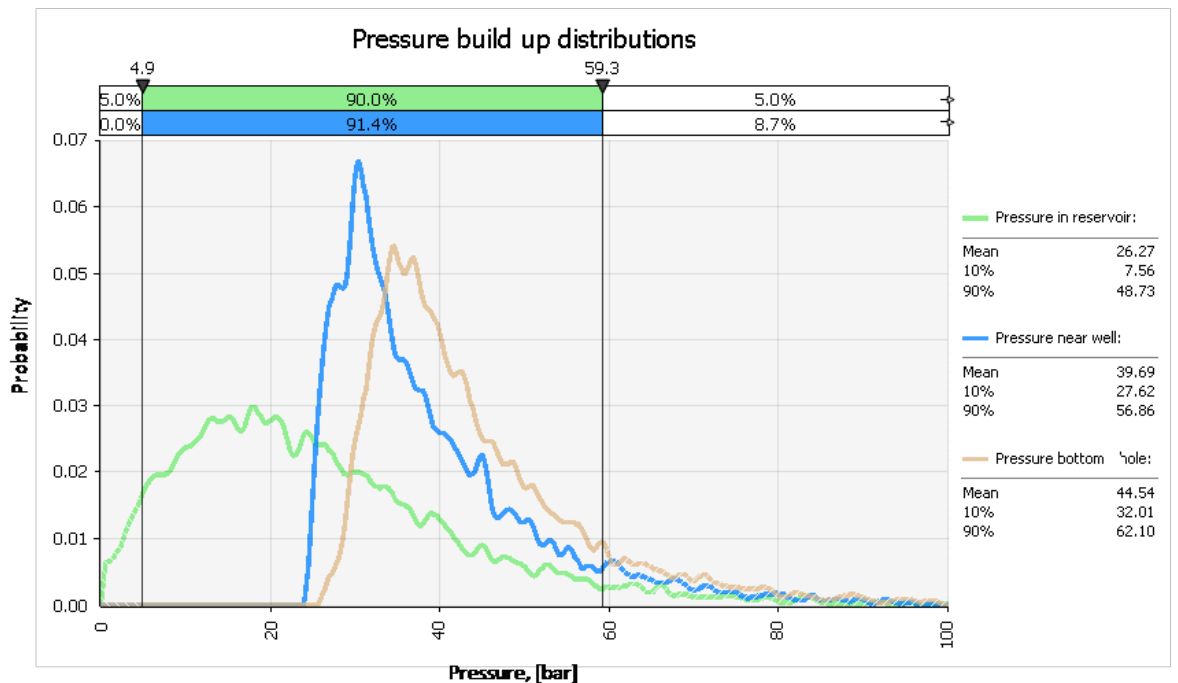


Figure 7-35: Pressure build-up distributions in reservoir, near well area and bottom hole.

DOCUMENT NO.: TL02-GTL-Z-RA-0001	REVISION NO.: 03	REVISION DATE: 01.03.2012	APPROVED:
-------------------------------------	---------------------	------------------------------	-----------

Table 7-14: Pressure build-up summary.

	Low	Base	High
Percentile	10%	Most likely	90%
Reservoir [bar]	8	26	49
Near well area [bar]	28	40	57
Bottom hole [bar]	32	45	62

7.5 Risk of fracturing

The risk of fracturing presented here is the risk of fracturing initiation occurring, given the target injection volumes. The pressure during injection can be monitored, and will not be allowed to exceed estimated fracturing levels. The practical consequence will instead be reduced injection rates and/or volumes. Therefore, instead of being considered a *risk of fracturing*, the probability can equally be considered a *risk of injection volume reductions*.

Given the uncertainty distribution in pressure build-up and the study described in chapter 5.5, the risk related to fracturing initiation of cap rock can be estimated.

To evaluate the probability of fracturing initiation of the cap rock in the injection area, pressure build-up in the bottom hole is used. This is because the cap rock right above the sand-well interface could potentially “see” pressures close to the bottom hole pressure. The study described in chapter 5.5 has done a detailed evaluation of the fracturing pressure of the cap rock in the area above the injection. The study suggests the following uncertainty distribution (bar) in Figure 7-36 of fracturing initiation pressure.

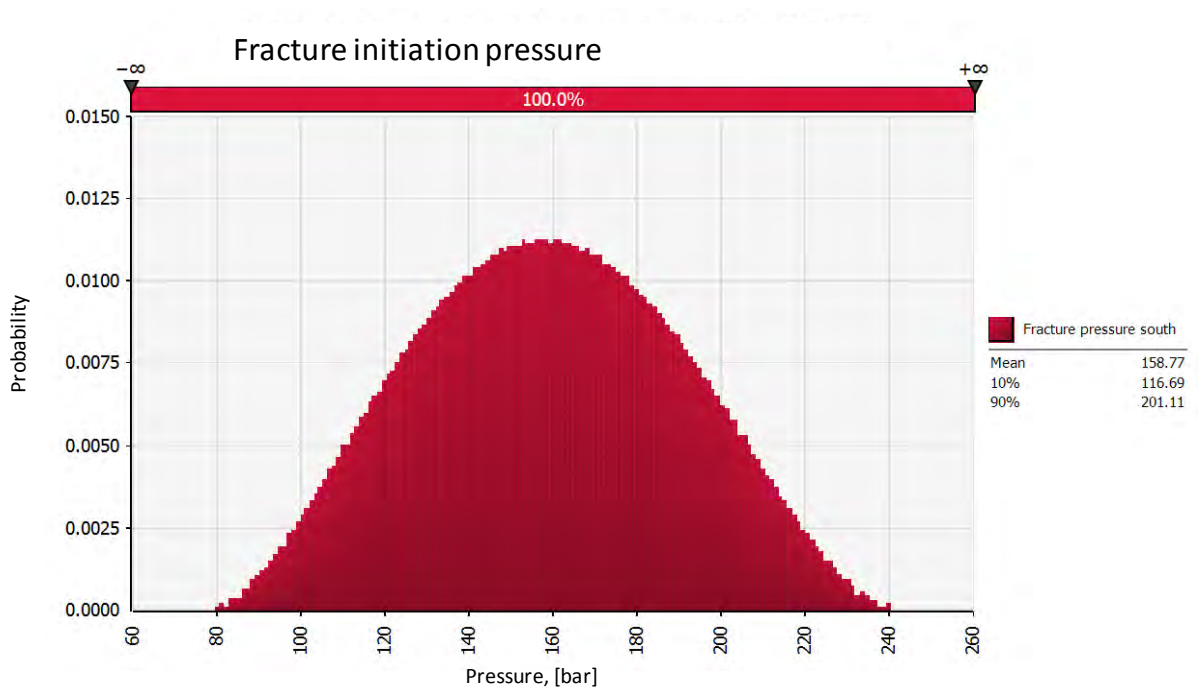


Figure 7-36: Uncertainty distribution of fracture pressure of cap rock in injection area (south).

DOCUMENT NO.: TL02-GTL-Z-RA-0001	REVISION NO.: 03	REVISION DATE: 01.03.2012	APPROVED:
-------------------------------------	---------------------	------------------------------	-----------

Figure 7-37 combines this distribution with the pressure build-up (bar) distribution for the well bottom hole from Figure 7-35.

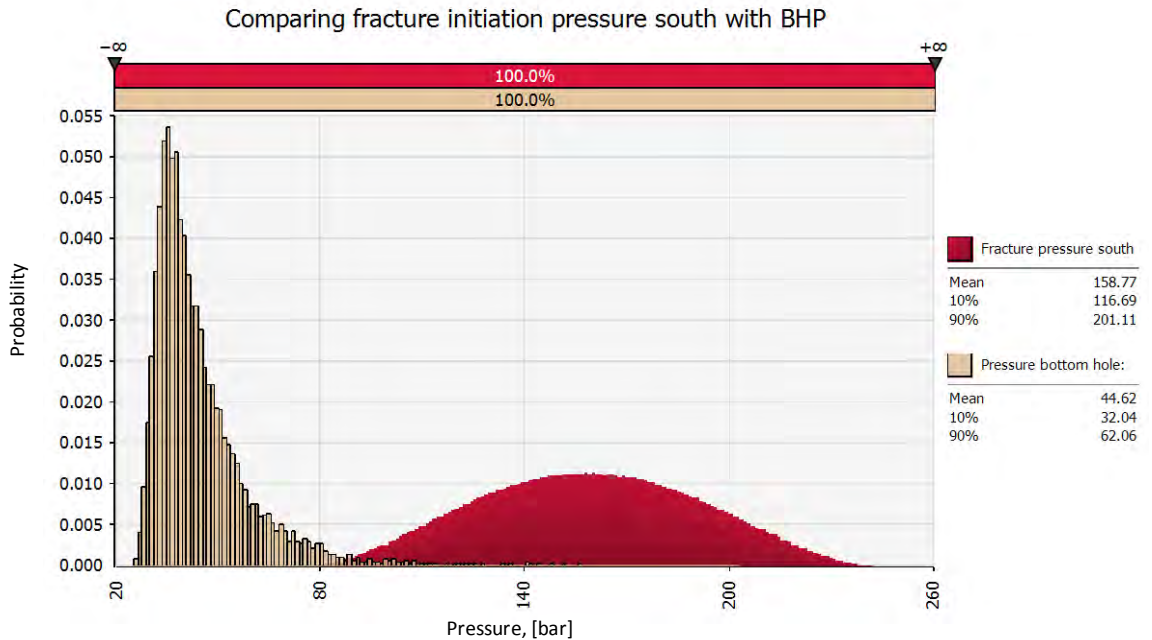


Figure 7-37: Fracture pressure and pressure build-up combined given injection of 160MtCO₂.

The probability of a fracturing can be illustrated by the area of intersection of the two distributions. Probability of the pressure build-up being above the fracturing pressure is from this derived to be 0.2%. The results show that with an injection rate of 3.2MtCO₂ over a 50 year period, the probability of fracturing initiation of the cap rock in the southern area is 0.2%.

7.6 Estimating the storage site capacity

As mentioned previously, by increasing the total injection volume of CO₂, the pressure build-up distributions will follow the basic compressibility equation and the whole distribution will be shifted to the right. The area of intersection with the fracture or fault reactivation pressure will therefore increase. As stated in evaluation criteria in chapter 3, there should be no significant risk of leakage. By defining “no significant” as 10% probability, injection volume can be increased until this number is reached. By increasing the total injection volume up to the convergence of 10% probability, the maximum storage capacity for Johansen storage site can be estimated.

By tripling the injection volume to the total of 480MtCO₂, the probability of fracturing the cap rock in injection area converges to 10%. Figure 7-38 shows the uncertainty distribution in reservoir pressure build when 480Mt is injected combined with fracturing pressure in the north. Expected pressure build-up in the reservoir increases from 26 bar to 49 bar. It is assumed there is no change in rate, only an increase in the injection period to 100 years. Simulations show that based on the reference simulation model, the CO₂ migration does not change significantly if the injection volume is doubled.

DOCUMENT NO.: TL02-GTL-Z-RA-0001	REVISION NO.: 03	REVISION DATE: 01.03.2012	APPROVED:
-------------------------------------	---------------------	------------------------------	-----------

This estimate of total storage capacity is uncertain and should be reviewed as a loose suggestion. Large geological uncertainties could affect this result and the model should be adjusted as more data is included from the well information and injection history.

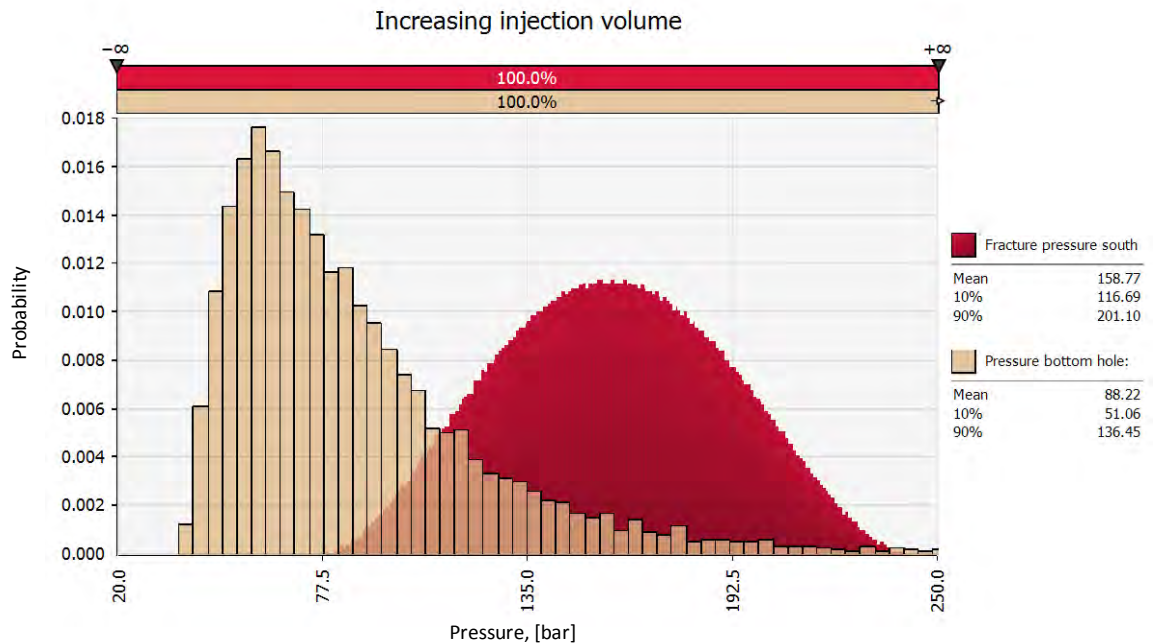


Figure 7-38: Fracture pressure and pressure build-up combined when increasing injection volume from 160Mt to 480MtCO₂.

7.7

Uncertainty summary

This chapter has described an approach to account for the main geological and reservoir uncertainties for the Johansen storage site and their effect on storage capacity. related to likelihood of fracturing cap rock fault reactivation. Given confirmation of the geological model through drilling of a well in the area, the risk and uncertainty analysis shows that the area is robust regarding storage capacity. Even if the exploration well shows thinner or less permeable Johansen Formation than expected, the analysis shows that there are enough potential upsides to ensure a safe storage of CO₂. Increasing the injection volume, the model shows a theoretical maximum capacity of 480Mt given the current data available.

The scenario of no Johansen present in injection area is not included in this study. The main uncertainties lie within the geological model and there will always be scenarios that this analysis cannot comprehend. The risk analysis should be a living model that will be updated as more well and historical data become available.

This uncertainty evaluation is focused on pore volume connectivity, pressure build-up and comparing it to a limiting fracturing or fault reactivation pressure. There is still risk linked to CO₂ migration paths and permeable leakage areas through the cap rock or fault zones. The migration shown in chapter 6.2 is strongly dominated by the geological picture. Although the reference model shows a safe CO₂ migration, structural and lithological changes to the geomodel could also change the confidence related to migration.

DOCUMENT NO.: TL02-GTL-Z-RA-0001	REVISION NO.: 03	REVISION DATE: 01.03.2012	APPROVED:
-------------------------------------	---------------------	------------------------------	-----------

8 RISK OF LEAKAGE

8.1 Introduction

Addressing leakage risk is about proactive measures taken to ensure that the storage is working as expected. By itself an assessment of leakage risk cannot guarantee safe storage, but it will increase the knowledge and awareness of risk factors (potential leakage pathways and possible consequences of a given leakage scenario) and thus decrease the leakage risk.

This sub-chapter addresses possible leakage pathways, seeks to address their probability of acting as conductors for CO₂ from the sub-surface storage site to the surface and possible consequences of a leakage.

Leakages can in general be described as small scale leakages and larger scale leakages. For small scale leakages these can lead to build-up of CO₂ in soils, result in depressions in the ground/sea-bottom and migration of CO₂ into overlying formations. At an offshore storage site local changes in pH-values (acidification of seawater) and impact on ecosystems could also occur.

For a larger leakage due to failure of a wellbore or well-cement a leakage could represent a health and safety risk to operational personnel around the wellbore. For offshore wells disturbance of marine sediments and marine ecosystems around the failed well could also represent a hazard risk.

The leakage risk varies with the life-time of the CO₂ storage project. The highest risk exposure is during injection (mainly due to increased sub-surface pressures). After injection has ceased the leakage risk decreases with time (DNV 2009).

CO₂ storage is regulated by the Norwegian Petroleum Law and the European Directive 2009/31/EC on the geological storage of CO₂¹. In order to comply with the EU directive on geological storage of carbon dioxide Gassnova has initiated a risk analysis focusing on the risk of leakage of CO₂ from the storage. The analysis has been performed by Scandpower with support from NGI and the work is documented in the report "*Hazard Identification and Risk Analysis of CO₂ storage at Lower Jurassic Johansen Formation*" (Gassnova-Scand 2012). The analysis is referred to as Report no: 101965/R1 in this chapter. A summary of the analytical approach, the assessments and conclusions regarding risks are presented below.

8.2 Risk acceptance criteria

According to article 4 of Directive 2009/31 "A geological formation shall only be selected as a storage site, if under the proposed conditions of use there is no significant risk of leakage, and if no significant environmental or health risks exist".

More specific risk acceptance criteria for CO₂ storage have not yet been implemented by Gassnova (industry best practice) or Norwegian authorities (legally binding criteria). The results of the leakage risk analysis are therefore evaluated based on the requirements of the EU directive and with the aim to ensure safe and sound operations.

¹ Twelve EU Member States implemented the CO₂ storage directive within the deadline June 2011 ([GCCSI, 01.07.2011](#)). Norway is due to implement the directive within 2013. A draft version of the Norwegian legislation for CO₂ storage has been circulated internally between departments and directorates under the name "*Forskrift om transport og utnyttelse av undersjøiske reservoarer på kontinentalsokkelen til lagring av CO₂*", but has not yet been made available for public or industry consultation.

DOCUMENT NO.: TL02-GTL-Z-RA-0001	REVISION NO.: 03	REVISION DATE: 01.03.2012	APPROVED:
-------------------------------------	---------------------	------------------------------	-----------

8.3 Analytical approach

Based on industrial experience and discussions between Gassnova, Ross Offshore, NGI and Scandpower the potential leakage pathways have been categorized as shown in Table 8-1.

Table 8-1 The table shows identified leakage pathways covered in this report

Leakage pathways	Described further in	Leakage risk depends on:	Conclusions
Identified faults	<p>Chapter 5.7.3 <i>“Fault reactivation study”</i>.</p> <p>Chapter 4.8 <i>“Fault seal assessment”</i>.</p> <p>Chapter 5.6.5 <i>“Cap rock leakage assessment”</i></p>	<p>Conducting properties, fault plane extent and reactivation potential</p>	<p>The fault seal assessment (Chapter 4.8) identifies an area of possible communication along the main fault between the TWGP and TWOP (central/northern study area).</p> <p>The cap rock is characterized by a low fault density.</p> <p>For faults with a fault throw larger than the seal thickness probabilities and estimated leakage rates are given in this chapter. Faults with a fault throw less than the seal thickness are considered to be safe in terms of communication to shallow layers (Yang and Aplin 2007). However, these faults may have a potential for hydraulic fracturing if injection pressures override fault reactivation threshold levels. Still, cemented fractures have proven to be stronger than the adjacent rock in laboratory tests.</p> <p>Based on a conservative and unlikely model, the minimum allowable pressure build-up at the injection well and Troll area is 200 bar and 120 bar, respectively, before the modelled faults reactivate. However, a more realistic model, assuming a normal stress regime, allows for pressure build-up in excess of 240 bar and 140 bar at the injection and Troll area, respectively.</p>
Possible un-identified faults	<p>Chapter 5.7.3 <i>“Fault reactivation study”</i></p> <p>Chapter 5.6.5 <i>“Cap rock leakage assessment”</i></p> <p>Report: <i>Hazard Identification and Risk Analysis of CO₂ storage at Lower Jurassic Johansen Formation</i>, Scandpower, Report no: 101965/R1</p>	<p>Conducting properties, fault plane extent and reactivation potential</p>	<p>Sub-seismic faults (~10m) are not considered a risk in terms of cross-fault leakage as the throws are of corresponding size.</p> <p>Note that the results from the Scandpower risk analysis show that leakages through sub-seismic faults are a relatively large contributor to the total risk picture (see Table 2). The study gives a total estimated expected % leaked CO₂ from un-identified faults and paleo fractures of 0.00834%, but notes that this number is expected to decrease with further seismic and geological evaluations.</p> <p>Further evaluations in this report (TL02-GTL-Z-RA-0001) have concluded that the leakage risk associated with possible un-identified faults and paleo fractures give a total expected % leakage less than 0.00834%. The quantification of expected leakage from un-</p>

DOCUMENT NO.: TL02-GTL-Z-RA-0001	REVISION NO.: 03	REVISION DATE: 01.03.2012	APPROVED:
-------------------------------------	---------------------	------------------------------	-----------

			identified faults is not re-assessed in this study, but the current knowledge base supports the argumentation that a total expected leak of 0.0101% from the Johansen storage complex is a conservative estimate.
Existing fractures	Chapter 5.6.5 <i>“Cap rock leakage assessment”</i>	Density of fractures, intersection of fractures, orientation of fractures, placement of fractures (in cap-rock), cementation (degree of cementation and cementation-CO ₂ reactions), conductive properties, extent	<p>The cap rock exhibits high angle fractures with a non-continuous nature. The fractures do not display any predominant orientation, indicating that they have an origin related to local pressure changes due to burial, compaction and pressure relief.</p> <p>For un-identified paleo fractures Report no: 101965/R1 recommends further studies on the interpreted fracture pattern². Such studies are expected to decrease leakage risks and give a lower expected % leakage than 0.00834%.</p> <p>See also induced fractures.</p>
Induced fractures	Chapter 5.7.4 <i>“Fracture Initiation”</i>	Density of fractures, intersection of fractures, orientation of fractures, placement of fractures (in cap-rock), cementation (degree of cementation and cementation-CO ₂ reactions), conductive properties, extent	It is considered that the lowest likely pressures build-up before leakage, through induced or activated fractures, into the overburden is 127 bar and 82 bar at the injection location and 31/2-1 well location respectively. The theoretical minimum case is considered to be too conservative. It is equally likely that injection pressures of 169-177 bar and 105-114 bar are allowable at the injection and 31/2-1 well locations before CO ₂ leakage occurs. This is also below the capillary entry pressure (> 250 bar) for the Drake Formation found through lab testing.
Connecting sand bodies	Chapter 4.8 <i>“Fault seal assessment”</i> Chapter 5.6.5 <i>“Cap rock leakage assessment”</i>	Sub-surface pressure, lithologies, heterogeneities, depositional environment	<p>The fault seal assessment (chapter 4.8) concludes that the sands of the Dunlin Group and the Brent Group are in juxtaposition with each other at a main fault between the TWGP and TWOP only. Here the risk of communication across and along the fault-plane is rather high (probably thin clay-coating).</p> <p>The fault assessment (chapter 4.8) strongly suggests that there is pressure communication between the Statfjord and the Johansen formations in a much larger area than included in the reference case model. This does not indicate a leakage route for CO₂ as Statfjord is below Johansen.</p>

² The Scandpower report argues that there are reasons to believe that the fracture patterns (interpreted as due to water escape in the cap rock and the reservoir) used as input to the Scandpower leakage risk analysis, might represent an artifact of the seismic acquisition and processing since the same structures are observed in the sandy layers (fracturing due to water escape will not develop in sandy layers).

DOCUMENT NO.: TL02-GTL-Z-RA-0001	REVISION NO.: 03	REVISION DATE: 01.03.2012	APPROVED:
-------------------------------------	---------------------	------------------------------	-----------

			<p>A southern injection location is chosen in order to avoid plume migration to the area of possible communication.</p> <p>More pressure communication between the Statfjord and Johansen formations than modelled in the reference case model will contribute to a lower overall leakage risk.</p>
Injection wells	<p>Chapter 8.3.13 <i>CO₂ well challenges</i></p> <p>Appendix: <i>Drilling & Well: Cement Design and Operational Practice</i></p>	<p>Cement, casing, materials, injection pressure, properties of CO₂ stream, sub-surface pressure</p>	<p>This studies identifies the following challenges with regards to CO₂ injection wells;</p> <ul style="list-style-type: none"> •Cement design and operational practice •Material choice with regards to corrosion (steel, fluids elastomers) •Barrier design and placement •Barrier monitoring •Well intervention
Through pores in cap rock	<p>Chapter 5.6.5 <i>“Cap rock leakage assessment”</i></p>	<p>Pressure build-up, cap rock properties, fluid properties</p>	<p>Chapter 5.6.5 concludes that the most significant risk of leakage through cap rock is via porous layers. The lower Drake Formation is treated as the main seal with the upper Drake as a contributing layer. The upper Drake Formation has a proven sand development in Troll wells in Quadrant 31, but these sands are believed to have a local extent and are not believed to pose any significant leakage risk in the study area south of the Troll field.</p> <p>Uncertainties related to the extent of sand bodies in the upper Drake Formation is a contributing cap rock sealing risk, but a mean thickness of the lower Drake Formation of 72 meters are deemed sufficient to seal the CO₂ plume also in the case of sand development in the upper Drake Formation.</p>
Capillary flow	<p>Gassnova-IRI 2011</p>	<p>Pressure build-up, rock properties, fluid properties</p>	<p>Leakage risk of capillary flow also gives the risk of CO₂-injection disturbing adjacent hydrocarbon reservoirs.</p> <p>In Gassnova-IRI 2011 mechanisms for leakage through capillary migration and diffusion have been evaluated. The evaluation concludes that there is no significant risk of leakage through capillary migration or diffusion.</p>
Abandoned wells		<p>Cement, casing, materials, sub-surface pressure, properties of plug</p>	<p>There are no abandoned wells within the vicinity of the plume migration path for any likely scenario.</p>
Chemical reaction between CO ₂ and cap rock/overburden	<p>Chapter 5.6.5 <i>“Cap rock leakage assessment”</i></p>	<p>Cap rock properties, fluid properties, pressure, temperature</p>	<p>A further leakage scenario is through acidic CO₂-brine dissolution of calcite cemented fractures in the shale constituting the cap rock (Bromhal, et al. 2010). In the well sample testing conducted by Iris (Gassnova-IRI 2011), a mean calcite percentage of 10% was measured by XRD analysis of bulk rock. This level is comparable to calcite percentages measured on Utsira cap rock (Kemp et al. 2001). The calcite is present in the natural mineral assemblage of the rock and is not believed to represent a significant risk to seal integrity.</p>

DOCUMENT NO.: TL02-GTL-Z-RA-0001	REVISION NO.: 03	REVISION DATE: 01.03.2012	APPROVED:
-------------------------------------	---------------------	------------------------------	-----------

			<p>The mineralogy of the cap rock based on cores from wells outside the investigated area shows that the expected composition of the Drake shale will be geochemically stable with little possibility of leakage.</p>
Catastrophic events	<p>Chapter 4.9 “Seismicity”</p> <p>Climatic conditions are not covered in this report, and should be addressed in a FEED study.</p>	Tectonic activity, climatic conditions	<p>Chapter 4.9 <i>Seismicity</i> summarizes relevant literature. There referred studies indicate that earthquakes in the study area are quite deep and terminate at the lower crustal body. The northern part of the study area has a higher frequency of earthquakes than the southern. The literature study concludes that seismicity is expected to have minimal impact on storage site integrity.</p> <p>The earthquakes in the study area terminate at the top of the lower crustal body and no indications of disturbance in Johansen, Statfjord and shallower formations are seen.</p> <p>Oil and gas accumulations in the nearby and more seismic active Tampen-area have remained contained in the respective reservoirs since Jurassic times.</p>
Heterogeneities in the cap rock/overburden	<p>Chapter 5.6.5 “Cap rock leakage assessment”</p> <p>Report: <i>AVO study</i> Western Geco, Gassnova-WGD 2011</p> <p>Report: <i>Apparent Gas Chimney in Block 31/8</i>, AkerGeo, Gassnova-AKS 2011</p> <p>Report: <i>Assessment of Gas Chimney</i>, Weatherford, Gassnova-WPC 2011</p> <p>Report: <i>Quick assessment of seismic evidence of leakage of the Johansen Formation</i>, VBPR, Gassnova-VBPR 2011</p>	Lithology, water/gas escape structures, pressure, fractures, geomechanical properties	<p>A gas anomaly (see Figure 5-76) observed on seismic could indicate a weak zone in the Drake Formation. Alternatively, the disturbance could be due to clay diapirism. The main conclusion from the Gassnova initiated studies is that there is no conclusive evidence of a deep gas chimney in block 21/8 (Gassnova-ROS 2011). The studies and well 31/8 underpin that the main migration pathways are further north than the observed anomaly.</p> <p>The assessments of features that may cause leakage through the cap rock suggest that the observed seismic anomalies might be dewatering structures formed by migrating fluids. Such features are often seen in sands above a polygonal fault system indicative of a palaeo-leakage system. Such a system has not been identified in the seismic data. As these features are formed at early stages of a clay burial they can be difficult to detect due to the healing properties of young and mobile clays. Another possibility is that they may be under the limit of seismic resolution or that such features are not present.</p> <p>No evidence of leakage has been found in the plume migration area.</p>

8.3.1 **CO₂ migration in the storage formation**

Based on available information from seismic investigations and previously drilled wells in the study area a geological model has been built. A black oil simulator has been run to model CO₂

DOCUMENT NO.: TL02-GTL-Z-RA-0001	REVISION NO.: 03	REVISION DATE: 01.03.2012	APPROVED:
-------------------------------------	---------------------	------------------------------	-----------

plume migration during and after injection, and NGI has simulated leakage rates for identified and expected leakage sources. The base case used in Report no: 101965/R1 is the injection of 3.2 Mt/yr for a period of 50 years adding up to a total of 160 Mt CO₂ injected. The simulation models give possible plume migration as a function of time and make it possible to identify potential leakage pathways. The identified leakage pathways are listed in .

The Scandpower leakage risk assessment recommend further verification of the geological model and plume simulations over a longer time period (5000 years as opposed to the current 500 year simulations). An injection exploration well would give further and more representative data for the geological model and subsequent dynamic models. Therefore, such a test well would also provide more confident and better leakage risk estimates.

8.3.2 **Leakages through faults and fractures**

Three major faults have been identified in the area surrounding the injection point; A Major western fault, the Troll West fault and the Troll East fault. These three are given special attention in Report no: 101965/R1.

The plume is expected to expose the major western fault after 42 years and the Troll West fault after 200 years. The Troll East fault will not be exposed in the base case simulation model, but with more pessimistic assumptions it may be exposed.

For each of these faults acting as potential leakage pathways, event trees have been developed to support the estimated probabilities. Figure 8-1 shows the “Troll West fault” event tree describing leakage through the major western fault. The branch probabilities in the event trees are based on expert judgments by NGI³ and Scandpower personnel.

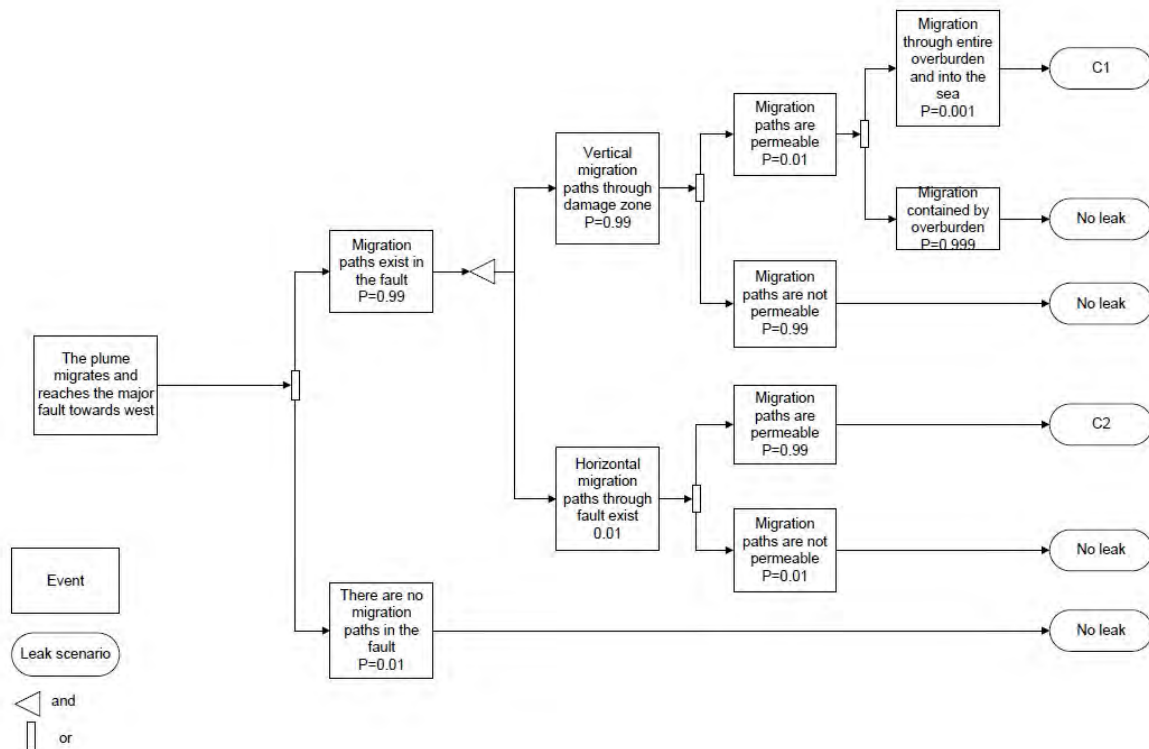


Figure 8-1 Event tree for the major western faults, the Troll West fault, with corresponding estimated probability of occurrence. The branch probabilities in the event trees are based on expert judgments by NGI and Scandpower personnel.

³ The clay-filled fault strength parameters were based on the NGI Mohr Coulomb results available at the time of modelling for clay laminated Cook Formation samples.

DOCUMENT NO.: TL02-GTL-Z-RA-0001	REVISION NO.: 03	REVISION DATE: 01.03.2012	APPROVED:
-------------------------------------	---------------------	------------------------------	-----------

For each event tree a number of corresponding leakage rates have been estimated. The leakage rates are generally time dependent. In addition calculations have been made for two different combinations of parameters to address uncertainty:

- Conditional probability 0.9: Fault length 1000m, permeability 10mD, anisotropic
- Conditional probability 0.1: Fault length 5000m, permeability 1000mD, isotropic

A summary of the identified leakage pathways, their associated leakage probabilities and expected % leakage is shown in Table 8-2. Some of the leak scenarios through faults may release a sizeable amount of CO₂ from the reservoir compared to the total amount injected. The highest expected percentage leakage from a sub-seismic fault or paleo fractures give a 0.0039% of the total injected amount, i.e. 6 240 tons. All analyzed sub-seismic faults and paleo fractures give an estimated leakage of 0.00834% of total injected amounts, i.e 13 344 tons of CO₂. Based on available information the number of subseismic faults and paleo fractures have been estimated to 2 per square kilometer. Since the number of faults and fractures exposed to the CO₂ plume is time dependent the scenarios have been calculated for 50 and 500 years after injection start. Two different combinations of parameters have been used to address uncertainty. In order to decrease leakage risk associated to paleo fractures it is recommended to do further studies on the interpreted fracture patterns (Report no: 101965/R1 suggests that these might represent an artifact of the seismic acquisition and processing).

8.3.3 Leakages through subseismic faults and paleo fractures

Subseismic faults and paleo fractures can be modeled in the same event tree. Based on available information the number of subseismic faults and paleo fractures have been estimated to 2 per square kilometer. Since the number of faults and fractures exposed to the CO₂ plume is time dependent the scenarios have been calculated for 50 and 500 years after injection start. As above two different combinations of parameters have been used to address uncertainty

DOCUMENT NO.: TL02-GTL-Z-RA-0001	REVISION NO.: 03	REVISION DATE: 01.03.2012	APPROVED:
-------------------------------------	---------------------	------------------------------	-----------

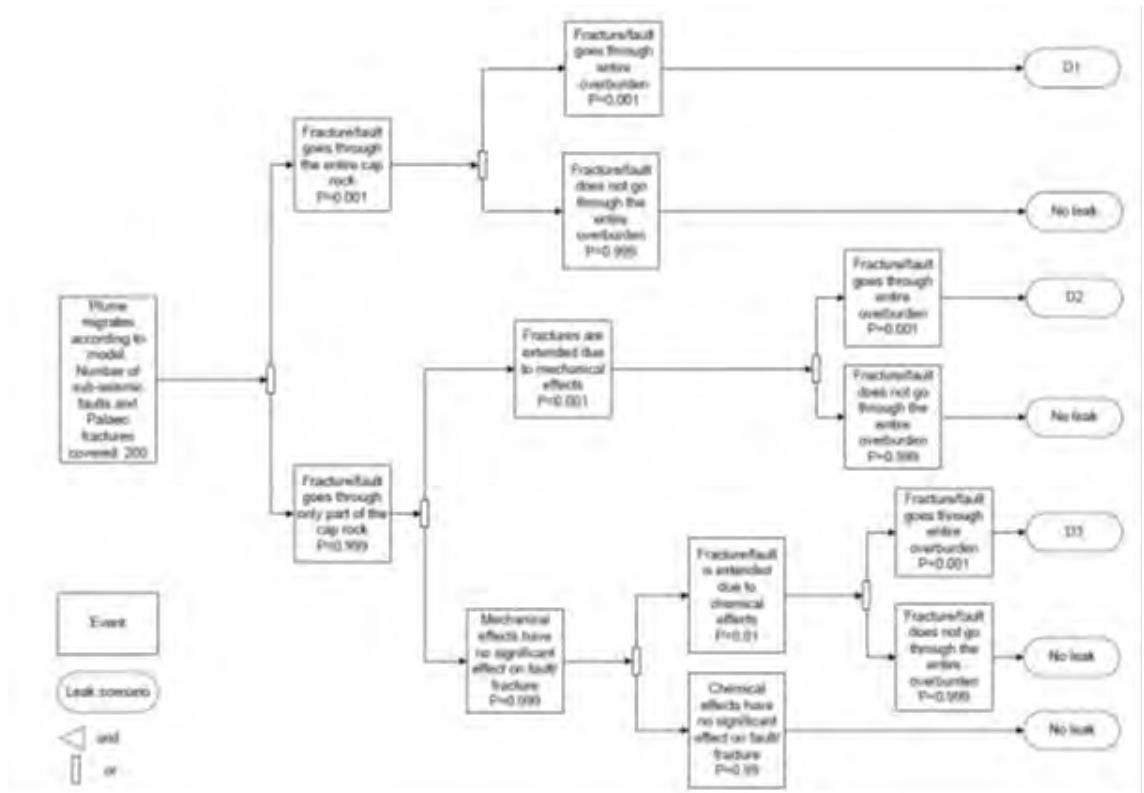


Figure 8-2 Event tree for paleo fractures

8.3.4 Leakage through injection wells

Leakage through injection wells can occur during drilling, injection and workover operations. Parameters affecting the probability of leakage from the injection well due to external causes are protection against falling objects and activity regarding the well head. Maintenance and modifications on the well head will cause the highest risk for damaging the well head.



The potential for wellbore leakage during injection depends in part on the quality of the original construction as well as geochemical and geomechanical stresses that occur over its life-cycle (Crow 2010)⁴.

The highest risk for leakage through active wells are believed to be whilst drilling wells after injection has commenced and during workover operations. Current known CO₂ blowouts are from the use of CO₂ injection for EOR purposes⁵ (Skinner 2003).

Figure 8-3 CO₂ snow at the wellhead during blow-out from a CO₂ injection in Hungary in 1991. The blow-out occurred when a workover operation at a CO₂ injector was commenced after a temporarily shut-down period. The BOP was almost fully stripped down when the well flooded. Picture courtesy of MOL

⁴ Crowther et al. (2010) found that the amount of fluid migration along the wellbore of the investigated 30-year old CO₂ production wells is probably small because: the amount of carbonation decreased with distance from the reservoir, cement permeability was low (0.3–30 microDarcy); the cement–casing and cement–formation interfaces were tight, the casing was not corroded, fluid samples lacked CO₂, and the pressure gradient between reservoir and caprock was maintained.
⁵ Only in U.S there are some 3000 CO₂ injection wells for use in EOR on land, the oldest from 1972.

DOCUMENT NO.: TL02-GTL-Z-RA-0001	REVISION NO.: 03	REVISION DATE: 01.03.2012	APPROVED:
-------------------------------------	---------------------	------------------------------	-----------

The probability of leakage through the injection well has been assessed based on statistics from the SINTEF Blowout Database for the North Sea. These are historical data based on oil and gas drilling. Such drilling are often commenced into over-pressurized zones and are such, initially, subject to higher risk exposure than the initial CO₂ injection wells which are drilled in assumed normal gradient conditions. But over a time period of 50 years drilling of new or additional injection wells in addition to work-over and re-completion operations will occur. Statistics from the database on blow-out occurrences for both work-over operations and exploration drilling are therefore believed to be representative for CO₂ injection wells in the North Sea⁶ (see (Gassnova-Scand 2012) for a discussion of representative databases). Two scenarios have been identified in accordance with information in the database:

- Full bore rupture, release rate 100 kg/s, corresponding probability 0.0023, Duration 62,66 days
- Restricted flow, release rate 25 kg/s, corresponding probability 0.0055, Duration 62,66 days

For both scenarios the duration until the release is stopped is estimated to be two months.

8.3.5 Leakage through abandoned wells

15 exploration wells penetrate the Johansen Formation inside a radius of approximately 45km from the 31/8 injection point. All of these are exploration wells abandoned according to prevailing requirements at the time of plugging, and an assessment has been made of the integrity of these. In general these old wells were found to be good. Some wells have issues regarding possible communication paths between reservoir segments, but this is not considered to be a challenge as it is outside the modelled plume migration area for modelled scenarios.

8.4 Probabilities and leakage rates

As described in Chapter 7.3 the risk of fracturing and fault reactivation is low in what is deemed as the most realistic model (assuming a normal stress regime and allowing for pressure build-up in excess of 240 bars in the injection area and 140 bars in the Troll area).

In the risk analysis (Report no: 101965/R1) it is assumed that the maximum pressure build up will not exceed 42 bars. By increasing or decreasing the injection volume, the leakage probability will change respectively.

All the analyzed scenarios are summarized in the table below. The leakage rates are generally time dependent, and the figures listed in the table are peak rates. The “expected % leaked” is the total leakage multiplied by the probability and given as a percentage of the total 160 Mt CO₂.

⁶ Note that the blow-out frequency for onshore CO₂ injection wells in the US is higher than those in SINTEFs database (see appendix 13.24 for further discussions).

DOCUMENT NO.: TL02-GTL-Z-RA-0001	REVISION NO.: 03	REVISION DATE: 01.03.2012	APPROVED:
-------------------------------------	---------------------	------------------------------	-----------

Table 8-2 The table shows the main leakage sources and their associated leakage probabilities are listed in the table below. Leakage rates have been calculated by NGI for each branch using a simulation model where the leakage rates for each branch have been calculated based on the probabilities and estimated leakage rates for each of the identified leakage sources. A summary of expected % leaked for each of the scenarios gives the total expected % leaked for each of the main leakage categories. Note that these results suggest that leakages through unidentified faults and paleo fractures are a relatively large contributor to the total risk picture. This leakage risk contribution is expected to decrease with more certain information. In addition the consequences of a leakage from such faults and fractures are very low and thus contributing less to total leakage risk than for example a leakage through an injection well.

Leakage source	Probability range (overall probability)	Peak leakage rate (kg/s)	Expected % leaked	Potential leak (tones)	Total (summarized) expected % leaked
Major Western Fault Fault Conduit width = 50	9,8E-9 to 7,1E-6	2.22 to 52.96	7.99E-7 to 6.15E-5	1.28 to 98.4	1.26E-4
Troll West Fault Also called TWOP/TWGP Fault Fault Conduit width = 50	9.8E-9 to 7.1E-6	8.88 to 52.96	7.99E-7 to 2.46E-4	1.28 to 393.6	3.68E-4
Induced fractures	5.0E-11 to 3.7E-7	1.11 to 94.8	3.77E-10 to 1.95E-6	0.000603 to 3.12	4.47E-6
Unidentified faults and paleo fractures	2.0E-7 to 1.5E-3	0.55 to 18.9	3.01E-6 to 8.68E-4	4.816 to 6240	8.34E-3
Injection well	2.25E-3 to 5.5E-3	25 to 100	4.65E-4 to 7.61E-4	744 to 1217.6	1.23E-3
Total					1.01E-2

For other identified leakage mechanism (Table 8-1) like reactivation of faults due to induced pressure, leakage through capillary penetration, leakage through injection well after injection period, leakage through abandoned wells and reduced cap rock integrity. Report no: 101965/R1 concludes with a negligible contribution to the leakage risk.

8.5 Leakage consequences

The consequences of CO₂ leakages from the CO₂ storage may be divided in three different categories: Possible human fatalities or injuries, local environmental consequences and global environmental consequences.

DOCUMENT NO.: TL02-GTL-Z-RA-0001	REVISION NO.: 03	REVISION DATE: 01.03.2012	APPROVED:
-------------------------------------	---------------------	------------------------------	-----------

8.5.1 **Human fatalities/injuries**

Elevated CO₂ concentrations (1-3% air by volume) cause no physical damage, but lead to rapid breathing, headaches, and tiredness. Above 3% incomplete gas exchange in the lungs causes CO₂ concentrations in the blood to increase and hence alter the pH of the blood. This condition is called hypercapnia and leads to brain malfunction, loss of consciousness and death at concentrations above 5-10% (Roberts et al. 2011).

Of the numerous publications addressing the health risk of CO₂ seeps, one by Roberts et al. 2011 is worth mentioning. Roberts et al. (2011) address natural CO₂ seeps in Italy and Sicily and find that human fatalities are strongly influenced by seep surface expressions, topography, wind speed, CO₂ flux and human behavior. The risk of an accidental human fatality from these continuous CO₂ seeps was calculated to be 10-8 year⁻¹ to the exposed population, - a value significantly lower than that of many socially accepted risks (Roberts et al. 2011). Seepage from CO₂ storage sites are modeled (Report no: 101965/R1 gives an average expected leakage of 0.89 tons per day) to be far less than that of Italian natural flux rates (an average of 10-100 tons CO₂ per day).

According to NIOSH and OSHA the limit for occupational exposure is 0,5%. IDLH (Immediate Dangerous to Life and Health) for CO₂ is 4%. At this concentration, if the exposure lasts for more than 30 minutes, it is considered that individuals will not be able to escape from death or permanent injury by their own.

The aerial spread in fault and fracture leakage sources and the potential (expected % leaked) for each of these sources give very low probabilities for accumulating critical CO₂ concentrations. Taking into account that a significant amount of CO₂ will never reach the sea surface due to e.g. dissolution of CO₂ in seawater and the large sea depth (3300m), it is concluded that these leakage scenarios do not represent any threats to humans. Report no: 101965/R1 concludes that *“Leakage of CO₂ from the faults/fractures will never reach the sea surface and thus will not be any risk for humans. The concentrations in air immediate above the sea surface will be far below any critical concentrations for humans as the gas is penetrating the sea surface across such a large area”* (a potential leakage is assumed to be distributed along the width and length of the fault plane in questions. See Appendix 13.24 for calculations and further discussions). Leakage scenarios via induced fractures are concentrated in the area of plume migration and where the formation is affected by pressure build-up⁷. As the total expected leak from such leakage sources are very low (0.00000447% of the total injected amount; see Table 2) and largely dispersed it is concluded that these leakage scenarios do not represent any threats to humans.

The most critical leakage will be a full blowout in connection with an injection well where an estimated maximum leakage rate is set at 100kg/s. In this scenario critical CO₂-concentrations could occur at the surface. If the blowout occurs due to workover/well operations from a surface vessel, the crew upon the vessel may be exposed to enhanced CO₂ concentrations. But due to the large sea depth and the fact that CO₂ is heavier than air, the probability of critical CO₂ concentrations at the topside of the surface vessel is negligible. In any case there must be emergency and contingency plans in place to handle possible blowouts and well-kicks for both well-interventions and drilling new injection wells.

8.5.2 **Local environmental consequences**

The leak scenarios through the cap rock/overburden areas are distributed over a large area, but in the case of a given leakage it will affect a constrained area. For the largest leak rates it will be a local area around the leak zone (fault/crack) near the sea bottom with a non-negligible

⁷ E.g. brittle and weak formations, areas with trapped stresses or areas under strain are believed to be the most zones where induced fractures develop first.

DOCUMENT NO.: TL02-GTL-Z-RA-0001	REVISION NO.: 03	REVISION DATE: 01.03.2012	APPROVED:
-------------------------------------	---------------------	------------------------------	-----------

reduction of the pH-value of the sea. Reduction of pH will have consequences for the organism close to sea bottom (benthic life). The estimated probabilities of such large scenarios are estimated to be low (see theTable 8-2). Thus the overall risk of such scenarios will be acceptable.

Blowouts in connection with injection wells are associated with a larger leakage rate and higher frequency. Insert number and compare with industrial study. During a blow-out CO₂ is believed to be concentrated in a narrow plume where most CO₂ reach the sea level as gas. In such a scenario some of the CO₂ in the subsea plume will be dissolved in the sea. Since sea water with dissolved CO₂ has a higher density than ordinary seawater it will most probably spread out due to gravity spreading given sufficient concentrations of dissolved CO₂. Locally dissolved CO₂ can form a local zone in the water column around the plume, and close to the sea bottom, with a non-negligible reduction of seawater pH-values. But due to the limited duration of these scenarios (well-control is re-gained after 2 months) combined with low probability (0.0023 according to Report no: 101965/R1) it is regarded as an acceptable risk of damage to the local environment.

8.5.3 Global environmental consequences

There is a large net reduction in release of CO₂ to atmosphere compared to no capture, for any of the identified scenarios.

For leakage through faults only part of the leaked CO₂ will enter the atmosphere. Estimated leakage rates have more of a seepage nature for more than 80% of the identified fault leakage sources (estimated leakage rates less than 20kg/s). In addition a portion of the leaked CO₂ will be trapped in shallower formations and/or the water column. But given the potential impact of un-recognized and prolonged leaks from faults measures to prevent such leaks should be taken and monitoring plans designed for detection (see Chapter 10).

Blowouts in connection with injection wells will have a larger leak rate and a higher frequency. CO₂ leakages in such scenarios will be concentrated in a narrow plume and enter the atmosphere. The total amount released is believed to be insignificant compared to the total amount injected and the global environmental consequences due to releases from injection wells are considered to be acceptable.

The main consequence in the evaluated scenarios is pH disturbances due to CO₂ dissolved in seawater. The largest of the identified releases could contribute to a general acidification of the ocean, but most of these scenarios have a very low probability so the risk of these scenarios is considered acceptable.

The risk for the global environment, taken into account all possible leakages, is considered to be well within acceptable levels.

8.6 Conclusion

Summing up all leakage scenarios gives a total expected leakage of 0.0101% of the injected CO₂ (0.89 t/d) over the modelled 500 years, which is well within acceptable levels. The highest leakage risk is associated with the injection well itself (with a total expected leakage of 0.00123% of total injected volumes).

The risk for humans in relation to leakages at sea bottom via the injection well is very low. The largest risk for people is related to possible topside blowouts which may happen during well workover/intervention. Measures should be taken during workover/intervention to decrease risk and adequate emergency and contingency plans should be implemented. Work operations on an injection well are anticipated to have an acceptable low risk.

DOCUMENT NO.: TL02-GTL-Z-RA-0001	REVISION NO.: 03	REVISION DATE: 01.03.2012	APPROVED:
-------------------------------------	---------------------	------------------------------	-----------

For other identified leakage mechanism (see Table 1) like reactivation of faults due to induced pressure, leakage through capillary penetration, leakage through injection well after injection period, leakage through abandoned wells and reduced cap rock integrity Report no: 101965/R1 concludes with a negligible contribution to the leakage risk.

Storage site integrity is considered high in the area surrounding the selected injection location. A competent cap rock (Drake Formation - shale) covers the whole storage area with an average thickness of 72m for the lower, most competent part of the shale. There are no abandoned wells within the vicinity of the plume migration path for any likely scenarios; neither is there any faults cutting through the cap rock that has an identifiable risk of leakage. Some fluid migration to Brent and possibly Sognefjord/Fensfjord should be expected across faults in the northern area. This will be positive for the storage complex as it reduces pressure build-up. Based on the risk evaluation above and the details in Report no: 101965/R1 it is concluded that the Johansen formation complies with the requirements in the EU directive that there shall be no significant risk of leakage and no significant environmental or health risk.

In order to reduce leakage risks the geological model could be verified further, in particular fractures and faults could be more closely investigated, and simulations could be ran for more than 500 years. An injection exploration well would give further and more representative data for the geological model and subsequent dynamic models. Such a test well would thus provide more confident, and better, leakage risk estimates.

As the main leakage risk is associated with the injection well it is recommended to address this leakage risk by taking adequate mitigating measures in terms of monitoring and operational attention. Drilling and work-over operations in overpressurized environments are challenging and in general the golden rule that “CO2 injected too fast in an inappropriate medium (driving too fast in the wrong direction on the highway) will eventually break your storage formation, wellbore and/or seal” applies.

DOCUMENT NO.: TL02-GTL-Z-RA-0001	REVISION NO.: 03	REVISION DATE: 01.03.2012	APPROVED:
-------------------------------------	---------------------	------------------------------	-----------

9 STORAGE SITE DEVELOPMENT, TECHNICAL CONCEPT

9.1 Storage Site Development

In 2008, on behalf of NPD, StatoilHydro performed a conceptual study (DG2) for transportation and storage of captured CO₂ from the flue gas from the Power Plant at Kårstø and the new full scale CO₂ Capture Plant Mongstad (CCM) in connection with the combined heat and power plant (Hagen and Melling et al 2008). The StatoilHydro conceptual study included a sub-study, undertaken by subcontractor Aibel to identify the extent of modification needed for Troll A to be a suitable host platform for operation of the subsea station at the Johansen location (StatoilHydro/Aibel).

Gassnova took the work further in maturing the concept by performing a FEED study contracted to Aker Solution in 2009 (Gassnova-Aker Solutions 2009). The scope was somewhat narrowed to cover mainly Utsira S, but also had a development on Johansen in mind (difference in water depth). The level of detailing corresponds to a large extent to what would have been required for a DG3/investment recommendation/PDO in a traditional petroleum field development setting.

The Ministry of Petroleum and Energy (MPE) by letter dated 29 January 2010 requested Gassco and Gassnova in cooperation to participate in development of a total value chain regarding the disposal of CO₂. Gassco has coordinated studies to evaluate transport solutions based on pipeline transport from Mongstad to one of four offshore storage locations in either the Johansen or Troll Kystnær formations as defined by Gassnova. These alternatives have been evaluated based on both the S-lay and the Reeling installation methods.

The Gassco work is based on results and recommendations from earlier concept studies performed in 2008 as detailed in DG3 document (Gassco), and pre-engineering work performed for the Kårstø transport solution as described in DG4 report (Gassco).

In connection with the change in focus from Kårstø to transport and storage of CO₂ from Mongstad CCM, further conceptual work for storage in Johansen Formation needed to be done. Gassnova contracted Odin/JP Kenny in October 2011 to conduct a feasibility study on identifying a viable design for a subsea system controlled from shore. Further main objectives of the study were:

- To identify benefits and disadvantages of a template and a cluster arrangement
- To identify and recommend on location for onshore located equipment for controls and chemicals handling and control centre
- To identify restrictions and technology gaps

9.2 Subsea Tie-back options

The development scenario is a subsea injection system for CO₂ storage located in 305m of water depth. Its position will be approximately 108km from the CO₂ capture plant (CCM) at Mongstad from where the CO₂ is captured from exhaust gas at the power plant. The CO₂ is piped offshore for subsea injection and storage in the Johansen Formation South.

Tie-back options for remote operation and control of the subsea system and supply of process conditioning chemicals are either the Troll A platform or a shore located facility. The distance from a subsea station for Johansen Formation South located in block 31/5 is approximately 34km to Troll A, and in the area of 100km to shore depending on the location chosen.

In combination with the study work already completed regarding the potential of utilising the Troll A platform as a power source/signal processing for the SCS, this solution or part solution should be considered, if not for the full planned 50 year design life, then possibly for a shorter,

DOCUMENT NO.: TL02-GTL-Z-RA-0001	REVISION NO.: 03	REVISION DATE: 01.03.2012	APPROVED:
-------------------------------------	---------------------	------------------------------	-----------

for example 25 year design life, at which time a replacement Subsea Controls Umbilical from onshore could be provided if the Troll Alpha platform was to be decommissioned in the interim period. This could also be linked with the likely design life of a Subsea Controls Umbilical.

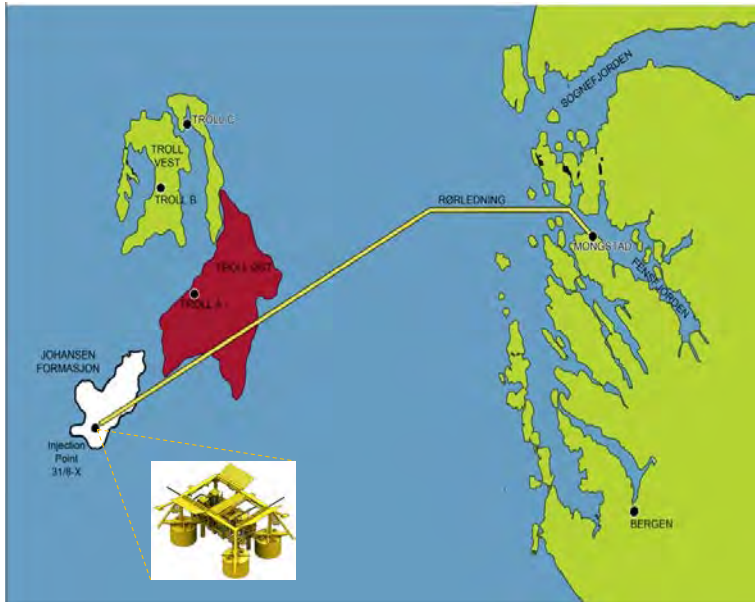


Figure 9-1: Field layout Mongstad - Johansen South.

9.2.1 **Host platform**

The conceptual study performed by StatoilHydro in 2008 included a study by Aibel to document all topside installation necessary for completion of umbilical tie-in to Troll A. The study aimed to find and estimate realisation of a solution enabling the platform to control and operate a subsea station with up to 2 new wells dedicated for CO₂ injection. The modification was found to be possible with no significant obstructions identified (StatoilHydro/Aibel).

It was assumed that existing J-tube (J10) could be used for the umbilical. Subsea topside control equipment and hydraulic package would be project supply included software and interface topside. Integrated Subsea Control Unit (SCU) into Safety Automation System (SAS/PCDA) and existing Operator Station (OS) will be detailed with regards to the automation discipline. MEG/MeOH would require a separate installed pump skid.

9.2.2 **Subsea Wells Controlled from Shore**

The shore located option was investigated in the feasibility study with Odin/JP Kenny.

For the purpose of this CO₂ Subsea Study it is assumed that the Subsea Controls Umbilical is tied-back to an onshore SCS Sub-Station at the Sture Terminal with further communication linkage back to the Mongstad Heat and Power Plant via an orbiting satellite. The overall study conclusions will recommend that further study work is performed to determine the suitability of these elementary assumptions.

The Subsea Controls System (SCS) will be sited onshore at a sub-station adjacent to the Subsea Controls Umbilical shore approach. For the purpose of this Subsea Study, Statoil’s Sture Terminal has been considered for the shore approach. There is little basis for this selection other than: Sture is closer to Mongstad; it already has an environmental slant (recovery of VOC); it already has linkage to Mongstad (LPG/naphtha Vestprosess pipeline). No contact has been made with Statoil regarding this terminal consideration. A transmitting Controls Station is

DOCUMENT NO.: TL02-GTL-Z-RA-0001	REVISION NO.: 03	REVISION DATE: 01.03.2012	APPROVED:
-------------------------------------	---------------------	------------------------------	-----------

assumed to be sited within the Mongstad Heat & Power Plant which will communicate to the Controls Sub-Station via an orbiting satellite link.

The SCS will remotely control all subsea aspects (CO₂ injection, subsea trees, hydraulic valves, chemical injection, instrumentation, CO₂ migration and leak detection).

Yet to be evaluated is any requirement for Subsea Controls Umbilical Subsea midline boosting bearing in mind the length of umbilical being considered.

9.3 **Technical Concept**

9.3.1 **System overview**

The subsea system is to be designed for a total of four subsea injection wells and includes a future option of tie-in of a future pipeline or a second drill location (with up to two injection wells) at a maximum distance of 10km from the first template and manifold subsea structure. The solution is based on diver-less technology to install and maintain the subsea facilities over the 50 year design life.

A topical solution will consist of one 4-wellslot integrated template and manifold subsea structure populated with two injection wells consisting of Xmas tree and wellhead systems with a subsea control system. The topside control system and chemicals equipment will be located on the selected tie-back platform with operational control performed via a communication link from the control room for the CO₂ capture plant at Mongstad. This solution was investigated in the Aker Solution FEED study.

An alternative solution is a cluster system comprising a manifold system with stack-outs for satellite wells. Pipeline spools and control umbilicals connect the satellite wells to the manifold. The topside control system and chemicals equipment may alternatively be located at a suitable shore based facility. Operational control may be performed via communication link from the control room for the CO₂ capture plant at Mongstad. This option will require a long control umbilical and may need a different design both for the umbilical and the distribution system for hydraulics and chemical fluid at the manifold. This is due to possible challenges with response time and transport of fluid over long distances. This solution is presently being investigated in a feasibility study with Odin/JP Kenny.

9.3.2 **Template Structure**

The basic philosophy for the Integrated Template Structure (ITS) is to limit the offshore installation operation by installing the template and protection structure together. It is also possible to include the Manifold Module in the combined lift. The structure enables tie-in operations either prior to or after drilling of the wells. The ITS will be designed for trawl loads and loads from dropped objects.

The template design has four injection well bay slots with a self sustained manifold that can be retrieved separately. The wells are drilled through the well slots where the conductors are guided and hung off during cementing of the conductor to the soil. The injection template will be designed to accommodate up to 4 injection trees. One well slot may be used as stack-out for a satellite well.

9.3.3 **Cluster System**

A cluster system is a flexible solution for handling of CO₂ from different sources, adding flexibility for future tie-ins and also allowing flexibility in the rig installation schedule. However, selecting a cluster option would result in more units being delivered and installed. The offshore installation is the driving factor, but also the area which has the largest fluctuation

DOCUMENT NO.: TL02-GTL-Z-RA-0001	REVISION NO.: 03	REVISION DATE: 01.03.2012	APPROVED:
-------------------------------------	---------------------	------------------------------	-----------

due to construction vessel rates and availability. The CAPEX and installation cost difference between a template solution and a cluster solution is in the area of 20-40 MNOK in advantage of template solution for two wells. The pipeline spool and control jumper will increase the total cost depending of the step-out distance to the satellite wells.

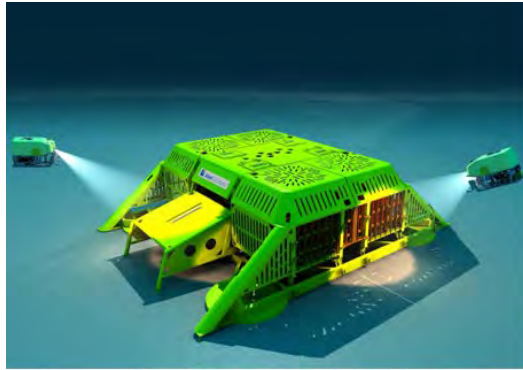


Figure 9-2: ITS solution.

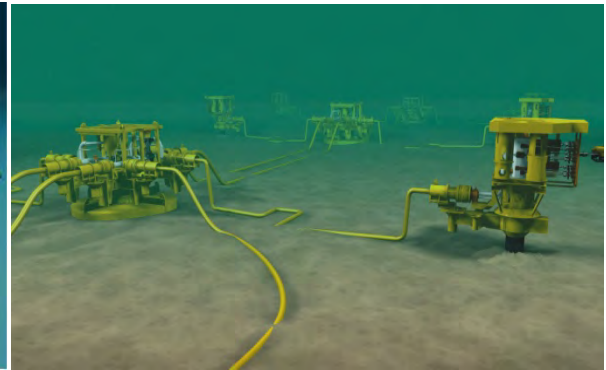


Figure 9-3: Cluster solution.

9.3.4 **Manifold**

The manifold will be prepared for future tie-in of a pipeline from an alternative source and will be equipped with two 12” manifold headers with a X-over system for distribution of the gas to the wells for storage or for export.

The manifold module will be designed as a unit that can be installed with the template and the manifold protection structure or as a separate installation should the template be used as a pre-drilling template.

The manifold will allow for connection of a temporary pig receiver/launcher on each of the injection headers. Possibility for tie-in of future wells will be catered for.

The manifold distributes the chemicals supplied from the host platform for conditioning of the subsea CO₂ injection, and the platform supplied electrical, fibre optics and hydraulic lines used to control and monitor the subsea facilities.

The manifold further contains a separate retrievable flow control module for each of the injection wells containing instrumentation for monitoring pressure, temperature and flow volume of the CO₂ being injected. The module also contains a choke valve for subsea choking of injection.

Finally, the manifold contains monitors to detect any CO₂ leakage within the subsea structure area.

9.3.5 **Pig Receiver**

The pig receiver modules will be designed to be separately installable and retrievable from the manifold and protection structure. The modules will contain all valves and stabs necessary to control fluid and pigs in accordance with the RFO concept, and will be used for pigging during initial testing, de-watering and subsequent inspection pigging.

DOCUMENT NO.: TL02-GTL-Z-RA-0001	REVISION NO.: 03	REVISION DATE: 01.03.2012	APPROVED:
-------------------------------------	---------------------	------------------------------	-----------

The pig modules will be independent from the tie-in tool. The template will cater for potential future inspection pigging. The preliminary concept for future inspection pigging of the CO₂ injection line is to perform this by utilising the CO₂ gas for driving the pig.

9.3.6 Wellhead System

The wellhead design provides the interface between the injection well and the Xmas tree and uses standard oil/gas industry subsea production system interfaces (UWD-15, 18 3/4" – 15,000 psi rated). Wellhead layout will be based on results from capacity and global analysis.

9.3.7 Xmas Tree System

The Xmas tree design provides the interface between the wellhead and the manifold distribution system. It is installed in the template injection well bay slot and utilises a standard oil/gas industry system design of a 10,000 psi, and temperature class T rated horizontal outlet tree with a nominal 5" internal sized bore and a 7" production tubing hanger interface.

The tree design was arrived at through a concept selection where the features required by the Gassnova specification were compared with the available tree configurations. The evaluation showed that a horizontal tree was the best solution to address the required design features with minimal risk.

The Xmas tree assembly will be designed in accordance with API 17D, PSL3 for injection service. An electro-hydraulic subsea production control system with ROV retrievable Subsea Control Module (SCM) will be used to control the Xmas tree functions.

Subsequently an 18-3/4" subsea BOP stack can be landed and locked on top of the Xmas tree. This allows for the installation of the tubing hanger and dual tubing hanger crown plugs into the tree through a standard marine riser/BOP and associated Landing String assembly. The upper plug acts as a secondary barrier and an internal sealing Tree Cap can thus be omitted.

9.3.8 Control System

The control system includes all equipment necessary for the safe operation and control of the subsea injection system and its interfaces. It covers the topside or costal located elements of the subsea system including the hydraulic unit (HPU), Subsea Power and Control Unit (SPCU), Master Control Station (MCS) and its software, the necessary tree and manifold and Flow Control Module (FCM) mounted controls elements, the transmitters and other data acquisition units and handling for the above well equipment.

The control system shall be as simple and robust as possible, consistent with field design life and reliability requirements. Redundancy shall enable the system to survive single point failures, thus facilitating normal operations until a backup plan is implemented. Local well leak monitoring and tie-in of seabed Permanent Monitoring System will be included in the design as well as establishing a programme for safe monitoring of injected CO₂.

The subsea control system utilises fibre optics for communication between topside and subsea, hydraulic power for remote valve operation and electrical power for operation of the subsea equipment. The fibre optic signals, hydraulic power and electrical power are provided by the equipment installed on the host platform or costal location together with a computer station as the control and monitoring operator interface.

A hydraulic, chemical, electrical and optical distribution system will be installed on the Manifold with the SCMs located on the Xmas trees. The SCMs will control the various valves and chokes for the well including those on the choke bridge and will directly monitor the various sensors for the well with the exception of the down-hole sensors. The Control System

DOCUMENT NO.: TL02-GTL-Z-RA-0001	REVISION NO.: 03	REVISION DATE: 01.03.2012	APPROVED:
-------------------------------------	---------------------	------------------------------	-----------

communications are superimposed onto the power distribution system to reduce the number of electrical conductors in the distribution system.

The Operator Station (OS) will be integrated with the host SAS system and will collect and process data from the SCU and present the information on a colour VDU monitor, allowing the operator to interact with the process system.

Primary subsea control will be from the MCS located on the host platform with a hang-off to an onshore system provided by an onshore contractor. The MCS shall also be connected to the platform operating system.

The philosophy for the control of the equipment from onshore is not fully developed at this stage of the project. However, the technology is available to facilitate secure and reliable communications and total control from an onshore control centre. This solution is presently being investigated in the feasibility study with Odin/JP Kenny.

Communication to onshore facilities will be agreed upon between Contractor, onshore Contractor and Topsides Contractor after executed bandwidth analysis and approved by Company during detailed design.

The ESD system will be defined as one system from inlet to capture plant via the host platform and down to and including the subsea systems. Effective and reliable communication of initiated ESD through all segments is therefore important.

The telemetry signals between the capture plant control room (CCR) and the host platform for the subsea wells will be transferred via a fibre optic cable system.

9.3.9 Alternative Control system – All Electric

An all electric control system for controlling an Xmas Tree with electric actuated valves replacing the hydraulic system has limited proof of successful operations. Due to the low number of installed units, it is not possible at this stage to claim “Proven in Use”. However, some areas of field-proven experience are multiple chokes and manifolds on production wells.

An electric-actuated subsea system enables precise valve control, providing optimum flow and production. For advanced applications like intervention, workover and processing, the electric controls system allows for increased response time and advanced sequence control.

Electric technology is suited to long distance tie-backs.

The main benefits of electric systems are reduced Capex for umbilicals, and zero-discharge to sea. They also simplify expansion and reconfiguration at a later stage. Improved uptime and the possibility to easily change electric actuators in case of failure are seen as great advantages together with the possibility to change out one electric Subsea Control Unit (eSCM) during operation when the redundant eSCM will take over the control.

One important factor with the electric trees is how easily field expansions can be performed, that is adding satellite trees and/or templates with more electric trees, particularly with the infrastructure available.

9.3.10 Umbilical System

An electro-hydraulic multiplexed control system located on the host installation will provide the operation and hydraulic supply for all seabed valves and chokes and will monitor and relay

DOCUMENT NO.: TL02-GTL-Z-RA-0001	REVISION NO.: 03	REVISION DATE: 01.03.2012	APPROVED:
-------------------------------------	---------------------	------------------------------	-----------

output from all downhole and seabed instrumentation to the topside or costal control room. The integrated service umbilical provides the distribution of the chemicals, fibre optics, hydraulic power and electrical power from the host installation to the subsea injection system. The umbilical will be designed with capacity for local well leak monitoring and tie-in of seabed Permanent Monitoring. The termination at the subsea injection system is at the manifold using a remote connection system.

9.3.11 Workover System

The completion system will enable future well intervention either from a rig or a light intervention vessel. The CO₂ injection wells will probably be completed utilising a Landing String system. However, the Xmas tree will be designed to interface a Lower Riser Package (LRP) with a Riser system which can be used for any downhole completion and intervention work including wireline, coiled tubing, flow testing or well clean-up.

The workover system interfaces with the subsea tree and tubing hanger, which forms parts of the upper completion. Upper completion consists of the well portion from (and including) the production packer and two SCSSVs will be installed. At least the upper valve will have the possibility to receive a back-up valve installed by wireline. Immediately below the production packer it will be possible to install a retrievable barrier plug, preferably by wireline.

The strategy is that completion tools will be provided by the subsea system equipment supplier on rental basis.

9.3.12 Drilling and Completion

For redundancy and to ensure maximum access to the CO₂ injection facilities, two wells will be planned for CO₂ injection into the Johansen Formation. The wells will be drilled either from a common subsea template or from two separate subsea structures. The following location is suggested:

Johansen S, well 31/8-1X 2 UTM 522842 E 6701175 N

The water depth will be approximately 305m at the location, which means that a semi-submersible drilling unit will have to be used. Preliminary well design suggests deviated wells with sub horizontal inclination through the reservoir. At the location, the top of reservoir is determined at 3050m and the base of the reservoir at 3201m. These depths are to be regarded as preliminary and will be subject to change with access to new data. Currently the wells are planned to be drilled to approximately 3900m MD MSL.

Drilling wells in this area does not normally include any special risks. The final casing points have to be picked based on the results from the appraisal well. The landing of the well in the reservoir combined with the barrier requirements/cap rock qualities will require some design iterations.

9.3.13 CO₂ Well Challenges

Wet CO₂, or CO₂ in solution, is a corrosive fluid. Specific attention is required for chemical degradation of well materials in CO₂ storage projects. The combination of CO₂ and water could result in:

- Chemical degradation of the cement thereby potentially enhancing porosity and permeability.
- Corrosion of the casing steel, creating pathways through the steel.

DOCUMENT NO.: TL02-GTL-Z-RA-0001	REVISION NO.: 03	REVISION DATE: 01.03.2012	APPROVED:
-------------------------------------	---------------------	------------------------------	-----------

All wells penetrating the cap rock are a potential leak path and the risk of having a leak must be reduced to a minimum.

- Old wells will require special attention well by well due to the nature of the barrier design and materials used.
- New wells can be designed “optimally”, but there must be a balance between new technology and operational risk. It does not help to pump CO₂ resistant cement if it cannot be placed efficiently, thereby establishing a qualified barrier.

In addition to the barrier elements, plans for barrier monitoring and remedial actions must be established for CO₂ injection wells (during and after injection), old wells and dedicated appraisal/monitoring wells penetrating the reservoir. As in all well operations the risk of barrier failure should be as low as reasonably practicable. Methods for establishing risk levels must be evaluated and selected. Compensating measures must be addressed if it is difficult to verify barrier status. This could be done by implementing monitoring technologies and methods.

Well intervention is likely to be necessary during the lifespan of the CO₂ injection. This could be due to workovers, data collection or re-establishment of barriers. A plan for how to perform these interventions must be in place with regards to equipment and methods.

The list below summarizes the currently identified challenges with regards to CO₂ injection wells;

- Cement design and operational practice
- Material choice with regards to corrosion (steel, fluids elastomers)
- Barrier design and placement
- Barrier monitoring
- Well intervention

Attached to this interim report (see separate document, Drilling & Well: Cement Design and Operational Practice) is a summary of the current industry status and recommendations regarding cement. It is further recommended that the remaining well related aspects listed above is addressed in due course before the operations commence to minimize the risk of leakage and ensure operational efficiency in the injection period.

9.3.14 Pipeline

Gassco has coordinated studies to evaluate transport solutions based on pipeline transport from Mongstad. The assumption is a 108km long 12” nominal ID pipeline from Mongstad to Johansen storage area. The pipe size is calculated for a flow of 3.2Mt/y. The pipeline design pressure is 250 bar at MSL and min/max design temperature -20/+50°C. The maximum operational pressure is defined as the design pressure less a margin. Based upon the DG4 analysis for the Kårstø – Utsira case this margin is currently set to 5 bar implying a maximum operating pipeline pressure of 245 bar. Maximum pump pressure from the CCM capture plant is 200 bar.

The pipeline provides the interface between the onshore CO₂ capture plant and the subsea facility, terminating at the manifold using a remote connection system consisting of a pipeline end termination unit and pipeline spool jumpers.

The pipeline facilities at the landfall comprise conventional pigging facilities with a combined pig launcher/receiver, an ESD valve to isolate the offshore pipeline from the onshore pipeline, blowdown/vent facilities for depressurising the pipeline and for venting possible off-spec CO₂ to the atmosphere, valves, piping, instrumentation, controls and utilities as required for the

DOCUMENT NO.: TL02-GTL-Z-RA-0001	REVISION NO.: 03	REVISION DATE: 01.03.2012	APPROVED:
-------------------------------------	---------------------	------------------------------	-----------

various landfall facility functions. CO₂ quantities shall be metered when leaving the Capture Plant.

The pipeline facilities at the downstream end of the pipeline comprise a removable combined pig receiver/launcher with associated valves and piping, and instrumentation and controls, all implemented on the subsea template or manifold structure downstream of the battery limit.

A PLET structure supports the tie-in interface between the spool and the pipeline. The tie-in to the template would then be via a Z-spool or an L-spool with one mechanical connector at either end, designed to take possible misalignment loads within the deflection capability of the spool.

9.3.15 Environmental Consideration – Open Loop Hydraulic System

The subsea control system will utilise an open loop hydraulic power system to operate remotely controlled valves on the Xmas tree and flow control module with hydraulic fluid vented to sea after valve operation. In addition, it should be expected that there will be a small amount of hydraulic fluid leakage as part of the valve quiescent state.

Safe and quick operation of Safety Valve and Xmas Tree valves is a superior aim for the hydraulic system, utilising either open or closed return system. In a closed system, back pressure in the return line can be experienced due to blockage (hydrate formation, bacteria growth, etc) or other conditions, and can cause valves to fail to operate. In order to reduce this risk, redundancy in the return system will be necessary. Redundancy in a closed system requires twice the length of tubing, and more valves and pumps. This makes the closed return system considerably more complex, with high probability for erroneous operations, and leading to necessary intervention and maintenance. This type of intervention lends itself to possible leaks to sea.

Introducing a closed return system using water based hydraulic fluid does not add any value to the environment in comparison to cost incurred and reduced reliability and regularity in operation. The hydraulic system to be adopted for the Gassnova CO₂ Storage project will be a vent-to-sea system where all exhaust fluid from valve operations is vented to the environment. Gassnova CO₂ injection wells will utilise a water-based hydraulic control fluid (typical Castrol Transaqua HT2) specifically formulated for use as the control medium in subsea and surface production control systems. The hydraulic fluid will be fully compliant with 2007 SFT environmental legislation for offshore chemicals in Norway and will contain no substitutable chemistry. The fluid will incorporate all the features that are required for operation in a wide range of equipment and operational conditions.

The amount of fluid discharge will depend on the number of times a valve is operated. However, once the subsea injection facility is commissioned valve operation is only necessary during routine barrier testing of a well. This is required every 6 months when a well is in normal operational mode. The hydraulic operated valves are typically of two type sizes - 2 1/16” and 5 1/8”, of which the master and wing valves for the injection and annulus bores will be barrier tested, in addition to the downhole safety valve (DHSV). In the operation phase the discharge to sea will be in the range of 0.7 to 1 m³/year per well.

9.3.16 Leak/emission monitoring

The Gassnova CO₂ injection project will meet the requirements for monitoring of CO₂ leaks in the newly endorsed EC directive (2009/31/EC) on geological storage of CO₂. Monitoring equipment will be installed at the wellhead and the subsea station may be used as tie-in point for Permanent Monitoring System for sea bed monitoring of CO₂ emission from the reservoir.

DOCUMENT NO.: TL02-GTL-Z-RA-0001	REVISION NO.: 03	REVISION DATE: 01.03.2012	APPROVED:
-------------------------------------	---------------------	------------------------------	-----------

Leak monitoring system at the wellhead is based on a very sensitive acoustic sensor and electronics. The acoustic energy picked up by the sensor is filtered using special developed algorithms. Filtering techniques are based on extensive testing performed in order to optimize sensitivity to leaks of CO₂ while at the same time minimizing the probability of false alarms. The magnitude of the filtered signals is mapped to MODBUS registers to allow trending on topsides SCADA system.

With traditional seismic shooting, there are long intervals between repeat surveys. With permanent monitoring, changes are identified immediately. The tasks can be solved with seismic nodes placed on the seabed in the actual area. These will send data about changes in the seabed continuously to a surface vessel, platform or a central onshore. In addition, these signals are combined with other input from oceanographic and environmental monitoring so that those responsible continuously have a good picture of suspicious changes in the seabed or the environment.

There are limitations to the range of suitability of Micro Seismic and active Shooting field seismic techniques for the utilisation on the Johansen Formation. The Micro Seismic has limitations as to what formation depths and upper geology stratum combinations can be monitored appropriately. This has to be determined on a case by case basis which typically includes geophysical data modelling. As an example, considering depth only, formations greater than 1500 to 2500m deep can prove to be problematic for micro seismic to detect any fracturing in the overburden / cap rock (the Johansen Formation is in the region of 3000m deep).

Detection of CO₂ leaks downhole by means of well annulus installed pH monitoring equipment technology is less well advanced than seabed acoustic leak monitoring. Leak detection is by a device which monitors the change in the annulus pH (presumably from a neutral pH to a lower acidic value in the event a CO₂ leak occurs. It is assumed the drillers, post well cleaning, will leave the annulus filled with a neutral pH fluid).

9.3.17 Installation

Installation of the subsea constructions and the umbilical will be part of Gassco scope and is described in Gassco Decision Gate 4 Report (Gassco)

9.3.18 Operation and Maintenance Strategy

The plan is to inject CO₂ into two injection wells. One well will be subject to injection at the time, with the second well as back-up and used for monitoring of the reservoir. One well may be a satellite well with maximum stack-out of 4km.

The assumption is made that there will be four full “pull tubing” type workovers over the life span of 50 years. Two of these will be mandatory, in that it is assumed that the Xmas trees will have to be pulled for inspection and re-certification (or replacement) after 25 years. The equipment will be designed for ROV access during installation, intervention and inspection.

Maintenance, inspection and monitoring (IMR) plans will be developed to ensure safety and availability of the facilities. The establishment of IMR activities and plans will initially be based upon the practical operation and maintenance experience for the same type of subsea equipment i.e. “generic maintenance concept”.

The Subsea equipment will be maintenance free. The Gassnova operation and maintenance strategy will be based on corrective maintenance. A safety/technical/economic review is to be performed in case of equipment failure and this will dictate method and time for maintenance.

DOCUMENT NO.: TL02-GTL-Z-RA-0001	REVISION NO.: 03	REVISION DATE: 01.03.2012	APPROVED:
-------------------------------------	---------------------	------------------------------	-----------

The inspection philosophy is to be based upon periodical survey programme. The intervention principle based upon continuously monitoring and control will give minimum need for intervention and down time on critical components.

The strategy is to utilize existing tools on a rental basis for all IMR activities.

9.4 **Cost Estimate**

9.4.1 **Project Development Cost**

The cost estimate has been prepared to ascertain the budget value of EPC and installation contracts (+/- 40%) on the basis of Trees, Controls, Remote connection system and Umbilicals. Costs have been taken from Contractor in-house estimates and benchmarked against recently completed and recently won projects (2009).

Cost estimates are here comparable to earlier estimate performed by Statoil. As indicated (+/- 40%) the uncertainties are large and considerable contingency need to be added. Major uncertainties are material cost (2009 figures), new technology and potential unidentified gaps

The cost estimate excluded items such as;

- Contractor management costs and personnel costs
- Marine warranty surveyor cost
- Construction all risk insurance policies
- Authority and legislation interfacing and management costs
- Equipment delivery, transportation and insurance costs from ex works to the final destination
- Value added tax (Mva etc)

Contingency to cover for uncertainty within the given scope, which may lead to a different design, is not included.

The cost estimate is based on a subsea template solution, with all major fabrication and design work conducted in Norway, and with all delivery points from various nominated North Sea ports or factories in Norway.

The preliminary overall project development costs for CO₂ transport and storage in the Johansen Formation with tie-in of umbilical to Troll A are presented in Table 9-1. The costs are in MNOK (2009) at an overall +/- 40% estimate and without tax, VAT or project reserves.

Table 9-1: Project development cost, 2009.

	Johansen S (34km)	
	One campaign	Two campaigns
Subsea facilities with 2 injection wells—one Template and one Umbilical	621	621
Installation of subsea Template and Umbilical	78	78
Troll A umbilical tie-in and topside modifications adjusted with 6% for price increase from 2008	94	94
Drilling and completion of wells	952	1014
Pipeline, pig receiver and onshore installation	1688	1688
Total, MNOK	3433	3495

DOCUMENT NO.: TL02-GTL-Z-RA-0001	REVISION NO.: 03	REVISION DATE: 01.03.2012	APPROVED:
-------------------------------------	---------------------	------------------------------	-----------

9.4.2 Drilling and Completion of Injection Wells

Either one or two rig mobilizations are built into the time and cost estimates for the wells. The latter is under the assumption that the major parts of the wells will be drilled one year, and that well completion will be done the following year, after tie-in of the pipeline.

A rig rate of US\$ 500,000 per day has been used for estimation of drilling and completion costs. The completion comprises open-hole sand screens and 25% chrome in all tubulars coming into contact with well fluids.

Drilling and completions costs are considered to be a $\pm 40\%$ cost estimate. The uncertainties are mainly related to:

- Well location/well path
- Rig availability and rig rates
- Exchange rates
- Drilling Operator’s overhead
- Cost for qualification of new technology

The calculated well costs include the development costs only, i.e. appraisal well cost and other costs incurred prior to final project go-ahead are not included. In

Table 9-2 an allowance of 22.5% has been included into all time estimates, and then a fixed contingency of 90 MNOK has been added to the drilling cost. This is equal to the cost of approximately 10 extra rig days plus the hardware cost of one re-drilled hole-section. The Operator’s overhead cost during drilling of the well has been suggested at 10% of the well cost before contingency. Furthermore, 35 MNOK is added to cater for the operating company’s planning and engineering activities prior to start-up of the drilling operation. This also covers probable development and qualification costs related to technology development within drilling and completion.

Table 9-2: Drilling and completion cost estimates.

	Johansen S	
	One campaign	Two campaigns
Shallow gas site survey	6	6
Drilling and completion of wells	836	893
Drilling Operator's overhead	75	80
Pre-engineering and technology qualification	35	35
Total, MNOK	952	1014

9.4.3 Operation and Maintenance Cost

Operation and maintenance costs for storage of CO₂ in the Johansen Formation area with Troll A as host platform for well control are presented in

Table 9-3.

Table 9-3: Operation and maintenance cost.

DOCUMENT NO.: TL02-GTL-Z-RA-0001	REVISION NO.: 03	REVISION DATE: 01.03.2012	APPROVED:
-------------------------------------	---------------------	------------------------------	-----------

Operation and maintenance	Cost MNOK
Maintenance of equipment on Troll A inc CO ₂ well operator's share of platform operations	13
Annual ROV inspection and maintenance of subsea facilities	5
Average annual cost of 4 workovers, spread over 50 years inc annual 4D seismic monitoring	40
Total annual operating cost	58

An organisation for operation of the well system needs to be established and the cost can be roughly estimated to 20 MNOK/year.

This cost estimate must be seen as indication as the operation is not organized or planned yet

Additional costs will appear for the monitoring effort, particularly 4D seismic and the monitoring of the marine environment. No effort has been made to cost these activities.

9.4.4 Storage cost

Assuming 5 Billion NOK of investment and 100 Mnok in yearly OPEX, the lifetime cost will amount to 10 Billion 2012 NOK. With a cumulative injection of 160 Mt the storage cost will be 60 NOK/t CO₂. A reduced rate from Mongstad will increase the cost pr. Tonne.

DOCUMENT NO.: TL02-GTL-Z-RA-0001	REVISION NO.: 03	REVISION DATE: 01.03.2012	APPROVED:
-------------------------------------	---------------------	------------------------------	-----------

10 MONITORING

The scope of this chapter is to highlight the challenges and specific issues regarding monitoring at Johansen and investigate how these issues can be dealt with according to the requirements in the relevant EU directive. Monitoring is focused on areas and features that are highlighted in the risk assessment as having an increased leakage potential.

10.1 Definition of terms

The EU directive offers the following definitions:

Storage site

Defined volume area within a geological formation used for the geological storage of CO₂ and associated surface and injection facilities.

Storage complex

Storage complex means the storage site and surrounding geological domain which can have an effect on overall storage integrity and security; that is, secondary containment.

10.2 Existing regulations

The requirements regarding monitoring and reporting of geologically stored CO₂ are listed in Article 12 to 14 in the “Storage Directive” (Directive 2009/31/EC). The operator of a storage site is required to document the quantity of CO₂ injected and stored, as well as ensure that the quality of the CO₂ stream is within the given requirements. Furthermore, the operator shall have a monitoring plan for the storage complex and surrounding area to ensure its integrity, and effectiveness of possible corrective measures. The criteria for the monitoring plan are listed in Annex II (Directive 2009/31/EC).

The required accuracy and positioning of the relevant monitoring and sampling points are listed in draft amendment (Directive 2010/345/EU) to (Directive 2007/589/EU), also called the MRG – Monitoring and Reporting Guidelines.

10.2.1 Monitoring

The monitoring plan shall be based on the risk assessment performed as part of the criteria for the characterization and assessment of the potential storage complex and surrounding area. Annex I of (Directive 2009/31/EC) Step 3.3 – states that the risk assessment shall contain both a *Hazard characterisation* and *Exposure assessment* and hence the monitoring plan shall be developed to monitor the most critical elements. Examples of these can be:

- Potential leakage pathways (e.g. faults, old wells)
- Critical parameters affecting potential leakage (e.g. reservoir pressure, injection pressure, plume extension)
- Secondary effects of storage including displaced formation fluids and new substances created through storage (e.g. displaced formation waters, change in pH)
- Physical structures associated with the project (e.g. wells and subsea structures)

The monitoring plan shall be split into phases representing the main stages of the project; baseline, operational and post-closure monitoring. It shall describe what, where and how each parameter is monitored together with a rationale for choice of monitoring technology (Best Available Technology – BAT).

10.2.2 Metering

The performance of the storage complex is monitored by measuring parameters at different locations in the capture, transport and storage complex. In addition to monitoring the amount of CO₂ stored to prevent over-injection, metering is necessary to document compliance with the

DOCUMENT NO.: TL02-GTL-Z-RA-0001	REVISION NO.: 03	REVISION DATE: 01.03.2012	APPROVED:
-------------------------------------	---------------------	------------------------------	-----------

greenhouse gas emission trading scheme (Directive 2003/87/EC). The rationale behind metering the CO₂ stream, the metering location and their required accuracy for CO₂ storage projects are currently given in (Directive 2010/345/EU) as a draft amendment to the guidelines for the monitoring and reporting of greenhouse gas emission (Directive 2007/589/EU). Metering requirements for stored CO₂ and CO₂ emitted through vents or leakages are given in the amendment. For the storage complex the requirements can be summarized as follows:

- Where Continuous Emission Measurement Systems (CEMS) are used, the uncertainty of the overall emission or flow over the reporting period shall be less than +/- 2.5% (Tier 4 in section 2 of Annex XII).
- The amount of emissions leaked from the storage complex shall be quantified for each of the leakage events with a maximum uncertainty over the reporting period of +/- 7.5%.

10.3 EU legislations applied to Johansen

In the following chapter a description is given of various monitoring technologies that may be applied for the Johansen Storage Complex. Some, if not all, of these are planned to be applied in order to fulfil the various directives as outlined above. However, both the technology and the legislations can be described to be in their infancy regarding CCS and considerable development is currently on-going in the industry to implement and mature new technology. The exact content of the monitoring and metering plan may therefore change depending on time of submission. Metering technology was outlined for the Utsira Storage Complex and the same technology is envisaged to be employed here (Gassnova-ROS. 2010). Metering technology will therefore not be further elaborated on.

Based on this storage evaluation and the risk assessment, the focus areas of a Monitoring, Meetering and Verfication programme for Johansen will be:

- Measuring the injected volumes and monitoring the CO₂ quality (subsea/downhole and onshore)
- Monitoring the CO₂ plume development. This will mainly be done by 4D seismic. Whether traditional 4D seismic will give adequate resolution of plume thickness, or permanently installed seabed monitoring, or other techniques can be utilized need further work.
- Monitor the reservoir pressure development (injection well and in monitoring well if applicable)
- Monitoring the facilities itself for leakage
- Monitoring marine life in the vicinity of the subsea and well area (highest risk of leakage)

10.3.1 Monitoring

Monitoring can be divided into baseline, operational, and post closure monitoring. The overall objective is to monitor the integrity of the transport network. Since CO₂ is a naturally occurring gas continuously seeping out of the sea bed, it will be desirable to monitor the area of the expected plume extension to establish a baseline survey. This should also be applicable for the transport network where the pipeline and trench should be surveyed prior to first fill to identify any naturally occurring CO₂.

Several monitoring techniques are available, but the monitoring aims should be carefully selected to cost-effectively improve understanding, predictive modelling and public acceptance. Techniques include CO₂ plume imaging, model calibration, and surface leak detection, all of which require baseline datasets to be available before injection commences. This will form the baseline monitoring plan. Comparison against subsequent time-lapsed datasets will then form part of the operational and post closure monitoring plan.

DOCUMENT NO.: TL02-GTL-Z-RA-0001	REVISION NO.: 03	REVISION DATE: 01.03.2012	APPROVED:
-------------------------------------	---------------------	------------------------------	-----------

10.3.2 **Monitoring area**

The monitoring plan will operate within an area of review (AOR) with sufficient extent to include any potential material impacts due to CO₂ storage. Displacement of brine is normally part of the AOR, but this will be very challenging to monitor as the Johansen Storage Complex is subsea. The AOR normally spans four distinct domains (geosphere, hydrosphere, biosphere and atmosphere). Emphasis is on the geosphere, which is defined as the subsurface domain below the seabed. The storage complex comprises a primary storage formation (Johansen/Cook formations), and a primary seal (Lower Drake Formation). A secondary seal (Draupne Formation) is interpreted and exists above the whole storage complex. Further up in the stratigraphy, the geosphere also contains additional deep saline aquifers (Brent Group and Viking Group). These are hydrocarbons bearing on other parts of the North Sea.

10.4 **Johansen specific monitoring needs**

The storage complex will have to be monitored both for leakage as well as plume control. Below applicable monitoring techniques are listed for each of these scenario.

10.4.1 **Identified leakage points**

A risk assessment has been carried out by Scandpower on behalf of Gassnova (Gassnova-Scand 2012). The study identified the injection well to have the highest leakage risk. This well integrity will be continuously monitored through the use of sensors and sniffers on the subsea installation (Gassnova-ROS. 2010).

Faults are potential leakage paths, but according to our fault seal study most of these faults are sealed (see chapter 5.4). The fault separating Troll West Oil Province (TWOP) and Troll West Gas Province (TWGP) (see Figure 10-1) where there is sand-sand connection could indicate a possible leakage path. The TWOP/TWGP fault is located 26.5km north of the preferred injection point and the plume is likely to reach it after more than 1000 years. This fault has a sand-sand connection between the upper sandstones of the middle Jurassic Brent Group and the sandstones of the lower Jurassic Johansen and/or Cook formations, but due to the shaley parts of the Drake Formation this fault is believed to be sealed with a shale sealing coat (shale/clay smear). A regional flow analysis should be performed to decide the likely migration path for such a leak. The resulting seabed location can then be specifically monitored for leakage at the appropriate time.

10.4.1.1 *Seabed monitoring*

For leakage detection at the sea bed, baseline monitoring over a period is required, to account for the seasonal variations in natural CO₂ seepage from the underground.

Several different methods for CO₂ detection exists and several are under development. One of the promising systems is the VideoRay Pro 3 XE Micro-ROV developed by BGR in collaboration with CO2ReMoVe. This remotely operated vehicle (ROV) allows for detection of leakage as well as sampling/measuring directly at the emanation site. It is tested successfully on naturally occurring gas emanations in Laacher See in 2010. The advantage with a ROV compared to, for example, a buoy-mounted system is that it is not restricted to the immediate proximity of its placement. Baseline data collection using such a mobile system should focus on areas over the faults mentioned in 10.4.

For monitoring at the injection site and other possible wells a buoy-mounted system for permanent monitoring is recommended.

10.4.2 **Monitoring for plume migration verification**

Top Johansen Formation at the suggested injection point is located at a depth of 3050m TVD and Base Johansen Formation is located at 3218m TVD. Top Johansen Formation is fairly flat

DOCUMENT NO.: TL02-GTL-Z-RA-0001	REVISION NO.: 03	REVISION DATE: 01.03.2012	APPROVED:
-------------------------------------	---------------------	------------------------------	-----------

in the expected plume area with no significant troughs or crests and the plume is hence expected to spread out thin over large areas with a tendency towards North-East. The plume movement will be monitored, although migration into high risk area or through the cap rock is unlikely. However, the injectors and possible MMV wells are potential leakage paths and will be monitored closely.

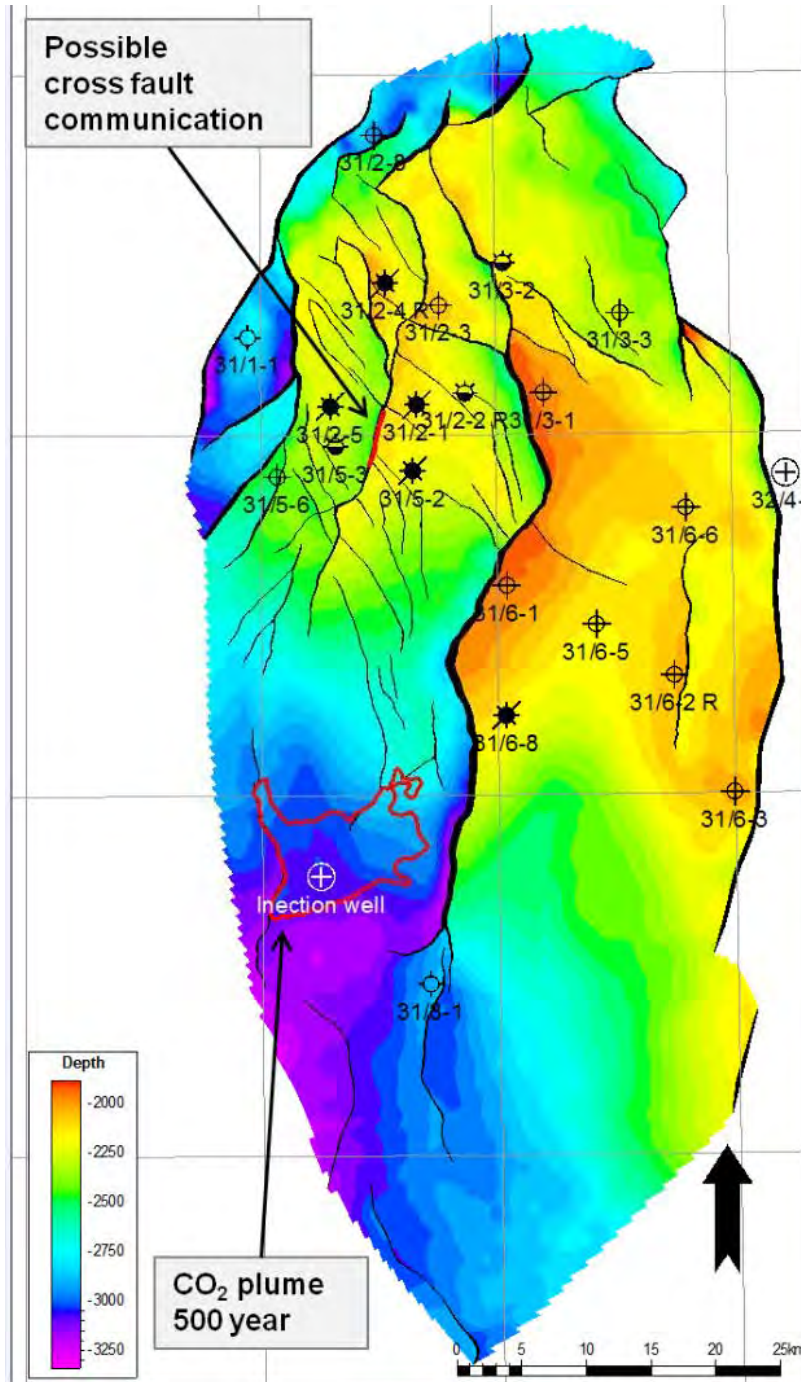


Figure 10-1: The southern parts of the Horda platform, suggested injection point and plume area after 500 years.

DOCUMENT NO.: TL02-GTL-Z-RA-0001	REVISION NO.: 03	REVISION DATE: 01.03.2012	APPROVED:
-------------------------------------	---------------------	------------------------------	-----------

10.4.2.1 *Seismic monitoring*

4D seismic

Seismic monitoring is employed all over the world, for monitoring oil reservoirs, EOR-operations and CO₂ storage.

4D controlled source seismic requires an initial acquisition of data (baseline 3D survey) and subsequent monitoring (monitoring line). The temporal spacing of the survey must be determined such that the requirements for monitoring are met. In the injection phase (operation phase) acquisition should be scheduled in order of years, based on the modelling. Post-injection (closure phase) surveys will typically be scheduled with several years interval. In the post-closure phase the monitoring can be kept at a minimum. For all monitoring phases the monitoring frequency must be intensified should there be significant discrepancy between plume behaviour and modelled plume spread, and an increased risk of leakage is detected.

For the baseline survey one should consider whether the survey should cover the predicted total extent of the plume in the injection period, or if one survey should act as a baseline for the subsequent survey. The expected pressure development in the storage complex should then be considered as this may influence the seismic signal.

The potential for plume monitoring using seismic is dependent on the pressure and saturation effects as a result of the CO₂ injection. A study conducted by Schlumberger shows that it is possible to interpret and follow the plume movement. The resolution is somewhat impaired at such depths (Gassnova-Schlumberger 2011) but tracking a plume with thickness from 15-20 metres is viable. The study is based on two 2D lines crossing at the injection point, a full 3D study is recommended to get an even better view of the method for monitoring the CO₂ plume development in the Johansen Formation.

Other storage projects have also shown that accumulation of thin CO₂ layers (beneath intrasand shales) give great seismic response even if their thickness is well below seismic resolution (e.g. Sleipner CO₂ storage project, Statoil).

VSP

Vertical seismic profiles (VSP) are defined as measurements made in a vertical borehole using geophones inside the wellbore and a source at the surface near the well. The advantage of this method is that the receivers are placed beneath the weathered surface zone and hence the attenuation of the high frequency waves is partially avoided. Thus, the resulting image of the underground is improved with higher resolution at higher frequencies than conventional seismic, but limited to the area surrounding the well. The signal to noise ratio is typically also much higher, due to quiet borehole environment and strong sensor coupling.

VSP is recommended to verify the interpretation of the 3D seismic, and to get a more precise image of the area around the injection well(s) and possible MMV well(s).

10.4.2.2 *Electro-magnetic*

CSEM

Controlled source electro magnetics (CSEM) is a complementary monitoring method where the response is reliant on the difference in the electric resistivity of the stored CO₂ compared to the baseline study. The method utilizes receivers that are deployed on the sea bottom and a dipole source emitting electromagnetic waves to be towed over the area of interest.

DOCUMENT NO.: TL02-GTL-Z-RA-0001	REVISION NO.: 03	REVISION DATE: 01.03.2012	APPROVED:
-------------------------------------	---------------------	------------------------------	-----------

A 1D study is carried out by Vestfonna Geophysical to evaluate the feasibility of CSEM as a monitoring method for CO₂ storage in the Johansen Formation. The resistivity of the water bearing reservoir (baseline) is approximated to 2 Ωm and two different models are run; one where the reservoir with CO₂ has a resistivity of 10 Ωm and one with a resistivity of 50 Ωm (Figure 10-2). CO₂ has much higher resistivity than water and different plume thicknesses and levels of CO₂ mixed with water will give different resistivity. The modelling is therefore done for the two resistivity values.

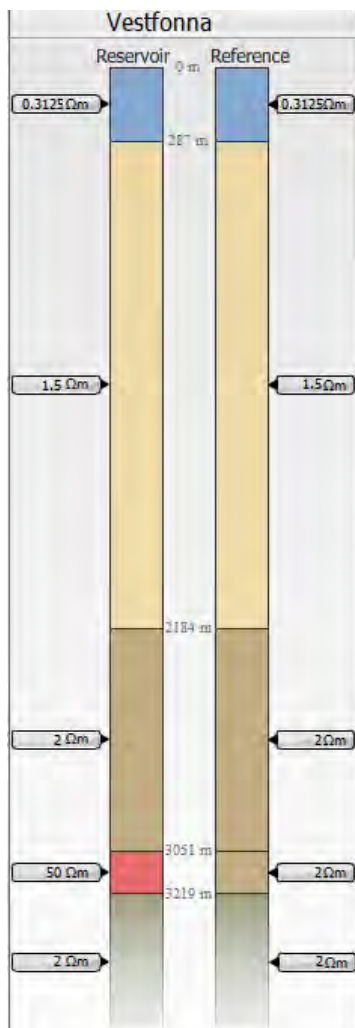


Figure 10-2: The 1D model set-up for the EM-modelling. The set-up is for the suggested injection point and the resistivity data is extrapolated from the available well data in the northern area of Horda Platform.

The initial results show that the method gives satisfactory results. See Figure 10-3 for the results of the modelling. 1D modelling does not take into account the possible variations in background resistivity, the spread of the plume, plume thickness and shape, nor does it include background noise. It is therefore recommended that a full 3D study be conducted.

DOCUMENT NO.: TL02-GTL-Z-RA-0001	REVISION NO.: 03	REVISION DATE: 01.03.2012	APPROVED:
-------------------------------------	---------------------	------------------------------	-----------

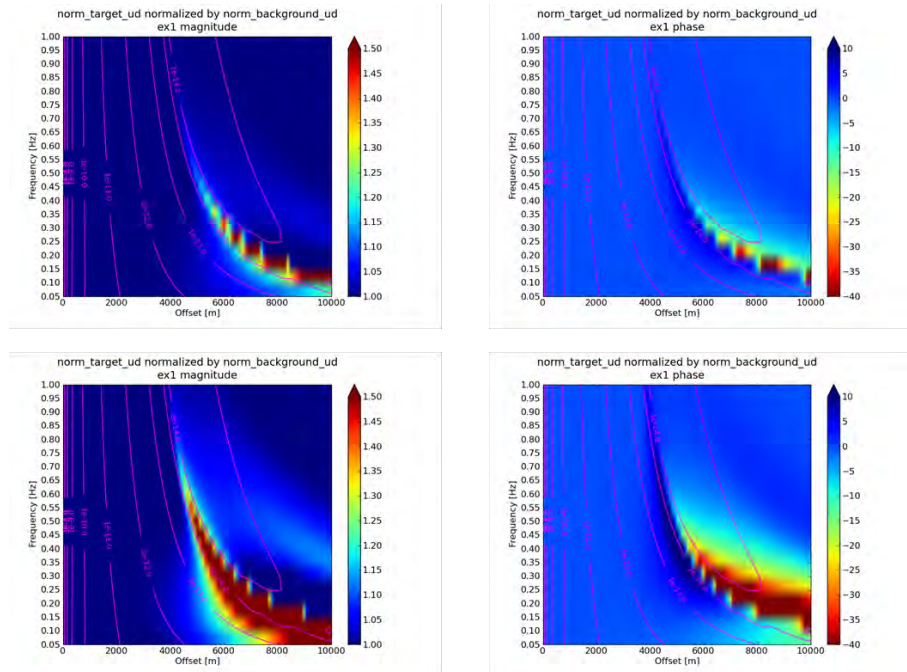


Figure 10-3: Results of 1D modelling. The figures to the left show the magnitude of the response normalized to the baseline at different frequencies emitted from the dipole source (top left 10 Ωm and bottom left 50 Ωm). The figures to the right show the phase difference between baseline and modelled cases (top right 10 Ωm and bottom right 50 Ωm). The visibility of the CO₂ saturated reservoir increase with decreasing frequencies (y-abcissa), this is expected due to the depth of the reservoir.

Crosswell EM

The Crosswell EM method is a potential approach to monitor the fluid distribution. For this method two wells placed less than 1000m (for openhole; for cased hole the distance is less) apart are needed. The method has been successfully demonstrated monitoring CO₂ floods in e.g. the Vacuum field (New Mexico, operated by ChevronTexaco).

A string of receivers are placed in one well and a transmitter (wire coil) is lowered into the other well and moved up and down. The wire coil broadcasts EM signals at a predefined frequency (normally between 10 and 400Hz). These signals are measured by the receivers and suitably averaged to improve the signal to noise ratio. The Crosswell EM method allows for imaging a roughly elliptical region between the wells.

10.4.3 **Other operational monitoring techniques**

10.4.3.1 *Downhole monitoring of microseismicity*

Passive seismic monitoring provides a possibility of continuous monitoring and near to real-time analyses of the gathered information. However, microseismic monitoring will only be able to image areas between the seismic event and the receivers, so deducing fluid related velocity changes is challenging. On the upside, passive seismic monitoring is an excellent technique for identifying injection induced deformation. Whether it is reactivation of old structures or new faults/fractures, there exist various methods to locate the hypocenter and even the fault plane and the orientation of the deformation. Microseismicity can potentially reveal the movement of the plume both in the reservoir and in the cap rock.

DOCUMENT NO.: TL02-GTL-Z-RA-0001	REVISION NO.: 03	REVISION DATE: 01.03.2012	APPROVED:
-------------------------------------	---------------------	------------------------------	-----------

The placement of three-component geophone sensors downhole into the vicinity of the cap rock will make it possible to detect any fracturing of the cap rock. The geophone sensors can be placed in the injection well, but the vibrations from injecting the CO₂ will be a major noise contributor and make interpretation of the data difficult. The best results will in such a set up be recorded when there are pauses in the injection. Placing the sensors in a geological sidetrack is a far better possibility, e.g. right above the cap rock to prevent drilling into it and hence compromise the seal.

Another possibility is placing the sensors in the replacement injector well or in a MMV well in the vicinity. The number of geophone sensors, together with the vertical spacing of them, decides the level of accuracy. The exact array of geophones must be decided based on the well/track used and at which depths the monitoring will focus, for the record; monitoring in other storage complexes are in the order 16 three-component geophones placed with 15m vertical spacing (Weyburn) and eight three-component geophones placed with 20m vertical spacing (Pembina Cardium).

Detection range is up to 1000m depending on the magnitude of the event and the placement and numbers of geophones.

The real-time data from the microseismic monitoring can be used for injection guidance. Steering injection by switching wells based on the realtime response from the reservoir can prevent unwanted pressure build-up. In a set-up with a cluster of injectors one can use the microseismic response as a guide and alternate between injectors to relieve pressure build up in areas.

10.4.3.2 *Land based monitoring of seismic events on the Horda platform*

An earthquake study has been conducted by Norsar (Gassnova-Norsar 2012). The study focused on analysing the natural seismicity on the Horda platform. Historic data from all the land based seismic sensors along the western coast of Norway were used in the analyses. The study concluded that the Horda platform is close to aseismic. However, the land based sensors are not good enough for precise location of the seismic events that occur offshore. For a more precise positioning of small seismic events on the Horda platform (down to magnitude -0.5) a dense cluster of sensors (called an array) is recommended to be placed at the station on Ask (which has the best readings with the current equipment, e.g. single sensor). This array should be operative a couple of years before injection, such that a good baseline is established. The relevance of such an array must be carefully investigated, but could be used to detect whether the injection leads to increased seismicity in the area, and hence be used as feedback to the injection process.

The depth of the Johansen/Cook formations, the integrity of the cap rock and the sealed faults indicate that storage in the expected plume area is safe and that no seepage to the sea bottom will occur. However, it is important to have a monitoring system available in the unlikely event of unexpected plume movement or detection of CO₂ movement above the seal. In such cases it is important to recognize the breach of the seal at an early stage such that baseline monitoring can be conducted before the hydrosphere is reached.

10.4.4 **Monitoring well**

If a verification well is drilled and it is not planned to be used as an injector, it should be investigated whether this can be instrumented as a monitoring well. Whether it is desirable to leave the well temporarily abandoned to facilitate intervention should be considered. Further should both injectors be permanently instrumented with downhole sensors to be able to function as monitoring well if/when they are not used for injection.

DOCUMENT NO.: TL02-GTL-Z-RA-0001	REVISION NO.: 03	REVISION DATE: 01.03.2012	APPROVED:
-------------------------------------	---------------------	------------------------------	-----------

11 IMPACT ASSESSMENT

This chapter gives a preliminary overview of the impact that the Johansen CO₂ Storage Site might have on the area. A proper Impact Assessment Study needs to be carried out in the final qualification phase.

CO₂ storage in the Johansen Formation will not bring new kind of operations into the area. The activity will be comparable to activities currently performed by the petroleum industry. The size of the operation at the nearby Troll field is 20 times larger.

The risk of CO₂ leakage from the storage itself is evaluated in detail and concluded to be extremely low. CO₂ exposure from the subsea facilities is regarded as very low. In spite of this, a monitoring programme will be set up for early detection of CO₂ exposure and its mitigation. A base line situation will be documented as reference for the later measurements.

The situations of the various aspects of impact are outlined in the following;

- The storage activity will not conflict directly with other industrial subsurface activities. The storage complex is situated under a large hydrocarbon accumulation. In the presence of hydrocarbon shows in the formation it could be argued that the porous formation could have functioned as a former migration pathway. However, there are no indications in the well data that the formation was involved in the hydrocarbon migration and trapping within the Troll field (Bretan, et al. 2011). This is also verified from studies performed on thin sections cut from core material from well 31/2-3 (Gassnova-IRI 2011).
- Exploration activities in the potential CO₂ injection area (northern part of block 31/8 and southern part of 31/5) have not indicated any HC accumulations in any geological formations. The latest exploration license is expected to be relinquished this year. Hence no further petroleum activities are foreseen and no potential conflict can be identified yet.
- Based on an extensive simulation effort it is expected that the CO₂ plume will spread slowly into the formation around the injector and tend to migrate northwards towards shallower areas. In the base case estimate it will take 500 years for it to get to areas under the Troll reservoir. If communication to the 500m shallower Troll field exists it will take many additional years to enter the field itself. Contamination of Troll gas during field life can therefore be excluded.
- The entering of brine, displaced by the CO₂ plume, into reservoir areas of Troll cannot be excluded. The extent will be limited and the effect positive in form of reservoir pressure support. The production at Troll is approximately 30 times larger (measured in reservoir volume) compared to the planned injected CO₂ volume. The pore volume of the Troll dynamic unit (aquifer and reservoir) is 5 times the size of the Johansen Formation unit.
- The impact on fishery will be quite limited. Restrictions will only be executed during installation and drilling. Two periods of half a year each, are expected with restrictions similar to those in the Troll area. The subsea installations at 300m depth will be protected for trawling. The pipeline will get buried.

An impact assessment programme was envisaged and is recommended for the next qualification phase. It must be planned in detail and agreed with the authorities before its execution. It is estimated to take one year.

DOCUMENT NO.: TL02-GTL-Z-RA-0001	REVISION NO.: 03	REVISION DATE: 01.03.2012	APPROVED:
-------------------------------------	---------------------	------------------------------	-----------

12 CONCLUSIONS AND RECOMMENDATIONS

This evaluation has contributed considerably to the maturity of Johansen Storage Complex as a CO₂ storage site. An injection location in block 31/8 is proposed in an area where the requested 160Mt of CO₂ will be safely stored for 10,000 years without any significant risk of leakage. The proposed location offers good plume control, is covered by a competent cap rock and is expected to have adequate injectivity to store the required yearly rate of 3.2Mt. The major uncertainty is in the sand quality in the injection area and hence injectivity. The proposed injection location is in no conflict with hydrocarbon or other interests in the area. No significant risk of leakage has been documented. The presence and confirmation of the storage formation must, however, be proven by a verification well as this is the highest remaining uncertainty for the project.

The maturation of the injection area has been done through extensive use of seismic interpretation and attribute analysis on both “normal” seismic data and inversion data. More specialised tools such as SVI Pro have also been used for detailed analysis regarding depositional environment and cap rock integrity. Together with a petrophysical evaluation of all wells in the area, it has been possible to propose a depositional model and associated reference case geological model with high confidence. Compared to traditional prospect evaluation, the proposed model has a 70% probability. The volumetric confidence in Johansen Storage Complex is high due to the likelihood of communication with other formations in the area. The success of the storage complex is, however, dependent on sand development suitable for injection at the proposed location in order to avoid migration into the higher risk areas in the north. Further maturing and increase of probability should be done by drilling of a well to confirm the model.

Storage site integrity is considered high in the area surrounding the selected injection location. A competent cap rock (Drake Formation - shale) covers the whole storage area with an average thickness of 72m for the lower, most competent part of the shale. The mineralogy of the cap rock based on cores from wells outside the investigated area shows that the expected composition of the Drake shale will be geochemically stable with little possibility of leakage. There are no abandoned wells within the vicinity of the plume migration path for any likely scenario, neither are there any faults cutting through the cap rock that has an identifiable risk of leakage. Migration towards and underneath the Troll reservoirs is unlikely for any scenario with the selected injection location. Some fluid migration to Brent Group and possibly Sognefjord/Fensfjord formations should be expected across faults in the northern area. This will be positive for the storage complex as it reduces pressure build-up. It will not be noticeable for Troll as volumetric difference is too large. An assessment has been made regarding a safe pressure increase in the area, where fault reactivation, fault generation and cap rock fracturing was investigated. The expected pressure build-up resulting from the injected volume is well below what is viewed as safe pressure build-up, and indicates that the storage capacity has the potential to be increased well beyond the 160 Mt investigated (possibly as high as 480 Mt). Simulation of plume spread associated with a doubling the injected volume does not show migration into any high risk areas for the first 500 years.

The storage site can be developed with a standard 4-slot subsea template and for the base case geological model, the desired yearly rate can be injected through one injection well. A minimum of two wells are recommended for back-up and reliability purposes. Expected development costs will be approximately 5 billion NOK (+/- 40% estimate) including two wells, pipeline and tie-in to Troll A. This gives a cost /tonnes of approximately 30 nok/tonne.

Monitoring of plume spread is possible using 4D seismic, although the depth of the reservoir and the lack of a defined trap make plume thickness resolution a challenge. Injection will be

DOCUMENT NO.: TL02-GTL-Z-RA-0001	REVISION NO.: 03	REVISION DATE: 01.03.2012	APPROVED:
-------------------------------------	---------------------	------------------------------	-----------

continuously monitored, while the surrounding sea and areas at risk will be monitored at regular intervals.

A verification well location is proposed as shown in Figure 14-1 in appendix A2. The proposed location is south of the injection well, but within the spit system. Reasoning for this proposed location is that it is important for the geological understanding to prove the existence of the spit system. The system is more developed in the proposed location, but injection this far south increases the risk of migration southwards in the storage complex.

Recommendations for further work

Further work is necessary in order to qualify the defined Johansen Storage Complex as a storage site, and to characterise the site according to requirements set out in the EU directive. The assessment is currently heavily based on seismic analyses, and the most important remaining work here will be drilling of a verification well to confirm the geological model, and to obtain fresh core and fluid samples from the actual injection area. Samples area necessary to characterise the storage complex to the extent required by EU and both storage formation and cap rock must be cored. This acquisition program will essentially provide:

- Pressure in area and any signs of depletion due to production from Troll
- Fluid samples for full geochemical description
- Permeability and injectivity data
- Cap rock in-situ fracturing strength through mini-frac test

A proposed location for an exploration well can be found in Appendix 2 together with a suggested formation evaluation programme. The possibility of re-using the verification well as an injection well, and the implication this may have on its location must be analysed prior to drilling. The scope of a possible injection test might need to be reassessed. At this stage just a short test is proposed to investigate permeability and the near bore area.

Should the verification well confirm the depositional model, preparation for investment decision can be initiated. Failure to confirm the proposed model will trigger a re-evaluation of the injection location and storage site development. .

Before a storage application can be filed following issues need to be documented:

- A full metering and monitoring plan
- Impact assessment study.

To fully comply with the EU Directive some detailed work must be done in several areas. The most important areas are:

- Regional flow analysis must be done to assess the impact on adjacent aquifers and to form basis for possible surface leak monitoring.
- Geomechanics and modelling of overburden for same purpose

The details in such program must be developed in a dialog with the Competent Authority.

If further work should be performed on the current dataset, it is recommended to be focused around understanding the large deviations in permeability obtained from the tested core material, and whether the data should be discarded or not. The results of this work will not have influence on the capacity estimation of the storage complex, but may influence the number of wells and length of reservoir sections needed per well to achieve the desired injectivity.

DOCUMENT NO.: TL02-GTL-Z-RA-0001	REVISION NO.: 03	REVISION DATE: 01.03.2012	APPROVED:
-------------------------------------	---------------------	------------------------------	-----------

REFERENCES

- Akaku. «IPTC 12304 numerical simulation of CO₂ storage in aquifers without trapping structures.» *Japex Research center*, 2008.
- Aker, E, M Angeli, E Skurtveit, og M Soldal. «Experimental percolation of supercritical CO₂ through a caprock.» *Energy Procedia 1*, 2009: 3351-3358.
- Aleman, P.B. «Acoustic impedance inversion of lower permian carbonate buildups in the permian basin, Texas.» Texas, 2004.
- Alles, S, A Busch, A Kronimus, B Krooss, H Stanjek, and J Wollenweber. "Caprock and overburden processes in geological storage: an experimental study on sealing efficiency and mineral alterations." *Proceedings of the 9th International Conference on Greenhouse Gas Control Technologies (GHGT-9)*. Washington DC: Energy Procedia 1 (1), 2008. 3469–3476.
- Alles, S, et al. "Carbon dioxide storage potential of shales." *International Journal of Greenhouse Gas Control* 2(3), 2008: 297-308.
- Bachu, S, C Hawkes, and P McLellan. "Geomechanical Factors Affecting Geological Storage of CO₂ in Depleted Oil and Gas Reservoirs." *Journal of Canadian Petroleum Technology*, 2005.
- Bao, Y, Q Liu, L Zhang, S Zhang, og R Zhu. *Effects of hydrocarbon physical properties on caprock's capillary sealing ability*. Dongying 257015, China: Geology Scientific Research Institute, SinoPec Shengli Oilfield Company, 2010.
- Bergmo, Per, and Erik Lindeberg. "Exploring geological storage sites for CO₂ from Norwegian gas power plants: Johansen formation." *GHGT-9*, 2009: 2945-2952.
- Berndt, C, S Bunz, and J Mienert. "Polygonal fault systems on the mid-Norwegian margin: A long-term source for fluid flow." *Subsurface Sediment Mobilization*, 2003, Geological Society of London Special Publication ed.
- Bjørkum, P.A, and O Walderhaug. "Geometrical arrangement of calcite cementation within shallow marine sandstones." *Earth-Science Reviews* 29 (1990): 145-161.
- Bjørkum, P.A, and P.H Nadeau. "Temperature controlled porosity/permeability reduction, fluid migration, and petroleum exploration in sedimentary basins." *Australian Petroleum Production & Exploration Association Journal* 38 (1998): 453-46.
- Bjørlykke, K. «Clay mineral diagenesis in sedimentary basins, a key to the prediction of rock properties. Examples from the North Sea Basin.» *Clay minerals*, 1998: 15-34.
- . "Petroleum Migration." *Petroleum Geoscience: From Sedimentary Environments to Rock Physics*, 2010.
- Bjørlykke, K, D.A Karlsen, and R Olstad. "Pore water flow and petroleum migration in the Smørbukk field area, offshore mid-Norway." *Hydrocarbon Seals - Importance for exploration and production*, 1997, NPF, Special Publication no.7 ed.
- Boggs Jr, S. *Principles of Sedimentology and Stratigraphy 2/E*. University of Oregon, 1995.
- Bolton, A, J Cartwright, and D James. "The genesis of polygonal fault systems: a review." *Subsurface Sediment Mobilization*, 2003: 216, 223-243.
- BP Petroleum Development Ltd . «Petrophysical study of Norwegian offshore continental shelf well 6507/10-1. » 1983.
- Bradley, H. «Petroleum Engineering Handbook 26-8.» I *Petroleum Engineering Handbook*, av H Bradley, chapter 26-8. 1987.
- Bretan, P, G Yielding, O.M Mathiassen, og T Thorsnes. «Fault-seal analysis for a CO₂ storage: an example from the troll area, Norwegian Continental Shelf.» *Petroleum Geoscience* 17 , nr. 2 (2011): 181-192.
- Bromhal, G.S, B.R Ellis, D.L McIntyre, og C.C Peters. «Changes in caprock integrity due to vertical migration of CO₂-enriched brine.» *Energy Procedia*, 2010.
- Caillet, G, J Connan, I Kaarstad, T. L Leith, og J Pierron. «Recognition of caprock leakage in the Snorre Field, Norwegian North Sea.» *Marine and Petroleum Geology* 10, 1993: 29-41.
- Charnock, M, J. P. G. Fenton, I Kristiansen, og A Ryseth. «Sequence stratigraphy of the Lower Jurassic Dunlin Group, northern North Sea.» *Sedimentary Environments Offshore Norway - Paleozoic to Recent*, 2001, NPF Special Publication 10. utg.: 145-174.
- Christie, P.A.F, and J.G Sclater. "Geological objections to an extensional origin for the Buchan and Witchground Graben in the North Sea (reply)." *Nature*, no. 287 (1980): 467-468.

DOCUMENT NO.: TL02-GTL-Z-RA-0001	REVISION NO.: 03	REVISION DATE: 01.03.2012	APPROVED:
-------------------------------------	---------------------	------------------------------	-----------

- Copestake, P, B. C Mitchener, M. A Partington, and J. R Underhill. "Biostratigraphic calibration of genetic stratigraphic sequences in the Jurassic-lowermost Cretaceous (Hettangian-Ryazanian) of the North Sea and adjacent areas." *Petroleum Geology of North-West Europe: Proceedings of the 4th Conference*. London: Geological Society, 1993. 371-386.
- Crow, W., Carey, J. W., Gasda, S., Williams, D. B, Celia, M. «Wellbore integrity analysis of a natural CO₂ producer.» *International Journal of Greenhouse Gas Control*, v 4, (International Journal of Greenhouse Gas Control, v 4, pp 186-197), 2010: pp 186-197.
- Cuisiat, F, L Grande, and K Høeg. "Laboratory testing of long term fracture permeability in shales." *SPE/ISRM Rock Mechanics Conference, 20-23 October*. Texas, 2002.
- Daniel, R.F, and J.G Kaldi. "Evaluating seal capacity of caprocks and intraformational barriers for the geosequestration of CO₂." PESA Eastern Australian Basins Symposium III, 2008.
- Deegan, C.E, and B.J Scull. "A proposed standard lithostrati-graphic nomenclature for the Central and Northern North Sea." Institute of Geological Sciences, 1977.
- Deutsch, C.V , and A. G Journel. *GSLIB Geostatistical Software Library and User's Guide*. 2nd. 1998.
- Dewhurst, D.N, Y.L Yang, and A.C Aplin. "Permeability and fluid flow in natural mudstones." In *Muds and Mudstones: Physical and Fluid-flow Properties*, by A.C Aplin, A.J Fleet and J.H.S Macquaker, 22-543. London: Geological Society Special Publications, 1999.
- Directive 2003/87/EC. «Directive 2003/87/EC Commission Decision...» u.d.
- Directive 2007/589/EU. «Directive 2007/589/EU Commission Decision establishing guidelines for the monitoring and reporting of greenhouse gas emissions...» u.d.
- Directive 2009/31/EC. "Directive 2009/31/EC of the European parliament and of the council of 23 April 2009 on the geological storage of carbon dioxide..." n.d.
- Directive 2010/345/EU. «Directive 2010/345/EU Commission Decision amending Decision 2007/589/EC.» u.d.
- Dreyer, T, M Whitaker, J Dexter, H Flesche, og E Larsen. «From spit systems to tide-dominated delta: integrated reservoir model of the Upper Jurassic Sognefjord Formation on the Troll West Field.» Redigert av A. G Dore og B Vining. *Petroleum geology: north-west Europe and global perspectives. Proceedings of the 6th Petroleum Geology Conference*. London: Geological Society, 2005. 423–448.
- Duke, W, L. «Geostrophic circulation or shallow marine turbidity currents? The dilemma of palaeoflow patterns in storm-influenced prograding shoreline systems.» *Journal of Sedimentary Petrology*, nr. 60 (1990): 870–883.
- Ehrenberg, S.N. «Relationship between diagenesis and reservoir quality in sandstones of the Garn Formation, Haltenbanken, mid-Norwegian continental shelf.» *AAPG Bulletin*, 1990: 1538-1558.
- . «Preservation of Anomalously high porosity in deeply buried sandstones by grain-coating chlorite: Examples from the Norwegian Continental Shelf.» *The American Association of Petroleum Geologists Bulletin*, 1993: 1260-1286.
- Evans, D, C Graham, A Armour, P Bathurst, og (eds). *Millennium Atlas: Petroleum Geology of the Central & Northern North Sea*. Geological Society London, 2003.
- Friedmann, S. J., and D. Nummedal. "Reassessing the Geological Risks of Seal Failure for Saline Aquifers and EOR Projects." *2nd Annual Conference on Carbon Sequestration*. Alexandria, VA, 2003.
- Gassco. «DG3 and DG4 studies.» u.d.
- Gassco. «PG23-BY.RF-08.14869; Study for CO₂ Transport from Kårstø and Mongstad, Decision Gate 3 Document.» u.d.
- Gassco. «PG24-KA.RF-09.24123; CO₂ Transport Network Decision Gate 4 (3+) Report.» u.d.
- Gassnova - TNO. «TL02-TNO-Q-RA-0001.» 2012.
- Gassnova. "3D AVO Seismic Inversion and Lithology Prediction West Troll Field, Norway." 2011.
- Gassnova. «Hazard Identification and Risk Analysis of CO₂ storage at Lower Jurassic Johansen Formation.» 2012.
- Gassnova-Aker Solutions. «Subsea FEED study Kårstø/Utsira S.» 2009.
- Gassnova-AKS. «TL02-AKS-P-RA-00001 Apparent Gas Chimney Block 31/8.» 2011.
- Gassnova-IRI. «TL02-IRI-P-RA-0001 Effekt av O₂ i CO₂ injeksjonsgass på undergruslagring av CO₂.» 2010.
- Gassnova-IRI. "TL02-IRI-P-RA-0002 Laboratory Rock Testing Programme." 2011.

DOCUMENT NO.: TL02-GTL-Z-RA-0001	REVISION NO.: 03	REVISION DATE: 01.03.2012	APPROVED:
-------------------------------------	---------------------	------------------------------	-----------

- Gassnova-Norsar. «Earthquake study for the Øygarden Fault Zone Northern North Sea.» 2012.
- Gassnova-POL. "TL02-POL-J-RA-00001 Seismic Acquisition GN1001." 2011.
- Gassnova-ROS. «TL02-2011-PP-00019 Gas Chimney Evaluation.» 2011.
- Gassnova-ROS. "TL02-GTL-G-RA-0002 Structure Geology of the Horda Platform." 2011.
- Gassnova-ROS. "TL02-ROS-G-TN-0001 Petrophysical Report - Johansen Formation." 2011.
- Gassnova-ROS. "TL02-ROS-X-RA-0002 Reservoir Parameter Study Report." 2011.
- Gassnova-ROS. "TL02-ROS-Z-RA-00001 SVI Pro Study." 2011.
- Gassnova-ROS. «TL02-ROS-Z-RA-0002 Johansen Subsurface Status Report.» 2010.
- Gassnova-ROS. «TL01-ROS-Z-RA-0001 Utsira South Subsea Development Report.» 2010.
- Gassnova-Scand. «Hazard Identification and Risk Analysis of CO2 Storage at Lower Jurassic Johansen Formation.» 2012.
- Gassnova-Schlumberger. "Seismic Monitoring Study." 2011.
- Gassnova-SIN. "TL02-SIN-P-RA-0001 Thermal, Shale Gauge Ratio and Overpressure Modelling in the Johansen Formation." 2011.
- Gassnova-VBPR. "Quick Assessment of Seismic Evidence of Leakage of the Johansen Formation." 2011.
- Gassnova-WGD. "TL02-2010-PP-00001 Western Geco - AVO Study." 2011.
- Gassnova-WGD. "TL02-WGD-G-RA-0001_01_002 Seismic Data Processing." 2011.
- Gassnova-WGD. «TL02-WGD-G-RA-0002 3D AVO Seismic Inversion and Lithology Prediction West Troll Field, Norway.» 2011.
- Gassnova-WPC. "TL02-WPC-Z-RA-00001 Assessment of Gas Chimney." 2011.
- Gibbons, K, T Hellem, og A Kjemperud. *Sequence architecture, facies development and carbonate-cemented horizons in the Troll Field reservoir, offshore Norway*. London: Geological Society, Special Publications , 1993, 1-31.
- Gouly, N.R, and R.E Swarbrick. "Development of polygonal fault systems: a test of hypotheses." *Journal of the Geological Society*, 2005.
- Gregersen, U, and N. P Johannessen. "The Neogene Utsira Sand and its seal in the Viking Graben area, North Sea." Danmarks og Grønlands Geologiske Undersøgelse Rapport, 2001, 100.
- Hagen, and Melling et al. "DG2 Report - (draft) CO2 Storage - Utsira/Johansen with appendix A-H K-Q." 2008.
- Hager, R.V, and J Handin. "Experimental deformation of sedimentary rocks under confining pressure: Tests at room temperature on dry samples." *American Association of Petroleum Geologists Bulletin* 42(12), 1957: 2892-2934.
- Hallam, A. «Eustatic control over major cyclic changes in Jurassic sedimentation.» *Geology Magazine*, 1963: 444-450.
- Hildebrand-Mittlefehldt, N. «Deformation near a fault termination, part II: A normal fault in shales.» *Tectonophysics* 64, nr. 3-4 (1979): 211-234.
- Ilyina, V. I. *Jurassic Palynology of Siberia*. Nauka, Moscow, 1985.
- Ingram, G.M, J. L Urai, and M. A Naylor. "Sealing processes and top seal assessment." *Hydrocarbon Seals: importance for Exploration and Production*, 1997, MPF Special Publication 7 ed.: 165-174.
- Jenkyns, H. C. «The early Toarcian (Jurassic) anoxic event: stratigraphic, sedimentary and geochemical evidence.» *American Journal of Science* 288 (1988): 101-151.
- Johannessen, P. N, and L. H Nielsen. "Spit-systems - an overlooked target in hydrocarbon exploration: the Holocene to Recent Skagen Odde, Denmark." *Geological Survey of Denmark and Greenland*. Vol. 10. 2006. 17–20.
- Kemp, S.J, J Bouch, and H.M Murphy. *Mineralogical characterisation of the Nordland Shale, UK Quadrant 16, northern North Sea*. British Geological Survey Commissioned Report, 2001, 52.
- Kestin, J., Khalifa, H. E., Abe, Y., Grimes, C. E., Sookiazian, H., Wakeham, W. A. "Effect of pressure on the viscosity of aqueous sodium chloride solutions in the temperature range 20-150 °C." *J. Chem. Eng. Data*, 1978: 328–336.
- Kumar. «SPE 89343 Simulating CO2 storage in deep saline aquifers.» *SPE*, 2005.
- Lindeberg, E, og P Bergmo. «The Long-Term Fate of CO2 Injected into an Aquifer.» *Proceeding of the 6th International Greenhouse Gas Control Technologies*. Kyoto, 2002.

DOCUMENT NO.: TL02-GTL-Z-RA-0001	REVISION NO.: 03	REVISION DATE: 01.03.2012	APPROVED:
-------------------------------------	---------------------	------------------------------	-----------

- Livbjerg, F, and R Mjøs. *The Cook Formation, an offshore sand ridge in the Oseberg area, northern North Sea. In: Collinson, J. D. (ed.) Correlation in Hydrocarbon Exploration.* London: Graham & Trotman, 1989.
- Marjanac, T. «Architecture and sequence stratigraphic perspectives of the Dunlin Group formations and proposal for new type and reference-wells.» *Sequence Stratigraphy of the Northwest European Margin*, 1995, Norwegian Petroleum Society (NPS), Special Publication 5. utg.: 143-165.
- Marjanac, T, and R. J Steel. "Dunlin Group sequence stratigraphy in the Northern North Sea: a model for Cook sandstones deposition." 1997: 276-292.
- Maver, K.G, Odegaard, and K.B Rasmussen. "Direct inversion for porosity of post stack seismic data." *European 3-D Reservoir Modelling Conference, 16-17 April.* Stavanger, 1996.
- McPherson, B.J.O.L, and P.C Lichtner. "CO2 sequestration in deep aquifers." *Proceedings of the First National Conference on Carbon Sequestration, 14-17 May.* Washington DC, 2001.
- Møllegaard, Eskil. *Seismotektonikk i nordlige Nordsjø.* Cand Scient Oppgave, Institutt for Geologi, Universitetet i Oslo, 2000.
- Monaghan, N, and R Iskander. *Petrophysics evaluation of the interval base Johansen formation to top Krossfjord formation in the Troll area.* ResLab Integration AS Report, 2009.
- Morad, S. *Carbonate cementation in sandstones: distribution patterns and geochemical evolution.* Special Publications International Association of Sedimentologists, 1998, 1-26.
- Morton, N. «Potential reservoir and source rocks in relation to Upper Triassic to Middle Jurassic sequence stratigraphy, Atlantic margin basins of the British Isles.» *Petroleum Geology Conference series.* 1993. 285-297.
- Nghiem, Shrivastava. *SPE 125848 Simulation of CO2 storage in saline aquifers.* 2009.
- Nikitenko, B. L, and B. N Shurygin. "Lower Toarcian black shales and Pliensbachian-Toarcian crisis of the biota of Siberian palaeo-seas." Edited by D. K. Thurston and K Fujita. *International Conference on Arctic Margins, Anchorage, Alaska.* Anchorage: US Department of the Interior Minerals Management Service, Alaska Outer Continental Shelf Region, 1992. 39.
- Norsk Saga. «Final Well Report 31/5 1&2.» 1985, NPD Factpages.
- Odin/JP Kenny. «Subsea Wells Controlled from Shore.» 2011.
- Parkinson, D. N. , and F. M. Hines. "The Lower Jurassic of the North Viking Graben in the context of western European Lower Jurassic stratigraphy." Edited by V. L. Felt, E. R. Johannessen, C. Mathieu and R. J. Steel. *Sequence Stratigraphy of the Northwest European Margin* (Norwegian Petroleum Society (NPF)), no. Special Publication 5 (1995): 97 - 107.
- Pruess, Spycher and. «CO2-H2O mixtures in the geological sequestration of CO2.II. Partitioning in chloride brines at.» *Geochimica et Cosmochimica Acta, vol 69, No. 13,* 2005: 3309-3320.
- Ramm, M, and A. E Ryseth. "Reservoir quality and burial diagenesis in the Statfjord formation, North Sea." *Petroleum Geoscience, Vol. 2,* 1996: 313-324.
- Santarelli, FJ, O Havmøller, and M Naumann. *Geomechanical Aspects of 15 Years Water Injection on a Field Complex: An Analysis of the Past to Plan the Future.* Society of Petroleum Engineers SPE 112944, 2008.
- Schlumberger. «Johansen CO2 Storage Complex Fault Stability Evaluation.» 2011.
- Sheriff, R.E, and L.P Geldhart. *Exploration Seismology Volume 2: Data Processing and Interpretation.* Cambridge: Cambridge University Press, 1987.
- Shurygin, B.N. «Lower and middle jurassic formations in the Anabar-Khatanga district (Northern Siberia).» *I New data on the stratigraphy and fauna of the Jurassic and cretaceous of Siberia,* av Sakd og Shurygin, 19-47. Institute of Geology and Geophysics, Novosibirsk, 1978.
- Skinner, L. «CO2 Blowouts: an emerging problem.» *World Oil,* 2003: 38-42.
- Soleimani, B, and A Zarvani. "Lithological and petrophysical evaluation of the caprock keybeds, Asmari Reservoir of Pazanan Oil Field, Zagros, Iran." *Songklanakarinn J. Sci. Technol* 31 (6), 2009: 655-660.
- Span, R., Wagner, W. «A New Equation of State for Carbon Dioxide Covering the Fluid Region from the Triple-Point Temperature to 100 K at Pressures up to 800 MPa.» *J. Phys. Chem. Ref. Data,* 1996: 1509 – 1596.

DOCUMENT NO.: TL02-GTL-Z-RA-0001	REVISION NO.: 03	REVISION DATE: 01.03.2012	APPROVED:
-------------------------------------	---------------------	------------------------------	-----------

- Spivey, J.P., McCain, W.D., Jr., North, R. «Estimating Density, Formation Volume Factor, Compressibility, Methane Solubility, and Viscosity for Oilfield Brines at Temperatures from 0 to 275oC, Pressures to 200 MPa, and Salinities to 5.7 mole/kg.» *JCPT*, 2004.
- StatoilHydro/Aibel. «Troll A Topside Study.» u.d.
- Steel, R.J. «Triassic-Jurassic mega sequence stratigraphy in the Northern North Sea: rift to post rift evolution.» Redigert av JR Parker. *Petroleum Geology of North-West Europe: Proceedings of the 4th Conference*. London: Geological Society, 1993. 299-315.
- Storvoll, V, K Bjørlykke, D Karlsen, og G Saigal. «Porosity preservation in reservoir sandstones due to grain-coating illite: a study of the Jurassic Garn Formation from the Kristin and Lavrans fields, offshore Mid-Norway.» *Marine and Petroleum Geology* , June 2002: 767-781.
- Suehiro, Y., M. Nakajima, K. Yamada, og M., Uematsu. «Critical parameters of $\{x\text{CO}_2 + (1 - x)\text{CHF}_3\}$ for $x = (1.0000, 0.7496, 0.5013, \text{ and } 0.2522)$.» *J. Chem. Thermodyn*, 1996: 1153-1164.
- Thomas, B.M, P Moller-Pedersen, M.F Whitaker, og N.D Shaw. «Organic facies and hydrocarbon distributions in the Norwegian North Sea.» I *Petroleum Geochemistry in Exploration of the Norwegian Shelf*, av B.M et al (eds) Thomas. London3-26: Graham & Trotman, 1985.
- van Wijngaarden, A.J, B.P Tjøstheim, and A Torp. *Regional effects of Troll Production*. Norsk Hydro Produksjon AS, 2007, 1-66.
- Vollset, J, and AG Doré. "A revised Triassic and Jurassic lithostratigraphic nomenclature for the Norwegian North Sea." *NPD-Bulletin No. 3*, 1984: 53.
- Vukalovich, M.P., Altunin, V.V. *Thermophysical Properties of Carbon Dioxide*. Collet's Publishers LTD. London & Wellingborough, 1969.
- Weiguo, L, JP Bhattacharya, Y Zhu, D Garza, and E Blakenship. "Evaluating delta asymmetry using three-dimensional facies architecture and ichnological analysis, Ferron 'Notom Delta', Capital Reef, Utah, USA." *Sedimentology*, 2010: 478-507.
- Wikipedia. "http://en.wikipedia.org/wiki/Carbon_dioxide." n.d.
- Wilkinson, M, R.S Haszeldine, and A.E Fallick. "Jurassic and Cretaceous clays of the northern and central North Sea hydrocarbon reservoirs reviewed." *Clay Minerals*, 2006: 151-186.
- Yang, Y, and A. C Aplin. "Permeability and petrophysical properties of 30 natural mudstones." *Journal of Geophysical Research* 112 (2007).
- Yielding, G, and P Bretan. *Fault Seal Study Johansen Formation, Troll Field*. Norwegian Petroleum Directorate, Badley Geoscience Limited, 2008.
- Yielding, G, N Lykakis, and J.R Underhill. "The role of stratigraphic juxtaposition for seal integrity in proven CO2 fault-bound traps of the Southern North Sea." *Petroleum Geoscience*, May 2011: 193-203.

DOCUMENT NO.: TL02-GTL-Z-RA-0001	REVISION NO.: 03	REVISION DATE: 01.03.2012	APPROVED:
-------------------------------------	---------------------	------------------------------	-----------

APPENDICES

A1 GAP Analysis

EU requirement	Chapter in report / status
<p>Step 1: Data Collection</p> <ul style="list-style-type: none"> “Sufficient data shall be accumulated to construct a volumetric and three-dimensional static (3-D)-earth model for the storage site and storage complex, including the cap rock, and the surrounding area, including the hydraulically connected areas.” 	
<i>geology and geophysics;</i>	<u>Chapter 4</u> 2D/3D seismic, well logs, core descriptions.
<i>hydrogeology (in particular existence of ground water intended for consumption);</i>	<u>n/a</u> No groundwater present offshore Norway. Hydrogeological evaluations not performed.
<i>reservoir engineering (including volumetric calculations of pore volume for CO₂ injection and ultimate storage capacity);</i>	<u>Chapter 4</u> Plugs from the single existing core in Johansen have been tested for capillary trapping potential and relative permeability effects. Also cores from nearest Cook formation have been tested. No information about formation water quality. Water quality assumed.
<i>geochemistry (dissolution rates, mineralization rates);</i>	<u>Chapter 4</u> Mineral composition for cap rock has been established based in nearest available core. No further studies done regarding changes in permeability, porosity as this is not view as critical for present stage of project. Also lack of data for location.
<i>geomechanics (permeability, fracture pressure);</i>	<u>Chapter 4 & 5</u> Fracture stability study done. Also samples from nearest available cap rock sampled and tested for mechanical strength.
<i>seismicity;</i>	<u>Chapter 4.9</u> Data from earthquake stations sampled and analysed by NORSAR.
<i>presence and condition of natural and man-made pathways, including wells and boreholes which could provide leakage pathways;</i>	All relevant and available information about all wells in area that could be affected by plume gathered. Status of wells regarding potential leakage assessed.

DOCUMENT NO.: TL02-GTL-Z-RA-0001	REVISION NO.: 03	REVISION DATE: 01.03.2012	APPROVED:
-------------------------------------	---------------------	------------------------------	-----------

<p><i>domains surrounding the storage complex that may be affected by the storage of CO₂ in the storage site; New GD: Field studies and surface studies;</i></p>	<p>EIA not part of this study.</p>
<p><i>population distribution in the region overlying the storage site;</i></p>	<p><u>n/a</u></p>
<p><i>proximity to valuable natural resources (including in particular Natura 2000 areas pursuant to Council Directive 79/409/EEC of 2 April 1979 on the conservation of wild birds(1) and Council Directive 92/43/EEC of 21 May 1992 on the conservation of natural habitats and of wild fauna and flora(2), potable groundwater and hydrocarbons);</i></p>	<p>Proximity to natural resources covered under point below.</p>
<p><i>activities around the storage complex and possible interactions with these activities (for example, exploration, production and storage of hydrocarbons, geothermal use of aquifers and use of underground water reserves);</i></p>	<p>Presence of Troll field wells mapped. No hydrocarbon potential in area. Dry well 31/8-1.</p>
<p><i>proximity to the potential CO₂ source(s) (including estimates of the total potential mass of CO₂ economically available for storage) and adequate transport networks.</i></p>	<p>Proximity to Mongstad established. This part of project is covered by Gassco. No further data gathered.</p>
<p>Step 2: Building the Static Model</p> <ul style="list-style-type: none"> The EU Storage Directive states: “Using the collected data, a three-dimensional static geological earth model, or a set of such models, of the candidate storage complex, including the cap rock and the hydraulically connected areas and fluids shall be built using computer reservoir simulators. The static geological earth model(s) shall characterize the complex.” 	
<p><i>geological structure of the physical trap;</i></p>	<p><u>Chapter 5.4</u> Explanation of mapping of cap rock and secondary cap rock.</p>
<p><i>geomechanical, geochemical and flow properties of the reservoir overburden (cap rock, seals, porous and permeable horizons) and surrounding formations;</i></p>	<p><u>Chapter 5.6</u> Only primary cap rock has been mapped for presence of porous layers in this phase. No full geological model with properties of all layers in overburden has been built. Primary cap rock found to be so competent that presence of additional seals in overburden has not been critical to recommending site for storage.</p>

<p>DOCUMENT NO.: TL02-GTL-Z-RA-0001</p>	<p>REVISION NO.: 03</p>	<p>REVISION DATE: 01.03.2012</p>	<p>APPROVED:</p>
---	-----------------------------	--------------------------------------	------------------

<p><i>fracture system characterization and presence of any human-made pathways;</i></p>	<p><u>Chapter 4.8, 5.6 and appendix xx (drilled wells).</u></p>
<p><i>horizontal and vertical extent of the storage complex;</i></p>	<p><u>Chapter 5.1</u> Defined in 5.1.</p>
<p><i>pore space volume (including porosity distribution);</i></p>	<p><u>Chapter 5.3, 5.4 and 5.5</u> Explanations of how the geological grid has been populated, and how this ties in with depositional model.</p>
<p><i>baseline fluid distribution;</i></p>	<p><u>Chapter 6.1</u> Pressures in Johansen assumed hydrostatic. This based on information from wells drilled in area. All wells drilled prior to production start at Troll so no info regarding depletion in Johansen.</p>
<p><i>The uncertainty associated with each of the parameters used to build the model shall be assessed by developing a range of scenarios for each parameter and calculating the appropriate confidence limits. Any uncertainty associated with the model itself shall also be assessed.</i></p>	<p><u>Chapter 7</u> Done as an integrated uncertainty assessment.</p>
<p><u>Step 3: Characterization of the Storage Dynamic Behaviour Johansen, sensitivity characterisation, risk assessment</u></p> <ul style="list-style-type: none"> • <i>The EU Storage Directive states that “The characterizations and assessment shall be based on dynamic modelling, comprising a variety of time-step simulations of CO₂ injection into the storage site using the three-dimensional static geological earth model(s) in computerized storage complex simulations”</i> • <i>Step 3.1: Characterisation of the storage dynamic behaviour; At least the following factors shall be considered:</i> 	
<p><i>possible injection rates and CO₂ stream properties;</i></p>	<p><u>Chapter 3</u> Evaluation criteria supplied by Gassnova.</p>
<p><i>the efficiency of coupled process modelling (that is, the way various single effects in the simulator(s) interact);</i></p>	<p><u>Chapter 6.1</u> This is also explained in parameter model and in Eclipse manual. Eclipse has not been coupled with any other simulation.</p>

<p>DOCUMENT NO.: TL02-GTL-Z-RA-0001</p>	<p>REVISION NO.: 03</p>	<p>REVISION DATE: 01.03.2012</p>	<p>APPROVED:</p>
---	-----------------------------	--------------------------------------	------------------

<i>reactive processes (that is, the way reactions of the injected CO₂ with in situ minerals feedback in the model);</i>	n/a Not covered in this phase of the work. Any possible negative effects on permeability and porosity will be captured uncertainty assessment. Issue not viewed as critical for this phase of project and will be more relevant for detailed engineering phase – after fresh core and fluid samples have been collected.
<i>the reservoir simulator used (multiple simulations may be required in order to validate certain findings);</i>	<u>Chapter 6.1</u> Reservoir Parameter report explains reasoning behind choice of simulator.
<i>short and long-term simulations (to establish CO₂ fate and behaviour over decades and millennia, including the rate of dissolution of CO₂ in water).</i>	<u>Chapter 6.2</u>
<i>pressure and temperature of the storage formation as a function of injection rate and accumulative injection amount over time;</i>	<u>Chapter 6.2</u>
<i>horizontal and vertical extent of CO₂ vs. time;</i>	<u>Chapter 6.2</u>
<i>the nature of CO₂ flow in the reservoir, including phase behaviour;</i>	<u>Chapter 6.2</u>
<i>CO₂ trapping mechanisms and rates (including spill points and lateral and vertical seals);</i>	<u>Chapter 6.2</u>
<i>secondary containment systems in the overall storage complex;</i>	<u>Chapter 5.6</u> No simulation regarding CO ₂ flow in overburden is presently done
<i>storage capacity and pressure gradients in the storage site;</i>	<u>Chapter 6.2/Chapter 7</u>

DOCUMENT NO.: TL02-GTL-Z-RA-0001	REVISION NO.: 03	REVISION DATE: 01.03.2012	APPROVED:
-------------------------------------	---------------------	------------------------------	-----------

<p><i>the risk of fracturing the storage formation(s) and cap rock;</i></p>	<p><u>Chapter 7</u> Invariably linked to how much capacity is stretched.</p>
<p><i>the risk of CO₂ entry into the cap rock;</i></p>	<p><u>Chapter 10.1</u> See also Scandpower report.</p>
<p><i>the risk of leakage from the storage site (for example, through abandoned or inadequately sealed wells);</i></p>	<p><u>Chapter 10.1</u> See also Scandpower report.</p>
<p><i>the rate of migration (in open-ended reservoirs);</i></p>	<p><u>Chapter 5.2</u> Will be done for Base case even though Johansen is not an open-ended reservoir. Rate of migration is dependent on dip of formation. Hard to establish when dip of structure varies throughout. But focusing on migration towards Troll.</p>
<p><i>fracture sealing rates;</i></p>	<p><u>Chapter 5.7</u></p>
<p><i>changes in formation(s) fluid chemistry and subsequent reactions (for example, pH change, mineral formation) and inclusion of reactive modelling to assess affects;</i></p>	<p>Not done for this phase of project. Not critical for storage site integrity.</p>
<p><i>displacement of formation fluids;</i></p>	<p>Convection modelled as far as this is important o increase understanding of amount of totally dissolved CO₂, Model not fine gridded enough to visualise this. Some displacement into Troll.</p>
<p><i>increased seismicity and elevation at surface level.</i></p>	<p>Not modelled – but assumptions about increased seismicity done. Elevation of surface level not critical for any installations in area due to distance and water depth.</p>

<p>DOCUMENT NO.: TL02-GTL-Z-RA-0001</p>	<p>REVISION NO.: 03</p>	<p>REVISION DATE: 01.03.2012</p>	<p>APPROVED:</p>
---	-----------------------------	--------------------------------------	------------------

<p>Step 3.2: Sensitivity characterisation</p> <ul style="list-style-type: none"> Multiple simulations shall be undertaken to identify the sensitivity of the assessment to assumptions made about particular parameters. The simulations shall be based on altering parameters in the static geological earth model(s), and changing rate functions and assumptions in the dynamic modelling exercise. Any significant sensitivity shall be taken into account in the risk assessment. 	<p>Chapter 7 Included in risk model.</p>
<p>Step 3.3: Risk assessment</p> <ul style="list-style-type: none"> Risk assessment shall comprise, inter alia, the following: <ul style="list-style-type: none"> Hazard characterisation Exposure assessment Effects assessment Risk characterisation 	
<p>Step 3.3.1: Hazard characterisation</p> <ul style="list-style-type: none"> Hazard characterisation shall be undertaken by characterising the potential for leakage from the storage complex, as established through dynamic modelling and security characterisation described above. This shall include consideration of, inter alia: 	
<p>potential leakage pathways;</p>	<p>Chapter 8.</p>
<p>potential magnitude of leakage events for identified leakage pathways (flux rates);</p>	<p>Chapter 8.</p>
<p>critical parameters affecting potential leakage (for example maximum reservoir pressure, maximum injection rate, temperature, sensitivity to various assumptions in the static geological Earth model(s));</p>	<p>Chapter 8.</p>
<p>secondary effects of storage of CO₂, including displaced formation fluids and new substances created by the storing of CO₂;</p>	<p>Chapter 8.</p>
<p>any other factors which could pose a hazard to human health or the environment (for example physical structures associated with the project);</p>	<p>Chapter 8.</p>

<p>DOCUMENT NO.: TL02-GTL-Z-RA-0001</p>	<p>REVISION NO.: 03</p>	<p>REVISION DATE: 01.03.2012</p>	<p>APPROVED:</p>
---	-----------------------------	--------------------------------------	------------------

<p>Step 3.3.2: Exposure assessment</p> <ul style="list-style-type: none"> Based on the characteristics of the environment and the distribution and activities of the human population above the storage complex, and the potential behaviour and fate of leaking CO₂ from potential pathways identified under Hazard characterization. (3.3.1) 	<p>n/a for this phase.</p>
<p>Step 3.3.3: Effects assessment</p> <ul style="list-style-type: none"> Based on the sensitivity of particular species, communities or habitats linked to potential leakage events identified under Step 3.3.1. Where relevant it shall include effects of exposure to elevated CO₂ concentrations in the biosphere (including soils, marine sediments and benthic waters (asphyxiation; hypercapnia) and reduced pH in those environments as a consequence of leaking CO₂). It shall also include an assessment of the effects of other substances that may be present in leaking CO₂ streams (either impurities present in the injection stream or new substances formed through storage of CO₂). These effects shall be considered at a range of temporal and spatial scales, and linked to a range of different magnitudes of leakage events. 	<p>n/a for this phase.</p>
<p>Step 3.3.4: Risk Characterisation</p> <ul style="list-style-type: none"> This shall comprise an assessment of the safety and integrity of the site in the short and long term, including an assessment of the risk of leakage under the proposed conditions of use, and of the worst-case environment and health impacts. The risk characterization shall be conducted based on the hazard, exposure and effects assessment. It shall include an assessment of the sources of uncertainty identified during the steps of characterization and assessment of storage site and when feasible, a description of the possibilities to reduce uncertainty. 	<p>Chapter 8</p>

<p>DOCUMENT NO.: TL02-GTL-Z-RA-0001</p>	<p>REVISION NO.: 03</p>	<p>REVISION DATE: 01.03.2012</p>	<p>APPROVED:</p>
---	-----------------------------	--------------------------------------	------------------

A2 Proposed Location and Formation Evaluation Programme for Exploration Well

Requirements to the wellbore are:

1. It shall be possible to cut a number of cores of minimum 8” OD size in Drake, Cook, and Johansen Formations (not expecting to penetrate Amundsen in southern area)
2. It shall be possible to conduct a miniature DST (pumping Formation fluids into the drill string from a well section isolated with two open hole packers) in the Johansen Formation.
3. TD will be at a minimum of 50m below Johansen, enabling wireline logging of the transition between Statfjord and Johansen.
4. The well shall be permanently plugged and abandoned upon completion of the data acquisition programme (depends on subsequent well duty).
5. The abandonment shall be done with the aim to withstand a possible intrusion of CO₂ into either the Johansen and/or the Cook Formation at the exploration well location (depends on subsequent well duty).

Data Acquisition

Data acquisition requirements are listed below. Note the data acquisition scope may be subject to change as result of new information or general maturing of the project.

Cuttings samples

To be collected every 10m from 20” (or 18 5/8”) shoe to TD, to the extent it does not conflict with other data acquisition.

Paleontology

To be reported from 20” (or 18 5/8”) shoe to TD

LWD

Formations	Conventional suite	Additional suite
Nordland Hordaland Rogaland	GR/Res/Cal	Den/Neu/DT
From top Shetland down to and including Brent	GR/Res/Den/Neu/DT/Cal	Image log (Den/GR/Resistivity images) Formation pressure
From top Drake to TD	GR/Res/Den/Neu/DT/Cal	NMR/DTSM/OrientCali Image log Formation pressure

Wireline logs

As back-up to LWD, the same logs as with LWD.

In addition, MDT with fluids sampling to be taken in the Cook Formation and Johansen Formation. It should also be considered to collect fluid samples in nearest permeable formation above Lower Drake to investigate change in chemistry across primary seal.

Formation strength

LOT or XLOT (to be determined) at casing points.

Mini frac tests to be conducted in Drake, Cook (no Amundsen expected) and Johansen Formations (optional, to be confirmed at later stage)

Mini DST or Injection Test

Optional - to be determined

DOCUMENT NO.: TL02-GTL-Z-RA-0001	REVISION NO.: 03	REVISION DATE: 01.03.2012	APPROVED:
-------------------------------------	---------------------	------------------------------	-----------

Coring

Conventional cores to be cut at:

- Inside Drake
- Transition Drake/Cook
- Inside Cook
- Transition Cook/Johansen
- In Johansen 2
- In Johansen 1
- Transition Dunlin (Johansen or Amundsen/Statfjord)

Sidewall coring

To be available as back-up in case of difficulties in recovering representative specimens of conventional cores

VSP

VSP or check-shots, to be determined

Cement verification

For the 9 5/8" casing, Schlumberger USIT log or similar (if available)

Abandonment cement plugs to be tagged and, if technically possible, pressure tested.

Geochemistry

It is assumed that sampling and analyses required for geochemical purposes is covered by the above. Specific needs will however be addressed at a later stage.

DOCUMENT NO.: TL02-GTL-Z-RA-0001	REVISION NO.: 03	REVISION DATE: 01.03.2012	APPROVED:
-------------------------------------	---------------------	------------------------------	-----------

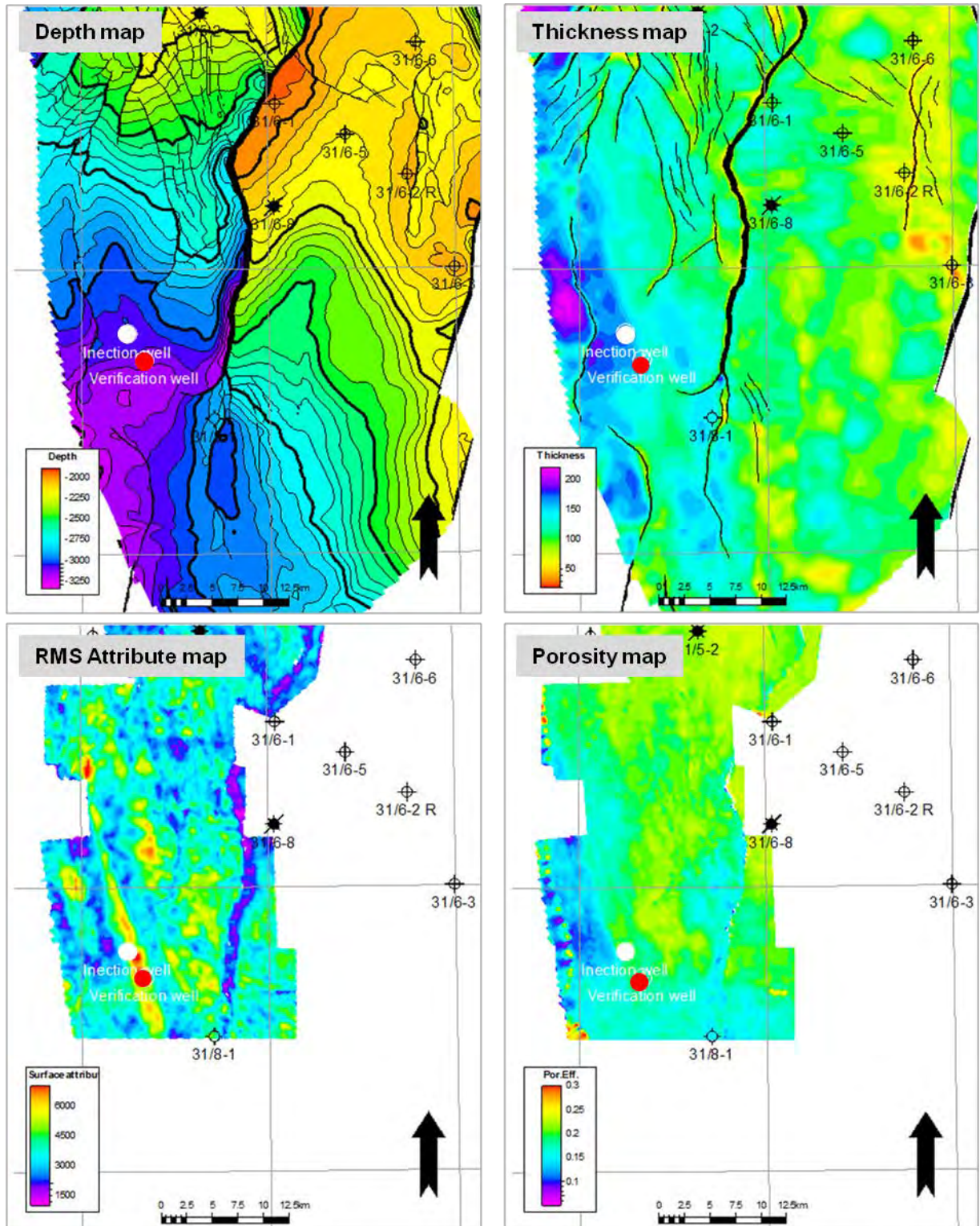


Figure 14-1 verification well location

DOCUMENT NO.: TL02-GTL-Z-RA-0001	REVISION NO.: 03	REVISION DATE: 01.03.2012	APPROVED:
-------------------------------------	---------------------	------------------------------	-----------

A3 Well to Seismic Calibration – Figures
 Figures related to Chapter 5.2.1

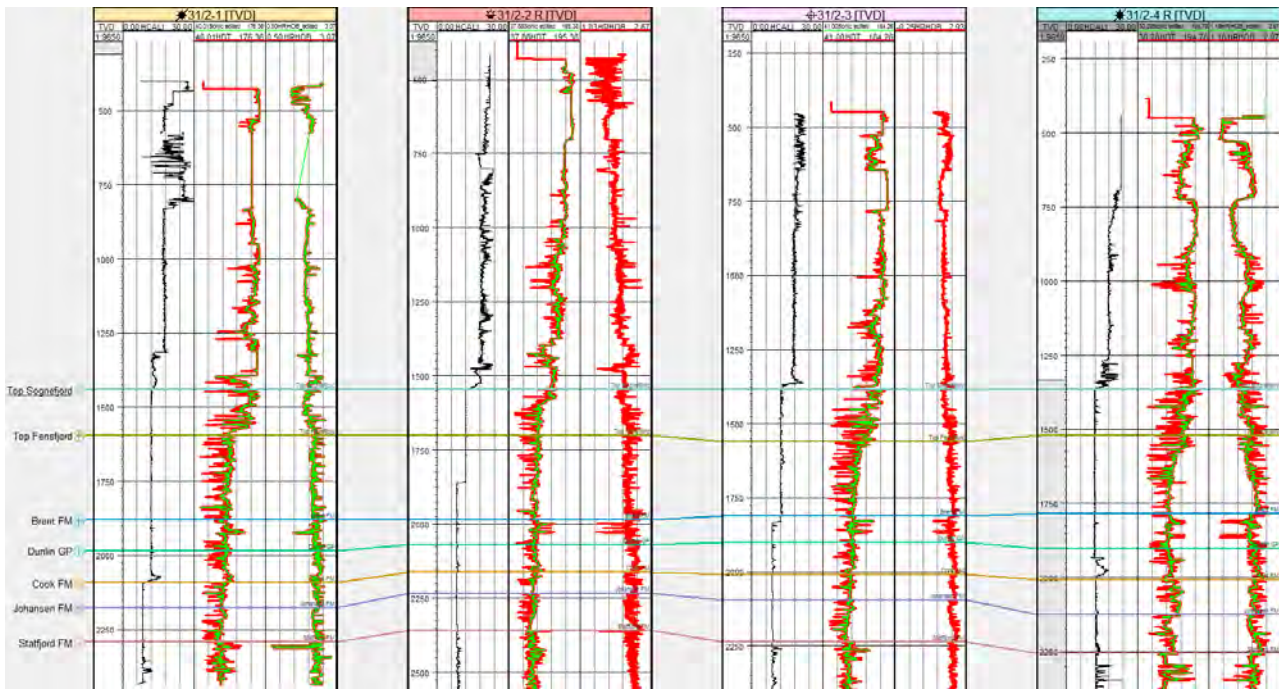


Figure 1: Input well log panels from wells (left to right) 31/2-1, 31/2-2 R, 31/2-3, 31/2-4 R with logs: caliper, sonic and density (left to right). Red log-curves are original logs and green curves are edited versions going into the seismic to well tie process.

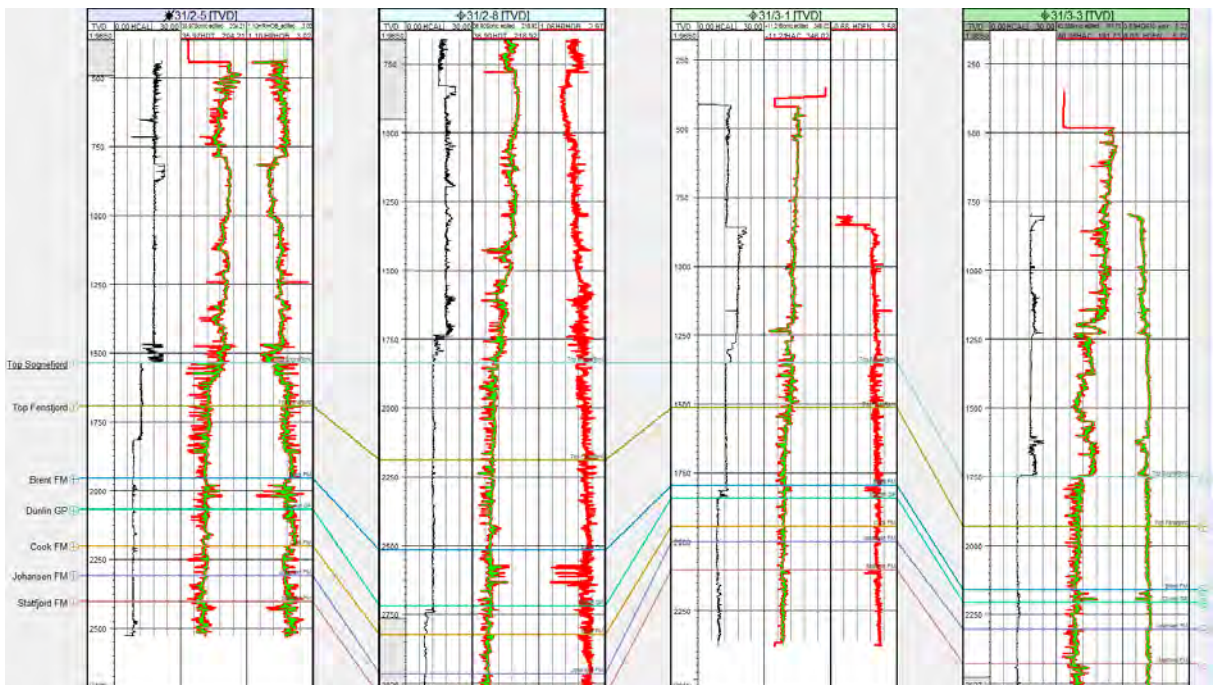


Figure 2: Input well log panels from wells (left to right) 31/2-5, 31/2-8 R, 31/3-1, 31/3-3 with logs: caliper, sonic and density (left to right). Red log-curves are original logs and green curves are edited versions going into the seismic to well tie process.

DOCUMENT NO.: TL02-GTL-Z-RA-0001	REVISION NO.: 03	REVISION DATE: 01.03.2012	APPROVED:
-------------------------------------	---------------------	------------------------------	-----------

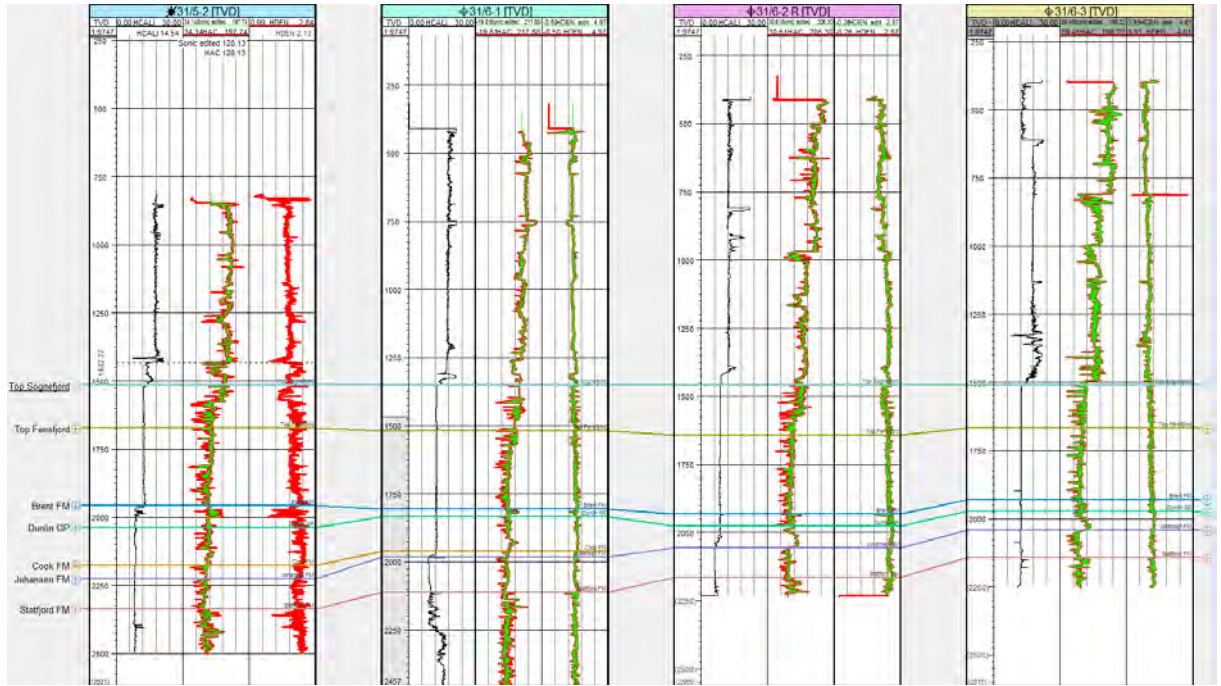


Figure 3: Input well log panels from wells (left to right) 31/5-2, 31/6-1, 31/6-2 R, 31/6-3 with logs: caliper, sonic and density (left to right). Red log-curves are original logs and green curves are edited versions going into the seismic to well tie process.

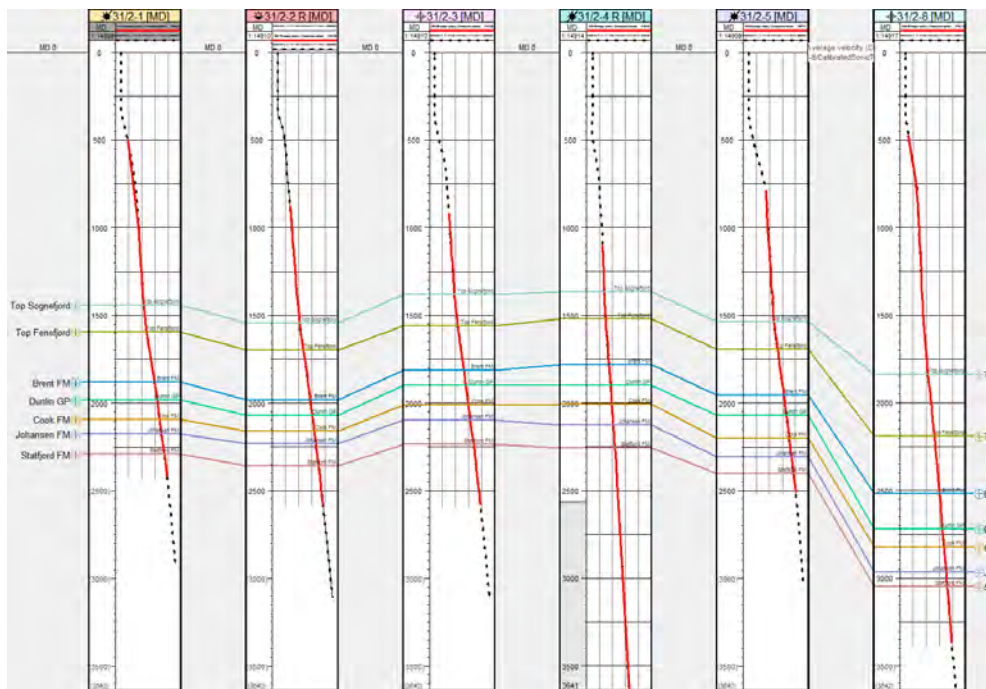


Figure 4: Average velocity from edited checkshots (red solid line) and calibrated sonic logs (stippled black line) from wells 31/2-1, 31/2-2 R, 31/2-3, 31/2-4 R, 31/2-5 & 31/2-8 (listed from left to right).

DOCUMENT NO.: TL02-GTL-Z-RA-0001	REVISION NO.: 03	REVISION DATE: 01.03.2012	APPROVED:
-------------------------------------	---------------------	------------------------------	-----------

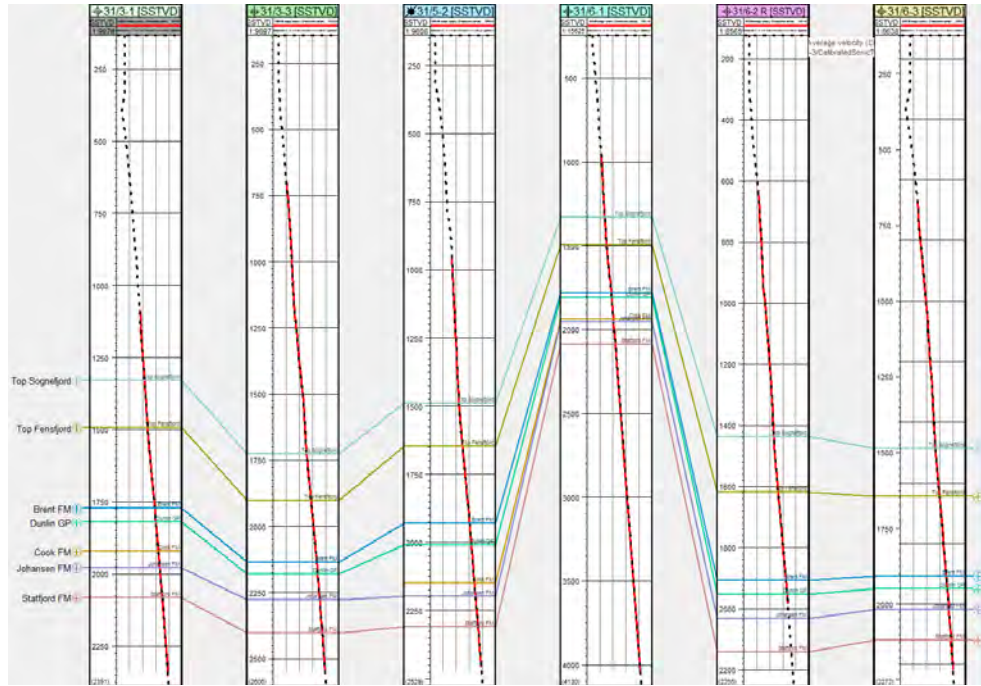


Figure 5: Average velocity from edited checkshots (red solid line) and calibrated sonic logs (stippled black line) from wells 31/3-1, 31/3-3 R, 31/5-2, 31/6-1, 31/6-2 R & 31/6-3 (listed from left to right).

DOCUMENT NO.: TL02-GTL-Z-RA-0001	REVISION NO.: 03	REVISION DATE: 01.03.2012	APPROVED:
-------------------------------------	---------------------	------------------------------	-----------

Time SRD	Well: 31/2-2 R	Well: 31/2-2 R	RC	Survey: GN10MI	ynthetic	Survey: GN10MI	Time SRD
ms	Log set: Log set 1	Log set: Log set 1		v1_full_fold_FM_Stac		v1_full_fold_FM_Stac	ms
1519	Calc AI (kPa.s/m)	13144	0	HGR (gAPI)150	-0.188	0.189	2835
1.5	HRHOB (g/cm3)	3					2835
147	Sonic edited (us/ft)	24					2835
				Inline	2835	2835	2835
				Xline	4789	4797	4805
				Inline	4807	4809	4817
				Xline	4817	4825	4825

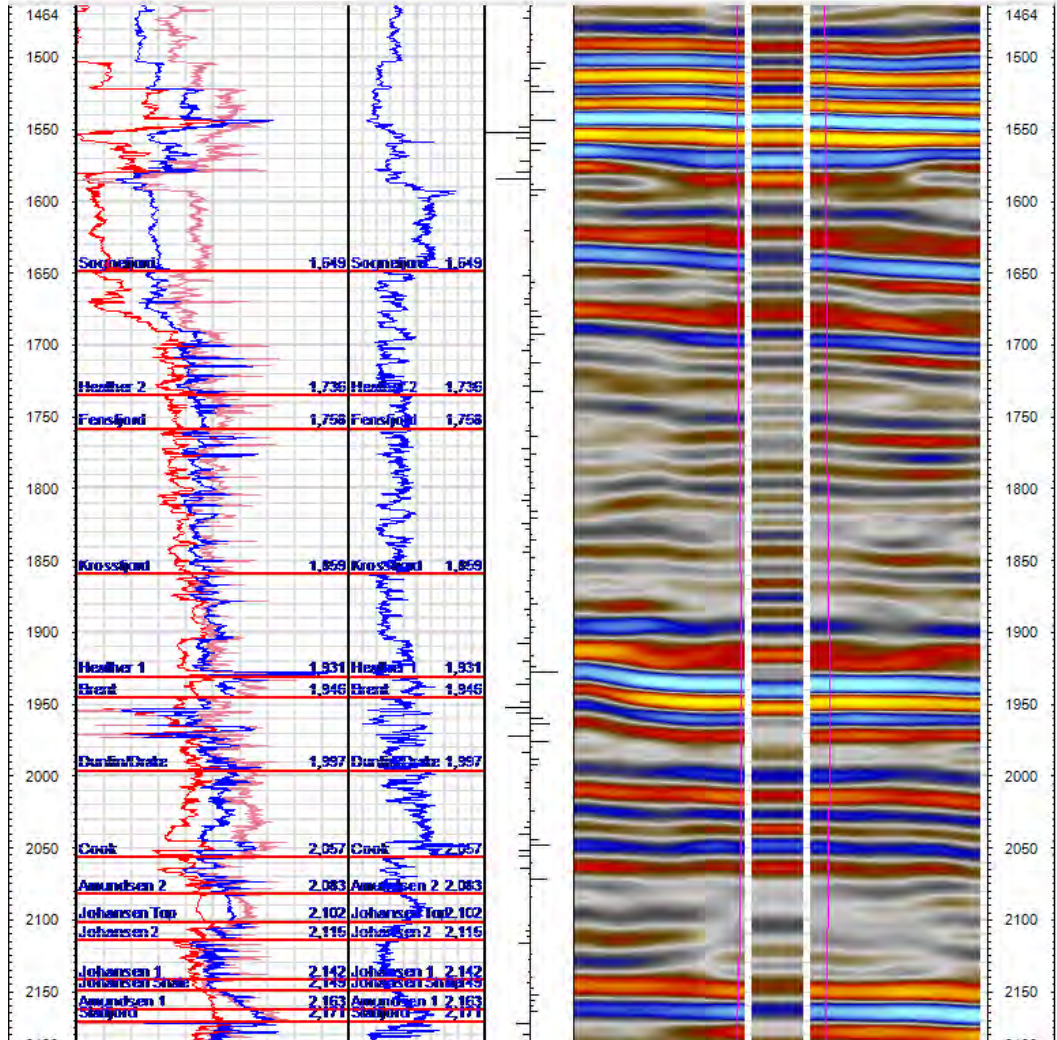


Figure 7: Synthetic seismogram panel from well 31/2-2R. From left to right; AI (calculated) - density and sonic in shared panel, Gamma ray log, Reflection coefficient log, split panel with synthetic seismogram in the middle flanked by extracted seismic along inline through well position.

DOCUMENT NO.: TL02-GTL-Z-RA-0001	REVISION NO.: 03	REVISION DATE: 01.03.2012	APPROVED:
-------------------------------------	---------------------	------------------------------	-----------

Time	Well: 31/2-3		Well: 31/2-3		RC	Survey: GN10MI			ynthetic	Survey: GN10MI			Time
SRD	Log set: Log set 1		Log set: Log set 1			vI_full_fold_FM_Stack				vI_full_fold_FM_Stack			SRD
ms						Inline	Inline	Inline	Inline	Inline	Inline	ms	
-621	Calc AI (kPa.s/m)	14138.0	HGR (gAPI)150	-0.54	RC0.548	3107	3107	3107	3107	3107	3107		
1.5	HRHOB (g/cm3)	3					Xline		Xline				
147	Sonic edited (us/ft)	24				4457	4465	4473	4475	4477	4485	4493	

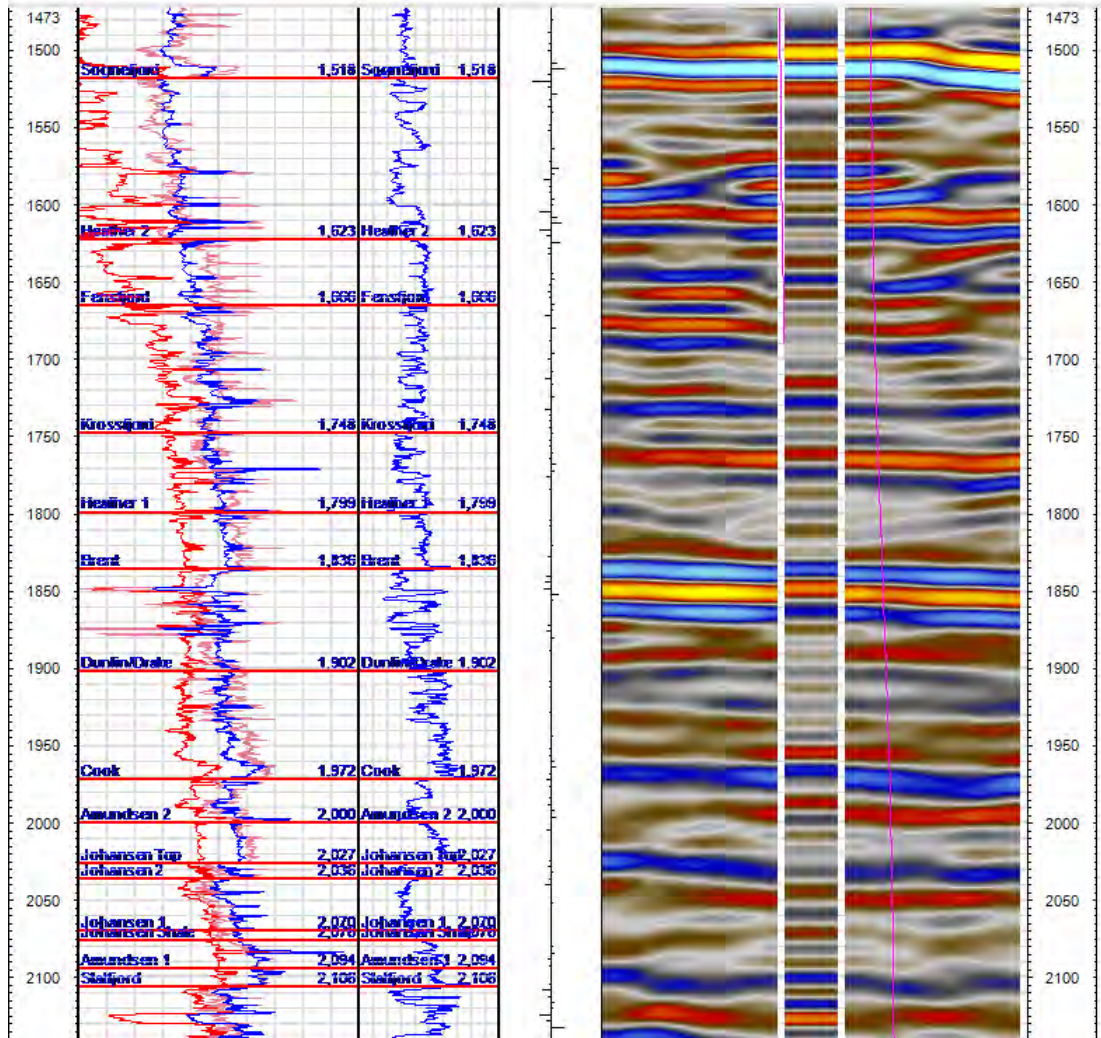


Figure 8: Synthetic seismogram panel from well 31/2-3. From left to right; AI (calculated) - density and sonic in shared panel, Gamma ray log, Reflection coefficient log, split panel with synthetic seismogram in the middle flanked by extracted seismic along inline through well position.

DOCUMENT NO.: TL02-GTL-Z-RA-0001	REVISION NO.: 03	REVISION DATE: 01.03.2012	APPROVED:
-------------------------------------	---------------------	------------------------------	-----------

Time	Well: 31/2-4 R	Well: 31/2-4 R	RC	Survey: GN10MI	ynthetic	Survey: GN10MI	Time
SRD	Log set: Log set 1	Log set: Log set 1		01_full_fold_FM_Stack		01_full_fold_FM_Stack	SRD
ms							ms
1904	Calc AI (kPa.s/m)	16112,0	HGR (gAPI)150	-0.00379	3174	3174	3174
1.5	HRHOB_edited (g/cm3)	3	HCALI (in)	20	3174	3174	3174
147	Sonic edited (us/ft)	24			3811	3819	3827
							3831
							3839
							3847

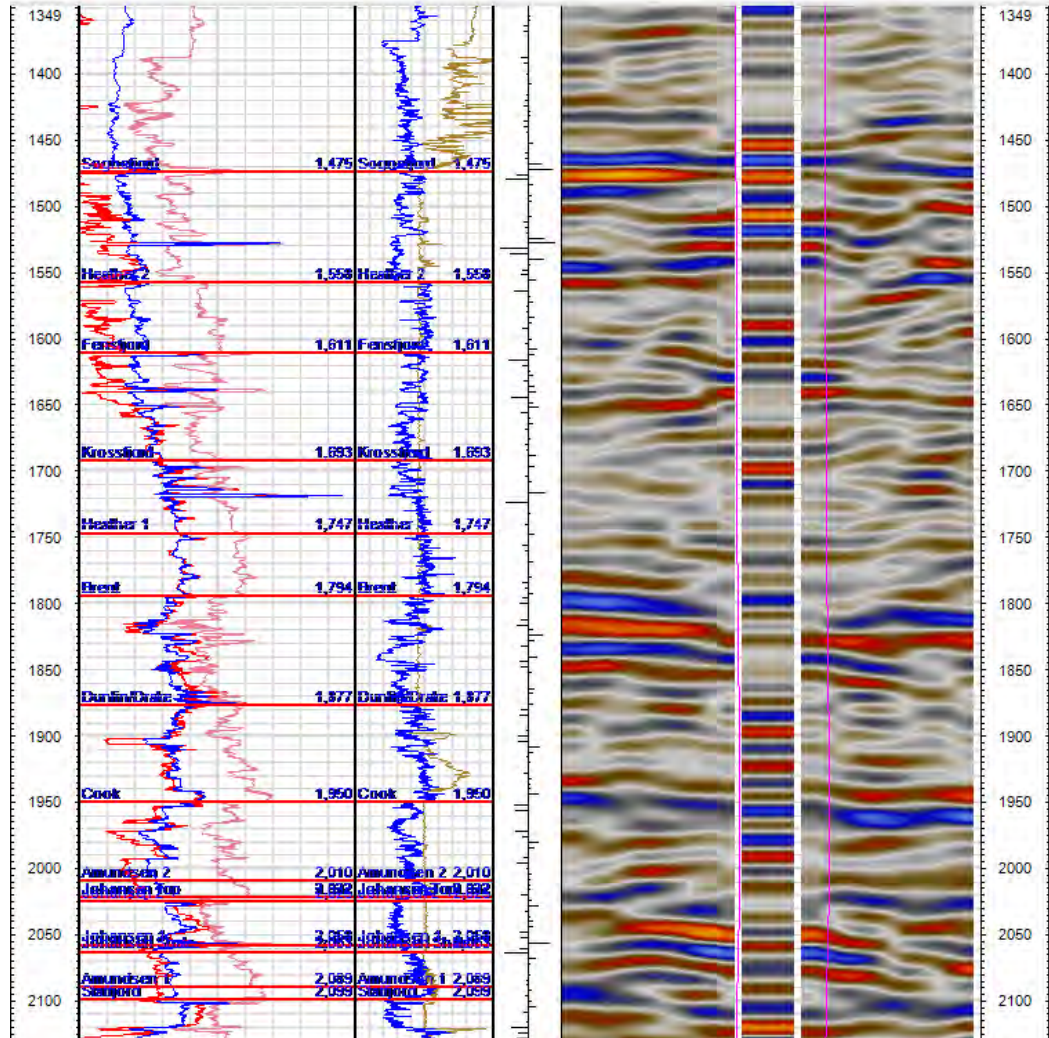


Figure 9: Synthetic seismogram panel from well 31/2-4R. From left to right; AI (calculated) - density and sonic in shared panel, Gamma ray log, Reflection coefficient log, split panel with synthetic seismogram in the middle flanked by extracted seismic along inline through well position. This well gives a poor match to synthetic seismograms compared with the other wells.

DOCUMENT NO.: TL02-GTL-Z-RA-0001	REVISION NO.: 03	REVISION DATE: 01.03.2012	APPROVED:
-------------------------------------	---------------------	------------------------------	-----------

Time	Well: 31/2-5		Well: 31/2-5		RC	Survey: GN10M1		ynthetic	Survey: GN10M1		Time
SRD	Log set: Log set 1		Log set: Log set 1			vI_full_fold_FM_Stac			vI_full_fold_FM_Stac		SRD
ms											ms
2041	Calc AI (kPa.s/m)	11716.0	HGR (gAPI)150	-0.80	13	2793	2793	Inline	2793	2793	
1.5	HRHOB_edited (g/cm3)	3						Xline			
147	Sonic edited (us/ft)	24				3119	3127	3135	Xline	3137	3155

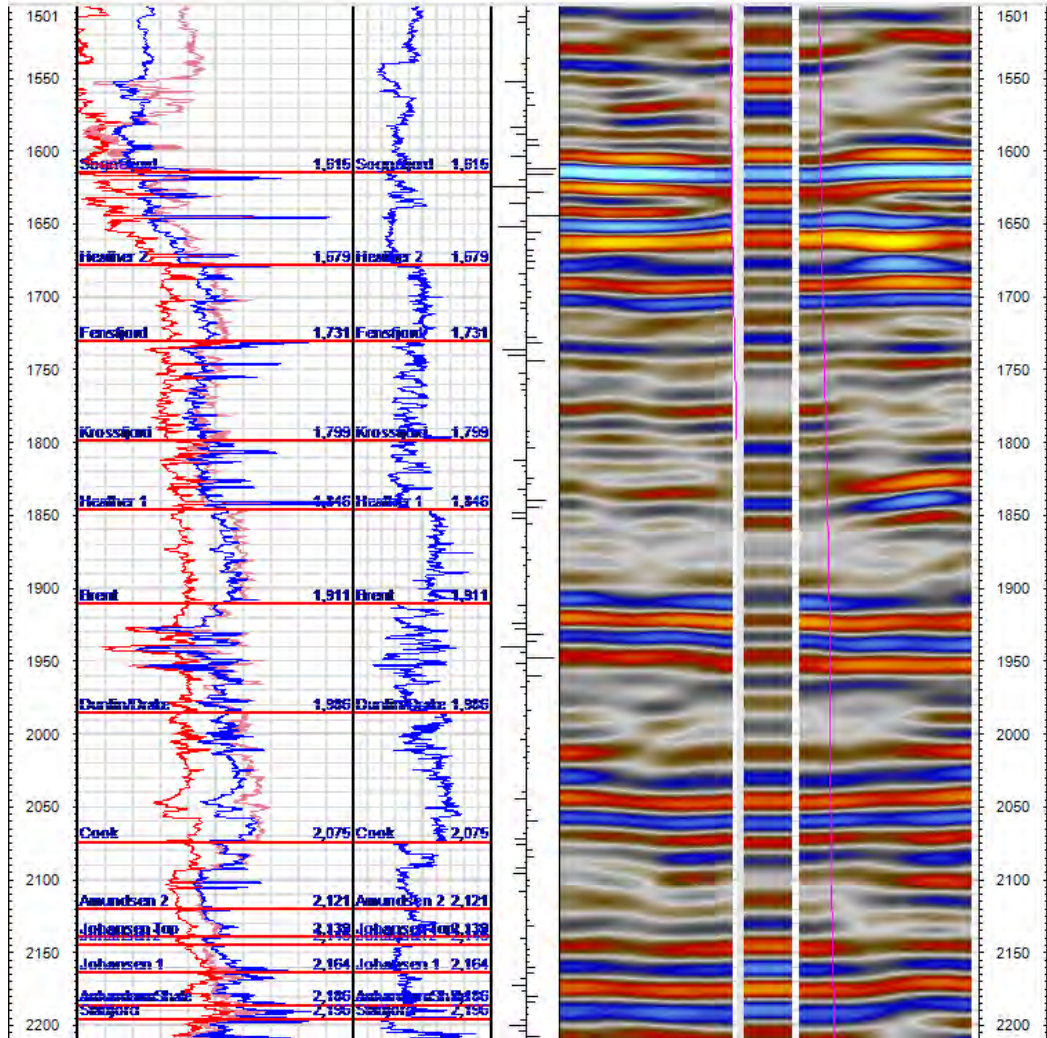


Figure 10: Synthetic seismogram panel from well 31/2-5. From left to right; AI (calculated) - density and sonic in shared panel, Gamma ray log, Reflection coefficient log, split panel with synthetic seismogram in the middle flanked by extracted seismic along inline through well position.

DOCUMENT NO.: TL02-GTL-Z-RA-0001	REVISION NO.: 03	REVISION DATE: 01.03.2012	APPROVED:
-------------------------------------	---------------------	------------------------------	-----------

Time	Well: 31/2-8		Well: 31/2-8	RC	Survey: 2D MN9103	Survey: 2D MN9103	Time
SRD	Log set: Log set 1		Log set: Log set 1		:: MN9103-310A [Real]	:: MN9103-310A [Real]	SRD
ms					Line	Line	ms
1173	Calc AI (kPa.s/m)	15993.0	HGR (gAPI)150	-0.20215	1 1 1 1 1 1 1 1 1 1	1 1 1 1 1 1 1 1 1 1	
1.5	HRHOB (g/cm3)	3			Trace	Trace	
147	Sonic edited (us/m)	24			2567 2571 2575	2577 2581 2585	

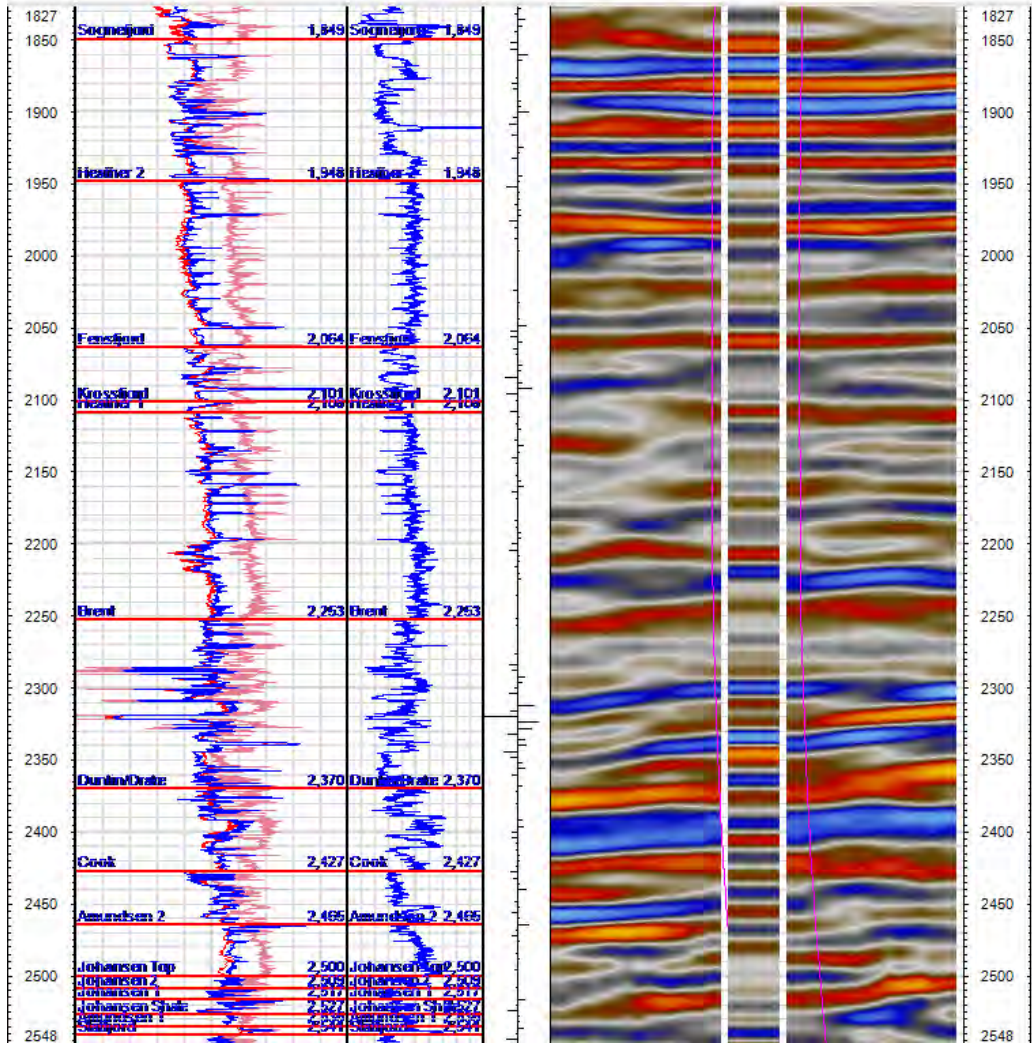


Figure 11: Synthetic seismogram panel from well 31/2-8. From left to right; AI (calculated) - density and sonic in shared panel, Gamma ray log, Reflection coefficient log, split panel with synthetic seismogram in the middle flanked by extracted seismic along inline through well position.

DOCUMENT NO.: TL02-GTL-Z-RA-0001	REVISION NO.: 03	REVISION DATE: 01.03.2012	APPROVED:
-------------------------------------	---------------------	------------------------------	-----------

Time	Well: 31/3-1		Well: 31/3-1	RC	Survey: GN10MI			ynthetic	Survey: GN10MI			Time
SRD	Log set: Log set 1		Log set: Log set 1		vI_full_fold_FM_Stac				vI_full_fold_FM_Stac			SRD
ms					Inline	2838	2838	Inline	2838	2838	2838	ms
-2383	Calc AI (kPa.s/m)	35995	OHGR_edit (gAPI#60)	-0.50379	2838	2838	2838	2838	2838	2838		
1.5	HDEN (g/cm3)	3			Xline	5765	5773	Xline	5776	5777	5786	5793
147	Sonic edited (us/ft)	24										

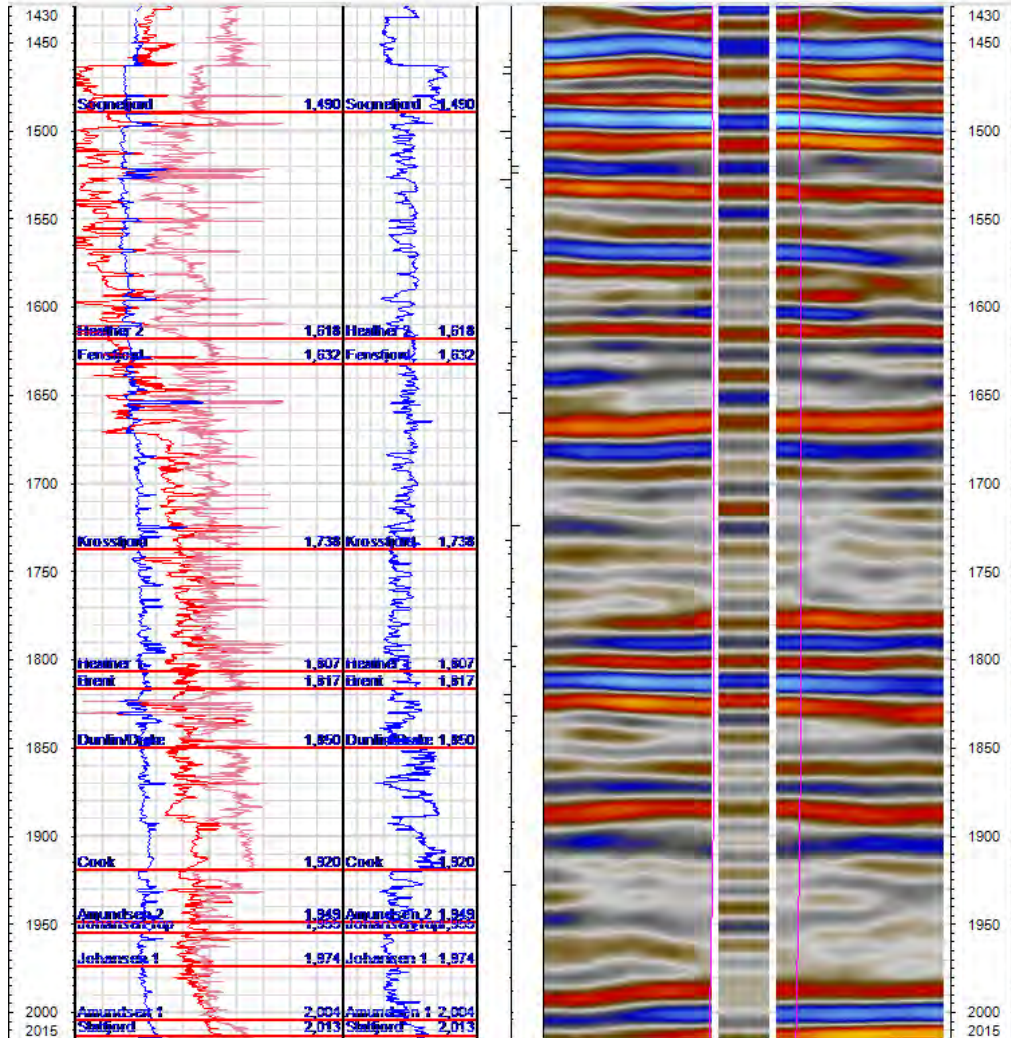


Figure 12: Synthetic seismogram panel from well 31/3-1. From left to right; AI (calculated) - density and sonic in shared panel, Gamma ray log, Reflection coefficient log, split panel with synthetic seismogram in the middle flanked by extracted seismic along inline through well position.

DOCUMENT NO.: TL02-GTL-Z-RA-0001	REVISION NO.: 03	REVISION DATE: 01.03.2012	APPROVED:
-------------------------------------	---------------------	------------------------------	-----------

Time	Well: 31/5-2		Well: 31/5-2		RC	Survey: GN10MI			ynthetic	Survey: GN10MI			Time
SRD	Log set: Log set 1		Log set: Log set 1			vI_full_fold_FM_Stac				vI_full_fold_FM_Stac			SRD
ms													ms
2568	Calc AI (kPa.s/m)	12886	0	HGR (gAPI)150	-0.202	2593	2593	2593	Inline	2593	2593	2593	
1.5	H DEN (g/cm3)	3							Xline	4159	4159	4159	
147	Sonic edited (us/ft)	24				4141	4149	4157	Xline	4161	4169	4177	

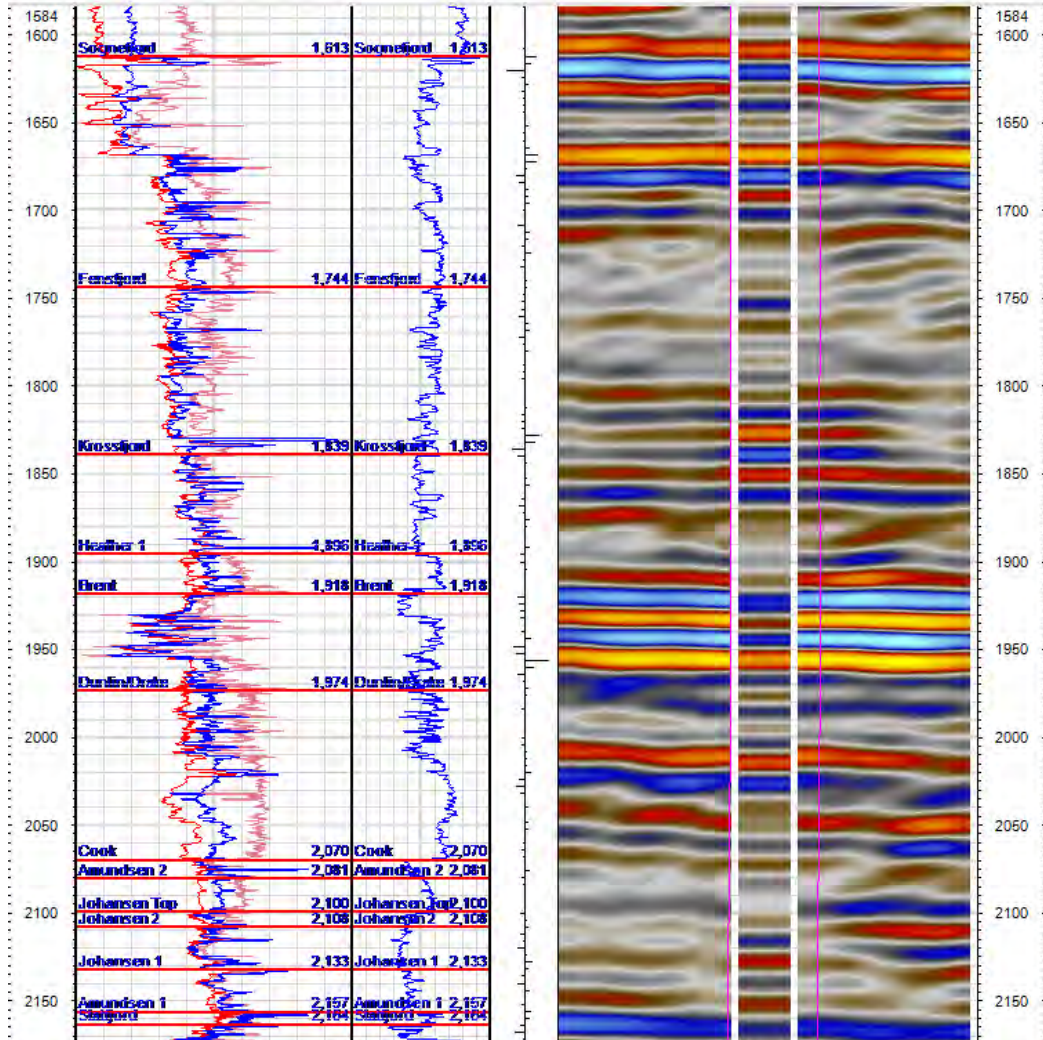


Figure 13: Synthetic seismogram panel from well 31/5-2. From left to right; AI (calculated) - density and sonic in shared panel, Gamma ray log, Reflection coefficient log, split panel with synthetic seismogram in the middle flanked by extracted seismic along inline through well position.

DOCUMENT NO.: TL02-GTL-Z-RA-0001	REVISION NO.: 03	REVISION DATE: 01.03.2012	APPROVED:
-------------------------------------	---------------------	------------------------------	-----------

Time	Well: 31/6-1		Well: 31/6-1		RC	-08-4D-TROLLCO2.S			Synthetic-08-4D-TROLLCO2.S			Time
SRD	Log set: Log set 1		Log set: Log set 1)-TROLLCO2.SG9202.)-TROLLCO2.SG9202.			SRD
ms						Inline	Inline	Inline	Inline	Inline	Inline	ms
-1150	Calc AI (kPa.s/m)	22068.0	HGR (gAPI)	150	-0.75	1897	1897	1897	1897	1897	1897	
1.5	HDEN_edit (g/cm3)	3					Xline	3300	Xline	3301	Xline	
147	Sonic edited (us/ft)	24				3292	3296	3300	3301	3302	3306	3310

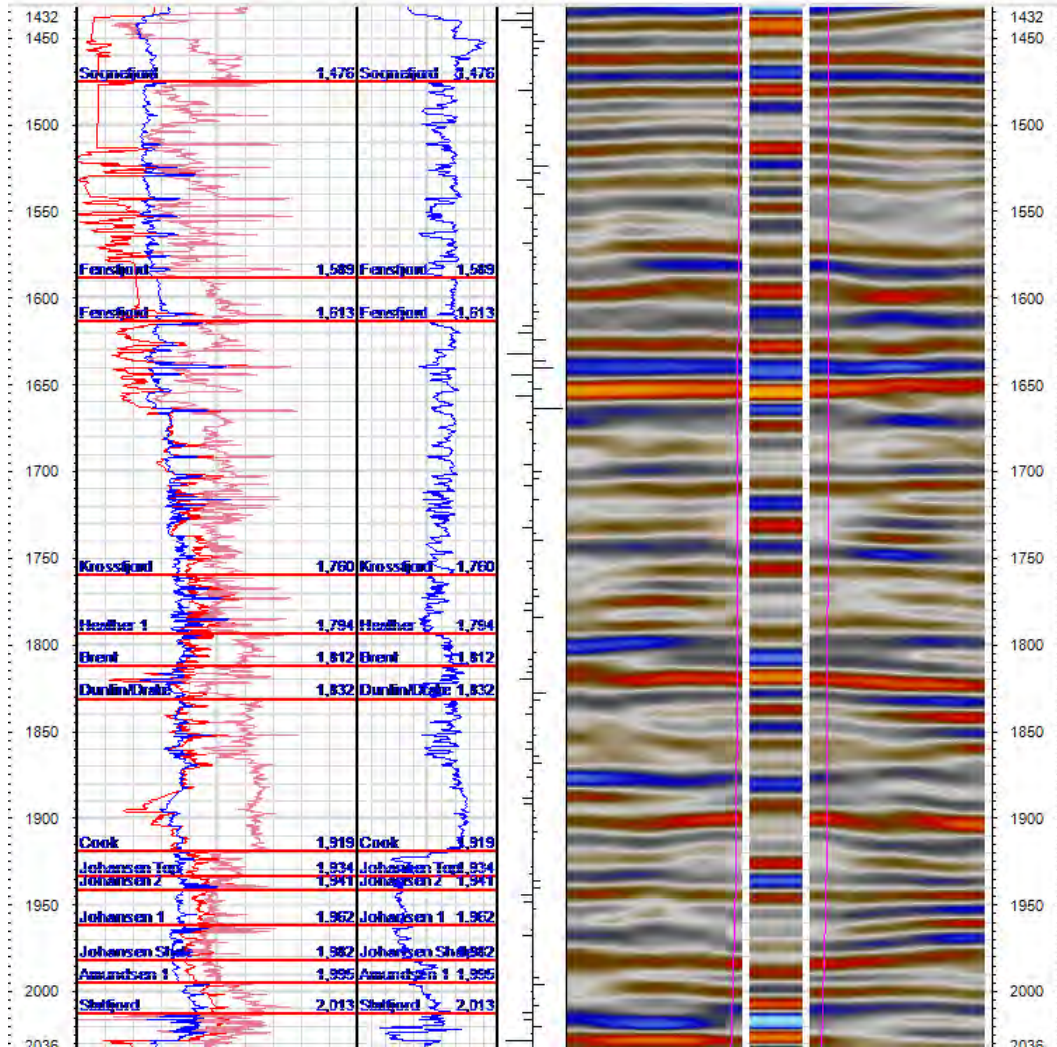


Figure 14: Synthetic seismogram panel from well 31/6-1. From left to right; AI (calculated) - density and sonic in shared panel, Gamma ray log, Reflection coefficient log, split panel with synthetic seismogram in the middle flanked by extracted seismic along inline through well position.

DOCUMENT NO.: TL02-GTL-Z-RA-0001	REVISION NO.: 03	REVISION DATE: 01.03.2012	APPROVED:
-------------------------------------	---------------------	------------------------------	-----------

Time	Well: 31/6-3		RC	Survey: 2D SHP91			Survey: 2D SHP91			Time
SRD	Log set: Log set 1			ic: SHP91-149A [Realiz			ic: SHP91-149A [Realiz			SRD
ms				Line	Line	Line	Line	Line	ms	
2154	Calc AI (kPa.s/m)	15752	0	1	1	1	1	1	1	
1.5	HDEN (g/cm3)	3		Trace	Trace	Trace	Trace	Trace		
147	Sonic edited (us/ft)	24		4366	4370	4374	4375	4376	4380	
								4384		

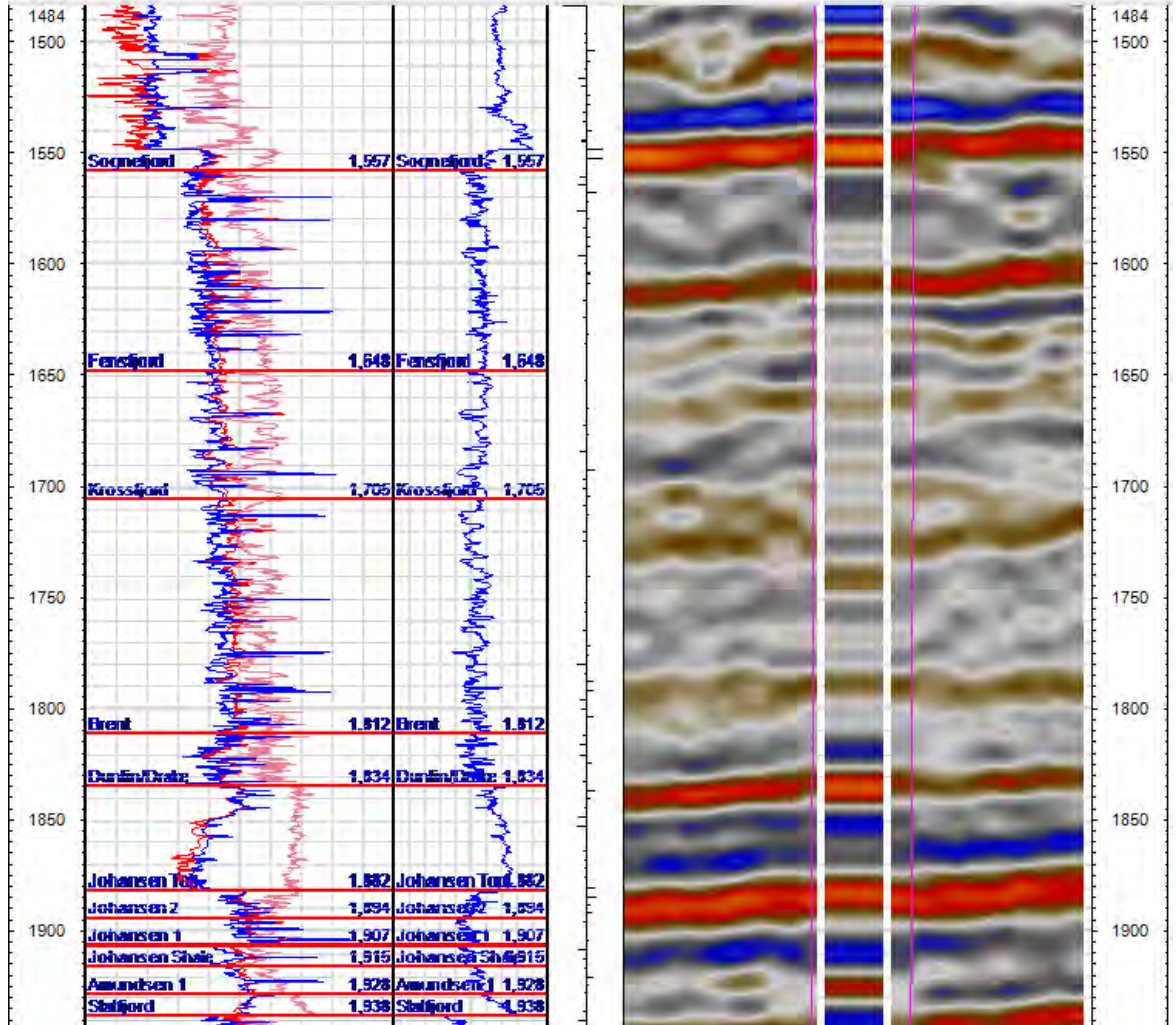


Figure 14-2: Synthetic seismogram panel from well 31/6-3. From left to right; AI (calculated) - density and sonic in shared panel, Gamma ray log, Reflection coefficient log, split panel with synthetic seismogram in the middle flanked by extracted seismic along 2D line through well position.

DOCUMENT NO.: TL02-GTL-Z-RA-0001	REVISION NO.: 03	REVISION DATE: 01.03.2012	APPROVED:
-------------------------------------	---------------------	------------------------------	-----------

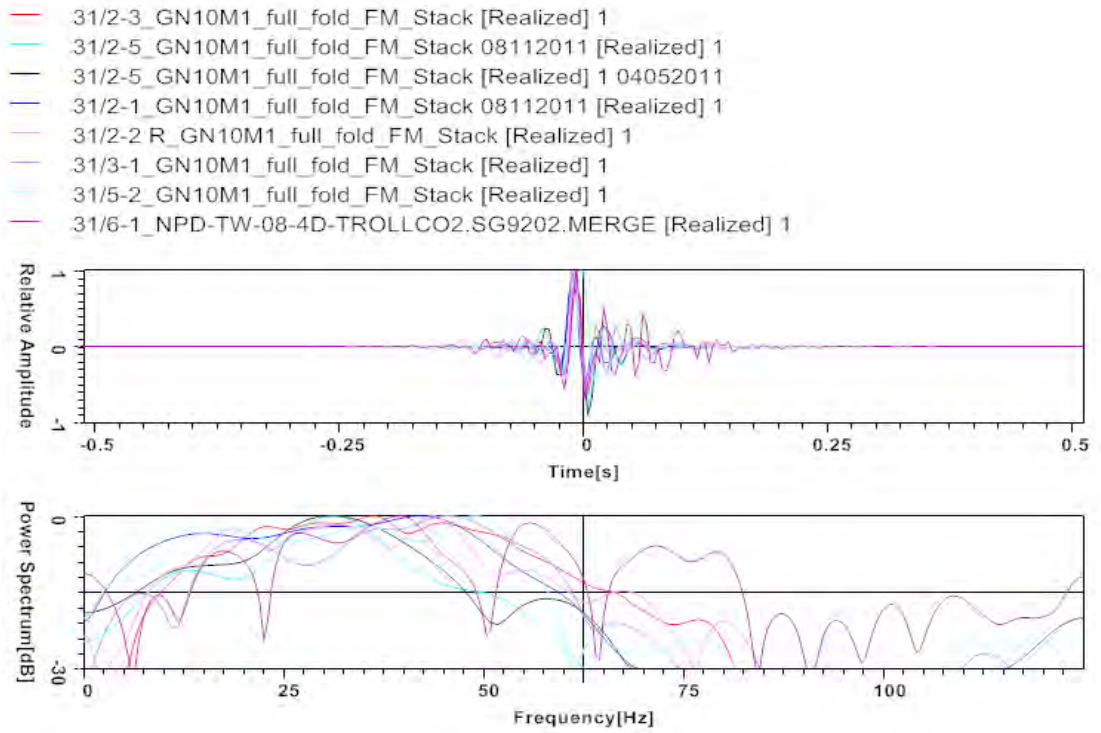


Figure 16: Extracted least square constant zero phase time domain wavelets from the GN10M1 & NPD-TW-08 3D surveys. The impulse responses (upper frame) show reasonably stable wavelets for each well position.

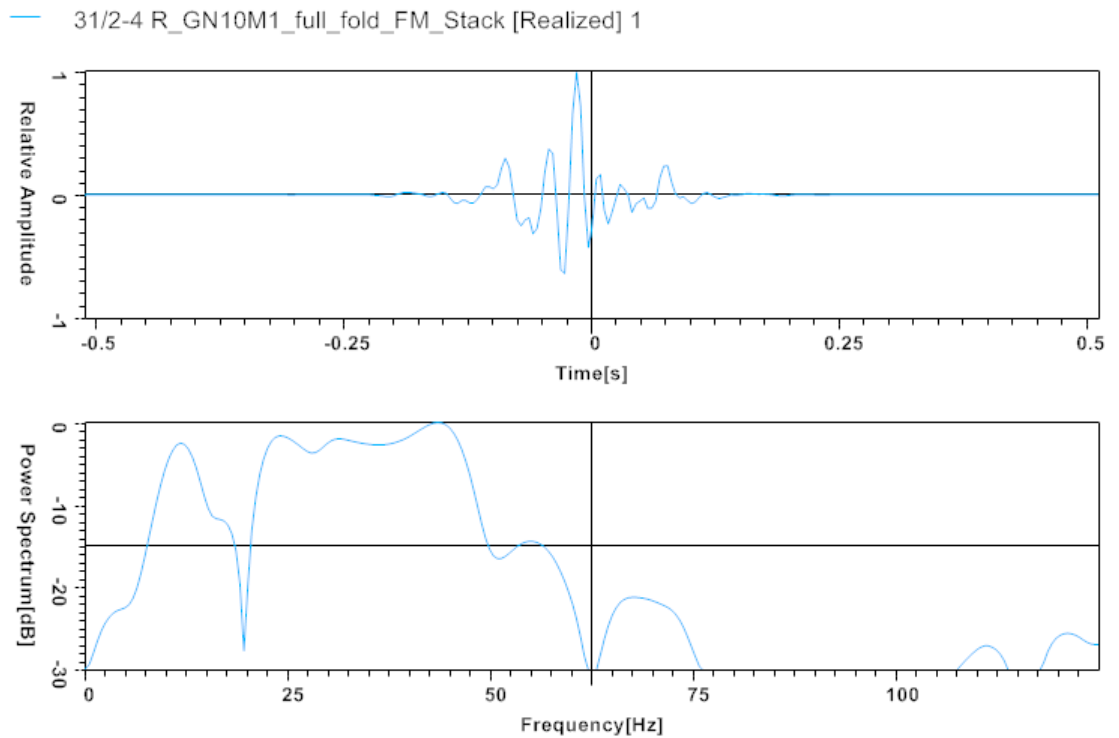


Figure 17: Extracted wavelet from 31/2-4R well show bad zero phase characteristics compared with the other wells (see Figure 9 and Error! Reference source not found.).

DOCUMENT NO.: TL02-GTL-Z-RA-0001	REVISION NO.: 03	REVISION DATE: 01.03.2012	APPROVED:
-------------------------------------	---------------------	------------------------------	-----------

A4 Johansen Storage Complex Time and Depth Maps

Figure list

- Figure 1 Seabed time map
- Figure 2 Seabed depth map
- Figure 3 Base Quarternary time map
- Figure 4 Base Quarternary depth map
- Figure 5 Base Pliocene time map
- Figure 6 Base Pliocene depth map
- Figure 7 Mid-Oligocene time map
- Figure 8 Mid-Oligocene depth map
- Figure 9 Green Clay time map
- Figure 10 Green Clay depth map
- Figure 11 Balder Fm time map
- Figure 12 Balder Fm depth map
- Figure 13 Shetland Gp time map
- Figure 14 Shetland Gp depth map
- Figure 15 Draupne Fm time map
- Figure 16 Draupne Fm depth map
- Figure 17 Sognefjord Fm time map
- Figure 18 Sognefjord Fm depth map
- Figure 19 Fensfjord Fm time map
- Figure 20 Fensfjord Fm depth map
- Figure 21 Brent Gp time map
- Figure 22 Brent Gp depth map
- Figure 23 Drake Fm time map
- Figure 24 Drake Fm depth map
- Figure 25 Lower Drake Fm time map
- Figure 26 Lower Drake Fm depth map
- Figure 27 Cook Fm time map
- Figure 28 Cook Fm depth map
- Figure 29 Upper Amundsen Fm time map
- Figure 30 Upper Amundsen Fm depth map
- Figure 31 Johansen Fm time map
- Figure 32 Johansen Fm depth map
- Figure 33 Lower Amundsen Fm time map
- Figure 34 Lower Amundsen Fm depth map
- Figure 35 Statfjord Fm time map
- Figure 36 Statfjord Fm depth map

DOCUMENT NO.: TL02-GTL-Z-RA-0001	REVISION NO.: 03	REVISION DATE: 01.03.2012	APPROVED:
-------------------------------------	---------------------	------------------------------	-----------

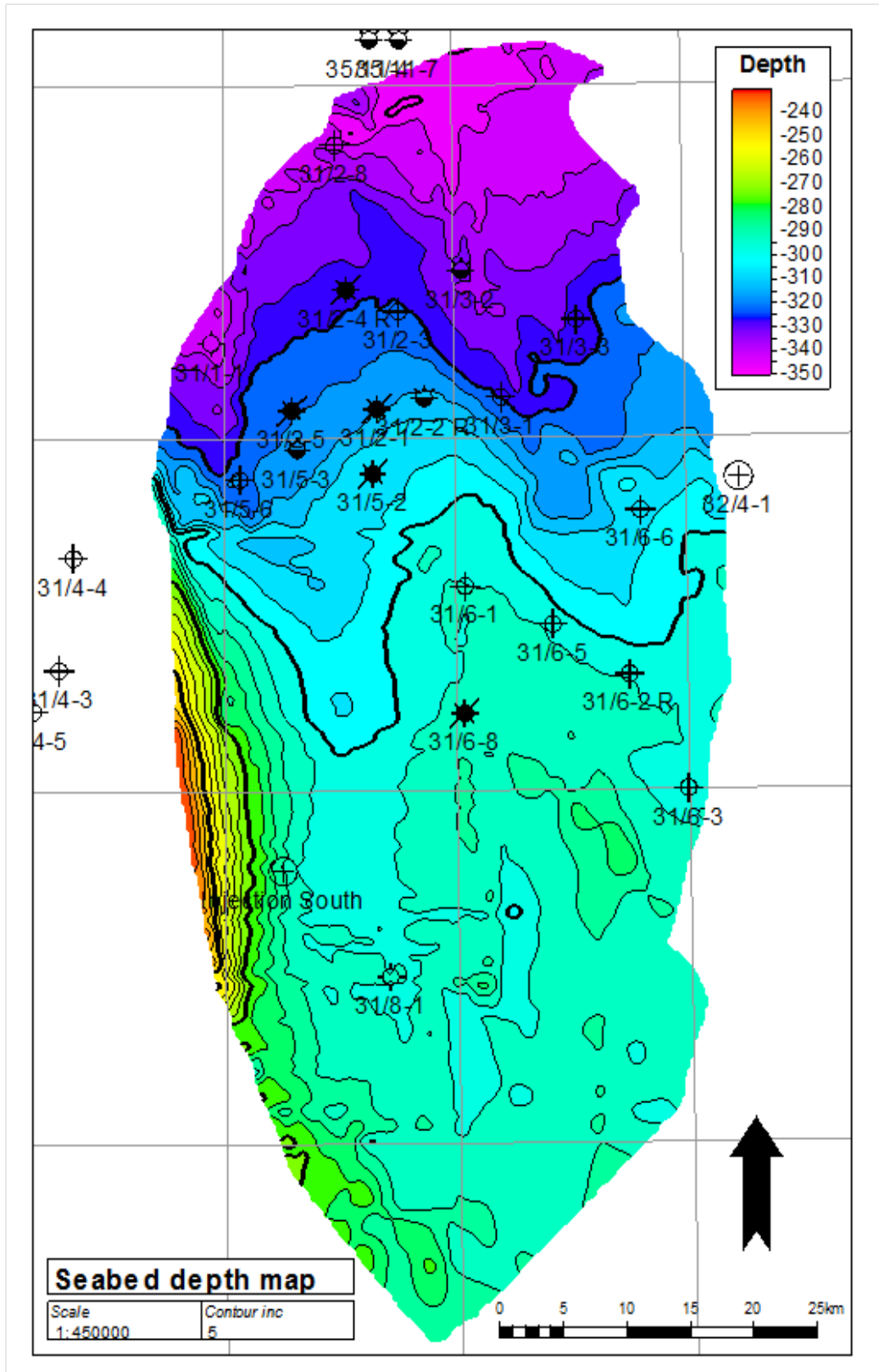


Figure 2: Seabed depth map.

DOCUMENT NO.: TL02-GTL-Z-RA-0001	REVISION NO.: 03	REVISION DATE: 01.03.2012	APPROVED:
-------------------------------------	---------------------	------------------------------	-----------

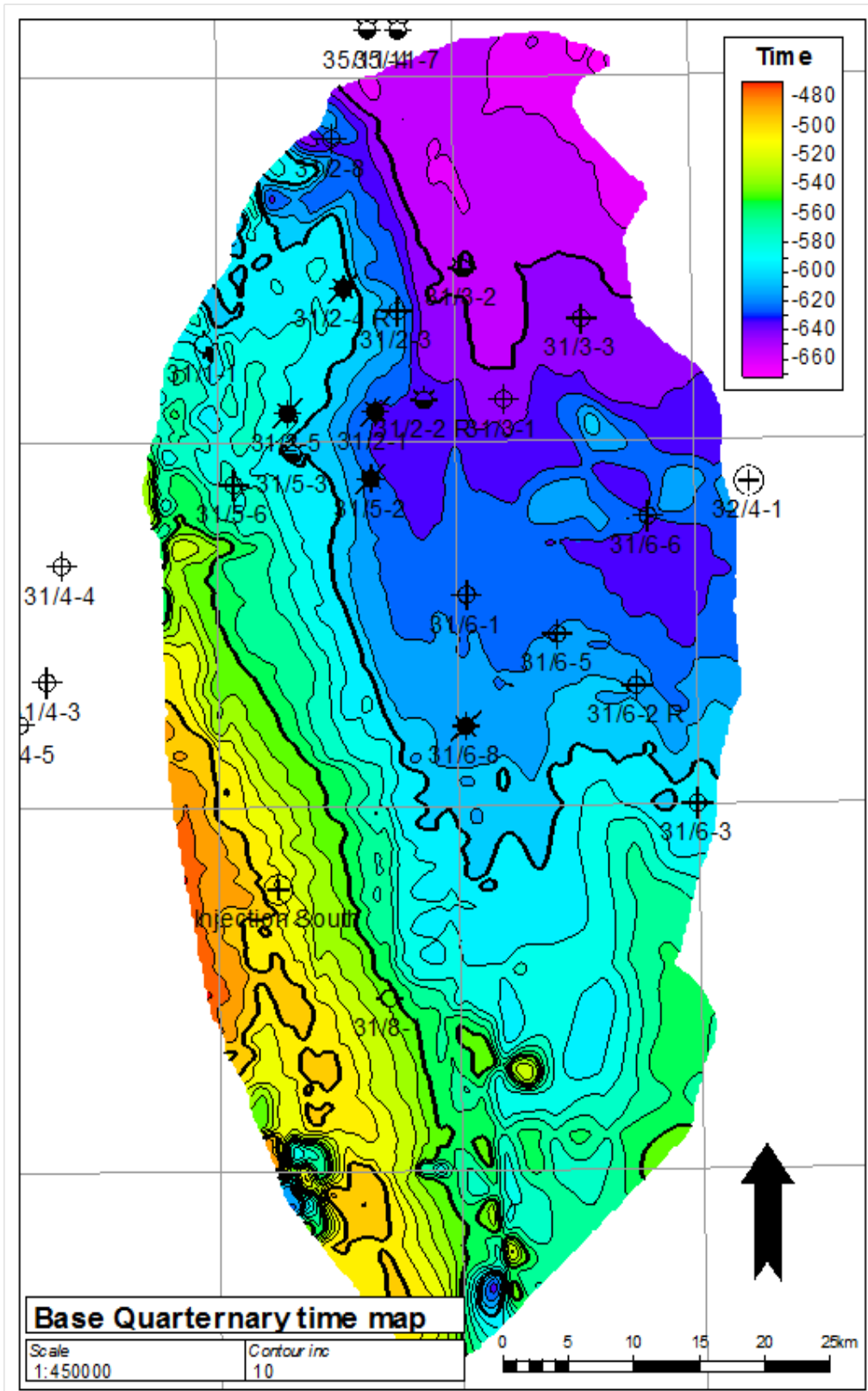


Figure 3: Base Quaternary time map.

DOCUMENT NO.: TL02-GTL-Z-RA-0001	REVISION NO.: 03	REVISION DATE: 01.03.2012	APPROVED:
-------------------------------------	---------------------	------------------------------	-----------

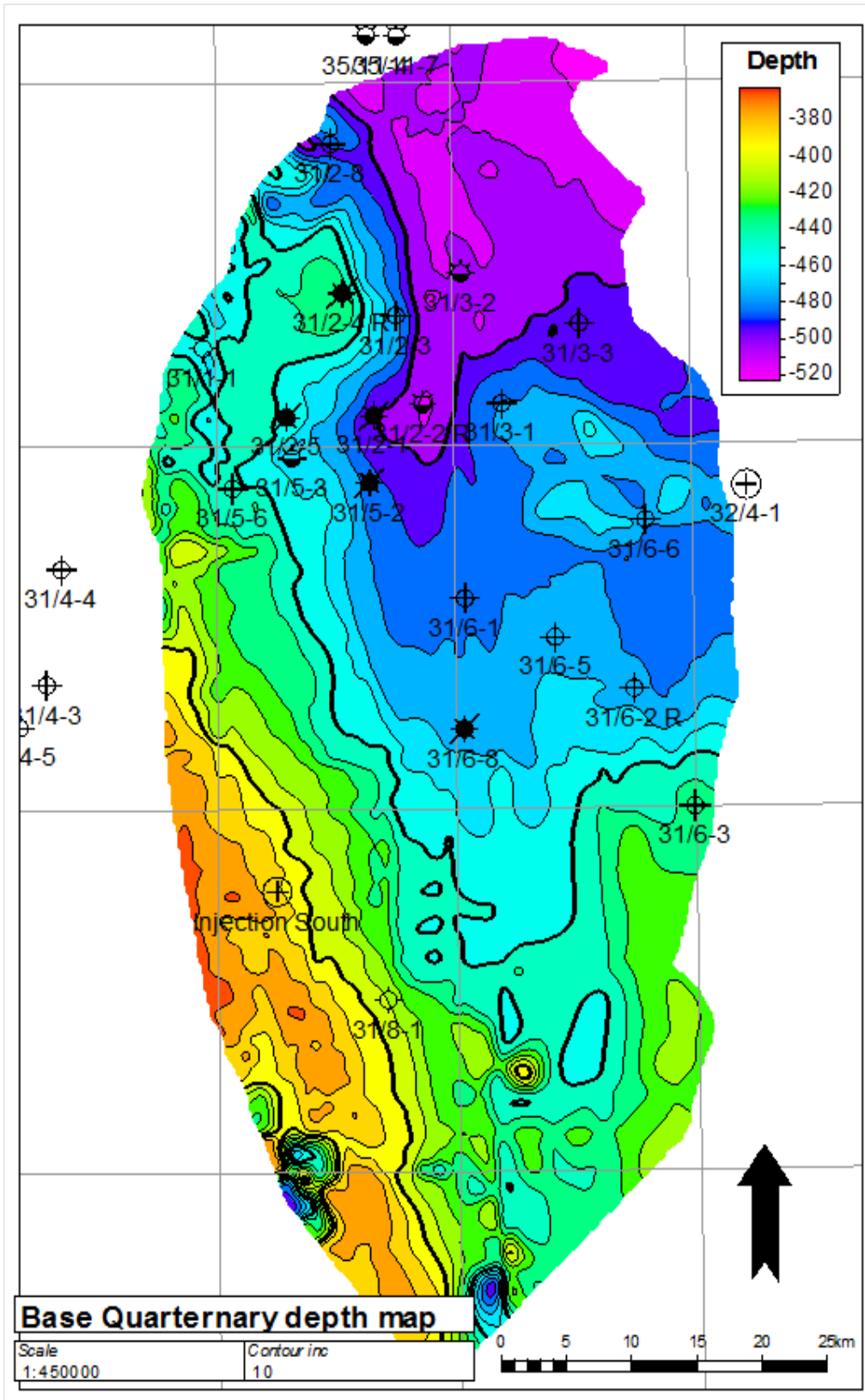


Figure 4: Base Quaternary depth map.

DOCUMENT NO.: TL02-GTL-Z-RA-0001	REVISION NO.: 03	REVISION DATE: 01.03.2012	APPROVED:
-------------------------------------	---------------------	------------------------------	-----------

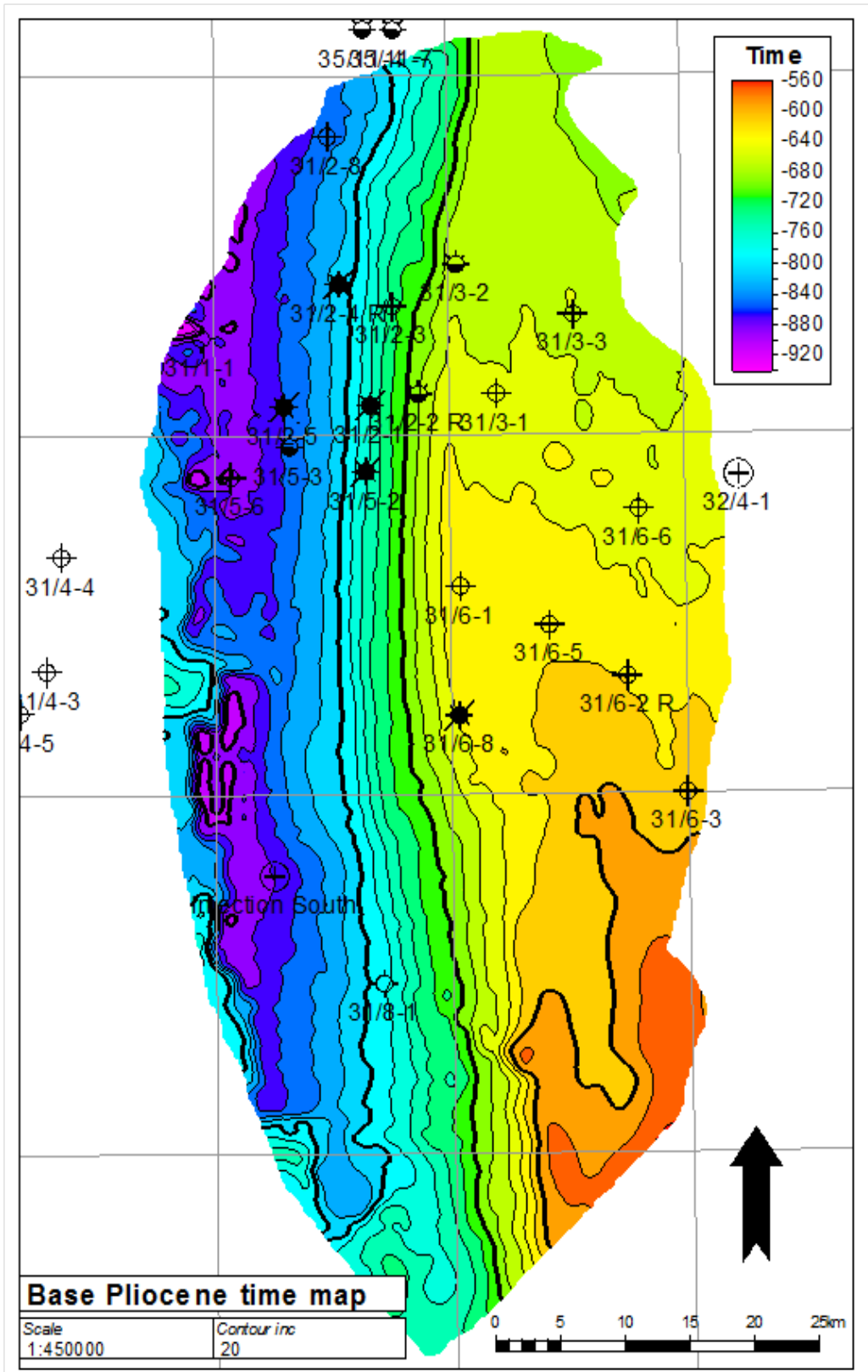


Figure 5: Base Pliocene time map.

DOCUMENT NO.: TL02-GTL-Z-RA-0001	REVISION NO.: 03	REVISION DATE: 01.03.2012	APPROVED:
-------------------------------------	---------------------	------------------------------	-----------

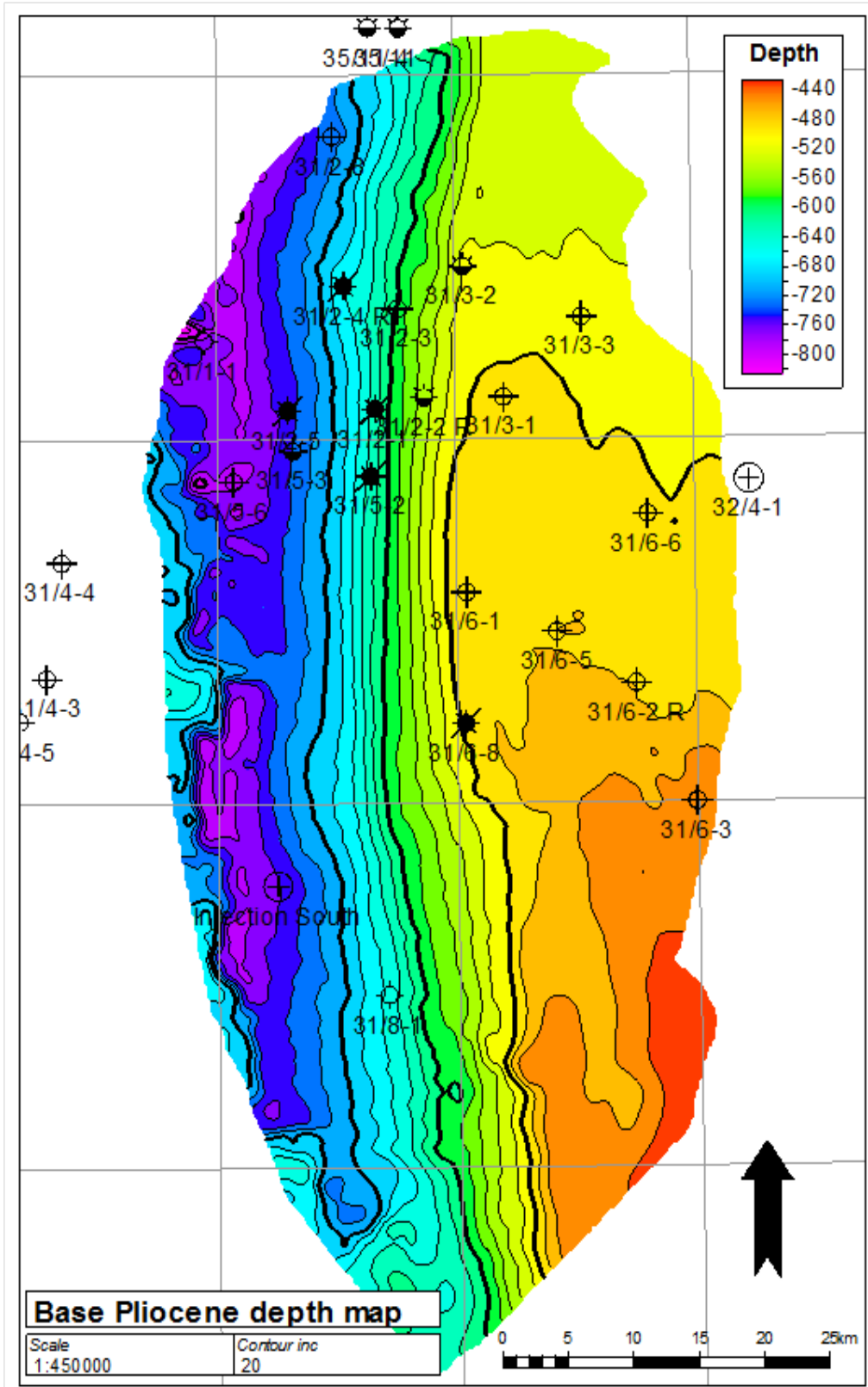


Figure 6: Base Pliocene depth map.

DOCUMENT NO.: TL02-GTL-Z-RA-0001	REVISION NO.: 03	REVISION DATE: 01.03.2012	APPROVED:
-------------------------------------	---------------------	------------------------------	-----------

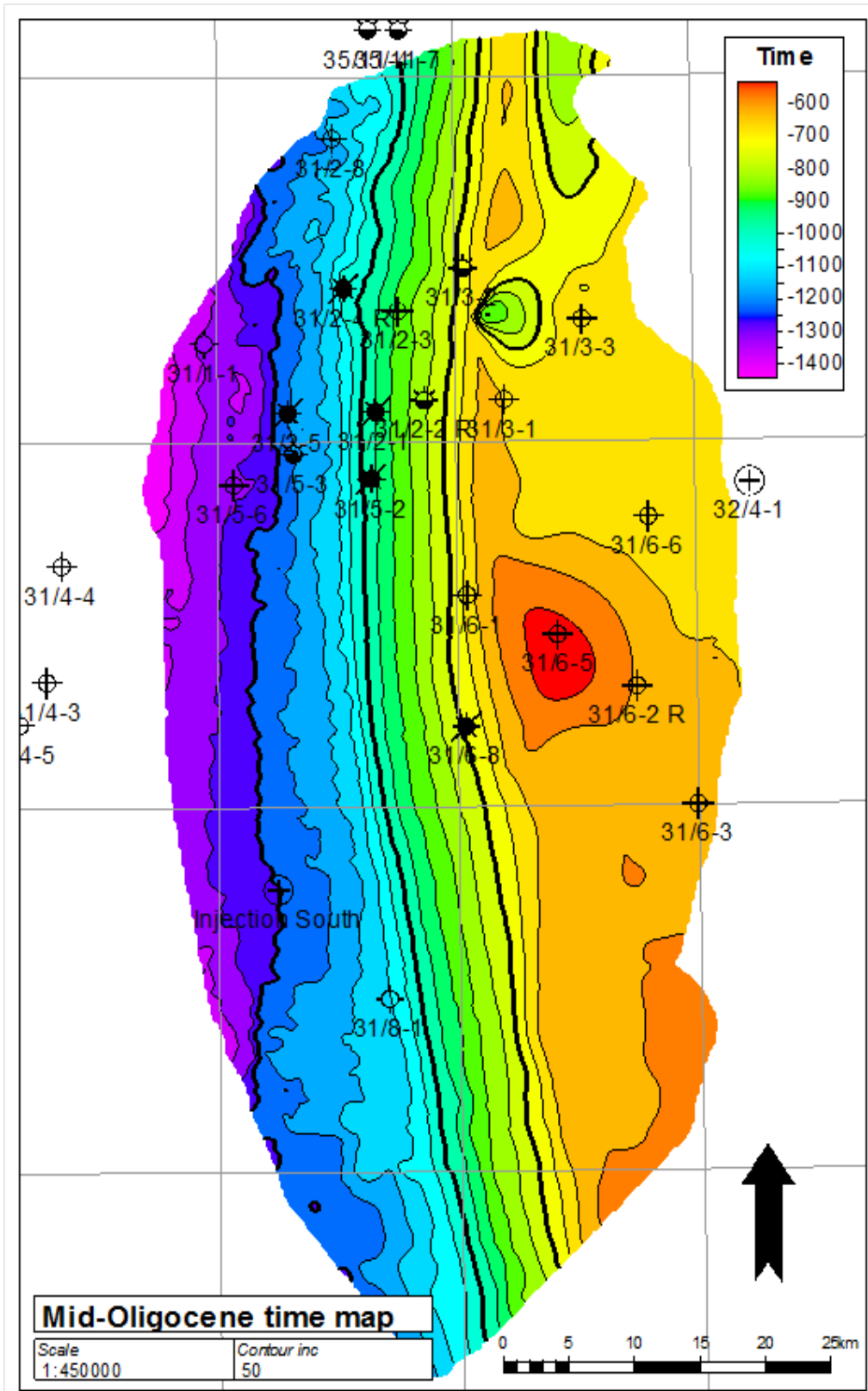


Figure 7: Mid-Oligocene time map.

DOCUMENT NO.: TL02-GTL-Z-RA-0001	REVISION NO.: 03	REVISION DATE: 01.03.2012	APPROVED:
-------------------------------------	---------------------	------------------------------	-----------

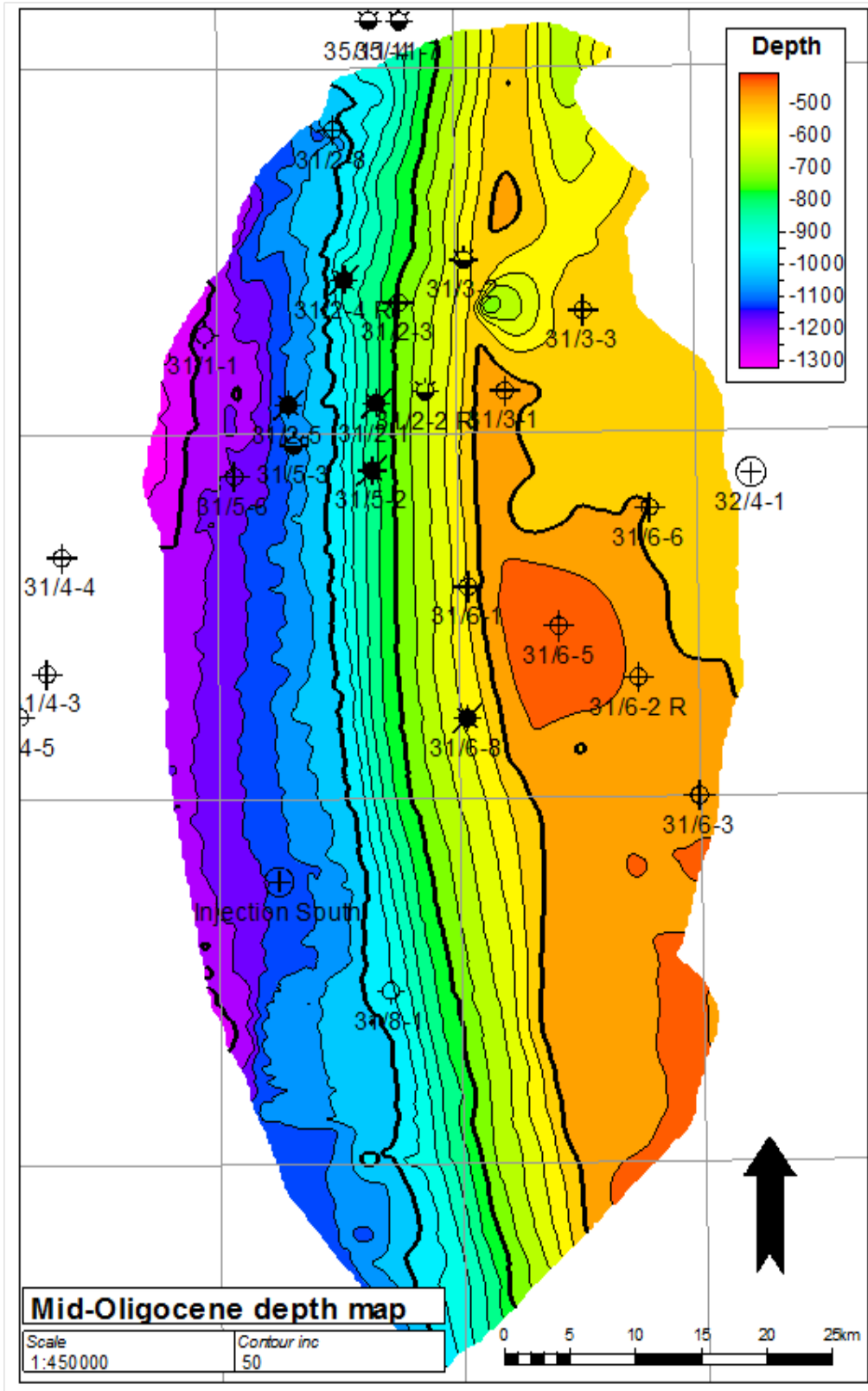


Figure 8: Mid-Oligocene depth map.

DOCUMENT NO.: TL02-GTL-Z-RA-0001	REVISION NO.: 03	REVISION DATE: 01.03.2012	APPROVED:
-------------------------------------	---------------------	------------------------------	-----------

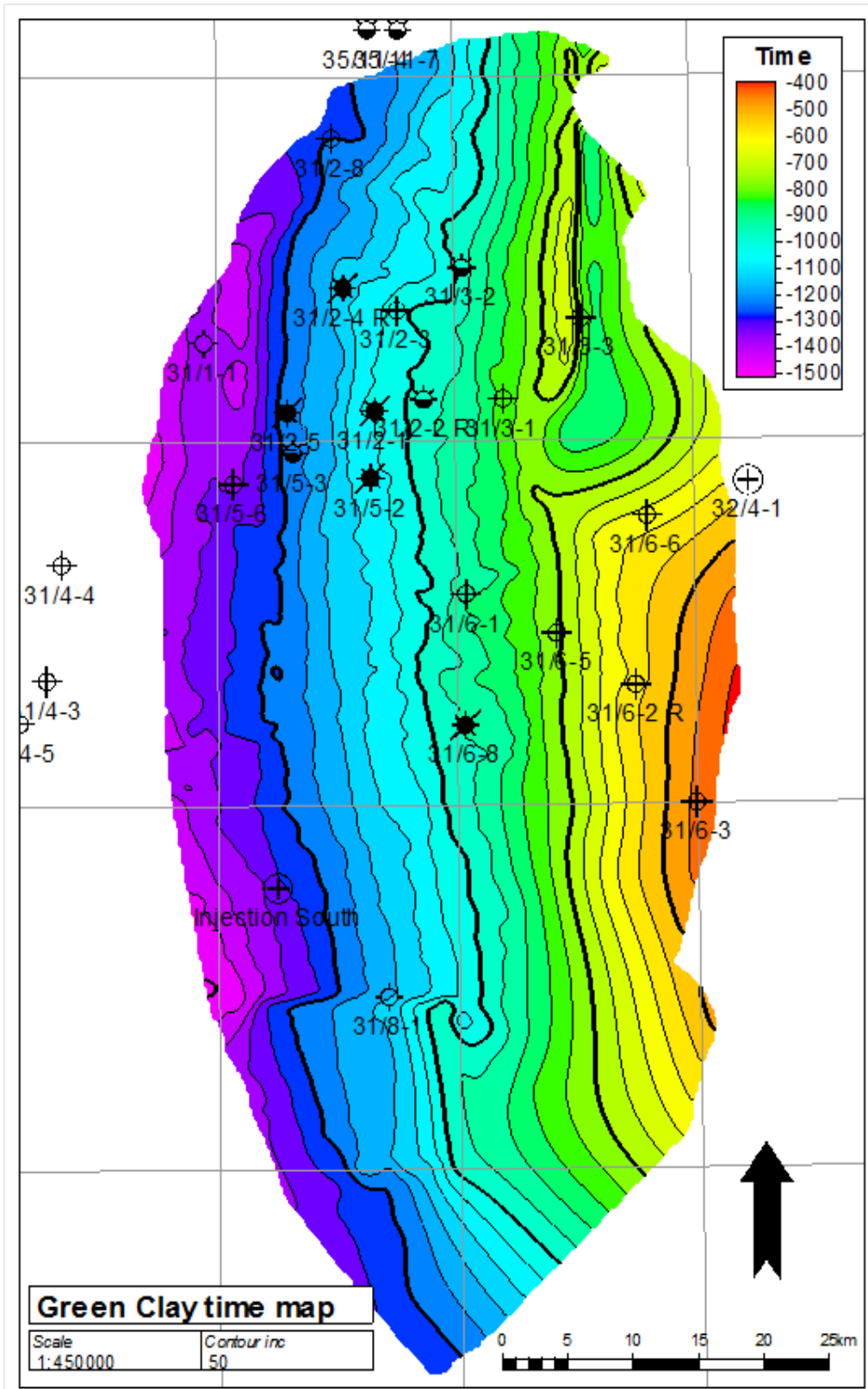


Figure 9: Green clay time map.

DOCUMENT NO.: TL02-GTL-Z-RA-0001	REVISION NO.: 03	REVISION DATE: 01.03.2012	APPROVED:
-------------------------------------	---------------------	------------------------------	-----------

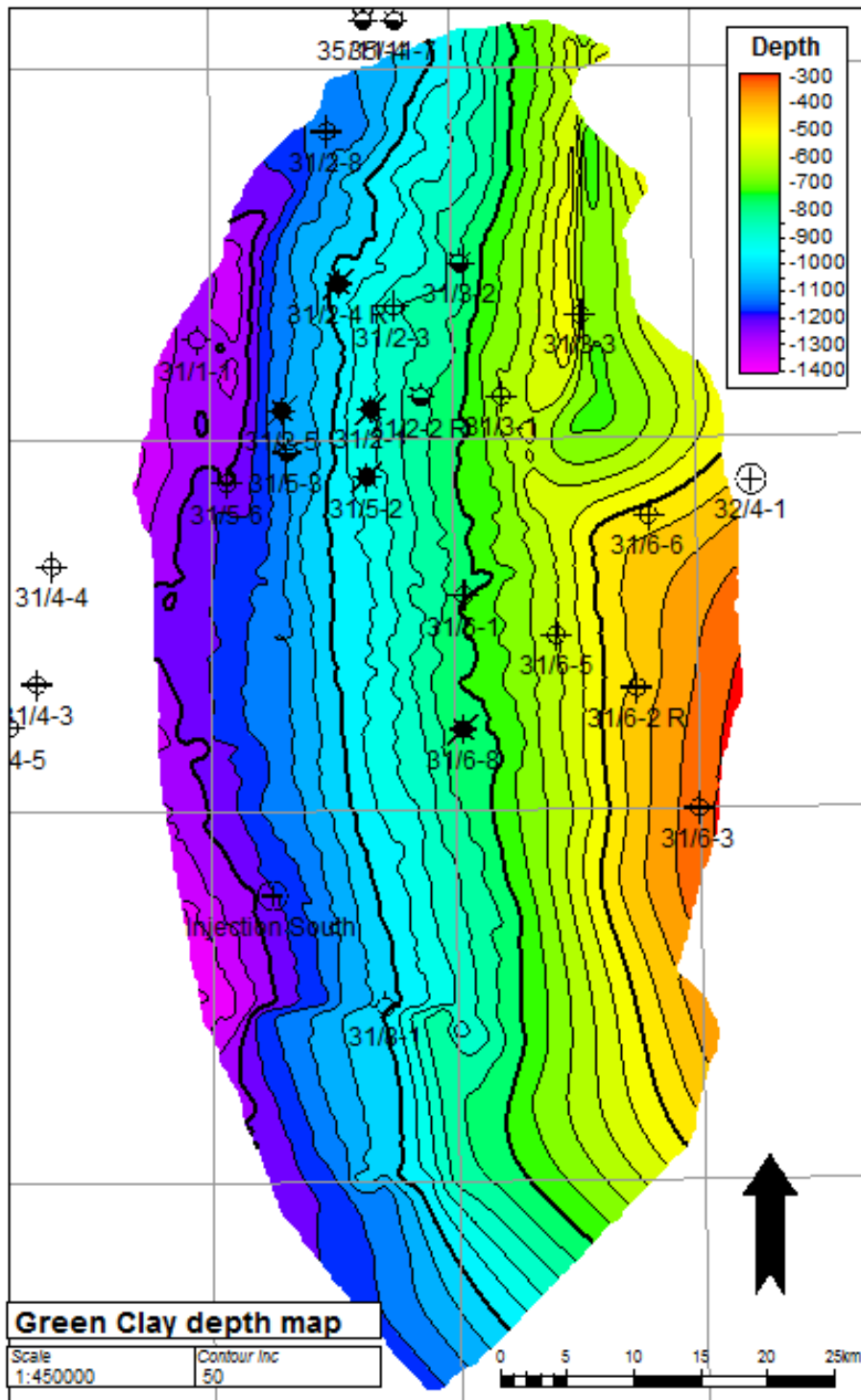


Figure 10: Green Clay depth map.

DOCUMENT NO.: TL02-GTL-Z-RA-0001	REVISION NO.: 03	REVISION DATE: 01.03.2012	APPROVED:
-------------------------------------	---------------------	------------------------------	-----------

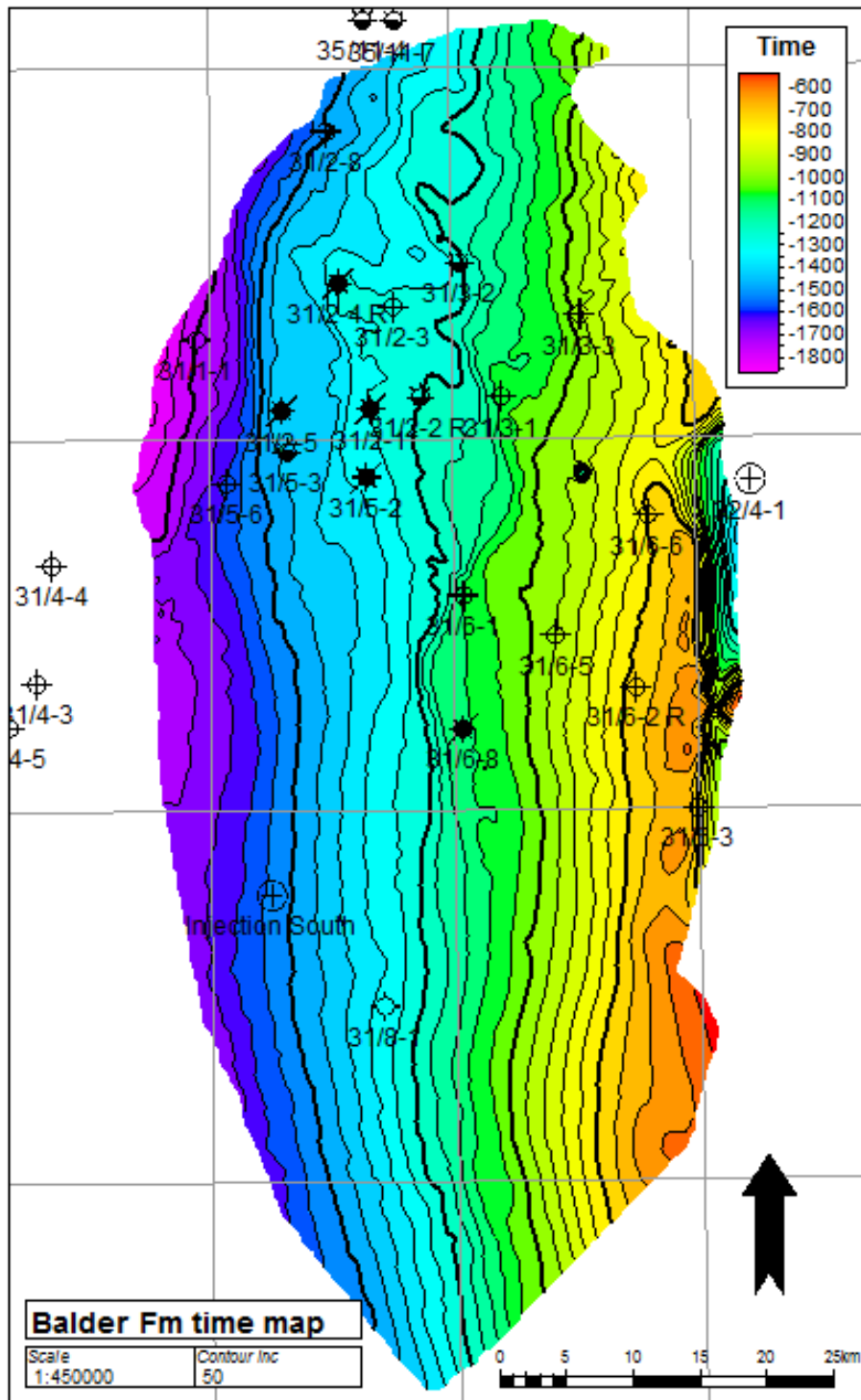


Figure 11: Balder Fm time map.

DOCUMENT NO.: TL02-GTL-Z-RA-0001	REVISION NO.: 03	REVISION DATE: 01.03.2012	APPROVED:
-------------------------------------	---------------------	------------------------------	-----------

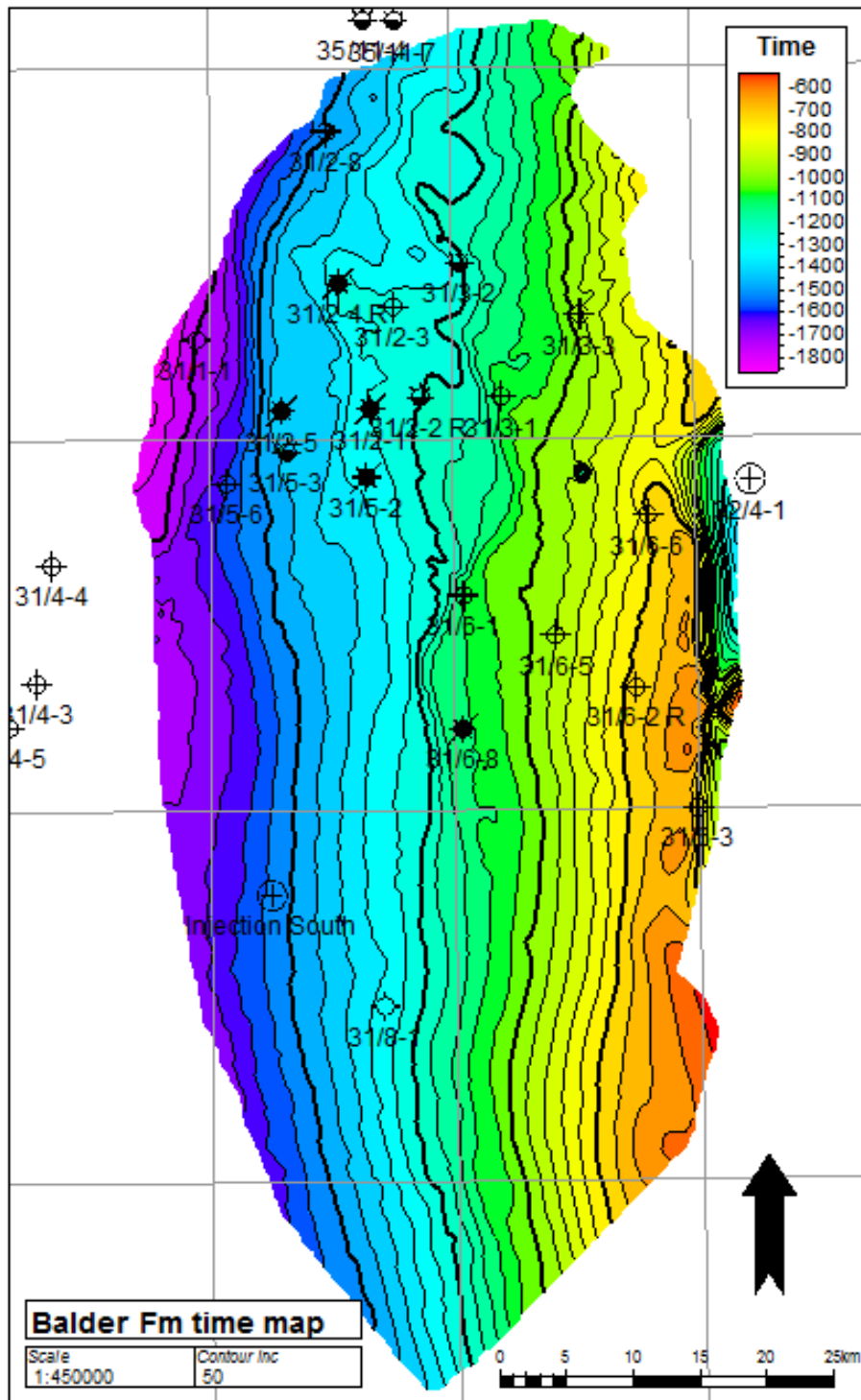


Figure 12: Balder Fm depth map.

DOCUMENT NO.: TL02-GTL-Z-RA-0001	REVISION NO.: 03	REVISION DATE: 01.03.2012	APPROVED:
-------------------------------------	---------------------	------------------------------	-----------

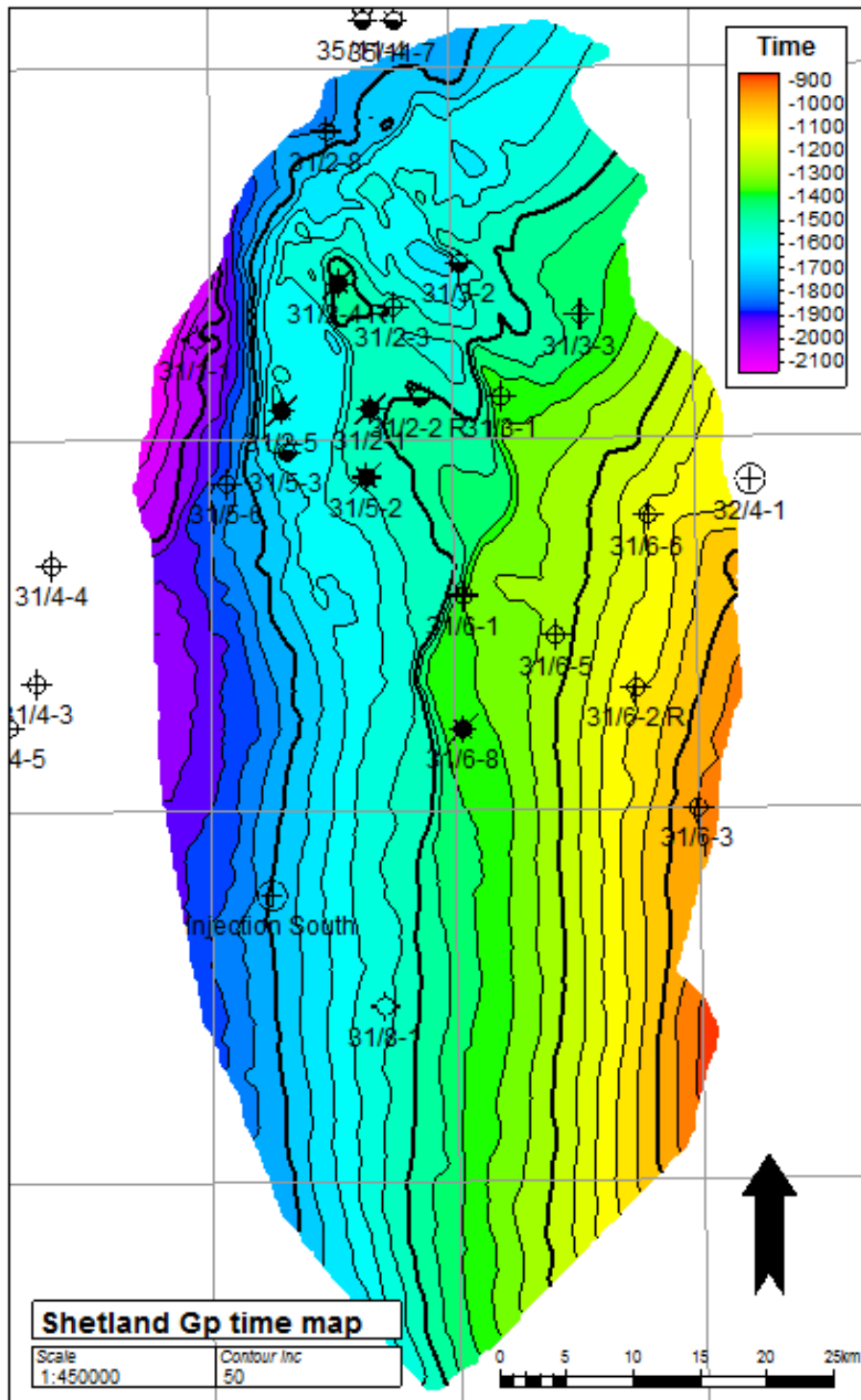


Figure 13: Shetland Gp time map.

DOCUMENT NO.: TL02-GTL-Z-RA-0001	REVISION NO.: 03	REVISION DATE: 01.03.2012	APPROVED:
-------------------------------------	---------------------	------------------------------	-----------

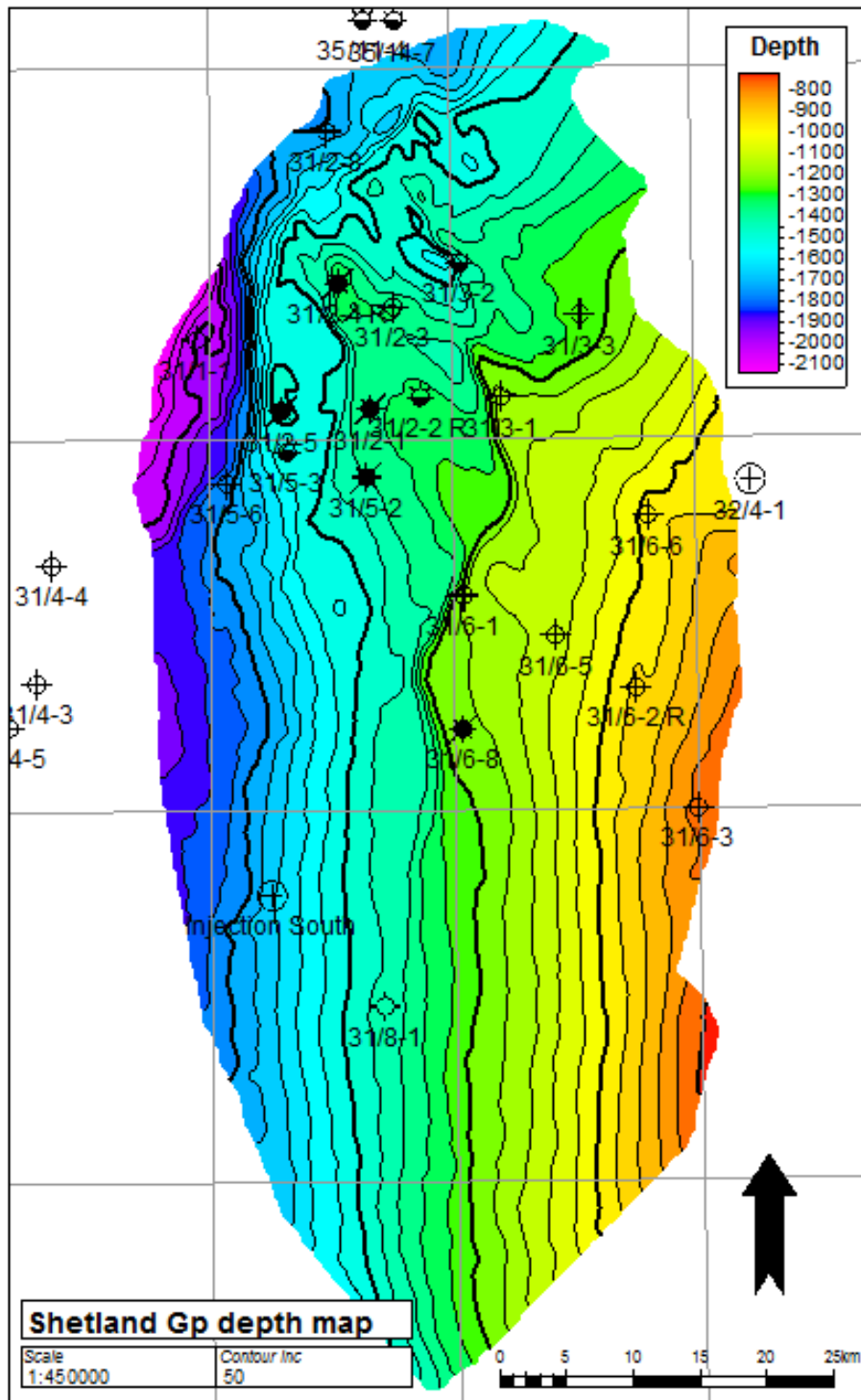


Figure 14: Shetland Gp depth map.

DOCUMENT NO.: TL02-GTL-Z-RA-0001	REVISION NO.: 03	REVISION DATE: 01.03.2012	APPROVED:
-------------------------------------	---------------------	------------------------------	-----------

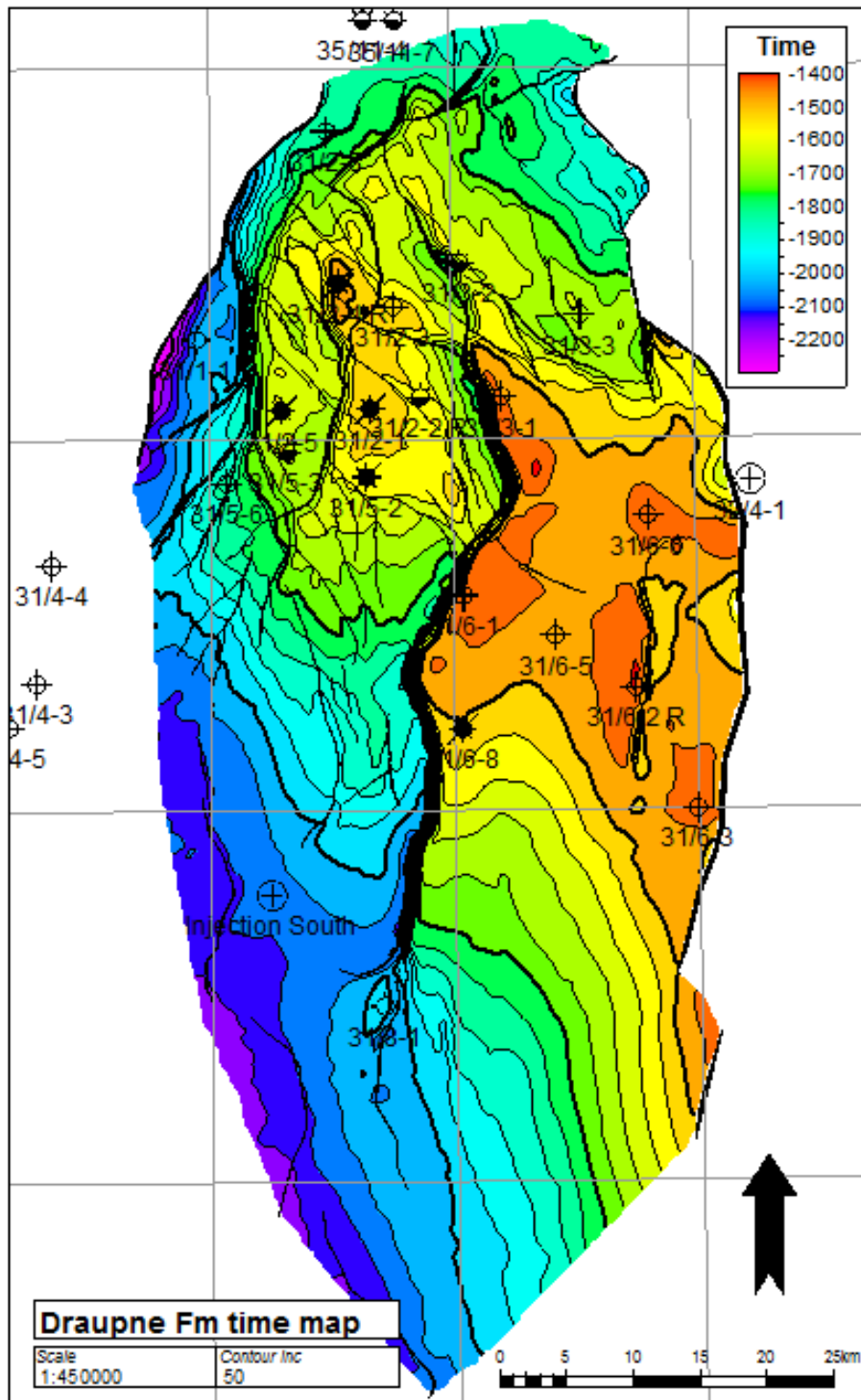


Figure 15: Draupne Fm time map.

DOCUMENT NO.: TL02-GTL-Z-RA-0001	REVISION NO.: 03	REVISION DATE: 01.03.2012	APPROVED:
-------------------------------------	---------------------	------------------------------	-----------

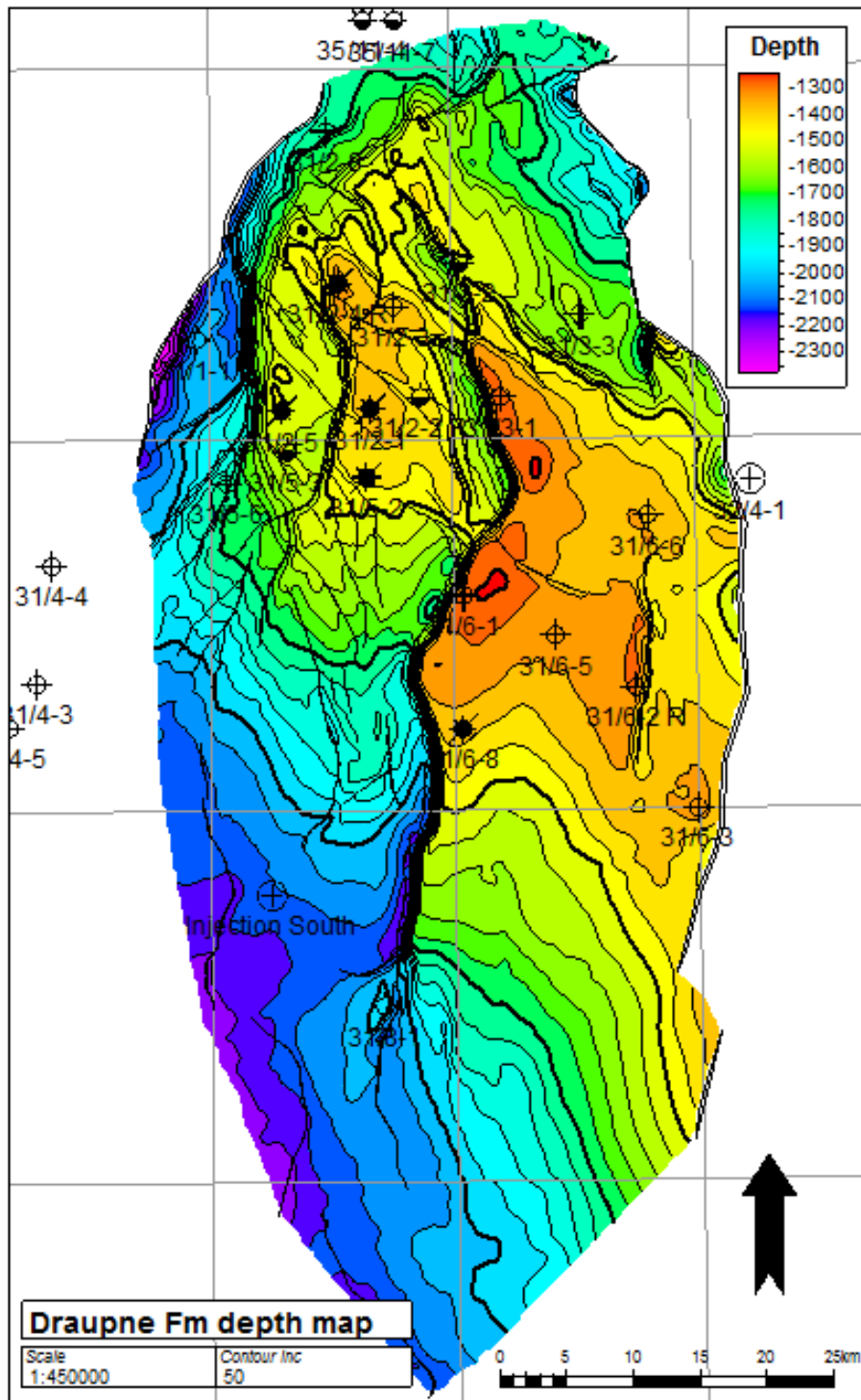


Figure 16: Draupne Fm depth map.

DOCUMENT NO.: TL02-GTL-Z-RA-0001	REVISION NO.: 03	REVISION DATE: 01.03.2012	APPROVED:
-------------------------------------	---------------------	------------------------------	-----------

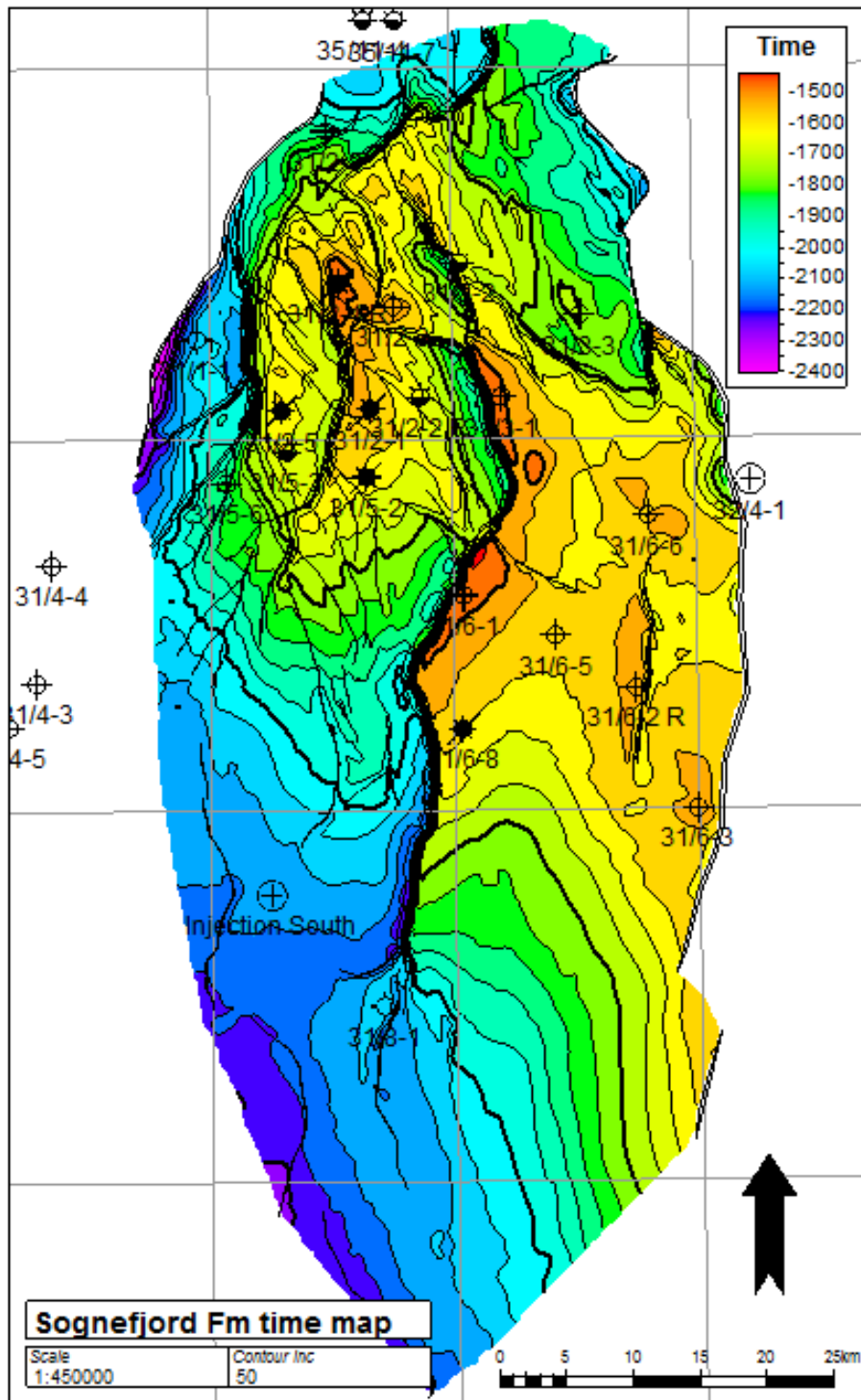


Figure 17: Sognefjord Fm time map.

DOCUMENT NO.: TL02-GTL-Z-RA-0001	REVISION NO.: 03	REVISION DATE: 01.03.2012	APPROVED:
-------------------------------------	---------------------	------------------------------	-----------

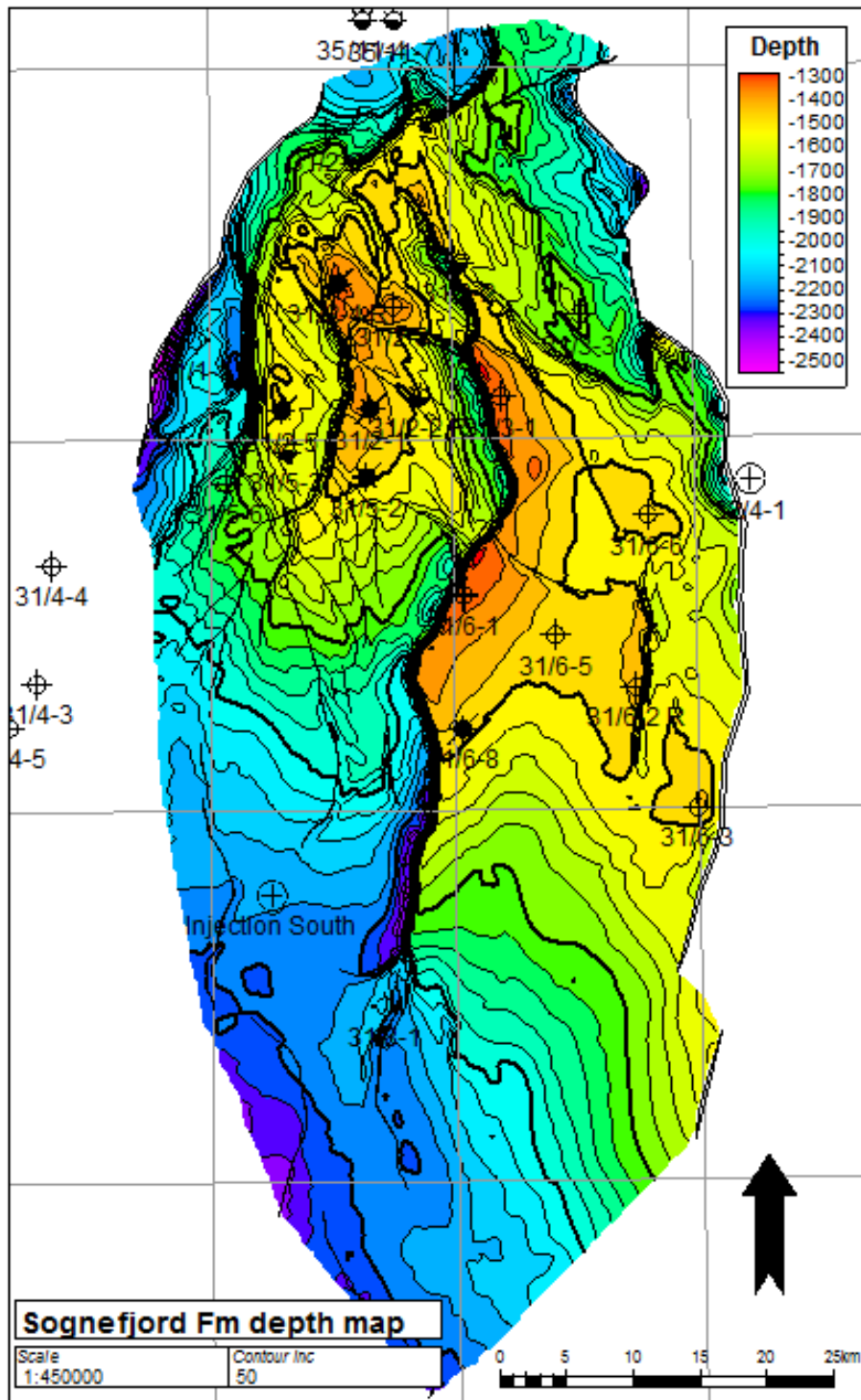


Figure 18: Sognefjord Fm depth map.

DOCUMENT NO.: TL02-GTL-Z-RA-0001	REVISION NO.: 03	REVISION DATE: 01.03.2012	APPROVED:
-------------------------------------	---------------------	------------------------------	-----------

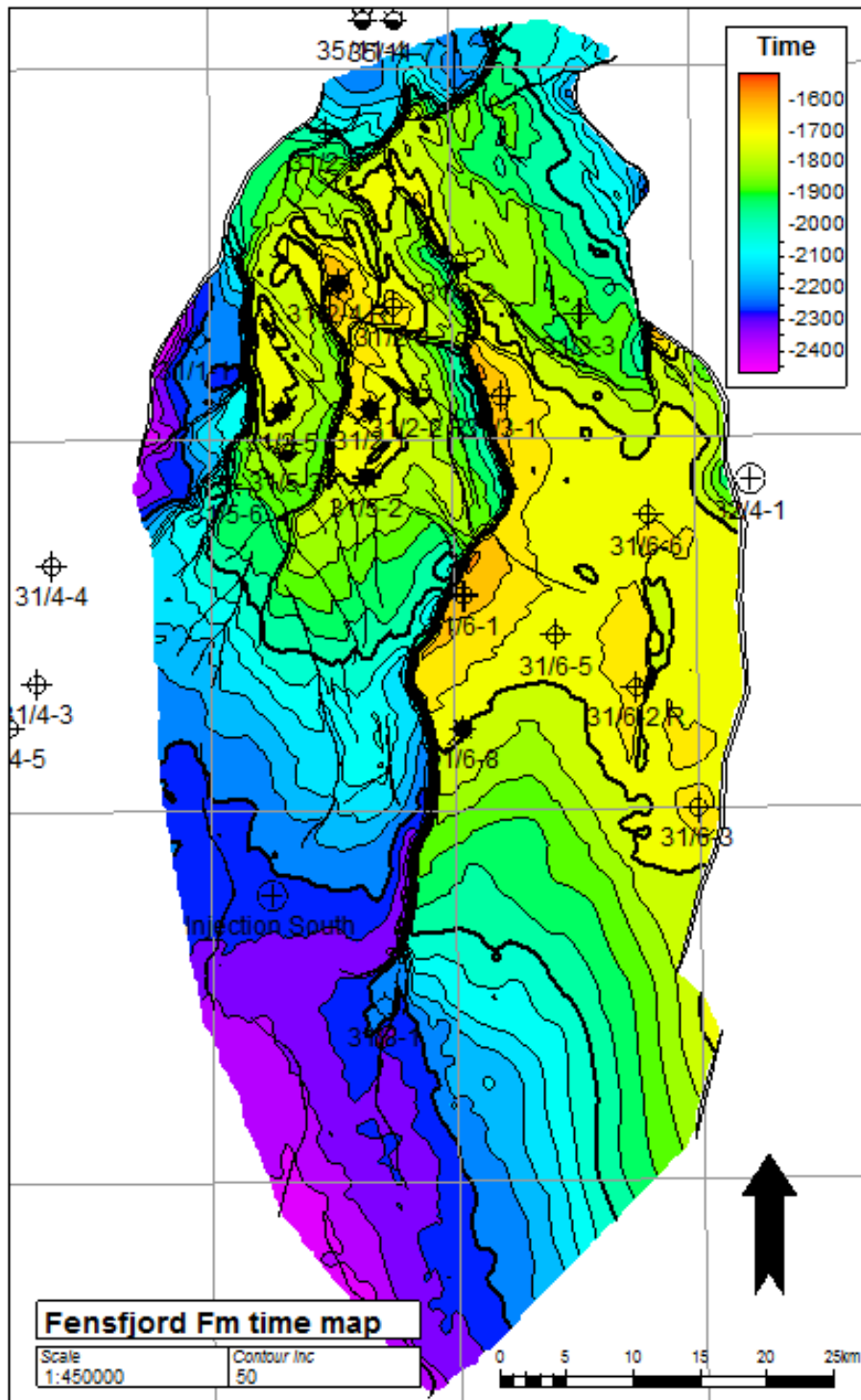


Figure 19: Fensfjord Fm time map.

DOCUMENT NO.: TL02-GTL-Z-RA-0001	REVISION NO.: 03	REVISION DATE: 01.03.2012	APPROVED:
-------------------------------------	---------------------	------------------------------	-----------

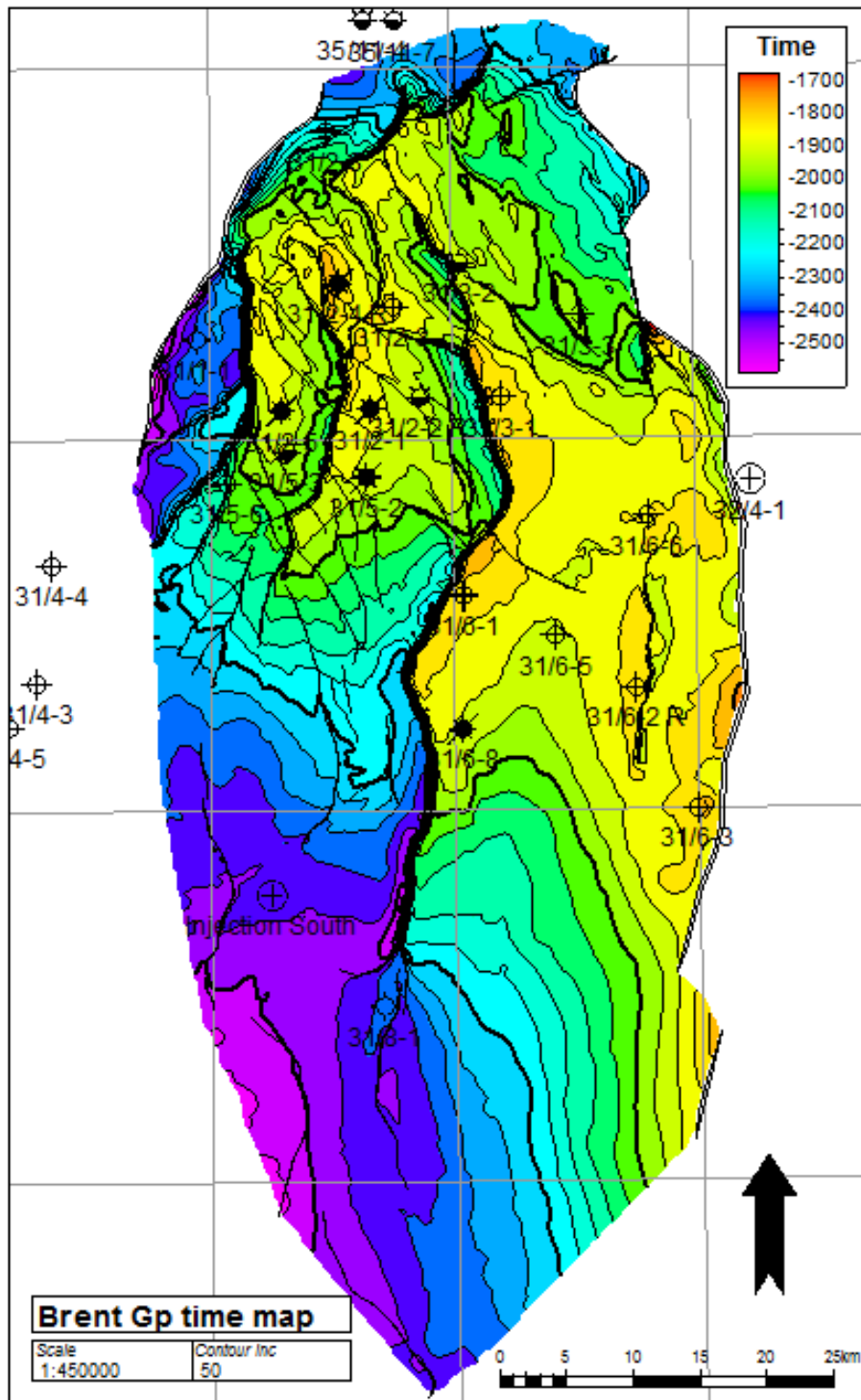


Figure 21: Brent Gp time map.

DOCUMENT NO.: TL02-GTL-Z-RA-0001	REVISION NO.: 03	REVISION DATE: 01.03.2012	APPROVED:
-------------------------------------	---------------------	------------------------------	-----------

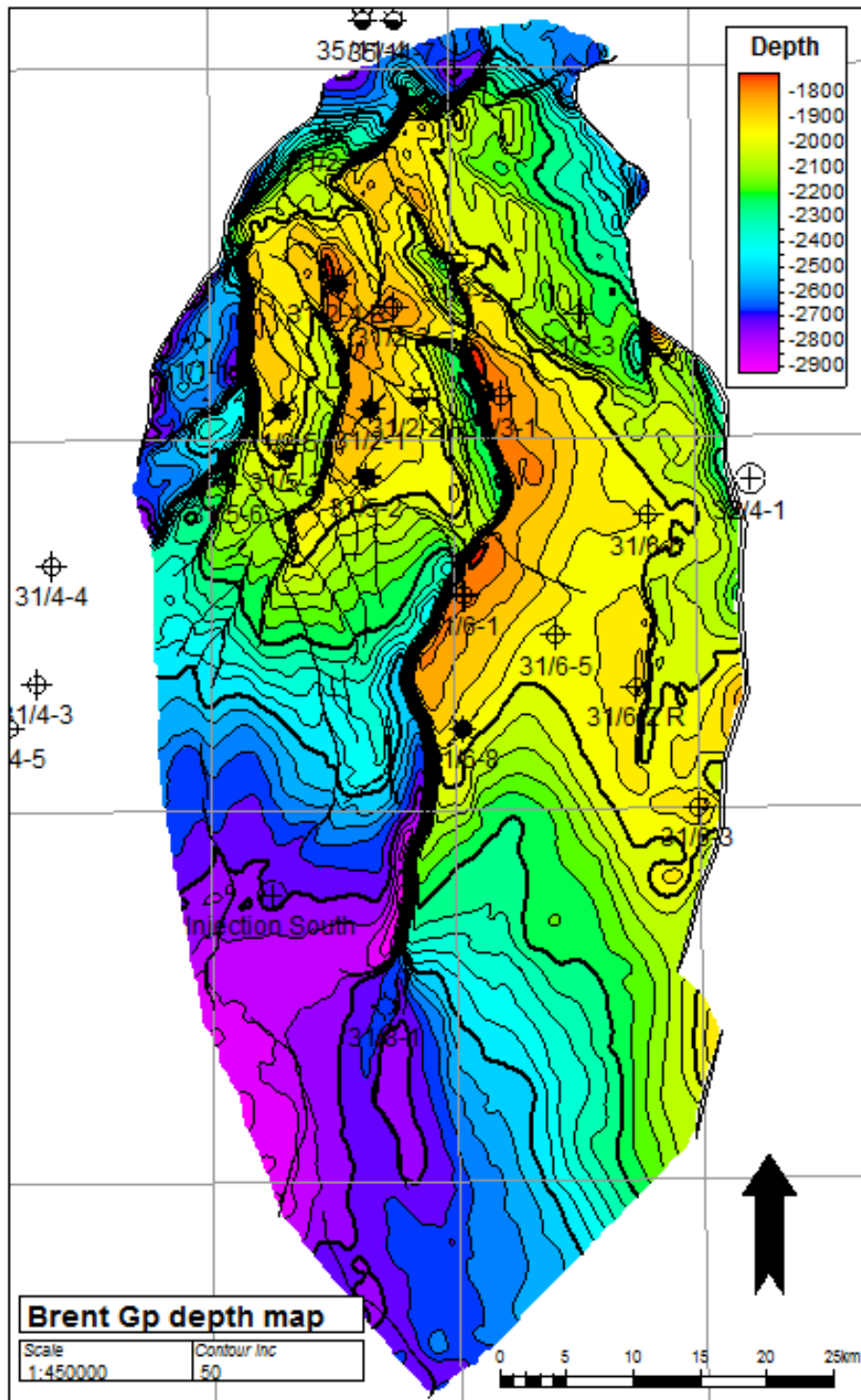


Figure 22: Brent Gp depth map.

DOCUMENT NO.: TL02-GTL-Z-RA-0001	REVISION NO.: 03	REVISION DATE: 01.03.2012	APPROVED:
-------------------------------------	---------------------	------------------------------	-----------

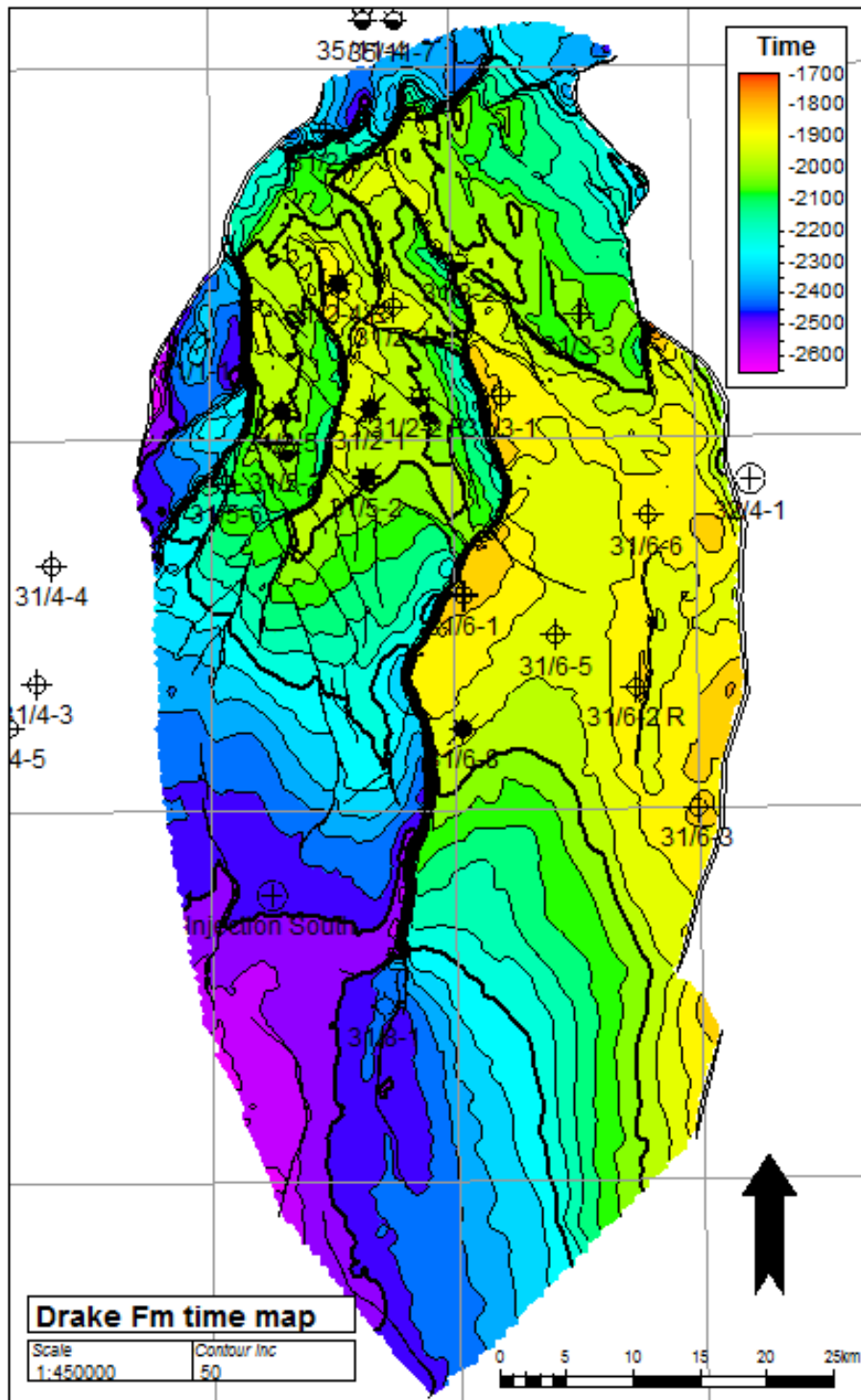


Figure 23: Drake Fm time map.

DOCUMENT NO.: TL02-GTL-Z-RA-0001	REVISION NO.: 03	REVISION DATE: 01.03.2012	APPROVED:
-------------------------------------	---------------------	------------------------------	-----------

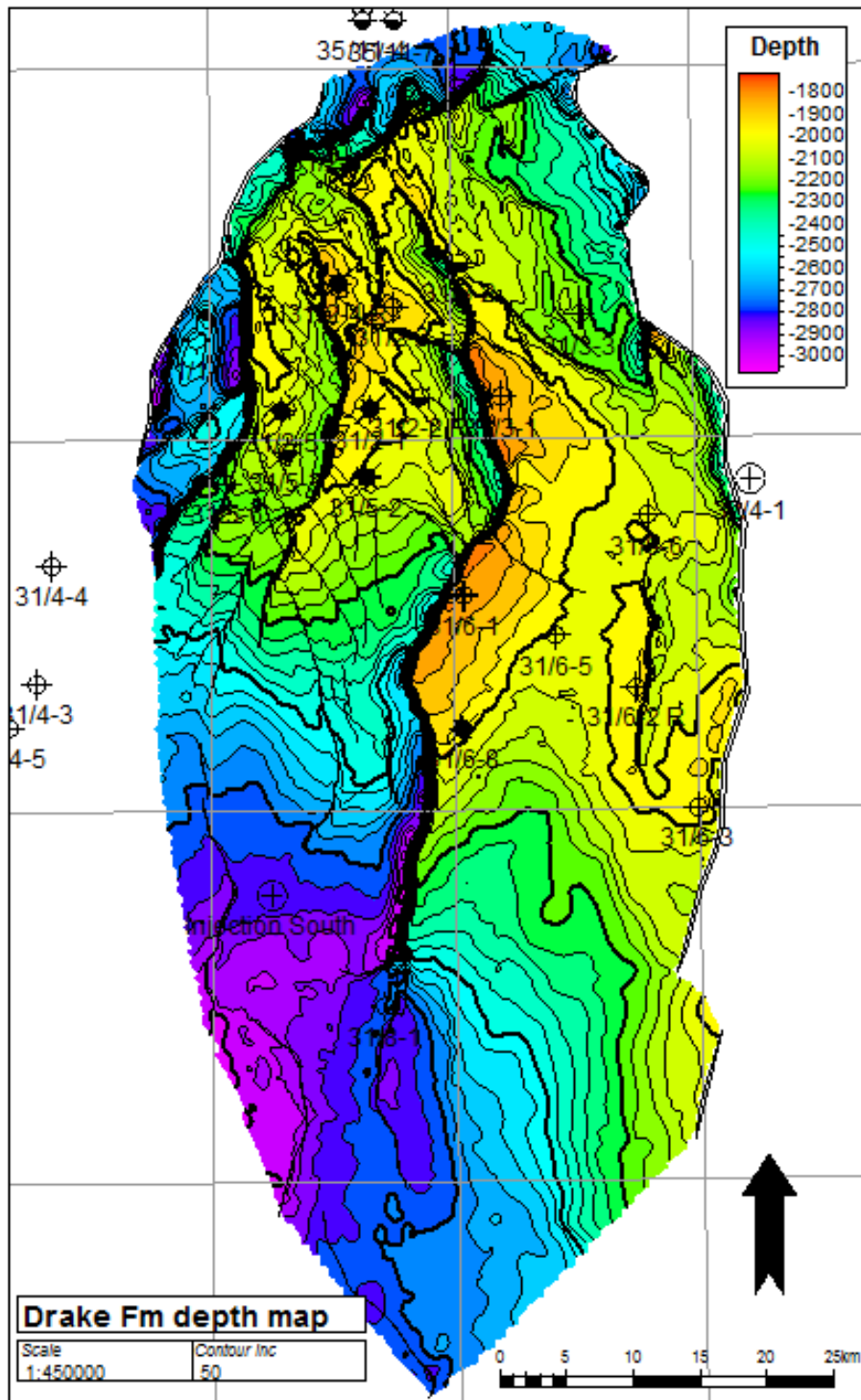


Figure 24: Drake Fm depth map.

DOCUMENT NO.: TL02-GTL-Z-RA-0001	REVISION NO.: 03	REVISION DATE: 01.03.2012	APPROVED:
-------------------------------------	---------------------	------------------------------	-----------

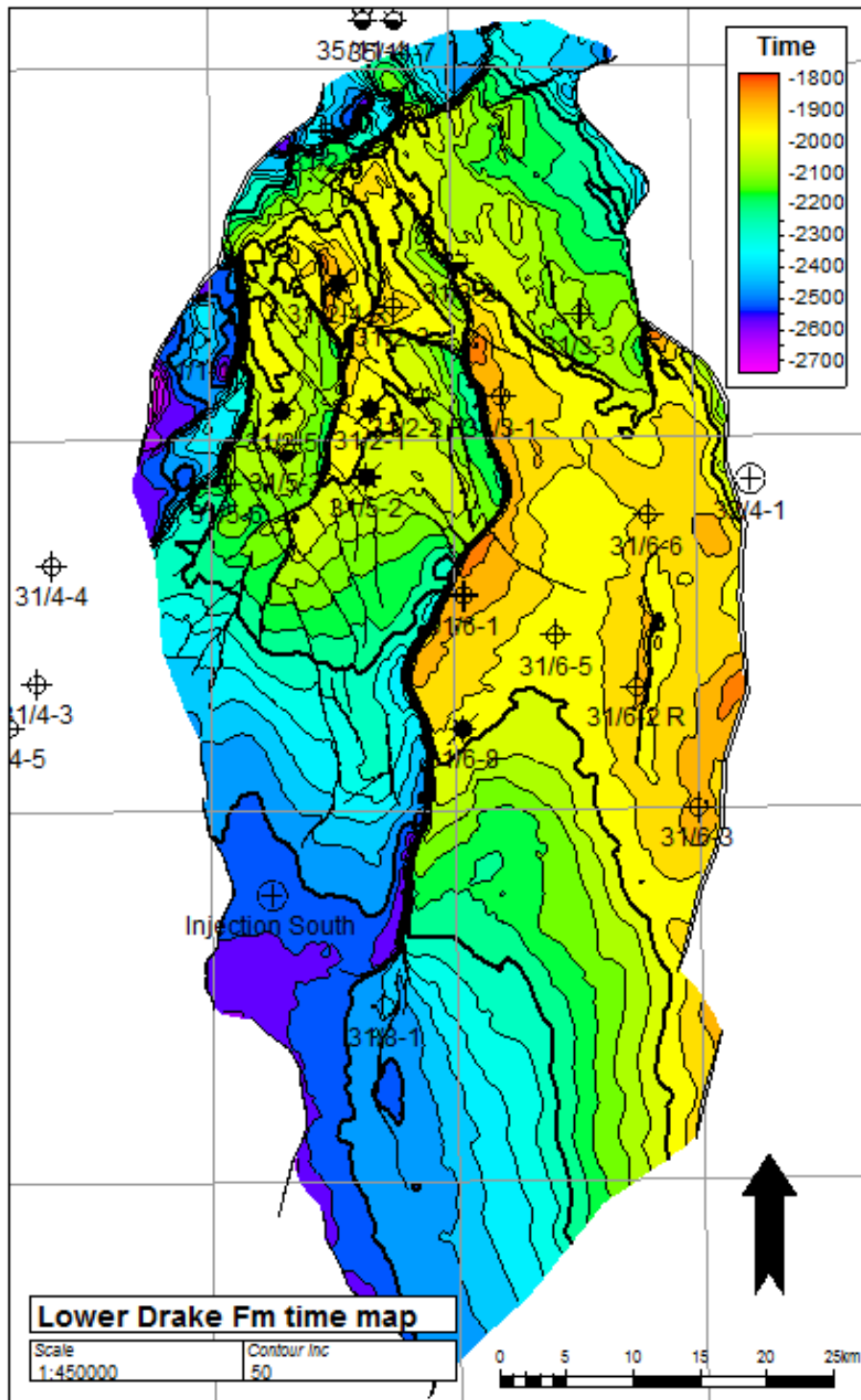


Figure 25: Lower Drake Fm time map.

DOCUMENT NO.: TL02-GTL-Z-RA-0001	REVISION NO.: 03	REVISION DATE: 01.03.2012	APPROVED:
-------------------------------------	---------------------	------------------------------	-----------

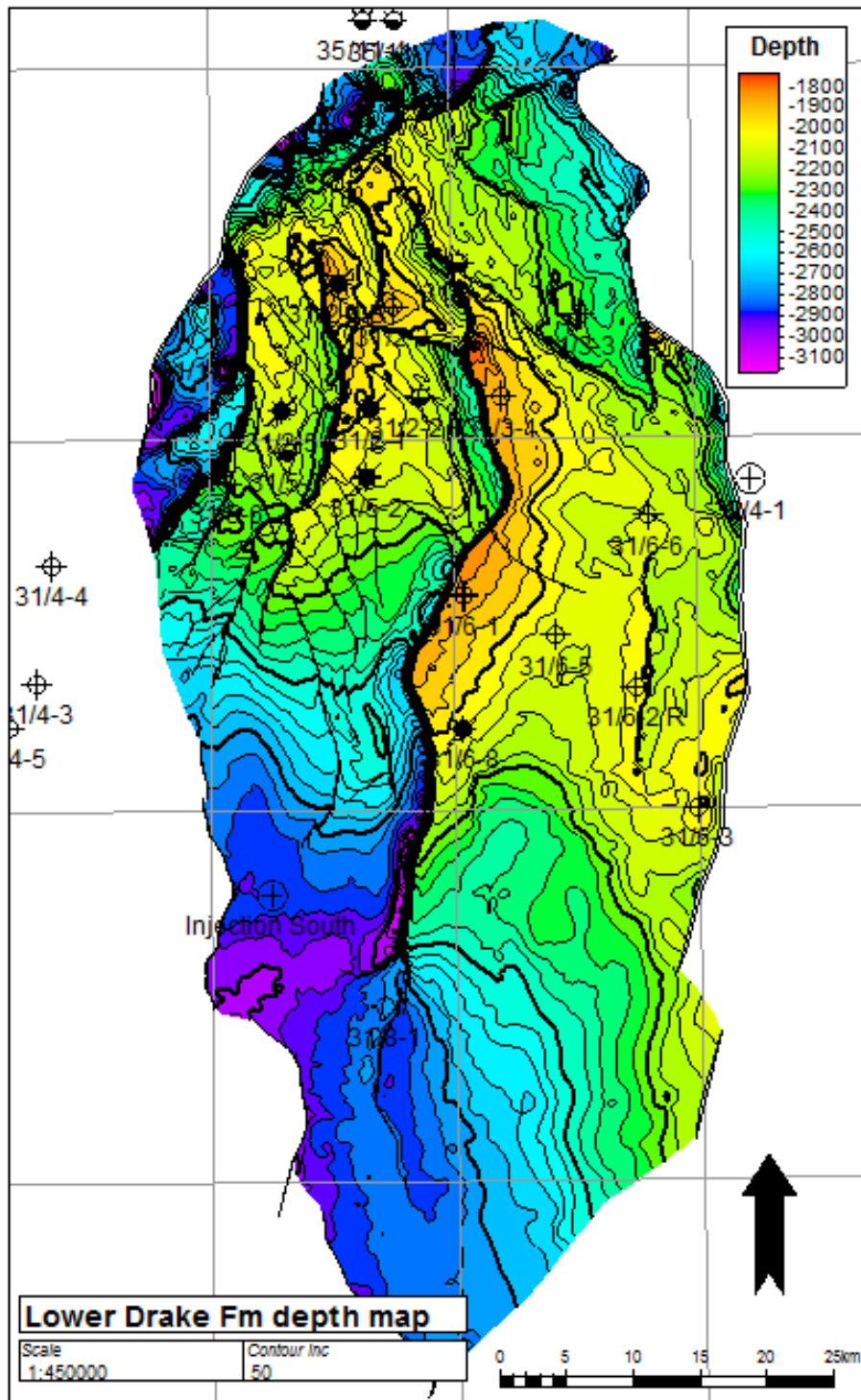


Figure 26: Lower Drake Fm depth map.

DOCUMENT NO.: TL02-GTL-Z-RA-0001	REVISION NO.: 03	REVISION DATE: 01.03.2012	APPROVED:
-------------------------------------	---------------------	------------------------------	-----------

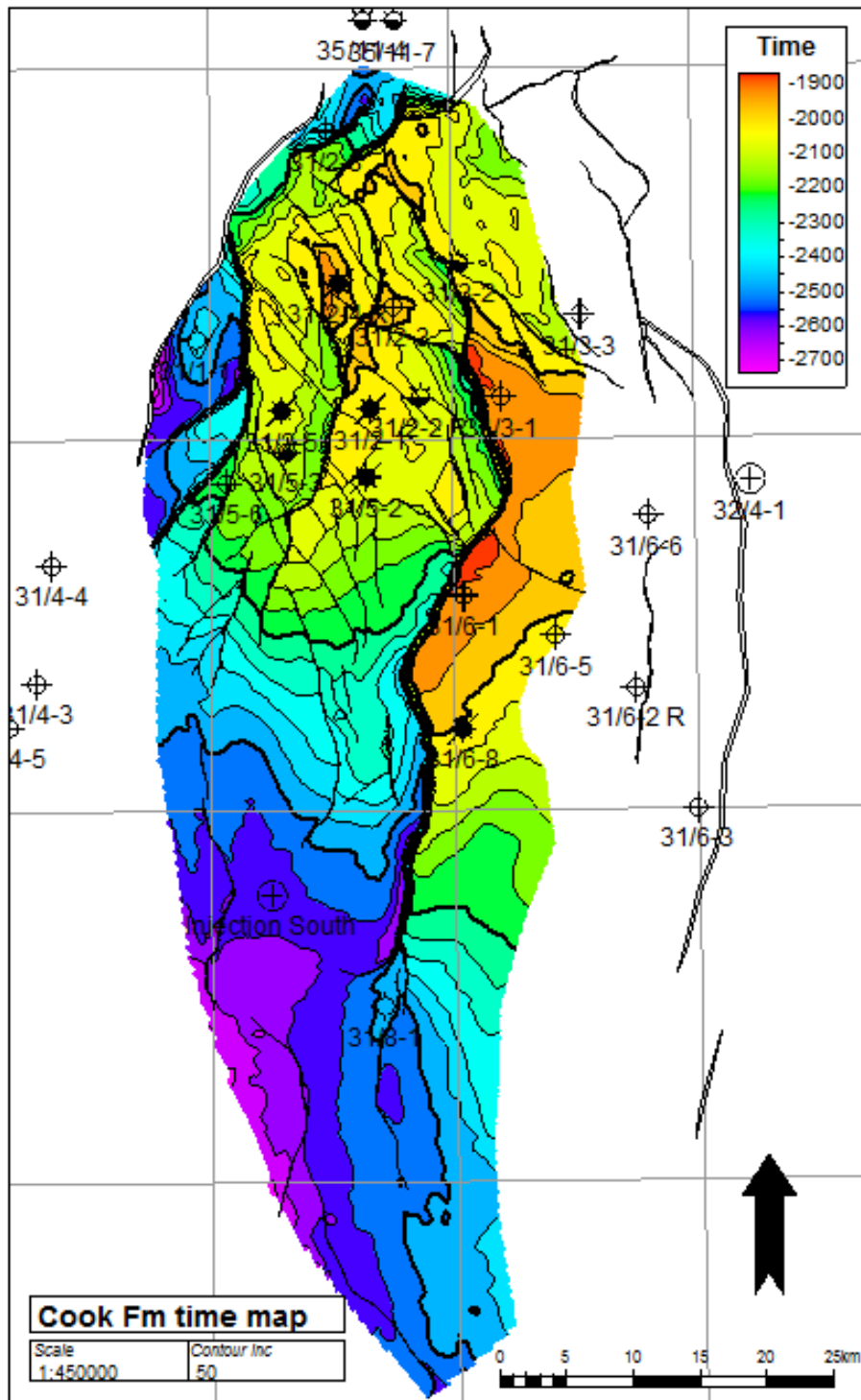


Figure 27: Cook Fm time map.

DOCUMENT NO.: TL02-GTL-Z-RA-0001	REVISION NO.: 03	REVISION DATE: 01.03.2012	APPROVED:
-------------------------------------	---------------------	------------------------------	-----------

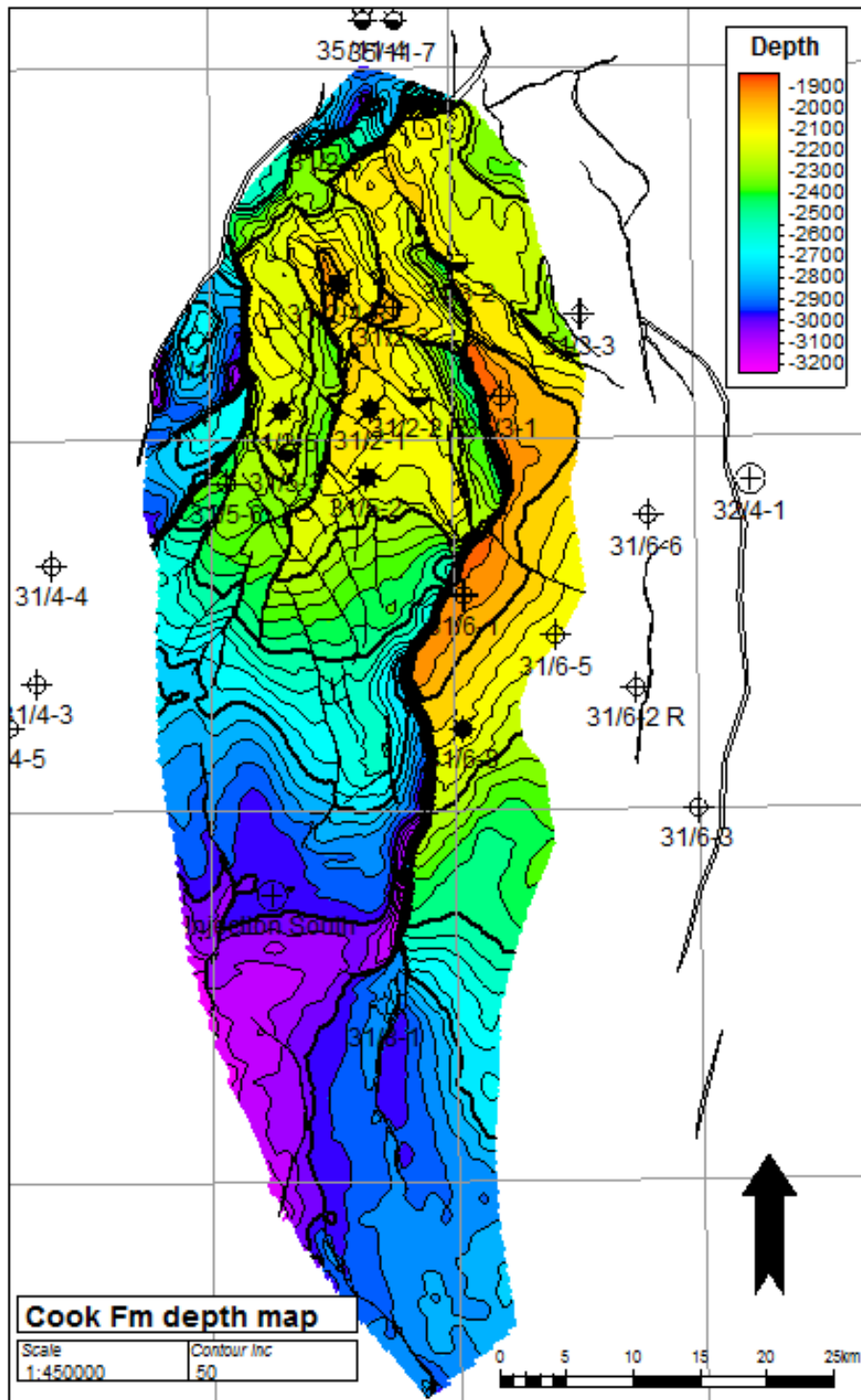


Figure 28: Cook Fm depth map.

DOCUMENT NO.: TL02-GTL-Z-RA-0001	REVISION NO.: 03	REVISION DATE: 01.03.2012	APPROVED:
-------------------------------------	---------------------	------------------------------	-----------

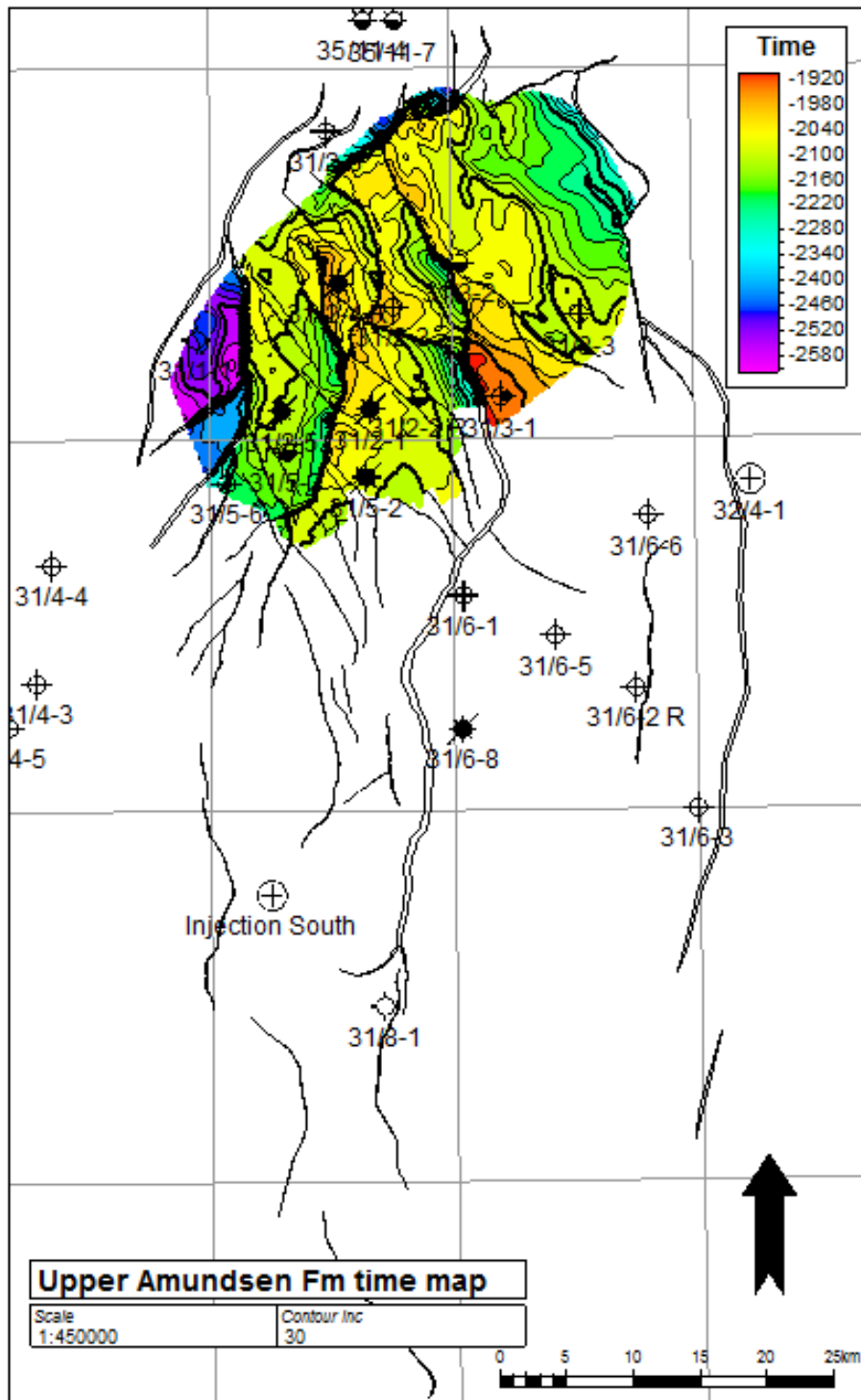


Figure 29: Upper Amundsen Fm time map.

DOCUMENT NO.: TL02-GTL-Z-RA-0001	REVISION NO.: 03	REVISION DATE: 01.03.2012	APPROVED:
-------------------------------------	---------------------	------------------------------	-----------

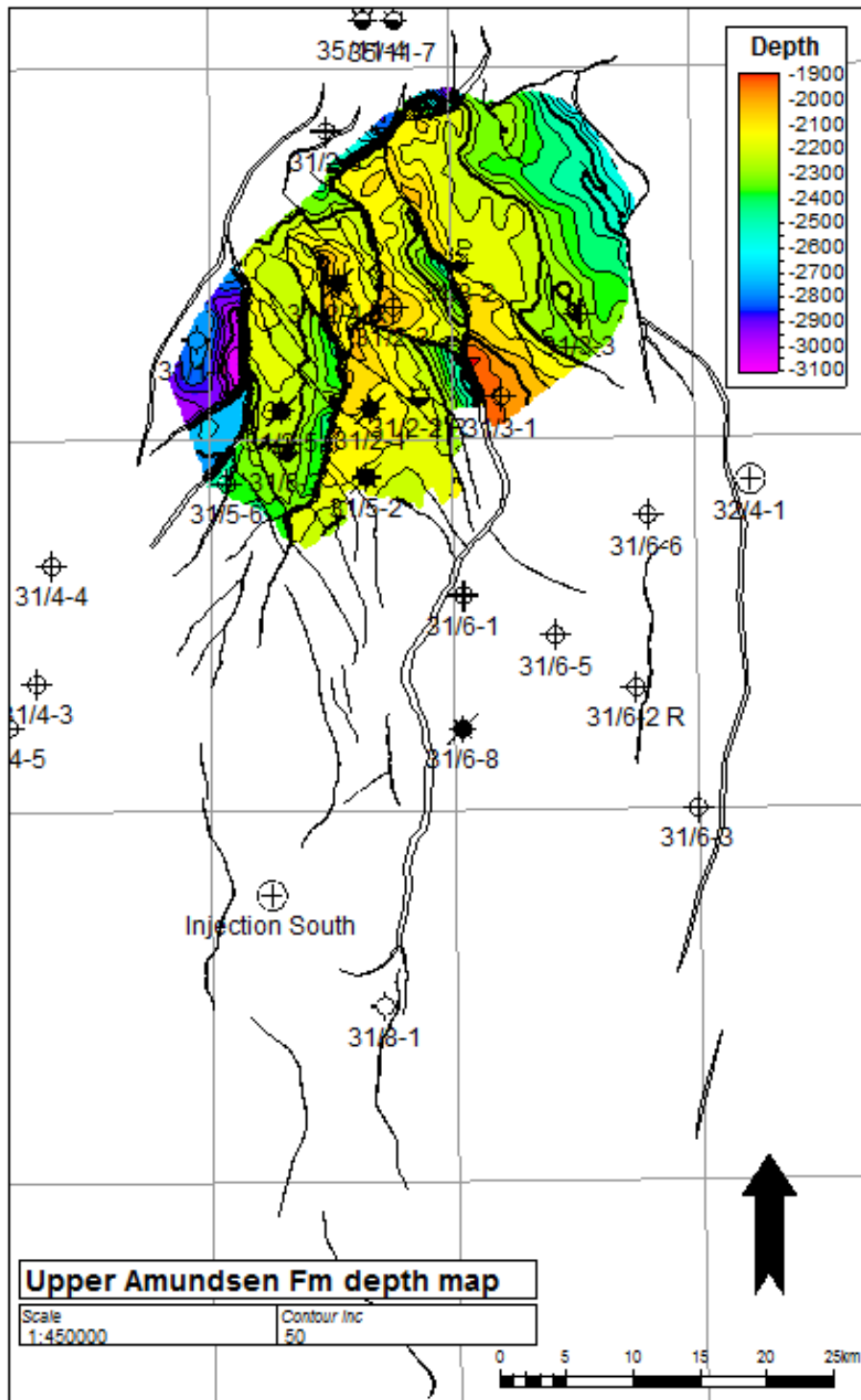


Figure 30: Upper Amundsen Fm depth map.

DOCUMENT NO.: TL02-GTL-Z-RA-0001	REVISION NO.: 03	REVISION DATE: 01.03.2012	APPROVED:
-------------------------------------	---------------------	------------------------------	-----------

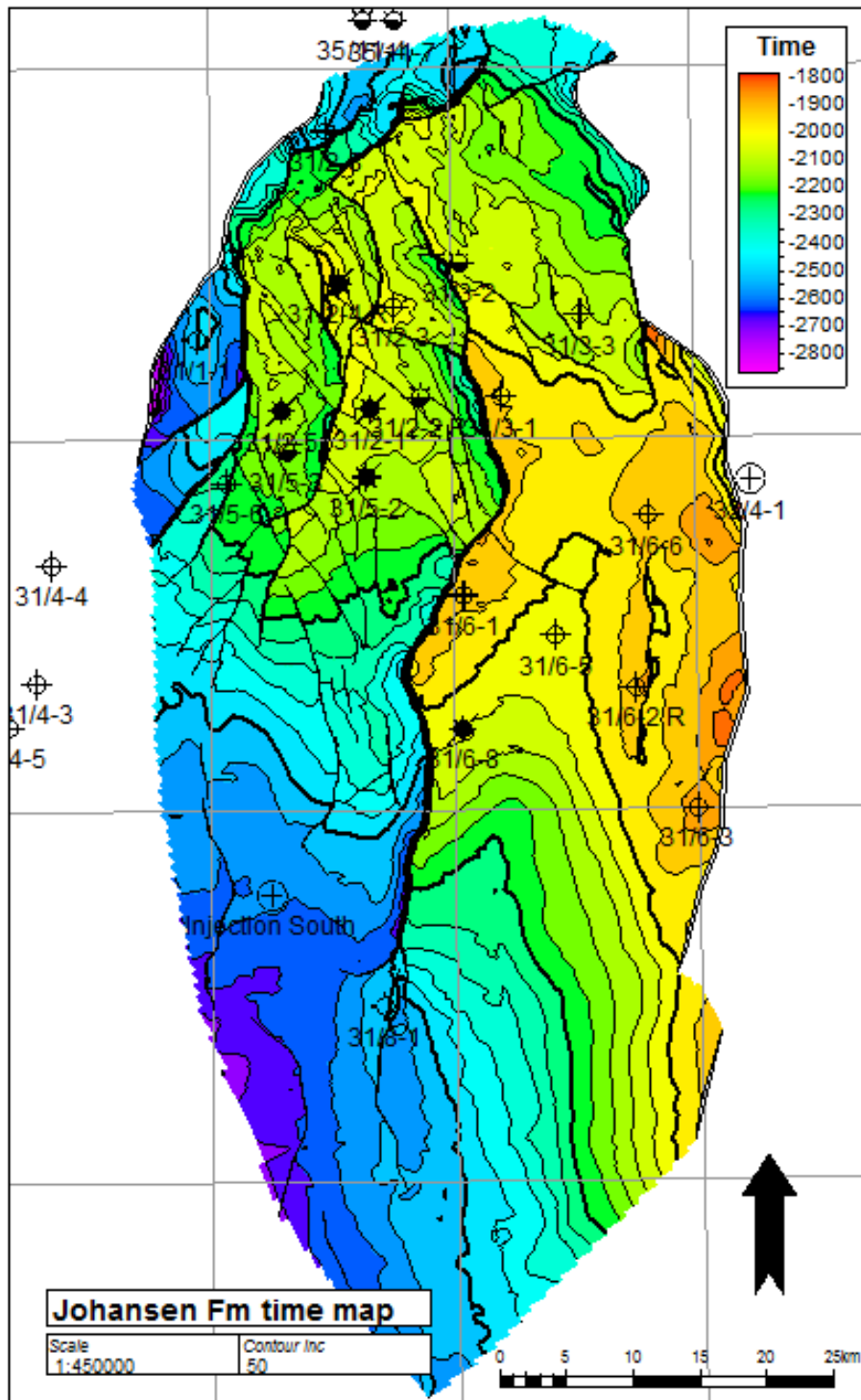


Figure 31: Johansen Fm time map.

DOCUMENT NO.: TL02-GTL-Z-RA-0001	REVISION NO.: 03	REVISION DATE: 01.03.2012	APPROVED:
-------------------------------------	---------------------	------------------------------	-----------

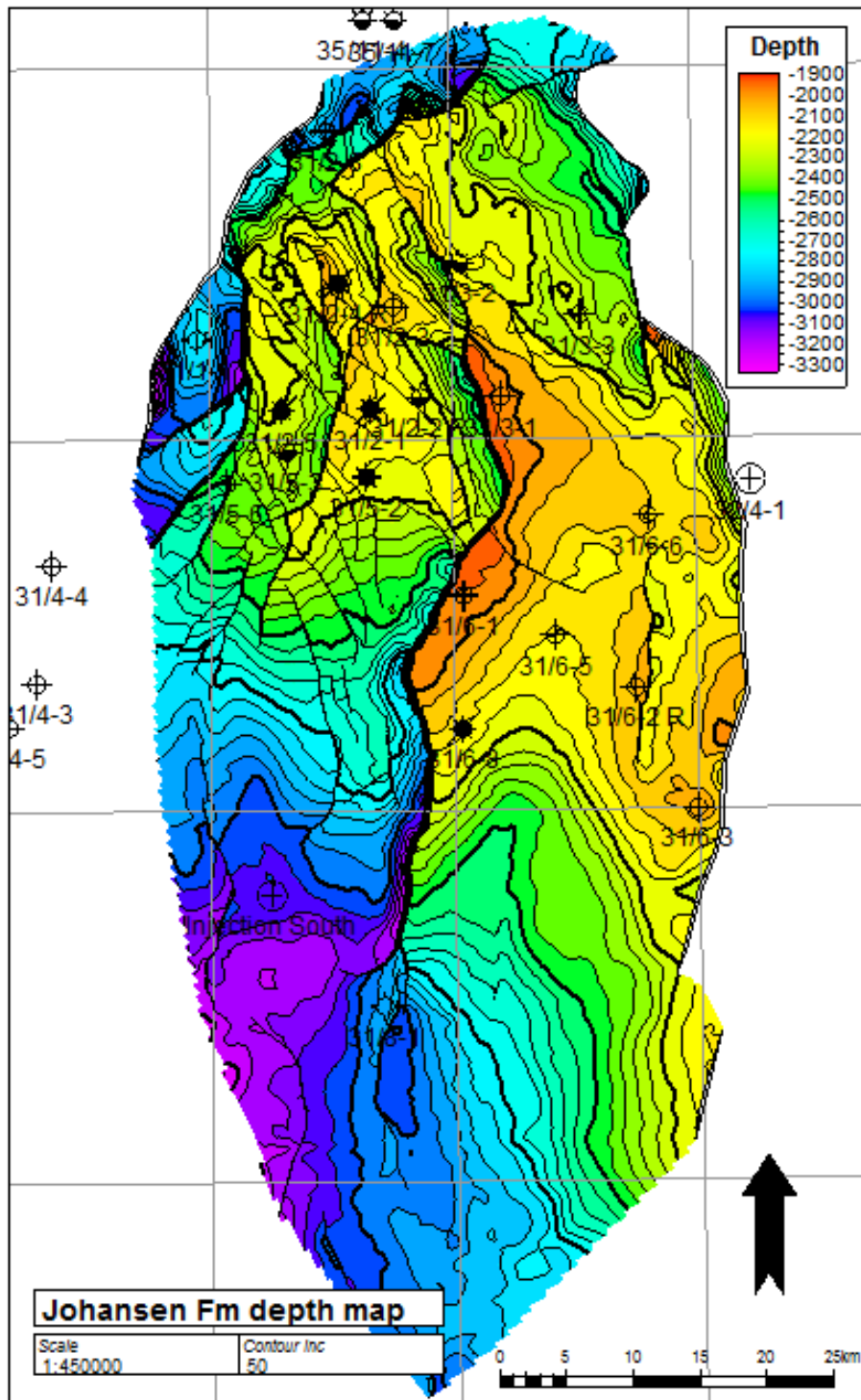


Figure 32: Johansen Fm depth map.

DOCUMENT NO.: TL02-GTL-Z-RA-0001	REVISION NO.: 03	REVISION DATE: 01.03.2012	APPROVED:
-------------------------------------	---------------------	------------------------------	-----------

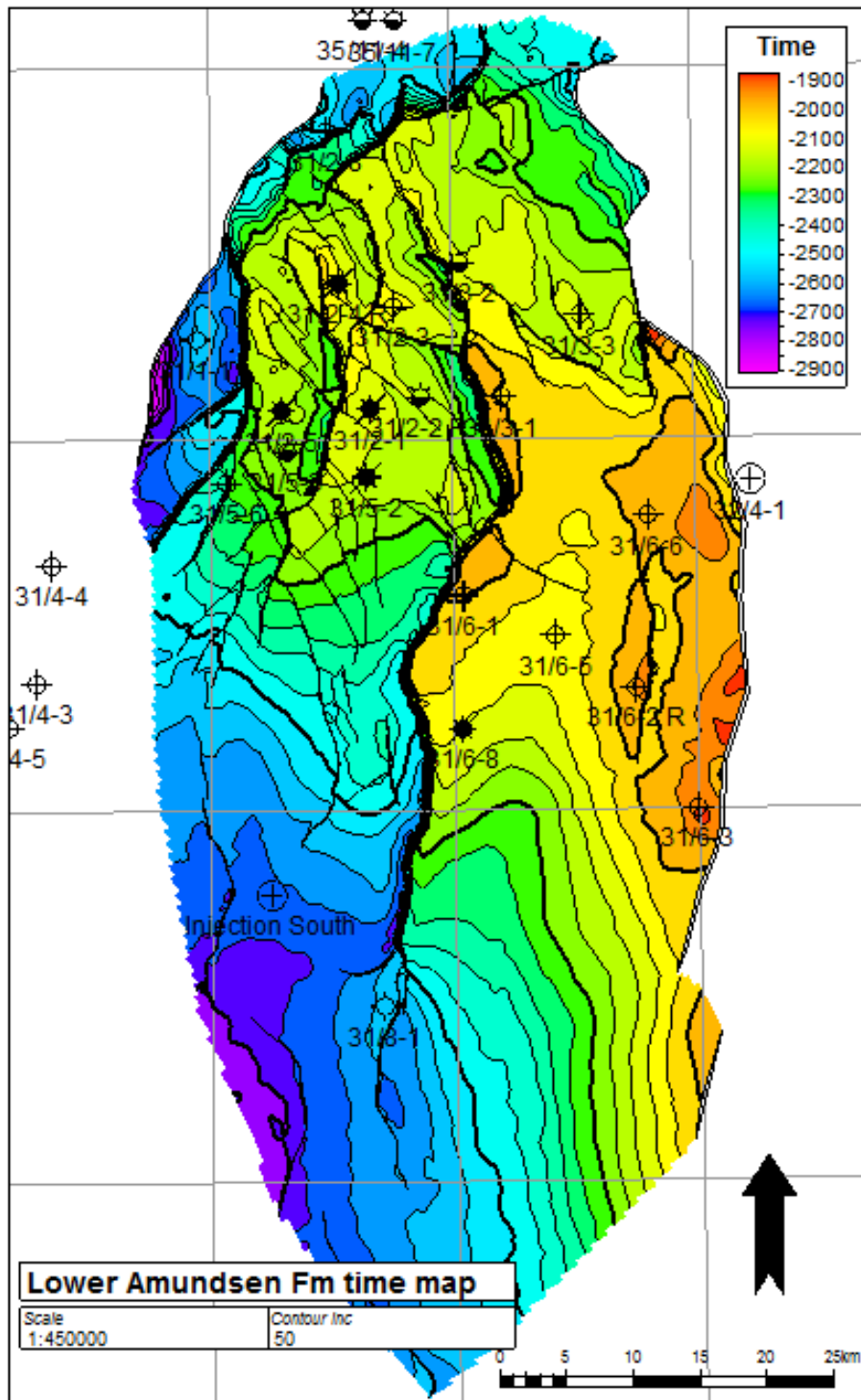


Figure 33: Lower Amundsen Fm time map.

DOCUMENT NO.: TL02-GTL-Z-RA-0001	REVISION NO.: 03	REVISION DATE: 01.03.2012	APPROVED:
-------------------------------------	---------------------	------------------------------	-----------

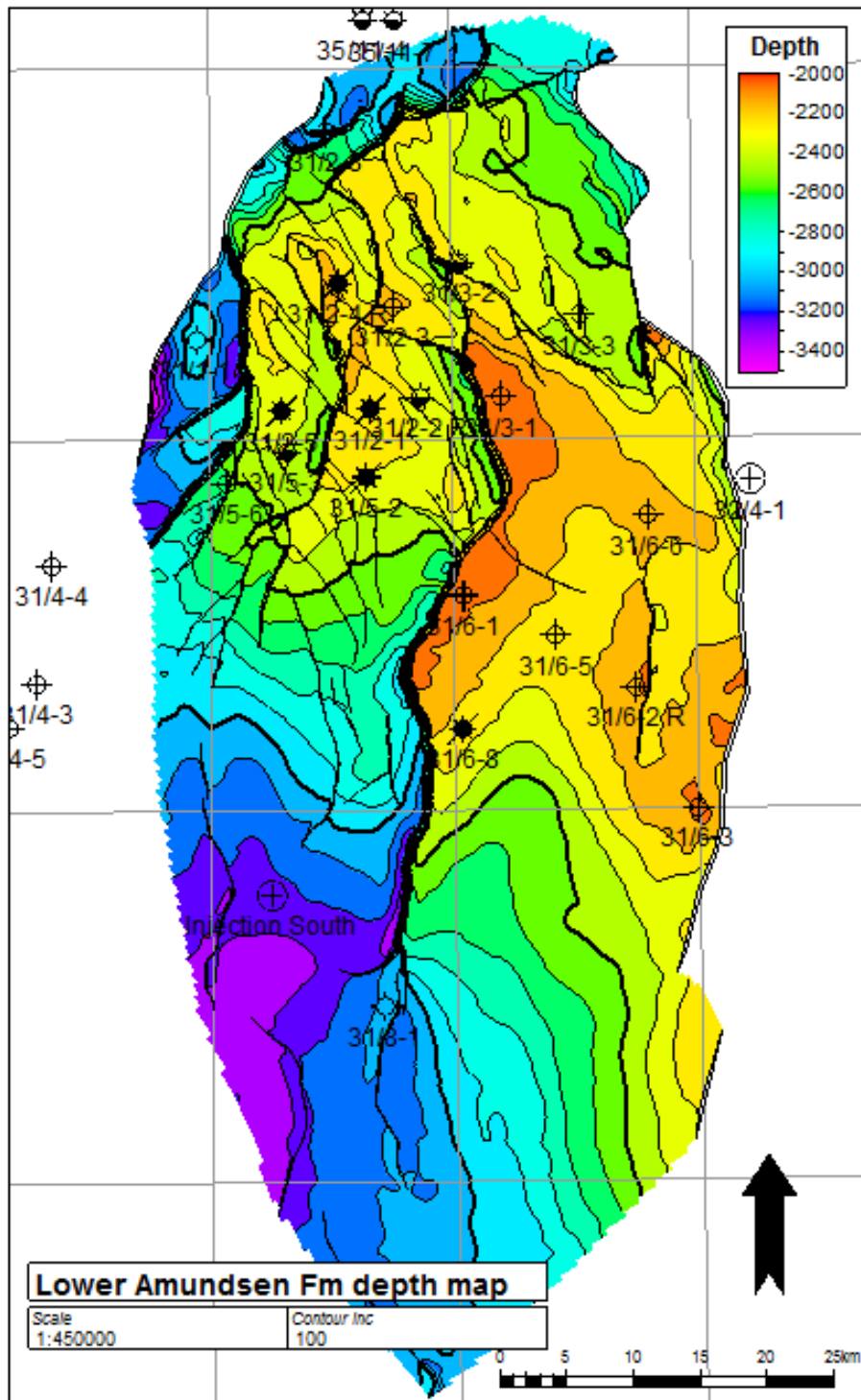


Figure 34: Lower Amundsen Fm depth map.

DOCUMENT NO.: TL02-GTL-Z-RA-0001	REVISION NO.: 03	REVISION DATE: 01.03.2012	APPROVED:
-------------------------------------	---------------------	------------------------------	-----------

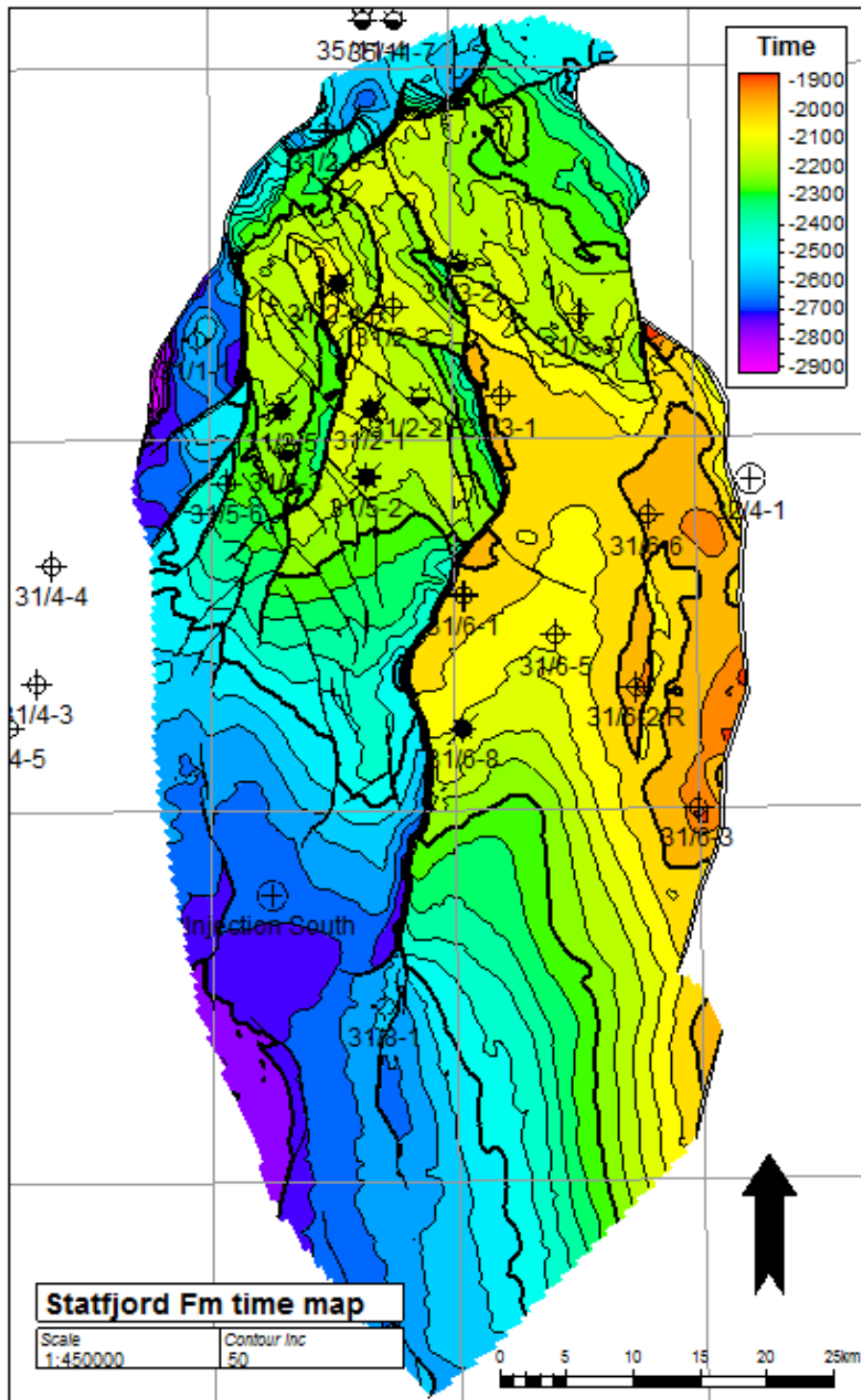


Figure 35: Statfjord Fm time map.

DOCUMENT NO.: TL02-GTL-Z-RA-0001	REVISION NO.: 03	REVISION DATE: 01.03.2012	APPROVED:
-------------------------------------	---------------------	------------------------------	-----------

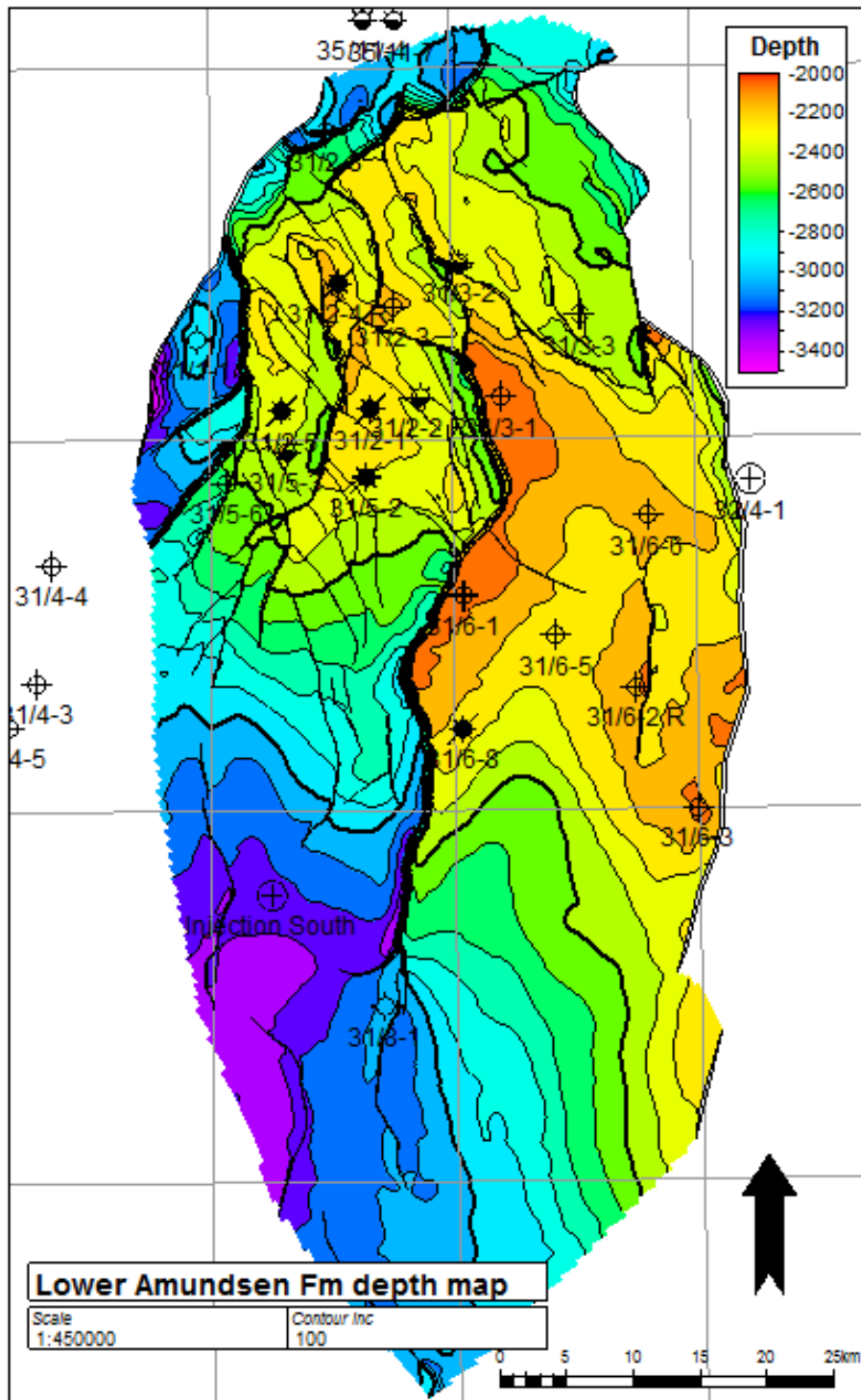


Figure 36: Staffjord Fm depth map.

DOCUMENT NO.: TL02-GTL-Z-RA-0001	REVISION NO.: 03	REVISION DATE: 01.03.2012	APPROVED:
-------------------------------------	---------------------	------------------------------	-----------

Velocity Modelling for Depth Conversion in Quadrant 31

Documentation of proprietary hiQbe®

for

GassNova

by

Aker Geo

Oslo, June 2011

DOCUMENT NO.: TL02-GTL-Z-RA-0001	REVISION NO.: 03	REVISION DATE: 01.03.2012	APPROVED:
-------------------------------------	---------------------	------------------------------	-----------

Summary

A hiQbe® 3D velocity model was made for Gassnova for the purpose of depth conversion in the quadrant 31 area. The model covers quadrant 31 from south to north, but is slightly offset in the east-west direction, starting mid-way in blocks 31/1, -4, -7 and -10 on the western side, and ending mid-way in blocks 32/1, -4, -7 and -10 on the eastern side. Figure 1 shows a base map of the hiQbe, with the stacking velocity and well data used, overplotting calibrated average velocity at 2000 ms TWT. A hiQbe® is a 3D velocity model which can be used directly in depth conversion. It is based on stacking velocities and check shots. The stacking velocities are balanced from survey to survey, then filtered to remove noise. Well calibration consists of anisotropy modelling and well tie. The quality of a hiQbe® depends on the quality and coverage of the input data. In this case the quality was good throughout, but the coverage was very variable, from excellent inside the 3D area to very loose in the 2D area. As a consequence, the hiQbe® is of high quality inside the 3D area, suitable for detailed depth conversion of structures and for well planning, and of lesser quality outside, suitable for regional depth conversions such as needed in an aquifer study.

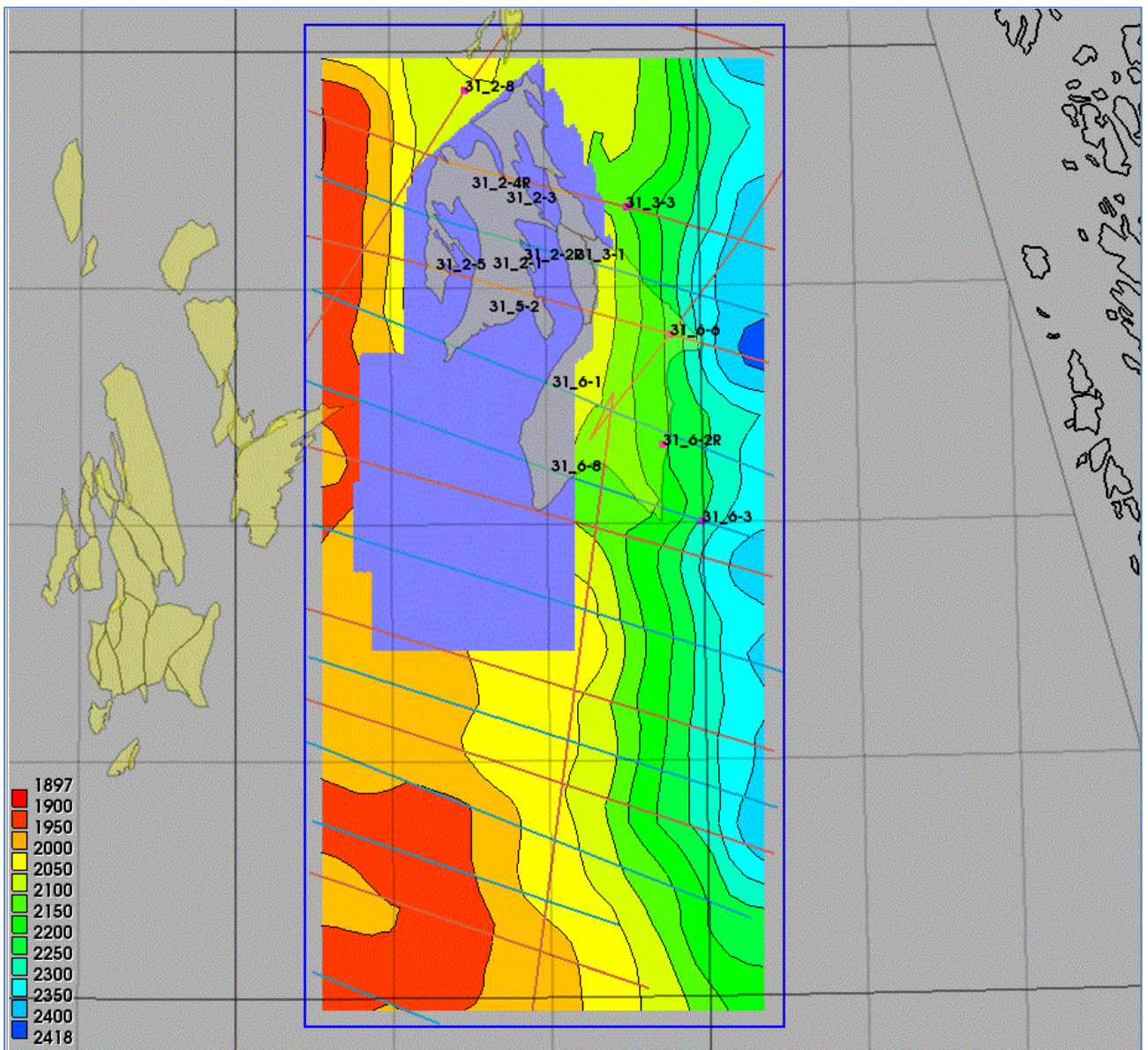


Figure 14-3: hiQbe base map with average velocity at 2000ms TWT.

DOCUMENT NO.: TL02-GTL-Z-RA-0001	REVISION NO.: 03	REVISION DATE: 01.03.2012	APPROVED:
-------------------------------------	---------------------	------------------------------	-----------

Data base

The data base consisted of stacking velocities from selected seismic surveys and check shots from selected wells. The surveys and wells used are listed in

Table 14-1 and

Table 142. The primary data set is GassNova’s 3D survey GN10M1.

The stacking velocity data from GN10M1 were provided in SEG-Y format, with file name GN10M1_STACKING_VELOCITY_50m.SEGY. The contents of the EBCDIC header are listed below (with blank lines omitted).

```
C01 CLIENT: GASSNOVA SF CONTRACTOR: WESTERNGECO
C02 AREA: W.TROLL FIELD QUAD 31 OFFSHORE NORWAY
C03 DATA TYPE: GN10M1 FINAL STACKING RMS VELOCITY CUBE
C04 VELOCITY GRID IS 50mX50m
C05 FORMAT: SEGY SAMPLE RATE: 20MS 201 SAMPLES/TR 4BYTE IBM FLOATING
C06 INLINE RANGE: 975 - 3783 INC 2
C07 XLINE RANGE: 1545-6521 INC 8
...
C35 XY COORDINATES MULTIPLIED BY 100
C36 CDPX BYTE181 I4, CDPY BYTE185 I4, INLINE BYTE189 I4, XLINE BYTE193 I4
C37 SURVEY NAME: GN10M1
C38 DATUM: ED50 PROJECTION: UTM CENTRAL MERIDIAN: 03 DEG E SPHEROID :INT 1926
C39 GRID ORIGIN:505030.0 6690221.0 - CELL SIZE: 12.5MX25M - AZIMUTH: 90DEG
C40 END EBCDIC
```

The other data, two 2D surveys and check shots from fourteen wells, are public domain data sets borrowed from Aker Geo’s internal data base. No data from these, neither in raw nor time sliced form, were given to GassNova. The only data set delivered to GassNova was the hiQbe®.

The responsibility with regards to GassNova’s right to use these data lies with GassNova. While such use should be permitted in Aker Geo’s opinion, as long as the raw data are not distributed to GassNova, we do not speak on behalf of the data owners, and we do not claim to interpret correctly the meaning of the regulations for use of public domain data in Norway.

Table 14-1: Survey list.

survey	type	size	line km	gathers	area km2
GN10M1	xytv	341329758	6024.3	22054	2119.8
nvgt-88	STK_VEL	0	539.6	282	6469.5
nvgti-3-92	STK_VEL	0	397	223	5625.2

Table 14: Well list.

well	points	well	points	well	points
31_2-2R	74	31_3-1	62	31_6-3	56
31_2-3	70	31_3-3	64	31_6-6	58
31_2-4R	114	31_5-2	52	31_6-8	48
31_2-5	68	31_6-1	92	31_2-1	64
31_2-8	84	31_6-2R	56		

DOCUMENT NO.: TL02-GTL-Z-RA-0001	REVISION NO.: 03	REVISION DATE: 01.03.2012	APPROVED:
-------------------------------------	---------------------	------------------------------	-----------

hiQbe processing sequence

The processing sequence has the following steps:

- Data preparation and QC
- Stacking velocity modelling
 - Survey to survey balancing
 - Statistical low-pass noise filter
- Well calibration
 - Anisotropy modelling
 - Well tie
- Output of well calibrated hiQbe®

The cube dimensions were 2km by 2km laterally and 50ms vertically, from 100ms to 4000ms.

Data preparation and QC

Figure 2 shows a Dix interval velocity QC display of the GN10M1 velocity field after format conversion from SEG-Y. The inline runs approximately through the middle of the 3D, through well 31/2-4R. Four time horizons from a regional Aker Geo map series are shown as thin blue lines; these are Seabed, Base Tertiary, BCU and Top Triassic. The Cretaceous pinches out from the south (right) to the north (left), and Base Tertiary and BCU almost coincide in the north (left) on top of the Troll field, where the Cretaceous section is very thin. We can see that the velocities are distinctly different in the Tertiary, Cretaceous and Jurassic. The dip of the Jurassic layers, as seen by the velocity cross-section, is correct. This is a good quality stacking velocity field.

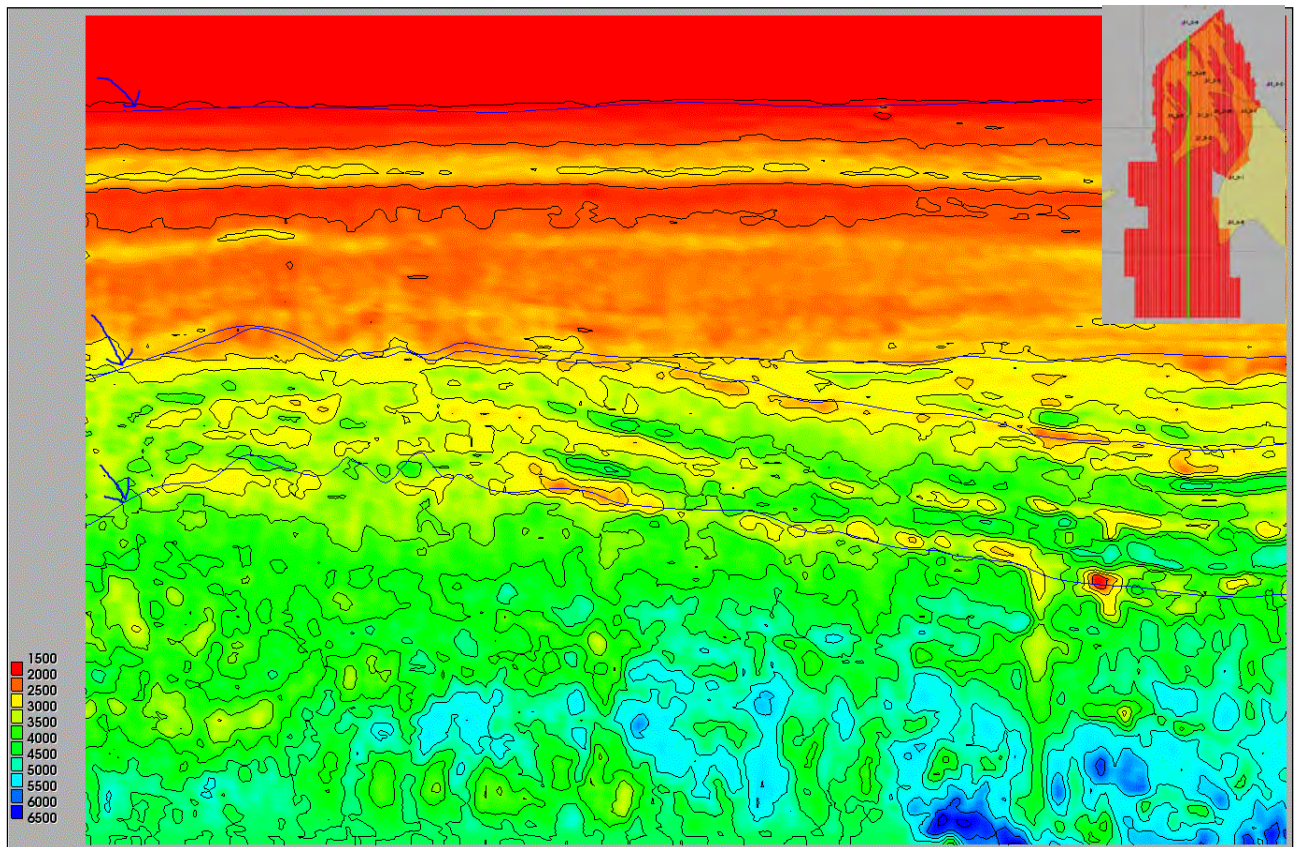


Figure 2: Dix interval velocity from GN10M1 on NS inline through well 31/2-4R.

DOCUMENT NO.: TL02-GTL-Z-RA-0001	REVISION NO.: 03	REVISION DATE: 01.03.2012	APPROVED:
-------------------------------------	---------------------	------------------------------	-----------

Stacking velocity modelling

Survey to survey balancing is illustrated in Figure 3. Velocity data from two partially overlapping surveys are seen from the side. In the original data, one has systematically higher velocities than the other. Balancing is done by keeping one fixed (the pink) and by multiplying the other (blue) with a scaling factor which causes the two data sets to line up. In this study, GN10M1 was fixed, and the two 2D surveys were balanced. Scaling factors were determined for each level in the cube.

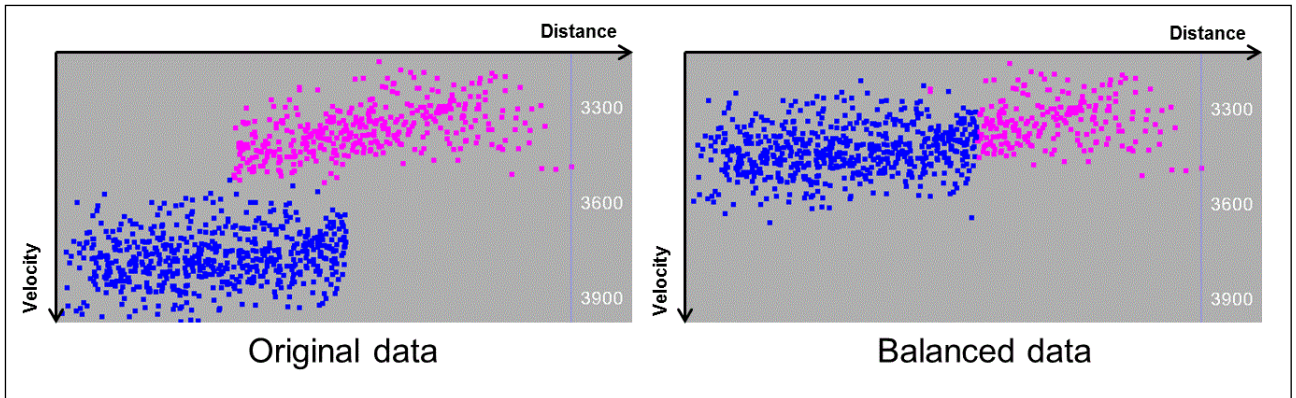


Figure 14: Survey to survey balancing.

Stacking velocities are seismic imaging parameters, and they are not always proportional to true velocity. When used for depth conversion, they contain noise which first must be removed. This is best done with a low pass statistical noise filter. The effect of this is seen when comparing Figure 14 (raw data) with Figure 4 4 (final hiQbe®). In Figure 4 left is east and right is north.

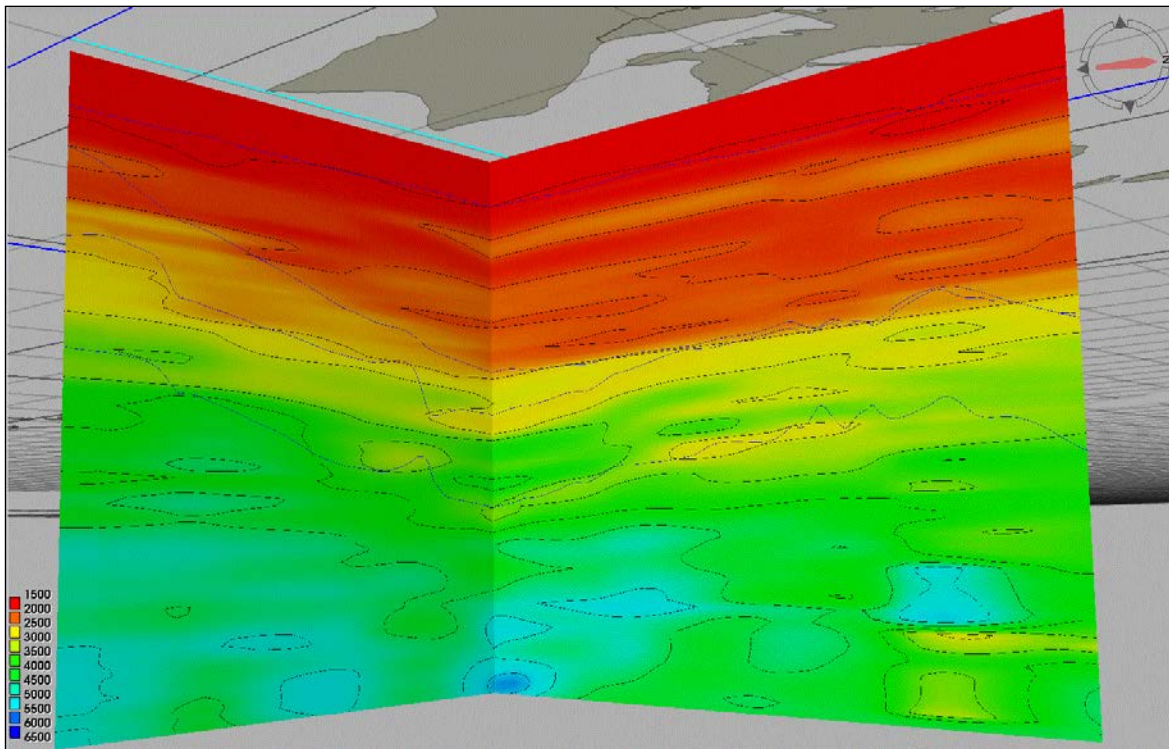


Figure 4: Interval velocity from the well calibrated average velocity cube.

DOCUMENT NO.: TL02-GTL-Z-RA-0001	REVISION NO.: 03	REVISION DATE: 01.03.2012	APPROVED:
-------------------------------------	---------------------	------------------------------	-----------

Figure 4 is a composite of two cross-sections, one north-south (along the same line as in Figure 3) and one east-west. The same time horizons are displayed. The east-west leg touches the southernmost tip of Troll East. This is a 3D perspective, and the velocity cross-sections start a little below MSL. The light blue line is the exact position of the east-west part, relative to the base map.

When comparing Figure 3 and Figure 4 we see that the former (raw data) is much crisper and more distinct than the latter (hiQbe®), but this is deceptive. The crisper raw data set has a lot more noise than the hiQbe®, and is not suitable for depth conversion. When modelling velocities for depth conversion there is a trade-off between resolution and depth conversion accuracy, and some of the resolution in the raw data must be sacrificed. It is therefore a good idea to keep the raw data, and to use that directly if the objective is “velocity inversion” (a term we use in Aker Geo), that is, to derive geological information from the velocity data by inverting them to a different domain.

The east-west leg of Figure 4 runs almost entirely through an area with sparse 2D seismic coverage. The pinch out of the Tertiary towards the coast has been picked up, but it is not quite accurately modelled at the left (eastern) edge. The velocity cross-section “flattens out” where there is still dip on the time horizons (thin blue lines). This is because the 2D line coverage is too sparse. This should be kept in mind when using the hiQbe®. The 2D data have given the hiQbe® very reasonable regional velocity trends outside of the 3D area, but the sparse 2D coverage limits the quality of the velocity model in some locations.

Well calibration

Anisotropy modelling is done by interpretation of a general scaling factor curve, which is used to convert the stacking velocity cube to the average velocity domain. The pink crosses in Figure 5 are average scaling factors from the wells, for each level. The red line is the digitized curve. The scaling factors are calculated (and applied) below Seabed, because the water leg is isotropic.

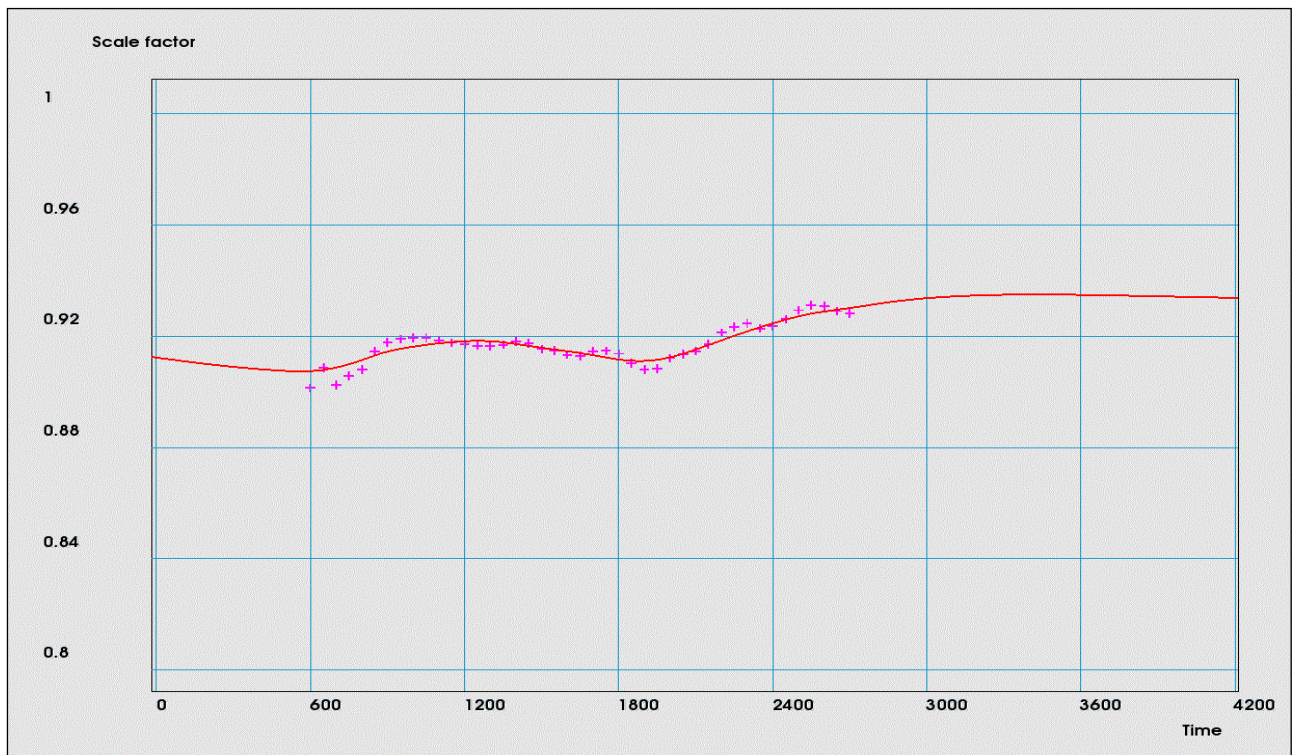


Figure 5: Anisotropy modelling.

DOCUMENT NO.: TL02-GTL-Z-RA-0001	REVISION NO.: 03	REVISION DATE: 01.03.2012	APPROVED:
-------------------------------------	---------------------	------------------------------	-----------

Well tie is first done in the scaling factor domain. Scaling factor well tie is equivalent to lateral mapping of anisotropy. It is done at each time level in the cube. Figure 6 shows the scaling factor grid at 2000ms. A large lateral radius has been used, in order to make values in wells in the same geological setting merge together into a continuous pattern.

The pattern at this level is not the same as at other levels. (There is not a systematic east flank effect.)

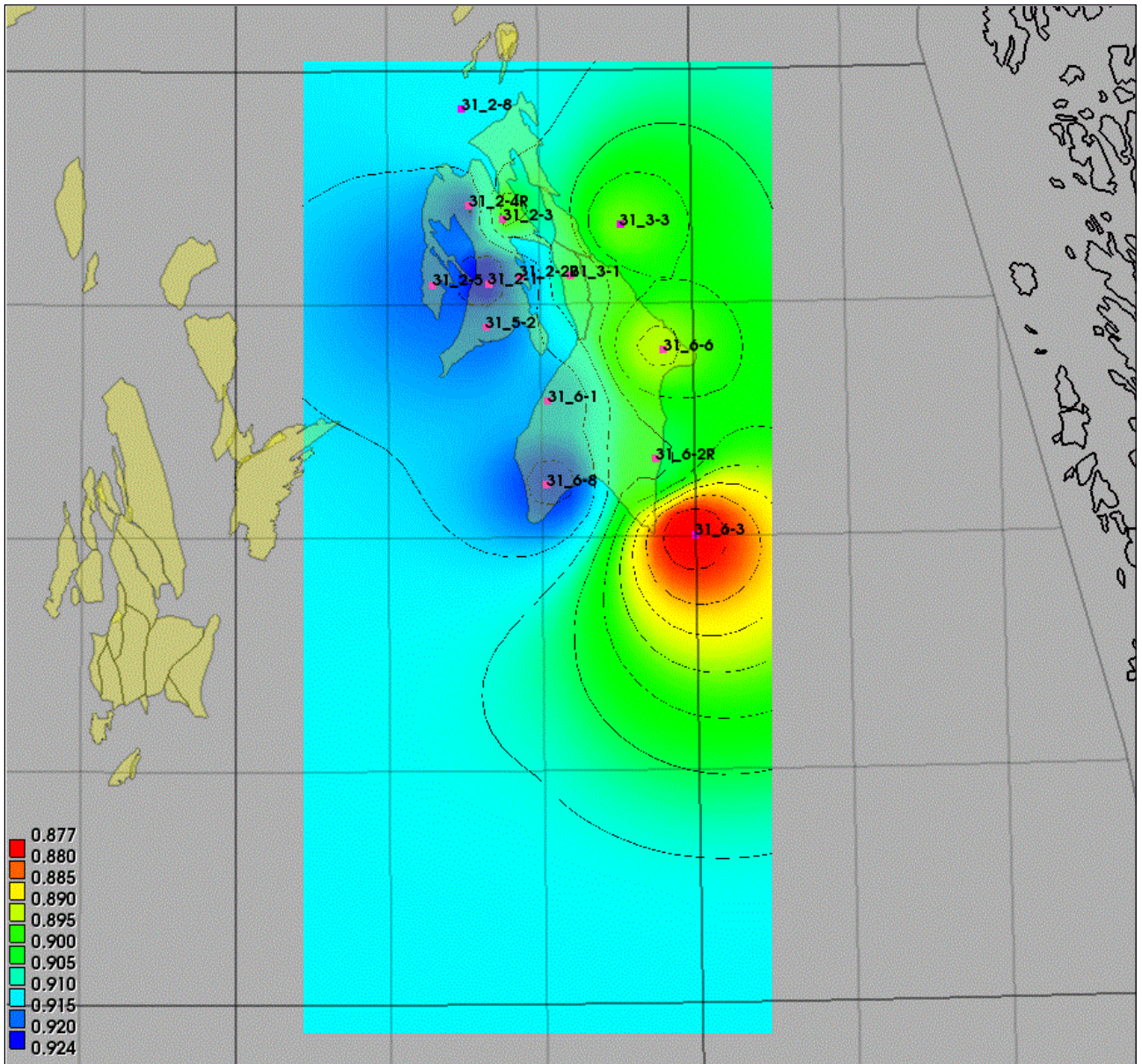


Figure 6: Scaling factor grid at 2000ms TWT.

The individual scaling factors can be considered to consist of two components, remaining stacking velocity noise at the well, and actual anisotropy. It is not always easy to tell these apart.

Another well tie in the average velocity domain is done after this, in order to eliminate numerical inaccuracies. The hiQbe® will therefore tie precisely to the wells, to the extent that it is possible with the 2km by 2km grid resolution.

DOCUMENT NO.: TL02-GTL-Z-RA-0001	REVISION NO.: 03	REVISION DATE: 01.03.2012	APPROVED:
-------------------------------------	---------------------	------------------------------	-----------

Depth conversion with the hiQbe®

The calibrated average velocity hiQbe® was delivered on SEG-Y format, ready to be imported to Petrel and used for depth conversion there.

Depth conversion with this cube in Petrel is straight forward. A time grid is converted directly to depth. For regional studies it is not necessary to do anything more than this. In local studies, where accurate seismic interpretations and well tops are available, it is recommended to finish the depth conversion with a depth well tie.

Depth conversion uncertainty

In this area of the North Sea, the velocity related depth conversion uncertainty can be expected to be within ±1% where the seismic data quality and coverage is good. By rule of thumb, this should apply to the 3D area above the level of Top Triassic. In the 2D area, or at deeper levels, or in parts of the 3D area with poor seismic data quality (if any), the uncertainty will be two to three times as large. This is an estimate of standard deviation of depth prediction error in wells, after elimination of any static shift.

This velocity uncertainty is related to the remaining stacking velocity noise in the hiQbe®, and can be expected to have the shape of a random field with a wavelength of between 3 and 5km. The appropriate method to use for volumetric uncertainty estimates is stochastic modelling.

For well prognoses it is often necessary to come up with a P₁₀ - P₉₀ estimate rather than the standard deviation. To convert to this we must multiply with 1.28 (1% becomes 1.28%). This assumes a normal distribution (which is as good a guess as any).

In a depth conversion there will also be uncertainty related to the seismic time interpretation and the well ties. This should be estimated by the interpreter and added to the velocity uncertainty.

DOCUMENT NO.: TL02-GTL-Z-RA-0001	REVISION NO.: 03	REVISION DATE: 01.03.2012	APPROVED:
-------------------------------------	---------------------	------------------------------	-----------

A6 Content Johansen Storage Complex Petrel Projects

Project data stored in USB disk delivered Gassnova.

SEISMIC INTERPRETATION FINAL

- Storage complex 2D and 3D database
- 2D and 3D time horizon and fault interpretation of the key horizons described in the seismic interpretation chapter (5.2.2).
- Key well database
- Main input for Storage Complex Description evaluations

CAP ROCK EVALUATION

- Project used for evaluation described in Chapter 5.6.
- Interpretation of the Upper and Lower Drake formations
- SVI-Pro cubes used for leakage evaluation
- Cap Rock fault interpretation
- Seismic attribute cubes and maps
- Inversion cubes and maps

GEOMODEL FINAL

- Project used for evaluation described in Chapter 5.3, 5.4, 5.5 and 5.8.
- Refined horizon and fault interpretation used in building the geomodel
- Well data (logs and correlations) from the petrophysical evaluation used for formation evaluation and building of the different property models (porosity and permeability)
- Seismic attribute cubes and maps
- Inversion cubes and maps
- Well correlations: logs and lithology interpretation
- Velocity models for depth conversion
- Inversion cubes and maps
- Various input used in the risk and volume connectivity evaluations

SVI-PRO

- Generated SVI-Pro cubes used for Fault Seal study and storage complex evaluation

GASSNOVA INVERSION RESULTS

- Resulting inversion cubes:
 - Acoustic impedance cubes with or without LFM
 - Density cubes with or without LFM
 - Different lithology cubes

4D MONITORING STUDY

- 4D monitoring seismic results

SINTEF_Petrel_final_results

- Basin modelling result from 3 2D lines:
 - Porosity data
 - Thermal development
 - SGR of major faults
 - Overpressure model

DOCUMENT NO.: TL02-GTL-Z-RA-0001	REVISION NO.: 03	REVISION DATE: 01.03.2012	APPROVED:
-------------------------------------	---------------------	------------------------------	-----------

RESERVOIR MODEL

- Reference simulation model for the Johansen Storage Complex as an Eclipse 100 data file. All include files (GRID, PROPS, SUMMARY and SCHEDULE) are included in one text document.
- Result files for simulations, simulated for 500 years (2014-2514) ready for import in Petrel

DOCUMENT NO.: TL02-GTL-Z-RA-0001	REVISION NO.: 03	REVISION DATE: 01.03.2012	APPROVED:
-------------------------------------	---------------------	------------------------------	-----------